



Province of British Columbia  
Ministry of Energy, Mines and  
Petroleum Resources  
Hon. Anne Edwards, Minister

MINERAL RESOURCES DIVISION  
Geological Survey Branch

# **GEOLOGICAL FIELDWORK 1993**

**A Summary of Field Activities  
and Current Research**

Editors: B. Grant and J.M. Newell

**PAPER 1994-1**

# MINERAL RESOURCES DIVISION

## Geological Survey Branch

Parts of this publication may be quoted or reproduced if credit is given. The following is the recommended format for referencing individual works contained in this publication:

Stephen J. Cook and Wayne Jackaman (1994): Regional Lake Sediment and Water Geochemistry Surveys in the Northern Interior Plateau, B.C. (93F/2, 3, 6, 11, 12, 13, 14); in *Geological Fieldwork 1993*, Grant, B. and Newell, J.M., Editors, *British Columbia Ministry of Energy, Mines and Petroleum Resources*, Paper 1994-1, pages 37-42.

### British Columbia Cataloguing in Publication Data

Main entry under title:

Geological fieldwork: - 1974 -

(Paper, ISSN 0226-9430)

Annual.

Issuing body varies: 1974-1980, Geological Division; 1981-1985, Geological Branch; 1986- , Geological Survey Branch.

Subseries, 1979- , of: Paper (British Columbia. Ministry of Energy, Mines and Petroleum Resources)  
"A summary of field activities of the Geological Division, Mineral Resources Branch."

ISBN 0381-243X=Geological fieldwork

1. Geology - British Columbia - Periodicals. 2. Geology, Economic - British Columbia - Periodicals. 3. Mines and mineral resources - British Columbia - Periodicals. I. British Columbia. Geological Division. II. British Columbia. Geological Branch. III. British Columbia. Geological Survey Branch. IV. British Columbia. Ministry of Energy, Mines and Petroleum Resources. V. Series: Paper (British Columbia. Ministry of Energy, Mines and Petroleum Resources)

QE187.G46

557.11'05

Rev. Dec. 1987



VICTORIA  
BRITISH COLUMBIA  
CANADA

JANUARY 1994

## FOREWORD

The 1993 edition of *Geological Fieldwork: A Summary of Field Activities and Current Research* is the nineteenth in this annual publication series. It contains reports on Geological Survey Branch activities and projects. The base budget of the Branch for the 1993/94 fiscal year is \$5.63 million. This budget has been supplemented by an additional \$469 000 from the Inter-Ministry Corporate Resource Inventory Initiative to prepare 1:250 000 scale mineral potential maps of Commission on Resources and Environment planning areas.

Regular readers will notice significant changes in the appearance of this year's volume. For the first time production to the camera-ready stage has been entirely by in-house "word processor". Authors have been responsible for the input, formatting and lay-out of their own papers.

The contents of this year's volume reflect the new emphasis of integrated multidisciplinary survey programs. Reports on two major integrated studies, the northern Vancouver Island and Interior Plateau projects are grouped together. Each section includes an overview paper and separate reports on bedrock mapping, surficial geology, applied geochemistry and aspects of metallogenesis. The geochemical components of these programs emphasized the study of natural acid drainage on northern Vancouver Island and the viability of lake-sediment sampling as an exploration technique in heavily drift-covered areas of the Interior Plateau.

Other major contributions to the Ministry's Economic Development Program include 1:50 000 mapping projects in the Yahk-Creston area of the East Kootenays, with emphasis on the Aldridge Formation which hosts the Sullivan orebody; the area surrounding the Goldstream mine in the northern Selkirk Mountains; and the Tulsequah area of north western British Columbia where exciting new discoveries have been made on the old Tulsequah Chief property. These programs are targeted on regions where existing reserves will be depleted before the turn of the century or, in the case of Tulsequah, where a past-producer appears headed for revitalization and the surrounding area has promise for new exploration opportunities. Three papers report on continuing research on the coalbed methane potential of British Columbia coals.

An important element of the Branch's 1993/94 program, the Mineral Potential Initiative, is not reported on in this volume as its objectives are geared to the publication of state of the art, stand-alone mineral potential maps at 1:250 000 scale. The first phase of the project, the assessment of the mineral potential of Vancouver Island, is complete.

This volume also includes thirteen papers from the Mineral Deposit Research Unit at The University of British Columbia, providing new insights into alkalic porphyry copper-gold deposits and volcanogenic massive sulphide deposits in the province with particular emphasis on the porphyries in the Ironmask batholith and massive sulphide deposits at Myra Falls on Vancouver Island, Tulsequah and Anyox on the Mainland Coast.

I would like to acknowledge the efforts of the Scientific Review Office for once again meeting tight publication deadlines; John Newell for his thorough and timely edits and Brian Grant for guiding the whole process.

*W.R. Smyth*  
*Chief Geologist*  
*Geological Survey Branch*  
*Mineral Resources Division*

# TABLE OF CONTENTS

	<i>Page</i>		<i>Page</i>
<b>FOREWORD</b> . . . . .	3	<b>REGIONAL GEOLOGY</b>	
<b>INTERIOR PLATEAU PROJECT</b>		<b>D.A. Brown, J.A. Bradford, D.M. Melville A.S. Legun, and D. Anderson:</b> Geology and Mineral Deposits of Purcel Supergroup in Yahk Map Area, Southeastern British Columbia (82F/1) . . . . .	129
<b>P.F. Matysek and P. van der Heyden:</b> 1993-1994 Update: Interior Plateau Program . . . . .	9	<b>J.M. Logan and J.R. Drobe:</b> Summary of Activities North Selkirk Project Goldstream River and Downie Creek Map areas (82M/8, 9 and Parts of 10) . . . . .	153
<b>L.J. Diakow and I.C.L. Webster:</b> Geology of the Fawnie Creek Map Area (93F/3) . . . . .	15	<b>M.G. Mihalynuk, M.T. Smith, K.D. Hancock and S. Dudka:</b> Regional and Economic Geology of the Tulsequah River and Glacier Areas (104K/12, & 13) . . . . .	171
<b>T.R. Giles and V.M. Levson:</b> Surficial Geology and Drift Exploration Studies in the Fawnie Creek Area (93F/3) . . . . .	27	<b>APPLIED GEOCHEMISTRY AND SURFICIAL GEOLOGY</b>	
<b>S.J. Cook and W. Jackaman:</b> Regional Lake Sediment and Water Geochemistry Surveys in the Northern Interior Plateau, B.C. (93F/2, 3, 6, 11, 12, 13, 14) . . . . .	39	<b>W. Jackaman:</b> B.C. Regional Geochemical Survey Program: Highlights from the 1993 Release (104M) . . . . .	201
<b>T.G. Schroeter and R.A. Lane:</b> Mineral Resources: Interior Plateau Project (93F/3 and parts of 93F/2, 6 & 7) . . . . .	45	<b>B. Bhagwanani and R.E. Lett:</b> The Sequential Extraction of Copper, Silver, Molybdenum, Iron and Manganese from Geochemical Standards and Selected Samples . . . . .	207
<b>VANCOUVER ISLAND PROJECT</b>		<b>COAL</b>	
<b>A. Panteleyev, P.T. Bobrowsky, G.T. Nixon and S.J. Sibbick:</b> Northern Vancouver Island Integrated Project . . . . .	59	<b>B.D. Ryan and M.F. Dawson:</b> Coalbed Methane Desorption Results from the Quinsam Coal Mine and Coalbed Methane Resource of the Quinsam Coalfield, British Columbia (92F/13, 14) . . . . .	215
<b>G.T. Nixon, J.L. Hammock, V.M. Koyanagi, G.J. Payie, A. Panteleyev, N.W.D. Massey, J.V. Hamilton and J.W. Haggart:</b> Preliminary Geology of the Quatsino - Port McNeill Map Areas, Northern Vancouver Island (92L/12, 11) . . . . .	63	<b>B.D. Ryan and M.F. Dawson:</b> Potential Coal and Coalbed Methane Resource of the Telkwa Coalfield, Central British Columbia (93L/11) . . . . .	225
<b>P.T. Bobrowsky and D. Meldrum:</b> Preliminary Drift Exploration Studies, Northern Vancouver Island (92L/6, 92L/11) . . . . .	87	<b>B.D. Ryan and F.M. Dawson:</b> Coalbed Methane Canister Desorption Techniques . . . . .	245
<b>A. Panteleyev and V.M. Koyanagi:</b> Advanced Argillic Alteration in Bonanza Volcanic Rocks, Northern Vancouver Island - Lithologic and Permeability Controls . . . . .	101	<b>PORPHYRY DEPOSITS - MDRU</b>	
<b>S.J. Sibbick:</b> Preliminary Report on the Application of Catchment Basin Analysis to Regional Geochemical Survey Data, Northern Vancouver Island (92L/3, 4, 5 and 6) . . . . .	111	<b>T.M. Fraser:</b> Hydrothermal Breccias and Associated Alteration of the Mount Polley Copper-Cold Deposit (93A/12) . . . . .	259
<b>V.M. Koyanagi and A. Panteleyev:</b> Natural Acid Rock-Drainage in the Red Dog/Hushamu/Pemberton Hills Area, Northern Vancouver Island (92L/12) . . . . .	119	<b>C.R. Stanley, J.R. Lang and L.D. Snyder:</b> Geology and Mineralization in the Northern Part of the Iron Mask Batholith, Kamloops, British Columbia (92I/9, 10) . . . . .	269

<b>C.R. Stanley:</b> Geology of the Pothook Alkalic Copper-Gold Porphyry Deposit, Afton Mining Camp, British Columbia (92I/9, 10) . . . . .	275	<b>R.W.J. Macdonald, T.J. Barrett, R.L. Sherlock, R.L. Chase, P. Lewis and D.J. Alldrick:</b> Geological Investigations of the Hidden Creek Deposit, Anyox, Northwestern British Columbia (103/P5) . . . . .	351
<b>J.R. Lang:</b> Geology of the Crescent Alkalic Porphyry Copper-Gold Deposit, Afton Mining Camp, British Columbia (92I/9) . . . . .	285	<b>R.L. Sherlock, T.J. Barrett, T. Roth, F. Childe, J.F.H. Thompson, D. Kuran, H. Marsden and R. Allen:</b> Geological Investigations of the 21B Deposit, Eskay Creek, Northwestern British Columbia (104B/9W) . . . . .	357
<b>L.D. Snyder and J.K. Russell:</b> Petrology and Stratigraphic Setting of the Kamloops Lake Picritic Basalts, Quesnellia Terrane, South-Central B.C. (92I/9, 15 and 16) . . . . .	297	<b>A.W. Kaip and D. Gaunt:</b> Geology and Alteration Zonation of the Hank Property, Northwestern British Columbia (104G/1, 2) . . . . .	365
<b>B.A. Lueck and J.K. Russell:</b> Silica-Undersaturated, Zoned, Alkaline Intrusions Within the British Columbia Cordillera . . . . .	311	<b>R.L. Sherlock, F. Childe, T.J. Barrett, J. Mortensen, P.D. Lewis, T. Chandler, P. McGuigan, G.L. Dawson and R. Allen:</b> Geological Investigations of the Tulsequah Chief Massive Sulphide Deposit, Northwestern British Columbia (104K/12) . . . . .	373
<b>VMS DEPOSITS - MDRU</b>		<b>EXTERNAL PUBLICATIONS AND UNIVERSITY RESEARCH</b>	
<b>M. Robinson, C.I. Godwin and S.J. Juras:</b> Major Lithologies of the Battle Zone, Buttle Lake Camp, Central Vancouver Island (92F/12E) . . . . .	319	External Publications by B.C. Geological Survey Branch Staff . . . . .	383
<b>T.J. Barrett, R.L. Sherlock, S.J. Juras, G.C. Wilson, R. Allen:</b> Geological Investigations of the H-W Deposit, Buttle Lake Camp, Central Vancouver Island (92F/12E) . . . . .	339	University Research in British Columbia . . . . .	385
<b>S. McKinley, J.F.H. Thompson, T.J. Barrett, R. Sherlock, R. Allen, C. Burge:</b> Geology of the Seneca Property, Southeastern British Columbia (92H/5W) . . . . .	345		

## 1993 - 94 UPDATE: INTERIOR PLATEAU PROGRAM

By Paul F. Matysek, B.C. Geological Survey Branch  
and  
Peter van der Heyden, Geological Survey of Canada

(B.C. Ministry of Energy, Mines and Petroleum Resources Mineral Strategy - Targeted Geology Program  
and Canada - British Columbia Mineral Development Agreement, 1991 - 1995)

**KEYWORDS:** Interior Plateau, regional geology, surficial geology, economic geology, lake sediment geochemistry, biogeochemistry, airborne geophysics, ground geophysics

### INTRODUCTION

The Interior Plateau program is a major geoscience initiative that is funded federally under the guidelines of the Canada - British Columbia Mineral Development Agreement and provincially by the Ministry of Energy, Mines and Petroleum Resources as part of its 1993 Mineral Strategy.

Prospective geological environments favourable for economic mineral deposits exist in areas adjoining the Interior Plateau study area (e.g., porphyry deposits such as Endako and Gibraltar, the Equity Silver deposit and epithermal precious metal deposits such as Silver Queen and Blackdome). Extrapolation of structural trends, plutonic suites and stratigraphy suggests that there is potential for similar, undiscovered economic deposits in the region.

Mineral exploration and development in the region has been severely hampered by a number of factors which include: poor infrastructure, inaccessibility, dense vegetation, extensive and variably thick glacial drift, a blanket of Miocene and younger lava flows, an obsolete geological database and lack of modern geophysical and geochemical coverage. As a result most of this region of central British Columbia is under-explored and consequently poorly understood and undervalued.

Staff of the Geological Survey of Canada (GSC) and the British Columbia Geological Survey Branch (BCGS) have conducted a number of integrated multi-disciplinary projects throughout the Interior Plateau region (Figure 1). Two key objectives of this undertaking are to provide new data to upgrade the existing geological, geochemical and geophysical databases and the development of new exploration models and technologies. The integration of the new geoscientific information will aid mineral exploration and better support mineral potential assessment and informed resource management and land-use decisions in the region.

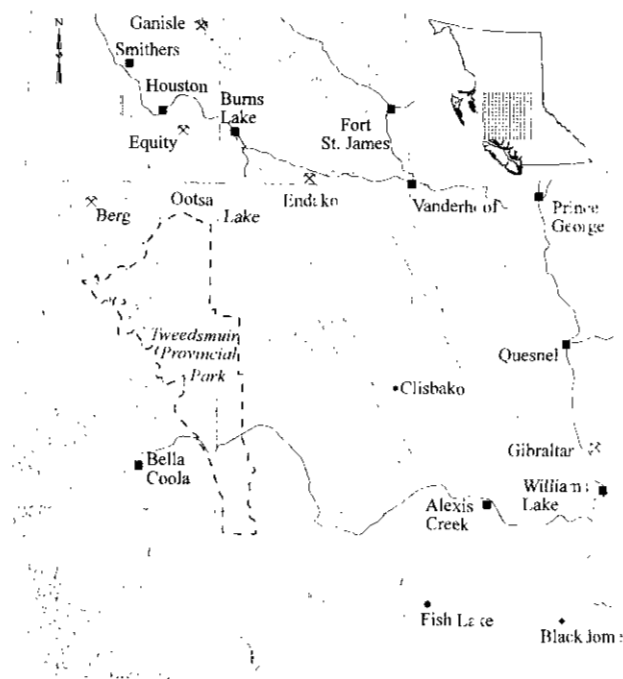


Figure 1. Producing mines (shown by diamonds) and other significant mineral deposits in the Interior Plateau region.

This report gives a brief overview and highlights of projects carried out by both the BCGS and GSC this past year. Annual reports and maps will be published for projects active during a given year. Geoscientists from both organizations meet semi-annually to review results and outline future and complimentary work. A final volume synthesizing the Interior Plateau program is planned for publication in 1995-96.

### REGIONAL BEDROCK MAPPING

A number of bedrock mapping surveys were conducted last summer to develop a better understanding of the stratigraphy structure and the geological controls of mineral deposits in the Interior Plateau.

Continuing southward from last year's 1:50 000 mapping of NTS map-sheet 93F/6, (Diakow *et al.*, 1993; Green and Diakow, 1993), Larry Diakow and Ian Webster (BCGS) conducted 109 traverses over 800 square kilometres of NTS map-sheet 93F/3 (Fawnie Creek; Diakow and Webster, 1994, this volume). The area hosts a number of mineral occurrences which include the Wolf prospect, a low sulphidation, adularia-sericite epithermal gold-silver deposit, the Fawn showing, a precious metal bearing epithermal vein and the Paw showing, a porphyry copper molybdenum occurrence.

The following significant features were noted during the course of mapping:

- Bedrock exposures subcrop account for about 15% of the total area; the remainder is mantled by glacial overburden.
- The basement succession consists of silica bimodal volcanic rocks and intravolcanic marine sedimentary rocks. New fossil collections suggest that this mixed volcano-sedimentary succession may be entirely Middle Jurassic (Bajocian to Callovian) in age.
- Quartz monzonite of the Late Cretaceous Capoose batholith, mapped last season in the Natalkuz Lake map area, extends southward into the Fawnie Creek map area. Porphyry copper, skarn and a new epithermal precious metal prospect are hosted by the altered country rocks near the pluton.
- The Fawnie Creek area is part of a roughly east-west trending zone of uplift encompassing the Fawnie and Nechako ranges. The uplift is delimited by several northeasterly trending structures. Uplift probably began as early as middle Cretaceous time and continued into the Late Cretaceous with the emplacement of the Capoose batholith.
- Two new epithermal precious metal prospects were discovered. The silicified rocks are Middle Jurassic in age. Occurrence 1 consists of pervasively silicified rocks exposed over an area 150 metres in diameter. Massive silica, with drusy lined cavities, is accompanied by sericite, barite and minor pyrite. It is exposed within a kilometre of the margin of the Capoose batholith. Occurrence 2 consists of isolated vein segments found in quartz-bearing rhyolite flows and minor ash-flow tuffs of probable Middle Jurassic age. The veins occur intermittently along a north-northeast trend. These showings are probably part of a zone of parallel veins that extends for a least 500 metres. The veins, up to 1.5 metres wide and 50 metres long, consist of massive and banded quartz, calcite and rare barite. Disseminated pyrite is the only sulphide observed. Geochemical results are pending.

In 1992, GSC geologists Peter van der Heyden and Arthur Calderwood commenced 1:50 000 mapping in the Charlotte Lake (93C/3) and Junker Lake (93C/4) map-sheets (van der Heyden *et al.*, 1993). In 1993 van der Heyden and Mustard completed 1:50 000 mapping of the Bussel Creek (92N/14 and Tatla Lake (92N/15) sheets.

The following notes summarize preliminary results of the 1993-94 field season (van der Heyden *et al.*, 1994):

- Auriferous arsenopyrite-quartz veins, hosted by small quartz diorite and felsite intrusions near Perkins Peak (Bussel Creek map area), occur in fault-bounded lenses below the base of a Late Cretaceous imbricate thrust zone. The quartz veins may be late-stage extension veins that formed perpendicular to thrust faults following compression. Other gold-bearing quartz veins in the study area also appear to be associated with thrust faults.
- Coast Belt plutons and metavolcanic rocks in the western part of the study area represent a Jura-Cretaceous magmatic arc which was situated outboard of the Tyaughton basin, and which was thrust over the basin in Late Cretaceous time along a major imbricate thrust zone. Preliminary geochronometry of a pluton from one of the higher thrust sheets, which was involved in the deformation, has yielded a 93 to 94 Ma crystallization age. A crosscutting apophysis of the large Klinaklini pluton yielded a preliminary 63 to 64 Ma emplacement age.
- Stikine Terrane, including the newly dated *ca.* 220 Ma Sapeye Creek pluton, may underlie the Tyaughton trough between the Yalakom and Tchaikazan faults.

Paul Metcalfe and Catherine Hickson (GSC) continued with their study of the stratigraphic succession and petrological relationships of the Early Tertiary felsic volcanic rocks which host epithermal mineralization discovered on the Baez and Clisbako claim groups near the headwaters of the Clisbako River. The study area comprises four 1:50 000 map sheets (93B/12, B/13, C/9 and /16). Metcalfe and Hickson (1994) determined that:

- Three volcanic assemblages are exposed in the Clisbako River area. The oldest undeformed units are felsic to intermediate volcanic flows and pyroclastic rocks, which host hydrothermal alteration and mineralization. These are overlain by an assemblage of intermediate to mafic lava flows.
- The area of outcrop of the felsic volcanic rocks and the overlying mafic assemblage is a circular highland area, approximately 40 kilometres in diameter. It is possible that this area is an eroded caldera, partially filled with younger basaltic lavas of the Chilcotin Group.

Catherine Hickson (GSC) completed the bulk of her mapping project in the Taseko Lakes map sheet (920) this summer. Her work concentrated on the stratigraphy of the Jackass Mountain Group in the Big Bar map area (920/1). Significant features from the mapping include:

- The Watson Bar thrust separates an upper plate of Jackass Mountain Group rocks from a lower plate of Jackass Mountain Group rocks and small Cretaceous (?) dioritic plutons. Plutons within the fault zone are strongly altered, including kaolinitic alteration of feldspars and oxidation of hornblende.

Further details can be obtained from Hickson *et al.*, 1994.

## MINERAL DEPOSIT STUDIES

Tom Schroeter and Bob Lane (BCGS) concentrated on the evaluation, description and classification of a variety of deposit types, and their geological settings. This year's effort comprised literature research and brief site investigations of the Wolf precious metal deposit, the Fawn (Gran) epithermal and skarn occurrences, and the Blackwater-Davidson "transitional" precious and base metal deposit.

They report that, in the Fawnie Creek (93F/3) region:

- Mineralization and alteration is of two ages: approximately 48 Ma (Wolf) and approximately 64 to 68 Ma (Blackwater-Davidson and Capoose)
- Mineralization is predominantly structurally controlled.
- The Wolf prospect is a low sulphidation, adularia-sericite epithermal gold-silver deposit with potential for bonanza and bulk mineable economic mineralization.

Further details on the Wolf and other mineral showings are documented by Schroeter and Lane (1994, this volume). Additionally, as part of a larger project initiated in 1991 to develop a regional metallogenic synthesis of the Interior Plateau, landsat imagery and publicly available drill-hole data files of the Energy Division of the Ministry are being examined to determine their potential for outlining structures and stratigraphic contacts.

## SURFICIAL GEOLOGY AND TILL GEOCHEMISTRY

Vic Levson and Tim Giles (BCGS) commenced a project in 1993 to map the surficial geology and complete a till geochemistry sampling program in the Fawnie Creek map area (93F/3; Giles and Levson, 1994, this volume). This project complements work done by Giles and Kerr (1993) and Proudfoot (1993) in the eastern portion of the Anahim Lake map area (93C/1, 8,

9, 16). Work included compiling a surficial geology map of the Fawnie Creek area, conducting stratigraphic and sedimentologic studies of the Quaternary deposits and defining the glacial history and ice-flow patterns. The till geochemistry portion of the program included collection of samples for a regional survey and development and refining of drift exploration methods by conducting detailed case studies around known mineral deposits.

Results to date indicate the following:

- Morainal sediments of the last glaciation are widespread and form a cover from a few to several metres thick in low-lying areas to less than 2 metres thick in upland regions.
- Glaciofluvial sediments are also common in the map area, occurring as eskers, kames, terraces, fans and outwash plains in valley bottoms and along valley flanks. They consist mainly of poorly to well-sorted, stratified, pebble and cobble gravels and sands in deposits up to 10 metres thick. Glaciolacustrine sediments are rare and occur on the east side of the Wolf property, in two valleys on the south side of Entiako Spur, and near Top Lake. There was one dominant ice-flow direction towards the east-northeast, modified by topographic control during both early and late stages of glaciation.
- Two hundred and ninety-nine samples were collected in 93F/3 at a density of 1 sample per 4 square kilometres. Samples were collected from the C mineral soil horizon, to reflect glacial dispersion processes. Approximately 100 pebbles were collected at till sample sites for lithologic analysis and provenance studies.
- Detailed case studies were completed at three mineral prospects: Wolf, Capoose and Blackwater-Davidson; two mineral showings: Fawn and Yellow Moose; and two newly discovered showings (Diakow and Webster, 1994, this volume). These studies were conducted to document mineral dispersion processes by glaciers and colluvial processes and to test methods of drift exploration. All till samples will be analysed by ICP-ES and INAA for more than 50 elements. Reports surficial geology, drift prospecting potential and till geochemistry maps are planned for publication in 1994.

Alaine Plouffe (GSC) is also engaged in a multi-year project that addresses regional surficial geochemistry and Pleistocene stratigraphy, ice-flow pattern indicators and till lithologies. The project area comprises the northwest quadrant of Taseko Lakes (920) and the northeast quadrant of Anahim Lake (93C). Reconnaissance sampling in the Taseko River valley, and a detailed survey in the Fish Lake area were completed in 1992 (van der Heyden *et al.*, 1993). In 1993, a total of 124 till and glaciofluvial sediment samples were collected and a number of ice-flow

indicators were measured. Most of the sampling was conducted along the major forestry roads on mapsheets 920/5 and 920/12. The silt plus clay size-fractions (<63 µm) of all samples collected in 1992 and 1993 will be analyzed by ICP-ES and by INAA. All project results including surficial geology and till geochemistry maps are planned for publication in 1994.

## **GEOCHEMISTRY SURVEYS AND STUDIES**

### **REGIONAL GEOCHEMICAL LAKE-SEDIMENT SURVEYS**

In preparation for planned regional geochemical surveys in the Interior Plateau, Steven Earle (1993) conducted a research study on the applicability of lake-sediment surveys for mineral exploration in the Nechako Plateau area and Steve Cook (1993) conducted a number of lake-sediment orientation surveys in the Vanderhoof-Houston region in 1992. Preliminary interpretation of the orientation data suggests:

- Lake sediments at Wolf Pond, Clisbako and Bentzi Lake clearly reflect the presence of nearby epithermal precious metal occurrences, containing maximum gold concentrations of 56 ppb, 16 ppb and 9 ppb, respectively. These concentrations are far in excess of the regional background of 1 ppb gold in lake sediments.
- More representative results will be obtained by the sampling of each lake and sub-basin during regional lake-sediment surveys.
- Sampling of near-shore organic sediments adjacent to drainage inflows is recommended in detailed/follow-up investigations.

An important outcome of these studies is the development of geochemical models for the transport and concentration of gold and other metals under a range of limnological conditions.

Incorporating recommendations from the orientation surveys Steve Cook and Wayne Jackaman (BCGS) conducted two regional lake-sediment and water geochemistry surveys this summer (Cook, 1994, this volume).

- The Fawnie survey covers map areas 93F/2 (Tsacha Lake) and 93F/3 (Fawnie Creek), where exploration has been centred on precious metal prospects such as the Wolf and Blackwater-Davidson occurrences.
- The Ootsa survey is centred on the Eocene volcanic basin south of Burns Lake and covers parts of map areas 93F/6 (Natalkuz Lake), 93F/11 (Cheslatta Lake), 93F/12 (Marilla), 93F/13 (Takysie Lake) and 93F/14 (Knapp Lake).

- A total of 460 sites were sampled over a combined area of approximately 3530 square kilometres at an average density of 1 site per 7.7 square kilometres.
- Sediment samples will be analysed for gold and 45 additional elements by a combination of atomic absorption spectroscopy and instrumental neutron activation analysis.
- Water samples will be analysed for uranium, fluoride, sulphate and pH.

Results, including data booklet, maps and floppy diskette, will be released in 1994. Follow-up of prospective anomalies as well as additional surveys of adjoining areas is planned for next year, with the eventual objective of completing Regional Geochemical Survey coverage of NTS map areas 93C (Anahim Lake), 93F (Nechako River) and 93K (Fort Fraser).

### **BIOGEOCHEMICAL SURVEYS**

Following up encouraging results from 1992 orientation surveys in the Clisbako River and Fish Lake areas (van der Heyden *et al.*, 1993) Colin Dunn (GSC) directed an airborne reconnaissance and a detailed follow-up ground biogeochemical survey this summer. The program's focus is to evaluate the effectiveness of biogeochemistry as a prospecting tool in this type of terrain.

A regional tree-top (lodgepole pine) survey was undertaken by helicopter in the Fish Lake area in early May. A total of 276 samples were obtained from a 1625 square kilometre area at a grid spacing of 2.5 kilometres. Detailed sampling in August has provided further insight into the response of tree chemistry to a zone of gold enrichment in overburden and bedrock, and helps to quantify levels that may be of significance to mineral exploration. Samples were air dried, then needles were separated from stems and the stems were reduced to ash at 470°C. Ash samples were analysed by INAA and ICP-ES for determination of over 50 elements.

Results from the regional survey and detailed studies show:

- Low levels of metals in tree tissues, but subtle multi-element anomalies define broad geochemical trends
- Chromium is enriched along a zone 12 kilometres long centred on Fish Lake
- Several zones of coincident enrichment (*i.e.*, >90th percentile values) of gold, arsenic and antimony, with spatially related zones of cesium and chromium in the eastern half of the survey area; and copper and molybdenum in the western half.
- Biogeochemical sampling profiles, using the outer bark of lodgepole pine, show that background levels of gold in ash are less than

10 ppb, whereas over zones of gold enrichment concentrations are 30 to 50 ppb gold.

Data have yet to be fully evaluated, but results indicate that biogeochemical surveys in this part of the province are likely to yield only weak enrichments of metals. However, the absolute concentrations are of less importance than the patterns of metal distributions.

## GEOPHYSICAL SURVEYS AND STUDIES

### AIRBORNE AEROMAGNETIC SURVEYS

Dennis Teskey (GSC) co-ordinated a regional aeromagnetic survey over the Chilcotin-Nechako region (93B, C, F and G) this summer. Processing and interpretation of the digital data will be followed by a publication of high-resolution total field maps at 1:100 000 scale and specific maps at 1:50 000 scale, scheduled for release in 1994. It is anticipated that geologic structures underlying the thin but extensive Miocene and younger flood basalts will be identified.

### AIRBORNE AND GROUND MULTIPARAMETER GEOPHYSICAL SURVEYS

Following up successful ground orientation surveys, Rob Shives, Bruce Ballantyne and Don Harris (van der Heyden *et al.*, 1993) conducted both a high-resolution airborne gamma ray spectrometry survey with accompanying total field magnetic and VLF-EM surveys as well as detailed ground follow-up investigations. The airborne survey consisted of two traverses 500 metres apart, over the Fish Lake and Clisbako River areas, using the GSC Skyvan fixed-wing aircraft. Ground follow-up consisted of gamma ray spectroscopy, rock and stream sediment and till sampling.

The following preliminary results have been noted:

- Strong potassium responses in at least two areas relate to unmapped felsic units within volcanics currently shown as Early to mid-Cretaceous and Miocene to Pleistocene olivine basalts (Hickson, 1993).
- Coincident magnetic and VLF anomalies define a north-trending linear which passes through the Fish Lake deposit and continues north along the west side of the Cone Hill intrusive complex.
- Tete Hill, a prominent circular topographic feature mapped as Cretaceous to Tertiary "Tete Hill granite (Riddell *et al.*, 1993) has strong circular magnetic and VLF responses. There is no airborne or ground spectrometric potassium anomaly associated with this feature. Field examination failed to find "granite" outcrops.

- Potassium concentrations in sulphide-bearing outcrops and intrusive phases are low and enrichment trends appear to be subtle.
- A small creek flowing into Fish Lake, yielding anomalous Regional Geochemical Survey gold concentrations (269 ppb gold, Jackaman *et al.*, 1992) was sampled by heavy mineral panning. Numerous fines (<100 µm) gold grains were recovered.

Results from these studies confirm that the airborne and ground geophysics techniques will directly aid bedrock and surficial mapping, geochemical interpretation and exploration.

## COMMENTS

Other information including discussions, poster displays and Open File maps will be made available at the 1994 Cordilleran Roundup. Provincial surveys and studies will be continuing next summer beginning with a one-day field trip illustrating significant geological, geochemical and geophysical features.

## ACKNOWLEDGMENTS

The authors would like to thank all project team members for their assistance. John Newell for a review of this paper and Wade Noble for formatting the manuscript.

## REFERENCES

- Cook, S.J. (1993): Preliminary Report on Lake Sediment Studies in the Northern Interior Plateau, Central British Columbia (93C, E, F, K, L); in Geological Fieldwork 1992, Grant, B. and Newell, J.M., Editors, B.C. Ministry of Energy, Mines and Petroleum Resources, Paper 1993-1, pages 475-481.
- Cook, S.J. (1994): Regional Lake-sediment and Water Geochemistry Surveys in the Northern Interior Plateau, B.C. (NTS 93F/2,3,6,11,12,13,14); in Geological Fieldwork 1993, Grant, B. and Newell, J.M., Editors, B.C. Ministry of Energy, Mines and Petroleum Resources, Paper 1994-1, this volume.
- Diakow, L.J. and Webster, I.C.L. (1994): Geology of the Fawnie Creek Map Area (93F/3); in Geological Fieldwork 1993, Grant, B. and Newell, J.M., Editors, B.C. Ministry of Energy, Mines and Petroleum Resources, Paper 1994-1, this volume.
- Diakow, L.J., Green, K., Whittle, J. and Perry, A. (1993): Geology of the Natalkuz Lake Area, Central British Columbia (93F/6); B.C. Ministry of Energy, Mines and Petroleum Resources, Open File 1993-14.
- Earle, S. (1993): Assessment of the Applicability of Lake Sediment Geochemical Surveys for Mineral Exploration in the Nechako Plateau Area of British Columbia: in Exploration in British Columbia 1992, B.C. Ministry of Energy, Mines and Petroleum Resources, pages 69-105.
- Giles, T.R. and Kerr, D.E. (1993): Surficial Geology in the Chilanko Forks and Chezacut Areas (93C/1,8); in

- Geological Fieldwork 1992, Grant, B. and Newell, J.M., Editors, *B.C. Ministry of Energy, Mines and Petroleum Resources*, Paper 1993-1, pages 483 - 490.
- Giles, T.R. and Levson, V.M. (1994): Surficial Geology and Drift Exploration Studies in the Fawnie Creek Area (93F/3.); in Geological Fieldwork 1993, Grant, B. and Newell, J.M., Editors, *B.C. Ministry of Energy, Mines and Petroleum Resources*, Paper 1994-1, this volume.
- Green, K.C. and Diakow, L.J.(1993): The Fawnie Range Project - Geology of the Natalkuz Lake Map Area; in Geological Fieldwork 1992, Grant, B. and Newell, J.M., Editors, *B.C. Ministry of Energy, Mines and Petroleum Resources*, Paper 1993-1, pages 57 - 67.
- Hickson, C.J. (1993): Geology of the Northwest quadrant, Taseko Lakes Map Area, West-central British Columbia; *Geological Survey of Canada*, Open File 2695.
- Hickson, C.J., Mahoney, J.B. and Read, P.B. (1994): Geology of the Big Bar Map Area: Facies Distribution in the Jackass Mountain Group; in Current Research, Part A, *Geological Survey of Canada*, Paper 94-1A, in press.
- Jackaman, W., Matysek, P.F. and Cook, S.J. (1992): British Columbia Regional Geochemical Survey - Taseko Lakes (NTS 920); *B.C. Ministry of Energy, Mines and Petroleum Resources*, B.C. RGS 35.
- Metcalfe, P. and Hickson, C.J. (1994): Preliminary study of Tertiary Volcanic Stratigraphy in the Clishako River Area, Central British Columbia; in Current Research, Part A, *Geological Survey of Canada*, Paper 1994-1A, in press.
- Proudfoot, D.N.(1993): Drift Exploration and Surficial Geology of the Clusko River (92C/9) and Toil Mountain (93C/16) Map Sheets; in Geological Fieldwork 1992, Grant, B. and Newell, J.M., Editors, *B.C. Ministry of Energy, Mines and Petroleum Resources*, Paper 1993-1, pages 491 - 498.
- Riddell, J., Schiarizza, P., Gaba, R., McLaren, G. and Rouse, J. (1993): Geology of the Mount Tatlow Map Area (92O/5, 6, 12); *B.C. Ministry of Energy, Mines and Petroleum Resources*, Open File 1993-8.
- Schroeter, T.G. and Lane, R.A. (1994): Mineral Resources: Interior Plateau Project (93F/3 and parts of 93F/2, 6, and 7); in Geological Fieldwork 1993, Grant, B. and Newell, J.M., Editors, *B.C. Ministry of Energy, Mines and Petroleum Resources*, Paper 1994-1, this volume.
- van der Heyden, P., Shives, R., Ballantyne, B., Harris, D., Dunn, C., Teskey, D., Plouffe, A. and Hickson, C. (1993): Overview and Preliminary Results for the Interior Plateau Program, Canada - British Columbia Agreement on Mineral Development 1991-1995; in Current Research, Part E; *Geological Survey of Canada*, Paper 93-1E, pages 73-79.
- van der Heyden, P., Mustard, P. and Friedman, R. (1994): Northerly Continuation of the Eastern Waddington Thrust Belt and Tyaughton Trough, Tatla Lake - Bussel Creek Map Areas, West-central British Columbia; in Current Research, Part A, *Geological Survey of Canada*, Paper 94-1A, in press.

# GEOLOGY OF THE FAWNIE CREEK MAP AREA

(NTS 93 F/3)

By Larry J. Diakow and Ian C.L. Webster

**KEYWORDS:** Regional geology, Interior Plateau, Hazelton Group, Naglico formation, Ootsa Lake Group, Capoose batholith, Epithermal prospects.

## INTRODUCTION

This report describes the results of 1:50 000-scale bedrock mapping conducted in the Fawnie Creek map area during 1993. This work is a component of the Interior Plateau project, which also includes surficial geology, lake sediment geochemistry and mineral deposits studies that were simultaneously conducted in the Fawnie Creek and adjoining map areas of the northern Interior Plateau region (see Giles and Levson, Cook and Jackaman, and Schroeter and Lane, 1994; this volume). The Interior Plateau project began in 1992 in collaboration with the Geological Survey of Canada, whose geoscience activities are discussed elsewhere (van der Heyden *et al.*, 1993). Bedrock mapping in the Fawnie Creek map area is an extension of work in the Natalkuz Lake map area to the north (Diakow *et al.*, 1993; Green and Diakow, 1993).

The aim of the project is to provide new geoscientific data in order to facilitate evaluation of mineral potential in the region. The bedrock program covers two main mineralized stratigraphic successions. Two new epithermal precious metal targets have been

identified in the older Middle Jurassic volcano-sedimentary rocks. Assessment of these rocks for massive sulphide potential requires additional study. Epithermal mineralization is also associated with Eocene volcanism, however hostrocks of this age have very limited distribution in the Fawnie Creek map area. Hydrothermally altered rocks are locally extensive along parts of the contact of the Late Cretaceous Capoose batholith. In the Fawnie Creek area there are skarn prospects, and a newly discovered zone of pervasively silicified Middle Jurassic strata near the pluton margin.

The Fawnie Creek map area is located in the Nechako Plateau near the geographic centre of British Columbia (Figure 1). Access to the area is from Vanderhoof, approximately 140 kilometres to the northeast, by the Kluskus-Ootsa Forest Service road. An important junction at 142 kilometres, marks the beginning of the Kluskus-Malapat Forest Service road, which in turn is intersected 4.5 kilometres away by the Van Tine road. A network of well-maintained logging roads developed throughout much of the topographically elevated Entiako Spur in the north, and the Naglico Hills in the south provides access to the main areas of bedrock. These ridges intersect the Fawnie Range, which trends southeast at the eastern margin of the Fawnie Creek area. Together they bound a central low-lying area occupied by Fawnie Creek and interconnected Laidman and Johnny lakes.

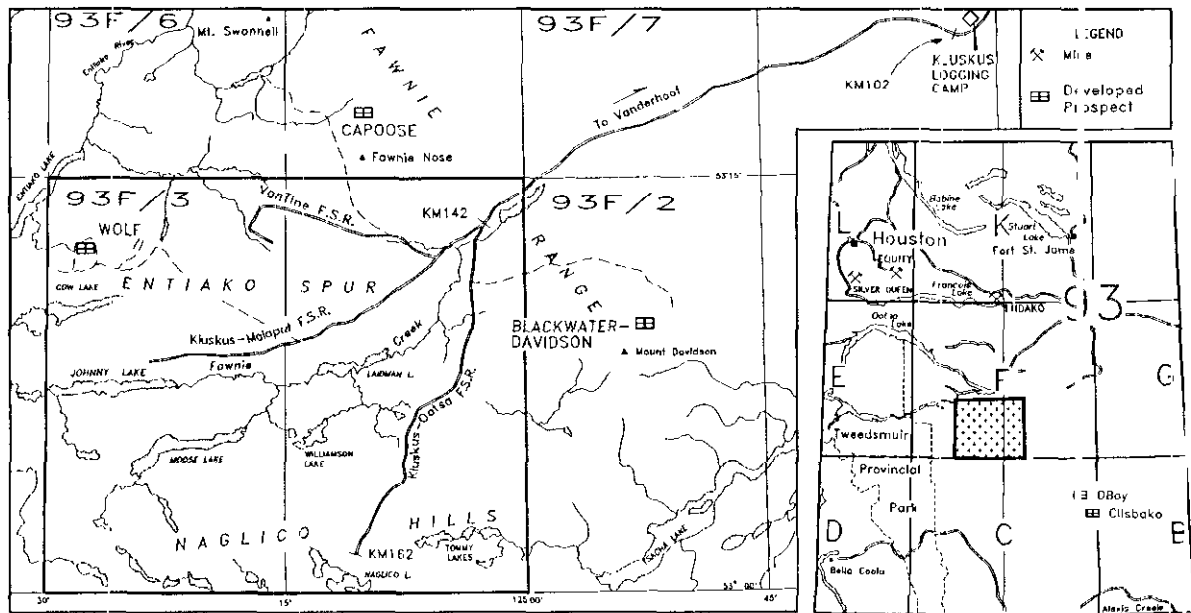


Figure 1. Location and road access to the Fawnie Creek map area.

## VOLCANIC AND SEDIMENTARY ROCKS

The Fawnie Creek area is part of a zone of regional uplift that includes the Fawnie Range, and the Nechako Range to the east. The oldest rock unit, informally named the Naglico formation, consists of flows and volcanoclastic rocks containing interbeds of Middle Jurassic sediments. Small hypabyssal stocks and sills of augite porphyry are believed to be cogenetic with parts of the Middle Jurassic volcanic succession. The Late Cretaceous Capoose batholith intrudes and alters the Jurassic rocks. Eocene volcanic rocks of the Ootsa Lake Group form scattered, relatively thin (< 200 m thick) outliers that rest unconformably on the Jurassic basement. Basaltic lava flows, of probable Miocene and younger age underlie mainly topographically subdued areas south and northwest of the Naglico Hills.

### MIDDLE JURASSIC

#### HAZELTON GROUP

##### NAGLICO FORMATION

The informal Naglico formation is named for silica-bimodal volcanic rocks and Bajocian intravolcanic sediments that appear to be gradationally overlain by marine sedimentary strata containing Callovian fossils in the topmost beds. These rocks underlie the entire Fawnie Creek area. Exposures are most continuous in the Naglico Hills; on the Entiako Spur the formation is less continuous and comprises a relatively thin blanket of thermally altered rocks in intrusive contact with the Capoose batholith. The altered rocks consist of an epidote-quartz-calcite  $\pm$  garnet assemblage. Regionally, recognition of the Jurassic versus Tertiary successions is aided by the ubiquitous presence of epidote, chlorite and quartz in the older rocks. These minerals are most evident lining fractures, as veins and incipient replacement of groundmass and primary minerals, particularly in rocks of basaltic to andesitic composition. In contrast, the Eocene rocks lack this altered mineral assemblage and overall, they have a fresher appearance.

The Naglico formation in the Fawnie Creek area is subdivided into two main lithostratigraphic divisions. The lower division is composed of crudely layered fragmental and lesser flow rocks of rhyolitic composition, and local maroon and green andesitic tuffs deposited in a subaerial environment. The upper division, which is significantly more widespread, is dominated by mafic and intermediate lavas. Marine sedimentary rocks are interlayered with these volcanic rocks and become predominant in the stratigraphically highest Middle Jurassic exposures. Except for the acid volcanic rocks, this mixed volcano-sedimentary succession is

lithologically similar to, and represents the southern extension of units J(v,s) and mJs, mapped in the Natalkuz Lake map area (Diakow *et al.*, 1993; Green and Diakow, 1993). The base of the Naglico formation was not observed; the upper surface is an erosional unconformity with Tertiary volcanic rocks.

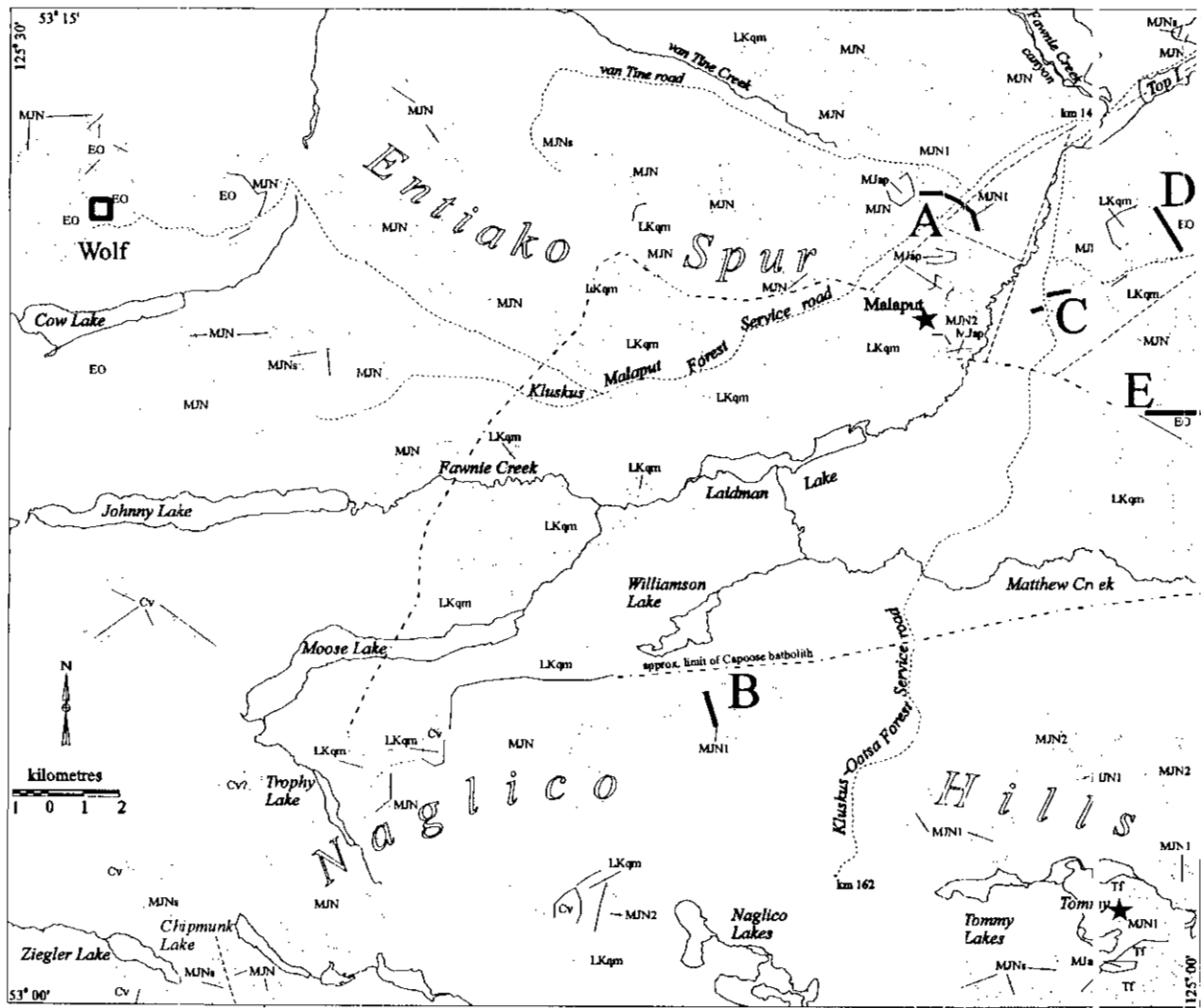
##### Rhyolitic Flows and Associated Pyroclastic Rocks (Unit MJN1)

The 150-metre reference section for the lower division is in a logged area adjacent to the 5-kilometre post of the Kluskus-Malaput Forest Service road (section A, Figure 2). The base is not exposed; however, the upper contact is sharp and conformable with the upper division, which includes pyroxene-phyric flows, and volcanoclastic and epiclastic rocks.

The rhyolitic rocks characteristically contain up to 3% rounded quartz phenocrysts. The lowest exposures of the reference section are rhyolites with light coloured flow laminae in a contrasting dark grey to black aphanitic groundmass (Plate 1A). Isolated outcrops of these distinctive lavas are found in the area between section A and the canyon of Fawnie Creek. Most of the section is made up of light grey fragmental rocks in typically thick, well-indurated beds devoid of internal structure. The beds are composed of lapilli and fewer block-sized fragments supported by a plagioclase-rich matrix (Plate 1B). The lithic fragments are mainly textural variants of plagioclase-porphyrific andesite, and some flow-laminated rhyolite. Several monzonitic fragments were also observed. Scarce, thin, welded zones within the otherwise massive unwelded tuffs have a compaction fabric defined by compressed lithic fragments (Plate 1C).

Rocks of the lower division crop out intermittently in a broad area between Williamson and Tommy lakes, about 20 kilometres south of reference section A. Semicontinuous outcrop of the rhyolitic unit and its apparent conformable upper contact were observed in a logged area south of Williamson Lake (section B, Figure 2). In general, rhyolitic rocks at this locality differ from those at section A by the prominence of flows and subordinate fragmental and epiclastic rocks. The flow textures vary between sparsely porphyritic and crowded porphyritic, depending on the relative abundances of resorbed quartz, and plagioclase phenocrysts. The pyroclastic rocks include well-bedded lapilli tuff and finer graded tuffs containing abundant quartz. Periodic reworking of the rhyolitic flows and tuffs has resulted in local interbeds of volcanic sandstone and conglomerate.

Rhyolitic flows and minor welded ash-flow tuff of undetermined thickness crop out sporadically in the heavily treed area adjacent to Tommy Lakes. Epithermal veins and vein stockworks are exposed at a number of closely spaced localities in the rhyolitic rocks; they require further work to assess their mineral potential (*see New Epithermal Precious Metal Prospects*).



**MIOCENE TO PLIOCENE - Chilcotin Group**

**Cv** Basalt flows, black, aphanitic and sparsely porphyritic with olivine and scarce coarse-grained plagioclase laths.

**EOCENE - Ootsa Lake Group**

**EO** Mainly rhyolite with lesser andesite flows, quartz-bearing lapilli tuffs, minor lacustrine tuffaceous siltstone.

**MIDDLE JURASSIC - Hazelton Group - Naglico formation**

**MJNs** Volcanic derived, feldspar-rich fine to coarse grained clastic sediments containing abundant fossils; minor interlayered ash tuff and argillite.

**MJN2** Augite-phyric basaltic and andesitic flows with associated compositionally similar lapilli and block tuffs; subordinate maroon tuffs with sparse quartz phenocrysts.

**MJN1** Rhyolitic lava, ash-flow tuff and lapilli tuff containing diagnostic round quartz phenocrysts; minor epiclastic sediments with detrital quartz; local maroon and green ash and lapilli tuffs.

**INTRUSIVE ROCKS**

**TERTIARY**

**Tf** Felsite sills, fine grained, granular, vitreous biotite.

**LATE CRETACEOUS**

**LKqm** Quartz monzonite, pink, equigranular to porphyritic, accessory biotite and hornblende; volumetrically minor phases include quartz porphyry and biotite-hornblende quartz diorite.

**MIDDLE JURASSIC**

**MJap** Mafic plugs containing diagnostic medium-grained augite and fine grained plagioclase phenocrysts.

**SYMBOLS**

- Geological contact.....
- Fault.....
- Potential epithermal prospect.....★
- Geological section.....
- Outcrop limit.....

Figure 2. Distribution of major lithologic units in the Fawnie Creek map area. The stars mark the Malaput and Tommy; two epithermal precious metal prospects discovered during the mapping program.

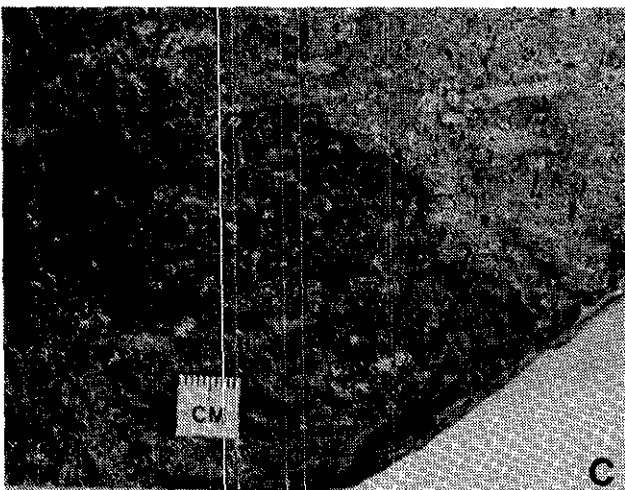
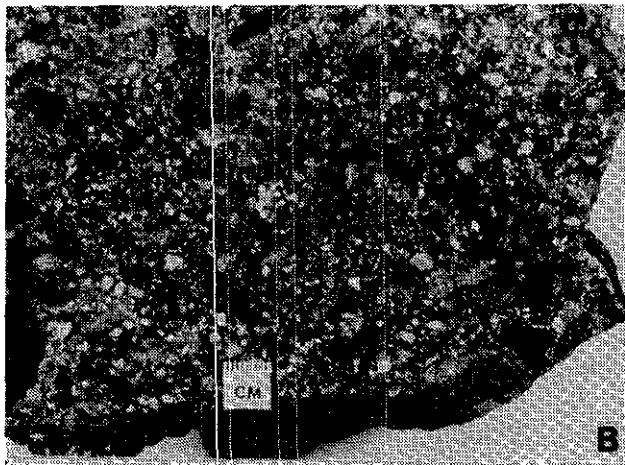
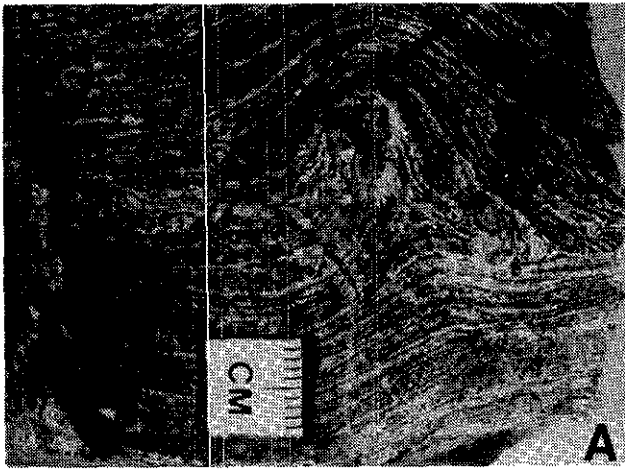


Plate 1. Representative rhyolitic rocks of the Middle Jurassic Naglico formation (unit MJN1). A) Finely laminated black lava flows found at the base of section A. B) Unwelded lapilli tuff is volumetrically the most significant rock type in section A. This rock characteristically contains round quartz grains, as shown immediately above the left side of the scale bar. C) Ash-flow tuff showing compaction foliation defined by compressed quartz-bearing cognate pyroclasts. This sample is from the Tommy Lakes area, where massive bedded quartz-bearing flows of unit MJN1 comprise the country rocks for epithermal quartz-barite-calcite veins and stockwork veinlets.

Southeast of section A, across the valley occupied by Fawnie Creek, quartz-bearing rhyolitic ash-flow tuff and lava are spatially associated with a significantly different rock sequence (section C, Figure 2). The stratigraphic position of these felsic rocks in relation to nearby isolated exposures of amygdaloidal, porphyritic and aphanitic andesite flows and volcanic conglomerate is unclear due to poor exposure. The conglomerate contains well-rounded clasts, some as large as 3 metres in diameter, of variants of porphyritic andesite and some welded dacite. Nearby and presumably a continuation of the section, the felsic rocks are about 25 metres thick at the base of a conformable overlying sequence composed of well-bedded, maroon and green fine-grained tuffs about 50 metres thick. Near the top, the tuffs are in contact with synvolcanic sediments and upsection they diminish to thin interbeds in the overlying sedimentary sequence (*see* Intravolcanic Sediments).

The rhyolitic sequence was probably deposited in a subaerial environment as suggested by welded ash-flow tuff and the absence of intercalated marine sedimentary rocks. In section C, where maroon tuffs underlie fossiliferous marine sediments, this relationship marks the transition from subaerial to shallow submarine deposition. The age of the rhyolitic sequence is unconstrained, but it is believed to be Middle Jurassic based on bivalves found in synvolcanic sediments at the upper gradational contact with volcanics at section C. Samples of rhyolitic rock from each of the three sections discussed were collected for U-Pb dating.

#### Augite-phyric Flows and Associated Pyroclastic Rocks (Unit MJN2)

The upper division is a lithologically varied succession dominated by andesitic flows and subordinate volcanoclastic rocks, and intravolcanic sedimentary rocks. This succession is regionally extensive, cropping out mainly in the Naglico Hills and Entiako Spur, but also scattered throughout the intervening low-lying area. To the north, in the adjacent Natakuz Lake map area, an identical correlative volcano-sedimentary sequence underlies a broad area east of, and including the Fawnie Range (Diakow *et al.*, 1993). Variations in thickness of the upper division are difficult to ascertain because of the combined effect of generally poor exposure in monotonous volcanic sections that lack markers, and suspected intraformational stratigraphic repetition caused by numerous faults with small displacements. The upper division strata appear to be about 250 metres thick above the Capoose batholith, in the central part of the Entiako Spur; the thickest accumulation is believed to comprise a southwest-inclined homocline, south-southeast of Moose Lake in the Naglico Hills.

Because of the internal lithologic variability in rocks of the upper division no single section is representative, however, certain lithological features persist over broad areas. The primary lithologies include dark green flows

of basalt and andesite. Vitreous augite phenocrysts, in amounts rarely exceeding 3% are ubiquitous, and a diagnostic feature of the andesitic flows. Plagioclase, the dominant phenocryst, varies in abundance. Some of the more common textural varieties include sparsely porphyritic, fine-grained crowded plagioclase porphyry to coarse-grained porphyry (Plate 2A,B). The flow succession also contains several other minor textural varieties. These include amygdaloidal lava with irregular, quartz-chlorite cavities, and dense, aphanitic basalt. Sometimes the basalt has resistant parallel ribs on the weathered surface, a feature that was observed in identical rocks in the Natalkuz Lake map area (Green and Diakow, 1993). Small-volume dacitic and rhyolitic lavas occupy relatively thin intervals in the more mafic succession.

Maroon and green pyroclastic rocks are interspersed with flows in the central part of the Entiako Spur. They are composed predominantly of lapilli tuff in which the lithic fragments and the matrix contain abundant plagioclase and subordinate chloritized mafic minerals. Quartz fragments are generally present, but because of their small size (< 2 mm) and low abundance (up to 2%) they can be easily overlooked. A somewhat different succession of fragmental rocks is found intimately layered with the augite porphyry flows in the central and eastern parts of the spur, and to the north-northeast across the headwaters of Van Tine Creek, in the Fawnie Range. They consist of lapilli and lesser block-tuffs dominated by plagioclase-rich pyroclasts with a fine-grained, crowded texture (Plate 2C). This distinctive texture is due to minute plagioclase up to 2 millimetres long in amounts up to 35 volume percent. Interbeds of ash tuff and rare accretionary tuff are also present. Accretionary lapilli were also found at another locality, in section B, where they are associated with bedded ash and lapilli tuffs that rest on crowded plagioclase ± pyroxene-porphyritic andesite flows. This sequence is capped by a cobble-boulder conglomerate containing locally derived rounded clasts of porphyritic andesite, and some quartz-bearing rhyolite eroded from the underlying lower division.

Fragmental rocks exposed mainly in the area between Chipmunk and Trophy lakes (local names) differ from those elsewhere in the map area, in that they consist mainly of aphanitic, off-white felsic(?) lapilli in a light green matrix. These rocks are commonly interlayered with augite-bearing andesite flows diagnostic of the upper division, and locally with welded dacite. The fragments are commonly subrounded, a feature that possibly reflects some post-depositional reworking. The interlayered relationship of these felsic rocks with andesitic flows is interpreted to suggest contemporaneous bimodal volcanism.

Deposition of much of the augite-phyric volcanic unit is presumed to be in a relatively shallow marine environment with local subaerial conditions, as indicated

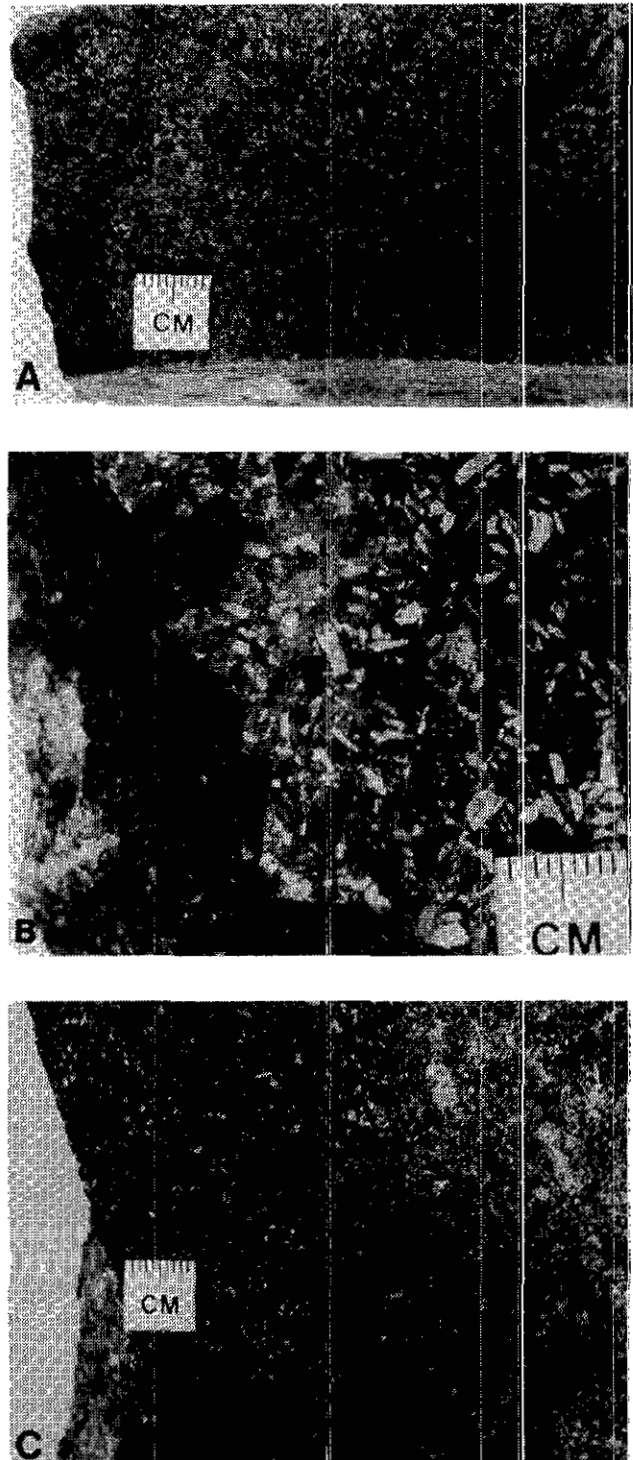


Plate 2. Representative augite-phyric rocks of the Middle Jurassic Naglico formation (unit MJN2). A) Typical fine-grained end-member "crowded" plagioclase porphyry lava composed of up to 40% plagioclase and sparse vitreous augite phenocrysts. B) The coarse-grained end-member flows contain plagioclase laths up to 5 millimetres long. Note the abundant vitreous augite evident as black grains. C) Monolithic "crowded plagioclase porphyry" lapilli tuff occur mainly in the eastern part of the Entiako Spur and into the Fawnie Range where they are interlayered with augite-phyric flows. Note the uniform fine-grained porphyritic texture of both the matrix and pyroclasts.

by rare accretionary lapilli. Evidence of marine deposition is based on a number of localities where the flows contain interbeds of volcanic-derived marine sedimentary rocks. These rocks are described in the following section. Despite textural variations, their bulk composition varies little in an area that encompasses the entire Fawnie Creek and much of the Natalkuz Lake areas. This broad distribution may reflect construction of a series of coalescing shield-like volcanoes in which there appears to have been a preponderance of tholeiite to weakly calcalkaline basalt (at present there is a small geochemical data set for flows in the Natalkuz Lake area. Rocks collected in the Fawnie Creek area had not been analysed in time for this report). Local concentrations of more felsic pyroclastic deposits probably indicate short-lived, more violent eruptive episodes or are coalescing deposits from a separate but nearby volcanic centre.

#### **Intravolcanic Sediments (Unit MJNs)**

Fossiliferous sedimentary rocks are randomly dispersed and stratigraphically conformable with andesitic rocks of the upper division. Generally the exposures are poor, and limited to angular debris churned up in roadcuts and logging cutblocks. Representative sections are exposed near the top of section A, and to the east of Fawnie Creek at section C. The main feature of the intravolcanic sediments is their immaturity, characterized by the high proportion of angular plagioclase and volcanic lithic detritus. The dominant lithologies include feldspathic sandstone and siltstone, tuffaceous argillite, locally prominent volcanic conglomerate and scarce limestone. Fossils are nearly always present, varying in abundance from a few belemnites and pelecypods to zones containing a rich and varied fauna that includes ammonites, gastropods, colonial corals, bryozoans and various bivalves. Preliminary fossil identifications by Dr. Howard Tipper of the Geological Survey of Canada indicate at least one early Bajocian collection; most are indeterminate or probable Middle Jurassic.

Near the top of section A, volcanogenic sedimentary rocks occupy an interval about 40 metres thick. They overlie rhyolitic rocks of the lower division, and the upper conformable contact is with coarse-grained, augite-phyric andesite flows. The base of the section is dominated by light green, tuffaceous siltstone and mudstone that alternate in differentially weathered, parallel beds between 5 millimetres and 3 centimetres thick. Convolute bedding and channels are observed in several intervals about 1.5 metres thick. These fine-grained rocks persist up-section to within about 20 metres of the upper contact where they comprise minor interbeds in a succession of thick, poorly sorted beds composed of subrounded to subangular pebble and cobble-sized detritus. Much of the detritus contains augite, derived from nearby augite-phyric volcanics. The interpretation drawn from these sediments is that the

lower fine-grained sequence may be waterlain airborne ash deposited, in part, on an unstable slope susceptible to slumping. The overlying coarser deposits suggest a transition to a higher energy environment, perhaps associated with local progradation of a volcanoclastic-epiclastic apron.

Stratigraphic section A varies markedly from section C, across the valley of Fawnie Creek. As described above and summarized here, the strata underlying the Entiako Spur to the northwest are predominately volcanic rocks representative of both divisions of the Naglico formation. Minor intravolcanic marine sediments are found exclusively in the upper division. The volume of volcanic rocks is significantly less in the area to the southeast of Fawnie Creek. Most notable is the relative absence of augite-bearing flows and associated volcanoclastic rocks. Instead, they are supplanted by an apparently distal sedimentary succession, at least 150 metres thick, which is cut by augite porphyry sills and dikes. Similar intrusions (unit MJap) are believed to be comagmatic feeders for upper division volcanic strata. Extrusive augite-bearing volcanic rocks may well have been erupted above the sediments, but removed during a regional erosional episode in the interval spanning Late Cretaceous and Eocene time. Although the upper contact of the sedimentary succession was not observed, the uppermost exposure of sediments crops out topographically beneath a nearby outlier of Eocene volcanic strata. North of Top Lake a correlative section of sedimentary rocks dips gently to the southeast, and barring a fault, it is interpreted to project down dip beneath a distant exposure of augite-bearing flows. Rhyolitic rocks prevalent at the base of section A apparently continue across the valley to section C where they comprise a minor depositional unit within a heterogeneous succession of intermediate flows and variegated maroon and green fine-grained tuffs conformably overlain by sediments. The bottom of this sedimentary section is a well-exposed gradational contact in which volcanogenic fine and coarse-grained sediments rest directly on ash tuff. An identical tuff bed is enclosed by sediments about 10 metres above the contact. The bottom of the lowest sedimentary bed provides evidence of synchronous volcanism and marine sedimentation as shown by volcanic conglomerate dominated by angular clasts occupying ball and pillow structures in an underlying bed of vitric and ash tuff (Plate 3A). Bivalves and belemnites are concentrated in a thin layer within the basal conglomerate. Up-section, angular, volcanic lithic fragments and abundant plagioclase grains in the sediments suggest erosion of a nearby volcanic source or penecontemporaneous volcanic activity. These coarse immature rocks appear to rapidly diminish up-section, passing into finer grained feldspathic siltstone and sandstone (Plate 3B), and are eventually replaced by tuffaceous argillite. Discrete off-white weathered layers, believed to be ash, impart a striped appearance where

they alternate with black argillite (Plate 3C). There are good exposures of these argillaceous rocks in rusty pyritic roadcuts between 143.5 and 146.5 kilometres on the Kluskus-Ootsa Forest Service road. They typically display uniform, parallel beds between 3 and 7 centimetres thick and contain calcareous concretions.

The recessive nature of the sedimentary rocks results in generally scattered exposures in section C. Although the section appears to be continuous, in reality a significant hiatus, spanning late Bajocian and Bathonian time is suspected. Belemnites and bivalves located at the base of the succession are not diagnostic, but based on lithology these rocks resemble early(?) Bajocian sediments found elsewhere in the upper division of the Naglico formation. At the top of the section, a fossil quarry contains a varied faunal assemblage that includes Callovian ammonites associated with abundant belemnites, pelecypods, brachiopods, and rare, star-shaped crinoid columnals. Comparable Callovian sediments are found at one other locality in the map area, about 1 kilometre north of Top Lake.

The strata at section C presumably represent the top of the Naglico formation preserved in the Fawnie Creek map area. Sedimentary rocks found in the upper division are interpreted to represent early Bajocian shallow-marine deposits within the influence of an active volcanic centre and followed in time by a significant increase in water depth and oxygen deficient conditions. This is indicated by the change from sediments rich in volcanic detritus at the base of the section to overlying parallel-bedded, pyritic tuffaceous argillite. By Callovian time a relatively shallow water near-shore environment was re-established giving way to feldspathic siltstone and sandstone replete with a diversified faunal assemblage.

A clastic succession, lithologically distinct from those previously described, is exposed in the area between Chipmunk and Ziegler lakes. To the east these rocks are faulted against andesite flows of the upper division; and to the west, they appear to be unconformably overlain by rocks of the Chilcotin Group. The succession is predominantly sorted sandstone that is interlayered with, and grades into, minor granule-pebble conglomerate. The arenaceous beds contain quartz, but lack high concentrations of detrital plagioclase, which distinguishes them from typical Bajocian and Callovian sandstones found elsewhere in the map area. The conglomerate beds are typically framework supported, characterized by well-rounded clasts. The clasts are mainly pale green siltstone, lesser black mudstone, and light grey chert. No fossils were found in these rocks, however, similar conglomeratic rocks conformably overlie a Bathonian or Callovian sedimentary sequence exposed along the eastern slope of the Fawnie Range (*cf.* unit mJs of Diakow *et al.*, 1993). A single, angular

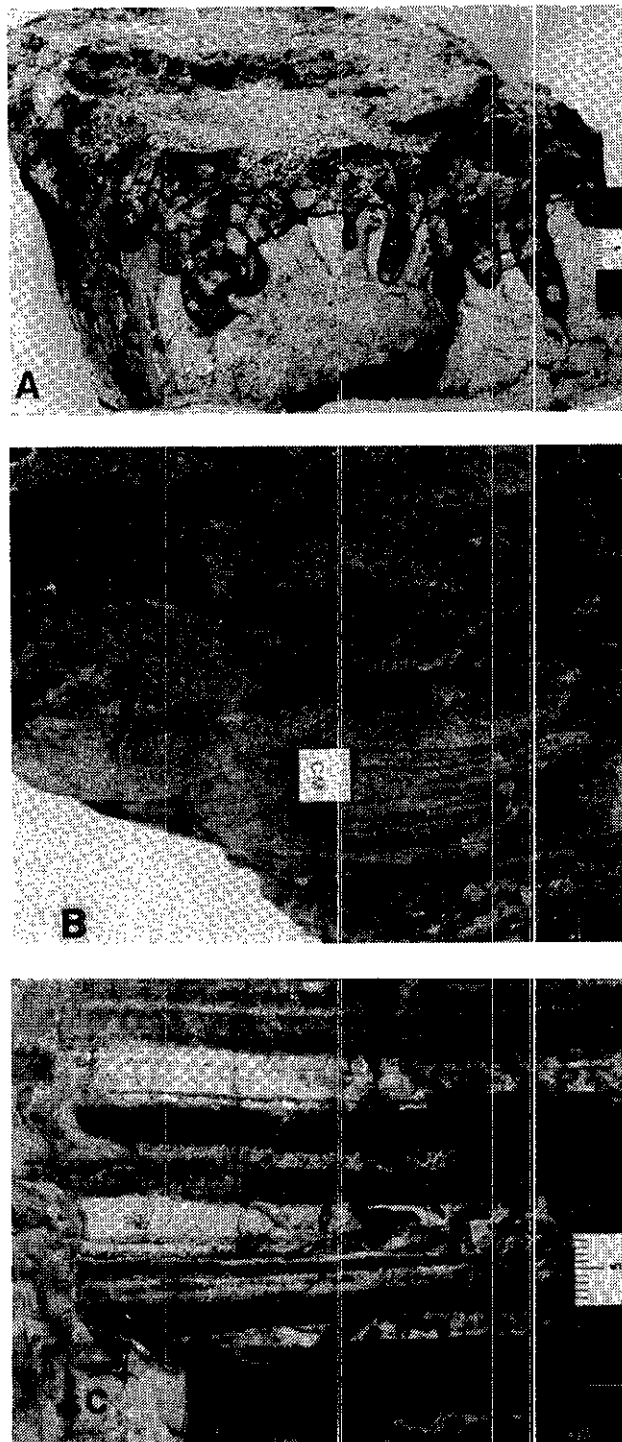


Plate 3. Volcanic-derived sedimentary rocks of the Naglico formation (unit MJNs). A) Sharpstone conglomerate and immature feldspathic sandstone overlying vitric ash tuff at the top of the underlying volcanics in section C. Load casts occur at the contact, highlighted by the black line. They provide evidence of synvolcanic sedimentation. Note necking of the lobes and the detached sediment-filled sphere enclosed by ash. B) Feldspathic sandstone, comprised mainly of angular plagioclase grains, is the dominant rock type of unit MJNs. In this example fine grained feldspathic sandstone and mudstone show flaser bedding. C) Parallel laminated white ash tuff interlayered with tuffaceous argillite. These rocks overlie coarser grained volcanic sediments and mark the transition in time to a deeper quiet water environment.

fragment of an identical conglomerate was found immediately upsection from Callovian sediments at section C; however, outcrop of this rock was not located.

## ***EOCENE***

### **OOTSA LAKE GROUP (UNIT EO)**

Volcanic rocks of the Ootsa Lake Group occur in three widely spaced localities. They cap three knolls north of Cow Lake, where they comprise the host rocks for the Wolf epithermal precious metal prospect, and two outliers are situated along the western slope of the Fawnie Range. It is uncertain whether the group was uniformly deposited over the intervening area and subsequently eroded or that these outliers represent areally restricted deposits erupted from separate volcanic centres. We favour the latter interpretation because there are significant lithologic differences in Eocene strata near Cow Lake compared to correlative rocks along the Fawnie Range. Furthermore, we believe that emplacement of the Capoose batholith elevated the central Entiako Spur forming a paleo-topographic high and consequently a local barrier for Eocene eruptives. The preserved Eocene volcanic sequences are relatively thin; about 150 to 175 metres thick north of Cow Lake and at least 155 metres thick in the Fawnie Range (section E, Figure 2). The succession may be somewhat thicker where it is exposed north of the access road to the Blackwell-Davidson prospect (section D, Figure 2). Volcanic rocks and a cogenetic subvolcanic intrusion at the Wolf prospect yield three K-Ar dates, on whole rocks, between  $47.6 \pm 1.7$  and  $49.9 \pm 1.7$  Ma (Andrew, 1988).

The lower contact of the Ootsa Lake Group apparently dips gently westward on the three isolated hills north of Cow Lake. A basal conglomerate crops out in a creek along the northwest-facing side of the westerly hill. On the central and easterly hills, the Ootsa Lake Group sits unconformably either on fossiliferous sedimentary rocks or pyroxene-bearing flows of the Naglico formation. A similar contact relationship apparently exists in the Fawnie Range where rocks of the Naglico formation, cut by quartz porphyry dikes (unit LKqp) and the Capoose batholith, crop out topographically below comparatively unaltered strata of the Ootsa Lake Group.

Eocene strata at the Wolf prospect generally dip southwest, but north and northeast-trending faults cause local deviations from this trend. The base of the succession is locally marked by an oligomictic orthoconglomerate about 20 metres thick. It is composed of well-rounded hornblende-biotite quartz monzonite and aplite clasts up to 1.3 metres in diameter. The texture and mineralogic features of the clasts suggest a local provenance from the Capoose batholith. The

conglomerate is overlain by tuff, which is part of a poorly exposed, predominantly pyroclastic section that comprises as much as 30% of the Eocene succession in the subsurface (personal communication, D. Heberlein, 1993). The tuffs include welded and non-welded zones in ash and lithic-rich beds, and some locally significant heterolithic breccia. Tuffaceous siltstone and sandstone of probable lacustrine origin form lenticular deposits conformable with the overlying rhyolite flows. These lavas comprise the stratigraphic top of the Eocene section, dominating the upper slopes and capping the three prominent knolls at the Wolf prospect. Despite their apparent spatial dominance, due to their resistance and relatively flat attitude, they make up only about 30% of the overall Eocene succession. The rhyolite flows contain up to 5% quartz, typically a few millimetres in diameter, orthoclase and abundant microscopic zircon. Although biotite is generally present elsewhere in rhyolitic rocks of the Ootsa Lake Group, it was not observed in the lavas at the Wolf property. Felsic tuffs and flows (units EO<sub>rt</sub> and EO<sub>r</sub> of Diakow *et al.*, 1993), believed to be correlative with rocks at the Wolf prospect, crop out sporadically along the Entiako River in the southeast corner on Natakuz Lake map area. Here rhyolite conformably overlies andesitic flows, which in turn, are unconformable on the Capoose batholith. These andesitic flows were not observed at the Wolf prospect, however, south of Cow Lake similar rocks underlie a cluster of low-lying knolls that pass at lower elevation into pyroxene-phyric rocks of the Naglico formation.

At the Wolf prospect, a sill-like body and rhyolitic dikes, interpreted as synvolcanic hypabyssal plutons, intrude the lavas. They have a medium to coarse-grained porphyritic texture imparted by plagioclase, potassium feldspar and quartz, listed in order of abundance. Hydrothermal alteration is extensive and locally intensive, as indicated by the destruction of primary volcanic textures in bleached rocks, and the introduction of silica as a pervasive replacement and veinlets (*see* Schroeter and Lane, 1994, this volume).

Three main lithologies make up the Ootsa Lake Group near the eastern boundary of the map area (sections D and E, Figure 2). At section E, off-white, laminated rhyolite flows, brecciated towards the top of the unit predominate near the base of a crudely bedded volcanic succession. The thin flow-laminae in these rocks are locally obscured by the overgrowth of spherulites, which coalesce and form discontinuous layers. Scarce lithophysae are also present. Typically these rhyolitic rocks have an aphyric texture, however, some contain sparse plagioclase, quartz and biotite phenocrysts. Andesite flows conformably overlie the rhyolite. They contain diagnostic plagioclase laths up to 6 millimetres long in a dark matrix. The uppermost part of section E is dominated by lapilli tuff characterized by 20% bipyramidal and broken quartz fragments between 1 and 4 millimetres in diameter. The lithic fragments are

typically dark brown and subangular, aphanitic and porphyritic volcanic rocks. These quartz-rich tuffs resemble a solitary outcrop mapped north of Entiako Lake (unit EOrt of Diakow *et al.*, 1993). They are also strikingly similar to tuff interbeds in a probable Jurassic volcano-sedimentary sequence exposed at the top of Mount Davidson.

Rhyolite and andesite flows predominate in the outlier north of access road to the Blackwater-Davidson mineral prospect (section D, Figure 2). The main difference between this succession and section E is that the quartzose tuff unit is absent. Other distinguishing lithologic features include round amygdules, filled with chlorite and opalescent silica, common in the overlying coarse-grained plagioclase phyric andesite flows. The underlying rhyolites are distinctly laminated, mauve and pale green, and contain beds of monolithic breccia.

## **MIOCENE and YOUNGER VOLCANIC ROCKS**

### **CHILCOTIN GROUP (UNIT MPCv)**

Relatively thin, sheet-like basalt flows, tentatively assigned to the Chilcotin Group, are generally found in topographically low-lying areas, below 1150 metres elevation, where exposure is obscured by glacial deposits. Commonly, where outcrop is sparse the presence of nearby flows is indicated by boulder fields. Abundant large boulders of basalt are found in the low-lying area south of the Naglico Hills. The subdued topography in the southwest part of the map area, between Ziegler Lake to the south and Johnny Lake to the north, is believed to be manifestation of basaltic sheet flows. The topographically highest flows outcrop in the centre of the Naglico Hills at about 1300 metres elevation. The basaltic lavas are generally massive and characteristically vesicular. They weather light brown, and fresh surfaces are black with a dense aphanitic texture. Fresh olivine is locally abundant; plagioclase laths between 1 and 1.5 centimetres long are present, but rarely.

## **INTRUSIVE ROCKS**

### **MIDDLE JURASSIC**

#### **AUGITE PORPHYRY (UNIT MJap)**

Augite porphyry plugs, typically less than 1.5 square kilometres in area, are exposed in the eastern part of Entiako Spur and south of Tommy Lakes. These plutons apparently intrude and bleach rocks of unit MJN2. Their main feature is subhedral augite phenocrysts, which comprise as much as 25% of the rock, and plagioclase microphenocrysts arranged in a felty texture (Plate 4).

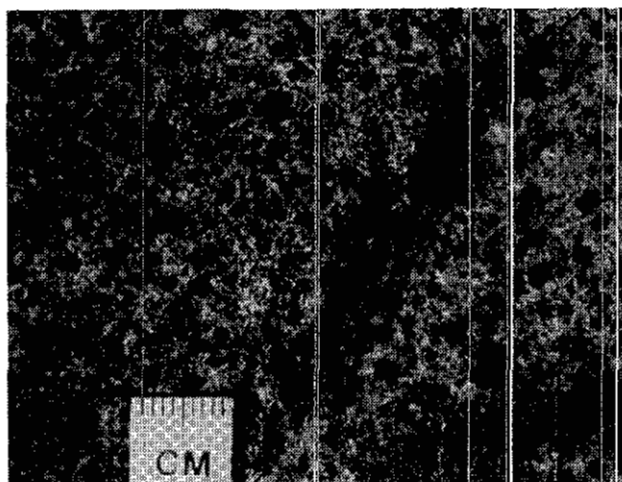


Plate 4. Type specimen of augite porphyry hypabyssal stock west of section A. The dark subhedral grains are vitreous augite phenocrysts supported by a matrix composed of randomly oriented plagioclase grains. These plutons are believed to be cogenetic with the augite-phyric volcanic rocks of unit MJN2.

The similar texture, mineralogy, and spatial relationship of these plutons with volcanic rocks of unit MJN2 are interpreted to suggest they may be cogenetic. A similar pluton south of Tommy Lakes is surrounded by sedimentary rocks of probable Middle Jurassic age, however, a contact was not observed. At one locality a remnant of a probable Eocene sill (unit Tf) rests directly on this pluton. Near section C, sedimentary rocks of unit MJN2 are cut by augite-phyric dikes and sills(?). No contacts were observed, and it is difficult to distinguish these so called sills from thin flows on the basis of texture and composition.

### **LATE CRETACEOUS**

#### **CAPOOSE BATHOLITH (UNIT LKqm)**

Quartz monzonite of the Capoose batholith outcrops in the extreme north of the map area, along Van Tine Creek, extending the body southward from the Natalkuz Lake map area (Diakow *et al.*, 1993). The batholith underlies as much as 150 square kilometres of the Fawnie Creek map area. It continues to the south beneath the Entiako Spur, cropping out extensively along its southern slope down to Laidman and Moose lakes, and beyond to its southern contact in the Naglico Hills. Thick glacial drift mantles the batholith in the valley east of Laidman Lake. However, the pluton is exposed in an incised creek valley, and north of Matthews Creek along the base of the Fawnie Range. Although the contact between the batholith and stratified rocks was not observed, the thermal effects on Jurassic strata are widespread, particularly in the central part of the Entiako Spur where volcanic rocks are variably replaced by an

assemblage of chlorite, epidote, silica and pyrite with or without garnet. The Capoose batholith has one reported K-Ar date of  $67.1 \pm 2.3$  Ma determined on biotite (Andrew, 1988). A site along the Kluskus-Malaput road was sampled this season. The rock contains both fresh biotite and hornblende which are suitable for K-Ar dating. A sample of biotite-hornblende quartz diorite (unit LKqd), which is locally intruded by quartz monzonite, will also be dated by the K-Ar method.

The main phase of the batholith is a homogeneous medium to coarse-grained, equigranular quartz monzonite. The rock is typically light pink and contains 35% quartz, roughly equal proportions of alkali feldspar and plagioclase, and about 10 to 15% combined fresh hornblende and biotite. Xenoliths in the pluton are abundant and composed of fine-grained porphyry with randomly oriented plagioclase laths less than 1 millimetre long and an interstitial anhedral mafic mineral, possibly hornblende.

At the east end of Moose Lake the quartz monzonite is gradational into a porphyritic monzonite. Plagioclase phenocrysts in this rock are subhedral and approximately 5 millimetres long, forming an interlocking aggregate with anhedral potassium feldspar, approximately 10% quartz, and 5% hornblende and biotite. A small isolated stock, south of the main body in the Naglico Hills, may represent yet another phase of the Capoose batholith. It consists for the most part of white, equigranular granodiorite with up to 15% chloritized mafic minerals. Pyrite is common in pyroxene-bearing flows of the Naglico formation cropping out east of the intrusive contact. Along the northern margin the pluton contains coarse-grained potassium feldspar phenocrysts, and chloritized plagioclase and biotite.

#### **BIOTITE-HORNBLLENDE QUARTZ DIORITE (UNIT LKqd)**

Biotite-hornblende quartz diorite forms isolated plugs and small stocks near the margin of, and rarely enclosed by, quartz monzonite of the Capoose batholith. Dikes of quartz monzonite and aplite are locally observed cutting the diorite. Typically these plutons are dark greyish green with a medium-grained equigranular texture. Hornblende, the dominant mafic mineral, commonly approaches 25% of the rock. Xenoliths in the diorite are generally quite rare except for one locality where pyroxene porphyry, which resembles Middle Jurassic lithologies, and other fine-grained dioritic fragments are abundant in zones of agmatite.

#### **QUARTZ PORPHYRY (UNIT LKqp)**

Quartz porphyry dikes and several plug-size plutons are found mainly east of Fawnie Creek. They cut Middle Jurassic sedimentary rocks; however, nowhere were they

observed cutting rocks of the nearby Ootsa Lake Group. These plutons are pink and characterized by 5 to 15% quartz phenocrysts. They also contain up to 5% hornblende, and subordinate biotite phenocrysts. Locally, small (< 1 cm diameter) mariolitic cavities suggest high-level emplacement. Based on their texture, composition and spatial association they are interpreted as subvolcanic apophyses projecting from the Capoose batholith.

### **TERTIARY**

#### **BIOTITE-BEARING FELSITE SILLS (UNIT TF)**

Greyish green fine-grained crystalline felsite sills that characteristically contain up to 5% vitreous biotite are confined to the area south and east of Tommy Lakes. Sporadic outcrops of these rocks in spatial association with rhyolite flows of the Naglico formation are found close to Tommy Lakes. In the extreme southeast corner of the study area these rocks comprise a laterally extensive sheet that is concordant with gently south dipping volcanic and sedimentary rocks of the Naglico formation, and an isolated remnant rests directly on an augite porphyry plug (unit MJap). The sills weather to porcellaneous, conchoidally fractured fragments. Sparse plagioclase phenocrysts, up to 4 millimetres long, are observed on the fine granular weathered surface.

### **STRUCTURE**

The Fawnie Creek area is part of a regional east-trending horst, the Nechako uplift, locally manifest as the Fawnie Range, Naglico Hills and Entiako Spur. Evidence of uplift is inferred from topographically highstanding basement rocks, mainly of Jurassic age, which to the south and north pass into extensive areas covered by Eocene and younger rocks. The lateral transition from old to young stratigraphy coincides with several inferred northeast-trending structures, which delimit the Fawnie and Nechako ranges to the north and south. These structures include the Nataalkuz fault, mapped to the north of the ranges (Diakow *et al.*, 1993); the Blackwater drainage system appears to follow a parallel structural zone to the south.

Uplift of the Middle Jurassic Naglico formation appears to be relatively uniform across much of the Nataalkuz Lake and Fawnie Creek map areas, as suggested by widely distributed augite-phyric lavas and intravolcanic sedimentary rocks. In the central Naglico Hills, the formation comprises a southwest-dipping homocline, however this trend in bedding is disrupted in the east near Tommy Lakes, where comparable Jurassic strata dip to the south. Significant variability in bedding

attitudes is also observed along the axis of the Entiako Spur. In the eastern part of the spur, the layered rocks dip in opposing directions across Fawnie Creek. Immediately west of Fawnie Creek, throughout section A, the beds dip at low to moderate angles northwest; farther west bedding attitudes change significantly from one ridge to another. Much of the variability is attributed to tilting along normal faults.

Faults in the Fawnie Creek typically trend north and northwest. Displacements are assumed to be small as they affect rocks mainly from the Naglico formation. Near the Wolf prospect, strata of the Ootsa Lake Group in contact with the underlying Naglico formation are disrupted by steeply dipping structures. Faults apparently occupy the two valleys between three knolls, causing the unconformable surface between Eocene and Jurassic basement to step down progressively toward the west. Jurassic sedimentary rocks in the vicinity of section C, east of Fawnie Creek, are truncated on the north by a steep, northwest-trending fault. The trace of this fault is lost where it intersects the Fawnie Creek valley, and field evidence suggests the structure does not extend directly across the valley. However, a fault which may be its northern extension is suspected to trace through the Fawnie Creek watershed where it turns sharply up-slope in the Fawnie Range. Interpretation of these segments as a continuous structure requires a crossfault with right-lateral motion, trending northeast through the valley occupied by Top Lake. There is little direct field evidence for such a fault, although it would be difficult to recognize as its trace would roughly parallel the strike of layered rocks in the area.

The high-level emplacement of the Late Cretaceous Capoose batholith into Jurassic rocks beneath the Entiako Spur generated numerous small-scale faults and fractures. Fracturing is most intense in the central part of the spur where the batholith is closest to the surface. Increased permeability in these rocks channelled the flow of hydrothermal solutions, as evidenced by widespread propylite, and more localized skarn alteration and pervasive silicification.

## ECONOMIC GEOLOGY

Except for epithermal vein and disseminated precious metal mineralization at the Wolf property, which is related to Eocene felsic magmatism, most mineral prospects in the Fawnie Creek and adjoining Nataalkuz Lake map areas occur near the margin of the Capoose batholith. Precious metal mineralization at the Capoose prospect, in the Nataalkuz Lake map area, is temporally and probably genetically related to the emplacement of batholith (Andrew, 1988). A similar spatial relationship exists in the Fawnie Creek map area where skarn and epithermal prospects occur in hydrothermally altered Middle Jurassic rocks near the

contact with the batholith. Two new epithermal targets, one a system of discordant veins and the other a zone of pervasive silicification, were discovered during the bedrock mapping program in volcanic rocks of the Naglico formation. Features of these occurrences are discussed in the following section. The setting of other known deposits in the Fawnie Creek map area is described elsewhere (Schroeter and Lane, 1994: this volume).

## NEW EPITHERMAL PRECIOUS METAL PROSPECTS

### MALAPUT (UTM 358470E, 5893455N)

The Malaput occurrence is in a gently sloping logged area accessed by a secondary road off of the Kluskus-Malaput Forest Service road. The occurrence consists of pervasively silicified rocks that crop out sporadically through apparently thin glacial drift in a zone measuring approximately 125 by 75 metres. Outcrops of the Capoose batholith occur about 1 kilometre to the northwest and comparatively unaltered green and maroon volcanic rocks, tentatively assigned to unit MJ11, are exposed about 50 metres to the east.

The altered rocks are composed mainly of fine-grained silica, in places accompanied by sericite and rare, crystalline barite. The texture of these rocks is typically massive with some irregular open cavities lined by drusy quartz. Finely disseminated pyrite, present in trace quantities, is generally oxidized resulting in a limonitic coating on weathered surfaces. About 50 metres to the east a solitary exposure of layered volcanic rocks contains bedding-parallel pyritiferous laminae.

The altered mineral assemblage is suggestive of a low-temperature, oxidized, epithermal setting. At present this alteration zone is poorly exposed; it requires additional work to assess its precious metal potential. A relatively flat site and the nature of alteration are amenable to an exploration program involving mechanized trenching and an induced polarization survey.

### TOMMY (UTM 363750E, 587650N)

The Tommy occurrence is actually three isolated quartz vein and stockwork veinlet occurrences found in the vicinity of Tommy Lakes in the southeast corner of the map area. At present, there are no roads in this area. It is occupied by tree-covered hills with generally poor rock exposures limited to their crests and steeper slopes. The veins occur in rhyolitic flows and lesser ash-flow tuff of unit MJ1.

The UTM grid coordinate cited above is for the largest of the veins. At this site a vertical quartz vein can

be traced discontinuously for 50 metres along a trend of 045°. The vein is typically less than 1.5 metres wide. The quartz is white, finely crystalline to massive, rarely banded along vein margins with drusy crystals growing inward toward the centre of some anastomosing veinlets. Sparry calcite sometimes occupies a void at the centre of the banded veins. Pyrite is present in trace amounts. Alteration of the country rocks is shown by minor reddening of the groundmass and plagioclase phenocrysts. Small outcrops of quartz can be traced intermittently for about 500 metres to the northeast.

Stockwork veinlets are exposed on a knoll due south of the easternmost of the Tommy Lakes. Prominent fractures and brecciated vein material trend northeast. Another system of stockwork veinlets crop out on a knoll near the centre of a recent forest burn, northeast of Tommy Lakes. These quartz veins are similar to others south of Tommy Lakes, however, they also contain crystalline barite.

Limited time was devoted to prospecting in the Tommy Lakes area during the course of bedrock mapping. We believe there is excellent potential for the discovery of additional epithermal quartz veins and their potential for precious metals is untested.

## ACKNOWLEDGMENTS

We were pleased to have had the opportunity to be accompanied in the field by Howard Tipper and Tom Richards. We thank them for enlightening discussions which improved our understanding of the regional geology. We also thank Howard for promptly identifying fossils while the mapping was in progress. We appreciate the logistical support and hospitality shown by Metall Mining Corporation on our frequent visits to the Wolf camp. In particular, discussions with Dave Heberlein regarding geology at the Wolf property were beneficial.

We are appreciative of the local ranchers - the Lamperts, Kestlers and Rempels who were supportive of our work in their backyard, and helped out when called on. Special thanks are extended to "Wrangler Walt" for introducing two greenhorns to horses, trail riding by star light, and "spike" sprinkled on bread. We thank Joyce of Northern Mountain Helicopters for her regularity with the morning radio call.

Hugh Jennings and Janet Riddell assisted in the project.

## REFERENCES

- Andrew, K.P.E. (1988): Geology and Genesis of the Wolf Precious Metal Epithermal Prospect and the Capoose Base and Precious Metal Porphyry-style Prospect, Capoose Lake Area, Central British Columbia; unpublished M.Sc. thesis, *The University of British Columbia*, 334 pages.
- Cook, S.J. and Jackaman, W. (1994): Regional Lake Sediment and Water Geochemistry Surveys in the Northern Interior Plateau, B.C. (NTS 93F/2,3,6,11,12,13,14); in *Geological Fieldwork 1993*, Grant, B. and Newell, J.M., Editors, *B.C. Ministry of Energy, Mines and Petroleum Resources*, Paper 1994-1, this volume.
- Diakow, L.J., Green, K., Whittles, J. and Perry, A. (1993): Geology of the Natakuz Lake Area, Central British Columbia (NTS 93F/6); *B.C. Ministry of Energy, Mines and Petroleum Resources*, Open File 1993-14.
- Giles, T.R. and Levson, V.M. (1994): Surficial Geology and Drift Exploration Studies in the Fawnie Creek Area (93F/3); in *Geological Fieldwork 1993*, Grant, B. and Newell, J.M., Editors, *B.C. Ministry of Energy, Mines and Petroleum Resources*, Paper 1994-1, this volume.
- Green, K.C. and Diakow, L.J. (1993): The Fawnie Range Project - Geology of the Natakuz Lake Map Area (93F/6); in *Geological Fieldwork 1992*, Grant, B. and Newell, J.M., Editors, *B.C. Ministry of Energy, Mines and Petroleum Resources*, Paper 1993-1, pages 57-67.
- Schroeter, T.G. and Lane, R.A. (1994): Mineral Resources (93F/3 and parts of 93F/2,6, and 7); in *Geological Fieldwork 1993*, Grant, B. and Newell, J. M., Editors, *B.C. Ministry of Energy, Mines and Petroleum Resources*, Paper 1994-1, this volume.
- van der Heyden, P., Shives, R., Ballantyne, B., Harris, D., Dunn, C., Teskey, D., Plouffe, A. and Hickson, C. (1993): Overview and Preliminary Results for the Interior Plateau Program, Canada - British Columbia Agreement on Mineral Development 1991-1995; in *Current Research, Part E; Geological Survey of Canada*, Paper 93-1E, pages 73-79.

**SURFICIAL GEOLOGY AND DRIFT EXPLORATION STUDIES IN THE  
FAWNIE CREEK AREA (93/F3).**

By T.R. Giles and V.M. Levson

**KEYWORDS:** Surficial geology, drift exploration, till, glaciofluvial outwash, glaciolacustrine sediments, applied geochemistry, mineral dispersion, dispersal trains.

**INTRODUCTION**

This paper describes the preliminary results of surficial geological mapping and till geochemistry sampling during the 1993 field season in the Fawnie Creek (93F/3) map area (Figure 1). This work is part of a larger program in the Interior Plateau that includes bedrock mapping, lake geochemistry and mineral deposit studies (see Diakow and Webster, Cook and Jackaman, and Schroeter and Lane, respectively, 1994, this volume). The program is designed to test the applicability of surficial geology data to drift prospecting in regions where mineral exploration has been hampered by thick drift cover. Neogene lava flows, an outdated geological database and a lack of modern geochemical and geophysical information have also hindered exploration in the area. Surficial geological mapping in the area was completed in order to understand the glacial history and provide a basis for design of a till geochemical sampling program. The projects main goals, designed to address these problems, are:

- to compile a 1:50 000 surficial geology map of the Fawnie Creek area (93F/3), conduct stratigraphic and sedimentologic studies of Quaternary deposits in the area, and define the glacial history and ice-flow patterns;
- to complete a regional (1:50 000) till sampling program and produce a series of till geochemistry and drift exploration potential maps for mineral exploration purposes; and
- to develop and refine methods of drift exploration applicable to the Interior Plateau region by conducting detailed case studies around known mineral deposits.

**STUDY AREA**

The Fawnie Creek map area lies within the Nechako Plateau, in the west-central part of the Interior Plateau. (Holland 1976). The Fawnie Range dominates the northeast corner of the map area, reaching elevations of over 1775 metres (5800 feet; Figure 2). Entiako Spur extends across the northern half of the region, with elevations dropping westward from 1750 metres (5700

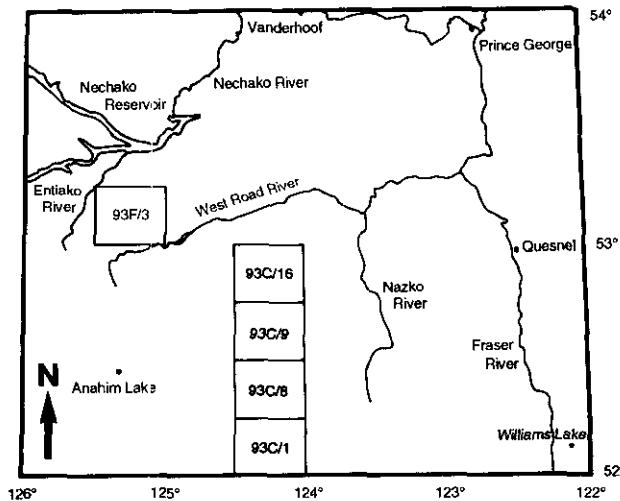


Figure 1. Location map of the Fawnie Creek (93F/3) map sheet. The 1992 study areas Chilanko Forks, Chezacut, Clusko River and Toil Mountain (93C/1, 8, 9, 16 respectively) are also shown (Giles and Kerr, 1993; Proudfoot, 1993).

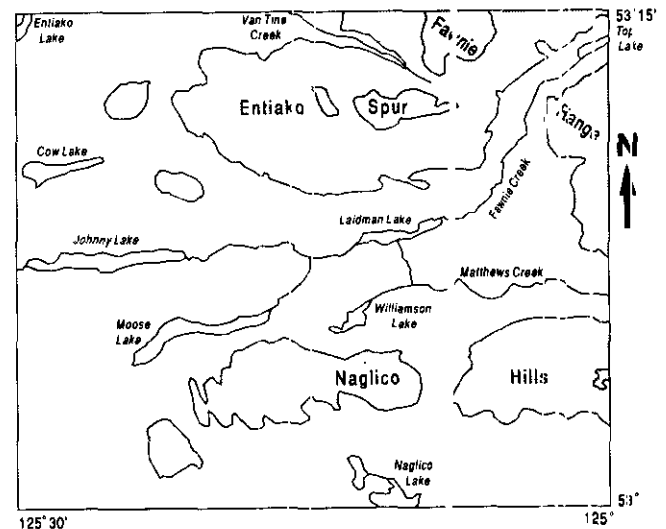


Figure 2. General physiography of the Fawnie Creek area. The light shading represents areas with elevations above 1200 metres (4000 feet) and the darker shading areas in excess of 1520 metres (5000 feet).

feet) to below 1200 metres (3900 feet). Fawnie Creek valley occupies the centre of the map area and flows from Top Lake at an elevation of around 1070 metres (3500 feet) southwest through Laidman and Johnny lakes. The Naglico Hills form the southern margin of the Fawnie Creek valley, reaching elevations of 1550 metres (5100 feet) in the east and 1370 metres (4500 feet) in the west and they, in turn, are bounded on the south by the valley of the Blackwater River. All valleys in the area are broad with gently inclined sides reflecting glacial modification, except Van Tine Creek (Figure 2) which is perpendicular to ice flow and has a sharp V-shaped valley.

During the last or Late Wisconsin glacialation, ice moved into the Fawnie Creek map area from the Coast Mountains before flowing north, northeast and east onto the Interior Plateau (Tipper, 1971). Coast Mountain ice extended as far east as the Fraser River before coalescing with Cariboo Mountain ice flowing to the west and northwest.

The study area is approximately 150 kilometres from Vanderhoof and is accessed by the Kluskus-Ootsa Forest Service road. Logging road access within the north half and southeast quarter of the map area is good but much of the west and southwest are accessible only by trails.

## METHODS

Surficial geology mapping was completed by interpretation of air photographs, field checking existing terrain map data (Tipper, 1954, 1963; Howes, 1976, 1977), and stratigraphic and sedimentologic studies of Quaternary exposures in the study area. Ice-flow history for the Fawnie Creek map area was largely deciphered from the study of crag-and-tail features, flutings and drumlins (Plates 1 to 3); striation measurements are also good local ice-flow indicators.

Till samples were collected for geochemical analysis in order to locate glacially dispersed mineralization present in the region. Regional sample locations were selected to obtain complete coverage of the map area, with the greatest density of samples along transects perpendicular to established ice-flow direction. In ice-parallel situations, where samples repeatedly represent the same terrain directly up-ice and therefore duplicate each other, wide-spaced sampling was used. An intermediate sample spacing was used on transects oblique to flow. Samples were collected from the C

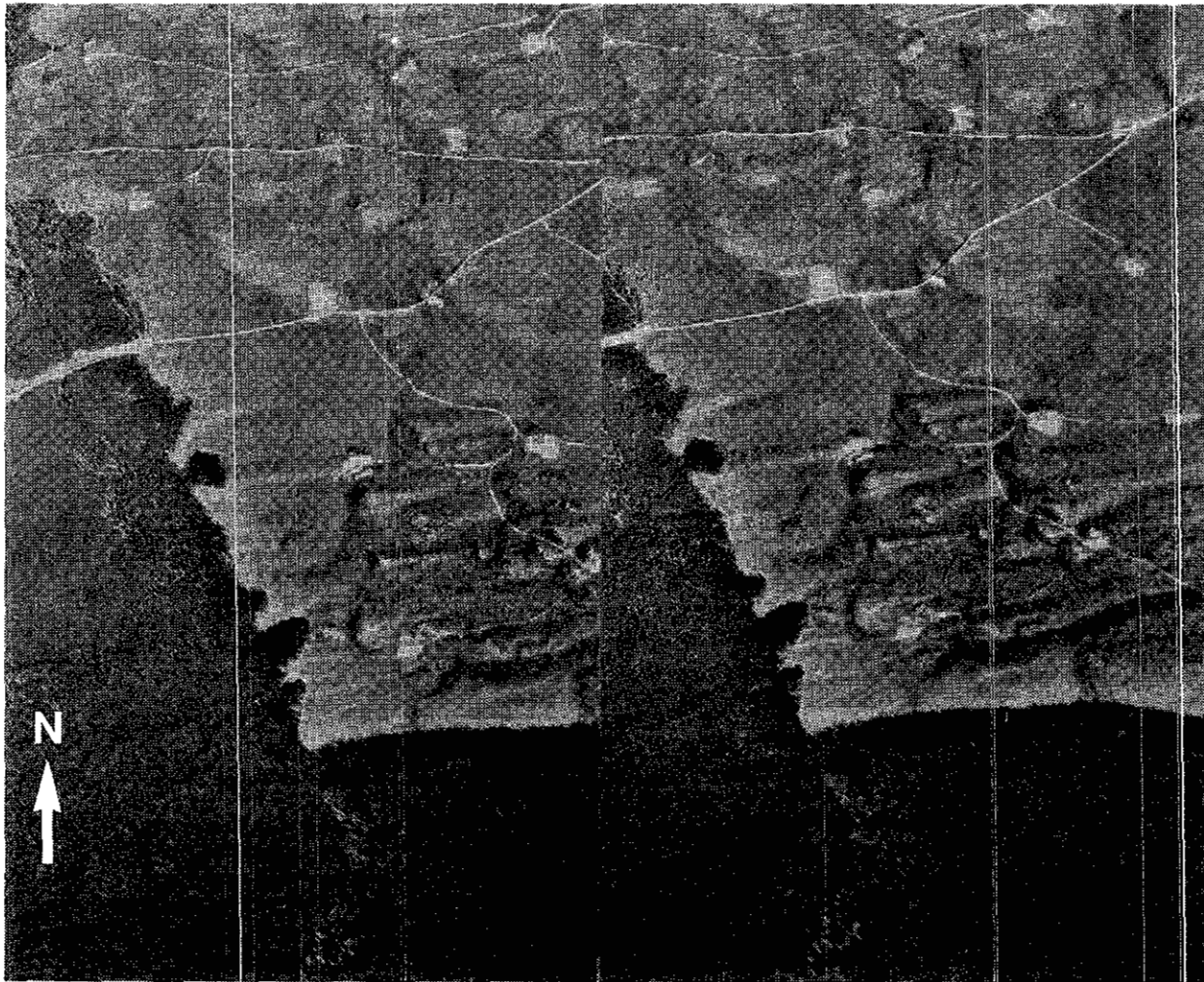


Plate 1. Stereo pair of air photographs of crag-and-tail features formed by glacial action on the north flank of the Naglico Hills near Williamson Lake. Note the consistent orientation of the linear tails toward the east in the down-ice flow direction. Note also how forest cover obscures glacial features in unlogged areas. Air photographs BCB 92048-68 and 69.

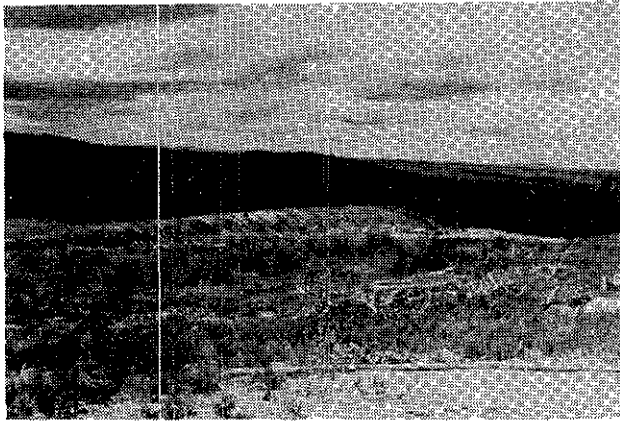


Plate 2: Crag-and-tail feature. A crag or knob of bedrock is exposed at the right (west) and the tail of sediment which filled the cavity beneath the ice is preserved to the left. Glacial ice-flow direction is from right to left ( $065^\circ$ ).

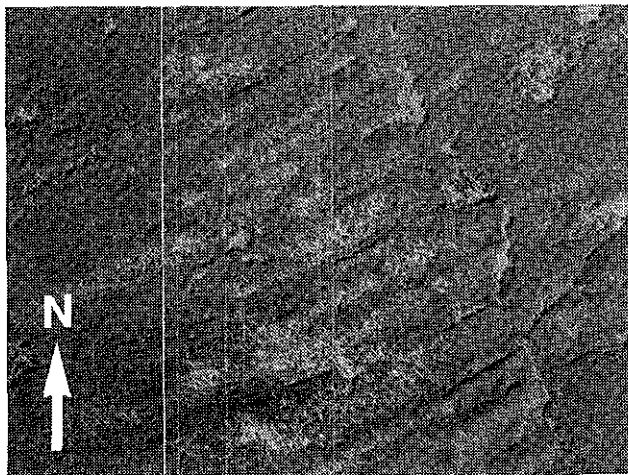


Plate 3: Air photograph of east-northeast oriented flutings reflecting regional ice-flow direction on the southwest side of Entiako Spur. Air photograph BCB 91087-160.

mineral soil horizon, which is comparatively unaffected by the pedogenic processes operative in the A and B soil horizons (Agriculture Canada Expert Committee on Soil Survey, 1987; Gleeson *et al.*, 1989). Sample sites consist of natural and man-made exposures (roadcuts, borrow pits, soil pits and trenches). Locations of sample sites were plotted on a 1:50 000 topographic base map with the aid of air photographs. A total of 229 till samples were collected throughout the study area (Figure 3) at a density of approximately one sample per 4 square kilometres. Higher density sampling was conducted in areas of perceived higher mineral potential and around known mineral prospects to provide a clearer understanding of glacial dispersion processes. At each sample site, data collected included descriptions of sediment type, primary and secondary structures, matrix texture, presence of fissility, compactness, total percentage and modal size of clasts, rounding of clasts, local slope, presence of striated clasts, and sediment genesis and thickness. Further information was noted on soil horizons, bedrock striae, bedrock lithology, clast provenance and abundance of mineralized erratics.

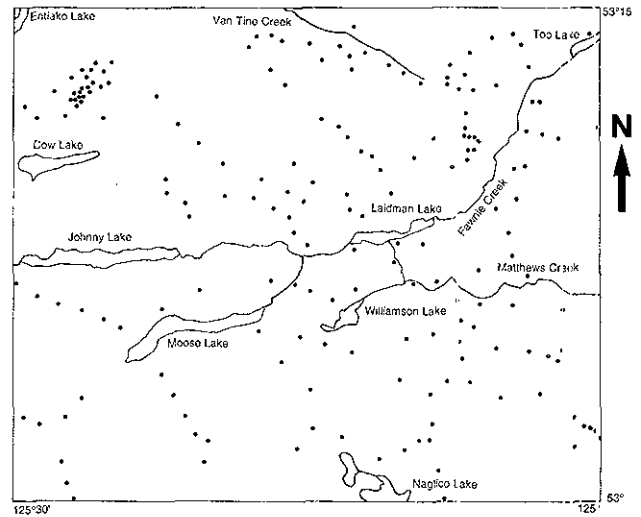


Figure 3: Location map of sample sites in the study area. The concentration of sites in the northwest corner reflects more detailed sampling completed in the vicinity of the Wolf prospect. Note the bias towards SE trending transects (perpendicular to regional ice-flow direction).

Detailed till and soil geochemistry sampling was conducted at three mineral prospects (Wolf, MINFILE 93F 045; Capoose, MINFILE 93F 039; and Blackwater-Davidson MINFILE 93F 037), two mineral showings (Fawn, MINFILE 93F 043; and Yellow Moose, no MINFILE) and two newly discovered prospects (no MINFILE; see Diakow and Webster, 1994) to document mineral (elemental and lithologic) dispersion processes (Table 1). Each site is unique in geomorphologic, sedimentologic or stratigraphic setting. Approximately 122 samples were collected along ice-parallel or ice-perpendicular, linear or fan-shaped traverses to document glacial dispersion and transport distance.

The most intensive survey was conducted at the Wolf epithermal gold-silver deposit. This included striation measurements to determine the local ice-flow history and a down-ice fan sampling program to gather information on mineral transport and dispersal. Samples were also taken up-ice from the prospect to determine background geochemical levels. Detailed sedimentologic and stratigraphic studies were conducted in numerous well-exposed trench sections in conjunction with a geochemical sampling program undertaken by University of British Columbia researchers (Delaney and Fletcher, in preparation). A steeply sloping trench with known bedrock geochemical values on the east side of the property was sampled in detail to document downslope dispersion in colluvial sediments.

Till samples were dried, split and sieved into three size fractions: 70 to 140 mesh (105 to 210  $\mu\text{m}$ ), 140 to 230 mesh (62.5 to 105  $\mu\text{m}$ ), and less than 230 mesh (less than 62.5  $\mu\text{m}$ ). All the <230 mesh fractions were analysed by instrumental neutron activation analysis (INAA) and inductively coupled plasma analysis (ICP) for 32 elements. The two coarser (105 to 210  $\mu\text{m}$  and 62.5 to 105  $\mu\text{m}$ ) fractions of samples taken during the detailed case studies, as well as several random samples from the

TABLE 1: DISPERSION STUDIES

Location	Deposit Type	Purpose	Samples	Sampling Design
Wolf	Epithermal Au-Ag	Glacial dispersion	40	Down-ice fan traverse
		Down-slope dispersion	24	Slope profile traverse
Mount Davidson	Transitional Au-Ag	Glacial dispersion	3	Linear down-ice traverse
Yellow Moose	High-level epithermal Hg-Au-Ag	Glacial dispersion	16	Down-ice fan traverse
Capoose	Transitional Au-Ag	Glacial dispersion	8	Linear down-ice traverse
Fawn	Epithermal Au-Ag	Glacial dispersion	12	Ice-flow perpendicular traverse
New discovery A	Unknown	Document lateral extent of deposit	11	Ice-flow perpendicular traverse
New discovery B	Unknown	Document lateral extent of deposit	8	Ice-flow perpendicular traverse

regional survey, were also analysed to investigate if mineral dispersion is similar in all size fractions during transport. One half of the sample splits was reserved for grain size and other follow-up analyses.

Approximately 100 pebbles were collected at till sample sites for lithologic analysis and provenance studies. Results will be used to investigate the relationship between bedrock geology and till clast lithology, glacial dispersion, rates of clast abrasion and rounding, and distances of travel. These data will be useful for tracing mineralized float to its source and to help determine bedrock lithology where exposure is limited due to drift cover.

## SURFICIAL GEOLOGY

### MORAINAL SEDIMENTS

Morainal deposits include all sediments deposited directly by or from glaciers with little or no reworking by water (Dreimanis 1989). Morainal sediments of the last glaciation occur throughout the Fawnie Creek map area and include lodgement and melt-out tills as well as glacial debris-flow sediments. Surficial geology mapping in the area shows that morainal sediments are the most widespread Quaternary deposits. They form a cover of variable thickness across much of the area and may occur as hummocky, kettled, fluted or relatively flat topography. Till thickness varies from a few to several metres in low-lying areas to less than 2 metres in upland regions and along steep slopes. Exposures of till up to 8 metres thick were observed in valleys perpendicular to the regional ice-flow direction (Figure 4, Section 93-9, Van Tine Creek). Exposures of till 1 to 2 metres thick are common on bedrock highs (Figure 4, Sections 93-1, 93-7, 93-15). In Fawnie Creek and Matthews Creek valleys, morainal sediments are largely buried by glaciofluvial outwash, fluvial and organic sediments.

Two distinct facies of morainal sediments are recognized: a compact, fissile, matrix-supported, sandy silt diamicton and a loose, massive to stratified, sandy diamicton. (Diamictons are defined as poorly sorted deposits consisting of mud, sand and gravel.) The first is interpreted to be basal lodgement and melt-out till and the latter to be glacial debris-flows and resedimented deposits. Basal tills seldom occur at the surface, usually being overlain by glacial debris-flow deposits and, on slopes, by resedimented diamictons of colluvial origin.

Basal tills are moderately to well compacted but range from weakly consolidated to very compact or overconsolidated. Moderate to strong platy fissility exists in the majority of the samples (Plate 4), although they are occasionally weakly fissile or nonfissile. Vertical jointing is common and blocky structures occur where the sediment has been exposed to the sun and is relatively dry (Plate 5). Weak to very strong oxidation of the till, characterized by reddish brown staining, is common and can occur pervasively or along vertical joint planes and horizontal partings. Subhorizontal slickensided surfaces are sometimes present, especially in clay-rich till.



Plate 4: Subhorizontal partings in massive diamicton interpreted as lodgement till.

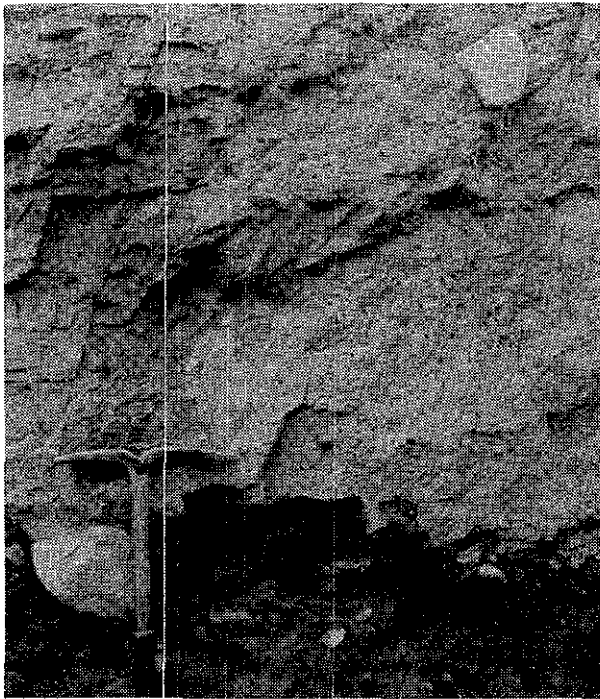


Plate 5: Melt-out till overlying proglacial outwash. Note the massive, resistant nature of the till.

Clasts in the basal tills range in size from small pebbles to large boulders with medium to large pebbles dominating most exposures. As much as 50% of the till may be comprised of clasts, but most exposures have between 10 and 30% clasts. Striated, faceted, embedded and lodged clasts are common and typically up to about 20% of the clasts are striated. Striated clasts are commonly flat lying and bullet shaped, and may be aligned parallel to ice-flow direction. Crude bedding locally visible in the tills, is indicated by higher percentages of small pebbles in some beds.

Lower contacts of basal till units vary from sharp and planar to gradational and irregular. Where till overlies competent bedrock that abraded slowly by sediment-rich basal ice, there is a clear and sharp contact. In some places, lower contacts are gradational with zones of broken, angular bedrock with little matrix, overlying fractured bedrock. Injections of till into bedrock fractures indicate high pressure conditions at the base of the ice during deposition. Occasionally, bedrock slabs have been lifted up into the body of the till; commonly they are folded and faulted but rarely are intact blocks preserved.

Diamictons of inferred debris-flow or colluvial origin (Plate 6) are loose to weakly compacted and are either massive or interbedded with stratified silt, sand or gravel. Clasts vary in size from small pebbles to large boulders but are usually medium to large pebbles. These diamictons typically contain 20 to 50% clasts although up to 70% are present locally. Subangular to subrounded clasts are most common, but local angular fragments dominate in some shallow exposures over bedrock. Up to 10% of the clasts are striated. Lenses and beds of sorted

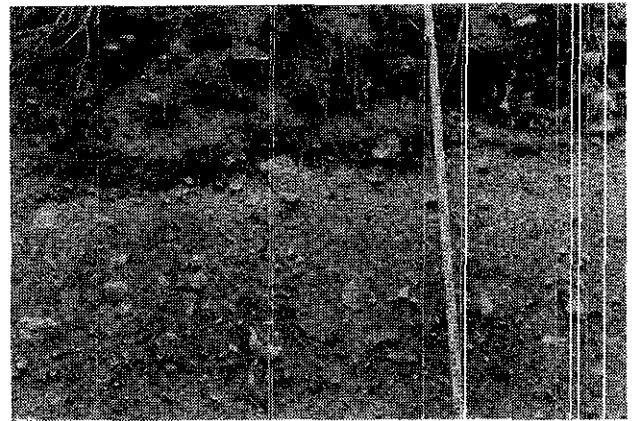


Plate 6: Loose, massive-appearing glacially-derived debris flow deposits overlain by sandy colluvium. Marked increments on measuring rod are labelled every 10 centimetres.

silt, sand and gravel occur in many exposures and may be continuous for up to 5 metres, although they are most frequently 10 to 100 centimetres wide. Debris-flow deposits may exhibit weak to very strong oxidization preferentially along the more permeable sand and gravel beds. Debris-flow units have gradational to clear lower contacts and typically overlie basal till.

## GLACIOFLUVIAL SEDIMENTS

Glaciofluvial sediments are common in the map area and occur as eskers, kames, terraces, fans and outwash plains in valley bottoms and along valley flanks. They consist mainly of poorly to well-sorted, stratified, pebble and cobble gravels and sands in deposits up to 10 metres thick. Thick sequences of glaciofluvial sands and gravels occur in large valleys (Fawnie, Matthews and Van Tine) (Figure 4, Section 93-9, Van Tine). Clasts are rounded to well rounded, vary in size from small pebbles to cobbles with rare boulders.

In upland areas on Entiako Spur, Naglico Hills and the Fawnie Range, postglacial glaciofluvial sands and gravels occur as a veneer or thin blanket, up to 2 metres thick, on top of till (Figure 4, Section 93-15). Structureless or crudely bedded, small-pebble to cobble, sandy gravel beds are common. Clasts may be up to boulder size, are frequently striated and vary from rounded to angular. Many of these deposits are interbedded with gravelly diamictons indicating that they are proximal outwash deposits.

Advance phase glaciofluvial sediments were observed at one site on the south side of Entiako Spur under till within a bedrock channel cut oblique to ice flow (Figure 4, Section 93-7). Horizontally stratified medium to coarse sand beds at the base of the section are erosionally truncated by a poorly sorted, crudely imbricated, clast-supported cobble gravel. Clay intraclasts, up to 10 centimetres in diameter occur in the gravel. These sediments are interpreted as proglacial, proximal braided-stream deposits.

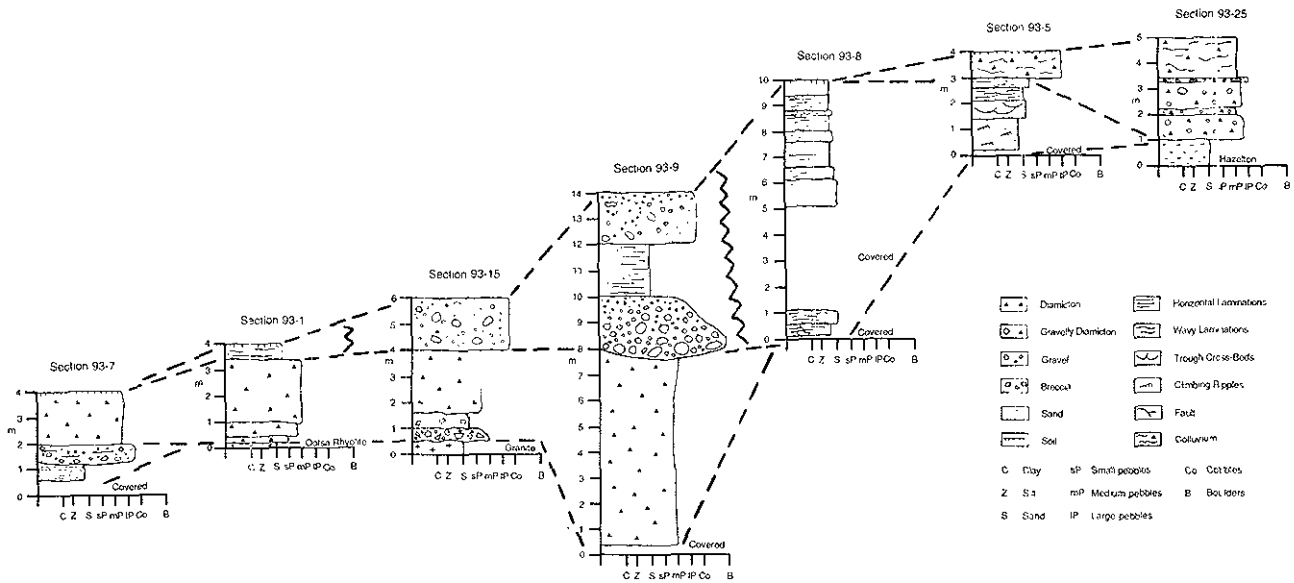


Figure 4. Representative stratigraphic columns of Quaternary deposits and interpretative correlation of main units in the study area.

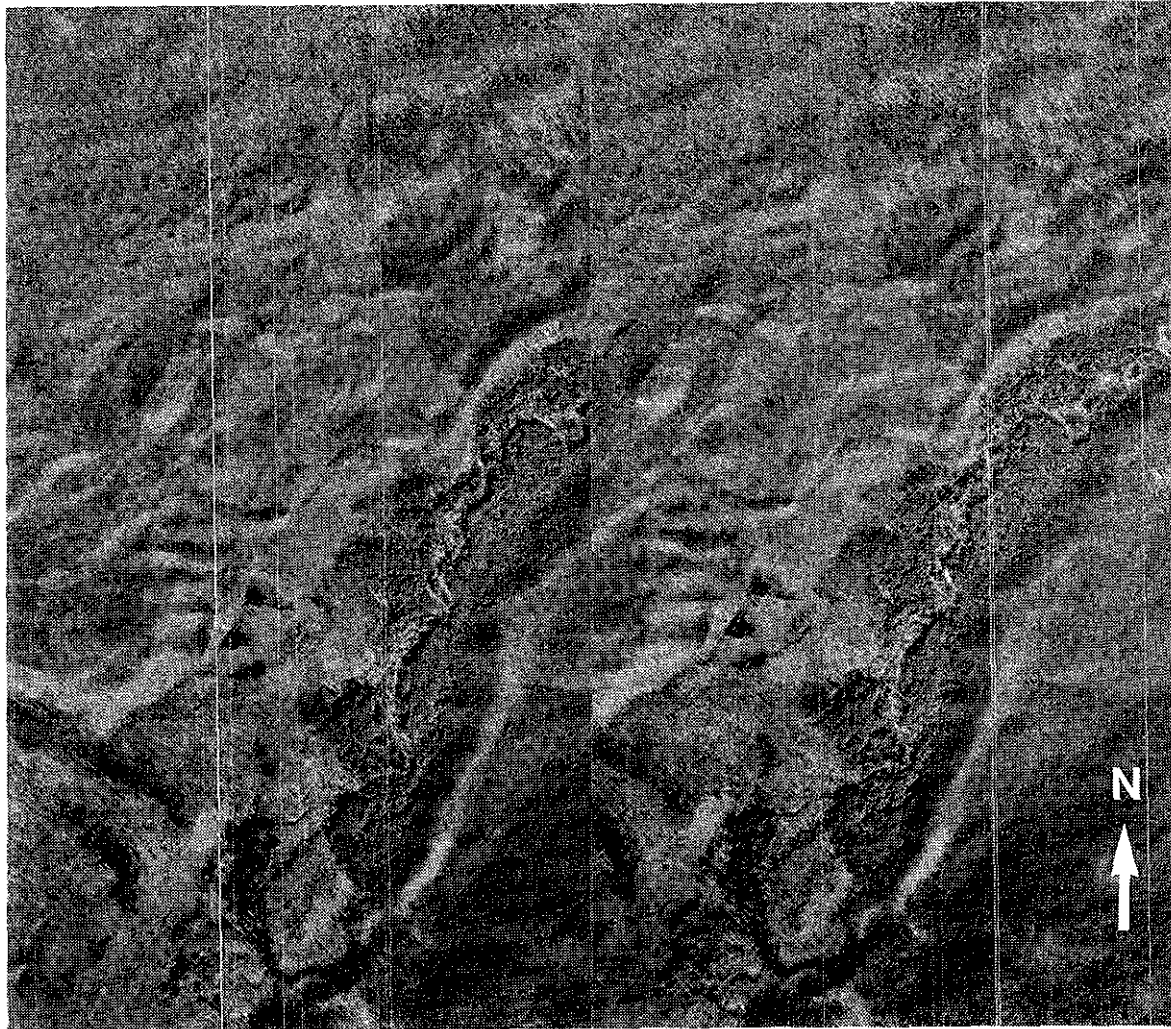


Plate 7: Stereo pair of the glaciofluvial complex southwest of Top Lake. Meltwater channels, gravel ridges and kettle depressions are visible. The incised, post-glacial Fawnie Creek valley extends from the right centre to the bottom centre of the plate. Air photographs BC 4281-153 and 154.

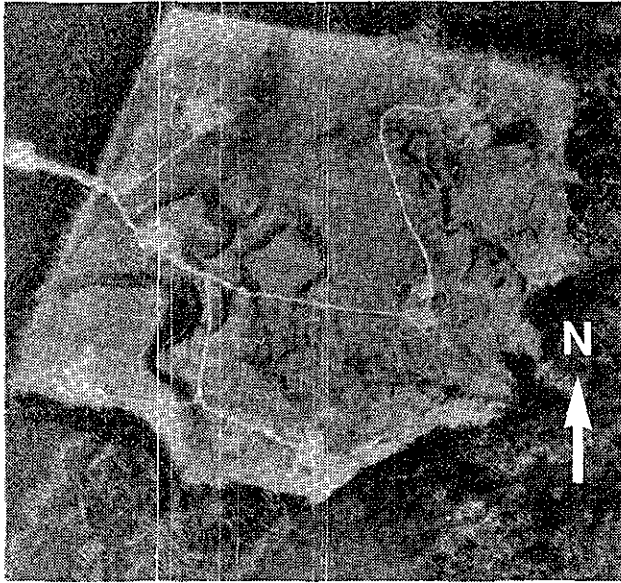


Plate 8: Meltwater channels developed near the margin of stagnating ice masses on the south side of the Entiako Spur. Air photograph BCE 91088-174.

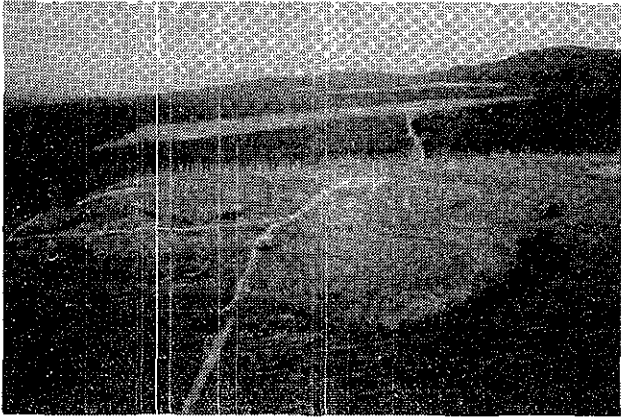


Plate 9: Oblique view, looking westerly, of meltwater channels seen in Plate 8.

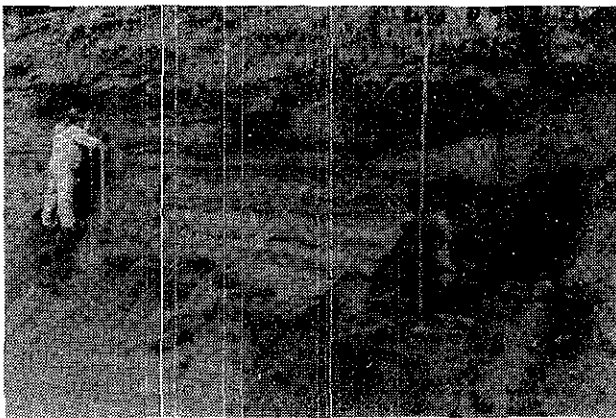


Plate 10: Well-sorted, ripple-bedded, fine to coarse sand in a coarsening upward sequence deposited in a small fan-delta on the south side of Entiako Spur.

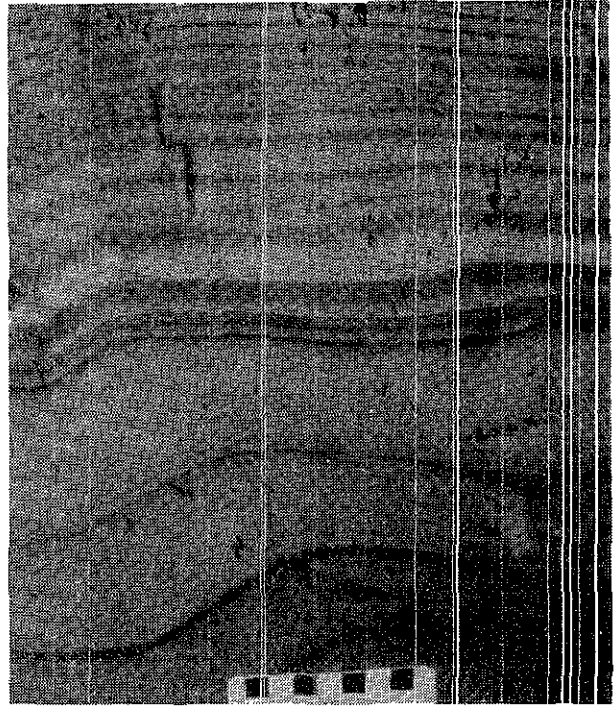


Plate 11: Depositional-stoss climbing ripples of the glaciolacustrine sand facies overlain by horizontally laminated fine sand, silt and clay. Scale is in centimetres.

Hummocky topography at the confluence of Van Tine and Fawnie valleys, consisting of ridges and knobs of sand and gravel with large kettles, indicates the presence of ice blocks within gravelly sediments during deposition of an outwash fan (Plate 7). On the southeast margin of Entiako Spur, large kame deposits and an extensive series of meltwater channels (Plates 8 and 9) developed parallel to the ice margin indicate prolonged ice stagnation and ablation. Moderately sorted, crudely bedded gravel and sand terraces high on the eastern margin of Fawnie valley are deposits of high-level ice-marginal channels formed during ice retreat or stagnation.

Approximately 20 kilometres to the northeast of the map area, there is a large esker complex at the junction of Top Lake and Chedakuz valley. The eskers are perpendicular to, and occur on the western margin of, the Chedakuz valley, indicating that they were formed by water from the Top Lake valley. As the glacier retreated up the Top Lake valley some ice masses remained in the Chedakuz valley and impounded drainage in the Top Lake valley. The glacial lake was able to drain subglacially and formed these large eskers.

### GLACIOLACUSTRINE SEDIMENTS

Glaciolacustrine sediments are found in only four places in the study area: on the east side of the Wolf prospect, in two valleys on the south side of the Entiako Spur (Figure 4, Section 93-5), and near Top Lake (Figure 2; Figure 4, Section 93-8). They can be divided into two facies based on grain size and structure: horizontally

bedded fine to coarse sand and horizontally laminated fine sands, silts and clays. A shallow-water fan-delta origin is proposed for the sand facies and the finer grained sediments are interpreted to be rhythmically bedded glaciolacustrine deposits.

The coarsest strata in the sand facies are horizontally bedded and trough cross-laminated medium to coarse sand beds up to 25 centimetres thick (Plate 10), commonly with fluid escape, flame and load structures. Parallel-laminated fine to medium sand beds, up to 10 centimetres thick, with dropstones, load structures, faults and deformed beds are common. Climbing ripples occur in well-sorted fine to medium sand beds, usually as a cap to underlying coarser strata. Beds of this facies commonly fine upwards from glaciofluvial gravels below to fine sand, silt and clay facies above.

Fine sands, silts and clays are thinly laminated, horizontally stratified and laterally extensive. Horizontally laminated, normally graded beds of fine sand and silt are the dominant sediments in this facies (Plate 11). Beds of fine sand up to 2 centimetres thick commonly form rhythmic couplets with silt beds,

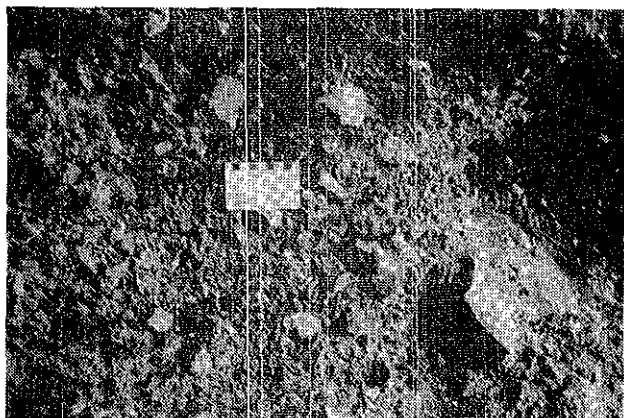


Plate 12: A typical exposure of unsorted, angular colluvial diamicton overlying on bedrock on a steep slope.



Plate 13: Air photograph of the postglacial alluvial fan which has deflected the outlet stream from Top Lake to the south side of the valley. Note the presence of one major channel and at least three abandoned channels. Air photograph BC 7807-311.

typically less than a centimetre thick. Fine sand and silt may occur in normally graded beds up to 20 centimetres thick. Clay beds are 1 to 5 centimetres thick. High-angle intraformational faulting is locally common, with displacements up to 10 centimetres.

### ***POSTGLACIAL FLUVIAL AND ORGANIC SEDIMENTS***

Fluvial sediments occur in valley bottoms throughout the area. They include reworked morainal and glaciofluvial deposits as indicated by stream exposures of glaciofluvial delta, terrace, kame and esker deposits, especially in the Fawnie Creek valley. Most streams in the area are meandering streams with gravel channels. Floodplains are dominated by fine sands, silts and organics. In upland areas small gravelly creeks have reworked glacial, glaciofluvial and colluvial sediments and locally are incised into bedrock. The flat, open terrain of Fawnie and Matthews Creek valleys is characterized by marshes and shallow lakes filled with organic sediment. In the southwest part of the map area the Fawnie valley broadens to over 15 kilometres wide. The organic deposits consist of decayed marsh vegetation with minor sand, silt and clay. Organic deposits also occur in the base of some valleys in low areas, as a thin veneer of decaying vegetation over cobble and boulder gravel.

### ***POSTGLACIAL COLLUVIAL AND ALLUVIAL FAN SEDIMENTS***

A thin veneer of weathered and broken bedrock clasts in a loose sandy matrix occurs on steep slopes throughout the area (Plate 12; Figure 4, Sections 93-25 and 93-5). These deposits grade downhill into a thicker cover of colluvial diamicton derived from both local bedrock and till. Colluvial veneers are common over tills on steep slopes. Colluvial diamictons are differentiated from till by their loose, unconsolidated character, the presence of coarse, angular clasts of local bedrock, crude stratification and lenses of sorted sand and gravel.

Several postglacial alluvial fans occur in the area; the largest and most active is located at the west end of Top Lake (Plate 13). There is a large catchment area upstream from an incised bedrock gully that forms the fan-head channel, and flashy discharge is typical. The alluvial fan has prograded across the western margin of Top Lake and has constrained the outlet stream to the southern side of the valley. Coarse cobble to boulder gravel is actively transported in the main fan channel. Evidence for rapid lateral migration of the modern channel was seen during the course of the field season. Heavy rainfall over a 2-day period resulted in bankfull conditions, channel migration and bank erosion in several areas. Up to several metres of channel aggradation occurred locally. Flooding caused extensive

damage, isolating a bridge in mid-stream by eroding the roadbed on either side. The main course of the channel spread across a plain approximately 50 metres wide where previously it had been contained in a channel 5 metres wide. Evidence for many such events on this and other fans in the area is indicated by numerous channel scars on the fan surfaces (Plate 13).

## ICE-FLOW HISTORY

Results of ice-flow studies in the area indicate that there was one dominant flow direction towards the east-northeast modified by topographic control during both early and late stages of glaciation. Striation measurements from exposed bedrock across the area typically indicate northeast to east flow, but range from 028° to 103°. Topographic control of ice-flow direction during early glacial phases is indicated by valley-parallel striae on bedrock surfaces that are buried by thick till sequences. At the Late Wisconsinan glacial maximum, ice covered the highest peaks in the region and movement appears to have been unaffected by topography, suggesting an ice thickness in excess of 1000 metres (3000 feet). Crag-and-tail features, drumlins and glacial flutings are present throughout the area and indicate flow towards the east and northeast during full glacial time. Cross-cutting striae in an easterly (075°) trending valley in the northeast part of the area record topographically influenced ice flow during waning stages of glaciation. Early flow is towards 045° and later flow at 075°. Similarly, in the southwest part of the area the full-glacial ice direction was determined to be 070° to 080° with later flow at 089° to 103°.

## SUMMARY OF GLACIAL HISTORY

Prior to glaciation, regional drainage was similar to present, westwards from Top Lake and Mount Davidson through the Fawnie valley into the Entiako River system. Advancing ice to the southwest caused flow to reverse and proceed to the east and north through the Top Lake valley. The first lobes of Late Wisconsinan Fraser glaciation ice advancing into the area were probably confined to major valleys. Drumlins, crag and tails, flutings and striations all indicate that when the glaciers were thick enough to be relatively unaffected by topography during full-glacial times, ice flow was east-northeasterly. At the margins of the advancing ice, coarse-grained proglacial outwash was deposited locally in the valley bottoms. Massive, matrix-supported, compact lodgement and melt-out tills were deposited by the advancing ice. During the final stages of deglaciation, loose, sandy gravelly diamictons were deposited on top of the tills by debris flows. Confined subglacial flow created small eskers in the bottom of Van Tine Creek and Fawnie Creek valleys and on the low-lying areas to the southwest of Moose Lake. In the Fawnie Creek valley the glacier downwasted and numerous meltwater channels were cut on the north side

of the valley (Plate 8). Gravelly outwash plains formed in the main valley bottoms as large volumes of sediment and water were removed from the ice margin.

This valley was the only outlet through the Fawnie Range for meltwaters from ablating ice south of the Entiako Spur. Stagnant ice masses to the northeast of the map area dammed meltwaters and caused formation of a glacial lake in the Top Lake region. A pitted delta formed where sediment-laden meltwaters entered the western margin of the lake at an elevation of around 1100 metres (3600 feet). Knob-and-kettle topography (Plate 13) indicates the presence of ice blocks within the deltaic sediments. Ten metres of rhythmically bedded sand and silt are exposed along the margin of Fawnie Creek valley suggesting sustained lake activity. A large esker complex is located at the eastern end of the Top Lake valley where meltwaters flowed under the stagnant ice masses in the Chedakuz valley.

Other smaller lakes also formed locally along the margins of the retreating ice. For example, in the Wolf area, glaciolacustrine sediments occur 75 metres above the base of a north-trending valley indicating local ice damming. In addition, meltwaters, flowing off the Entiako Spur on the north side of the Fawnie valley, were dammed by stagnant ice creating short-lived glacial lakes in the side valleys. A sequence of cobble-boulder gravel, fining upward to stratified fine sand, silt and clay, exposed in one of the valleys, records the change from a glaciofluvial to a glaciolacustrine environment. In another valley, a thick section of well-sorted, well-bedded, rippled fine to coarse sand is exposed in a coarsening upward sequence which suggests delta progradation into a lake.

## EXPLORATION IMPLICATIONS

Exploration programs in drift covered regions must rely on an understanding of glacial processes and the glacial history of the area (Coker and DiLabio, 1989). *Glaciers moving across mineralized bedrock erode and incorporate mineralized debris into the ice mass. Dilution of the mineralization occurs down-ice and forms a dispersal train within the till. The dispersal train may be strongly anomalous but very small at the head (source) and becomes less anomalous but much larger towards the tail. Dispersal train anomalies may be hundreds to thousands of times larger than the original bedrock source and form large targets for geochemical exploration (DiLabio, 1990). Dispersal trains are commonly very thin in comparison with their length and have clear lateral and vertical contacts with the surrounding till. In the simplest case of unidirectional ice-flow, mineralized material at a point source will be eroded, transported and redeposited to produce a ribbon-shaped dispersal train parallel to ice flow (Fox *et al.*, 1987; Gravel *et al.*, 1991). Variations in the ice-flow direction, caused by topographic irregularities or changing dynamics at the base of the ice may cause the anomaly to curve or to form a fan-shaped dispersal train. In more complex areas, where there have been numerous*

flow directions during glaciation or multiple glaciations, the anomaly may be widespread and difficult to trace to the source.

Sampling of basal tills rather than other types of surficial materials is recommended in this region for several reasons:

- Basal tills are deposited in areas directly down-ice from their source and therefore mineralized materials dispersed within the tills can be more readily traced to their origin than can anomalies in other sediment types. Processes of dispersion in ablation tills, glaciofluvial sands and gravels, and glaciolacustrine sediments are more complex and they are typically more distally derived than basal tills.
- The dominance of one main regional ice-flow direction throughout much of the last glacial period has resulted in a simple linear, down-ice transport of material. This makes tracing of basal till anomalies to source relatively easy compared to regions with a more complex ice-flow history.
- Due to the potential for the development of large dispersal trains, mineral anomalies in basal tills may be readily detected in regional surveys.

To reflect mechanical dispersion processes, samples should be collected from the C mineral soil horizon. This horizon remains comparatively unaffected by pedogenic processes which occur in the A and B horizons. Poor results of some traditional geochemical soil sampling programs may be due to indiscriminate sampling of B and even Ae horizons. Sedimentologic data should be collected at all sample sites in order to distinguish till from glacial debris-flow, colluvium, glaciofluvial or glaciolacustrine sediments. These sediments have different processes of transportation and deposition which must be recognized in order to understand associated mineral anomaly patterns. For example, local variations will be reflected in some sediments while regional trends may be evident in others. Analysis of these sediments will be useful only if their origin is understood.

A basic understanding of ice-flow direction, glacial dispersal patterns, and transportation distances is required for successful drift exploration programs. Interpretation of data with respect to glaciation may provide the explorationist with new avenues to explore for bedrock sources of mineralized float or geochemically anomalous soil samples.

## ACKNOWLEDGMENTS

The authors would like to thank Larry Diakow, Ian Webster, Hugh Jennings, Janet Riddell, Tom Schroeter, Bob Lane, Steve Cook and Paul Matysek for their cooperation on this integrated program. We also extend thanks to Dave Heberlein and all the Metallgesellschaft camp at Wolf, and Karl Schiemann and Tom Richards

and the rest of the Cogema camp at Kenney Dam. John Newell offered constructive remarks which improved the manuscript.

## REFERENCES

- Agriculture Canada Expert Committee on Soil Survey (1987): The Canadian System of Soil Classification, Second Edition; *Agriculture Canada*, Publication 1646.
- Coker, W.B. and DiLabio, R.N.W. (1989): Geochemical Exploration in Glaciated Terrain: Geochemical Responses; in Proceedings of Exploration '87: 3rd Biennial International Conference on Geophysical and Geochemical Exploration for Minerals and Groundwater, Garland, G.D., Editor, *Ontario Geological Survey*, Special Volume 3, pages 336-383.
- Cook, S.J. and Jackaman, W. (1994): Regional Lake-sediment and Water Geochemistry Surveys in the Northern Interior Plateau, B.C. (93F/2, 3, 6, 11, 12, 13, 14); in *Geological Fieldwork 1993*, Grant, B and Newell, J.M., Editors, *B.C. Ministry of Energy, Mines and Petroleum Resources*, Paper 1994-1, this volume.
- Delaney, T.A. and Fletcher, W.K. (in preparation): Soil and Till Geochemistry at the Wolf Property, Central B.C.
- Diakow, L.J. and Webster, I.C.L. (1994): Geology of the Fawnie Creek Map Area (93F/3); in *Geological Fieldwork 1993*, Grant, B and Newell, J.M., Editors, *B.C. Ministry of Energy, Mines and Petroleum Resources*, Paper 1994-1, this volume.
- DiLabio, R.N.W. (1990): Glacial Dispersal Trains; in *Glacial Indicator Tracing*, Kujansuu, R. and Saarnisto, M., Editors, *A.A. Balkema*, Rotterdam, pages 109-122.
- Dreimanis, A. (1989): Tills: Their Genetic Terminology and Classification; in *Genetic Classification of Glacial Deposits*, Goldthwait, R.P. and Matsch, C.L., Editors, *A.A. Balkema*, Rotterdam, pages 17-83.
- Fox, P., Cameron, R. and Hoffman, S. (1987): Geology and Soil Geochemistry of the Quesnel River Gold Deposit, British Columbia; in *Geoexpo '86*, Elliot, I.L. and Smee, B.W., Editors, *The Association of Exploration Geochemists*, pages 61-67.
- Gleeson C.F., Rampton, V.N., Thomas, R.D. and Paradis, S. (1989): Effective Mineral Exploration for Gold Using Geology, Quaternary Geology and Exploration Geochemistry in Areas of Shallow Till; in *Drift Prospecting*, DiLabio, R.N.W. and Coker, W.B., Editors, *Geological Survey of Canada*, Paper 89-20, pages 71-96.
- Giles, T.R. and Kerr, D.E. (1993): Surficial Geology in the Chilanko Forks and Chezacut Areas (93C/1, 8); in *Geological Fieldwork 1992*, Grant, B. and Newell, J.M., Editors, *B.C. Ministry of Energy, Mines and Petroleum Resources*, Paper 1993-1, pages 483-490.
- Gravel, J.L., Sibbick, S. and Kerr, D. (1991): Geochemical Research, 1990: Coast Range - Chilcotin Orientation and Mount Milligan Drift Prospecting Studies (92O, 92N, 93N); in *Geological Fieldwork 1990*, *B.C. Ministry of Energy, Mines and Petroleum Resources*, Paper 1991-1, pages 323-330.

- Holland, S.S. (1976): Landforms of British Columbia, A Physiographic Outline; *B.C. Ministry of Energy, Mines and Petroleum Resources*, Bulletin 48.
- Howes, D.E. (1976): Fawnie Creek Terrain Map, *B.C. Ministry of Environment, Lands and Parks*.
- Howes, D.E. (1977): Terrain Inventory and Late Pleistocene History of the Southern Part of the Nechako Plateau; *B.C. Ministry of Environment Lands and Parks*, RAB Bulletin 1.
- Proudfoot, D.N. (1993): Drift Exploration and Surficial Geology of the Clusko River (93C/9) and Toil Mountain (93C/16) Map Sheets; in *Geological Fieldwork 1992*, Grant, B. and Newell, J.M., Editors, *B.C. Ministry of Energy, Mines and Petroleum Resources*, Paper 1993-1, pages 491-498.
- Schroeter, T.G. and Lane, R.A. (1994): Mineral Resources: Interior Plateau Project (93F/3 and parts of 93F/2, 6 and 7); in *Geological Fieldwork 1993*, Grant, B. and Newell, J.M., Editors, *B.C. Ministry of Energy, Mines and Petroleum Resources*, Paper 1994-1, this volume.
- Tipper, H.W. (1954): Geology of Nechako River British Columbia (93F); *Geological Survey of Canada*, Map 1131A.
- Tipper, H.W. (1963): Nechako River Map-area, British Columbia; *Geological Survey of Canada*, Memoir 324
- Tipper, H.W. (1971): Glacial Geomorphology and Pleistocene History of Central British Columbia; *Geological Survey of Canada*, Bulletin 196.

## NOTES



**REGIONAL LAKE SEDIMENT AND WATER GEOCHEMISTRY SURVEYS  
IN THE NORTHERN INTERIOR PLATEAU, B.C. (93F/2,3,6,11,12,13,14)**

By Stephen J. Cook and Wayne Jackaman

**KEYWORDS:** Applied geochemistry, lake sediments, lake waters, Nechako Plateau.

## INTRODUCTION

The Interior Plateau Project is a multidisciplinary investigation of bedrock geology, glacial history, and till and lake sediment geochemistry of parts of the Nechako and Fraser plateaus in the Northern Interior. Matysek and van der Heyden (1994, this volume) provide an overview of the project. Mineral exploration of this area has been limited by extensive drift cover, poor exposure and a young volcanic cover. As well, geological information is either nonexistent or obsolete.

Two regional lake sediment and water geochemistry surveys (Figure 1) were carried out by the Geological Survey Branch in the Nechako Plateau area during 1993, as a component of the Interior Plateau Project. The Fawnie survey covers 1:50000 NTS map areas 93F/2 (Tsacha Lake) and 93F/3 (Fawnie Creek), where exploration has been centred on precious metal prospects such as the Wolf (MINFILE 093F 045) and Blackwater-Davidson (MINFILE 093F 037) occurrences. The second, or Ootsa survey is centred on the Eocene volcanic basin south of Burns Lake and covers parts of NTS map areas 93F/6 (Natalkuz Lake), 93F/11 (Cheslatta Lake), 93F/12 (Marilla), 93F/13 (Takysie Lake) and 93F/14 (Knapp Lake). A total of 460 sites were sampled over a combined area of approximately 3530 square kilometres at an average density of 1 site per 7.7 square kilometres (Table 1). The survey areas were selected on the basis of their mineral potential. Concurrent bedrock and surficial geology mapping (Diakow and Webster, 1994; Giles and Levson, 1994) and mineral deposit studies (Schroeter and Lane, 1994, all this volume) were conducted in the western part of the Fawnie survey area. The Eocene volcanic basin offers a favourable but relatively unexplored environment for epithermal precious metal deposits.

The subdued topography, poor drainage and abundance of lakes in the Nechako Plateau make lake sediments an ideal geochemical exploration medium, and Earle (1993) has demonstrated the usefulness of lake sediment geochemistry in the area. Many regional surveys have been conducted, including those of mineral exploration companies, Spilsbury and Fletcher (1974), Hoffman (1976) and Gintautas (1984). They are an

effective tool to delineate both regional geochemical patterns and anomalous metal concentrations related to mineral occurrences. For example, sediment geochemistry reflects the presence of a bulk silver prospect near Capoose Lake (Hoffman, 1976; Hoffman and Fletcher, 1981) and and porphyry copper-molybdenum mineralization near Chutani Lake (Mehrtens, 1975; Mehrtens *et al.*, 1973), and has been successful in locating gold-silver mineralization at the Wolf occurrence (Andrew, 1988). Orientation studies conducted by the senior author in 1992 (Cook, 1993a,b) near the Wolf, Clisbako and Holy Cross epithermal precious metal occurrences have shown that elevated concentrations of gold (max: 56 ppb, 16 ppb and 9 ppb, respectively), arsenic and other elements occur in adjacent lake sediments (Cook, 1994).

This report provides only a general overview of the regional lake sediment surveys, the first such publicly funded surveys to be undertaken in British Columbia since the 1986 surveys of NTS map areas 93E (Whitesail Lake) and 93L (Smithers) (Johnson *et al.* 1987a,b). Results and interpretation, including data booklet, maps and floppy diskette, will be released in 1994.

## DESCRIPTION OF THE STUDY AREAS

### LOCATION AND ACCESS

The Fawnie survey area covers about 1880 square kilometres and is located approximately 50 kilometres south of Highway 16 and the town of Fraser Lake. There is only limited road access into the field area. The Kluskus-Ootsa and Kluskus-Malapat Forest Service roads provide access to much of the northern part of 93F/3 from Vanderhoof and Fraser Lake, while the Blue Road extends into the easternmost part of the survey area in 93F/2. Two of the major mineral occurrences, the Wolf and Blackwater-Davidson prospects, are road accessible. The Alexander Mackenzie trail crosses the southeast part of the survey area along the Blackwater River.

The Ootsa survey area lies north of the Fawnie area and covers about 1650 square kilometres south of Burns Lake. The irregular shaped area is bounded by Ootsa and Natalkuz lakes of the Nechako Reservoir in the south, and extends northwest to the Uncha Lake area. The northern boundary is about 25 kilometres south of Burns

Lake. There is considerably more logging activity in the Ootsa area than in the more remote Fawnie area, and hence better road access. The Kluskus-Nataalkuz ('500' road), Marilla and Holy Cross-Binta Forest Service roads cross the survey area and provide access from Vanderhoof, Fraser Lake and Burns Lake.

### **BEDROCK GEOLOGY AND MINERAL DEPOSITS**

The survey areas lie within the Stikinia Terrane. Bedrock geology of the Fawnie survey area has been mapped by Tipper (1963) and, in part, by Diakow and Webster (1994, this volume). Most of the area is underlain by volcanic and sedimentary rocks of the Lower to Middle Jurassic Hazelton Group. These are intruded by Cretaceous granitic rocks of the Capoose batholith and overlain by Eocene volcanics of the Ootsa Lake Group, Oligocene and Miocene volcanics of the Endako Group and Miocene-Pliocene basalt flows. In contrast, the Ootsa survey area covers most of the

northwest-trending belt of Ootsa Lake Group felsic volcanic rocks mapped by Tipper (1963) on the north side of the Nechako Reservoir. This unit, comprising a differentiated succession of Eocene andesitic to rhyolitic flows and pyroclastic rocks, underlies about 65 to 70% of the area. Other rock units, particularly Endako Group volcanics, are less extensively exposed.

The metallogeny and mineral deposits of the Fawnie area are outlined by Schroeter and Lane (1994, this volume). Epithermal precious metal deposits in Ootsa Lake volcanics and transitional precious metal deposits associated with the Capoose batholith are the most promising exploration targets. Interest in the potential for epithermal and related deposits has increased in recent years, and both the Wolf and Blackwater-Davidson prospects occur within the Fawnie survey area. The Wolf prospect is a low sulphidation adularia-sericite epithermal gold-silver occurrence (Schroeter and Lane, 1994, this volume), currently under exploration by Metall Mining Corporation, and is hosted by felsic flows, tuffs and subvolcanic porphyries. Mineralization occurs as

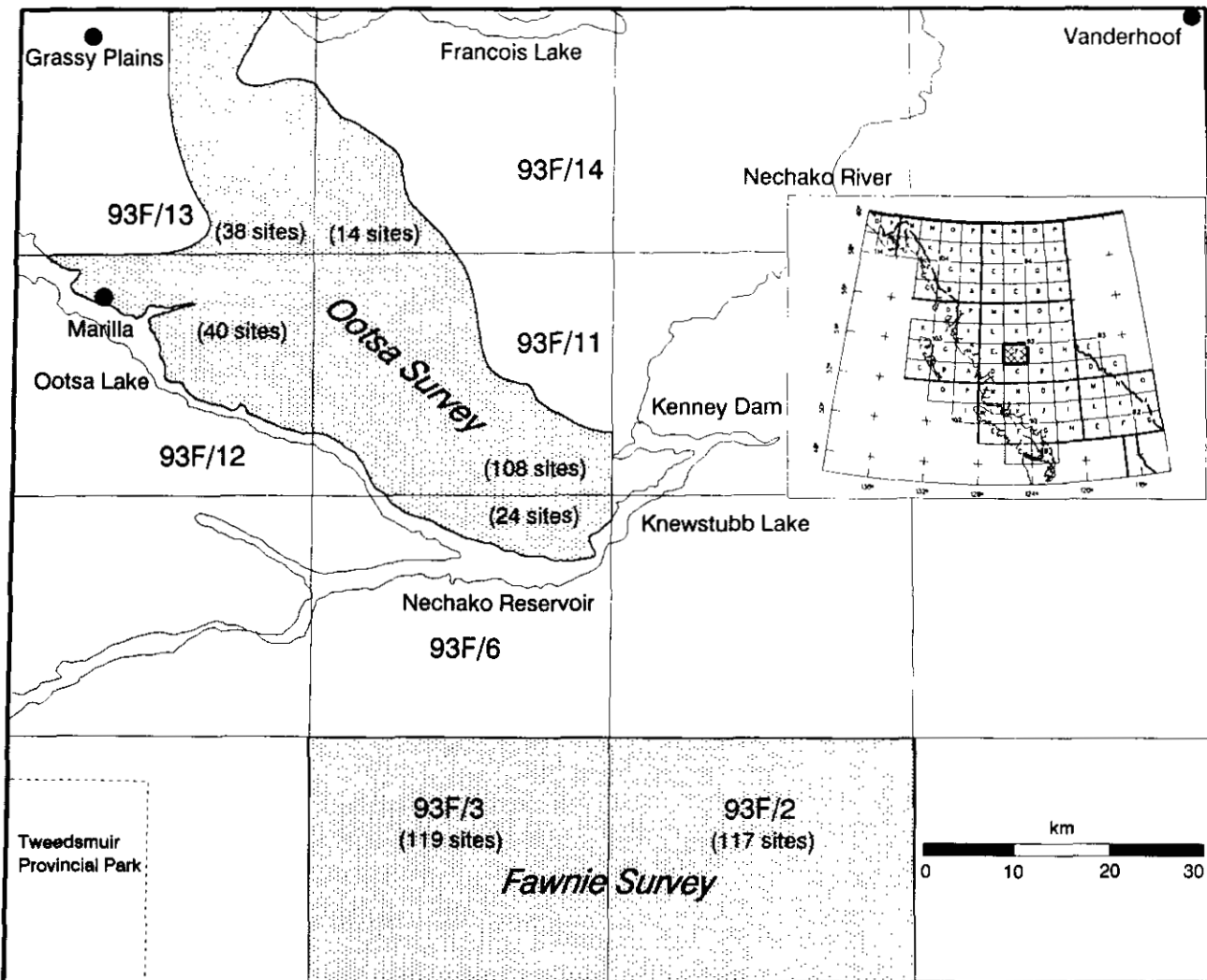


Figure 1. Locations of 1993 Interior Plateau lake sediment surveys in NTS map area 93F (Nechako River), showing the number of sites in each 1:50,000 NTS map area.

quartz-carbonate veins, silicified stockworks and hydrothermal breccia zones. Anomalous silver, zinc, arsenic and molybdenum concentrations in sediment of a nearby lake led to the discovery of the prospect (Dawson, 1988). The Blackwater-Davidson prospect is a structurally controlled transitional gold-silver-zinc-lead-copper occurrence (Schroeter and Lane, 1994, this volume). There is little information available on the metallogeny of the Ootsa survey area, and there are no precious metal occurrences within this area currently recorded in MINFILE. However, exploration for epithermal deposits is in progress in the region (Cogema Ltd.).

## PHYSIOGRAPHY AND SURFICIAL GEOLOGY

The surficial geology and glacial history of the Fawnie area have been documented by Giles and Levson (1994, this volume). Much of the region is drift covered although some areas, particularly the Naglico Hills in 93F/3, have considerable outcrop. Most of the survey area lies within the Nechako Plateau, although a small area southeast of Tsacha Lake and the Blackwater River falls within the Fraser Plateau (Holland, 1976). Topography is dominated by the subparallel ridges of the Fawnie and Nechako ranges, with Mount Davidson (elev: 1852 m) and Kuyakuz Mountain (elev: 1781 m) forming maximum elevations, respectively. The Entiako Spur and Naglico Hills are also prominent topographic highs. A wide variety of physiographic regimes, ranging from rocky subalpine peaks to boggy lowlands along the Blackwater River and Fawnie Creek, occur throughout the area. Active first-order streams are relatively uncommon. Lakes are not uniformly distributed; they are numerous in parts of the Naglico Hills, but absent in large expanses of the Fawnie Range and Entiako Spur. The area within the Fraser Plateau is predominately flat lying and characterized by abundant bogs but few lakes.

The Ootsa survey area lies wholly within the Nechako Plateau and, like the Fawnie area, has extensive drift cover. It is less mountainous than the Fawnie area, with most of the plateau surface at an elevation of 900 to 1100 metres. The Devils Thumb (elev: 1287 m) forms a prominent topographic high. The Ootsa area has a more rugged and hummocky topography; lakes are more evenly distributed across the landscape, and there are fewer small ponds and lowlands.

## SURVEY METHODOLOGY

### SAMPLE COLLECTION

Helicopter-supported sample collection in the Fawnie survey area was carried out during the period June 15-18, 1993, while collection in the Ootsa area was carried out in the period September 17-19. A sediment sample and a water sample were systematically collected

TABLE 1. SUMMARY OF 1993 INTERIOR PLATEAU LAKE SEDIMENT SURVEYS. SAMPLING DENSITY IS IN SITES PER SQUARE KILOMETRE.

Survey	NTS	Area (square km)	Sampling Density sites	Samples	
Fawnie	93F/2,3	1880	8	236	251
Ootsa	93F/6,11,12,13,14 (parts thereof)	1650	7.4	224	238
Totals		3530	7.7	460	489

at each site. A total of 251 sediment and water samples were collected from 236 sites in the Fawnie area, and 238 sediment and water samples were collected from 224 sites in the Ootsa area (Table 1). Average site density was approximately 1 per 8.0 square kilometres in the Fawnie area *versus* 7.4 square kilometres in the Ootsa area. Helicopter sampling rates averaged 10.5 sites per hour in the Fawnie survey and 12 sites per hour in the Ootsa survey.

## SEDIMENTS

Sediments were sampled from a float-equipped Bell 206 helicopter using a Hornbrook-type pedo sampler, and placed in Kraft paper bags. Standard National Geochemical Reconnaissance (NGR) sampling procedures, as discussed by Friske (1991) were used. On the basis of results of 1992 orientation studies in the region (Cook, 1993a,b), the surveys incorporate some departures from standard lake sediment sampling strategies used elsewhere in Canada for the NGR program, particularly pertaining to overall site density and the number of sites sampled per lake.

First, every lake and pond in the survey area was sampled, rather than sampling only a selection of lakes at a fixed density (*ie.* 1 site per 13 km<sup>2</sup>). Sediment at even small ponds may contain anomalous metal concentrations revealing the presence of nearby mineralization such as that at the Wolf prospect (Cook, 1994). In practice, some small ponds were not sampled due to unfavourable landing conditions. Samples were also not collected from the centres of very large and deep lakes (*ie.* > 10 km<sup>2</sup>, or more than 40 m deep) such as Tsacha, Uncha, Binta and Lucas lakes, nor from reservoir areas such as Ootsa or Cheslatta lakes which have been altered by the creation of the Nechako Reservoir. Organic soils from swamps and bogs were also avoided.

Secondly, centre-lake sediment samples were collected as per standard NGR procedure, but sediment from the centres of all major known or inferred sub-basins was also collected to investigate the considerable

trace element variations which may exist among sub-basins of the same lake. The extent of these variations is illustrated by the molybdenum distribution in sediments of Tatin Lake (Figure 2), a large (4.5 km long) lake situated about 6 kilometres north of Endako, adjacent to the Ken porphyry molybdenum-copper occurrence (MINFILE 093K 002). This lake was sampled during 1992 orientation studies (Cook, 1993a). Molybdenum concentrations in centre-basin sediments vary from 7 ppm in the centre of the lake, to 12 ppm and 23 ppm in the western and eastern sub-basins, respectively. These variations may be controlled at least partly by limnological differences among the sub-basins. Consequently, up to five sites were sampled from some of the larger lakes in the Fawnie and Ootsa surveys. Lake bathymetry maps in unpublished reports of the Fisheries Branch, Ministry of Environment, Lands and Parks, were consulted prior to sampling several of the larger lakes such as Kuyakuz, Moose and Johnny lakes to aid in site location and to avoid wasting helicopter time over extremely deep basins.

## WATERS

Water samples were collected in 250-millilitre polyethylene bottles using a custom-designed sampling apparatus. Waters were sampled from approximately 15 centimetres below the lake surface to avoid collection of surface scum, and precautions were taken to minimize suspended solids. The purpose of the water sampling differed between the two survey areas. Waters from the Ootsa area were collected for standard RGS analysis (pH, U, F, SO<sub>4</sub>), but those from the Fawnie area were

collected as a pilot study of regional trace element concentrations in lake waters. Consequently, all Fawnie survey water bottles were rinsed three times with distilled water at the Analytical Sciences Laboratory, Victoria, prior to use, and transported to the field in sealed plastic bags to ensure a high level of cleanliness. Analytical tests conducted on acidified and unacidified distilled water blanks, prior to field work, showed no measurable contamination of the waters by the containing bottles.

## FIELD OBSERVATIONS

A variety of field observations were recorded at each site using Geological Survey of Canada lake sediment cards (Garrett, 1974). These included observations pertaining to the sample itself, including depth, colour, composition and odour, as well as those regarding the lake and immediate area, including lake size, general topography and potential sources of contamination. The absence or presence of suspended solids in water samples was also noted. Lake names used on either NTS topographic maps or the Vanderhoof Forest District map were included where applicable.

## SAMPLE PREPARATION AND ANALYSIS

### SEDIMENTS

Sediment samples were initially field dried and, when sufficiently dry to transport, shipped to Bondar-Clegg and Company, North Vancouver (Fawnie survey),

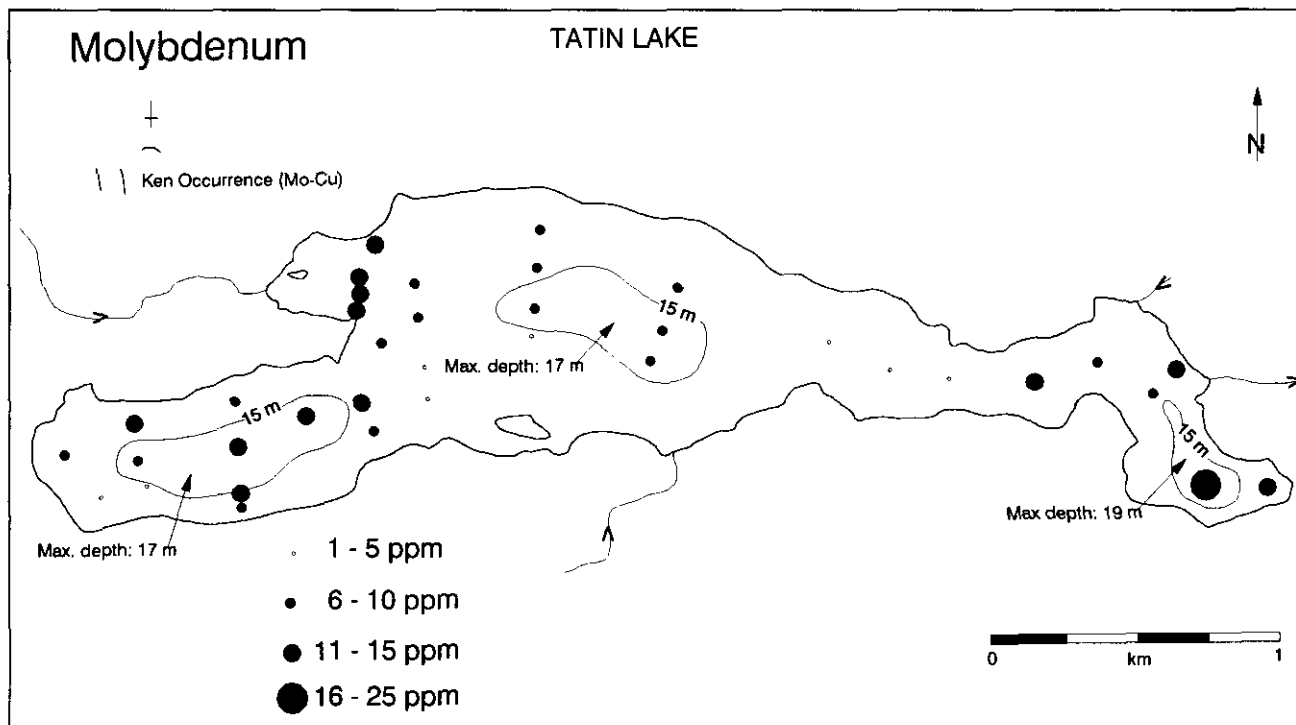


Figure 2. Molybdenum (ppm) distribution in sediments of Tatin Lake (93K/03), north of the village of Endako, showing variations in metal content between various sub-basins (15 metre contour). Bathymetry modified after Walsh (1977).

and Rossbacher Laboratory Ltd., Burnaby (Ootsa survey) for final drying at 40°C. The sample preparation procedure will comprise two steps. First, the sample will be disaggregated inside a plastic bag with a rubber mallet. The entire sample, to a maximum of 250 grams, will then be pulverized to approximately -150 mesh (~100 microns) in a ceramic ring mill, and two analytical splits (10 g and 30 g) taken from the pulverized material.

One split of each prepared sediment sample will be submitted to a commercial laboratory and analyzed for zinc, copper, lead, silver, molybdenum, cobalt, arsenic, antimony, mercury, iron, manganese, nickel, bismuth, cadmium, fluorine and vanadium using atomic absorption spectroscopy (AAS). Loss on ignition will also be determined. A second 30 gram split will be analyzed for gold, arsenic, antimony and 30 additional elements using instrumental neutron activation analysis (INAA) at a second commercial laboratory. Details of digestion and analytical procedures for individual elements will be given in the Open File data releases.

## WATERS

Water samples from the Fawnie area were kept cool in a refrigerator and filtered to 0.45 microns at the Analytical Sciences Laboratory, Victoria. Samples will be analyzed at a commercial laboratory for a range of elements, including copper, zinc, molybdenum and arsenic, as well as for pH and SO<sub>4</sub>. No special preparation procedures were applied to Ootsa area waters, which will be analyzed for the standard RGS water suite (pH, U, F, SO<sub>4</sub>) at a second commercial laboratory.

Acidity was also determined on all samples in the Analytical Sciences Laboratory using a Corning model Checkmate 90 pH meter. A pH frequency distribution for the Ootsa area is shown in Figure 3. Lake waters are predominately of near-neutral pH, with a median value of

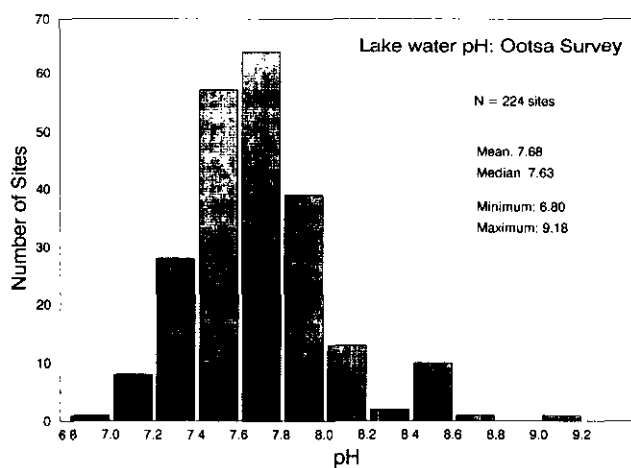


Figure 3. Frequency distribution of pH values in Ootsa survey lake waters.

7.63 (Range: 6.80 to 9.18). Nevertheless, slightly alkaline pH values of 8.00 or greater occur at 27 sites, with pH values of 8.40 or greater at 12 of these. The highest pH (9.18) occurs in a small lake east of Yellow Moose Lake (93F/6) in the southernmost part of the survey area, while the largest grouping of slightly alkaline lake waters is near Marilla in the western part of the area (Figure 1).

## QUALITY CONTROL PROCEDURES

Each block of twenty sediment samples contains seventeen routine samples, one field duplicate sample, one blind duplicate sample and one control standard in accordance with standard Regional Geochemical Survey (RGS) quality control procedures. Field duplicate sites are chosen randomly during fieldwork. Blind, or analytical, duplicate samples are taken from the field duplicate in each block following sample preparation, and reinserted into the suite to monitor analytical precision. Blind duplicates are not used in the water suite; a distilled water blank is inserted to monitor analytical contamination.

## SUMMARY

Two lake sediment surveys (460 sites) were conducted in map area 93F in the northern Interior, with Open File data release scheduled for 1994. Additional surveys of adjoining areas are planned for next year, with the eventual objective of completing Regional Geochemical Survey coverage of NTS map areas 93C (Anahim Lake), 93F (Nechako River) and 93K (Fort Fraser). Regional geochemical surveys are only one component of ongoing applied geochemical research in the northern Interior. The development of new or improved geochemical exploration methods applicable to the region is also an important objective of the Interior Plateau project. Consequently, it is anticipated that previous lake sediment orientation studies (Cook, 1993a; 1994) will be complemented in 1994 by formulation of follow-up guidelines for lake sediment anomalies, and by additional research into the relative effectiveness of other geochemical sampling media in the region.

## ACKNOWLEDGMENTS

The authors thank R.E. Lett of the Analytical Sciences Laboratory for his helpful assistance, and P.F. Matysek for his support of the project and comments on the manuscript. Special thanks are extended to M. King of White Saddle Air Services, Takla Lake, and J. Meier, Northern Mountain Helicopters, Vanderhoof, for their skillful flying. P.W. Friske of the Geological Survey of Canada, Ottawa, loaned sampling gear. B. Bhagwanani, Analytical Sciences Laboratory, filtered the lake water samples and did the pH determinations.

## REFERENCES

- Andrew, K.P.E. (1988): Geology and Genesis of the Wolf Precious Metal Epithermal Prospect and the Capoose Base and Precious Metal Porphyry-style Prospect, Capoose Lake Area, Central British Columbia; unpublished M.Sc. thesis, *The University of British Columbia*, 334 pages.
- Cook, S.J. (1993a): Preliminary Report on Lake Sediment Studies in the Northern Interior Plateau, Central British Columbia (93C, E, F, K, L); in Geological Fieldwork 1992, Grant, B. and Newell, J.M., Editors, *B.C. Ministry of Energy, Mines and Petroleum Resources*, Paper 1993-1, pages 475-481.
- Cook, S.J. (1993b): Controls on Lake Sediment Geochemistry in the Northern Interior Plateau, British Columbia: Applications to Mineral Exploration; *Canadian Quaternary Association*, Biennial Meeting, Program with Abstracts and Field Guide, page A10.
- Cook, S.J. (1994): Gold Distribution in Lake Sediments near Epithermal Gold Occurrences in the Northern Interior Plateau, British Columbia; in Proceedings of the Drift Prospecting Workshop, *B.C. Ministry of Energy, Mines and Petroleum Resources*, Special Volume.
- Dawson, J.M. (1988): Geological and Geochemical Report on the Wolf Property, Omenica Mining Division, British Columbia; *B.C. Ministry of Energy, Mines and Petroleum Resources*, Assessment Report 16995.
- Diakow, L.J. and Webster, I.C.L. (1994): Geology of the Fawnie Creek Map Area (93F/3); in Geological Fieldwork 1993, Grant, B. and Newell, J.M., Editors, *B.C. Ministry of Energy, Mines and Petroleum Resources*, Paper 1994-1, this volume.
- Earle, S. (1993): Assessment of the Applicability of Lake Sediment Geochemical Surveys for Mineral Exploration in the Nechako Plateau Area of British Columbia; in Exploration in British Columbia 1992, *B.C. Ministry of Energy, Mines and Petroleum Resources*, pages 69-106.
- Friske, P.W.B. (1991): The Application of Lake Sediment Geochemistry in Mineral Exploration; in Exploration Geochemistry Workshop, *Geological Survey of Canada*, Open File 2390, pages 4.1-4.20.
- Garrett, R.G. (1974): Field Data Acquisition Methods for Applied Geochemical Surveys at the Geological Survey of Canada; *Geological Survey of Canada*, Paper 74-52.
- Giles, T.R. and Levson, V.M. (1994): Surficial Geology and Drift Exploration Studies in the Fawnie Creek Area (93F/3); in Geological Fieldwork 1993, Grant, B. and Newell, J.M., Editors, *B.C. Ministry of Energy, Mines and Petroleum Resources*, Paper 1994-1, this volume.
- Gintautas, P.A. (1984): Lake Sediment Geochemistry, Northern Interior Plateau, British Columbia; unpublished M.Sc. thesis, *University of Calgary*, 175 pages.
- Hoffman, S.J. (1976): Mineral Exploration of the Nechako Plateau, Central British Columbia, Using Lake Sediment Geochemistry; unpublished Ph.D. thesis, *The University of British Columbia*, 346 pages.
- Hoffman, S.J. and Fletcher, W.K. (1981): Detailed Lake Sediment Geochemistry of Anomalous Lakes on the Nechako Plateau, Central British Columbia - Comparison of Trace Metal Distributions in Capoose and Fish Lakes; *Journal of Geochemical Exploration*, Volume 14, pages 221-244.
- Holland, S.S. (1976): Landforms of British Columbia - A Physiographic Outline; *B.C. Ministry of Energy, Mines and Petroleum Resources*, Bulletin 48.
- Johnson, W.M., Hornbrook, E.H.W. and Friske, P.W.B. (1987a): National Geochemical Reconnaissance 1:250 000 Map Series - Whitesail Lake, British Columbia (NTS 93E); *B.C. Ministry of Energy, Mines and Petroleum Resources*, RGS 16.
- Johnson, W.M., Hornbrook, E.H.W. and Friske, P.W.B. (1987b): National Geochemical Reconnaissance 1:250 000 Map Series - Smithers, British Columbia (NTS 93L); *B.C. Ministry of Energy, Mines and Petroleum Resources*, RGS 17.
- Matysek, P.F. and van der Heyden, P. (1994): 1993-94 Update-Interior Plateau Project; in Geological Fieldwork 1993, Grant, B. and Newell, J.M., Editors, *B.C. Ministry of Energy, Mines and Petroleum Resources*, Paper 1994-1, this volume.
- Mehrtens, M.B. (1975): Chutanli Mo Prospect, British Columbia; in Conceptual Models in Exploration Geochemistry, Bradshaw, P.M.D., Editor, *Association of Exploration Geochemists*, Special Publication No. 3, pages 63-65.
- Mehrtens, M.B., Tooms, J.S. and Troup, A.G. (1973): Some Aspects of Geochemical Dispersion from Base-metal Mineralization within Glaciated Terrain in Norway, North Wales and British Columbia, Canada; in *Geochemical Exploration 1972*, Jones, M.J., Editor, *The Institution of Mining and Metallurgy*, pages 105-115.
- Schroeter, T.G. and Lane, R.A. (1994): Mineral Resources: Interior Plateau Project (93F/3 and parts of 93F/2,6, and 7); in Geological Fieldwork 1993, Grant, B. and Newell, J.M., Editors, *B.C. Ministry of Energy, Mines and Petroleum Resources*, Paper 1994-1, this volume.
- Spilisbury, W. and Fletcher, W.K. (1974): Application of Regression Analysis to Interpretation of Geochemical Data from Lake Sediments in Central British Columbia; *Canadian Journal of Earth Sciences*, Volume 11, pages 345-348.
- Tipper, H.W. (1963): Nechako River Map-area, British Columbia; *Geological Survey of Canada*, Memoir 324.
- Walsh, M.G. (1977): Tatin Lake; *B.C. Ministry of Environment, Lands and Parks*, unpublished Fisheries Branch internal report.

## MINERAL RESOURCES: INTERIOR PLATEAU PROJECT (93F/3 and parts of 93F/2, 6 & 7)

By T.G. Schroeter and R.A. Lane

**KEYWORDS:** Economic geology, Interior Plateau, Hazelton Group, Ootsa Lake Group, epithermal, transitional, stratabound, porphyry Mo-Cu, skarn, landsat imagery.

### INTRODUCTION

The Interior Plateau physiographic region of central British Columbia extends in a northwesterly trending direction for over 400 kilometres. The area covers 93F/3 and parts of 93F/2, 93F/6 and 93F/7, approximately 110 kilometres southwest of Vanderhoof. Access is by Forest Service roads from Vanderhoof, where the Kluskus road, together with the Van-Tine spur road and mining roads, provide access to the Wolf, Paw, Fawn, Capoose, Buck and Blackwater-Davidson properties (Figure 1).

The northwestern region of the plateau is the focus for this assessment of economic potential for base and precious metal deposits in Lower to Middle Jurassic (Hazelton Group) and Tertiary (Ootsa Lake Group) volcanic and volcanoclastic rocks and associated intrusive rocks (e.g., Cretaceous Capoose batholith).

In general, the region has similarities to the Basin and Range structural province in Nevada (extensional block faulting). Furthermore, the Babine area, to the northwest, which is separated from the Interior Plateau by the Skeena Arch, has a similar structural style.

To date the mineral deposits component of the Interior Plateau project has concentrated on the evaluation, description and classification of a variety of deposit types in the study area. Particular attention was paid to host-rock lithologies, controls to mineralization, metallic and gangue mineralogy, timing of events and the relationship of mineralization to structure and plutonism. In the past, mineral exploration in the area has been hampered by: abundance of glacial drift cover, extensive cover of Neogene lava flows, relatively poor access, an obsolete geological database, and the lack of modern geophysical or geochemical survey data. Most of the area remains un-staked.

Epithermal, transitional, skarn, porphyry and stratabound (?) styles of mineralization have been identified and are described in this paper.

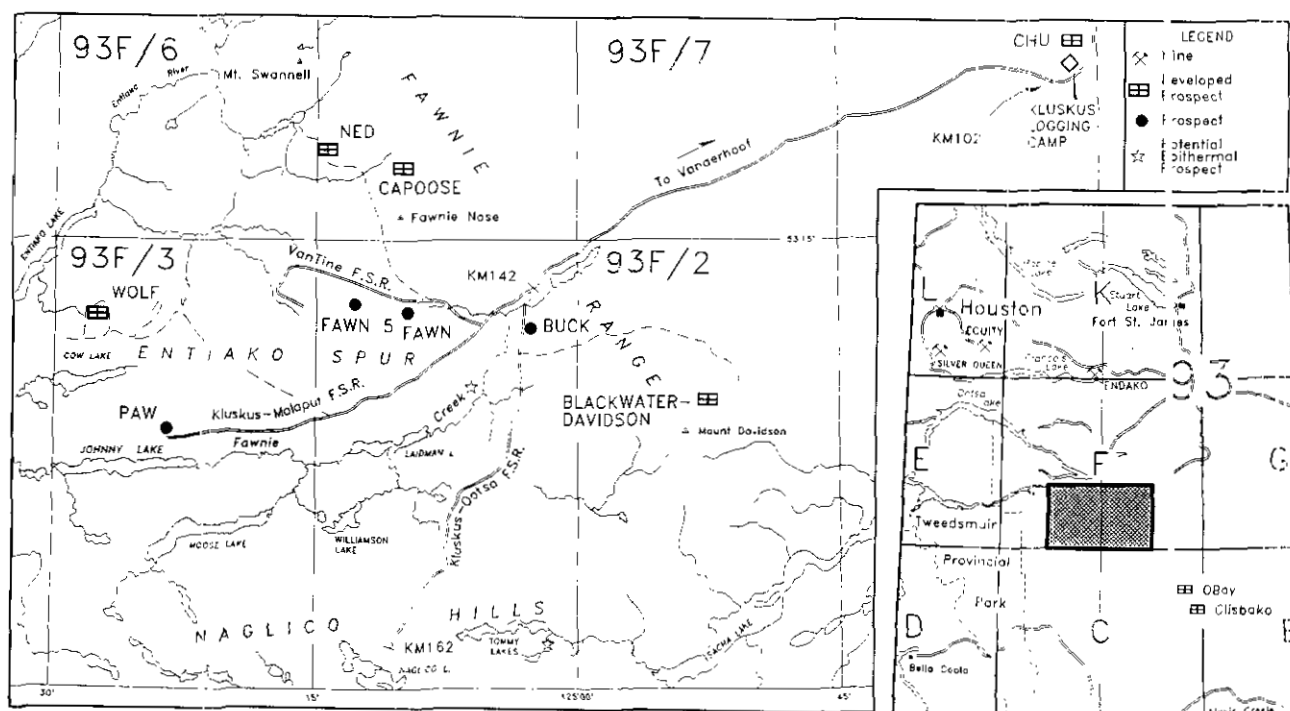


Figure 1. Location map of the Interior Plateau study area, showing the locations of metallic mineral prospects and showings. Prospects (boxes) and showings (dots) discussed in the text are located. Two new epithermal alteration zones (stars) were discovered during regional mapping (Diakow and Webster, 1994, this volume). Two operating mines, Equity Silver and Endako, as well as two epithermal prospects, Oboy and Clisbako, located outside the current field area, are shown for reference, Forest Service roads are shown as solid bold lines and four-wheel-drive roads are shown as dashed lines.

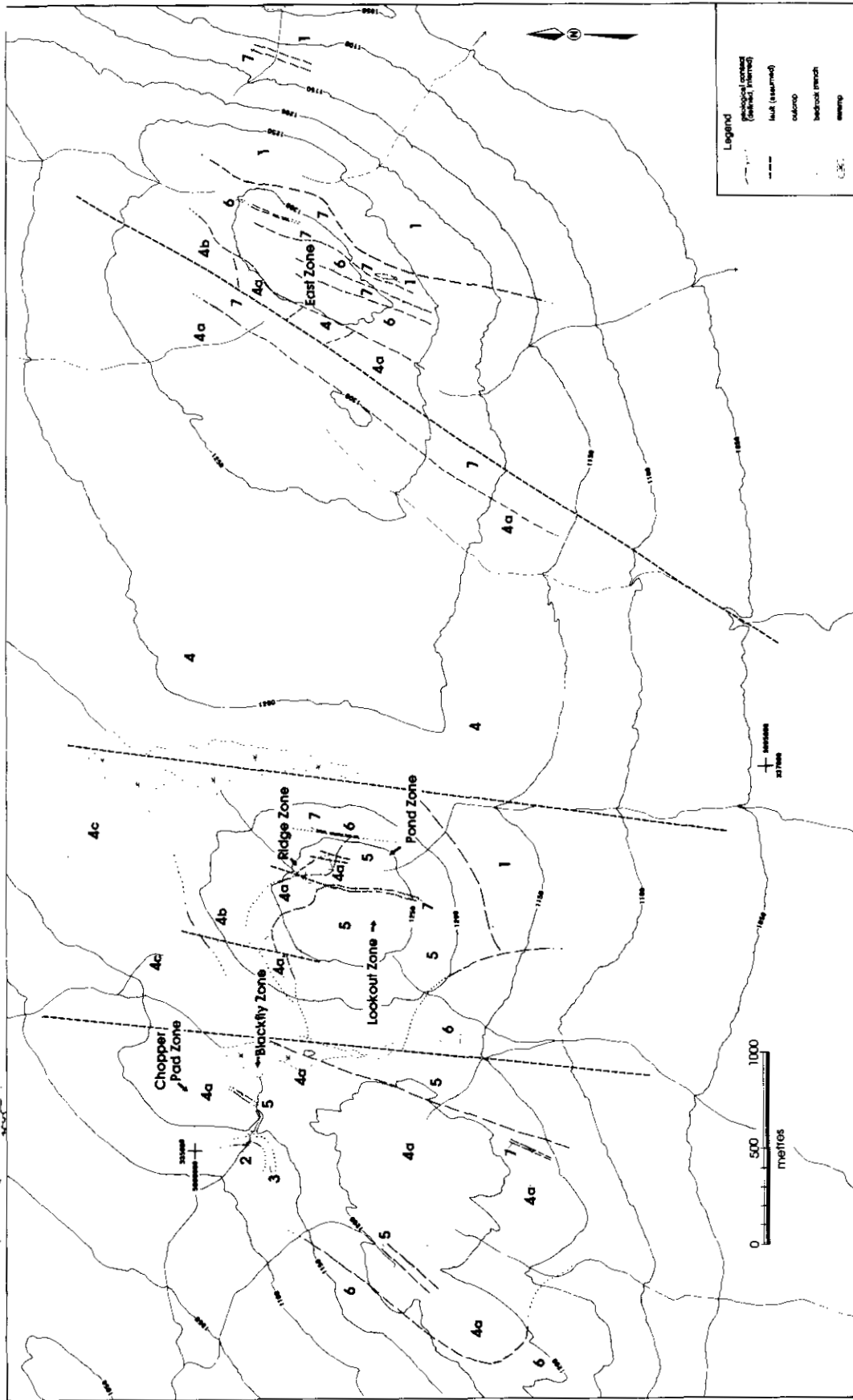


Figure 2. Simplified geological map of the central part of the Wolf epithermal gold-silver deposit and location of anomalous zones. Legend: **Jurassic Hazelton Group**, 1 = pyroxene-phyric andesite flows and minor argillaceous interbedded mudstones, siltstones and sandstones. **Tertiary Ootsa Lake Group**, 2 = basal(?) polymictic conglomerate; 3 = intermediate lapilli tuff; 4 = rhyolite package (4a = proximal rhyolite flows, tuffs and breccias; 4b = tuffaceous siltstones and mudstones, 4c = distal ignimbrites, densely welded to non-welded); 5 = maroon quartz feldspar porphyry; 6 = grey feldspar porphyry; 7 = quartz eye porphyry.

## EPITHERMAL DEPOSITS

Two epithermal precious metal prospects (Wolf and Fawn), hosted by Tertiary rhyolitic volcanic and related hypabyssal rocks and by Lower to Middle Jurassic Hazelton Group intermediate to acidic volcanic and volcanoclastic rocks respectively, are described in this paper. Two new epithermal prospects were discovered during the course of regional mapping at a scale of 1:50 000 (Diakow and Webster, 1994, this volume).

There is potential for both high-grade bonanza (*e.g.*, Blackdome; Republic, Washington; Sleeper, Nevada) and bulk-mineable (*e.g.*, Round Mountain, Nevada) deposits.

### WOLF [MINFILE 093F 045]

The Wolf prospect is a low-sulphidation, adularia-sericitic epithermal gold-silver deposit hosted by Upper Cretaceous to Oligocene Ootsa Lake Group sedimentary, rhyolitic volcanic and genetically related hypabyssal rocks. The property is approximately 130 kilometres southwest of Vanderhoof and consists of 198 mineral claim units in a 13 claim blocks between Cow Lake to the south and Entiako Lake to the northwest (Figure 1). The claims were originally staked in 1983 to cover prominent knobs of hydrothermally altered felsic volcanic rocks that crop out east of a silver-zinc-arsenic-molybdenum lake-sediment anomaly. The property is currently being explored by Metall Mining Corporation under option from Lucero Resource Corporation.

Remnants of a possible flow-dome complex form three areas of prominent relief extending from west to east across the property (Figure 2). These three resistant features are separated by northerly trending extensional faults that down-drop fault blocks toward the west. The Ootsa Lake Group at Wolf consists of the following sequence of rocks. A basal(?) polymictic boulder conglomerate rests unconformably on a basement of Jurassic Hazelton Group epiclastic sedimentary rocks and pyroxene-phyric andesite flows. Pale green vitric and lapilli tuffs, tuff breccias and tuffaceous siltstones conformably overlie the conglomerate. Tuffaceous rocks are in turn conformably overlain by rhyolite flows and autoclastic breccias (proximal), ignimbrites (distal) and rhyolitic tuffs. These are intruded by quartz-eye rhyolite that may, in part, be equivalent to the extrusive rocks. Grey feldspar porphyry and maroon quartz feldspar porphyry sills and dikes (also possible feeders to eroded Ootsa Lake rhyolites) intrude the volcanic pile. Late quartz-eye porphyry dikes cut all other rock types.

A Middle Eocene age of between  $47.6 \pm 1.7$  and  $49.9 \pm 1.7$  Ma has been established for rhyolite flows and felsic intrusives using K-Ar dating methods (Andrew, 1988). Wolf volcanic rocks are subalkaline with a high-potassium calcalkaline affinity and are dominantly hypersthene-cordierite normative (Andrew, 1988). The rhyolite package may represent a felsic volcanic centre in, or along, the margin of a resurgent caldera complex.

Mineralization and alteration are structurally controlled. Mineralization occurs in northerly trending quartz (carbonate) veins (Lookout and Pond zones), siliceous stockworks (Blackfly, Chopper Pad and East zones) and hydrothermal breccia zones (Ridge zone), and as a strat-abundant unit of pervasively silicified and brecciated rhyolite and tuffaceous sediments (Ridge zone) capped by a maroon quartz feldspar porphyry sill (Plate 1). Chalcedonic colloform banding (Plate 2), comb structures and drusy cavities are typical; bladed quartz textures, silica replacement of original calcite or barite (Plate 3), indicate that boiling occurred during the evolution of a high-level, epithermal system.

Sulphide mineralization is only weakly developed; very fine grained disseminated pyrite never exceeds 0.5% of the rock by volume. Traces of fine-grained chalcopyrite are rare. Other metallic minerals include micron-sized electrum, native silver, aguilarite ( $Ag_4SeS$ ), naumannite ( $Ag_2Se$ ), acanthite ( $Ag_2S$ ), digenite ( $Cu_5S_5$ ) and galena (Andrew, 1988). Soil and rock geochemistry show there is generally a lack of arsenic, antimony and mercury in the mineralized system. However, anomalous arsenic and mercury values occur at the Blackfly zone.

The highest grades of mineralization appear to occur in zones that have undergone repeated episodes of brecciation and silicification. Better gold grades are associated with grey to brown, banded chalcedonic silica and very fine grained disseminated pyrite (Plate 4). The most encouraging results to date have been at the Ridge zone where trenching across the zone yielded 8.49 grams per tonne gold and 42.21 grams per tonne silver over 7.5 metres (Cann, 1984). Another trench across the zone returned assays of 2.69 grams per tonne gold and 14 grams per tonne silver over 26.5 metres (D.R. Heberlein, personal communication, 1993). Diamond drilling by Minnova in 1992, before it was taken over by Metall Mining, outlined a zone of continuous mineralization with a minimum strike length of 300 metres, down-dip extension of at least 270 metres and true thickness of at least 7 metres. The best drill intersection (ddh WF-92-10) through the zone assayed 2.32 grams per tonne gold over 9.1 metres (D.R. Heberlein, personal communication, 1993).

Alteration on the property is characterized by moderate to intense silica replacement of permeable horizons in tuffaceous rhyolitic rocks. At the contact between rhyolite and the maroon quartz feldspar porphyry sill both rock types have been wholly replaced by white sugary quartz. The sill may have acted as an impermeable cap to ascending silica-rich hydrothermal fluids. Below this zone of intense silicification is a well developed multi-stage hydrothermal breccia that is weakly to moderately silicified (Plate 5). Some of the breccia clasts have been replaced by clay minerals. Areas of silicification are generally flanked by zones of argillic alteration that are particularly well-developed in porphyritic intrusions adjacent to faults where megacrystic plagioclase phenocrysts are replaced by clay. Clay mineralogy consists dominantly of kaolinite and lesser illite and montmorillonite (Andrew, 1988). Adularia has been identified, but it is not common (D.R. Heberlein, personal communication).

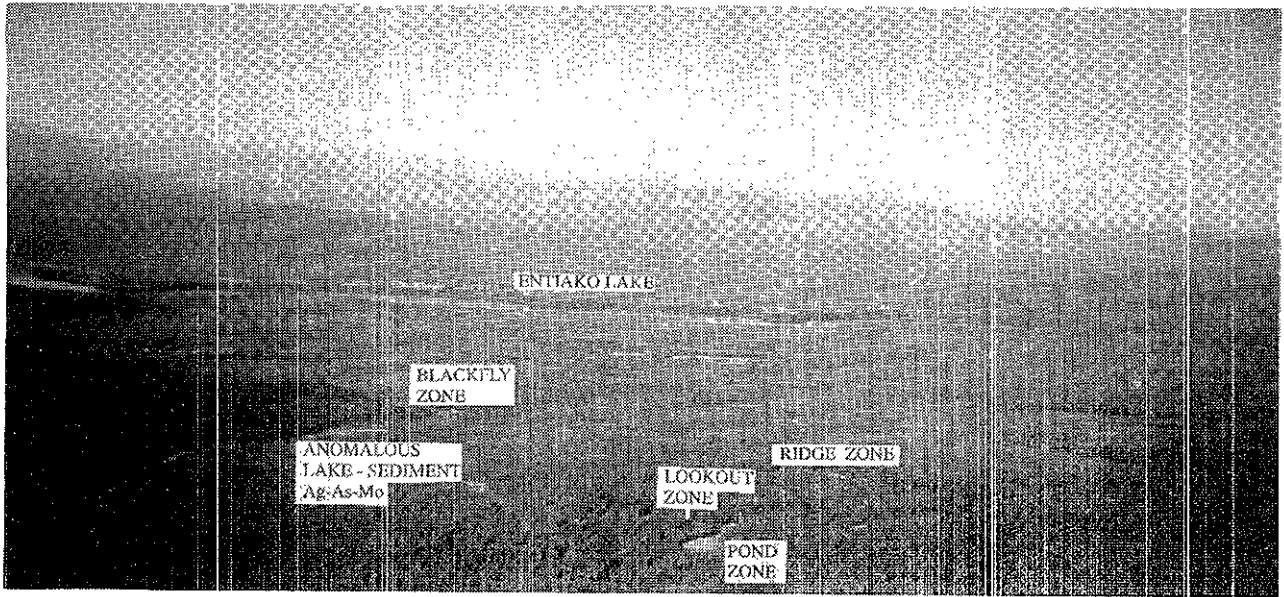


Plate 1. Looking north over the Wolf property. (Photo by K. Pride.)

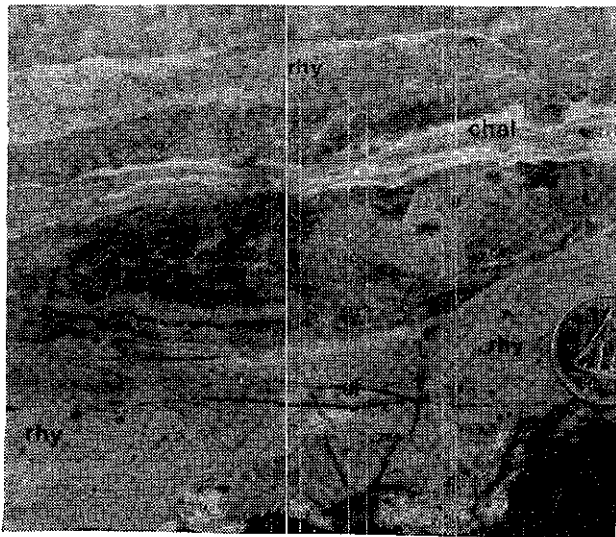


Plate 2. Banded chalcidonic quartz vein silicified quartz-phyric rhyolite, Ridge zone, Wolf property.

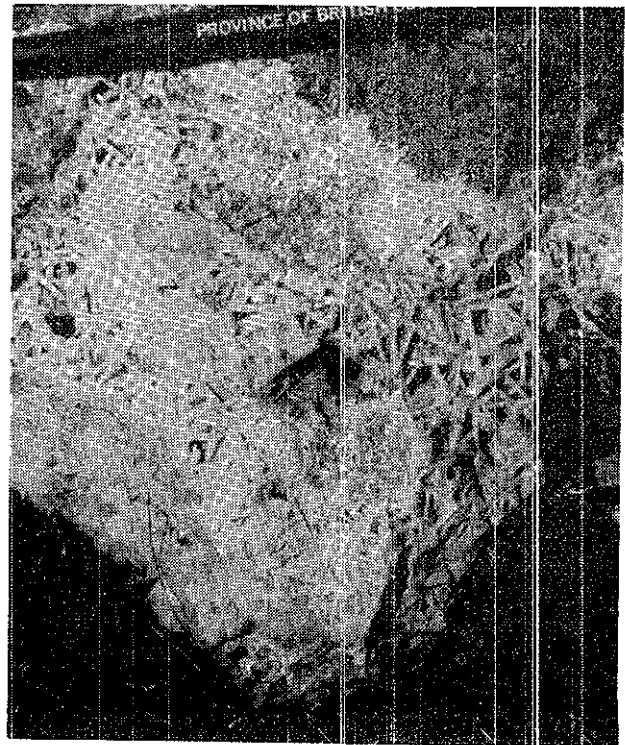


Plate 3. Bladed silica (after barite or calcite, indicative that boiling has occurred) in quartz-phyric rhyolite, Ridge zone, Wolf property.

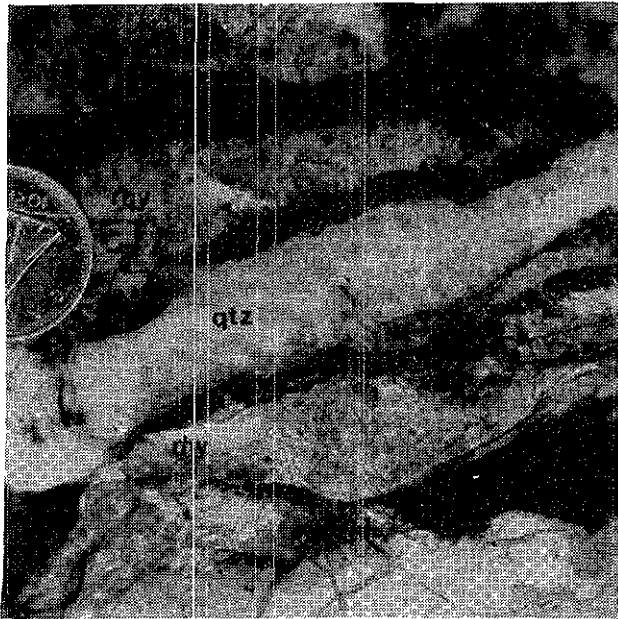


Plate 4. Banded quartz vein with dark grey (sulphide/sulphosalt/electrum?) borders in brecciated quartz-phyric rhyolite, Ridge zone, Wolf property.



Plate 5. Banded chalcedonic quartz veinlets in mineralized breccia, Ridge zone, Wolf property.

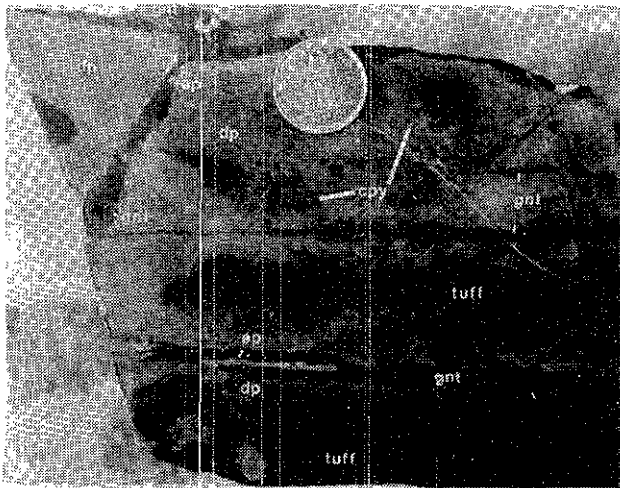


Plate 6. Diopside-garnet-epidote exoskarn with fragments of Hazelton Group crystal tuff, Fawn property.

1993). Clays, sericite, chlorite and minor secondary potassium feldspar occur as narrow alteration envelopes along the walls of sharply defined quartz (carbonate) veins. Manganese oxide commonly lines fractures; iron oxide staining and Liesegang rings occur locally.

The potential for future discoveries and continuing exploration success at the Wolf prospect is considered to be excellent.

#### **FAWN (GRAN) [MINFILE 093F 043]**

The Fawn prospect is located on the eastern end of Entiako Spur. The property, owned by Western Keltic Resources Inc., consists of 100 mineral claim units centred approximately 6 kilometres north of the east end of Laidman Lake and 4.5 kilometres west of Fawnie Creek (Figure 1). Access is provided by the Kluskus-Malaput and Van-Tine Forest Service roads.

The Fawn claim group is underlain by felsic to intermediate volcanic and sedimentary rocks of the Lower to Middle Jurassic Hazelton Group and by dioritic to granodioritic intrusive rocks (Figure 3). The volcanic suite consists of a lower felsic package consisting mainly of heterolithic rhyolite tuff breccia and an upper mainly andesitic package consisting of lapilli tuff, tuff breccia and pyroxene-phyric flows. Local lenses of thinly bedded, interbedded mudstone, limy siltstone and (lapilli) tuffs occur within the andesitic package. Tuffaceous siltstones are exposed at the transition between felsic and andesitic volcanics. Strata are broadly folded around north and northeast-trending axes (Smith and Hoffman, 1984) and have gentle to moderate dips.

Rocks throughout the property are weakly to moderately metasomatized. Epidote, chlorite, calcite and garnet occur along fracture planes, as medium to coarse-grained aggregates, and locally, as altered rims of breccia clasts (Plate 6).

Intrusive rocks of two different ages have been identified. The first, a fine to medium-grained equigranular, locally intensely fractured and pyritic granodiorite to di-

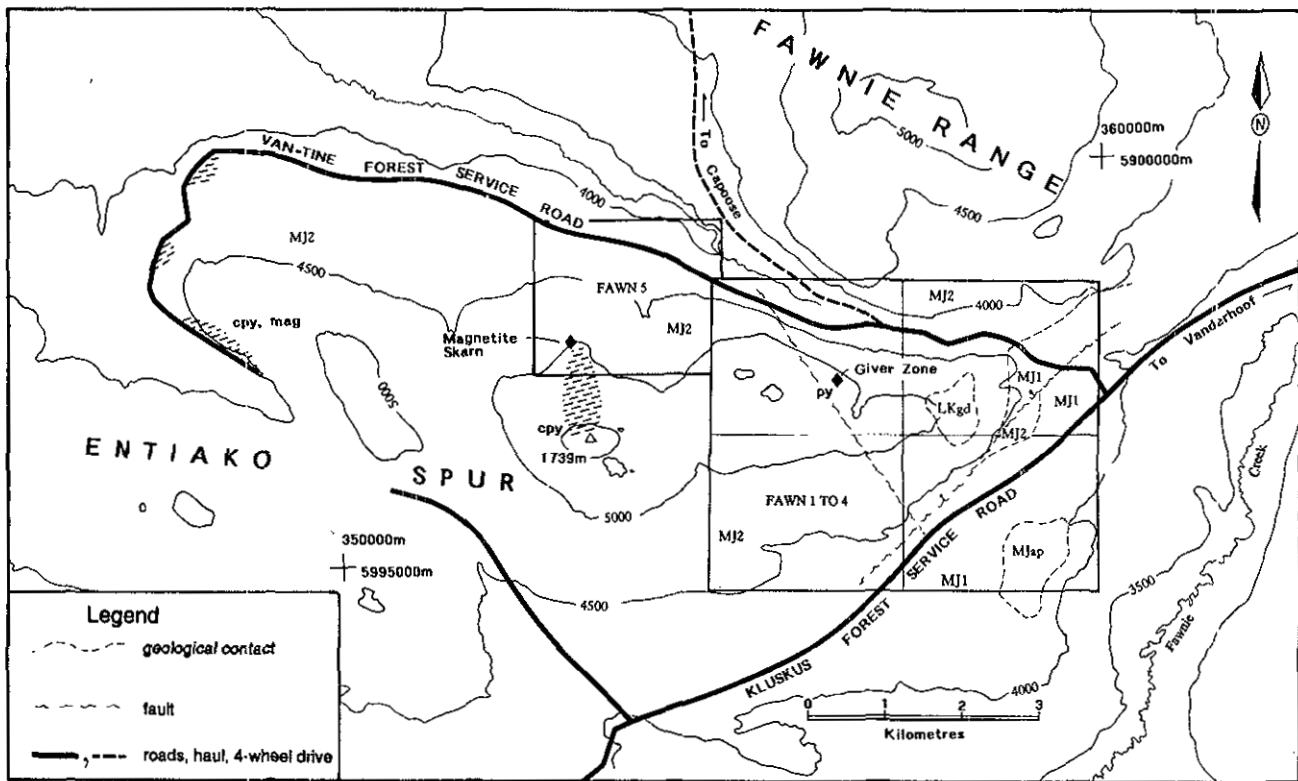


Figure 3. Simplified geological map of the Fawn claims. Legend: **Jurassic Hazelton group**; MJ1, (lower) felsic tuffs, flows and breccias; MJ2 (upper) intermediate to mafic tuffs, flows and pyroclastic rocks with minor sedimentary lenses; MJap, augite porphyry. **Cretaceous Quanchus intrusions**, LKgd, granodiorite. Hatched pattern signifies outcrop to suboutcrop of garnet-pyroxene-epidote magnetite (mag) chalcocopyrite (cpy) skarn and biotite hornfels. Pyrite (py) in quartz veins occurs at the Giver zone (diamond) and massive magnetic skarn (diamond) on the Fawn 5 claim. Geology after Diakow and Webster (1994, this volume).

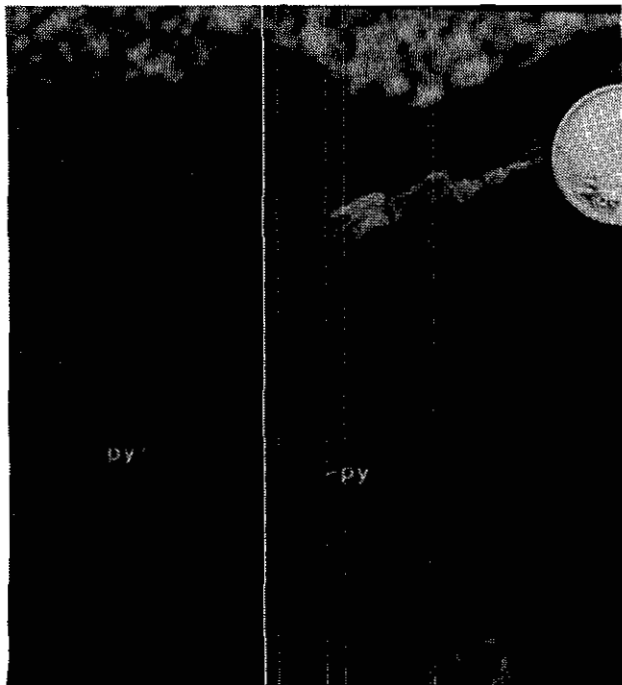


Plate 7. Banded silica with drusy cavities, Giver showing, Fawn property.

rite stock, cuts Hazelton Group volcanic rocks and may be part of the Quanchus Plutonic Suite or an apophysis (or cupola?) of the Capoose batholith (67.1±2.3 Ma) that underlies the relatively thin veneer of Hazelton Group rocks on the property. The second, a suite of porphyritic felsic dikes, cuts all other rock types including the diorite, and may be feeders to the Ootsa Lake (Awmack, 1991) rhyolitic volcanics that crop out elsewhere in the region.

Showings on the property are of two types: precious metal bearing epithermal veins and magnetite±chalcocopyrite, garnet-pyroxene-epidote exoskarn (skarn mineralization will be discussed in a later section).

Epithermal style mineralization and alteration have been exposed by limited trenching on the Giver zone in the northern part of the claim group (Plate 7). North to northeast-trending quartz-carbonate-pyrite±barite veinlets cut a northwesterly trending intensely silica, sericite and clay-altered zone. A continuous chip sample over an 8.2-metre width averaged 623 ppb gold and 7.1 ppm silver; grab samples from early 1980s BP Minerals test pits yielded values up to 12.9 grams per tonne gold and 25.0 grams per tonne silver (Awmack, 1991). The veins are also geochemically anomalous in arsenic, lead and zinc. Approximately 2100 metres east of the Giver zone, a quartz-sulphide vein is exposed along the contact between a felsic dike and diorite stock indicating that the

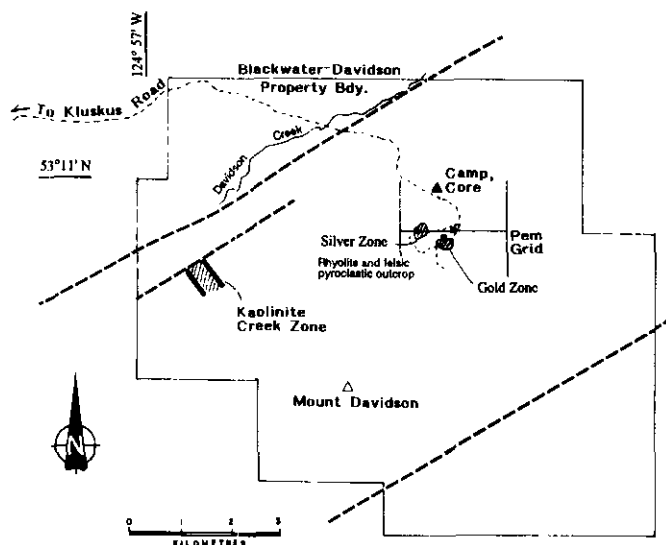


Figure 4. Sketch map of the Blackwater-Davidson property and surrounding area, showing the location of the Gold and Silver zones on the Pem grid and the Kaolinite Creek zone (after Allen, 1992).

mineralization is younger than either intrusive event (Awmack, 1991).

### TRANSITIONAL DEPOSITS

Structurally controlled, polymetallic base and precious metal bearing deposits formed at moderate depths where strongly saline, high-temperature hydrothermal fluids of magmatic origin were active (*i.e.*, transitional upwards from the porphyry copper environment to the epithermal environment). Two such deposits (Blackwater-Davidson and Capoose) exhibit several similar features, including: the occurrence of metasomatic (secondary) garnet in rhyolite, metallic (including sulphosalts) and gangue mineralogy, ore textures (*i.e.*, replacement "spherules"), and widespread phyllic and argillic alteration.

The Equity Silver mine is a classic example of a transitional deposit in British Columbia.

### **BLACKWATER-DAVIDSON (PEM)** **[MINFILE 093F 037]**

The Blackwater-Davidson property is located approximately 7 kilometres northeast of Mount Davidson, about 160 kilometres south of Vanderhoof (Figure 1). Access to the property is by a 17-kilometre four-wheel-drive road that extends eastward from Kilometre 146 on the Kluskus Forest Service road. The property comprises 22 claims totalling 304 mineral claim units that are wholly owned by Granges Inc. Outcrop on the property accounts for less than 1% of the area. Consequently most information has been obtained from diamond drilling and geophysical surveys. Reports by Allen (1992, 1993) summarise results of the most recent work programs.

The Mount Davidson area was covered by a regional geochemical sampling program completed by Granges in 1973. Stream sediment lead-zinc-silver anomalies led to

staking of the Pem claim in 1977. Granges conducted geophysical and soil geochemistry surveys intermittently from 1977 to 1984. A total of 31 core holes and 34 reverse circulation holes were drilled between 1985 and 1987. They identified two areas of mineralization, the Gold and Silver zones (Figure 4). Additional claims were staked in 1985, 1987 and 1991 and in 1992, Granges conducted detailed geological mapping, geochemical sampling, geophysical surveys (IP, magnetic and VLF-EM) and drilled five core holes on the Pem claim.

Most of the work to date has focused on the Pem grid where an area of high resistivity is flanked by a chargeability high and is coincident with a base metal - silver soil geochemistry anomaly. The Gold and Silver zones are both within a zone of high chargeability.

The claims are underlain primarily by Jurassic Hazelton Group stratigraphy consisting of an interbedded succession of argillite, siltstone and sandstone, as well as an intercalated sequence of rhyolitic to dacitic and andesitic to trachyandesitic tuffs, lapilli tuffs, breccias, and flows. Bedding attitudes are rarely apparent, but were seen are flat-lying or gently dipping to the west. Possible Ootsa Lake Group rhyolitic lapilli tuff crops out in the south and southwest of the property. Tertiary Endako Group amygdaloidal andesite flows unconformably overlie Hazelton Group strata in the northwest corner of the claim group.

Structures on the property, interpreted primarily from magnetic data, include subvertical northeast and northwest-trending faults dipping steeply southwest. The significance of these structures is not known, however the Gold and Silver zones occur in a structural block roughly 6 kilometres wide, bounded by northeast-trending faults (Figure 4).

The Gold zone has been interpreted as a structurally controlled, easterly trending, steeply dipping zone up to 70 metres across with a strike length of about 300 metres (Allen, 1992). Disseminated and shear-hosted mineralization occur in felsic lapilli tuffs, breccias and flows that have been affected by mainly phyllic (quartz-sericite-chlorite) and argillic (kaolinite) alteration over a minimum strike length of 900 metres and an undefined width. Mineralization does not appear to be lithologically controlled. There is an apparent correlation of higher gold content with the presence of pyrite with or without pyrrhotite. The most encouraging diamond-drill hole intersections include: hole DAV-11, 14.28 grams per tonne gold across 6.3 metres, and 48.3 grams per tonne gold across 1.3 metres (Zbitnoff, 1988) and hole BD-92-35, 0.72 gram per tonne gold across 47.5 metres (Allen, 1993). A conspicuous 17-metre section of drill core from hole BD-92-33 exhibits about 20% black spherules, up to 8 millimetres in diameter, commonly with 1 to 2-millimetre cores of pyrite±sphalerite (Plate 8). Between spherules, the host rock contains 5 to 8% fine-grained disseminated sphalerite, pyrite and galena. A similar texture and mineralogy is present at the Capoose prospect, approximately 30 kilometres to the west, where drill-indicated reserves are estimated at 28117 000 tonnes grading

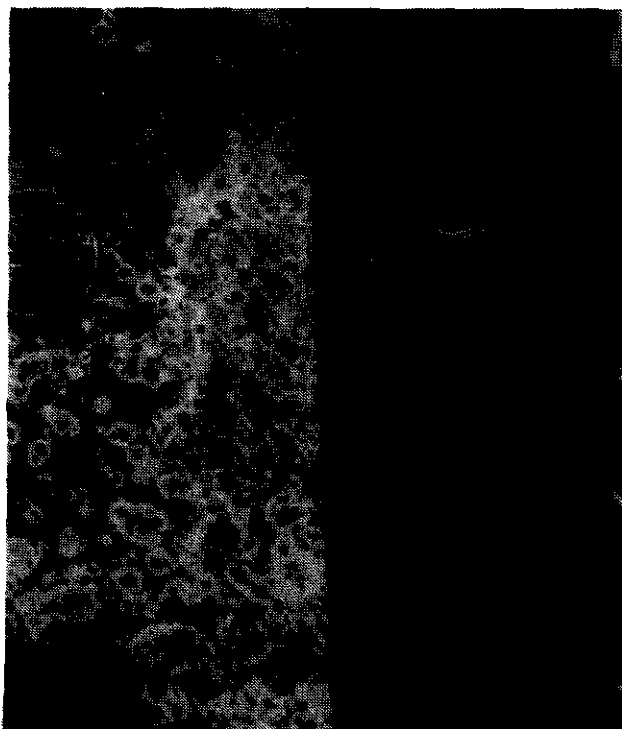


Plate 8. 'Spotted' texture in rhyolite. Dark 'spots' are nuclei growths or diffusion replacements by sulphides/sulphosalts/electrum. The mineralogy of light-coloured 'spots' cored by metallic minerals is unknown, Blackwater-Davidson property (ddh BD-92-33 at 59 metres).

0.52 gram per tonne gold and 37.7 grams per tonne silver (Granges Inc., Annual Report, 1984). Sulphides also occur in several massive (mainly pyrite) zones, in breccias, along fractures, in quartz-lined amygdules, and as replacements of garnet (?) and lapilli up to 1 centimetre in diameter, and in late cross-cutting stringers of sphalerite±galena (± carbonate). Total sulphide content is estimated at about 5% and includes 3 to 4% sphalerite, 1 to 2% pyrite and pyrrhotite, and traces of galena, arsenopyrite, chalcopyrite, tetrahedrite, boulangerite and marcasite(?).

The Silver zone is approximately 500 metres northwest of the Gold zone; its relationship to the Gold zone is not known. It is interpreted to be a relatively flat lying body up to 70 metres thick and is open to the northwest. The Silver zone contains an estimated reserve of 6 million tonnes grading 37 grams per tonne silver and 0.05 gram per tonne gold at a shallow depth (Allen, 1992).

Approximately 600 metres west of the Gold zone subcrop of felsic lapilli tuff-breccia contains individual grains and aggregates of red-brown garnet. The garnets occur in both matrix and fragments, and may have replaced original mafic grains. They are postulated to be products of metasomatism due to the contact thermal effect of the Capoose batholith which is thought to underlie the showings at no great depth. Garnets have not been observed in the Gold or Silver zones.

The felsic pyroclastic rocks that host this zone are typically moderately phyllically altered to patches of fine-grained green sericite±montmorillonite plus trace amounts of quartz, chlorite, dolomitic or ankeritic carbonate and garnet. Manganese oxide and, to a lesser extent, iron oxide, commonly stain fracture surfaces.

Local zones of potassic alteration (quartz-biotite sericite, clays and minor secondary potassium feldspar), dominated by secondary biotite, occur within the phyllic zones. Mineralized zones exhibit sodic depletion and silica enrichment; potassium levels are elevated in areas of alteration. Traces of tourmaline and rutile have been identified in thin section and specular hematite is relatively common (Allen, 1993).

At "Kaolinite" Creek, 3.5 kilometres west of the Pem grid, a fault-bounded zone of kaolinite-altered quartz-phyric tuff, 400 metres wide, overlies rhyolite that contains up to 5% disseminated pyrite and traces of sphalerite and pyrrhotite.

Analogies for this type of system might be the Capoose, Equity Silver and Red Mountain deposits.

### STRATABOUND DEPOSITS (?)

The stratigraphy of Middle Jurassic Hazelton Group rocks, in at least part of the Interior Plateau area, is similar to the rocks that host the gold-rich Eskay Creek stratabound deposit, north of Stewart, and might suggest the potential for stratabound deposits in the Interior Plateau. However, two significant differences are: most of the Hazelton Group volcanic rocks in the study area are subaerial (with a more felsic component), and the apparent lack of small, structurally controlled basins filled with argillaceous sedimentary rocks.

### BUCK [MINFILE 093F 050]

The Buck property is located immediately east of the Fawn claim group (Figure 1). The Buck 1 to 4 claims consist of 80 units that straddle the southwest-flowing Fawnie Creek and the Kluskus Forest Service road. Access to the showings is by a network of four-wheel drive roads that lead to logging clear-cuts within the claim group.

The claims were staked in 1991 and are owned by Western Keltic Mines Inc. In 1982 the same ground, known as the Rocks claims, was investigated by BP Minerals Ltd. (Holt, 1982). It conducted geological mapping, soil and rock geochemistry and trenching focusing on sulphide-bearing ankeritic breccias. There was no recorded work on this ground between 1983 and 1990. In 1992 exploration consisted of geological mapping, prospecting and geochemical sampling and new zones of sulphide mineralization were discovered.

The main area of interest is underlain by a mixed succession of Jurassic Hazelton Group mafic and felsic volcanic and sedimentary rocks that generally strike northerly with gentle to moderate easterly dips. Exposures of rusty weathering, pyritic, dark grey argillites and siltstones are conformably overlain by rhyolitic tuffs and

tuff breccias that resemble those to the west on the Fawn property, with the notable exception that breccias on the Buck property contain abundant clasts of the underlying argillite and siltstone as well as clasts of rhyolite and porphyry. Fine to coarse-grained clastic sedimentary rocks conformably overlie the rhyolite package. Dikes and sills of augite-phyric andesite cut the sedimentary and felsic volcanics and may be feeders to augite-phyric andesite flows that are exposed up-section on both the Fawn and Buck properties.

Stratabound sulphide mineralization is reported to occur in the Rutt zone within a northerly trending clay-sericite-chlorite-silica-altered felsic lapilli tuff unit that has been traced for over 400 metres (Caulfield, 1992). Up to 15% disseminated sphalerite, pyrite and pyrrhotite are present within the altered tuff. Traces of chalcopyrite were also noted. Sphalerite also occurs as a cement or matrix to discrete layers of lapilli. The width of the mineralized horizon is not known but a 3.0-metre chip sample within the zone yielded 2.01% zinc and 306 ppm copper; precious metal values are negligible.

The L14S Trench zone is centred about a kilometre due south of the Rutt zone and consists of ankerite breccia with weakly anomalous zinc, lead, copper, gold and silver geochemical values.

## SKARN DEPOSITS

Infiltration metasomatism related to intrusion of the Capoose batholith has resulted in the formation of iron exoskarn. A large area of metasomatized Hazelton rocks has been identified along the eastern contact of the Capoose batholith. The principal gangue minerals are pyroxene, garnet and epidote. Magnetite is predominant with minor chalcopyrite, pyrrhotite, pyrite and arsenopyrite.

### *FAWN 5 [MINFILE 093F 053]*

Magnetite skarn mineralization occurs in Hazelton Group andesitic pyroclastic rocks on the Fawn 5 claim block at an elevation of approximately 1525 metres (Figure 1). Several outcrops of massive magnetite define an arcuate, generally southeast-trending band of magnetite-rich skarn that appears to be relatively flat lying. Massive to semimassive magnetite with traces of chalcopyrite, is exposed over a width of at least 20 metres and the zone may reach 300 metres in apparent width (Smith and Hoffman, 1983). Calcisilicate mineralogy includes garnet, pyroxene, epidote and actinolite. Up-slope and to the south, epidote-chlorite alteration (magnetite, garnet and pyroxene) of the host pyroclastics is moderate to intense and widespread. Locally, epidote-rich bands have developed along a trend of 070°/75N. These bands mimic bedding and are probably replacements of tuffaceous layers.

Approximately 5 kilometres west of the claim boundary the westerly extension of the Van-Tine Forest Service road (Figure 1) has exposed limy tuffaceous, fossil-bearing sedimentary and intermediate pyroclastic breccias

and lapilli tuffs of the Middle to Upper(?) Hazelton Group. Locally well-developed zones of garnet-pyroxene-epidote infiltration skarn are flanked by dark brown to black biotite hornfels that is all but completely devoid of its original texture. Weak to moderate hornfelsing is widespread. Sulphide mineralization is sparse and averages less than 0.5% of the rock by volume. Pyrite, pyrrhotite, arsenopyrite and traces of chalcopyrite occur as fracture fillings and as disseminations in biotite hornfels and skarn. Locally, remnant lapilli have been partly replaced by pyrrhotite. These new outcrops extend the known thermal effect of the Capoose batholith a minimum of 5 kilometres farther to the west of the magnetite skarn showing on the Fawn 5 claim.

## PORPHYRY OCCURRENCES

The calcalkaline Capoose batholith and associated stocks underlie a large area. Zones of intense pyritization with minor chalcopyrite and molybdenite have been identified.

### *PAW [MINFILE 093F 052]*

This new showing is at the end of the Kluskus-Malapat Forest Service road approximately 5 kilometres southeast of the Wolf property (Figure 1). It is covered by the Paw 1 sixteen-unit claim block owned by Perry Crunenberg. It was staked for the first time in July, 1992. The occurrence consists of a single outcrop of medium-grained, equigranular granodiorite to diorite. Fracture controlled and disseminated sulphide mineralization consists of 3 to 4% pyrite and traces of molybdenite and chalcopyrite. Apparently there has been no work done on the property.

### *NED [MINFILE 093F 039]*

The Ned porphyry molybdenum-copper occurrence is located approximately 115 kilometres southwest of Vanderhoof and is centred 3 kilometres southeast of Capoose Lake (Figure 1). Granges Inc. last conducted field work on the property in 1979 and the claims have since been allowed to lapse. The occurrence is north of the study area (NTS 093F/06E) and was not investigated in 1993.

The property is underlain by biotite quartz diorite and quartz monzonite of the Cretaceous Capoose batholith (67±2.3 Ma). Mineralization consists of disseminated and vein pyrite, molybdenite and traces of chalcopyrite. The best assay was obtained from a chip sample across 5 metres which returned 0.046% molybdenite and 0.03% copper with negligible gold and silver (Zbitr off, 1978).

### *CHU, C (CH) [MINFILE 093F 001, 004]*

The CHU porphyry prospect is located 90 kilometres south-southwest of Vanderhoof and straddles the Kluskus Forest Service road at the Kluskus logging camp (Kilome-

tre 102). Exploration work, carried out from 1969 to 1975 by Rio Tinto Canadian Exploration Ltd., and from 1980 to 1985 by Granges, identified porphyry molybdenum-copper mineralization and a precious and base metal vein target, respectively. Placer Dome Inc. optioned the property in 1990 and in 1991 conducted geological mapping, soil geochemical and geophysical surveys on the property. In 1992 the company completed a 12-hole diamond drilling program to evaluate the potential for a porphyry copper-molybdenum deposit. Placer Dome did not undertake a field program in 1993.

The property is underlain by andesitic volcanic and fine-grained sedimentary rocks of the Lower to Middle Jurassic Hazelton Group. Monzonite to diorite of unknown age has intruded and hornfelsed the Hazelton rocks near the contact. Propylitic alteration consisting of chlorite, epidote and calcite is widespread.

The main area of interest is defined by coincident copper-gold geochemical anomalies, an induced polarization chargeability high, and a high magnetic anomaly (Edwards and Campbell, 1992). Mineralized drill core exhibits strong bleaching, veining and pyritization. Disseminated and fracture-controlled pyrite, up to 15%, minor chalcopyrite and traces of molybdenite occur in both intrusive and volcanic/sedimentary country rocks. Sphalerite and galena are present in late quartz-carbonate veinlets.

## LANDSAT IMAGERY

As a potential aid to field mapping and consequently the study of mineral deposit settings, a brief report on Landsat Imagery has been prepared by J.A. Turner of MineQuest Exploration Associates Ltd. The products consist of two landsat photo enlargements at 1:1 000 000 scale, each covering an area of 92 by 88 kilometres at a resolution of 30 metres, and a mylar overlay showing the traces of lineaments. The image was derived from the Thematic Mapper LANDSAT 5 satellite. The area of coverage is centred near Mount Davidson in the Chilcotin area (NTS 93C, 93F). General interpretations of linear and circular features are:

- large circular features may be remnant volcanic centres.
- northwest-trending lineaments (30 to 100 kilometres in length) suggest major fault systems.
- northeast-trending lineaments are assumed to be deep (crustal?) structures.
- prominent easterly trending lineaments are defined by long narrow lakes (e.g., Johnny Lake and Laidman Lake) and are interpreted to postdate other structures.
- weakly developed northerly trending lineaments occur on the Wolf property and in the area of the Fawnie Range (e.g., Capoose)
- small circular features (some with radiating linears) are common throughout the area.

Unfortunately, ground truthing of the features noted above was not carried out due to time constraints in the

field. The data will be examined in more detail over the winter months with possible follow-up next season.

## ENERGY DIVISION FILES

As part of a larger project to produce a regional metallogenic synthesis of the Interior Plateau, initiated by the authors in 1991, data on file with the Energy Division of the B.C. Ministry of Energy, Mines and Petroleum Resources in Victoria were examined and compiled. Further compilation and interpretation of data is planned for the winter months. cursory examination suggests the potential for outlining several structures and stratigraphic contacts (especially at depth). The data on file have been submitted by oil and gas companies for assessment purposes during exploration programs, carried out mainly in the early 1980s but also dating back to the 1960s.

## ACKNOWLEDGMENTS

Metall Mining Corporation and Fox Geological Consultants Ltd. are gratefully acknowledged for providing excellent tours of their respective properties in the area, including open discussions specific to their projects. Also, private company reports made available by Granges Inc. and Western Keltic Mines Inc. have aided the study greatly.

## REFERENCES

- Allen, G.J. (1992): Geology, Geochemistry and Geophysics Report on the Blackwater-Davidson Property; *B.C. Ministry of Energy, Mines and Petroleum Resources*, Assessment Report 22654, 27 pages.
- Allen, G.J. (1993): Diamond Drilling Report on the Blackwater-Davidson Property; unpublished report, *Granges Inc.*, January, 1993, 25 pages.
- Andrew, K.P.E. (1988): Geology and Genesis of the Wolf Precious Metal Epithermal Prospect and the Capoose Base and Precious Metal Porphyry-style Prospect, Capoose Lake Area, Central British Columbia; unpublished M.Sc. thesis, *The University of British Columbia*, 334 pages.
- Awmack, H.J. (1991): Geological, Geochemical and Geophysical Report on the Fawn Property; *B.C. Ministry of Energy, Mines and Petroleum Resources*, Assessment Report 21927, 155 pages.
- Cann, R.M. (1984): Wolf Claims: Geology, Geochemistry and Trenching, 1984; *B.C. Ministry of Energy, Mines and Petroleum Resources*, Assessment Report 13968, 27 pages.
- Caulfield, D. (1992): Geological and Geochemical Report on the Buck 1 - 4 Claims; *B.C. Ministry of Energy, Mines and Petroleum Resources*, Assessment Report 22569, 12 pages.
- Diakow, L.J. and Webster, I.C.L. (1994): Geology of the Fawnie Map Area (93F/3), in *Geological Fieldwork 1993*, Grant, B. and Newell, J.M., Editors, *B.C. Ministry of Energy, Mines and Petroleum Resources*, Paper 1994-1, this volume.
- Edwards, K. and Campbell, T. (1992): Assessment Report for the CH 10-16 Mineral Claims; *B.C. Ministry of Energy, Mines and Petroleum Resources*, Assessment Report 22027, 89 pages.

Holt, E. (1982): Fawnie Creek Geochemical Report on the Rocks Mineral Claim; *B.C. Ministry of Energy, Mines and Petroleum Resources*, Assessment Report 10787, 17 pages.

Smith, M. and Hoffman, S. J. (1983): Geological and Geochemical Report on the Gran 7 Claim; *B.C. Ministry of Energy, Mines and Petroleum Resources*, Assessment Report 12032, 58 pages.

Zbitnoff, G.W. (1978): Report on the Ned Claim; unpublished report, *Granges Inc.*

Zbitnoff, G.W. (1988): Diamond Drilling Report on Pem Claim, #554; *B.C. Ministry of Energy, Mines and Petroleum Resources*, Assessment Report 17032, 97 pages.

## NOTES

## NORTHERN VANCOUVER ISLAND INTEGRATED PROJECT

By A. Panteleyev, P.T. Bobrowsky, G.T. Nixon and S.J. Sibbick

**KEYWORDS:** Northern Vancouver Island, regional geology, surficial geology, drift exploration, economic geology, hydrothermal alteration, mineral deposits, exploration geochemistry.

### INTRODUCTION

The Northern Vancouver Island project is one of five new integrated studies resulting from the Ministry's 1993 *Mineral Strategy*, an initiative intended to revitalize base metal exploration in the province. Northern Vancouver Island (Figure 1) was chosen as an ideal starting point for a two-year study because the region has been assessed to have high mineral potential. Also, although the area has an established mining base and infrastructure, ore reserves at Island Copper mine are rapidly being depleted and closure is imminent.

The project typifies the integrated approach taken in these "targeted" geoscience programs. The project includes bedrock and surficial geological mapping; water, till and bedrock geochemistry; and alteration and mineral deposits studies. This work is supported by specialized stratigraphic, geochronological and remote sensing investigations by investigators from the Geological Survey of Canada, universities and the Canadian Centre for Remote Sensing.

Recent geological work that provides a foundation for the project includes regional geological mapping in the Mahatta Creek map area (92L/5) by Nixon *et al.* (1993a, 1993b) and Hammack and Nixon (1993), till geochemistry investigations in Quatsino map area, (92L/12) by Kerr *et al.* (1992) and mineral deposits and related natural acid drainage studies to the west of Island Copper mine by Panteleyev and Koyanagi (1993) and Koyanagi and Panteleyev (1993).

The economic geology of northern Vancouver Island is dominated by mineral deposits in Jurassic volcanic rocks of the Bonanza Group and the coeval rocks of the Island Plutonic Suite. These units define an Early Jurassic island arc, much akin to some present day western and southwestern Pacific volcanic arcs. Important mineral deposits in this setting are typically porphyry copper with related peripheral base and precious metal vein and replacement deposits, as well as skarn deposits. A fine Northern Vancouver Island example is Island Copper mine, a major porphyry copper deposit of superior quality by British Columbia standards. Major prospects are the Hushamu porphyry copper deposit (EXPO claims), 26 kilometres to the west

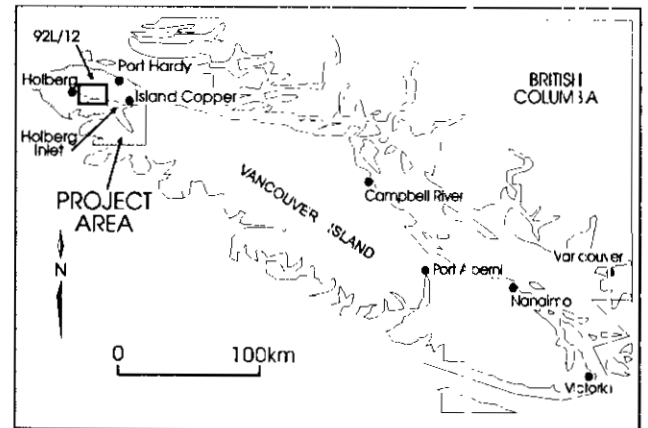


Figure 1. Location map.

of Island Copper mine and the smaller Red Dog deposit, 37 kilometres west-northwest of the mine. Hushamu is a large, but lowgrade copper-gold-molybdenum deposit; geological reserves within a larger resource are 172.5 million tonnes with an average grade of 0.28 % copper, 0.34 gram per tonne gold and 0.009 % molybdenum (Jordex Resources Inc. report, 1993). Red Dog mineral reserves are 31.2 million tonnes with an average grade of 0.313 % copper, 0.45 gram per tonne gold and 0.007 % molybdenum (Crew Natural Resources Ltd. prospectus, 1992). Skarn deposits include the past-producing mines at Yreka, a copper-gold-silver deposit 9 kilometres northwest of Port Alice, and the Merry W dow, Kingfisher and Old Sport copper-iron-gold deposits near Benson Lake, 16 kilometres southeast of Port Alice. The potential for precious and base metal replacement and epithermal-type occurrences is the new and current exploration focus in the region.

### COMPONENT STUDIES WITHIN THE INTEGRATED PROJECT

The four component fields of study in this integrated project: regional mapping, surficial geology, economic geology and exploration geochemistry, are summarized elsewhere in this volume by Nixon *et al.*, Bobrowsky and Meldrum, Panteleyev and Koyanagi, and Sibbick, respectively. Fieldwork in Northern Vancouver Island is expected to continue in 1994.



Plate 1. Northern Vancouver Island targeted geological study 1993; integrated project team. Left to right: Garry Payie, Graham Nixon, Jack Hamilton and Jan Hammack, regional mapping; Victor Koyanagi, regional mapping and economic geology; Jessie (in front), regional mapping and bear patrol; Peter Bobrowsky, surficial geology; Andre Panteleyev, economic geology; Bill McMillan, manager. Missing: Dan Meldrum and Wayne Jackaman. Photograph taken overlooking Nahwitti Lake.

## REGIONAL MAPPING

The regional bedrock geological mapping team, (Plate 1) investigated the central and eastern half of Quatsino map area (92L/12) and the western quarter of the adjoining 92L/11 map area. The area mapped at 1:20 000 scale for publication at 1:50 000 scale, covers approximately 800 square kilometres between Holberg and Port Hardy on the north to within 12 kilometres of Port Alice on the south. It contains the Island Copper mine and most of the significant known mineral deposits in the region. Samples were collected for petrochemistry, petrography, assay, isotopic dating, macrofossil and microfossil (conodont and radiolaria) identification.

Geological units recognized in the map area include the Upper Triassic Karmutsen volcanics, Parson Bay sediments and Quatsino limestone; the Lower Jurassic Bonanza volcanics with surprisingly little interbedded sedimentary material; the Jurassic Island Plutonic Suite and associated porphyries; Cretaceous sediments believed to be equivalent to the Longarm Formation (Kyuquot Group); and rare Tertiary dikes. The Bonanza volcanics were subdivided into major stratigraphic units that are mappable at 1:50 000 scale. The map units include a

succession of rhyolitic lavas and ash-flow tuffs intercalated with plagioclase-augite-phyric and rarely hornblende-phyric intermediate to mafic lavas, tuffs and tuff-breccias. The structure of the area is dominated by northwesterly striking, southwesterly dipping stratigraphic packages and right-lateral faulting. The rocks have undergone at least one episode of post-Lower Jurassic flexural-slip folding. The distinctive acid sulphate alteration found over large areas to the west of Island Copper mine and north of Holberg Inlet is hosted, to a large degree, by the Bonanza rhyolitic units.

## SURFICIAL GEOLOGY

Quaternary geological investigations were conducted in NTS map areas 92L/6 (Alice Lake) and 92L/11 (Port McNeill) in order to provide surficial geology data and interpretations to assist mineral exploration. This work attempts to integrate overburden studies into traditional base and precious metal exploration strategies. Surficial geology was mapped at 1:50 000 scale on a regional reconnaissance level throughout the two map sheets. A till geochemistry program was conducted in the western half of the same map sheets (92L/6 and 92L/11). In total, 178 sites were sampled for drift and pebble

samples; eight fabric locations were evaluated and another 16 paleoflow directional locations were documented. This study proposes to generate surficial geology maps and derivative exploration products currently termed "sample media confidence maps". This work will lead to the development of regional drift-exploration models.

Mapping has determined that all major sediment types are present in the study area and patterns in sediment type distribution and thickness are clearly discernible. For example, marine and glaciomarine deposits are restricted to coastal areas below the 35-metre contour. In the eastern part of the map area, the subdued topography is predominately underlain by ground moraine containing both supraglacial and subglacial till deposits. Thickness is variable but generally ranges between 5 and 20+ metres. A greater amount of bedrock is exposed to the west. There, sediment tends to be primarily a thin colluvium that rarely exceeds a few metres in thickness. Ice flow was regionally to the northwest with ice originating on the mainland in the Coast Mountains. The last glaciation occurred between 20 000 and 14 000 years ago.

## ***ECONOMIC GEOLOGY***

The mineral deposit studies focus on genetic models for intrusion-related mineralization in the northern belt of Bonanza volcanics and Island intrusions of the Jurassic Bonanza volcanic island arc. The distinction in arc terranes between epithermal and porphyry copper environments of mineralization is largely one of convenience for exploration rather than one of reality; there can be overlap. Zones of advanced argillic, acid sulphate alteration, with or without enargite and other high sulphidation assemblages, may mark the high-level near-surface expression of intrusive-related mineralized hydrothermal systems. The hydrothermally altered rocks can be hosts for precious metal and/or copper deposits or be barren hypogene leakage from concealed, deeper porphyry copper deposits. The large amount of acid leaching that occurs in the most strongly altered rocks needs to be carefully studied and interpreted in order to understand its origins. Generally only zones of alteration resulting from magmatic-hydrothermal processes are favourable for exploration. Similar looking acid-leached siliceous and clay-altered rocks produced by steam-heated (boiling) groundwaters and supergene processes are rarely mineralized.

The weathering of sulphide-rich deposits by surface leaching leads to the generation of acidic groundwaters and extensive (supergene) clay alteration. The leached rocks, together with the hydrothermally altered rocks, are commonly marked by visually striking limonite staining, clay alteration, acidic waters and surface deposits of bog iron (ferricrete blankets). The challenge in exploration is to identify commonly overlapping zones of supergene and hydrothermal alteration and identify ore controls.

## ***EXPLORATION GEOCHEMISTRY***

A follow-up of Regional Geochemical Survey (RGS) data released in 1989 (Matysek *et al.*, 1989) focused on geochemical anomalies in Bonanza Group rocks and their potential for hosting porphyry copper, transitional acid sulphate and epithermal mineralization. Emphasis was placed on the less prominent anomalies which originated in Bonanza rocks, especially those close to intrusive bodies. Of the six anomalous areas selected and inspected, only two had mineral properties located within their drainages. Further interpretations for collected samples are awaiting analytical results.

An analysis of the areal coverage of the RGS was undertaken through the use of catchment basin analysis. Catchment basins, also known as drainage basins, represent the land area drained by a particular creek or stream. Two hundred and ninety-four catchment basins sampled in the Regional Geochemical Survey in map area 92L/SW were digitized as polygons. Calculations reveal that these drainage basins range from 0.6 to 20 square kilometres in area. Only 54 % of the land area of 92L/SW is covered by these catchment basins. More importantly, approximately 46 % of the map area is *not* covered by the RGS sampling. There is, therefore, a large amount of unsurveyed, undetermined ground remaining. Mineralization in unsurveyed areas might be indicated by geochemical patterns expressed in drainages that border the untested areas.

## ***COMMENTS***

Preliminary results of field surveys were presented at a widely advertised public meeting in Port Hardy on August 27. An ensuing field-trip illustrated stratigraphic, lithologic, hydrothermal alteration and other features of interest. Other information including discussions, poster displays and Open File maps will be made available at the 1994 Cordilleran Roundup.

## ***ACKNOWLEDGMENTS***

It is a pleasure to acknowledge the cooperation and assistance the project team received from Bill Newman, Government Agent; John Fleming and Alan Reeves, Island Copper mine; Peter Dasler, on behalf of Jordex Resources Inc.; Neil leNobel, BHP Minerals (Canada) Ltd.; Bob Anderson, Crew Natural Resources Ltd.; Western Forest Products Ltd. and Tribune Timber Limited.

## ***REFERENCES***

- Hammack, J.L. and Nixon, G.F. (1993): Mineral Potential of the Mahatta Creek Map Area NTS 92L5; *B.C. Ministry of Energy, Mines and Petroleum Resources*, Mineral Potential Map 1993-1, 1:50 000 map.

- Kerr, D.E., Sibbick, S.J. and Jackaman, W. (1992): Till Geochemistry of the Quatsino Map Area (92L/12); *B.C. Ministry of Energy, Mines and Petroleum Resources*, Open File 1992-21, 15 pages plus appendices.
- Koyanagi V.M. and Panteleyev, A. (1993): Natural Acid-drainage in the Mount McIntosh/Pemberton Hills Area, Northern Vancouver Island (92L/12); in *Geological Fieldwork 1992*, Grant, B. and Newell, J.M., Editors, *B.C. Ministry of Energy, Mines and Petroleum Resources*, Paper 1993-1, pages 445-450.
- Matysek, P.F., Gravel, J.L. and Jackaman, W. (1989): 1988 Regional Geochemical Survey, Stream Sediment and Water Geochemical Data, NTS 92L/102I - Alert Bay - Cape Scott; *B.C. Ministry of Energy, Mines and Petroleum Resources*, RGS 23.
- Nixon, G.T., Hammack, J.L., Hamilton, J.V. and Jennings, H. (1993a): Preliminary Geology of the Mahatta Creek Area, Northern Vancouver Island (92L/5); in *Geological Fieldwork 1992*, Grant, B. and Newell, J.M., Editors, *B.C. Ministry of Energy, Mines and Petroleum Resources*, Paper 1993-1, pages 17-35.
- Nixon, G.T., Hammack, J.L., Hamilton, J.V. and Jennings, H. (1993b): Preliminary Geology of the Mahatta Creek Area, Northern Vancouver Island (92L/5); *B.C. Ministry of Energy, Mines and Petroleum Resources*, Open File 1993-10, 1:50 000 map.
- Panteleyev, A. and Koyanagi, V.M. (1993): Advanced Argillic Alteration in Bonanza Volcanic Rocks, Northern Vancouver Island - Transitions Between Porphyry Copper and Epithermal Environments (92L/12); in *Geological Fieldwork 1992*, Grant, B. and Newell, J.M., Editors, *B.C. Ministry of Energy, Mines and Petroleum Resources*, Paper 1993-1, pages 287-294.



**PRELIMINARY GEOLOGY OF THE QUATSINO - PORT McNEILL MAP  
AREAS, NORTHERN VANCOUVER ISLAND (92L/12, 11)**

**By G. T. Nixon, J. L. Hammack, V. M. Koyanagi, G. J. Payie, A. Panteleyev,**

**N. W. D. Massey, J. V. Hamilton, B. C. Geological Survey Branch**

**and J. W. Haggart, Geological Survey of Canada**

**KEYWORDS:** Regional geology, Bonanza Group, Vancouver Group, Karmutsen Formation, Quatsino Formation, Parson Bay Formation, Kyuquot Group, Coal Harbour Group, Island Plutonic Suite, stratigraphy, structure, mineralization, epithermal, acid sulphate alteration

**INTRODUCTION**

Regional geological mapping at 1:50 000-scale on northern Vancouver Island began in 1992 in the Mahatta Creek area (92L/5; Nixon *et al.*, 1993a and b) and continued in 1993 under the umbrella of a multidisciplinary program to further evaluate the base and precious metal potential of an area of known mineralization and established infrastructure (Panteleyev *et al.*, 1994). The only major operating mine in the area, the Island Copper open-pit operation of BHP Minerals (Canada) Limited, is scheduled to close in 1996 when reserves of copper-molybdenum-gold ore are expected to be exhausted. The area is a prime exploration target for base and precious metals associated with porphyry, epithermal and acid sulphate or high-sulphidation hydrothermal systems (Panteleyev, 1992; Panteleyev and Koyanagi, 1993, 1994). The majority of these systems are associated with the Early to Middle Jurassic Island Plutonic Suite and Early Jurassic Bonanza Group rocks. The regional mapping component of this study focused primarily on potential ties between mineralization and key elements of the Bonanza volcanic stratigraphy. The preliminary findings reported here demonstrate a distinct and regionally persistent relationship between felsic horizons in the volcanic pile and acid sulphate alteration assemblages variably endowed in base and precious metals. These results have an important bearing on applicable mineral deposit models and exploration strategies (Panteleyev and Koyanagi, 1994).

The area mapped (800 km<sup>2</sup>) encompasses the Quatsino sheet (92L/12) north and east of Holberg Inlet and the easternmost part of the Port McNeill sheet (92L/11), and extends from the community of Holberg east to Port Hardy and south towards Port Alice (Figure 1). Most of the area is accessible by a well-maintained network of logging roads and by boat in the protected waters of Rupert, Holberg and Neroutsos inlets. The area

is covered by the 1988 Regional Geochemical Survey (RGS; Matysek *et al.*, 1989); 1:50 000-scale (Maps 1734G, 9770G) and 1:250 000-scale (Map 7220G) aeromagnetic surveys; a 1:50 000-scale surficial geology map (Kerr, 1992); and drift prospecting studies (Kerr and Sibbick, 1992; Kerr *et al.*, 1992). Follow up of "untested" RGS anomalies in the 92L/102I map sheets is reported by Sibbick (1994) and recent surficial geological studies by Bobrowsky and Meldrum (1994). In addition, work is continuing on the application of *in situ* analysis of naturally acidic stream drainages as an exploration technique (Koyanagi and Panteleyev, 1993, 1994).

**TECTONIC SETTING AND REGIONAL GEOLOGY**

Northern Vancouver Island lies in the southern part of the Wrangellia tectonostratigraphic terrane which is bounded on the east by plutonic rocks of the Coast Belt and underplated on the west by the Pacific Rim and Crescent accretionary terranes (Wheeler and McFeeley, 1991). Amalgamation of Wrangellia to the Alexander Terrane to form the Insular Superterrane appears to have occurred as early as Late Carboniferous time (Gardner *et al.*, 1988). Subsequent accretion of the Insular Superterrane to inboard terranes of the Coast and Intermontane belts may have occurred as late as the mid-Cretaceous (Monger *et al.*, 1982) or as early as the mid-Jurassic when a single superterrane may have been accreted to the North American continental margin (van der Heyden, 1991). There is an accumulating body of geophysical evidence (T. J. Lewis, C. Love and T. Hamilton, personal communications, 1993) to suggest that since this accretionary event, the northern tip of Vancouver Island may have been involved in the formation of the Queen Charlotte Basin, a Tertiary trans-tensional province related to oblique convergence of the Pacific and Juan de Fuca plates with the North American plate (Riddiough and Hyndman, 1991). The southern boundary of this extensional regime appears to be marked by the northeasterly trending Brooks Peninsula fault zone which is coincident with Tertiary dike swarms (Nixon *et al.*, 1993a) and young (8 to 2 Ma) calcalkaline lavas of the Alert Bay volcanic belt (Figure 1). The tectonic setting of the Alert Bay suite has been linked to a descending plate-edge effect associated with a stand-off

# REGIONAL GEOLOGY NORTHERN VANCOUVER ISLAND

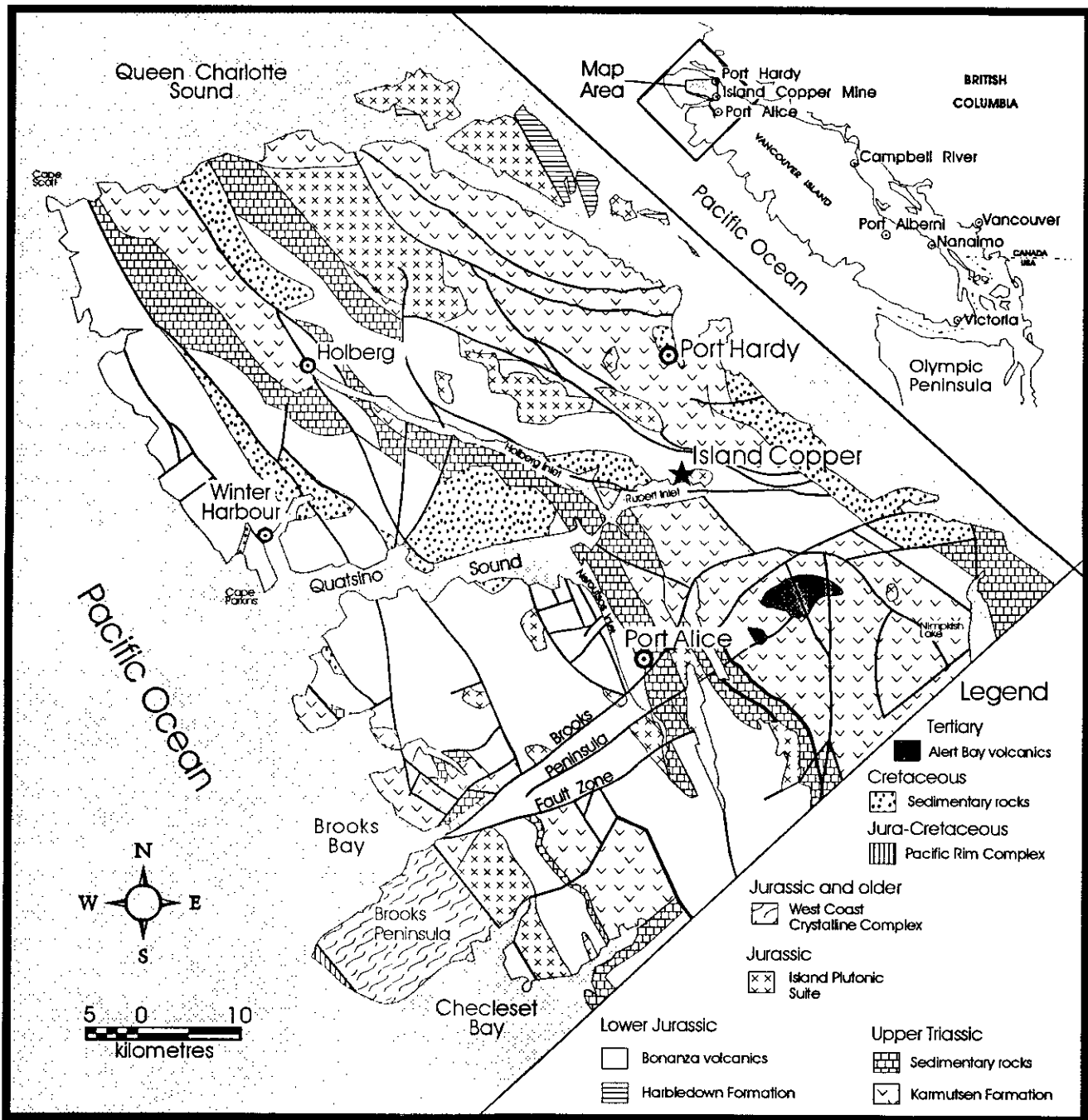


Figure 1. Generalized geology of northern Vancouver Island (modified after Muller *et al.*, 1974). Shaded inset shows location of map area.

the Pacific - Juan de Fuca - North America triple junction off the Brooks Peninsula in the recent past (*i.e.* prior to about 1 Ma; Bevier *et al.*, 1979; Armstrong *et al.*, 1985).

Pertinent aspects of the regional geology of the Quatsino Sound area were summarized by Nixon *et al.* (1993a). The area is largely underlain by fault-bounded

blocks of homoclinal strata that belong to the Upper Triassic and Lower Jurassic Vancouver and Bonanza groups, respectively, and that are intruded by Early to Middle Jurassic plutons of the Island Plutonic Suite

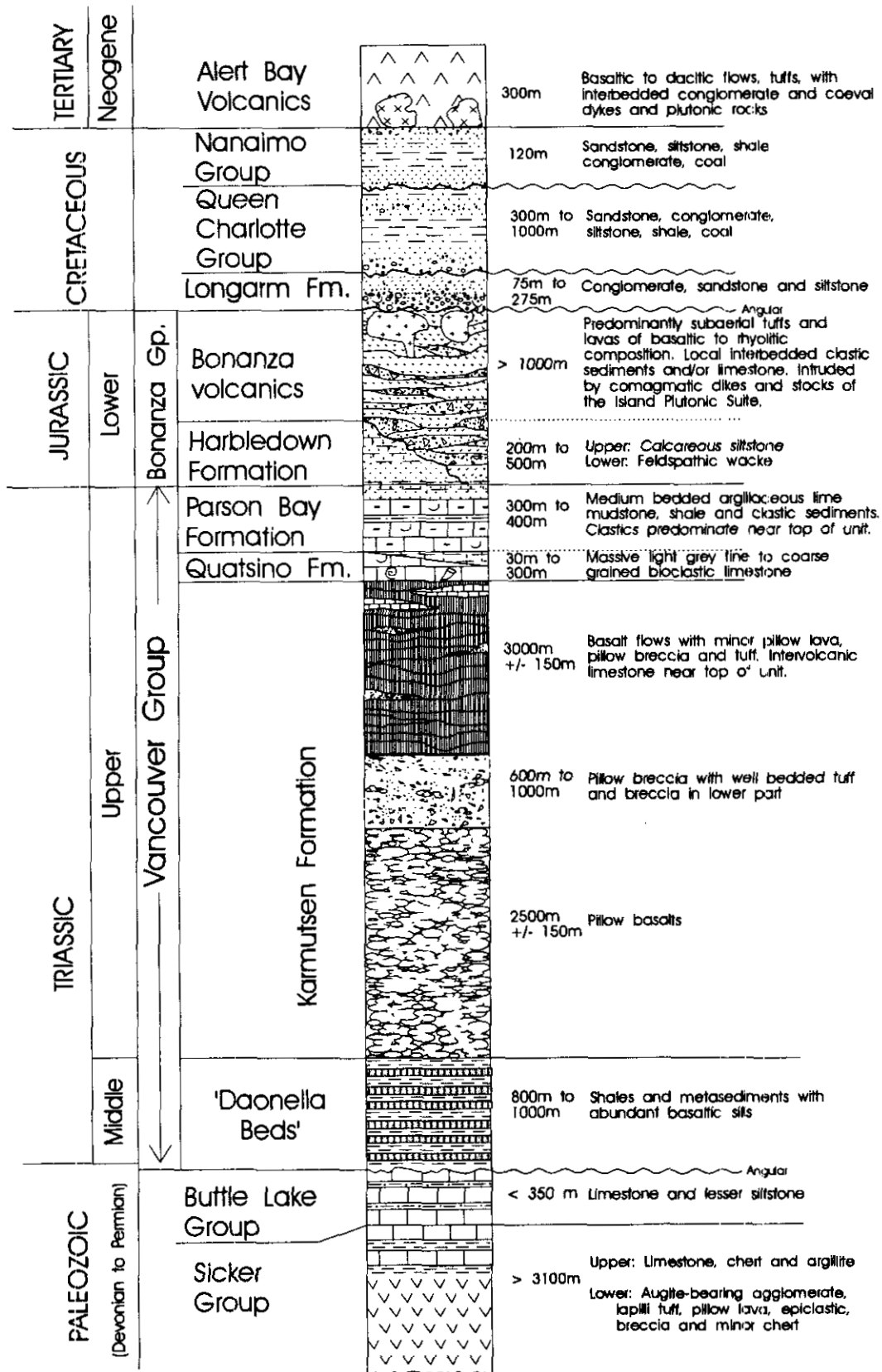


Figure 2. Regional Mesozoic-Cenozoic stratigraphy of northern Vancouver Island (modified after Muller *et al.*, 1974, 1981).

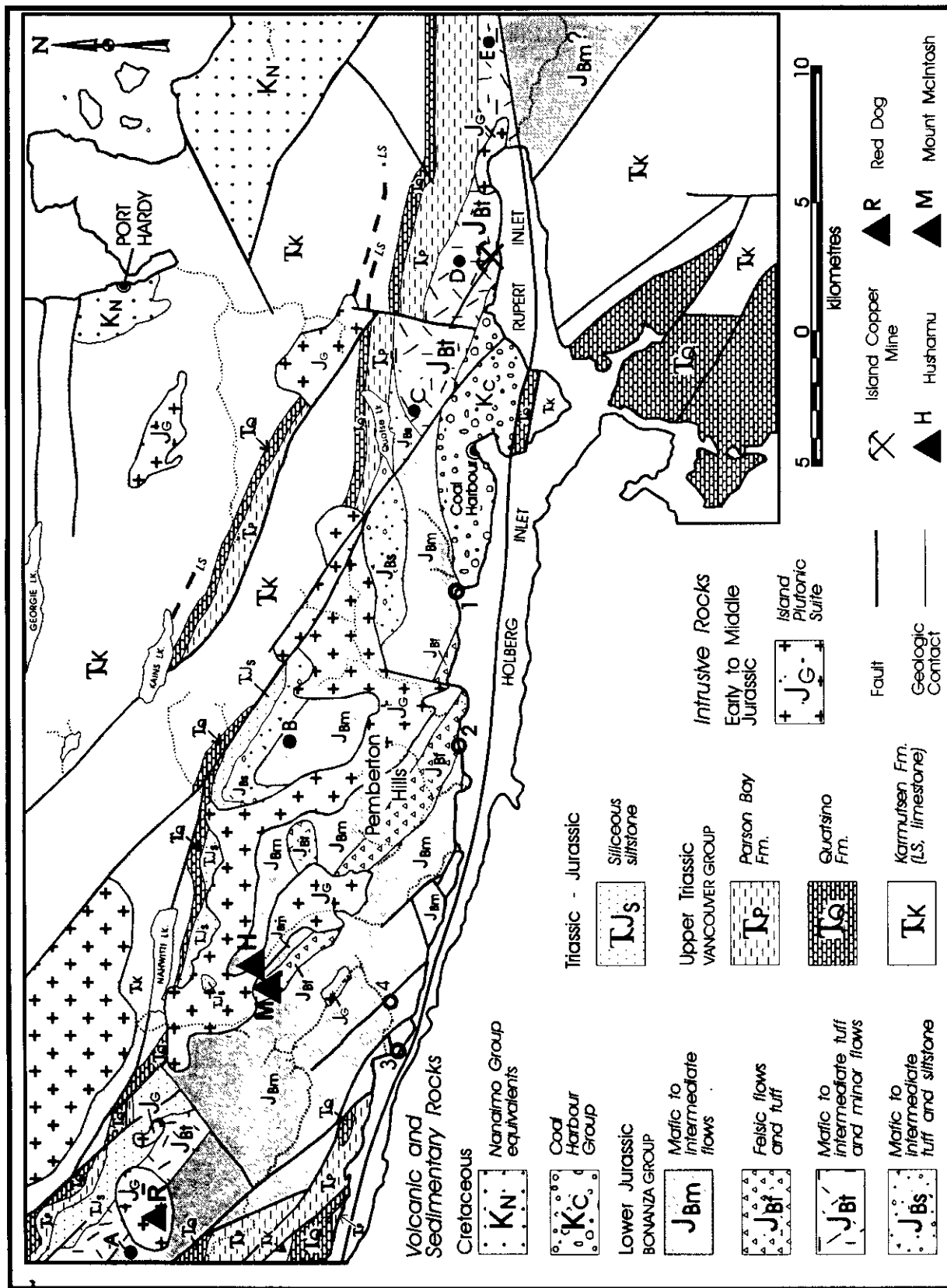


Figure 3. Generalized geology of the Quatsino - Port McNeill map area showing major porphyry deposits and an epithermal prospect (triangles); locations of stratigraphic sections (circles) given in Figure 4, and localities of Cretaceous and Jurassic-Cretaceous strata described in the text.

(Muller *et al.*, 1974, 1981; Figures 1 and 2). Island-arc volcanic and sedimentary rocks of Devonian to Early Permian age and Middle Triassic marine sediments that form the basement of Vancouver Island are not exposed in the project area, and are described elsewhere (e.g. Monger *et al.*, 1991). The oldest rocks in the area belong to the Upper Triassic Karmutsen Formation, a thick pile of tholeiitic submarine pillow basalts, breccias and tuffs capped by a subaerial succession of basaltic flows with minor limestone interbeds (Figure 2). The lavas have been interpreted in terms of flood basalt volcanism related to rifting of the older Paleozoic arc sequences, namely the Sicker and Buttle Lake groups (Muller *et al.*, 1974; Jones *et al.*, 1977; Barker *et al.*, 1989). Overlying the Karmutsen Formation is the upper Carnian to middle Norian Quatsino limestone which passes upward into Norian carbonates and clastics of the Parson Bay Formation. The Triassic rocks in turn are overlain by a thick sequence of subaqueous to subaerial arc volcanic and intercalated marine sedimentary rocks of the Lower Jurassic (Sinemurian-Pliensbachian) Bonanza Group. In part, these strata are correlative with non-calcareous "argillites" and greywackes of the Harbledown Formation found farther east across Johnstone Strait and on islands in Queen Charlotte Sound (Figure 1). To date, the Harbledown Formation has not been recognized as a mappable unit on northern Vancouver Island. The lower Mesozoic stratigraphy is intruded by Early to Middle Jurassic granitoids of the Island Plutonic Suite believed to be at least partly comagmatic with Bonanza Group volcanic rocks. Cretaceous marine and nonmarine strata were deposited as clastic wedges on deformed and denuded volcano-plutonic complexes of the Bonanza arc. Felsic to mafic Tertiary dikes and Neogene volcanics of the Alert Bay suite were emplaced in an anomalously near trench, fore-arc environment associated with the Brooks Peninsula fault zone (Armstrong *et al.*, 1985).

## STRATIGRAPHIC NOMENCLATURE

Although problems with stratigraphic nomenclature are known to exist (Nixon *et al.*, 1993a), no formal revision of the Lower Mesozoic stratigraphy of northern Vancouver Island is attempted at this time. In general, we have adopted the nomenclature of Muller *et al.* (1974 and 1981). However, new lithostratigraphic units mappable at 1:50 000 scale are described below and underscore the need for more detailed study of strata at the Triassic-Jurassic boundary and within the Bonanza Group. Ongoing studies of conodonts and radiolaria conducted by Michael Orchard (Geological Survey of Canada) and Fabrice Cordey, respectively, are attempting to address these problems.

With regard to the Cretaceous rocks of northern Vancouver Island, Jeletzky (1976) and Muller *et al.* (1974) have used different stratigraphic nomenclature. Although Jeletzky (*ibid.*) recognized similarities between the Cretaceous lithologic and paleontological successions of Quatsino Sound and those of Queen Charlotte Islands (Sutherland Brown, 1968), he preferred to consider the

former as distinct. Consequently, he introduced new stratigraphic nomenclature for some rock units in the Quatsino Sound region (e.g. Coal Harbour Group). In contrast, Muller *et al.* (1974) and Muller and Roddick (1983) applied Sutherland Brown's nomenclature for the Cretaceous sequences of the Queen Charlotte's to Vancouver Island. However, our preliminary work does appear to substantiate previously proposed differences between the Cretaceous successions in these areas (see also Haggart, 1993), and so we have retained some of Jeletzky's (1976) recommendations, at least until a formal stratigraphic revision of the Cretaceous rocks of northern Vancouver Island is undertaken.

## STRATIGRAPHY

The lower Mesozoic stratigraphic units in the Quatsino - Port McNeill map area form a generally westward-dipping, westward-facing homocinal succession with a conspicuous northwesterly trending structural grain that is shared by major faults and plutons in the region (Figure 3). Outliers of Cretaceous strata occur in the vicinity of Coal Harbour and along the shores of Holberg Inlet. Tertiary dikes are distributed throughout the area but no extrusive equivalents of the Alert Bay volcanics have been identified.

## KARMUTSEN FORMATION

The Karmutsen Formation underlies most of the northern and eastern parts of the map area where it forms subdued hummocky terrain (Figure 3). The succession is composed of dark greenish grey to purplish grey and maroon, hematitic basaltic lava flows with minor intercalated pillows, pillow breccias and hydroclastite deposits, and minor subvolcanic intrusions. It appears that only the predominantly subaerial, uppermost part of the Karmutsen Formation is exposed. The lavas are commonly massive and amygdaloidal with little evidence of internal cooling joints. Flow contacts are observed locally and marked by flow breccias (comparatively rare), a thin zone of hackly jointing at the chilled base of a flow, or textural differences such as phenocryst content or a dense glassy (devitrified) flow base resting on an amygdaloidal flow top. Flow thickness varies from as little as 1 metre to over 6 metres. Two distinct geometries of internal amygdule concentrations have been observed. The most common occurrence is a planar arrangement of amygdules in zones of variable width that are oriented parallel to flow contacts and provide a good indication of paleohorizontal (Plate 1). Pipe amygdules are also locally well developed and intersect these planar horizons at right angles (Plate 2). The latter are usually attributed to vaporization of surface water as hot lavas pass over wet ground, and both sets of features are well known in subaerial flood-basalt provinces. Amygdule infillings include quartz (rarely amethystine varieties) epidote, chlorite, carbonate and zeolite.



Plate 1. Laminar amygdaloidal horizons in Karmutsen basalt, 3.5 kilometres due south of the Island Copper mine across Rupert Inlet (93JHA1-16). These structures provide a good approximation to paleohorizontal. Pen is 16 centimetres long.

The majority of Karmutsen lavas are aphanitic to finely porphyritic (plagioclase <2 mm) with seriate textures; however, medium porphyritic (plagioclase 2-5 mm) lavas are relatively common and coarsely plagioclase-phyric variants (euhedral to subhedral laths measuring 0.5-2 cm) with hiatal textures appear near the top of the succession where they are intercalated with the other lava types as well as interflow limestones. The porphyritic lavas typically exhibit either a trachytoid texture of flow-aligned feldspars or glomeroporphyritic intergrowths in which a radiate or petal-like arrangement of plagioclase laths are ordered about a common nucleus. Local accumulations of plagioclase crystals (up to 40 volume %) are locally evident within individual flows.

Subaqueous basalt sequences occur throughout the map area but form extremely localized accumulations and thus appear to have no regional stratigraphic significance. In pillowed sequences, individual pillows rarely exceed 2 metres in length and at one locality a transition from pillowed basalt to massive flow is evident. Broken pillow fragments (<0.5 m) are distributed chaotically in pillow breccias and finer grained, poorly sorted hyaloclastite deposits. Finely comminuted interpillow material and hyaloclastite debris are locally cemented and veined by white zeolites. Other common vein minerals encountered in the Karmutsen Formation include quartz, epidote, chlorite and carbonate. Disseminated pyrite is widespread and especially common near intrusive contacts; chalcopryrite and native copper have also been observed. The degree of metamorphism of Karmutsen basalts in the map area has yet to be established from thin section studies. Farther west in the Mahatta Creek sheet (Nixon *et al.*, 1993a),



Plate 2. Pipe amygdules coalescing upward into a planar amygdule-rich horizon in a Karmutsen lava flow, 6 kilometres north-northeast of the eastern end of Rupert Inlet (93JHA10-2). The pipe amygdules form a lineation oriented approximately perpendicular to paleohorizontal.

prehnite-pumpellyite grade assemblages are widespread, and upper greenschist or lowermost amphibolite-grade facies appear in the thermal aureoles of intrusions of the Island Plutonic Suite.

#### INTRA-KARMUTSEN LIMESTONE

Two thin (<90 m) horizons of inter-volcanic, pale grey to buff-weathering limestone have been recognized near the top of the Karmutsen Formation. The main exposures form scattered outcrops in the low ground north of the Island Copper mine and roadcuts at the eastern end of Kains Lake (Figure 3). The dominant lithologies comprise thickly to thinly bedded limy mudstone, wackestone with more than 10% oolites set in a micritic matrix, and grain-supported packstone with a calcareous mud matrix. Bedding-parallel stylolites are found in micritic layers and some of the coarser grained beds contain rip-up clasts of black mudstone. Clearly, deposition took place in a shallow, near-shore environment periodically influenced by tidal currents.

## QUATSINO FORMATION

The Quatsino Formation generally comprises a pale to medium grey or buff-weathering, thickly bedded or massive lime mudstone, typically medium to dark grey on fresh surfaces. Rarely, the limestone is thinly bedded with undulose bedding surfaces, or laminated, where an argillaceous or silty component is commonly present. Elongate to irregular black chert concretions, usually less than 12 centimetres across, may locally exhibit a preferred orientation with their long dimensions parallel to the layering. Although the limestone is usually unfossiliferous, sparse coral fragments and crinoid stems, and rare ammonites and poorly preserved bivalves, have been observed. Recrystallization of Quatsino limestone is fairly common near faults and at the margins of plutons. In some exposures south of Nahwitti Lake, for example, the limestone has been recrystallized to a pale grey weathering, medium-grained marble with calcite crystals up to 3 millimetres in diameter. Anastomizing veins of calcite, and rarely quartz, are locally abundant near fault zones, and stylolites may be well developed on bedding planes.

The Quatsino - Parson Bay contact is well exposed in the Goodspeed River southwest of the Red Dog porphyry deposit at the boundary of the map area. Here, the top of the Quatsino Formation is a gradation from massive lime mudstone through a layer of oolitic grainstone 2 metres thick into 3 metres of massive algal mats with minor oolitic interbeds. This shallow intertidal to subtidal carbonate sequence is overlain by thin to medium-bedded lime mudstone and argillaceous lime mudstone with thin calcareous mudstone interbeds that define the base of the Parson Bay succession. Although oolitic horizons have been identified elsewhere in the Quatsino Formation, they appear to be relatively rare in the map area, and for the most part a carbonate basin/platform facies appears to be the dominant assemblage (Desrochers, 1989).

## PARSON BAY FORMATION

At least two distinct sedimentary facies of the Parson Bay Formation have been recognized in the map area: a predominantly calcareous facies at the western edge; and a weakly calcareous to non-calcareous facies in the northern and eastern parts of the area (Figures 3 and 4).

The western facies of the Parson Bay Formation is well exposed along the Goodspeed River and shores of Holberg Inlet. It consists of a faulted and folded succession of grey to buff-weathering, thin to medium-bedded micritic limestone, argillaceous limestone, calcareous siltstone and mudstone, and fine-grained calcareous sandstone with lesser thin shale interbeds. Lithologies exposed on Holberg Inlet contain abundant fossils including belemnites, bivalves and indeterminate Upper Triassic ammonoids (Arcestids; E. T. Tozer, personal communication, 1993). Similar lithologies in the Goodspeed River section contain graded bedding and

crosslamination. Bivalves identified by E. T. Tozer (personal communication, 1993) as *Halobia* (Carnian to middle Norian) and *Monotis subcircularis* Gabb (upper Norian, Cordilleranus zone) are locally prolific on shaly partings. The latter fossil locality appears to lie about 450 metres above the top of the Quatsino Formation; however, the stratigraphy here is complicated by northwest-trending mesoscopic folds. The contact with underlying massive limestone of the Quatsino Formation is transitional, as already described, and limestone layers at the base of the Parson Bay Formation contain abundant bivalves believed to be *Halobia*.

The northern facies of the Parson Bay Formation crops out along a northwesterly trending belt which extends from Red Dog through the Nahwitti River valley to Quatse Lake and beyond. The unit occupies areas of low relief and outcrops are generally sparse. The apparent stratigraphic setting of this facies at a number of localities along strike is shown in Figure 4. Estimated thicknesses are of the order of 400 to 600 metres except in the Nahwitti River area where structural thinning may have played a significant role. The northern facies may be tentatively subdivided into a lower predominantly calcareous to weakly calcareous sequence, and an upper predominantly non-calcareous succession. The lower part of the sequence consists of intercalated dark grey to black, generally thin to medium-bedded lime mudstone, argillaceous lime mudstone, laminated calcareous siltstone and shale. The upper part comprises thinly laminated, fissile, carbonaceous black shale and lesser dark grey siltstone. In the Red Dog - Nahwitti area, the transition from calcareous to non-calcareous lithologies is not exposed but appears to occur close to the top of the Quatsino Formation. Thin (1 cm) layers of buff-weathering micritic limestone occur sporadically throughout the section but form only a minor component of the stratigraphy. Bivalves identified as *Halobia* (E. T. Tozer, personal communication, 1993) are locally abundant near the transition from carbonate to shale-dominated sedimentation (sections A, B and D, Figure 4). In the east (section E), thickly bedded crystal tuffs or immature volcanic sandstones occur in the upper part of the succession where ammonoids and bivalves, tentatively identified as *Weyla*, are found in non-calcareous black shale interbeds. Although these strata are included here within the Parson Bay Formation, they may represent the base of a predominantly Lower Jurassic tuffaceous succession which is poorly exposed in this area.

## SILICEOUS SILTSTONE UNIT

A distinctive unit of siliceous siltstone overlies the Parson Bay Formation in the west and is relatively well exposed in the Red Dog - Nahwitti River area where it has an apparent thickness of 400 to 500 metres (sections A and B, Figure 4). These rocks were previously incorporated within the Parson Bay Formation by Muller *et al.* (1974) and Muller and Roddick (1983). The dominant lithologies are a pale grey to buff-weathering,

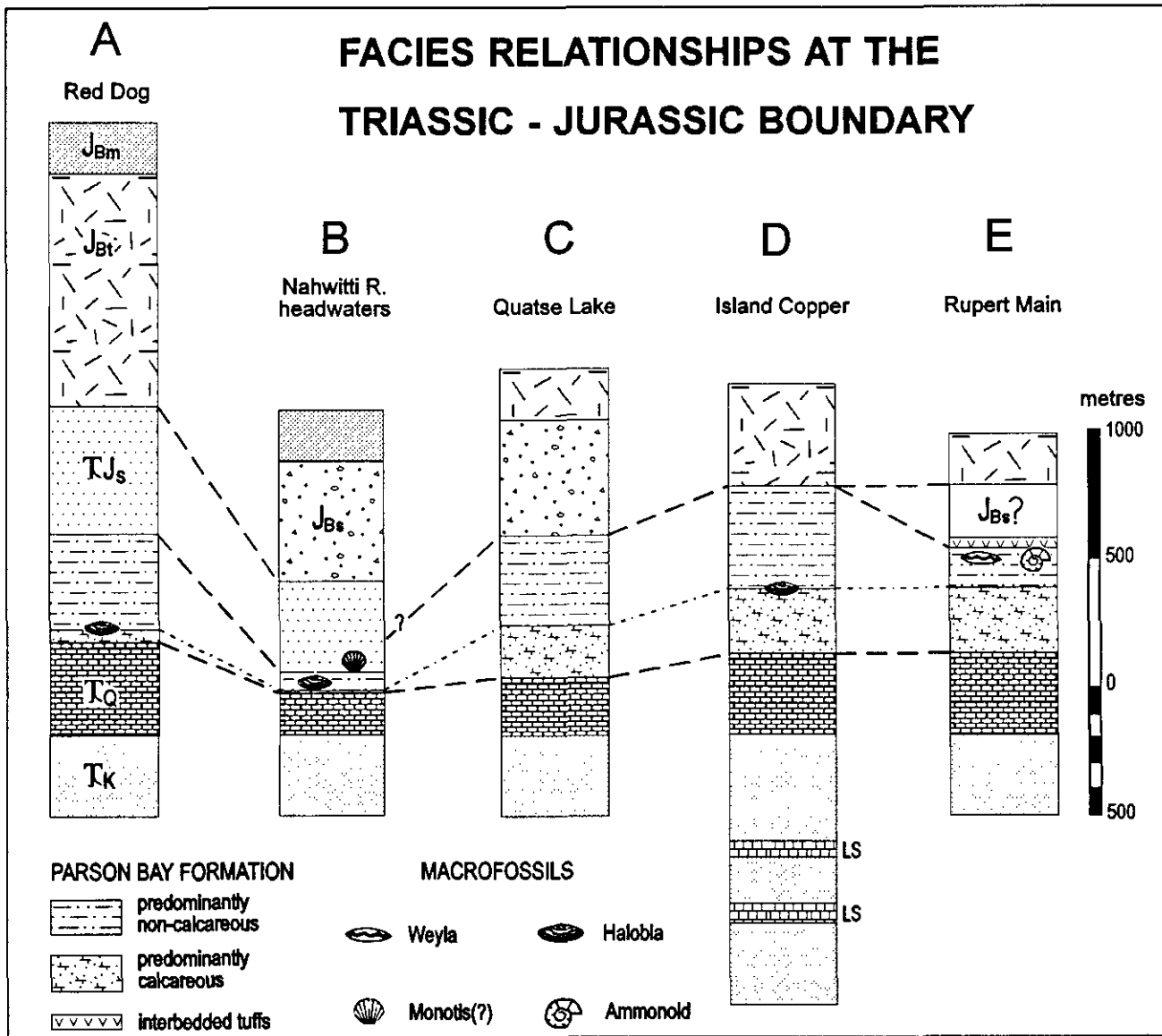


Figure 4. Apparent stratigraphy of Upper Triassic - Lower Jurassic sedimentary and volcaniclastic sequences showing facies variations. Thicknesses were estimated from geological relationships; lithologic patterns and locations of sections A-E are shown on Figure 3.

thinly bedded siliceous siltstone with dark grey shale partings up to 5 millimetres thick, and rare lenticular limestone units several metres in length. The lower part of the section contains rare calcareous mudstone layers (<10 cm thick), and siltstones high in the sequence appear to be more tuffaceous. North of Red Dog, the base of this unit is marked by a heterolithic volcanic conglomerate containing subrounded clasts of aphanitic to plagioclase-porphyrific mafic to intermediate rocks.

The latter bed appears to rest conformably on fine-grained clastics at the top of the Parson Bay Formation. South and west of Nahwitti Lake, the siltstones are locally hornfelsed and bleached near the margins of Island Plutonic Suite granitoids, and contain appreciable amounts of pyrite, and locally pyrrhotite, in veins and disseminations associated with white to purple-green skarn alteration. Quatsino limestone in this area has been recrystallized to a medium-grained marble; however,

limestone pods within the siltstone unit have retained their micritic character. Despite the effects of alteration, imprints of a bivalve that may be *Monotis* are prolific in certain shale horizons in the lower part of the section. Thus, it is tentatively suggested that the siliceous siltstone unit is uppermost Triassic (upper Norian) to lowermost Jurassic in age.

### BONANZA GROUP

The Bonanza Group may be conveniently described in terms of two stratigraphic entities: a predominantly subaqueous epiclastic-pyroclastic succession at the base of the group which can be correlated regionally; and an overlying, predominantly subaerial succession comprising felsic and mafic to intermediate flow and pyroclastic units that may have more restricted

significance. In total, the apparent thickness of the Bonanza Group exceeds some 3.5 kilometres, and most of this is subaerial.

## LOWER BONANZA STRATIGRAPHY

The base of the Bonanza Group is defined by a mixed succession of epiclastic and pyroclastic rocks which appears to conformably overlie the Parson Bay Formation in the east, and the siliceous siltstone unit in the west. The relative proportions of fine-grained clastics interbedded with coarser epiclastic and pyroclastic rocks locally define a sediment-tuff unit, or a predominantly pyroclastic unit, at or near the base of the Jurassic succession.

### Sediment-Tuff Unit

The sediment-tuff unit is exposed at the base of the Bonanza succession between Nahwitti and Quatse lakes (sections B and C, Figure 4). The base of this unit appears to be completely gradational with underlying siliceous siltstones and fine-grained clastics recur at intervals throughout the succession. However, it is distinguished from underlying siliciclastics by its overall coarser clastic nature and obvious pyroclastic component. The lithologies that are found are quite diverse. Medium grey-green heterolithic volcanic conglomerates contain rounded to subrounded clasts (<20 cm in diameter) of mafic to intermediate volcanic rocks, including plagioclase-phyric and amygdaloidal flows, and rare cobbles of hornblende porphyry. Dark greenish grey, thick to medium-bedded, predominantly monolithic volcanic breccias, tuff-breccias and lithic lapilli tuffs contain largely angular fragments of mafic to intermediate composition measuring up to 20 centimetres in length with most less than 6 centimetres. Accidental lapilli include rare aphanitic siliceous rocks that may be rhyolitic in composition. Clasts in the coarser monolithic deposits tend to be framework supported and may largely represent lag concentrates formed during pyroclastic flow emplacement. Finer grained interbedded clastic materials include thinly bedded to laminated tuffaceous sandstone and siltstone, crystal and crystal-vitric tuff, and siliceous siltstone, and locally exhibit sedimentary structures such as load casts. The volcanic sandstones and crystal tuffs are generally rich in plagioclase; the latter locally contain euhedral augite and possibly hornblende.

### Tuff Unit

The tuff unit is a predominantly pyroclastic succession that overlies siliceous siltstones in the Red Dog area and appears to rest on Parson Bay sediments in the vicinity of the Island Copper mine (sections A, C and D, Figure 4). This unit contains similar coarse pyroclastic-epiclastic lithologies as the sediment-tuff unit and may in part be correlative with it. The dominant lithologies are dark greenish grey, massive or thickly bedded heterolithic to monolithic lapilli tuffs, tuff-breccias, volcanic breccias and conglomerates, and minor crystal tuffs and volcanic sandstones. Clasts include aphanitic to amygdaloidal mafic rocks, plagioclase and

augite-phyric intermediate rocks, and rare aphanitic felsic volcanics and black shale. The tuff unit is considered to form part of a shoaling-upward succession deposited by submarine pyroclastic flow and epiclastic phenomena operating in a near shore (nearly emergent?) environment.

## MIDDLE TO UPPER BONANZA STRATIGRAPHY: PEMBERTON HILLS AREA

Mafic to intermediate flows found near the top of the Lower Bonanza succession described above mark the transition from a predominantly submarine to predominantly subaerial island-arc environment. The exact nature of this transition is not well documented at present due to generally poor exposure and the complexities associated with pluton emplacement and faulting. The middle to upper part of the the Bonanza stratigraphy is documented with reference to a type section in the Pemberton Hills region where access is best (Figure 5).

### Unit A

The uppermost part of the Bonanza stratigraphy in the Pemberton Hills area (unit A, Figure 5) is represented by a fairly monotonous sequence of dark greenish grey to reddish grey intermediate to mafic lava flows with apparently minor interbedded pyroclastic and sedimentary material. The lavas are predominantly fine (phenocrysts <2 mm) to medium (phenocrysts >2<5 mm) porphyritic varieties containing euhedral to subhedral plagioclase and pyroxene (largely augite); aphanitic and more coarsely porphyritic (phenocrysts <7 mm) flows are less common. The most phenocryst-rich flows contain 30 to 40% plagioclase and up to about 10% pyroxene. Flow breccias are typically well developed at the margins and internal jointing is locally pronounced. The joint pattern appears to correlate with total phenocryst content which may vary conspicuously within the same flow unit. Centimetre-scale platy jointing is well developed in phenocryst-poor flows or flow interiors whereas blocky joint patterns characterize phenocryst-rich flows or parts of flows. The more aphanitic lavas locally exhibit fine amygdaloidal textures with chlorite and hematite infillings. Major element geochemical analyses reported previously by Panteleyev and Koyanagi (1993, Table 2-7 1) and reproduced here (analyses 1-5, Table 1) indicate a rather restricted range of basaltic andesite to andesite compositions.

Intercalated clastic horizons in unit A provide valuable structural markers but outcrops are sparse. Thickly bedded tuff-breccias and lithic lapilli-tuffs contain angular to subrounded, variably oxidized and altered clasts (<20 cm in diameter) of the lavas which host them, and rare accidental fragments of hornblende porphyry. Their finely comminuted matrices usually carry euhedral to broken crystals of plagioclase and/or pyroxene. Thinly bedded to laminated, crystal-rich volcanic sandstones locally exhibit crossbedding and soft-sediment deformation features.

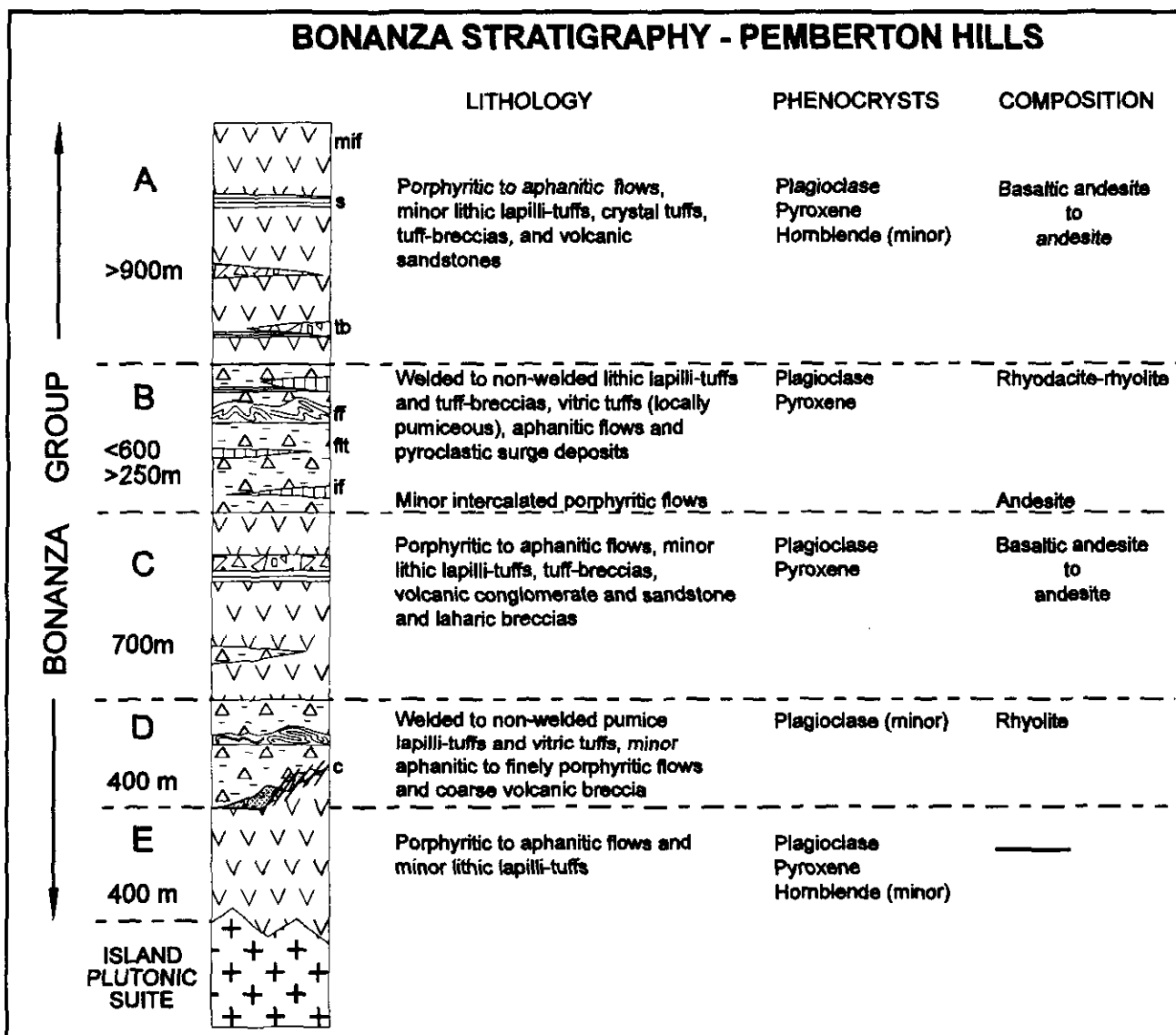


Figure 5. Schematic stratigraphy of the Bonanza Group in the Pemberton Hills area (see Figure 3). Key to lithologic patterns: mif, mafic to intermediate flows; s, volcanic sandstones; tb, tuff-breccias; ff, felsic flows; flt, felsic lapilli tuffs; if, intermediate flows; c, caldera margin.

#### Unit B

The upper felsic volcanic package (unit B, Figure 5) has a strike length of at least 25 kilometres and forms a southwesterly trending line of resistant knolls and ridges extending from Mount McIntosh to Holberg Inlet (Figure 3). The dominant lithologies are pale grey to white or buff-weathering ash-flow tuffs and viscous flows with minor proportions of intermediate lavas. The felsic rocks are variably altered rhyolites and rhyodacites (analyses 6-17, Table 1); intercalated porphyritic flows are basaltic andesite in composition (analyses 18 and 19, Table 1).

The lapilli tuffs are characterized by abundant angular to subangular clasts of aphanitic rhyolite, some with pronounced flow laminations, and a minor proportion of aphanitic to porphyritic mafic-intermediate volcanic rocks set in a finely comminuted vitroclastic matrix. These rocks locally grade downward, probably

within the same flow unit, into texturally similar tuff-breccias where accessory rhyolitic blocks measure up to 15 centimetres in diameter. The lithic population generally constitutes 15 to 25% by volume of the deposit with clasts ranging from 2 to 6 centimetres. Welding is usually not obvious in outcrop. However, flattened grey-green pumice lapilli are a conspicuous component of ash-flow tuffs exposed near the southwestern end of the unit (Wanokana Creek). At one locality in the Pemberton Hills (headwaters of Youghpan Creek), lithic lapilli-tuff grades upward into welded vitric tuff which in turn is overlain by a thin (0-12 cm) layer of bedded tuff followed by another ash-flow unit of welded vitric tuff. Locally, the latter unit has eroded through the layered horizon into the unit below. Internally, the layered vitric horizon is very thinly bedded to laminated and locally exhibits trough cross-stratification. Welding in the enveloping ash-flow tuff units is bedding parallel and continues without break where the stratified layer is missing. The

TABLE 1

## WHOLE-ROCK MAJOR ELEMENT COMPOSITIONS, BONANZA GROUP

No.	Sample	Unit <sup>1</sup>	SiO <sub>2</sub>	TiO <sub>2</sub>	Al <sub>2</sub> O <sub>3</sub>	Fe <sub>2</sub> O <sub>3</sub>	MnO	MgO	CaO	Na <sub>2</sub> O	K <sub>2</sub> O	P <sub>2</sub> O <sub>5</sub>	LOI	Total	SiO <sub>2</sub> <sup>*</sup>
1	92AP01/1-1	A	51.90	0.83	17.67	8.17	0.18	2.96	7.89	3.24	1.36	0.24	4.77	99.21	54.96
2	92AP01/2-2	A	50.79	1.01	17.09	9.54	0.19	2.91	9.47	2.75	0.22	0.20	5.25	99.42	53.93
3	92AP11/5-53	A	51.47	0.80	17.50	9.12	0.19	4.50	7.74	3.05	1.04	0.20	3.69	99.30	53.83
4	92AP01/5-5	A	54.14	0.86	16.60	8.13	0.16	2.60	5.01	3.42	1.25	0.17	7.16	99.50	58.63
5	92AP13/10-68	A	55.28	0.86	18.74	6.80	0.27	2.44	7.52	3.15	1.13	0.19	3.07	99.45	57.36
6	91AP41a	B	73.80	0.83	18.67	0.08	0.00	0.00	0.08	0.00	0.01	0.12	6.05	99.64	78.85
7	91AP20/6-95	B	96.34	1.67	0.95	0.17	0.00	0.00	0.01	0.00	0.00	0.01	0.59	99.74	97.17
8	93GNX14-2-6	B	78.62	0.87	6.59	2.22	0.01	0.05	0.32	0.38	1.17	0.19	9.02	99.45	86.94
9	93GNX15-4	B	70.07	0.56	9.92	9.47	0.01	0.06	0.12	0.14	0.14	0.10	9.35	99.96	77.33
10 <sup>†</sup>	92AP19/1-109	B	60.54	1.11	15.49	10.63	0.00	0.00	0.17	0.00	0.01	0.23	11.22	99.40	68.66
11 <sup>†</sup>	92AP19/1-110	B	70.16	1.45	18.65	1.34	0.00	0.02	0.16	0.00	0.01	0.20	7.42	99.41	76.27
12 <sup>†</sup>	92AP19/1-111	B	86.24	2.04	2.03	7.94	0.00	0.00	0.03	0.00	0.00	0.04	2.53	100.85	87.71
13 <sup>†</sup>	92AP19/1-112	B	93.90	2.81	2.13	0.74	0.00	0.00	0.03	0.00	0.00	0.03	1.12	100.76	94.24
14 <sup>†</sup>	92AP19/1-113	B	63.66	0.84	17.06	7.09	0.00	0.25	0.16	0.00	1.36	0.20	9.06	99.68	70.25
15 <sup>†</sup>	92AP19/1-114	B	66.68	0.67	12.92	8.55	0.00	0.21	0.14	0.00	1.51	0.21	8.38	99.27	73.36
16 <sup>†</sup>	92AP19/1-115	B	63.38	1.05	6.95	7.47	0.13	2.46	6.11	0.30	0.36	0.11	10.81	99.13	71.76
17	93GNX10-1	B	70.93	0.69	19.64	0.27	0.01	0.05	0.10	0.06	0.04	0.10	7.88	99.77	77.19
18	92AP19/2-119	B	49.23	0.90	19.21	9.01	0.19	3.05	10.03	2.63	0.44	0.20	4.45	99.34	51.88
19	92AP19/2-120	B	48.34	0.86	17.76	9.22	0.26	3.26	6.09	5.24	0.31	0.19	7.94	99.47	52.81
20	92VKO8-1	C	54.46	0.77	17.49	8.60	0.20	3.57	7.61	2.84	1.32	0.23	2.64	99.73	56.09
21	92AP16/1-77	C	55.64	0.83	17.54	8.52	0.16	3.01	7.31	3.05	1.72	0.23	1.76	99.77	56.77
22	92AP20/8-128	C	54.36	0.81	15.97	8.05	0.19	4.94	3.65	3.04	1.95	0.15	6.22	99.33	58.38
23 <sup>†</sup>	92AP19/1-116	C	54.59	0.94	15.51	7.46	0.11	5.78	3.36	1.01	1.13	0.21	9.11	99.21	60.59
24 <sup>†</sup>	92AP19/1-117	C	56.74	0.83	16.02	8.44	0.17	4.48	3.56	2.62	2.60	0.17	3.60	99.23	59.33
25 <sup>†</sup>	92AP19/1-118	C	55.84	0.83	15.84	8.38	0.08	4.30	4.54	2.29	1.07	0.17	5.92	99.26	59.63
26	92AP21/7-132	C	53.48	0.78	15.95	8.36	0.25	5.88	6.63	2.66	1.80	0.15	3.55	99.49	55.74
27	92VKO8-4	D	74.22	0.27	13.05	2.09	0.11	0.86	1.72	3.27	1.87	0.08	1.84	99.38	76.09
28	92AP16/7-83	D	69.80	0.30	14.60	2.52	0.12	1.34	2.40	3.32	2.86	0.07	2.05	99.38	71.71

<sup>1</sup> See Figure 5

Data from Panteleyev and Koyanagi (1993).

\* Recalculated to 100% anhydrous with total Fe as Fe<sub>2</sub>O<sub>3</sub>.

† Borehole samples labelled according to increasing depth from 10 to 16 and 23 to 25.

textural and stratigraphic relationships of the bedded tuff horizon are consistent with features found in pyroclastic surge deposits.

The pyroclastic flow deposits pass laterally along strike, and are locally overlain or interbedded with, aphanitic rhyolite flows (and dikes) with locally well-preserved flow laminations and flow folds. Flow breccias are relatively common and contain rounded to angular blocks of dense aphanitic flow material; some of these breccias carry pumiceous blocks with partially preserved tube vesicles.

The andesitic lavas are a minor but distinctive component of this unit. They are dark greenish grey, strongly porphyritic flows carrying blocky to lath-like plagioclase (<7 mm) and pyroxene (<2 mm) phenocrysts that form up to 15 and 10 modal percent respectively. Platy jointing oriented parallel to the flow foliation is locally quite pronounced.

### Unit C

The upper rhyolitic sequence is underlain by a succession of dark green-grey to maroon mafic to

intermediate lavas interbedded with relatively minor proportions of epiclastic and pyroclastic rocks of similar composition. Most of the volcanic rocks range from andesite to basaltic andesite in composition (analyses 20-26, Table 1). The lavas are usually porphyritic with plagioclase (<5 mm) and pyroxene (<3 mm) phenocrysts typically forming up to 35% by volume of the rock. Flow breccias are observed locally and the more porphyritic varieties exhibit flow laminations and well-developed flow folds due to their high apparent viscosity (Plate 3). A thickly bedded conglomerate with well-rounded cobbles of volcanic rocks occurs near the middle of the succession and thinly bedded tuffaceous sandstones are found near the base. Lithic lapilli-tuffs and tuff-breccias contain matrix-supported, angular to subrounded clasts of porphyritic to aphanitic lavas. Rare lahars breccias contain a similar population of clasts up to 0.5 metre in diameter, supported by a brick-red clay-rich matrix.

### Unit D

The only known outcrops of the lower rhyolitic unit occur north of the Pemberton Hills at the northern



Plate 3. Flow fold in porphyritic andesite flow, Bonanza Group (unit C, Figure 5); quarry 0.4 kilometre northeast of the Wann Knobs, Pemberton main logging road (93GNX10-2). The high apparent viscosity of this flow is due to its crystal-rich nature.

extremity of the logging road system (H600 road). The sequence is dominated by pale grey to buff-weathering ash-flow tuffs with minor airfall deposits and rhyolitic flows or dikes that are variably propylitized and clay-altered. Analytical data for two fairly fresh samples indicate rhyolitic compositions (analyses 27 and 28, Table 1).

The airfall deposits are thinly bedded vitric and crystal tuffs with some normally graded interbeds that consistently face and dip to the southwest. Flow or dike material is commonly flow laminated and aphanitic or finely porphyritic (<2 mm) with several percent feldspar phenocrysts. The lapilli tuffs are conspicuously pumiceous with dark grey-green, variably flattened pumice lapilli defining non-welded to welded textures. Their lithic population rarely exceeds 5% by volume of finely crystalline to porphyritic intermediate to felsic volcanic rocks.

Complex stratigraphic and structural relationships are exposed in roadcuts along the southeastern edge of the main outcrop area. A distinctively coarse heterolithic breccia at the base of the succession contains angular to subrounded blocks up to 3 metres across set in a finely comminuted dark greyish green matrix. This framework-supported breccia contains clasts of aphanitic and plagioclase-phyric basaltic to intermediate rocks, some of which were clay-altered or propylitized prior to brecciation, and sparse fragments of flow-banded rhyolite. This layer represents a debris flow or landslide deposit most likely associated with a vent-forming eruption. This deposit is overlain by, and in gradational contact with, non-welded pumiceous tuff that grades upward into partially welded lapilli tuff. Further south

and a little higher in the section, welded vitric tuff, a pumice-poor horizon within the lapilli tuff sequence, overlies aphanitic intermediate volcanic rocks of unit E. The contact is sharp and depositional with no break in welding. The lack of a flow-top breccia at this contact implies that either a period of erosion preceded deposition of the pyroclastic flows or that deposition occurred on the surface of a rotated block. At the northeastern limit of exposure, these intermediate flows are faulted against the lapilli tuffs and underlying volcanic breccia by one of a series of en echelon east-northeasterly trending faults (and subparallel mafic dikes). These faults are no doubt responsible for the rotation of welded fabrics in the lapilli tuffs at this locality which strike at high angles to regional bedding trends and dip moderately to steeply (30-60°) west and north. This fault-controlled margin with local evidence for (catastrophic?) deposition of coarse volcanic breccias immediately preceding ash-flow deposition is consistent with relationships typical of caldera margins. A partially exhumed caldera source-region in which the felsic pyroclastic rocks of unit E are preserved as an intracaldera facies would also explain the restricted extent of pyroclastic deposition. This interpretation requires a disconformity between units C and E along strike.

#### Unit E

Stratigraphically beneath the lower rhyolitic package, and best exposed in roadcuts north and east of the Hushamu porphyry (Figure 3), is a sequence of dark grey-green and medium grey to pinkish grey intermediate to mafic flows and flow breccias. The more altered rocks near intrusive contacts are buff to rusty weathering due to disseminated pyrite. Plagioclase-phyric lavas of andesitic composition appear to be the dominant lithology; no analyses of these rocks are currently available. Some of these rocks carry phenocrysts of hornblende (< 3mm) and xenoliths of hornblende diorite. At this time, it is not clear whether the latter lithologies are indeed part of the stratigraphy or a porphyritic phase of the Island Plutonic Suite.

#### BONANZA VOLCANISM: A PREDOMINANTLY SUBAERIAL SETTING

The onset of Bonanza volcanism is marked by a coarsening-upward sequence of intercalated marine, epiclastic and pyroclastic deposits which marks the gradual emergence of a volcanic island arc in the Early Jurassic. In the Quatsino - Port McNeill map area, this sequence is marked by the siliceous siltstone unit which overlies Parson Bay lithologies in the northwestern part of the map area, the overlying tuff-siltstone unit which we have tentatively assigned to the lowermost Jurassic, and the tuff unit which is well developed in the east. The persistence of oxidized massive flows and flow breccias at intervals throughout the Bonanza stratigraphy, the occurrence of welded tuffs within felsic pyroclastic sequences, the apparent lack of pillowed sequences and hyaloclastite deposits, and dearth of marine incursions

within the volcanic pile indicate that Bonanza volcanism occurred in a predominantly subaerial setting. This contrasts little with the Mahatta Creek area where intra-Bonanza marine sedimentary rocks and pillow breccias have been documented but are nevertheless scarce (Nixon *et al.*, 1993a). In the present map area, large volumes of porphyritic lavas, predominantly andesite and basaltic andesite, are the main component of the Bonanza succession. Of the two felsic volcanic packages identified in the Pemberton Hills area, the upper unit is the most widespread and marks a significant episode of rhyolitic volcanism. Both felsic horizons represent the products of flow-dome and caldera complexes associated with what appear to be relatively small volumes of pyroclastic flow material. They are also important from a mineral potential standpoint as discussed later.

## CRETACEOUS ROCKS

Lower Cretaceous strata equivalent in part to the Longarm Formation, as well as the younger Coal Harbour Group, are exposed principally on the shoreline along Holberg and Rupert inlets, and for short distances inland where outcrops are sparse (Figure 3). Additional exposures of Upper Cretaceous strata (Nanaimo Group equivalents) are found on the east coast in Port Hardy and vicinity. Throughout the Quatsino - Port McNeill map area, it is evident that both nonmarine and marine facies are represented in the Cretaceous succession.

### STRATA EQUIVALENT TO THE LONGARM FORMATION

Lower Cretaceous strata of approximately Hauterivian-Barremian age crop out at various localities around Holberg Inlet. The strata were noted by Jeletzky (1976), who studied small exposures in Apple Bay, and they were subsequently correlated with the Longarm Formation of the Queen Charlotte Islands by Muller *et al.* (1974) based on age relationships. Although Valanginian-Barremian strata near the entrance to Quatsino Sound (Winter Harbour area; Figure 1) are indeed similar to typical Longarm Formation rocks of the Queen Charlotte Islands, those in Holberg Inlet are lithologically distinct. For this reason, we treat the latter as "Longarm Formation equivalents".

Longarm Formation equivalent strata in Holberg Inlet consist of sandstone, pebble conglomerate, siltstone and, locally, coal seams up to approximately 10 centimetres in thickness. The strata are best displayed along the shoreline of Holberg Inlet in exposures some 5 and 10 kilometres west of Coal Harbour at Apple Bay and near Henriksen Point (localities 1 and 2 respectively, Figure 3), and appear to form an overall fining-upward sequence. The base of the Longarm Formation equivalent strata has not been observed but, based on facies and structural relationships, the succession is inferred to rest unconformably on volcanic rocks of the Bonanza Group.

The stratigraphically lowest units of this package consist of massive, medium to thinly bedded sandstone,

locally pebble rich, with interstratified coal seams and abundant plant debris. These rocks grade upward into medium-bedded, trough cross-stratified to massive sandstone, and finally into hummocky cross-stratified, medium to fine-grained sandstone. Measurements of trough cross-stratification in the coarser sandstone bodies indicate southeasterly to southwesterly directed paleocurrents. Resistant, hummocky cross-stratified sandstone beds in the upper part of the sequence at Apple Bay are interstratified with less resistant and poorly exposed marine siltstone and mudstone units, giving the appearance of a sandstone-rich succession; in fact, the fine-grained facies predominate and reflect a continuation of the trend towards increasing water depth seen throughout the Cretaceous section. Thus, the exposures of Longarm Formation equivalent strata in Holberg Inlet appear to comprise a single overall fining-upward sequence. The Hauterivian-Barremian age of Longarm Formation equivalent strata recognized to date in Holberg Inlet is based on ammonite faunas, and inoceramid and trigoniid bivalves (summarized in Muller *et al.*, 1974).

### COAL HARBOUR GROUP

The base of the Coal Harbour Group has not been observed at Coal Harbour, but is inferred to rest unconformably on volcanic rocks of the Bonanza Group (see summary in Jeletzky, 1976). The lowest strata consist of massive conglomerate with minor lenses of coarse-grained channel sandstone (*i.e.* Blumberg Formation of Jeletzky, 1976; the 'coarse arenite unit', which Jeletzky believed to underlie the Blumberg Formation, is here interpreted as sandstone lenses within the Blumberg Formation conglomeratic succession). Earlier mapping by staff at the Island Copper mine identified a basal contact of Blumberg Formation conglomerate resting on the Bonanza Group (J. Fleming and A. Reeves, unpublished data), but this exposure has subsequently been paved over. The conglomerate is succeeded up-section by trough cross-stratified sandstone intercalated with siltstone, minor conglomerate and minor coal.

The overall fining-upward facies trend noted in Jeletzky's (1976) measured section of the Blumberg Formation southwest of the Island Copper minesite is duplicated on the shore at Coal Harbour. Measurements of trough cross-stratified sandstone of the Blumberg Formation in both these sections indicate southeasterly to southwesterly paleocurrent trends, similar to those determined for the Longarm equivalent strata.

The age of the Coal Harbour Group is poorly constrained and relies on the identification of palynomorphs of late Early Cretaceous (Albian) age made by Hopkins (in Jeletzky, 1976) and collected from the section southwest of the Island Copper mine.

### STRATA EQUIVALENT TO THE NANAIMO GROUP

Strata equivalent in age to the Nanaimo Group of

southern Vancouver Island (Muller and Jeletzky, 1970) crop out in the northeastern part of the map area (Figure 3). The strata were studied previously by Jeletzky (1969) and Muller and Jeletzky (1970). Most exposures are found in recent roadcuts in the town of Port Hardy, and along the shoreline southeast of the town. The strata comprise gently dipping, shallow-marine to nonmarine facies, and include medium to coarse-grained sandstone and pebble conglomerate, siltstone and minor coal. Although no contact with older rocks has been seen, structural relationships suggest that the succession rests with angular unconformity on Karmutsen Formation volcanic rocks. The age of Nanaimo Group equivalent rocks in the map area is late Upper Cretaceous (approximately Campanian), as determined from marine molluscs (Jeletzky in Muller and Jeletzky, 1970).

### ***SEDIMENTARY ROCKS OF UNCERTAIN AFFINITY (JURASSIC-CRETACEOUS)***

Sedimentary rocks previously mapped as Lower Cretaceous Longarm Formation by Muller *et al.* (1974) along the north shore of Holberg Inlet just east of the mouth of Clesklagh Creek (locality 3, Figure 3) consist of vertically dipping, southward-younging, interstratified tuffaceous sandstone and volcanic conglomerate, flow breccias of andesitic composition, and minor thin coal seams. The age of these rocks is presently unknown but given the predominance of volcanoclastic debris and their compositional immaturity, they appear more likely to belong to the Bonanza Group.

A faulted, northeasterly dipping stratigraphic section exposed along logging roads above, and east of, Clesklagh Creek (locality 4, Figure 3) consists of a basal unit of coarse-grained pebbly volcanic sandstone, locally containing rhynchonelliform brachiopods and apparently interstratified with andesitic volcanic rocks. These strata appear to be overlain by several tens of metres of silty mudstone containing belemnite fragments. The mudstone section is in turn overlain by a thick sequence of marine to nonmarine(?), cross-stratified sandstone and siltstone which forms the top of the section. The age of the brachiopods found at the base of the section is presently unknown but brachiopods of this general type are common in Lower to Middle Jurassic rocks of the Insular Belt (H.W. Tipper, personal communication, 1993). It is therefore possible that the Clesklagh Creek strata may also belong to the Bonanza Group.

### **INTRUSIVE ROCKS**

Intrusive rocks in the map area comprise stocks and batholiths of the Island Plutonic Suite and their associated porphyritic phases, and mafic to felsic dikes and sills of Karmutsen, Bonanza and Tertiary age. Potassium-argon isotopic determinations summarized by Muller *et al.* (1974) on hornblende and biotite from intrusions of the Island Plutonic Suite in the map area yield dates between 145 and 169 Ma [Middle Jurassic

(Bathonian) to the Jurassic-Cretaceous boundary according to the time scale of Harland *et al.*, 1990]. These dates are generally considered to be too young and reflect minimum (cooling) ages only. Rubidium-strontium isochron dates of  $177 \pm 10$  Ma (Muller, 1977) and approximately 180 Ma (dated by R. L. Armstrong; J. Fleming, personal communication, 1992) provide better estimates of actual intrusion ages (*i.e.* latest Early to earliest Middle Jurassic).

### ***ISLAND PLUTONIC SUITE***

Granitoid rocks of the Island Plutonic Suite underlie sizeable areas of subdued relief in the central and northwestern parts of the map area. The principal rock types are pale grey to buff-weathering, generally medium-grained and equigranular, hornblende-bearing diorite or monzodiorite and quartz monzodiorite to granodiorite (nomenclature after Le Maitre, 1989). Propylitic and argillic alteration assemblages and skarning are locally well developed at their margins. Crosscutting fractures and veins are commonly filled with chlorite, hematite, epidote, quartz, kaolin, zeolites and, rarely, potassium feldspar.

The southern margin of the Nahwitti batholith north of Nahwitti Lake (Figure 3) is composed of coarse to medium-grained (2-6 mm) equigranular biotite-bearing hornblende quartz diorite to monzodiorite containing about 5% modal quartz and up to 20% hornblende. A marginal zone about a kilometre wide contains subequal proportions of biotite and hornblende and sparse xenoliths of feldspathic amphibolite. The granitoid rocks are extremely fresh and have been sampled for Ar-Ar dating. Conventional K-Ar dates on hornblende and biotite separates taken from the southern margin of the batholith range from 154 to 169 ( $\pm 8$ ) Ma (summarized in Muller *et al.*, 1974).

The Red Dog stock is a crowded feldspar porphyry with a finer grained, less porphyritic phase along its eastern margin and an equigranular quartz diorite phase whose contact relationships have not been observed. Blocky to lath-shaped feldspars averaging 3 to 5 millimetres in length and reaching 15 millimetres comprise up to 35 modal % of the rock together with chloritized hornblende (10%) and sparse quartz (1-2%). The finely crystallized mesostasis is grey to black. Three small stocks of diorite and "quartz-eye" granodiorite occur east of Red Dog (only one is shown on Figure 3); extensive hornfelsing of their hostrocks suggests that these bodies are more extensive at depth although not necessarily connected.

The large plutonic body south of Nahwitti Lake, referred to here as the Wanokana batholith, apparently extends from Hepler Creek in the west through Hushamu to Wanokana Creek in the east where it is disrupted by faulting (Figures 3 and 6). The Wanokana intrusion and its wallrocks are much more propylitized and clay-altered than the southern margin of the Nahwitti batholith. In the vicinity of Hepler Creek, the rock is a medium to coarse-grained (<7mm), equigranular hornblende quartz

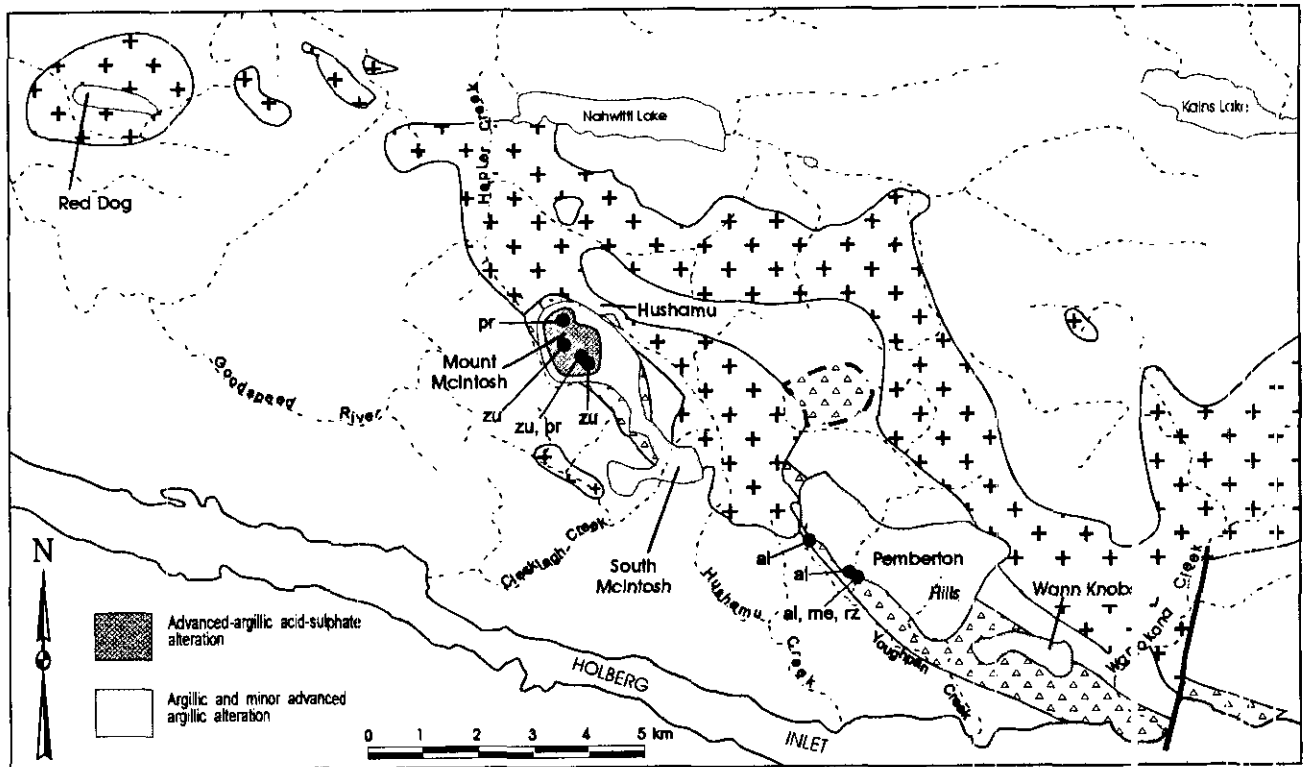


Figure 6. Geologic setting of acid sulphate alteration assemblages and X-ray diffraction sample sites.

monzodiorite to quartz diorite containing variable proportions of quartz (5-20 modal %) and partially chloritized hornblende (<15 modal %), with a plagioclase:potassium feldspar ratio approaching 2:1. These relatively quartz-rich rocks are also found along the northern margin of the pluton in outcrops east of Nahwitti Lake. On ridges north and east of the Hushamu deposit, dark grey-green, fine to medium-grained diorites and andesitic country rocks are extensively pyritized (2-10 volume % pyrite), and are difficult to tell apart in areas of more intense alteration. A similar fine-grained marginal phase is also exposed farther south in streams draining the northern flank of South McIntosh and high on the eastern flank of the lower Hushamu Creek valley (Figure 6). In these areas, a chloritic fine-grained marginal diorite grades into a medium-grained hornblende diorite with increasing distance from the contact. These rocks contain abundant disseminated pyrite (up to 10 volume %) and are partially altered to clay minerals. Exposures near Wannokana Creek are largely medium-grained (<5 mm) equigranular hornblende monzodiorite or diorite that may be weakly porphyritic with plagioclase reaching 8 millimetres. Minor leucocratic monzodiorite with less than 10% modal hornblende and rare medium-grained syenite with up to 70% potassium feldspar, 15% plagioclase and 15% hornblende ± biotite are also observed. A dark greenish grey fine to medium-grained hornblende-bearing dioritic phase again occurs along the northern contact with pyritic and propylitized andesitic volcanics several kilometres due north of the Wann Knobs (Figure 6). Two K-Ar determinations on biotite from Hepler Creek and

the northern margin of the batholith southwest of Nahwitti Lake yield dates of  $145 \pm 5$  and  $159 \pm 5$  Ma, respectively (Muller *et al.*, 1974).

Two small plutons farther east intrude the Karmutsen Formation. The Quatse stock northeast of Quatse Lake (Coal Harbour intrusion of Muller *et al.*, 1974) is a medium-grained hornblende monzodiorite or diorite with as much as 20 to 25% modal amphibole and less than 15% potassium feldspar. The southeastern margin of the intrusion is appreciably propylitized with thin anastomizing late-stage veins of kaolin cored with quartz. The Glenlion stock, exposed in roadcuts along the Holberg - Port Hardy road and in the headwaters of Glenlion Creek for which it is named, is a medium to coarse-grained, equigranular to weakly porphyritic (<7 mm) hornblende diorite. Intrusion breccias (agmatites) and concentrations of angular to subangular xenoliths of Karmutsen lavas occur at its margins; these mafic wallrocks are generally pyritized and locally silicified. Rare centimetre-scale modal layering of hornblende and feldspar is developed within zones up to several metres wide that parallel the ductily sheared margins of younger dikes.

The Island Copper intrusion is a well north-west-trending, northerly dipping dike-like body in the order of 100 to 150 metres wide that is probably an offshoot of the stock at the eastern end of Rupert Inlet. The dike is a quartz feldspar porphyry with phenocrysts of rounded to partially embayed quartz (<1 cm; 5-15 modal %), subhedral, locally glomerophytic, plagioclase (<4 mm; <30%) and minor altered mafic phenocrysts set in a fine-grained quartzofeldspathic groundmass. The Rupert

stock is a medium to coarse-grained, equigranular to porphyritic granodiorite containing up to 30% modal quartz, 60% feldspar and about 10% chloritized hornblende. Outcrops in the eastern part of the intrusion locally exhibit intense argillic alteration. Detailed descriptions of the geology of these intrusions are given by Cargill *et al.* (1976). A K-Ar date on biotite from the Rupert stock yielded an apparent crystallization age of  $154 \pm 6$  Ma (Muller *et al.*, 1974).

## MINOR INTRUSIONS

The majority of dikes and sills in the map area are microdiorite or aphanitic to plagioclase  $\pm$  pyroxene-porphyritic mafic to felsic equivalents of Bonanza Group volcanic rocks. Intrusions of Karmutsen age have only rarely been identified; a fine-grained basaltic sill with well-developed columnar jointing is exposed in a roadcut about 1.4 kilometres east of Georgie Lake. Dikes and sills of fine to medium-grained diorite to quartz monzodiorite or granodiorite are associated with intrusions of the Island Plutonic Suite. Hornblende-bearing porphyritic intrusions are widespread in the Bonanza Group and Upper Triassic sedimentary succession and commonly occur as marginal phases of granitoid plutons or crosscutting dikes. Pale grey weathering, coarsely porphyritic dikes of quartz (<1.5 cm) and plagioclase (<1 cm), rarely accompanied by hornblende (<1.5 cm) with hiatal to seriate textures are found southwest of Quatse Lake and on Rupert Main logging road southeast of Rupert stock, and represent apophyses of nearby granitoids of the Island Plutonic Suite. Hornblende plagioclase porphyries are generally medium porphyritic (<5 mm) with euhedral hornblende (<15%) and plagioclase (<20%) phenocrysts. Coarse hornblende ( $\pm$  plagioclase) porphyries have hiatal textures with large (<2 cm) euhedral amphibole phenocrysts set in a quartzofeldspathic microcrystalline to fine-grained groundmass. Soft-sediment deformation features have been observed at the base of sills intruding thinly bedded Bonanza sediments and within intrusion breccias cutting Parson Bay clastics north of Island Copper. These breccias comprise angular to subrounded clasts (<20 cm) of hornblende porphyry and xenoliths of siltstone and limestone derived from the underlying Quatsino Formation. A well-chilled, sparsely hornblende-phyric groundmass in the core of the intrusion is replaced by a black shaly matrix at the margin. Locally, contorted xenoliths of thinly bedded sediment are also observed. These textures imply that intrusion began in Early Jurassic time before Upper Triassic sediments were completely consolidated. In fact, angular xenoliths of hornblende porphyry and medium-grained diorite have been found in the basal Bonanza flow and tuff unit exposed along the Coal Harbour - Port Hardy road.

## TERTIARY DIKES

Some dozen or so mafic dikes of presumed Tertiary

age are distributed throughout the map area. They appear to be less prolific here than farther south in the vicinity of the Brooks Peninsula fault zone (Nixon *et al.*, 1993a), although this observation may be more apparent than real. The dikes are up to 3 metres wide and are distinguished by their fresh appearance, blocky jointing and dark rusty brown, spheroidal weathering. Fresh surfaces are dark grey, and there are both aphanitic and plagioclase-phyric (<15% phenocrysts) varieties. Amygdules may be filled with carbonate and pyrite, and flow-laminated margins are common. Dikes of rhyolitic as well as basaltic composition cut the Cretaceous rocks at several localities in Apple Bay and Coal Harbour. Most of these dikes dip steeply to moderately ( $90$ - $60^\circ$ ) and strike  $015$  to  $070$  or  $315$ . A whole-rock K-Ar determination for a basaltic dike on East Stragglng Island in Holberg Inlet yielded an Early Oligocene date of  $32.3 \pm 1.6$  Ma (Muller *et al.*, 1974).

## STRUCTURE

The structural style in the Quatsino - Port McNeill area is dominated by block faulting. Strata within individual fault blocks typically have a consistent dip and facing direction toward the south to southwest, describing a northwesterly trending homocline. On a regional scale, the area makes up part of the western flank of the Victoria arch, a northwesterly trending anticlinorium which is known to culminate east of Nimpkish Lake, southeast of the study area (Muller *et al.*, 1974). The northwesterly structural grain is further emphasized by prominent northwesterly trending transpressional faults. In all, three phases of deformation have been recognized in the map area, but have not yet been analyzed in detail. Comments on the main events are offered below.

### PHASE 1: POST-EARLY JURASSIC TO PRE-CRETACEOUS DEFORMATION

The earliest phase of deformation is related to an east to northeast-directed compressional event which resulted in regional tilting of the Lower Jurassic and older strata to form the Victoria arch. This was accompanied by flexural-slip folding and the development of northwesterly trending thrust faults. Early northeast-directed compression is indicated by the presence of a locally well-developed, northwesterly striking, stylolitic cleavage in Quatsino limestone.

### PHASE 2: POST-MID TO (?)PRE-LATE CRETACEOUS DEFORMATION

A second deformational episode postdates deposition of mid-Cretaceous Coal Harbour Group sediments and may predate deposition of the Upper Cretaceous Nanaimo Group. This episode was caused by a period of intense strike-slip faulting and lesser thrusting, which resulted from northerly directed compression. Faults formed

during this episode are the dominant northwesterly trending structures in the area and, in many cases, have produced significant drag folding, particularly where adjacent units are well bedded. The most obvious of these are northwesterly striking, high-angle oblique-slip faults which have a right-lateral and south-up sense of motion. The faults cause most of the stratigraphic repetitions that occur in the map area. The Holberg fault, a curvilinear south-side-up thrust, for the most part hidden beneath Holberg Inlet except near Coal Harbour (Figure 3), formed during this phase of deformation in response to northward-directed stresses. This important structure places Upper Triassic strata on the south side of the inlet adjacent to mid-Cretaceous and older strata on the north side of the inlet. The most convincing kinematic indicator for movement on the Holberg fault is the presence of many northerly verging, gently plunging drag folds in its footwall. This sense of motion is also demonstrated by minor coaxial thrust faults and a well-developed stylolitic cleavage in limestones in the footwall. Some of the major northwesterly trending, right-lateral oblique-slip faults in the area are splays off the Holberg fault; for example, faults near the western limit of mapping. Other major faults with a similar sense of motion include the Kains Lake and Nahwitti Lake faults.

### ***PHASE 3: TERTIARY DEFORMATION***

The most recent phase of deformation in the area is represented by northwesterly to north-northwesterly directed extension which postdates the deposition of Upper Cretaceous Nanaimo Group sediments. This phase is represented by minor northeasterly to east-northeasterly striking normal faults which affect Upper Cretaceous and older strata. Reactivation of pre-existing strike-slip faults occurred, but appears to be rare. Tertiary dikes intruded during this phase of deformation commonly strike toward the northeast, although this is not the only observed orientation.

### ***LITHOLOGIC CONTROLS ON STRUCTURAL STYLE***

The Karmutsen volcanic rocks form a rigid coherent mass that has deformed by strictly brittle mechanisms; faults and shear fractures are common. Bedding-parallel slip is rare due to an apparently high degree of cohesion along flow contacts. Beds were tilted during the earliest phase of deformation described above, but later faulting does not appear to have caused significant rotation of bedding. This has resulted in a bedding orientation which is remarkably consistent throughout the map area (Figure 7).

Limestone of the Quatsino Formation has accommodated strain by both brittle and ductile mechanisms. This unit typically dips moderately to the southwest or south except where the beds have been dragged into flexural-slip folds in response to faulting

(Figure 7). Pressure solution to form stylolite seams is common in most limestone outcrops and, together with associated calcite veins, has probably resulted from tectonic thickening. Quatsino limestone reaches extreme apparent thicknesses in the region east of Jeroutsos Inlet and Quatsino Narrows. These anomalous thicknesses are at least partly due to folding and thrust fault repetitions in this area.

Shale, siltstone and limestone of the Farson Bay Formation have largely accommodated strain by bedding-parallel shear. This has resulted in the development of mesoscopic folds which are particularly evident adjacent to fault zones (Figure 7). The shale facies of the Farson Bay Formation, which crops out in the northwest part of the map area, may have controlled faulting, locally to some degree as this facies is found in the footwall of several megascopic faults.

Volcanic rocks of the Bonanza Group have deformed predominantly by shear. This unit is characterized by very broad zones of intensely sheared rock adjacent to megascopic faults. Commonly these rocks dip moderately to the south or southwest but they are locally dragged adjacent to faults giving bedding attitudes a more random orientation (Figure 7). Part of this pattern may well reflect syn-Bonanza structural complexities such as caldera formation.

### ***ECONOMIC GEOLOGY***

The Quatsino - Port McNeill map area contains economically important porphyry copper-niobium-gold deposits, including the Island Copper mine, and base and precious metal skarns in addition to mineralization associated with epithermal acid sulphate alteration zones which are the current focus of exploration. In all, a total of 83 mineral occurrences are listed in the MINFILE database, which is the principal source of grade and tonnage information given below.

### ***SKARNS***

Most of the 18 or so mineral occurrences in the area that are classified as skarns, largely lead-zinc and copper skarns (G. E. Ray, personal communication, 1993), are developed at the margins of plutons that intrude Quatsino limestone or limestone interbeds near the top of the Karmutsen Formation. The most significant of these is the Caledonia deposit, situated at the eastern extremity of the Wanokana batholith northwest of Quatse Lake, where chalcopyrite occurs in an epidote-garnet-actinolite skarn in Quatsino limestone. Based on underground development, inferred reserves total some 68 000 tonnes grading 704 grams per tonne silver, 6.1% copper, 7.45% zinc and 0.6% lead. Several other skarn occurrences are also enriched in silver and a few contain gold assaying up to 0.3 gram per tonne in grab samples. A skarn occurrence within intra-Karmutsen limestones at the southeastern end of the Quatse stock has also been noted. The limestones here have been recrystallized and

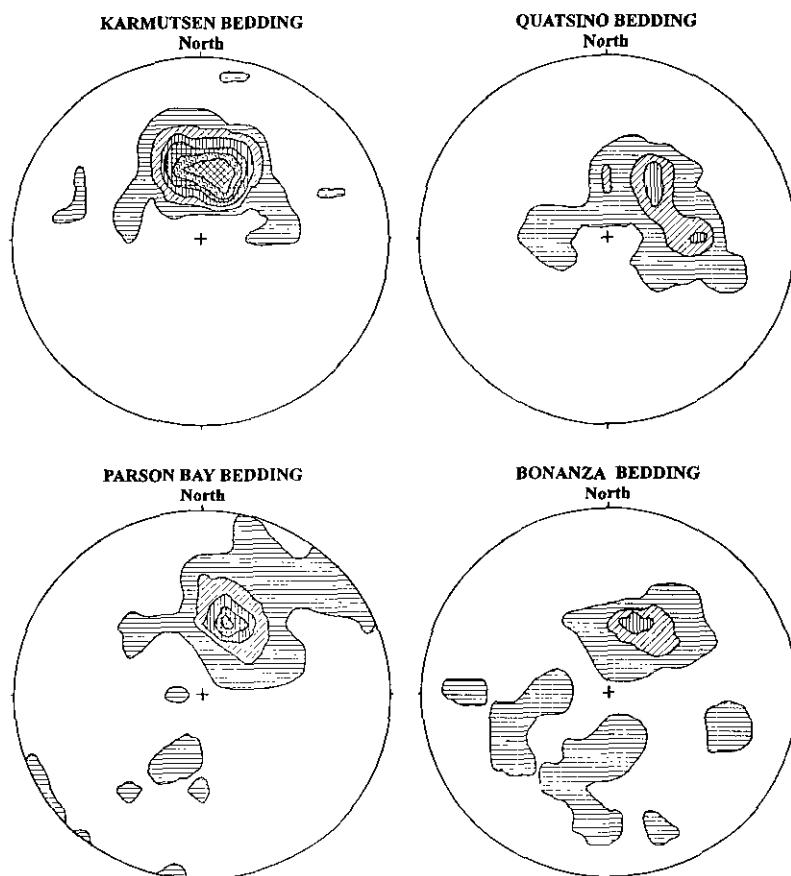


Figure 7. Poles to bedding for Karmutsen Formation; Quatsino Formation; Parson Bay Formation; and Bonanza Group. Contoured using the Schmidt method (3% points per 1% area).

replaced by a coarse-grained diopside-garnet-magnetite exoskarn with minor epidote, tremolite? and calcite, and disseminated chalcopyrite, pyrite and malachite. Locally, centimetre-scale magnetite-rich zones are interlayered with garnet-diopside zones.

## PORPHYRY DEPOSITS

Porphyry deposits have been, and continue to be, one of the main exploration targets in the region. The Island Copper mine of BHP Minerals (Canada) Limited is an arc-related porphyry copper-molybdenum-gold deposit hosted by a quartz feldspar porphyry dike of the Island Plutonic Suite and andesitic flows and pyroclastic rocks near the base of the Bonanza Group. The geology and mineralization are described in detail by Cargill *et al.* (1976) and summarized by Perello *et al.* (1989) and Panteleyev and Koyanagi (1993). Briefly, three main stages of alteration and mineralization have been recognized. An early stage represented by a stockworked core of quartz-magnetite-amphibole-sodic plagioclase that grades outward into a biotite-magnetite zone followed by a chlorite zone and an outermost epidote zone; a superimposed, structurally controlled intermediate stage related to the formation of a quartz stockwork and sericite-chlorite-kaolinite alteration assemblages; and a late stage involving generation of hydrothermal breccias under extreme base-leaching

conditions resulting in a pyrophyllite-dumortierite-sericite-kaolinite alteration assemblage. The main copper mineralization occurred during the early stage, and was closely followed by the main episode of molybdenum mineralization. The ore minerals, chiefly chalcopyrite and molybdenite with sparse bornite, sphalerite and galena, occur in fractures and locally as disseminations. Pyrite is two to three times as abundant as chalcopyrite, and magnetite is the most abundant oxide mineral. Rhenium is recovered from molybdenite concentrates in reported concentrations of up to 2400 ppm. Reserves were initially estimated at 257 million tonnes grading 0.52% copper, 0.017% molybdenum and 0.22 gram per tonne gold (Perello *et al.*, 1989). Mining began in 1971 and up to the end of June 1993 over 319 million tonnes of ore had been mined with the recovery of over 1 billion kilograms of copper, 25 million kilograms of molybdenum, 32.5 million grams of gold and 262 million grams of silver. The mine is tentatively scheduled to close in 1996.

Large zones of argillic and advanced argillic alteration are associated with porphyry deposits in the western part of the area. The Red Dog stock (described above) is host to a small porphyry copper-molybdenum-gold deposit concentrated in a quartz-magnetite breccia, the remnants of an acid-leached pyrophyllite-kaolinite-quartz "cap", in the central part of the intrusion (Figure 6). Economic minerals include chalcopyrite, molybdenite, bornite and traces of covellite. The deposit

TABLE 2

SOME CHARACTERISTIC ACID-SULPHATE ALTERATION MINERALS IDENTIFIED IN THE BONANZA GROUP BY X-RAY DIFFRACTION\*

<u>Mineral</u>	<u>Ideal Formula</u>
Pyrophyllite	$Al_2Si_4O_{10}(OH)_2$
Alunite	$KAl_3(SO_4)_2(OH)_6$
Natroalunite	$(Na>K)Al_3(SO_4)_2(OH)_6$
Zunyite	$Al_{13}Si_5O_{20}(OH,F)_{18}Cl$
Diaspore	$AlO(OH)$
Kaolinite/dickite	$Al_4Si_4O_{10}(OH)_8$
Jarosite	$KFe_3(SO_4)_2(OH)_6$
Rozenite	$FeSO_4 \cdot 4H_2O$
Melanterite	$FeSO_4 \cdot 7H_2O$

\* A. Panteleyev, unpublished data

has a drill-indicated reserve of 31.2 million tonnes grading 0.313% copper, 0.446 gram per tonne gold and 0.007% molybdenum (Crew Natural Resources Limited, Prospectus). The Hep and Hushamu porphyry deposits are situated at the margin of the Wanokana batholith (Figure 6). Geological reserves at the Hushamu are reported to be 172.5 million tonnes grading 0.28% copper, 0.34 gram per tonne gold and 0.009% molybdenum. The Hep deposit is reportedly located at the intersection of two shear zones estimated to contain 45 350 tonnes of material with an average grade of 0.80% copper.

**ACID SULPHATE ALTERATION AND MINERALIZATION**

Hydrothermal alteration and mineralization of the acid sulphate or high-sulphidation type in the Quatsino map area has been described previously by Panteleyev and Koyanagi (1993, 1994). They pointed out that these mineralized systems are entirely hosted by Bonanza volcanic rocks. Their argillic and advanced argillic alteration zones, as modified here, are shown in Figure 6, together with preliminary results of X-ray diffraction studies (Panteleyev, unpublished data). It is clear that the distribution of acid sulphate alteration coincides precisely with the trend of the upper rhyolitic unit of the Bonanza Group. This alteration certainly affects underlying basaltic andesite and andesite flows (unit C, Figure 5) but not the overlying lavas (unit A), with the apparent exception of one locality due west of South McIntosh where a rhyolite dike is exposed. It therefore seems likely that there is a fundamental genetic relationship between the felsic volcanic rocks and the development of acid sulphate alteration assemblages in the Bonanza Group.

The nature and origin of the hydrothermal fluids and the economic and gangue minerals that characterize these systems have recently been summarized by Panteleyev (1992) and placed in the context of specific deposit types that may exist on Northern Vancouver Island. It is evident that magmatic fluids play an important role in generating the extreme base-leaching conditions that characterize these copper-gold-silver mineralizing systems, some of which may have genetic, spatial and temporal relationships to subvolcanic porphyry copper deposits at depth. Alteration minerals commonly found in acid sulphate assemblages and that have been identified in the map area include pyrophyllite, alunite/natroalunite, zunyite, kaolinite, dickite, rozenite, jarosite, melanterite, sericite, illite, paragonite and native sulphur (Table 2; Figure 6). In addition, Panteleyev and Koyanagi (1993) sampled a vein occurrence overlooking Youghpan Creek that contained native gold coexisting with alunite (possibly schlossmacherite, an arsenian variety of alunite). A characteristic feature of this style of alteration is the relatively high abundance of pyrite which is largely responsible for the high acidity of natural drainages in the area (Koyanagi and Panteleyev, 1993, 1994). Felsic flow and pyroclastic rocks containing some 5 to 20% finely disseminated pyrite/marcasite are fairly common, and locally, more massive layers with up to 80% sulphides have been observed.

There is clear textural evidence for the felsic nature of the volcanic protolith at localities scattered throughout the argillically altered upper rhyolitic unit, with the notable exception of Mount McIntosh, where the advanced argillic overprint is strongest. Relict flow laminations and, rarely, flow folds, and pyroclastic textures, including welding, can readily be identified within the widespread argillic alteration at the Wann Knobs and in the Pemberton Hills, as detailed earlier.



Plate 4. Thin, clay-altered rhyolite dike cutting more intensely altered and locally brecciated rhyolite host. Note irregular dike margins and dispersed inclusions of brecciated and altered wallrock. Upper rhyolite (unit B), Bonanza Group, Mount McIntosh (93GNX22-3).

Where primary textures have been obliterated, the rock is reduced to a white-weathering, compact homogeneous microcrystalline mass or a vuggy porous siliceous rock locally infilled with secondary silica and clay minerals.

At Mount McIntosh, destruction of primary volcanic textures is much more complete in a widespread zone of advanced-argillic acid sulphate alteration. Here, pyrophyllite coexists with alunite, zunyite, diaspore and kaolinite, and metallic minerals include abundant pyrite, local enargite and traces of chalcopyrite, covellite, chalcocite and bornite (Figure 6; Panteleyev and Koyanagi, 1993, 1994). A compact to vuggy, microcrystalline silica-clay mottled rock forms extensive outcrops along the drill-road system high on the east side of the ridge. Locally, hydrothermal alteration breccias form at least two generations of narrow (<1 m wide) irregular dike-like bodies that crosscut the mottled siliceous rocks. Relict primary textures, including aphanitic flow breccias and flow laminations, are rarely preserved west of the roads along the crest of the ridge. The variably altered siliceous rocks are intruded locally by thin (<25 cm wide) rhyolitic dikes, some of which



Plate 5. Rhyolite dike with relict flow laminations (left) cut by altered hydrothermal breccia (right), South McIntosh (93GNX21-4).

carry rounded phenocrysts of quartz. Most of these dikes have sharp planar contacts; however, one has an irregular contact and a well-developed flow lamination, and incorporates screens and xenoliths of intensely altered wallrock (Plate 4). These dikes clearly postdate the advanced argillic alteration but appear to have been affected by late-stage argillic alteration, particularly at their margins. Other features of note include small restricted zones of intense quartz stockworking, and open-space fillings incompletely sealed by thinly layered, crustiform silica-hematite precipitates that contour these irregular channelways.

Some of the alteration features described above are also observed in a rhyolite dike intruding andesitic flows west of South McIntosh, and this outcrop provides an instructive record of protolith destruction. The aphanitic dike is 10 metres wide and offset across a high-angle (Tertiary?) fault trending 070. Pervasive hydrothermal alteration and devitrification have preferentially affected the pale greyish green margins of the dike. Flow laminations parallel to the contact are preserved locally in the less altered, darker grey core of the intrusion. These laminar flowage structures are crosscut by breccias with sharp to gradational contacts and angular fragments (<20 cm) of variably rotated rhyolite (Plate 5). Some flow-laminated rhyolite clasts at the margins of these breccias can be pieced back together and into their hostrock, providing clear evidence that brecciation and alteration took place after consolidation and cooling as opposed to during emplacement. These hydrothermal breccias bear a striking resemblance to the late crosscutting breccia dikes at Mount McIntosh.

#### CHEMICAL EFFECTS: PRELIMINARY OBSERVATIONS

Analytical data for hydrothermally altered rhyolitic protoliths given in Table 1 show variable leaching of

base, alkali, and other metals depending on the specific nature and degree of the alteration. Assuming a starting composition of relatively fresh Bonanza rhyolite (e.g. analysis 27, Table 1), felsic protoliths at Mount McIntosh exhibit: extreme leaching of sodium, potassium, calcium, magnesium and manganese, and, in this example, iron, with concomitant gains in aluminum, titanium and volatiles (analysis 6, Table 1); and extreme depletion of all metals except titanium which has been added to the rock (analysis 7). Note that in the latter case, and in similarly altered samples near the top of a drill hole in the Pemberton Hills (analyses 18c and d, Table 1), the balance of gains and losses of major element oxides does not require significant introduction of silica into the rock, and the process appears to be one in which leaching of all components takes place with the notable exception of titanium and residual silica. As titanium is clearly mobile in the fluids that generate these acid sulphate alteration assemblages, this constituent cannot be used as a conserved element in attempts to reconstruct the composition of the protolith.

#### AGE OF THE MINERALIZATION AND ALTERATION: A LOWER JURASSIC EPITHERMAL SYSTEM

There is some evidence to suggest that the acid sulphate alteration and mineralization occurred contemporaneous or penecontemporaneous with extrusion of Bonanza rhyolites. The most direct evidence occurs at Mount McIntosh where rhyolite dikes postdate the advanced argillic overprint. The recognition of flow breccias and flow laminations in the rhyolitic rocks and the presence of open-space fillings indicate that Mount McIntosh most likely represents a rhyolitic flow-dome complex. Rhyolite dikes intruded after the initial phases of dome extrusion represent a renewed period of internal inflation as a new pulse of magma ascended from depth. As noted above, these dikes postdate an episode of epithermal mineralization associated with advanced argillic acid sulphate alteration. As the bulk of the acid sulphate alteration is restricted to the upper Bonanza rhyolite unit, epithermal fluids were either particularly active during this period of felsic subaerial volcanism, or this is simply a reflection of the overall proximity of these rhyolitic rocks to their source vents. If the acid sulphate epithermal systems are indeed linked with porphyry copper mineralization at depth, as the presumed coeval nature of intrusions of the Island Plutonic Suite might suggest, then precious metal deposits transitional between the porphyry and epithermal environments ought to be hosted by rocks stratigraphically beneath the upper rhyolitic unit. In the overall context of Bonanza stratigraphy, as defined here (Figure 5), units C through E would be prime exploration targets for these "transitional" types of deposit. It is also intriguing to note that the two most significant porphyry copper-molybdenum-gold deposits in the area, at Island Copper and Red Dog, have intruded similar stratigraphic levels near the base of the Bonanza Group. Significant mineralization at the Red Dog deposit is intimately

associated with a silicified and brecciated host that exhibits advanced argillic alteration (pyrophyllite-quartz-kaolinite). Perhaps this siliceous rock represents a residue of extreme acid leaching formed in a "transitional" or epithermal environment that has since been partially engulfed and overprinted by higher level porphyry emplacement and mineralization.

#### ACKNOWLEDGMENTS

We owe a great debt of gratitude to all those who offered advice and assistance in the field, and participated in informative (sometimes downright lively!) discussions on the geology. John Fleming and Alan Reeves of BHP Minerals (Canada) Limited kindly made available geological compilations and docking facilities at the Island Copper mine; Peter Dasler (Daiwan Engineering Limited) shared his knowledge of the region; Mike Orchard (Geological Survey of Canada) made conodont collections (we hope!); Fabrice Cordey collected radiolaria (or at least "features"); Doug Archibald (Department of Geological Sciences, Queen's University) collected samples for Ar-Ar dating; and Tim Tozer (Geological Survey of Canada) made fossil identifications. We would also like to thank Western Forest Products Limited and Tribune Bay Logging Limited for safe access to the area; Donna Blackwell, Alan Gilmore and Bill Newman (Government Agent in Port Hardy) for logistics and expediting services; and John Newell and Brian Grant for editorial comments. Our sincere appreciation is extended to all those who attended the end-of-season workshop in Port Hardy for stimulating geological discussions, particularly those that took place on the field trip.

#### REFERENCES

- Armstrong, R. L., Muller, J. E., Harakal, J. E. and Muehlenbachs, K. (1985): The Neogene Alert Bay Volcanic Belt of Northern Vancouver Island, Canada: Descending-plate-edge Volcanism in the Arc-trench Gap; *Journal of Volcanology and Geothermal Research*, Volume 26, pages 75-97.
- Barker, F., Sutherland Brown, A., Budahn, J. R. and Plafker, G. (1989): Back-arc with Frontal Arc Component Origin of Triassic Karmutsen Basalt, British Columbia, Canada; *Chemical Geology*, Volume 75, pages 81-102.
- Bevier, M. L., Armstrong, R. L. and Souther, J. F. (1979): Miocene Peralkaline Volcanism in West Central British Columbia - Its Temporal and Plate Tectonics Setting; *Geology*, Volume 7, pages 389-392.
- Bobrowsky, P. T. and Meldrum, D. (1994): Preliminary Drift Exploration Studies, Northern Vancouver Island (92/06 and 11); in *Geological Fieldwork 1993*, Grant, B. and Newell, J. M., Editors, *B. C. Ministry of Energy, Mines and Petroleum Resources*, Paper 1994-1, this volume.
- Cargill, D. G., Lamb, J., Young, M. J. and Rugg, E. S. (1976): Island Copper, in *Porphyry Deposits of the Canadian*

- Cordillera, Sutherland Brown, A., Editor, *Canadian Institute of Mining and Metallurgy*, Special Volume 15, pages 206-218.
- Desrochers, A. (1989): Depositional History of Upper Triassic Carbonate Platforms on Wrangellia Terrane, Western British Columbia, Canada; *American Association of Petroleum Geologists*, Bulletin 73, pages 349-350.
- Gardner, M. C., Bergman, S. C., Cushing, G. W., MacKevett, E. M. Jr., Plafker, G., Campell, R. B., Dodds, C. J., McClelland, W. C. and Mueller, P. A. (1988): Pennsylvanian Pluton Stitching of Wrangellia and the Alexander Terrane, Wrangell Mountains, Alaska; *Geology*, Volume 16, pages 967-971.
- Haggart, J. W. (1993): Latest Jurassic and Cretaceous Paleogeography of the Northern Insular Belt, British Columbia; in *Mesozoic Paleogeography of the Western United States II*, Dunne, G. C. and McDougall, K. A., Editors, *Society of Economic Paleontologists and Mineralogists (Pacific Section)*, Book 71, pages 463-475.
- Harland, W. B., Armstrong, R. L., Cox, A. V., Craig, L. E., Smith, A. G. and Smith, D. G. (1990): A Geologic Time Scale 1989; *Cambridge University Press*, Cambridge, England.
- Jeletzky, J. A. (1969): Mesozoic and Tertiary Stratigraphy of Northern Vancouver Island, British Columbia (92E, 92L, 102I); *Geological Survey of Canada*, Paper 69-1A, pages 126-134.
- Jeletzky, J. A. (1976): Mesozoic and Tertiary Rocks of Quatsino Sound, Vancouver Island, British Columbia; *Geological Survey of Canada*, Bulletin 242.
- Jones, D. L., Silberling, N. J. and Hillhouse, J. (1977): Wrangellia - A Displaced Terrane in Northwestern North America; *Canadian Journal of Earth Sciences*, Volume 14, pages 2565-2577.
- Kerr, D. E. (1992): Surficial Geology of the Quatsino Area (92L/12); *B. C. Ministry of Energy, Mines and Petroleum Resources*, Open File 1992-6, scale 1:50 000.
- Kerr, D. E. and Sibbick, S. J. (1992): Preliminary Results of Drift Exploration Studies in the Quatsino (92L/12) and the Mount Milligan (93N/1E, 93O/4W) Areas; in *Geological Fieldwork 1991*, Grant, B. and Newell, J. M., Editors, *B. C. Ministry of Energy, Mines and Petroleum Resources*, Paper 1992-1, pages 341-347.
- Kerr, D. E., Sibbick, S. J. and Jackaman, W. (1992): Till Geochemistry of the Quatsino Map Area (92L/12); *B. C. Ministry of Energy, Mines and Petroleum Resources*, Open File 1992-21, scale 1:50 000.
- Koyanagi, V. M. and Panteleyev, A. (1993): Natural Acid-drainage in the Mount McIntosh/Pemberton Hills Area, Northern Vancouver Island (92L/12); in *Geological Fieldwork 1992*, Grant, B. and Newell, J. M., Editors, *B. C. Ministry of Energy, Mines and Petroleum Resources*, Paper 1993-1, pages 445-449.
- Koyanagi, V. M. and Panteleyev, A. (1994): Natural Acid-drainage in the Red Dog - Hushamu - Pemberton Hills Area, Northern Vancouver Island (92L/12); in *Geological Fieldwork 1993*, Grant, B. and Newell, J. M., Editors, *B. C. Ministry of Energy, Mines and Petroleum Resources*, Paper 1994-1, this volume.
- Le Maitre, R. W. (Editor) (1989): A Classification of Igneous Rocks and Glossary of Terms; *Blackwell Scientific Publications*.
- Matysek, P. F., Gravel, J. L. and Jackaman, W. (1989): 1988 British Columbia Geochemical Survey, Stream Sediment and Water Geochemical Data, NTS 92L/102I - Alert Bay/Cape Scott; *B. C. Ministry of Energy, Mines and Petroleum Resources*, RGS 23.
- Monger, J. W. H., Price, R. A. and Tempelman-Kluit, D. J. (1982): Tectonic Accretion and the Origin of the Two Major Metamorphic and Plutonic Belts in the Canadian Cordillera.; *Geology*, Volume 10, pages 70-75.
- Monger, J. W. H., Wheeler, J. O., Tipper, H. W., Gabrielse, H., Harms, T., Struik, L. C., Campbell, R. B., Dodds, C. J., Gehrels, G. E. and O'Brien, J. (1991): Cordilleran Terranes in Upper Devonian to Middle Jurassic Assemblages; in *Geology of the Cordilleran Orogen in Canada*, Gabrielse, H. and Yorath, C. J., Editors, *Geological Survey of Canada*, Geology of Canada, Number 4, pages 281-327.
- Muller, J. E. (1977): Evolution of the Pacific Margin, Vancouver Island, and Adjacent Regions; *Canadian Journal of Earth Sciences*, Volume 14, pages 2062-2085.
- Muller, J. E. and Jeletzky, J. A. (1970): Geology of the Upper Cretaceous Nanaimo Group, Vancouver Island and Gulf Islands, British Columbia; *Geological Survey of Canada*, Paper 69-25.
- Muller, J. E. and Roddick, J. A. (1983): Geology Alert Bay - Cape Scott, British Columbia; *Geological Survey of Canada*, Map, 1552A, scale 1:250 000.
- Muller, J. E., Cameron, B. E. B. and Northcote, K. E. (1981): Geology and Mineral Deposits of Nootka Sound Map Area (92E), Vancouver Island, British Columbia; *Geological Survey of Canada*, Paper 80-16.
- Muller, J. E., Northcote, K. E. and Carlisle, D. (1974): Geology and Mineral Deposits of Alert Bay - Cape Scott Map Area, Vancouver Island, British Columbia; *Geological Survey of Canada*, Paper 74-8.
- Nixon, G. T., Hammack, J. L., Hamilton J. V. and Jennings, H. (1993a): Preliminary Geology of the Mahatta Creek Area, Northern Vancouver Island (92L/5); in *Geological Fieldwork 1992*, Grant, B. and Newell, J. M., Editors, *B. C. Ministry of Energy, Mines and Petroleum Resources*, Paper 1993-1, pages 17-35.
- Nixon, G. T., Hammack, J. L., Hamilton J. V. and Jennings, H. (1993b): Preliminary Geology of the Mahatta Creek Area (92L/5); *B. C. Ministry of Energy, Mines and Petroleum Resources*, Open File 1993-10, scale 1:50 000.
- Panteleyev, A. (1992): Copper-gold-silver Deposits Transitional Between Subvolcanic Porphyry and Epithermal Environments; in *Geological Fieldwork 1991*, Grant, B. and Newell, J. M., Editors, *B. C. Ministry of Energy, Mines and Petroleum Resources*, Paper 1992-1, pages 231-234.

- Panteleyev, A., Bobrowsky, P. T., Nixon, G. T. and Sibbick, S. J. (1994): Northern Vancouver Island Integrated Project; in Geological Fieldwork 1993, Grant, B. and Newell, J. M., Editors, *B. C. Ministry of Energy, Mines and Petroleum Resources*, Paper 1994-1, this volume.
- Panteleyev, A. and Koyanagi, V. M. (1993): Advanced Argillic Alteration in Bonanza Volcanic Rocks, Northern Vancouver Island - Transitions Between Porphyry Copper and Epithermal Environments (92L/12); in Geological Fieldwork 1992, Grant, B. and Newell, J. M., Editors, *British Columbia Ministry of Energy, Mines and Petroleum Resources*, Paper 1993-1, pages 287-293.
- Panteleyev, A. and Koyanagi, V. M. (1994): Advanced Argillic Alteration in Bonanza Volcanic Rocks, Northern Vancouver Island - Lithologic Associations and Permeability Controls (92L/12); in Geological Fieldwork 1993, Grant, B. and Newell, J. M., Editors, *B. C. Ministry of Energy, Mines and Petroleum Resources*, Paper 1994-1, this volume.
- Perello, A., Arancibia, O., Burt, P., Clark, A. H., Clarke, C., Fleming, J., Himes, M. D., Leitch, C. and Reeves, A. (1989): Porphyry Cu-Mo-Au Mineralization at Island Copper, Vancouver Island, B. C.; *Geological Association of Canada, Cordilleran Section, Porphyry Copper Workshop*, Vancouver, April (Abstract).
- Riddihough, R. P. and Hyndman, R. D. (1991): Modern Plate Tectonic Regime of the Continental Margin of Western Canada; in *Geology of the Cordilleran Orogen in Canada*, Gabrielse, H. and Yorath, C. J., Editors, *Geological Survey of Canada*, Geology of Canada Number 4, pages 435-455.
- Sibbick, S. J. (1994): Preliminary Report on the Application of Catchment Basin Analysis to Regional Geochemical Survey Data, Northern Vancouver Island (92L/SW); in Geological Fieldwork 1993, Grant, B. and Newell, J. M., Editors, *B. C. Ministry of Energy, Mines and Petroleum Resources*, Paper 1994-1, this volume.
- Sutherland Brown, A. (1968): Geology of the Queen Charlotte Islands, British Columbia; *B. C. Ministry of Energy Mines and Petroleum Resources*, Bulletin 54.
- van der Heyden, P. (1991): A Middle Jurassic to Early Tertiary Andean-Sierran Arc Model for the Coast Belt of British Columbia; *Tectonics*, Volume 11, pages 82-97.
- Wheeler, J. O. and McFeely, P. (Compilers) (1991): Tectonic Assemblage Map of the Canadian Cordillera and Adjacent Parts of the United States of America; *Geological Survey of Canada*, Map 171A, scale 1:2 000 000.

## NOTES

**PRELIMINARY DRIFT EXPLORATION STUDIES, NORTHERN VANCOUVER ISLAND (92L/6, 92L/11)**

By Peter T. Bobrowsky and Dan Meldrum

**KEYWORDS:** Drift exploration, Quaternary, surficial geology, terrain, glaciations, till geochemistry, pebble lithologies, facies analysis, diamicton, drift thickness, Vancouver Island, Late Wisconsinan, Holocene

- derive interpretive exploration products currently termed "sample media confidence maps".

This paper provides a brief summary of the 1993 fieldwork activities, a progress report on the analyses currently in progress and several preliminary conclusions relevant to the project objectives.

**INTRODUCTION**

Quaternary geological investigations were undertaken in NTS sheets 92L/6 (Alice Lake) and 92L/11 (Port McNeill) as part of an integrated resource assessment program on Northern Vancouver Island (see Panteleyev *et al.*, 1994, this volume, for a review of the program; Figure 1).

**BACKGROUND**

The northern Vancouver Island area was selected for detailed study by the Geological Survey Branch as a region of under-explored mineral potential. A variety of deposit types occur in the area, but the most significant are gold-bearing porphyry copper-molybdenum deposits including the Island Copper mine at the east end of Rupert Inlet, and several well-known mineral occurrences (e.g. Red Dog and Hushamu/Mount



Figure 1. Location map of 1993 drift exploration study.

The aim of the Quaternary geology aspects of the project was to provide surficial geology data that would be useful in expanding current areas of exploration as well as stimulate long-term exploration activities. Specifically, the Quaternary geology project consisted of several components which sought to:

- document the Quaternary geological history of the study area.
- map the surficial geology at 1:50 000 scale.
- complete a regional drift - exploration project centred on till geochemistry sampling.
- develop drift-exploration models for the region.
- generate surficial geology maps.

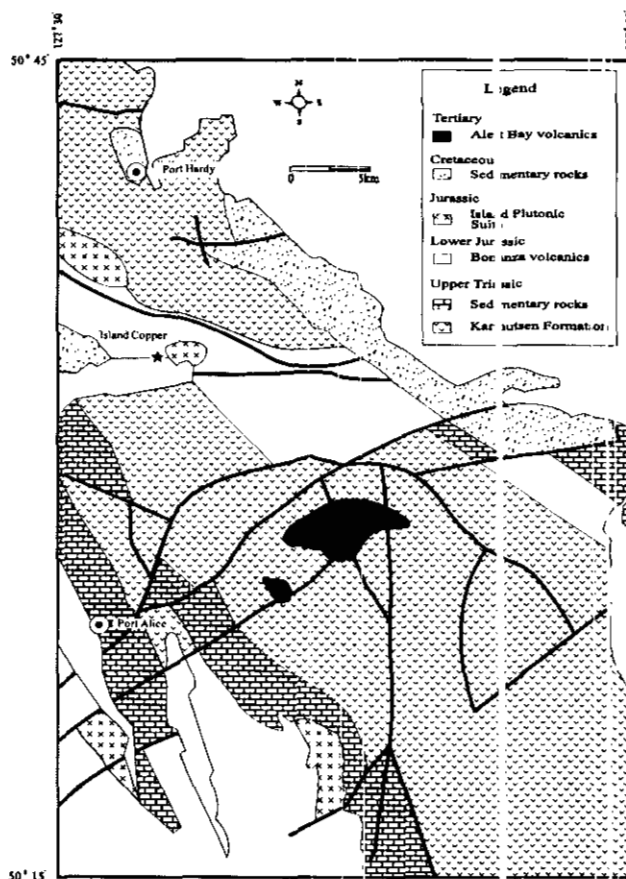


Figure 2. Generalized bedrock geology map.

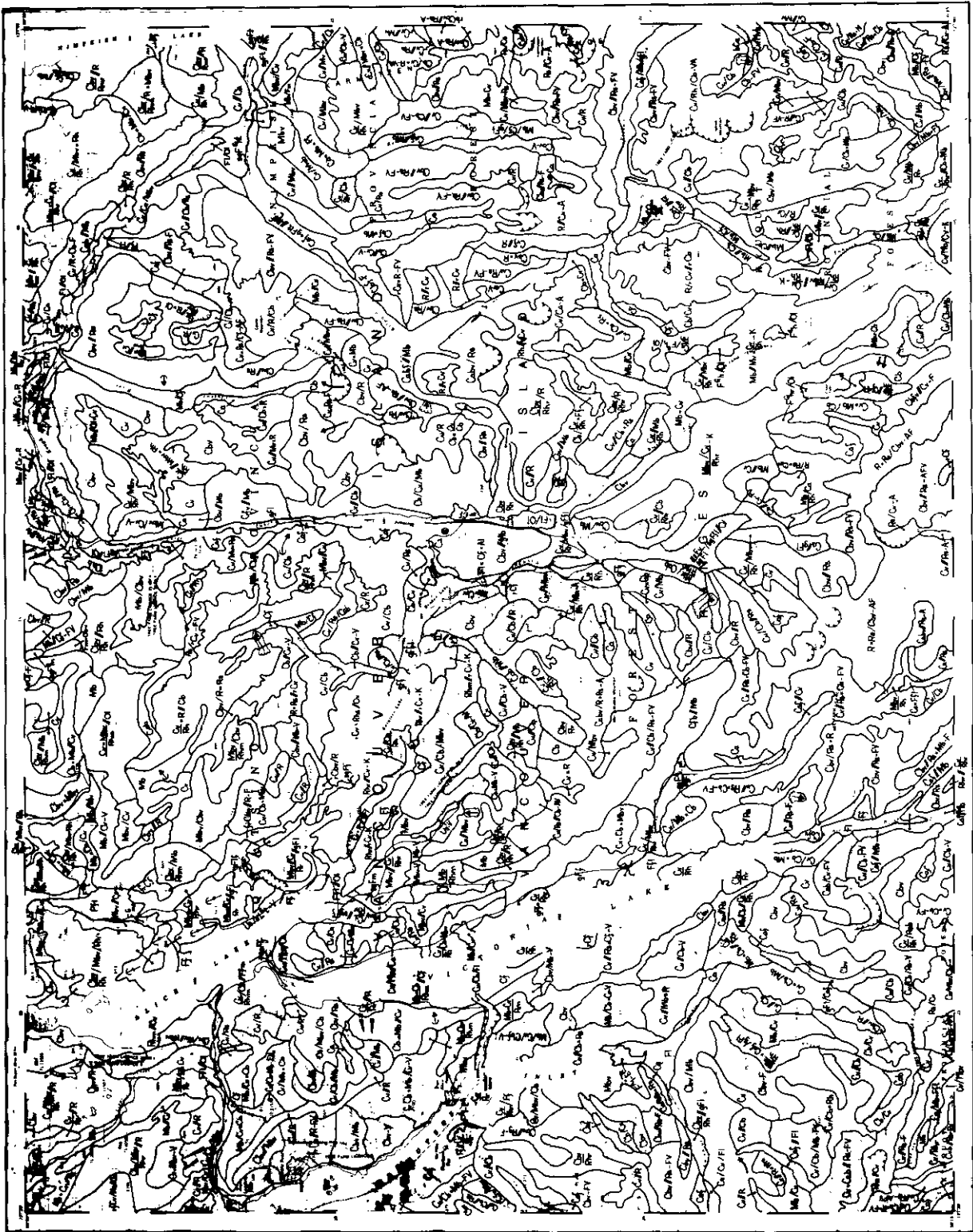


Figure 3. Terrain geology map, NTS 92L/6 (Alice Lake). This 1:50 000 scale map provides morphological landform data. See Howes and Kenk (1988) for legend details.



Figure 4. Terrain geology map, NTS 92L/41 (Port McNeill). This 1:50 000 scale map provides morphological information data. See Howes and Kenk (1988) for legend details.

McIntosh) between Port Hardy and Holberg. Mineral deposit studies have been ongoing since 1991 in 92L/12 (Quatsino; Panteleyev, 1992; Panteleyev and Koyanagi, 1993, 1994, this volume). They now conclude that much of the copper-gold mineralization found in the extensive zones of argillic alteration are a product of hydrothermal alteration of the Bonanza volcanic rocks. These acid-sulphate alteration zones are often hosted by rhyolitic units (Nixon *et al.*, 1994, this volume). Bedrock geological mapping at 1:20 000 scale, which started in 1992 with 92L/5 (Mahatta Creek; Nixon *et al.*, 1993), has been extended northward into 92L/12 and the western margin of 92L/11. Bedrock mapping results indicate that part of the Bonanza volcanics can be subdivided into units mappable at 1:50 000 scale, consisting of rhyolitic lavas and ash-flow tuffs (Nixon *et al.*, 1994, this volume). Geochemical data were collected in 1988 for 92L as part of the Regional Geochemical Survey (Gravel and Matysek, 1989) and again in 1993 with detailed follow-up work of significant anomalies. Although many anomalies are evident, this work also concludes that only 54% of the area in 92L/SW is realistically covered by Regional Geochemical Survey data (Sibbick, 1994, this volume). Till samples were obtained in 1991 for 92L/12 (Kerr *et al.*, 1992) and new samples were collected this year in the west half of 92L/6 and 92L/11. Surficial geology mapping at 1:50 000 scale was completed for 92L/12 in 1991 (Kerr, 1992). Fieldwork during the 1993 season extended the surficial mapping at a similar scale into all of 92L/11 and 92L/6. The primary intent of this wide mapping focus was to overlap the Bonanza volcanics which extend south-eastward from Island Copper (Figure 2).

## METHODS

Research in the area first involved interpretation of the surficial sediments using air-photographic study at a scale of 1:50 000 (photo suites BC77114). Terrain geology maps, which provide morphological landform data, were produced in 1980 at a scale of 1:50 000 for map sheets 92L/6 and 92L/11 (Figures 3 and 4). The air-photograph evaluation was used in conjunction with the existing morphological landform data portrayed on the terrain maps to construct preliminary surficial geology maps.

Field research was restricted to the western half of the two map sheets which were easily accessed by an extensive logging road network covering most of the region. Ground-truthing of the sediments portrayed on the preliminary surficial maps was accomplished by examination of exposures in road cuts, hand-dug pits and stream banks. Several hundred exposures were examined. Detailed descriptions including deposit types, unit thickness and extent, structures, contacts, texture, sorting, compaction, clast content, and weathering were

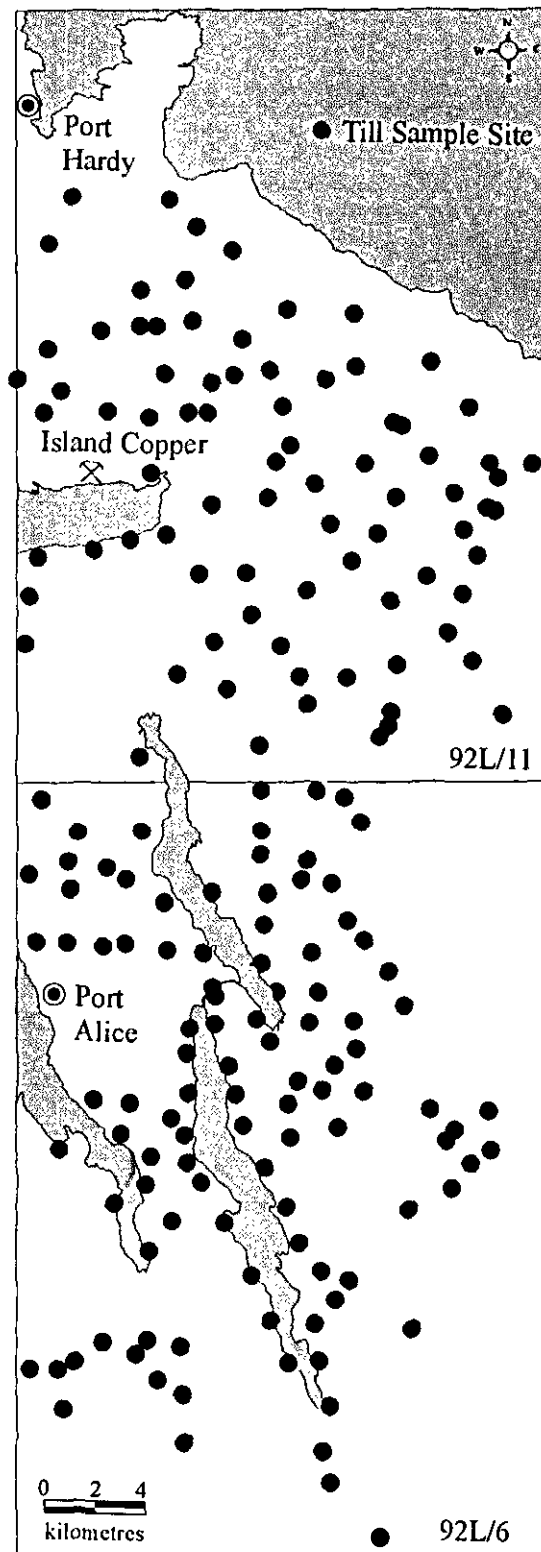


Figure 5. Drift sample location map. This map shows the location of 178 formally designated stops in the west half of maps NTS 92L/6 and 92L/11.

TABLE 1

## DRIFT SAMPLE FREQUENCY DISTRIBUTION AND SUMMARY STATISTICS

	SAMPLE DEPTH <sup>a</sup>	PERCENT CLASTS <sup>b</sup>	MEAN CLAST <sup>c</sup>	MAX CLAST <sup>d</sup>	SECTION HEIGHT <sup>e</sup>	OXID. DEPTH <sup>f</sup>	NUMBER SAMPLES <sup>g</sup>
FACIES A	2.3	25.9	6.0	61.2	4.0	0.9	77
FACIES B	1.7	33.3	8.5	63.2	3.2	0.8	24
FACIES C	1.7	37.2	9.1	52.3	2.9	1.4	49
FACIES D	1.8	41.0	10.4	47.4	2.8	1.4	21
OTHERS	-	-	-	-	-	-	7
TOTAL	-	-	-	-	-	-	178

a-depth below surface in metres  
 b-field estimated clast content  
 c-mean clast size in centimetres  
 d-average maximum clast size in centimetres  
 e-mean height of mappable exposure in metres  
 f-mean depth of contact to oxidation in metres  
 g-sample size

taken at 188 formally designated stops (Figure 5). Facies analysis of the unconsolidated sediments observed at each stop was used in the verification of the surficial map units and in the interpretation of sediment genesis.

As part of the reconnaissance drift-exploration program, bulk sediment samples (4-10 kg/sample) were collected at 178 designated stops for till geochemistry analysis. Mean sampling depth below ground surface ranged from 1.7 to 2.3 metres depending on the facies (Table 1).

Given a total land area actually sampled of about 860 square kilometres, sampling density was approximately 1 per 500 hectares (1 per 5 km<sup>2</sup>). Samples were stored in heavy-mil plastic bags. An additional ten duplicate drift samples were collected (about 1 in every 18 samples) for quality control tests. The principles of drift exploration are well summarized by Kauranne *et al.* (1992). Pebble samples (+100 clasts/sample and 5-10 cm in size) for clast lithologic analysis were also collected at 167 designated stops. The method and theory of pebble lithology analysis is described by Clark (1987) and Strobel and Faure (1987). Paleoflow indicators (e.g. fabrics, striations, crossbedding) were measured at 24 locations for either glacial or nonglacial deposits (Plates 1, 2 and 3). The importance and use of paleoflow indicators in drift studies is explained by Kujansuu and Saarnisto (1990).

In the laboratory, bulk-sediment samples were removed from their bags and air-dried at 25 to 30°C for a minimum of 48 hours, then crushed and sieved through stacked Tyler sieves to obtain the -230 mesh fraction. Representative splits of these fine-fraction samples were then submitted for aqua regia - inductively coupled plasma emission spectroscopy (ICP-ES) and instrumental neutron activation (INA) analysis. Geochemical results are pending. Pebble samples were split and will be categorized according to identifiable lithologies; results are also pending.



Plate 1. Glacially striated volcanic bedrock; paleoflow toward bottom.



Plate 2. Steeply dipping foreset beds of glaciofluvial delta. This postglacial deposit indicates that in this area, meltwater flowed towards the west as ice retreated eastward.

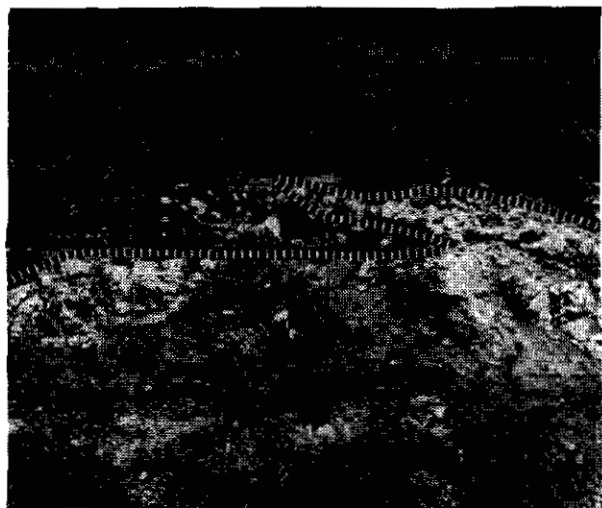


Plate 3. Attenuated plane of local bedrock (traced by dashed line) in subglacial till deposit indicates glacial flow to the west (to left). Subglacial thrusting mechanism is indicated, which is one method of incorporating debris into basal ice.

## RESULTS

### TERRAIN DISTRIBUTION

The study area encompasses approximately 1500 square kilometres of land which is differentially covered by varying combinations of sediments dominated by till, outwash and colluvium. A quantitative evaluation of the morphological landform data contained on the two terrain maps indicates that the major sediments occur in unequal proportions (Table 2; Figure 3). Colluvium is the most abundant throughout, covering approximately 49% (850 km<sup>2</sup>) of the area, but predominates in the west and south where relief is high and gravitational processes are accentuated. Ground moraine covers an additional 23% (332 km<sup>2</sup>) and occurs primarily in the north and

southeast where relief is generally subdued. Glaciofluvial deposits are also common, representing 12% (147 km<sup>2</sup>) of the total sediment cover; they are widely distributed, with an obvious concentration in the north-central part of the region. Fluvial sediments are not as common, covering only 5% (68 km<sup>2</sup>) of the map, and are restricted in their distribution to topographic lows occupied by modern rivers and streams. The remaining 11% (157 km<sup>2</sup>) of land surface consists of bedrock outcrops and lacustrine, glaciolacustrine, marine and organic accumulations.

### DRIFT THICKNESS

Drift thickness is highly variable, but generally predictable on the basis of the landforms present. In the high-relief areas to the west, colluvial veneers and blankets, 1 to 3 metres thick, occur directly down-slope from bedrock outcrops. Farther down-slope, till veneers or blankets overlain by colluvial veneers occur in thicknesses up to 10 metres. Depressions between the topographic highs are sedimentologically complex, containing variable thicknesses of till often covered by outwash. The latter deposits can reach thicknesses in excess of 30 metres. In the low-relief, eastern part of the study area, there are blankets of till more than 100 metres thick, and occasionally covered by thinner accumulations of outwash. Non-random drilling by BHP-Minerals Canada Ltd. provides useful regional data on overburden thickness. The frequency distribution of 448 drill holes relative to 10-metre increments of depth is positively skewed (Figure 6). Over half of the holes (249) drilled in the area encountered less than 10 metres of unconsolidated sediment; mean depth in this range is 5 metres. An additional 29% (129) of the holes encountered bedrock between 11 and 30 metres below surface. The remaining 15% of the drill holes exceeded 30 metres in depth. These data indicate most

TABLE 2  
TERRAIN DATA DISTRIBUTION FOR NTS 92L/6, 11\*

PRIMARY GENETIC MATERIAL	NTS 92L/6		NTS 92L/11		TOTAL STUDY	
	AREA COVERED (km <sup>2</sup> )	PERCENT	AREA COVERED (km <sup>2</sup> )	PERCENT	AREA COVERED (km <sup>2</sup> )	PERCENT
A	0.0	0.00	6.4	1.05	6.4	0.52
C	704.9	74.77	145.8	23.78	850.7	49.28
F	28.7	3.04	39.8	6.50	68.5	4.77
FG	7.8	0.83	139.7	22.77	147.5	11.80
M	137.3	14.56	195.4	31.85	332.7	23.20
O	0.0	0.00	21.3	3.47	21.3	1.74
R	61.9	6.56	1.4	0.23	63.3	3.40
U	2.1	0.22	2.3	0.37	4.4	0.30
W	0.1	0.01	61.2	9.98	61.3	5.00

\* see Howes and Kenk (1988) for legend to terrain categories. Only major genetic classes listed here.

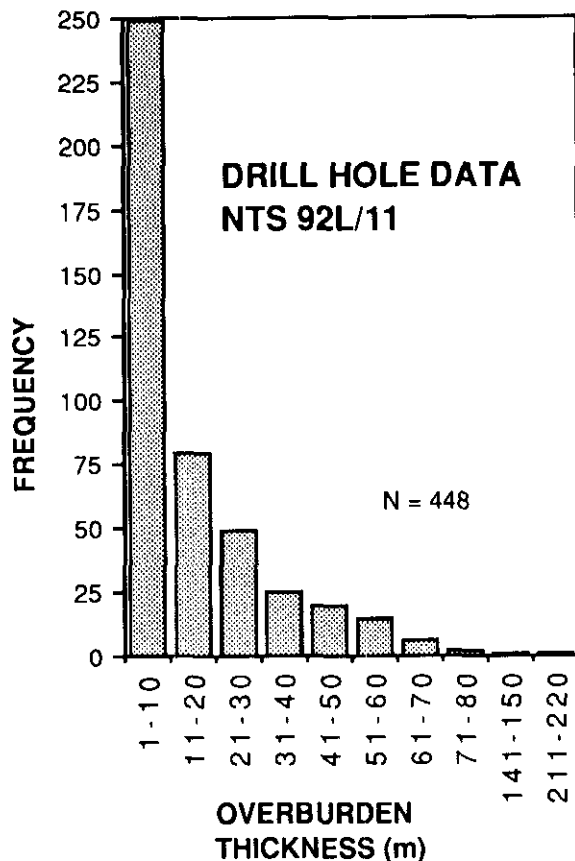


Figure 6. Histogram showing the frequency distribution of the drill hole relative to 10 m depth categories for overburden thickness.

accumulations categorized as blanket are of moderate depth. One hole east of Rupert Inlet passed through 215 metres of unconsolidated sediment. This hole and a 146-metre hole 600 metres to the north, are probably within a glacially over-deepened valley (fjord?) extending east from Rupert Inlet and associated with the Holberg fault. This scenario resembles the structurally controlled and glacially over-deepened valleys found in the southern interior of the province (cf. Bobrowsky *et al.*, 1993). In the latter case, ore deposits are sometimes associated with the glacially eroded tectonic structures.

## SEDIMENTOLOGY

Successful drift-exploration is based on the accurate identification and interpretation of the sediments sampled (Shilts, 1993). Four diamicton facies were identified in the study area based on objective criteria including texture, structure, consolidation, permeability, percentage clasts, clast shape and surface markings, lithologies, fabric, basal contact where evident, surface expression/landform, and position relative to other sediments. Sampling was largely restricted to various

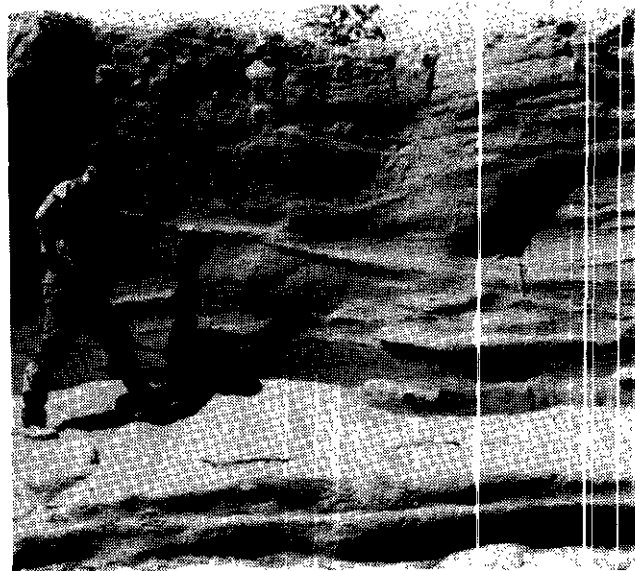


Plate 4. Horizontally laminated and planar tabular sand beds of glaciofluvial complex.

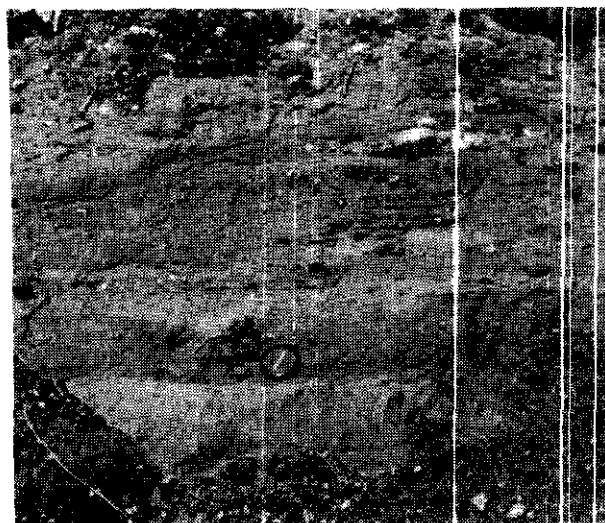


Plate 5. Inner-bay terrigenous facies of a glaciomarine environment.

diamicton facies, although other types of sediments were described, including those interpreted as representing glaciofluvial, glaciolacustrine, fluvial and marine environments (Plates 2, 4, 5 and 6). The primary attributes of the diamicton facies are described below.

Facies A is a cohesive, compact, dense, matrix-supported diamicton. The facies is generally massive, very poorly sorted and primarily grey to olive grey in colour. Clast content is low (average of 77 samples is 26%), consisting mainly of subrounded but occasionally subangular or rounded small pebbles; striations and faceting are also common. The pebble fabric is strong and bullet-shaped boulders are present. Some lithologies are mainly of local provenance, but exotics are present.

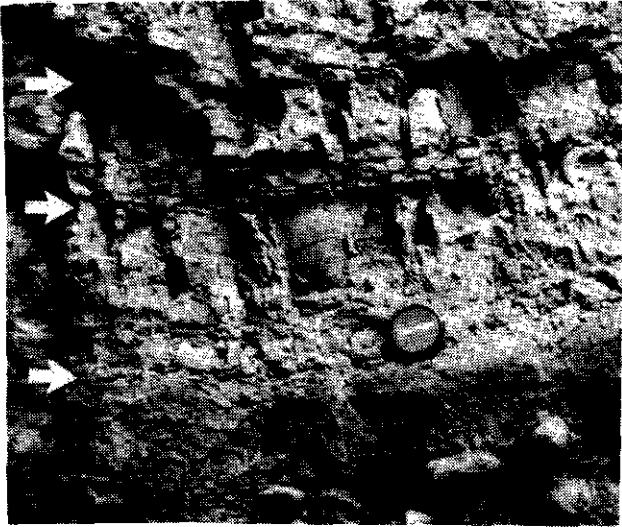


Plate 6. Rhythmic silty clay and clayey silt beds representing a postglacial lacustrine deposits. Rhythmite pairs occur between sets of arrows.



Plate 7. Example of facies A sediments interpreted as subglacial till deposit. See text for detailed facies description. Note massive nature of the matrix-supported diamict.

Deposit thickness is variable and ranges from 1 to more than 10 metres. The basal contact of the facies varies from sharp to indeterminate, the surface weathering is minimal and the base of the soil contact is usually abrupt. Facies A commonly overlies bedrock and is interpreted as representing a subglacial till deposit (Plate 7).

Facies B is a loose, soft to hard, poorly sorted and massive, matrix-supported diamict. It is primarily olive grey to brown in colour. The clast content is moderate (average of 24 samples is 33%), consisting mainly of subangular to subrounded stones ranging in size from pebble to boulder; the latter are often abundant.



Plate 8. Example of facies B sediments interpreted as supraglacial till deposit. Note large cobbles and boulders winnowed out of the deposit. See text for detailed facies descriptions.



Plate 9. Example of facies C sediments (above dashed line) overlying facies A. Former interpreted as colluviated till deposit. See text for facies description.

The pebble fabric is moderately strong, with rare striated clasts and an absence of faceting. Stone lithologies include both local and exotic types. Deposits are generally 1 to more than 3 metres thick, and the basal contact varies from gradational to indeterminate. Surface weathering is usually deep, and the basal contact of the soil is often diffuse. This facies usually overlies facies A and rarely overlies bedrock. Facies B is interpreted as representing supraglacial till deposits (Plate 8).

Facies C is a loose, soft, poorly sorted, matrix to clast-supported diamict. The facies is massive to crudely bedded and primarily olive - brown to brown in

colour. Clast content is high (average of 49 samples is 37%), consisting rarely of striated or faceted stones, which are angular to subrounded in shape. Clasts are primarily pebble to boulder in size, and are mainly local but occasionally exotic in lithology. Deposits are generally 1 to 3 metres thick, displaying a gradational to sharp basal contact. Surface weathering is usually evident throughout, and if a soil is present, the contact is diffuse. This facies overlies facies A, B or bedrock. Facies C is interpreted as representing colluviated till (Plate 9).

Facies D is a very loose, soft, poorly sorted, clast-supported diamicton. The facies is massive to crudely bedded and primarily brown in colour. The clast content is high (average of 21 samples is 41%), consisting mainly of angular to very angular, cobble to boulder sized stones which lack striations and faceting. The pebble fabric is poor, represented almost entirely by local lithologies. Deposits are generally 1 to 2 metres thick, and the basal contact is sharp. Surface weathering is usually present throughout and the base of the soil contact is diffuse. Facies D usually overlies bedrock and is interpreted as representing bedrock colluvium.

All four of these diamicton facies represent first derivatives of erosion and deposition (primary indicator facies). Analytical results of samples obtained from these deposits must be interpreted separately, but all can be confidently used in the recognition and evaluation of buried mineral occurrences. Less reliable sediments are second derivative products which have undergone additional transportation and redeposition (glaciofluvial) or even third derivative products (glaciolacustrine or glaciomarine; cf. Shilts, 1993).

Table 1 provides the frequency distribution of drift exploration samples relative to the above facies. Viewed in terms of importance, reliability or confidence for interpreting drift data (geochemistry, pebble lithology, etc.) the facies can be ranked as follows: facies A, facies D, facies B, facies C followed by other second and third-derivative sediments. It is evident from this distribution, that most of the drift samples collected will provide reliable data for exploration purposes as only 4% of the samples are not representative of the four primary diamicton facies.

## GEOLOGICAL HISTORY

### QUATERNARY

The Quaternary geological history of northern Vancouver Island combines the effects of short-term episodic glaciation during the Late Wisconsinan and the gradual evolution of landscapes during the Holocene. Early descriptions by Dawson (1887) recognized the significant contribution of glacial activity to the landscape relief, bedrock erosion and sediment redistribution observed in the area, but overlooked much of the postglacial influence.

Howes (1981, 1983) concluded that northern Vancouver Island had been glaciated twice during the Quaternary on the basis of drill-hole evidence for an

"older till" underlying interglacial sediments and Fraser Glaciation drift. In the absence of multiple till sections indicating more than one glaciation, Kerr and Sibbick (1992) concluded that the area north of Quatsino Sound had been glaciated only once, most likely during the Late Wisconsinan. However, given the evidence presented by Howes, this interpretation is clearly unfounded. Nonetheless, the near-surface sediments observed in this study and by Kerr and Sibbick relate to the last phase of glaciation and deglaciation; Port McNeill till and Port McNeill deglacial sediments, respectively.

Approximately 25 000 years ago, ice began to accumulate in several centres of British Columbia, including central Vancouver Island and the Coast Mountains north of Vancouver. As climatic conditions deteriorated, ice on the mainland expanded eastward into the interior and westward into the Strait of Georgia and Queen Charlotte Strait, whereas ice on Vancouver Island expanded locally to occupy topographic lows. Continued climatic deterioration resulted in a significant net transfer of water from the oceans to the ice sheets. This resulted in a eustatic lowering of sea level, a thickening of the ice mass up to 2 kilometres in the straits and 700 metres on Vancouver Island and a concomitant glacio-isostatic depression of the land surface to a maximum of about 200 metres (Clague *et al.*, 1982; Clague, 1983; Howes, 1983). Surrounding this depression was a forebulge which moved westward in unison with the advancing ice sheet. At approximately  $20\ 500 \pm 330$  years BP (GSC-2505), the coast east of Port Hardy and Port McNeill may have been depressed up to 100 metres, thereby inundating nearly 15% of the eastern study area with glaciomarine conditions. Isostatic depression on the west side of the island was also about 100 metres (Luternauer *et al.*, 1989). Glaciomarine sediments were deposited in submerged areas adjacent to the advancing glaciers. At the height of glaciation in this area, about 15 000 years ago, the Cordilleran ice sheet captured local ice masses and the dominant flow of ice was west to northwest, well beyond the present limit of land. During this period thick sequences of subglacial till were deposited in depressions and thinner veneers on topographic highs. Ice began to disappear from the area about  $13\ 630 \pm 310$  years BP (WAT-721); depositing blankets of supraglacial debris in areas of *in situ* ice decay and thin but widespread accumulations of glaciofluvial sediments in areas of active retreat.

An accelerator mass spectrometry world date of  $10\ 650 \pm 350$  years BP (RIDDL-984), from a submarine vibrocore obtained in the Pacific Ocean 20 kilometres north of Vancouver Island, provides good evidence for a period of very low sea levels at this time; 25 metres below present levels. The dated material comes from a paleosol surface subsequently buried below marine sediments (Luternauer *et al.*, 1989).

### HOLOCENE

A variety of geological processes have been actively modifying the landscape during the last 10 000 years.

Most notably, the *in situ* modification of all surficial sediments through the process of pedogenesis. Northern Vancouver Island is covered by podzolic soils. Indeed, the strongly acidic bedrock in this area favors the development of these aluminum and iron-rich soils. Sulphides in the parent materials are easily oxidized and removed through groundwater leaching and are often replaced by *in situ* oxidates, such as limonite, which absorb heavy metals. Iron which precipitates in the lower B-horizon sometimes forms a distinct "hard-pan" containing complex salts of fulvic acids (Kauranne *et al.*, 1992; Plate 10). Early researchers sampled the B-horizon because of this metal concentration, but this practise simply adds soil formation variation factors to the geochemistry interpretation. The mean basal depth for pedogenic oxidation varies from 0.8 to 1.4 metres depending on the facies identified (Table 1). For this reason, all sampling in this study was restricted to fresh, unweathered C-horizon or parent material profiles. The average depth of the samples ranged from 1.7 to 2.3 metres below surface, also depending on the facies identified.

Fluvial and mass-wasting processes also act on the surface environment of this area. Creeks, streams and rivers are ubiquitous, providing an efficient mechanism for removing and redepositing significant volumes of sediment. Mass-wasting processes and deposits were observed in abundance in the study area, particularly in the west half, where the high relief and wet climate promotes slope instability.

## DRIFT EXPLORATION MAPS

A number of attributes which characterize surficial sediments must be evaluated during drift exploration studies. Unfortunately, this is not always possible in field situations nor is it possible in the pre-field planning stage. Two attributes, sediment genesis and thickness, which are very important factors to consider in drift exploration work can be evaluated from air-photographic interpretation and then used in the planning process of drift sampling. The first factor follows Shilts (1993), who recognizes that drift sampling media can be ranked from excellent to poor according to genesis: first derivative products (*e.g.* till), second derivative products (*e.g.* outwash) and third derivative products (*e.g.* glaciolacustrine). This ordering emphasizes the importance of proximity to bedrock source and the transport history of sediments in affecting the integrity of samples. Similarly, the greater the thickness of a deposit the further the sampling surface is from the underlying bedrock.

Using the above two parameters, as portrayed in the information on a terrain map, we developed a series of genesis/thickness data pairs. To improve user interpretation, we then categorized our data pairs in the terrain units from 1 (excellent) to 5 (poor), as an indication of their utility and reliability in providing interpretable drift results. A 1 or 2 category terrain polygon implies that the explorationist can have a higher

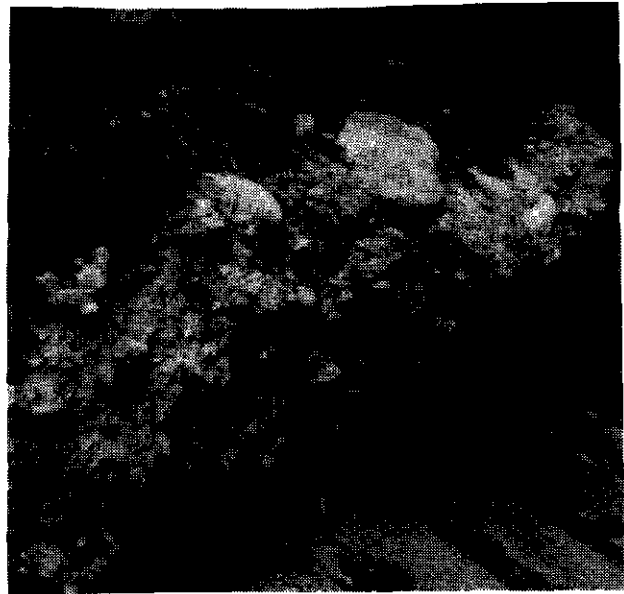


Plate 10. Hard pan formed in near surface gravel accumulation as a result of iron precipitation in Podzolic soil.

level of confidence in the interpretation of drift results in contrast to data retrieved from a 4 or 5 category polygon. For lack of a better term, we have tentatively called this style of map a "sample media confidence map". Industry response to an earlier variation of this method suggested that the original three categories should be expanded to further emphasize subtle variations in the deposits; hence, we have chosen five categories. Figure 7 is a sample media confidence map for 92L/11. The genesis / thickness pairs developed in this study which comprise the five individual categories are listed in the illustration.

The samples collected in this study are distributed over most of the categories, but occur primarily in categories 1 and 2. As such, we feel confident that the integrity of the data derived from the drift sampling program is high. Most samples come from sediments which have undergone short transport distances, have simple transport histories, or occur as thin deposits and therefore offer a good reflection of the potential for mineralization in the region.

## SUMMARY

Quaternary geology plays an important role in mineral exploration studies in areas of glaciated terrain. The principles of drift exploration rely on an accurate understanding of the regional geological history, the distribution of various types of sediment, the genesis of individual deposits and the relationship of sediment cover to bedrock lithology (Liverman, 1992). Terrain and surficial geology mapping provides a first step toward attaining these goals. Ground-truthing, including stratigraphic and sedimentologic descriptions using facies analysis further the exploration process by identifying deposit genesis. Following this, detailed sampling for till geochemistry and pebble lithologies can

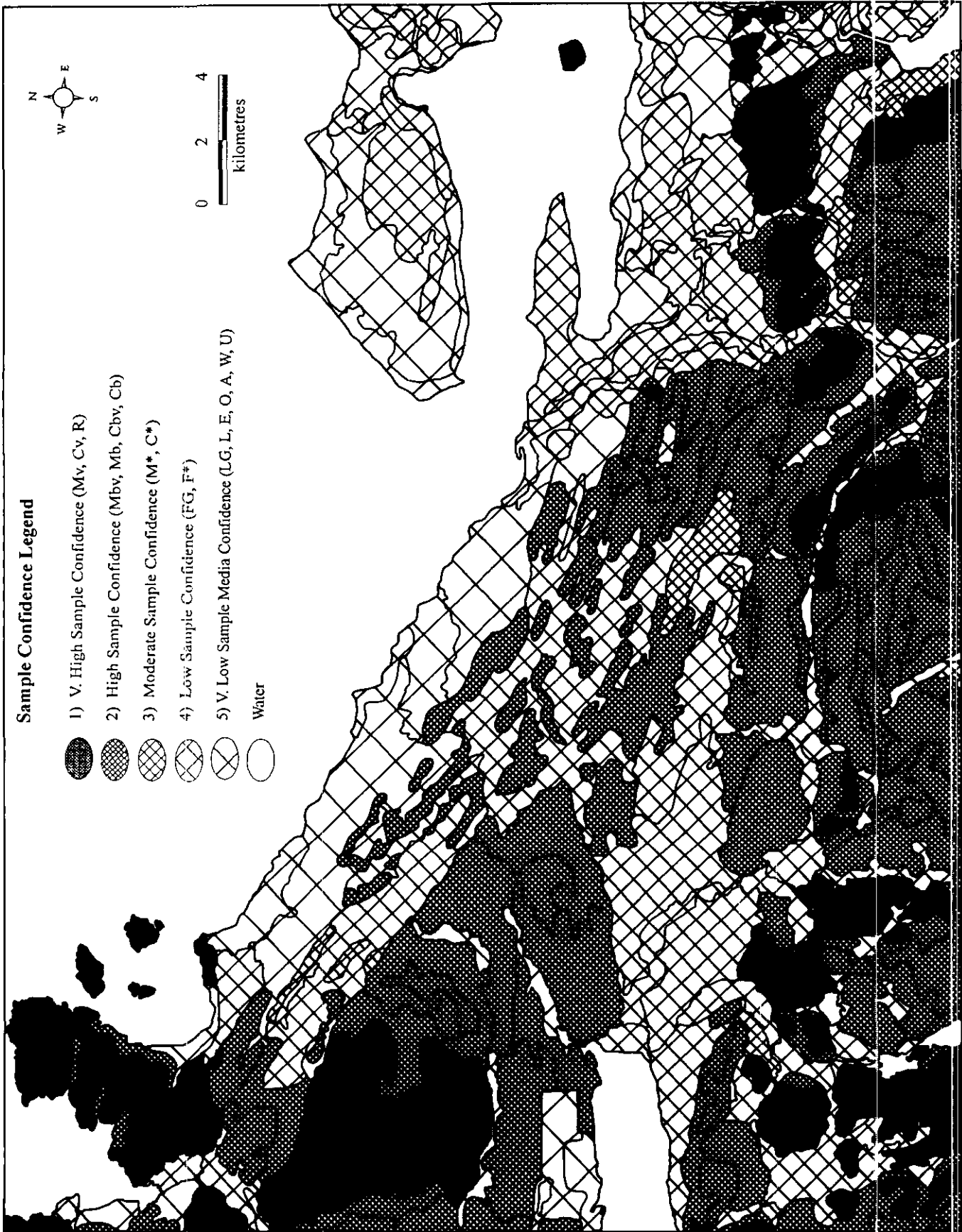


Figure 7. Sample media confidence map for NTS 92L/11. Preferred polygons for drift exploration studies are lower number categories (i.e. 1 to 3).

then be productively collected (cf. Coker and DiLabio, 1989). Successful interpretation of these data provides the final link between surficial geology and the exploration for buried mineral occurrences.

Terrain and surficial geology mapping must precede drift exploration studies which rely on till geochemistry and pebble lithology analysis. Such mapping not only identifies where preferred sediments occur, but also provides information regarding drift thickness and paleoflow direction. The identification of distinct glacial and nonglacial facies must be used in drift-exploration strategies, to ensure that comparability in results can be maintained. One recent study of glacial dispersal of till constituents showed clearly how flow paths and transport distances varied according to the different types of morainic landforms identified (Aario and Peuraniemi, 1992). Adequate sampling density suited to the objectives of the project must also be determined. The sampling density in this study (1 per 5 km<sup>2</sup>) was intended to provide reconnaissance level data as a basis for further exploration activity at more detailed scales. Assuming average transport lengths of 1.0 kilometre for geochemical anomalies (cf. Salminen and Hartikainen, 1985) and 10.0 kilometres for pebble lithologies (cf. Gillberg, 1967), the data collected in this study exceed the reconnaissance level study and approach local-scale accuracy.

It is the intent of this project to next study the results of the geochemical analyses and pebble lithology counts in relation to the facies and landforms sampled. We expect to establish quantitative dispersal decay curves and glacially dispersed geochemical anomalies characteristic of the northern Vancouver Island environment. We further intend to integrate this information with our knowledge of drift thickness (based on drill-hole data and "sample media confidence maps") to generate mineral drift - exploration models unique to this area and test the models during the next field season.

## ACKNOWLEDGMENTS

Productive discussions regarding bedrock geology, mineralization and geochemistry were gladly provided by the Northern Vancouver Island project geologists including A. Panteleyev, G.T. Nixon, S.J.N. Sibbick and W.J. McMillan. The authors appreciate the access to BHP Minerals data graciously provided through J. Fleming. This paper benefited substantially from the editorial comments of J.M. Newell, and formatting skills of Wade Noble.

## REFERENCES

- Aario, R. and Peuraniemi, V. (1992): Glacial Dispersal of Till Constituents in Morainic Landforms of Different Types; *Geomorphology*, Volume 6, pages 9-25.
- Bobrowsky, P.T., Kerr, D.E., Sibbick, S.J.N. and Newman, K. (1993): Drift Exploration Studies, Valley Copper Pit, Highland Valley Copper Mine, British Columbia: Stratigraphy and Sedimentology (92I/6, 7, 10 and 11); in *Geological Fieldwork 1992*, Grant, B. and Newell, J.M., Editors, *B.C. Ministry of Energy, Mines and Petroleum Resources*, Paper 1993-1, pages 427-437.
- Clague, J.J. (1983): Glacio-isostatic Effects of the Cordilleran Ice Sheet, British Columbia, Canada; in *Shorelines and Isostasy*, Smith, D.E., Editor, *Academic Press*, London, pages 321-343.
- Clague, J.J., Harper, J.R., Hebda, R.J. and Howes, D.E. (1982): Late Quaternary Sea Levels and Crustal Movements, Coastal British Columbia; *Canadian Journal of Earth Sciences*, Volume 19, pages 597-618.
- Clark, P.U. (1987): Subglacial Sediment Dispersal and Till Composition; *Journal of Geology*, Volume 95, pages 527-541.
- Coker, W.B. and DiLabio, R.N.W. (1989): Geochemical Exploration in Glaciated Terrain: Geochemical Responses; in *Proceedings of Exploration '87*, Garland, J.D., Editor, *Ontario Geological Survey*, Special Volume, 3, pages 336-383.
- Dawson, G.M. (1887): Report on a Geological Examination of the Northern Part of Vancouver Island, B.C.; *Geological Survey of Canada*, Annual Report 1886, Part B, 129 pages.
- Gillberg, G. (1967): Further Discussion of the Lithological Homogeneity of Till; *Geologiska Föreningen Stockholm Förhandlingar*, Volume 89, pages 29-49.
- Gravel, J.L. and Matysek, P.F. (1989): 1988 Regional Geochemical Survey, Northern Vancouver Island and Adjacent Mainland (92E, 92K, 92L, 102I); in *Geological Fieldwork 1988*, *B.C. Ministry of Energy, Mines and Petroleum Resources*, Paper 1989-1, pages 585-592.
- Howes, D.E. (1981): Terrain Inventory and Geological Hazards: Northern Vancouver Island; *B.C. Ministry of Environment, Lands and Parks*, APD Bulletin 5.
- Howes, D.E. (1983): Late Quaternary Sediments and Geomorphic History of Northern Vancouver Island, British Columbia; *Canadian Journal of Earth Sciences*, Volume 20, pages 57-65.
- Howes, D.E. and Kenk, E. (1988): Terrain Classification System for British Columbia, Revised Edition; *B.C. Ministry of Environment, Lands and Parks*, MOE Manual 10.
- Kauranne, K., Salminen, R. and Eriksson, K. (1992): Regolith Exploration Geochemistry in Arctic and Temperate Terrains; *Handbook of Exploration Geochemistry*, Volume 5, *Elsevier*, Amsterdam, 443 pages.
- Kerr, D.E. (1992): Surficial Geology of the Quatsino Area, NTS 092L/12, scale 1:50 000; *B.C. Ministry of Energy, Mines and Petroleum Resources*, Open File 1992-6.
- Kerr, D.E. and Sibbick, S.J. (1992): Preliminary Results of Drift Exploration Studies in the Quatsino (92L/12) and the Mount Milligan (93N/1E, 93O/4W) Areas; in *Geological Fieldwork 1991*, Grant, B. and Newell, J.M., Editors, *B.C. Ministry of Energy, Mines and Petroleum Resources*, Paper 1992-1, pages 341-347.
- Kerr, D. E., Sibbick, S.J. and Jackaman, W. (1992): Till Geochemistry of the Quatsino Map Area (92L/12); *B.C. Ministry of Energy, Mines and Petroleum Resources*, Open File 1992-21.
- Kujansuu, R. and Saarnisto, M. (Editors) (1990): Glacial Indicator Tracing; *Balkema*, Rotterdam.
- Liverman, D.G.E. (1992): Application of Regional Quaternary Mapping to Mineral Exploration, Northeastern Newfoundland, Canada; *Transactions Institution of Mining and Metallurgy*, Section B: Applied Earth Science, Volume 101, pages B89-B98.
- Luternauer, J.L., Clague, J.J., Conway, K.W., Barrie, J.V., Blaise, B., and Mathewes, R.W. (1989): Late Pleistocene Terrestrial Deposits on the Continental Shelf of Western Canada: Evidence for Rapid Sea-level Change at the End of the Last Glaciation; *Geology*, Volume 17, pages 357-360.
- Nixon, G.T., Hammack, J.L., Hamilton, J. and Jennings, H. (1993): Preliminary Geology of the Quatsino Sound Area, Northern Vancouver Island, 92L/5; in *Geological*

- Fieldwork 1992, Grant, B. and Newell, J.M., Editors, *B.C. Ministry of Energy, Mines and Petroleum Resources*, Paper 1993-1, pages 17-35.
- Nixon, G.T., Hammack, J.L., Koyanagi, V.M., Payic, G., Panteleyev, A., Massey, N.W.D., Hamilton, J.V. and Haggart, J.W. (1994): Preliminary Geology of the Quatsino - Port McNeill Map Area, Northern Vancouver Island (92L/12, 11); in *Geological Fieldwork 1993*, Grant, B. and Newell, J.M., Editors, *B.C. Ministry of Energy, Mines and Petroleum Resources*, Paper 1994-1, this volume.
- Panteleyev, A. (1992): Copper-Gold-Silver Deposits Transitional between Subvolcanic Porphyry and Epithermal Environments; in *Geological Fieldwork 1991*, Grant, B. and Newell, J.M., Editors, *B.C. Ministry of Energy, Mines and Petroleum Resources*, Paper 1992-1, pages 231-234.
- Panteleyev, A. and Koyanagi, V.M. (1993): Advanced Argillic Alteration in Bonanza Volcanic Rocks, Northern Vancouver Island - Lithologic Associations and Permeability Controls; in *Geological Fieldwork 1992*, Grant, B. and Newell, J.M., Editors, *B.C. Ministry of Energy, Mines and Petroleum Resources*, Paper 1993-1, pages 287-292.
- Panteleyev, A. and Koyanagi, V.M. (1994): Advanced Argillic Alteration in Bonanza Volcanic Rocks, Northern Vancouver Island - Lithologic and Structural Controls; in *Geological Fieldwork 1993*, Grant, B. and Newell, J.M., Editors, *B.C. Ministry of Energy, Mines and Petroleum Resources*, Paper 1994-1, this volume.
- Panteleyev, A., Bobrowsky, P.T., Nixon, G.T. and Sibbick, S.J. (1994): Northern Vancouver Island Integrated Project; in *Geological Fieldwork 1993*, Grant, B. and Newell, J.M., Editors, *B.C. Ministry of Energy, Mines and Petroleum Resources*, Paper 1994-1, this volume.
- Salminen, R. and Hartikainen, A. (1985): Glacial Transport of Till and its Influence on Interpretation of Geochemical Results in North Karelia, Finland; *Geological Survey of Finland*, Bulletin 335, 48 pages.
- Salonen, V.-P. (1988): Application of Glacial Dynamics, Genetic Differentiation of Glaciogenic Deposits and their Landforms to Indicator Tracing in the Search for Ore Deposits; in *Genetic Classification of Glaciogenic Deposits*, Goldthwait, R.P. and Matsch, C., Editors, *Balkema*, Rotterdam, pages 183-190.
- Shilts, W.W. (1993): Geological Survey of Canada's Contributions to Understanding the Composition of Glacial Sediments; *Canadian Journal of Earth Sciences*, Volume 30, pages 333-353.
- Sibbick, S.J.N. (1994): Preliminary Report on the Application of Catchment Basin Analysis to Regional Geochemical Survey Data, Northern Vancouver Island (92L/SW); in *Geological Fieldwork 1993*, Grant, B. and Newell, J.M., Editors, *B.C. Ministry of Energy, Mines and Petroleum Resources*, Paper 1994-1, this volume.
- Strobel, M.L. and Faure, G. (1987): Transport of Indicator Clasts by Ice Sheets and the Transport Half-distance: A Contribution to Prospecting for Ore Deposits; *Journal of Geology*, Volume 95, pages 687-697.

## NOTES

# ADVANCED ARGILLIC ALTERATION IN BONANZA VOLCANIC ROCKS, NORTHERN VANCOUVER ISLAND - LITHOLOGIC AND PERMEABILITY CONTROLS

By Andre Panteleyev and Victor M. Koyanagi

**KEYWORDS:** Economic geology, Bonanza volcanics, porphyry copper, copper-gold, epithermal, advanced argillic, acid sulphate, alunite, kaolinite, hydrothermal alteration, mineral deposits, mineralization.

## INTRODUCTION

Hydrothermally altered rocks containing advanced argillic alteration are being studied in British Columbia (Panteleyev, 1992; Panteleyev and Koyanagi, 1993) as part of an investigation of acid sulphate type epithermal mineralization and intrusion-related base and precious metal mineralization in settings transitional between porphyry copper and epithermal environments. The initiation of an integrated team project in northern Vancouver Island as part of the Ministry's 1993 *Mineral Strategy* enabled a revisit to the area and led to additional studies of the advanced argillic alteration and acid sulphate mineralization in Bonanza volcanic rocks to the west of the Island Copper mine in the Quatsino map area (NTS 92L/12; Figure 1). For a discussion of a related study of the generation of natural acid drainage in this mineralized environment, see Koyanagi and Panteleyev (1994, this volume). A summary of the integrated project (Panteleyev *et al.*, 1994, this volume) and more detailed descriptions of the other project components - surficial geology, bedrock geology and exploration geochemistry, are contained elsewhere in this volume (Bobrowsky and Meldrum, 1994; Nixon *et al.*, 1994; Sibbick, 1994).

## HYDROTHERMAL ALTERATION

Large areas of clay-altered, and locally intensely acid leached siliceous rocks, are found in the belt of Bonanza volcanic rocks to the north of Holberg Inlet (Figure 2). The most intense hydrothermal alteration, including advanced argillic assemblages, is evident in the region from the Pemberton Hills westward to Mount McIntosh, a distance of 15 to 30 kilometres to the west-northwest of Island Copper mine. A second zone of similar alteration occurs even farther west along the regional trend of the Bonanza hostrocks at the Red Dog property and to the west of it, about 6 to 7 kilometres to the north of the village of Holberg. The alteration is most evident in the rhyolitic Bonanza map-units but also occurs in the

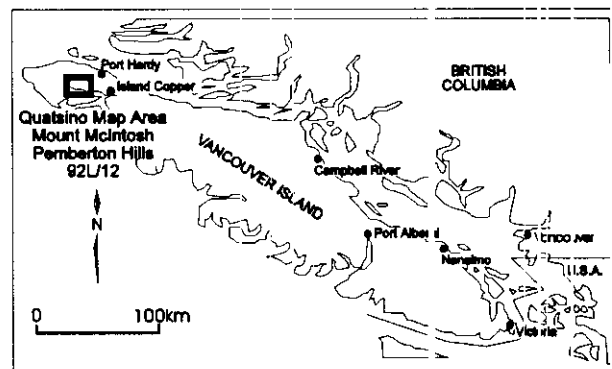


Figure 1. Location map; project area is north of Holberg Inlet in NTS 92L/12.

immediately underlying, feldspar-phyrific, basic to intermediate volcanic rocks and, to a lesser extent, some of the adjoining intrusive bodies of the Island Plutonic Suite. The relationship between regional stratigraphic map units and the hydrothermally altered rocks is discussed in Nixon *et al.* (1994, this volume).

The advanced argillic alteration is characterized by the presence of kaolinite, dickite, alunite and pyrophyllite. Other associated minerals confirmed by X-ray diffraction analysis are abundant quartz, diaspore [AlO(OH)], zunyite [Al<sub>13</sub>Si<sub>5</sub>O<sub>20</sub>(OH,F)<sub>18</sub>Cl], various micas including sericite, muscovite and illite; lesser smectite, paragonite, gypsum, anhydrite, natroalunite, sulphur and rutile; and minor topaz, (? meta-halloysite, arsenian alunite (schlossmacherite) and tridymite.

The clay-rich hydrothermal alteration assemblages all contain some quartz. It is derived from both residual and, less commonly, added silica. Major alteration assemblages are: quartz + kaolinite; quartz + dickite ± pyrophyllite and/or kaolinite, all with or without alunite, diaspore, zunyite and minor mica; and quartz + alunite ± kaolinite. Peripheral rocks, both underlying and lateral to the clay-altered zones, contain pervasive zones with swelling-type, mixed-layer smectite clay species (montmorillonite) as well as extensive propylitic alteration characterized by albite, chlorite, epidote, carbonate, pyrite and zeolite. The propylitic rocks, in places, are crosscut by fracture-controlled sericitic and kaolinitic alteration.

Strongly altered rocks are bleached and chalky appearing. Where relict clay-altered plagioclase is present, the rocks can be determined to be derived from basaltic to andesitic protoliths. The more intense

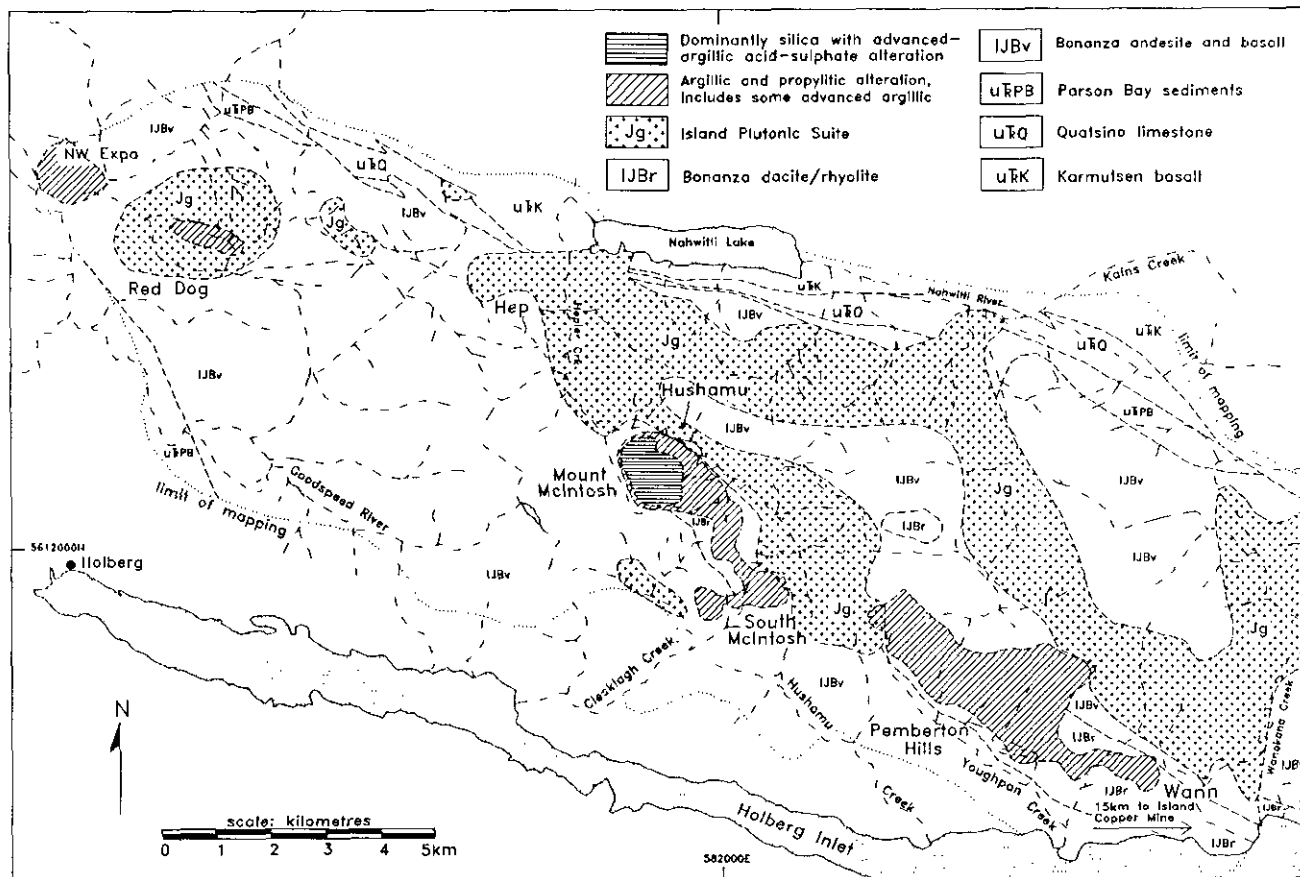


Figure 2. Generalized geological map units after Nixon *et al.* (1994), alteration zones and major mineral deposits north of Holberg Inlet in Quatsino map area 92L/12.

alteration in both feldspar-phyric and rhyolitic rocks creates a mottled rock with grey-buff-pink clay patches in grey, fine-grained to microcrystalline siliceous groundmass. The mottled anhedral, but generally equant, clay patches range in size from a few millimetres to a few centimetres in diameter. In thin section, they consist of aggregates of fine-grained clay minerals, mainly kaolinite. Streaks and irregular veins of kaolinite, quartz, diaspore or alunite and patches of zunyite crosscut the mottled rocks. In some outcrops, the rocks consist, in large part, of quartz stockworks, veins and patches of pervasive silica replacement. The most intensely leached rocks are made up of almost entirely quartz (>90%) and voids that give rise to a vuggy or "slaggy" texture or, less commonly, a friable, granular "sponge rock" appearance. This vuggy silica with attendant volume reduction of the altered hostrock is the characteristic siliceous residuum of intensely acid leached rocks in high sulphidation epithermal systems (White, 1991; Sillitoe, 1993). These highly porous rocks typically have 10 to 30% voids surrounded by fine, granular, interlocking, crystalline quartz grains. Other minerals present in various amounts are kaolinite/dickite, alunite and minor zunyite, rutile or other optically indeterminate iron-titanium minerals. The altered rocks commonly contain fine-grained pyrite; some silicified areas within the clay-altered zones contain 15% or more pyrite or, less commonly, specular hematite.

These residual, acid-leached textures are evident in the flow-banded rhyolite and other rhyolitic units, in feldspar-phyric basalt and basaltic andesite and, rarely, in some (quartz) diorite and monzonite stocks. Much, if not most, of the silica in these intensely altered rocks has been liberated from the breakdown of the hostrock silicate mineral grains. Remobilized and hydrothermally added silica is evident in places in the form of quartz veins and stockworks as well as crystalline and chalcedonic crusts and overgrowths in vugs and cavities.

Silica is also present as the main matrix component in many breccias and pervasively silicified or quartz-veined clasts in some crosscutting hydrothermal breccias, notably the youngest. The younger breccias tend to have rounded, strongly milled, hydrothermally altered polyolithic clasts. In many breccias, fine-grained pyrite is a major matrix component.

## PETROCHEMISTRY

Chemical compositions of typical Bonanza volcanic rocks and their altered equivalents in the map area were previously reported (Panteleyev and Koyanagi, 1993, Table 2-7-1, page 289) as major oxide data, including loss-on-ignition (LOI), CO<sub>2</sub>, S and FeO. Additional analyses of the same sample suite, with the corresponding minor element data, are shown in Table 1.

TABLE 1: MINOR ELEMENT ANALYSES FOR TYPICAL HOST ROCKS; CORRESPONDING DATA FOR WHOLE ROCK ANALYSES PUBLISHED IN GEOLOGICAL FIELDWORK 1992, PAGE 289.

SAMPLE NUMBER	Map Unit* Type**	Rock Type**	UTM		S %	Au ppb	Cu	Pb	Zn	Ni	Mo	Cr	As	Sb	Ba	Sr	Rb	Zr	Y	Nb	Ta	Th	U	Ce	Cs	Hf	Sc	V	La	Nd	Sm	Eu	Tb	Yb	Lu	
			East	North																																
Unaltered																																				
92AP01/1-1	1	1	578214	5612680	0.004	<2	37	6	100	6	<1	23	<0.5	0.1	706	622	<10	107	30	<5	<0.5	2.2	1.7	33	<1	3	20	142	17	16	4.3	1.3	0.7	2.9	0.47	
92AP01/2-2	1	1	578159	5611115	0.001	<2	41	5	90	9	<1	28	<0.5	0.1	267	487	<10	106	29	<5	<0.5	2.2	2.0	34	<1	4	34	227	17	23	5.1	1.5	0.9	3.5	0.48	
92AP11/5-53	1	1	578534	5612376	0.004	4	41	4	80	12	<1	26	1.9	0.1	469	589	<10	98	26	<5	<0.5	2.1	<0.5	38	2	3	26	183	16	13	4.4	1.5	0.7	3.1	0.51	
92AP8/5-30	1	1	576128	5617652	0.010	5	13	3	110	149	<1	444	4.4	3.5	450	698	<10	59	21	<5	<0.5	0.5	<0.5	12	<1	2	45	258	4.3	12	2.7	1.2	<0.5	2.4	0.39	
92AP5/8-18	1	1	581873	5616109	0.010	3	50	3	70	23	<1	42	<0.5	0.2	355	505	<10	81	23	<5	<0.5	1.8	<0.5	26	<1	<1	32	221	12	9	3.4	1.3	<0.5	3.0	0.50	
92AP01/5-5	1	2	578644	5611570	0.001	<2	28	5	80	4	<1	21	<0.5	0.1	789	381	<10	114	28	<5	1.3	3.0	2.0	40	2	4	27	196	18	19	4.6	1.6	0.8	3.9	0.56	
92AP13/10-68	1	2	582167	5611310	0.11	<2	83	8	65	3	<1	15	1.4	0.1	461	459	<10	158	32	5	<0.5	3.3	2.3	38	<1	5	18	155	16	13	4.3	1.3	1.0	3.5	0.55	
92AP20/8-128	1	2	586784	5609612	0.040	<2	56	4	77	9	<1	24	<0.5	0.3	613	245	18	134	30	5	<0.5	3.1	1.6	30	<1	2	19	175	14	13	3.4	0.9	0.6	2.9	0.45	
92AP21/7-132	1	2	589941	5608133	0.003	<2	58	4	70	55	<1	147	<0.5	0.1	657	464	11	139	28	5	<0.5	3.6	1.4	37	<1	4	26	191	16	13	3.8	1.2	0.6	2.9	0.49	
92AP16/1-77	1	2	586791	5610934	0.014	<2	135	4	74	7	<1	24	1.1	0.2	631	598	<10	133	31	<5	<0.5	2.9	<0.5	34	<1	3	16	146	17	15	3.9	1.3	0.6	2.8	0.46	
92VKO8-1	1	2	585921	5611889	0.10	<2	45	3	78	8	<1	34	5.8	1.0	467	653	20	120	29	<5	<0.5	2.1	1.2	31	2	3	15	69	15	15	3.6	1.3	<0.5	2.9	0.44	
92VKO8-4	1	3	585900	5612159	0.24	<2	16	4	29	3	<1	10	2.5	0.5	562	332	29	167	22	<5	1.4	5.2	2.1	42	<1	4	3.2	18	24	14	2.7	0.8	0.6	2.5	0.40	
92AP16/7-83	1	3	585130	5612360	1.09	<2	8	3	37	4	<1	16	2.6	0.4	774	394	30	167	23	<5	1.6	4.3	1.8	39	<1	4	3.5	32	21	14	2.4	0.8	<0.5	2.1	0.33	
92AP07/1-27	2	1	578376	5617526	0.007	<2	44	3	120	71	<1	125	1.4	0.3	41	371	<10	143	35	10	2.9	1.1	<0.5	35	<1	4	48	386	12	16	5.7	2.1	1.1	4.0	0.60	
92AP22/1-140	2	1	579223	5618229	0.013	5	111	3	78	87	<1	241	<0.5	0.1	46	409	<10	98	25	8	0.8	0.7	1.0	15	<1	2	27	281	6.5	10	2.9	1.0	<0.5	1.9	0.26	
Spilitized Matched Pair																																				
92AP19/2-119	1	1	586779	5608443	0.003	<2	51	3	78	33	<1	21	<0.5	0.1	542	588	<10	99	28	<5	1.3	1.8	0.8	32	<1	3	28	222	14	18	4.2	1.5	0.6	3.2	0.49	
92AP19/2-120	1	4	586779	5608443	0.006	<2	53	6	77	4	<1	19	<0.5	0.3	329	478	<10	93	27	<5	<0.5	1.7	1.0	27	<1	1	27	196	13	16	4.1	1.5	<0.5	3.2	0.51	
Hydrothermally Altered																																				
91AP41a	1	4	580931	5613075	0.050	10	20	8	14	1	20	24	3.0	<0.5	16	16	<10	125	<10	<5	<15	<15	<15	<15	<5	<5	83	<15								
91AP20/6-95	1	4	580931	5613075	0.020	<5	5	<6	8	1	11	22	2.0	2.0	27	26	249	12	15	<15	<15	<15	<15	<5	<5	<5	<5	<5								
92AP19/1-109	1	4	587379	5609236	8.16	10	150	17	14	15	<1	34	8.5	4.1	780	558	<10	196	24	6	<0.5	7.1	1.6	57	<1	7	33	189	26	23	7.5	1.9	1.2	3.7	0.64	
92AP19/1-110	1	4	587379	5609236	0.19	8	25	23	6	2	3	29	1.1	1.9	375	315	<10	234	27	7	1	6.8	2.7	62	<1	8	18	195	28	29	9.0	2.4	1.3	3.4	0.55	
92AP19/1-111	1	4	587379	5609236	0.10	16	67	4	10	2	14	26	1.6	2.7	108	33	<10	360	13	14	1.8	4.8	3.2	7	<1	13	9	113	2.1	5	0.6	0.4	<0.5	2.6	0.46	
92AP19/1-112	1	4	587379	5609236	0.04	11	14	9	3	<2	13	24	6.3	2.7	106	157	<10	512	21	18	4.2	7.4	4.3	10	<1	18	13	100	3.5	18	1.5	0.7	<0.5	4.5	0.76	
92AP19/1-113	1	4	587379	5609236	5.78	<2	130	16	45	6	<1	14	24	1	1203	259	17	254	40	8	1.5	8.6	4.4	64	<1	8	16	114	30	20	6.8	1.7	1.1	5.2	0.81	
92AP19/1-114	1	4	587379	5609236	6.87	<2	114	39	12	14	2	10	13	0.4	1862	503	20	220	33	<5	1.2	7.8	3.1	66	<1	8	13	95	31	21	6.1	1.8	0.9	4.9	0.79	
92AP19/1-115	1	4	587379	5609236	6.99	4	167	30	70	24	5	21	1.7	0.5	40	41	<10	164	30	8	1.2	4.0	2.0	34	<1	6	16	177	18	14	4.6	1.6	0.9	3.8	0.62	
92AP19/1-116	1	4	587379	5609236	1.72	<2	35	3	42	12	4	31	4.4	0.1	103	147	11	197	42	7	1.3	6.8	2.1	66	3	4	27	185	30	26	7.4	1.7	1.4	4.3	0.15	
92AP19/1-117	1	4	587379	5609236	0.57	<2	72	4	34	9	<1	28	6.3	0.5	630	300	30	191	35	8	1.5	5.8	2.9	37	2	6	21	170	20	19	5.4	1.4	<0.5	4.1	0.64	
92AP19/1-118	1	4	587379	5609236	1.82	<2	136	4	18	9	<1	29	1.5	0.9	366	288	11	184	38	6	<0.5	6.4	2.6	51	4	5	23	176	24	23	5.7	1.7	0.9	4.2	0.69	

\* Map Unit: 1 = Bonanza volcanics; 2 = Karmutsen basalt;

\*\* Rock Type Classification from TAS diagram: 1 = basalt; 2 = basalt/andesite; 3 = rhyolite/dacite; 4 = hydrothermally altered

All values in ppm except where noted

Analytical Methods: Sr, Rb, Zr, Y, Nb, Cr - XRF on fused disk (B.C. GSB laboratory)

As, Au, Sb, Ce, Cs, Sc, Ta, Th, U - thermal neutron activation (Activation Laboratories Limited)

Ba, V - XRF pressed pellet (Cominco Research Laboratories)

Assay for Cu, Pb, Zn, Ni, Mo, Ag - hv hydrofluoric - nitric - hydrochloric - hydrogen peroxide - ammonium persulfate

Elements not detected (below detection limit): Hg <1ppm, Ir <5ppm, Bi <3ppm except for samples 92AP19/1-109 @ 17ppm and 92AP19/1-115 @ 64ppm, all Ag <= 0.2ppm

91AP41a: F = 2800ppm, Hg <20 ppb, Te <0.3 ppm; 91AP20/6-95: F = 660ppm, Hg = 60ppb, Te <0.3ppm

Note for petrochemical studies and calculations of mass balance/flux, that titanium and possibly other immobile elements do not appear to be conserved, but rather are enhanced in the most strongly altered rocks. This observation is consistent with the modal abundance of rutile and other titanium species in the vuggy, siliceous rocks. Zirconium is probably not conserved either in the most silicified rocks, with up to 512 ppm zirconium in association with 2.8% TiO<sub>2</sub>, but only 21 ppm yttrium.

## MINERALIZATION

### PORPHYRY COPPER DEPOSITS

Porphyry copper deposits are the dominant mineral deposit type in the belt of Jurassic Bonanza volcanics and Island intrusions in northern Vancouver Island. The 'volcanic-type' porphyry copper deposit (Sutherland Brown, 1976; McMillan and Panteleyev, 1988) at Island Copper mine is a superior copper-gold-molybdenum mine by British Columbia standards. Porphyry copper prospects with established mineral reserves are those at the Hushamu and Red Dog deposits, 26 and 37 kilometres respectively, to the west of Island Copper mine. Other prospects in the large EXPO claim block at which significant exploration has been done include the NW Expo, HEP and a number of other showings. Skarn deposits in the map area, mainly near Nahwitti Lake, are hosted by Parson Bay, Quatsino and basal Bonanza units; they have received attention in the past for their base metal potential, and recently for precious metals.

### ISLAND COPPER

The Island Copper deposit has been described by Fleming (1992), drawing on the previous descriptions of Perello *et al.* (1989) and Cargill *et al.* (1976). The following description is extracted from these works. The mineralization is related to Early Jurassic (*circa* 180 Ma) rhyodacitic quartz feldspar porphyry dikes and related hydrothermal breccias. Initial ore reserves were estimated at 257 million tonnes at an average grade of 0.52% copper and 0.017% molybdenum. At the start of mining, in the near-surface and north end of the mine, gold grades in excess of 0.4 gram per tonne were common; they have diminished during the course of deeper mining. The average gold content (head-grade) for the mine will be about 0.18 gram per tonne (Fleming, 1992). The porphyry copper mineralization is characterized by stockworks, breccias, veinlets, disseminations and fractures with quartz, pyrite, chalcopyrite, molybdenite, magnetite, amphibole (tremolite/actinolite), biotite, chlorite, albite, sericite, epidote and calcite. Some breccias contain quartz, sericite, pyrophyllite, kaolinite and dumortierite, and there are extensive late stage veinlets with zeolite, calcite and hydrocarbon compounds.

Mineralization took place in both the central quartz feldspar porphyry dike and the andesitic hostrocks. The porphyries were emplaced at various stages. Early intrusions are quartz veined, strongly altered and mineralized; later intrusive rocks have fewer quartz veins and are less mineralized. The margins of the porphyritic intrusions are marked by well-mineralized breccias of various types. Intrusive breccias with rounded wallrock and porphyry fragments form hydrothermal pipes or dike-like bodies. Intrusion breccias with clasts contained in an igneous matrix are also present. The younger breccias with pyrophyllite, kaolinite, sericite and dumortierite occur in the uppermost and northern parts of the deposit. They contain quartz feldspar porphyry fragments and are interpreted to be phreatomagmatic hydrothermal bodies.

Hydrothermal alteration assemblages are centred on and zoned away from the central porphyry intrusions. The central, and early, alteration is a quartz-amphibole-magnetite assemblage with biotite, albite, apatite and much of the sulphide mineralization. This alteration grades outward into chlorite-pyrite ± magnetite, albite, calcite and further away, a propylitic assemblage characterized by abundant epidote. Mine staff regard this central, largely intrusion-hosted, chalcopyrite-rich mineralization to be a 'potassic' alteration due to the presence of abundant magnetite, biotite and hairline fractures filled with potassium feldspar (J. Fleming, personal communication, 1991). An intermediate stage alteration with quartz-sericite ± chlorite and kaolinite is associated with stockworking that grades locally into brecciation. It crosscuts, overlaps and locally flanks the central alteration zone. This intermediate stage has introduced some additional pyrite, molybdenite and chalcopyrite as fracture fillings. The late stage alteration is characterized by pyrophyllite, kaolinite and a distinctive, blue-coloured dumortierite-bearing, advanced argillic assemblage for which this deposit is renowned. It forms a carapace over much of the ore zone and is thought to be a very shallow, subvolcanic feature.

### HUSHAMU

The Hushamu deposit consists of two partially overlapping components. The deeper part of the prospect, the Hushamu deposit *sensu stricto*, is a porphyry copper-gold-molybdenum deposit. Mineral reserves are stated to be 172.5 million tonnes with an average grade of 0.28% copper, 0.34 gram per tonne gold and 0.009% molybdenum (Dasler *et al.*, in preparation). The porphyry copper zone is exposed along the valley bottom near a small lake known locally as Hushamu Lake. The intermediate to uppermost part of the deposit, on Mount McIntosh, is transitional into an enargite-bearing, acid sulphate, high-sulphidation epithermal zone. A description of the deposit by Perello (1992) refers to multiple stage stockworks with quartz-magnetite-chalcopyrite-pyrite fracture fillings and disseminations hosted by feldspar and feldspar-quartz porphyries and andesitic volcanics. At least part, if not most, of the deposit to the north of Hushamu Lake is

hosted by diorite to quartz diorite of the Island Plutonic Suite. The most intense alteration in the diorite is seen as fractures and quartz stockworks carrying magnetite, amphibole, pyrite and chalcopyrite and surrounded by alteration envelopes containing albite, chlorite and epidote. Elsewhere, pervasive chlorite, albite and illitic clays are predominant. This alteration is locally overprinted by quartz-sericite  $\pm$  kaolinite and rutile alteration with associated pyrite and minor chalcopyrite (Perello, 1992).

## RED DOG

The Red Dog deposit has reported geological reserves of 31.2 million tonnes with an average grade of 0.313% copper, 0.446 gram per tonne, gold and 0.007% molybdenum (Crew Natural Resources Ltd., prospectus, 1992). The principal minerals of economic importance are chalcopyrite and molybdenite. In addition, fine-grained bornite and traces of (primary) covellite have been noted. The deposit is centred on Red Dog Hill, in an east-southeast-trending zone of silicification and quartz-eye, quartz feldspar and 'syenitic' dike intrusions within a larger feldspar-hornblende-phyric stock of medium-grained diorite to monzonite composition. Other investigators have described the altered rocks in the mineralized zone as 'andesite'. If this is the case, the strongly altered rocks are either andesitic dikes or pendants within the larger stock, 2 kilometres in diameter. Hydrothermal alteration in the mineralized zone has produced silicified breccias and stockworks of dominantly crystalline quartz and magnetite  $\pm$  pyrite or quartz with either pyrite or hematite. Some of the hematite is strongly magnetic, suggesting an intermediate  $Fe_2O_3$  phase is present - maghemite ( $\gamma Fe_2O_3$ ). Hostrocks to the silica-rich altered zones are themselves silicified and have albitic plagioclase, sericite and variable chlorite, epidote and ankeritic carbonate. Crosscutting steeply dipping, east-trending fracture sets and altered bands contain quartz, pyrophyllite, sericite and kaolinite. These advanced argillic alteration sections appear to be, at most, a few metres wide. Late fractures and veins with pink laumontite selvages and calcite filling are abundant around the margins of the deposit.

## HEP

In the area between the Red Dog and Hushamu deposits to the south and west of Nahwitti Lake, there is a belt about 7 kilometres long that contains propylitically altered Bonanza volcanic rocks. Within this belt are zones with pyritic stockworks, and locally, magnetite-amphibole  $\pm$  hematite and widespread albitic alteration. The HEP prospect exemplifies this style of alteration. The MINFILE records (92L/078) describe the HEP occurrence as "(intruded) volcanics with propylitic, argillic and silicified units with widespread chlorite-epidote-zeolite". Pyrite, magnetite, chalcopyrite, molybdenite and lesser bornite are reported to be present, mainly as fracture fillings in sheared rocks. Some new logging roads to the north and northwest of the Hushamu

deposit and southwest of Nahwitti Lake expose notably widespread albitization in roadcuts and quarry pits. The albitization is recognized as a bone-white to buff, 'cherty-appearing', hard, vein-like to pervasive alteration that destroys original rock textures and fabrics in the andesitic, dioritic and thin-bedded sedimentary hostrocks. The albitic bleaching within larger zones of pervasive chlorite wallrock alteration is accompanied by fracture and vein-filling pyrite, epidote, calcite and minor white fine-grained micas. This is a more intense form of the regionally extensive propylitic alteration that is commonly peripheral to many of the other Island intrusions in the study area. In the lower intensity propylitic zones there is commonly widespread, but overall sparse development of hairline to thin quartz and quartz-calcite veinlets, some containing pyrite and minor chalcopyrite, galena and sphalerite. Widely spaced fractures and stockworks with calcite and the zeolite minerals laumontite or stilbite are common throughout the area.

## HIGH-SULPHIDATION EPITHERMAL DEPOSITS

High sulphidation (Hedenquist, 1987) epithermal mineralization, also known as acid sulphate (Heald *et al.* 1987), Nansatsu-type and a number of other terms (White, 1991, and references therein), is present in some of the siliceous, advanced argillic alteration zones studied. The most notable are those at Mount McIntosh and in the Pemberton Hills area (Pantelov and Koyanagi, 1993; Perello, 1992, and other unpublished company reports). Mineralization consists predominantly of pyrite as veins, disseminations, breccia matrix, crystalline open-space filling and massive to semi-massive rock replacements. Marcasite is present locally, generally as banded veinlets and fine-grained overgrowths on pyrite grains and rims on rock fragments in breccias. Pyrite commonly forms 5 to 10 volume per cent of the rock; there can be as much as 30% and locally, more. Typical high-sulphidation assemblages, those derived from strongly oxidized hydrothermal fluids with high sulphur to metal ratios, have deposited small amounts of enargite, chalcocite, covellite and bornite. Iron oxide minerals are locally abundant as both magnetite and hematite. The abundance of iron oxides is generally inverse to the amount of pyrite present. 'Limonitic' minerals, including goethite, lepidocrocite, other amorphous hydrous ferric oxides, earthy hematite and jarosite (Blanchard, 1966) are abundant. The minerals are thought to be mainly supergene although a hypogene origin for some of the crystalline limonite might be argued. The presence of limonite at depths of 200 metres or more, demonstrates the great extent to which groundwaters have been able to penetrate and leach the mineralized zones. Minor alteration minerals present are rutile, other opaque and semi-opaque iron-titanium (?) oxides, iron sulphates (melanterite and rozenite) and native sulphur.

## MOUNT MCINTOSH

The landscape and geology at Mount McIntosh are an expression of the upper part of the Hushamu porphyry copper system - a high temperature, advanced argillic alteration zone. The peak of the mountain is the uppermost part of the system, complete with hydrothermal and phreatomagmatic breccias. The strongly silicified, vuggy, acid-leached rocks there with underlying weakly developed high-sulphidation mineralization appear to be the epithermal part of the porphyry-related system. To the southeast about a kilometre, at the South McIntosh zone, there is an east-trending, steeply dipping silica-kaolinite-alunite 'ledge' 1300 metres long. This zone, 20 to 100 metres wide, is discordant with the trend of the host volcanic units. It defines a rhyolitic dike intrusion or swarm of intrusions and their coincident autobrecciated, magmatic-hydrothermal to magmatophreatic equivalents. Alteration in the core of the zone produced vuggy, mainly residual, silica rock with fine-grained crystalline to patchy alunite and kaolinite. The silicified rocks are surrounded by clay-altered rocks. They grade outward over a few metres from zones of dominantly kaolinite into zones with illite-chlorite, chlorite and finally, the widespread propylitic alteration with epidote, calcite and late laumontite veins that is prevalent in the area. Fine-grained pyrite, which locally constitutes up to 15% of the clay-altered rocks, is apparently the only sulphide present.

## PEMBERTON HILLS

In the Pemberton Hills area there is exploration interest in, from east to west, the Wann property and the Pemberton East and West Pemberton zones of the EXPO claims. Hydrothermal alteration in the area is dominated by pervasive kaolinite, and locally, alunite as bedding replacement, fracture and breccia-matrix fillings. Locally there is considerable, although not pervasive, acid leaching with residual vuggy silica textures. In places the porous rocks contain native sulphur; locally it constitutes up to 5% of the rock. Perello (1992) reports the occurrence of diaspore, anhydrite and widespread illite and (peripheral) chlorite.

Two types of pyritic mineralization are associated with the advanced argillic alteration (Figure 3). In one type, siliceous breccias and pyritic stockworks crosscut the rhyolitic and underlying interlayered intermediate to mafic rocks and dioritic to monzonitic intrusions that make up the Pemberton Hills. In one locality immediately west of Youghan Creek, one of the pyritic stockworks contains native gold together with arsenian alunite (schlossmacherite) (Panteleyev and Koyanagi, 1993). In the creek bed 250 metres to the northeast, there is also much stockworking and breccia-matrix replacement by pyrite, marcasite and the iron sulphate minerals melanterite and rozenite. The second style of mineralization is stratabound pyritic replacement of fragmental beds within the basal part of the rhyolite unit

and its underlying tuffaceous succession. The tuffaceous rocks comprise laminated to thin and thickly bedded tuffaceous sandstone, wackes, carbonaceous mudstones and minor conglomerates. The most visually impressive mineralization is present as massive to semi massive pyritic replacements. These have an evident lithologically determined, bedding-porosity permeability control. Permeable horizons at a regional or district scale are mainly along the contact zone of the lapilli tuff and breccia units of the basaltic to intermediate Bonanza volcanics and the overlying rhyolite map units (see Nixon *et al.*, 1994, this volume). In more detail, as evident in diamond-drill cores, the rhyolitic units are replaced along permeable, coarse airfall pyroclastic members and the brecciated flow units that are capped by less permeable, welded ash-flows. Clasts of massive sulphide (pyrite) occur in some of the lapilli tuff and breccia basal members of the rhyolite unit. Some of the sulphide clasts have rims of fine-grained marcasite. This is the best evidence observed that mineralization took place repeatedly in a near-surface, subaerial environment as a synvolcanic process early in the history of rhyolite unit deposition. The subaerial setting negates the possibility, despite the similarity in appearance, that the pyritic replacements in the fragmental rhyolitic rocks and underlying tuffaceous beds are 'Kuroko-type' massive sulphide mineralization. Generally, base and precious metal values in these pyritic, siliceous, clay-altered rocks are uninspiring. Small amounts of chalcocite and covellite have been noted in a few diamond-drill cores. The copper minerals are probably primary rather than supergene as they are associated with minor amounts of enargite.

## STRUCTURAL CONTROLS

The distinctive advanced argillic hydrothermal alteration occurs in permeable rocks above high-level magma chambers that have given rise to extrusive rhyolite, coeval quartz feldspar and feldspar porphyry dikes and possibly the underlying (altered) dioritic stocks. There are abundant rhyolitic units in the Bonanza stratigraphic section throughout northern Vancouver Island but in Quatsino map area the rocks are only locally clay-altered and, even less commonly, have undergone advanced argillic alteration. The larger scale control on alteration in the study area might well be faults that control the distribution of the bedded, tuffaceous sedimentary map unit that underlies rhyolites of the Pemberton Hills. The existence of a maar diatreme complex in this area has been suggested by Perello (1992). However, project regional mapping (Nixon *et al.*, 1994, this volume) shows that the tuffaceous sediment unit occupies a linear map trend and the rocks are neither equant nor circular in their distribution as would be the case in a maar setting. The bedded rocks are more likely deposited in a graben, or similar fault-bounded basin, possibly a caldera or series of nested calderas, along the trend of the andesitic volcanic arc. The rhyolite assemblage that overlaps the structurally

bounded tuff-inundated basin forms the thick flow-dome complexes with flanking welded and coarse pyroclastic deposits that define the Pemberton Hills. Within this structural setting, the most important control on movement of hydrothermal fluids and on alteration is the inherently high permeability of coarse subaerial pyroclastic, and possibly lacustrine, volcanoclastic rocks as well as the structurally imposed permeability.

Additional permeability has been created by the congruency of high and low-angle faults, late dike emplacements and the extensive systems of fractures and hydrothermally brecciated and leached rocks that acted as effective fluid conduits. Explosive hydrothermal fluid conduits, presumably above intrusive bodies, are marked by clusters of small, individual breccia bodies or breccia complexes. Those on Mount McIntosh are considered by Perello (1992) to be of various ages and are, in part, intramineral in age. The breccias contain mineralized fragments of various lithologies and are cut by moderately mineralized, quartz-veined porphyry dikes, younger breccias and pebble breccias. Most commonly observed in the intensely altered, silicified rocks are late, crosscutting, strongly milled pebble breccias in which there are abundant pervasively silicified clasts. A number of the most strongly leached, vuggy silica zones, commonly containing breccias, trend westerly and crosscut the regional east-southeasterly trending lithologic and alteration patterns. Within these zones, individual subvertical quartz veins and open space fractures and dilations commonly form at 070°.

Other sites of mineralization with some degree of structurally focused fluid flow are lithologic contacts, commonly those between intrusive stocks and their volcanic hostrocks; unconformities, notably those inferred between the andesitic and rhyolitic or bedded tuffaceous successions; and permeable interstratal beds, especially those in contact with impermeable units that act as aquitards.

## GENETIC INTERPRETATIONS

A current hypothesis is that the extensive clay alteration and related high-sulphidation copper-gold-silver epithermal mineralization in the study area are derived from fluids generated by intrusions of the Island Plutonic Suite. The intrusions are considered to be coeval and cogenetic with the rhyolitic, upper units of the Bonanza volcanic assemblage. The implicit genetic relationship between the subvolcanic high-sulphidation

epithermal and porphyry copper mineralization is being tested. Age relationships are being determined by radiometric dating of intrusive hostrocks and hydrothermal alteration minerals using K-Ar and <sup>40</sup>Ar-<sup>39</sup>Ar techniques. Preliminary age determinations from a few of the samples submitted for age determinations are shown below (Table 2). The results to date suggest that either the porphyry copper mineralization is considerably younger than any Early Jurassic Bonanza subvolcanic events, or the radiometric ages are reset by thermal overprinting.

Sources of hydrothermal fluids and the genesis of the mineral deposits can be interpreted from light stable isotopic studies. Preliminary results from a 20-sample suite submitted for analysis indicate that there is much variation in 'clay' minerals. The range in values from 4.6 to 12.7 per mil δ<sup>18</sup>O is possibly due to combining both hypogene and supergene clays in the sample suite. The values of δD show a very narrow range from -49 to -77 per mil, possibly indicative of origin in warm latitudes. Work on additional clay, quartz, sericite, hornblende and alunite mineral separates is ongoing and genetic interpretations await the completion of the analyses.

## DISCUSSION

Much of the advanced argillic alteration observed in the study area, and the associated (weakly developed) high-sulphidation mineralization, appears to be magmatic-hydrothermal in origin, is related to intrusions and took place during late porphyry copper mineralization and hydrothermal brecciation. Examples are the Mount McIntosh and Red Dog deposits. This type of mineralization in the upper part of porphyry copper-gold deposits is commonplace in western Pacific island arcs (Sillitoe, 1989), Chile (Sillitoe and Camus, 1991), and elsewhere (Mitchell, 1992). In the Pemberton Hills area, strongly pyritized, siliceous rocks containing crystalline, pink alunite in veins, stockworks and as breccia matrix appear to be a similar alteration. This, too, is likely to be magmatic-hydrothermal in origin, at least in part. But elsewhere in the Pemberton Hills, where native sulphur is abundant, sulphate minerals are present, and much of the kaolinite and alunite occurs as fine-grained to massive, white, bedding-plane replacements, there is a strong likelihood that the alteration and attendant acid leaching are derived from vapour-dominated groundwater systems. There is little potential for ore deposition in this 'geothermal' setting,

TABLE 2. PRELIMINARY RADIOMETRIC DATES.

Island Plutonic Suite - Hushamu stock:	sericite (alteration)	~171 Ma	<sup>40</sup> Ar- <sup>39</sup> Ar plateau age
Island Plutonic Suite - Hushamu stock:	hornblende	~172 Ma	<sup>40</sup> Ar- <sup>39</sup> Ar plateau age
(or plagioclase-hornblende porphyry dike)			
Island Intrusive Suite - Mead Creek stock:	hornblende	168 ± 4 Ma	K/Ar conventional dating
K/Ar age by J. Harakal, the University of British Columbia; Argon plateau dates from P. Reynolds, Dalhousie University			

but ample barren pyrite can be deposited. Sillitoe (1993) outlines how to recognize the various alunites present in the different geological environments and describes other shallow features of epithermal deposits. The origins of alunite and acid sulphate alteration, and the implications on ore potential of their genetic differences in advanced argillic zones, are reviewed by Rye *et al.* (1992) and Thompson (1992).

Enlightening examples that emphasize the large size of the advanced argillic alteration and related high-sulphidation mineralization that is possible are contained in the discussions of the Negros-Masbate arc (Mitchell and Leach, 1991) and Mankayan district, Lepanto deposit (Garcia, 1991), the Philippines. Note that the lateral extent of acid leaching and mineralization commonly far exceed their vertical dimensions. In the Negros-Masbate region, silicified, acid-leached rocks, mostly unmineralized except for pyrite, marcasite, sulphur and some sulphate minerals, form prominent topographic features over a distance of about 300 kilometres along the trend of the andesitic arc (Mitchell, 1992). At Lepanto, a silicified ledge containing enargite-gold mineralization within a zone of advanced argillic alteration occurs over a distance of 6 kilometres (Garcia, 1991). The size and origins of other, similar zones of recent alteration and mineralization in the Philippines are summarized in studies of active geothermal wells and fields by Reyes (1990). Her discussions are especially revealing about the detailed mineralogy, alteration zoning, structural controls and both the lateral and vertical extents of acid leaching in recent and active, acidic hydrothermal systems. In comparison, the size and geometry of the advanced argillic alteration systems in our study area very closely resemble many of the features in the Tongonan, Palinpinon and other wells she describes. Figure 3 incorporates some of Reyes' observations into a model for the geometric and fluid-flow relationships of typical northern Vancouver Island advanced argillic zones.

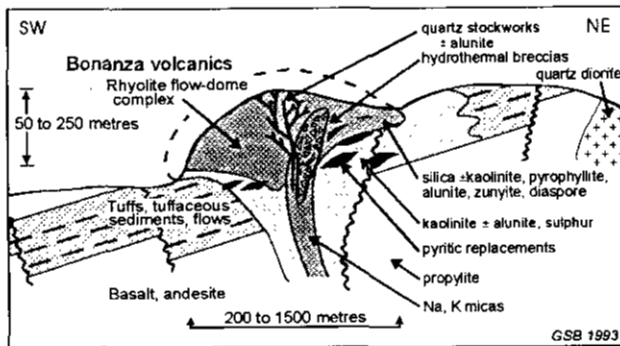


Figure 3. Schematic relationships between permeable lithologies, volcanic structures, hydrothermal conduits and mineralization in the Pemberton Hills; adapted, in part, from Reyes (1990).

Mitchell (1992) illustrates the spatial relationships between mineralized magmatic-hydrothermal systems and barren vapour-dominated, acid leaching environments in 'perched aquifers'. The relationships of mineralized and barren alteration zones with respect to

the (hydrothermal) groundwater table, as described by Mitchell, are illustrated on Figure 4. In this model, the intrusion of epizonal stocks or dike complexes initiates magmatic fluid flow and produces a central porphyry-type mineralized zone with peripheral, meteoric fluid-dominated propylitic alteration. Magmatic acidic gases at depth and in the higher level fluid conduits, as well as gas condensates near surface, form acid sulphate alteration with accompanying acid leaching of the hostrocks. The resulting, commonly stacked, zones of advanced argillic alteration can be later mineralized below the water table by magmatic hydrothermal fluids but are barren nearer the surface in the zone of 'boiling' vapour-dominated fluids and groundwater dilution.

Other recent investigations concerning the origins of advanced argillic and acid sulphate alteration, with instructive discussions about exploration for epithermal deposits in this setting, are those by White and Hedenquist (1990), Matsuhisa *et al.* (1991) and Giggensch (1992).

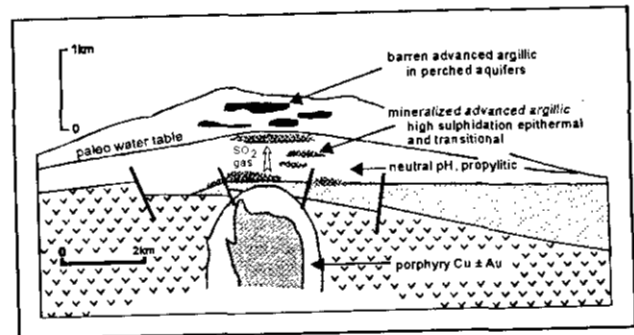


Figure 4. Generalized model for advanced argillic lithocaps showing the relationships between intrusions, porphyry copper deposits, alteration zones and the (hydrothermal) water table; after Mitchell (1992).

## ACKNOWLEDGMENTS

It is a pleasure to acknowledge the cooperation and assistance offered in the field and the interest in our work shown by John Fleming and Alan Reeves, Island Copper mine; Peter Dasler, on behalf of Jordex Resources Inc.; Neil leNobel, BHP Minerals (Canada) Ltd.; Bob Anderson on behalf of Crew Natural Resources Ltd., and Byron Richards, JB Engineering Limited. We thank Mac Chaudry for his high quality X-ray diffraction determinations and the preparation of clean mineral samples for isotopic analysis. Age determinations are being conducted by Peter Reynolds, Dalhousie University and Joe Harakal, the University of British Columbia. Stable isotope analyses are being done by Karlis Muehlenbachs, University of Alberta.

## REFERENCES

- Blanchard, R. (1966): *Interpretation of Leached Outcrops; Nevada Bureau of Mines, Bulletin 66.*

- Bobrowsky, P.T. and Meldrum, D. (1994): Preliminary Drift Exploration Studies, Northern Vancouver Island; in Geological Fieldwork 1993, Grant, B. and Newell, J.M., Editors, *B.C. Ministry of Energy, Mines and Petroleum Resources*, Paper 1994-1, this volume.
- Cargill, D.G., Lamb, J., Young, M.J. and Rugg, E.S. (1976): Island Copper; in Porphyry Deposits of the Canadian Cordillera, Sutherland Brown, A., Editor, *Canadian Institute of Mining and Metallurgy*, Special Volume 15, pages 206-218.
- Dasler, P.G., Young, M.J., Perello, P.G. and Giroux, G. (1995): The Hushamu Porphyry Copper-Gold Deposit; in Porphyry Deposits of the Northwestern Cordillera of North America, Schroeter, T.G., Editor, *Canadian Institute of Mining, Metallurgy and Petroleum*, Special Volume 46, in preparation.
- Fleming J. (1992): Porphyry Copper-Molybdenum-Gold Mineralization at Island Copper, Vancouver Island, B.C.; in Porphyry Copper Model, *Northwest Mining Association*, 1992 Short Course, Tucson, Arizona and Spokane, Washington, 7 pages.
- Garcia, J.S., Jr. (1991): Geology and Mineralization Characteristics of the Mankayan Mineral District, Benguet, Philippines; in High-temperature Acid Fluids and Associated Alteration and Mineralization, Matsuhisa, Y., Aoki, M. and Hedenquist, J.W., Editors, *Geological Survey of Japan*, Report No. 277, pages 21-30.
- Giggenbach, W.F. (1992): Magma Degassing and Mineral Deposition in Hydrothermal Systems Along Convergent Plate Boundaries; *Economic Geology*, Volume 87, pages 1927-1944.
- Heald, P., Hayba, D.O. and Foley, N.K. (1987): Comparative Anatomy of Volcanic-hosted Epithermal Deposits: Acid-sulfate and Adularia-sericite Types; *Economic Geology*, Volume 82, pages 1-26.
- Hedenquist, J.W. (1987): Mineralization Associated with Volcanic-related Hydrothermal Systems in the Circum-Pacific Basin; in Transactions, Fourth Circum-Pacific Energy and Mineral Resources Conference, Singapore, Horn, M.K., Editor, *American Association of Petroleum Geologists*, pages 513-524.
- Koyanagi, V.M. and Panteleyev, A. (1994): Natural Acid Rock Drainage in the Red Dog/Hushamu/Pemberton Hills Area, Northern Vancouver Island, (92L/12); in Geological Fieldwork 1993, Grant, B. and Newell, J.M., Editors, *B.C. Ministry of Energy, Mines and Petroleum Resources*, Paper 1994-1, this volume.
- Matsuhisa, Y., Aoki, M. and Hedenquist, J.W., Editors (1992): High-temperature Acid Fluids and Associated Alteration and Mineralization, *Geological Survey of Japan*, Report No. 277, 111 pages.
- McMillan, W.J. and Panteleyev, A. (1988): Porphyry Copper Deposits; in Ore Deposit Models, Roberts, R.G. and Sheahan, P.A., Editors, *Geoscience Canada*, Reprint Series 3, pages 45-58.
- Mitchell, A.H.G. (1992): Andesitic Arcs, Epithermal Gold and Porphyry-type Mineralization in the Western Pacific and Eastern Europe; *The Institution of Mining and Metallurgy*, Transactions, Volume 101, pages B125-B138.
- Mitchell, A.H.G. and Leach, T.M. (1991): Epithermal Gold in the Philippines: Island Arc Metallogeny, Geothermal Systems and Geology; *Academic Press Inc.*, London, 457 pages.
- Nixon, G.T., Hammack, J.L., Koyanagi, V.M., Payie, G., Panteleyev, A., Massey, N.W.D., Hamilton, J.V. and Haggart, J.W. (1994): Preliminary Geology of the Quatsino - Port McNeill Map Area, Northern Vancouver Island, (92L/12, 11); in Geological Fieldwork 1993, Grant, B. and Newell, J.M., Editors, *B.C. Ministry of Energy, Mines and Petroleum Resources*, Paper 1994-1, this volume.
- Panteleyev, A. (1992): Copper-Gold-Silver Deposits Transitional Between Subvolcanic Porphyry and Epithermal Environments; in Geological Fieldwork 1991, Grant, B. and Newell, J.M., Editors, *B.C. Ministry of Energy, Mines and Petroleum Resources*, Paper 1992-1, pages 231-234.
- Panteleyev, A. and Koyanagi, V.M. (1993): Advanced Argillic Alteration in Bonanza Volcanic Rocks, Northern Vancouver Island - Transitions Between Porphyry Copper and Epithermal Environments; in Geological Fieldwork 1992, Grant, B. and Newell, J.M., Editors, *B.C. Ministry of Energy, Mines and Petroleum Resources*, Paper 1993-1, pages 287-293.
- Panteleyev, A., Bobrowsky, P.T., Nixon, G.F. and Sibbick, S.J. (1994): Northern Vancouver Island Integrated Project; in Geological Fieldwork 1993, Grant, B. and Newell, J.M., Editors, *B.C. Ministry of Energy, Mines and Petroleum Resources*, Paper 1994-1, this volume.
- Perello, J.A. (1992): Comments on the Exploration Potential for Epithermal Au and Cu at McIntosh, South McIntosh, and West Pemberton, Expo Claims, Vancouver Island, British Columbia, *BHP Minerals Canada Ltd.*, unpublished company report, 19 pages.
- Perello, J.A., Arancibia, O.N., Burt, P.D., Clark, A.H., Clarke, G.A., Fleming, J.A., Himes, M.D., Litch, C.E.B. and Reeves, A.T. (1989): Porphyry Cu-Mo-Au Mineralization at Island Copper, Vancouver Island, B.C.; *Geological Association of Canada*, Mineral Deposits Division Workshop, Vancouver, Abstract.
- Reyes, A.G. (1990): Petrology of Philippine Geothermal Systems and the Application of Alteration Mineralogy to their Assessment; *Journal of Volcanology and Geothermal Research*, Volume 43, pages 279-309.
- Rye, R.O., Bethke, P.M. and Wasserman, M.D. (1992): The Stable Isotope Geochemistry of Acid Sulfate Alteration; *Economic Geology*, Volume 87, pages 225-262.
- Sibbick, S.J. (1994): Preliminary Report on the Application of Catchment Basin Analysis to Regional Geochemical Data, Northern Vancouver Island, (92L/SW); in Geological Fieldwork 1993, Grant, B. and Newell, J.M., Editors, *B.C. Ministry of Energy, Mines and Petroleum Resources*, Paper 1994-1, this volume.
- Sillitoe, R.H. (1989): Gold Deposits in Western Pacific Island Arcs: The Magmatic Connection; in The Geology of Gold Deposits: The Perspective in 1988, *Economic Geology*, Monograph 6, pages 274-291.

- Sillitoe, R. H. (1993): Epithermal Models: Genetic Types, Geometric Controls and Shallow Features; *in* Mineral Deposit Modeling, Proceedings IUGS/UNESCO Deposit Modeling Conference, 8th IAGOD Symposium, Ottawa, 1990, *Geological Association of Canada*, in press.
- Sillitoe, R.H. and Camus, F. (1991): A Special Issue Devoted to Gold Deposits in the Chilean Andes; *Economic Geology*, Volume 86, pages 1153-1345.
- Sutherland Brown, A. (1976): Morphology and Classification; *in* Porphyry Deposits of the Canadian Cordillera, Sutherland Brown, A., Editor, *Canadian Institute of Mining and Metallurgy*, Special Volume 15, pages 44-51.
- Thompson, A.J.B. (1992): Alunite Compositions and Textures: Relationships to Precious Metal Mineralization; *Mineral Deposits Research Unit, The University of British Columbia*, Short Course #8, 26 pages.
- White, N.C. (1991): High Sulphidation Epithermal Gold Deposits: Characteristics and a Model for their Origin; *in* High-temperature Acid Fluids and Associated Alteration and Mineralization, Matsuhisa, Y., Aoki, M. and Hedenquist, J.W., Editors, *Geological Survey of Japan*, Report No. 277, pages 9-20.
- White, N.C. and Hedenquist, J.W. (1990); Epithermal Environments and Styles of Mineralization: Variations and their causes, and Guidelines for Exploration; *in* Epithermal Gold Mineralization of the Circum-Pacific: Geology, Geochemistry, Origin and Exploration, II, Hedenquist, J.W., White, N.C. and Siddeley, G., Editors, *Journal of Geochemical Exploration*, Volume 36, pages 445-474.



**PRELIMINARY REPORT ON THE APPLICATION OF CATCHMENT BASIN ANALYSIS TO REGIONAL GEOCHEMICAL SURVEY DATA, NORTHERN VANCOUVER ISLAND (NTS 92L/03, 04, 05 AND 06)**

By S.J. Sibbick

**KEYWORDS:** Regional Geochemical Survey, applied geochemistry, Vancouver Island, catchment basin, Bonanza Group, copper, gold.

**INTRODUCTION**

Meaningful techniques for presenting geochemical data from regional stream sediment surveys have long been a difficulty for explorationists. Contouring and image analysis methods can create artifacts which misrepresent the data whereas its display as point values may not portray the spatial variation inherent to the data set. Further, the geochemistry of a stream sediment sample is often most influenced by the geology of the sediment source area. Coding the sample site by its underlying geology may not accurately represent the site and may result in the misidentification of anomalies.

An effective solution to this problem is to utilize the catchment basin of each sample site to define its zone of influence (Bonham-Carter and Goodfellow, 1986). This method can be used to:

- Define the actual areal coverage of a survey.
- Reclassify the geological influence on each sample based on its source area.
- Redefine the thresholds which separate anomalous from background populations.

Bonham-Carter and Goodfellow (1986) successfully used this method to predict the presence of lead-zinc occurrences using stream sediment data in the Nahanni River area (NTS 1051) of the Yukon and Northwest Territories. In a related study, Bonham-Carter *et al.* (1987) compared a variety of methods for representing the geology within each catchment basin in the Cobequid Highlands, Nova Scotia.

Catchments sampled in the course of the Regional Geochemical Survey (RGS) program in the 92L/SW (NTS 92L/03, 04, 05 and 06) map area have been digitized in order to evaluate this method. This area was selected for the following reasons:

- Bonanza Group rocks, the primary target for mineral exploration in the region, are the

most areally extensive lithology in 92L/SW (Figure 1).

- Regional Geochemical Survey coverage within this area is typical for northern Vancouver Island.
- 92L/SW is a relatively unexplored, frontier area with poor access and is therefore amenable to the use of Regional Geochemical Survey data for definition of exploration targets.

**REGIONAL GEOLOGY AND MINERALIZATION**

The 92L/SW map area is underlain primarily by Lower Jurassic Bonanza Group volcanic and volcanoclastic rocks and Triassic basalts of the Karmutsen Formation (Muller *et al.*, 197-). Upper Triassic limestones of the Quatsino Formation and clay to clastic sediments of the Parsons Bay Formation are exposed in the eastern section of the map area; Parsons Bay Formation also outcrops in the western edge of 92L/SW. To the southwest, Jurassic to Cretaceous sediments of the Pacific Rim Complex form the Brooks Peninsula. Granitoid intrusives of the Island Plutonic Suite are exposed throughout the map area (Nixon *et al.* 1993).

One hundred and two mineral occurrences are known in the 92L/SW map area (Hulme *et al.*, 1993). The major types of known metallic deposits are iron and copper skarns, precious metal epithermal systems and copper-molybdenum porphyries. Six of these occurrences are past producers, including the Merry Widow camp and the Yreka mine. The only active operation at present is the Benson Lake limestone quarry, located east of Victoria Lake.

**REGIONAL GEOCHEMICAL SURVEY**

The 92L/SW map area was sampled as part of RGS 23 (NTS 92L/102I) in 1988 (Gravel and Matysek, 1989). Moss-mat sediments and stream waters were collected

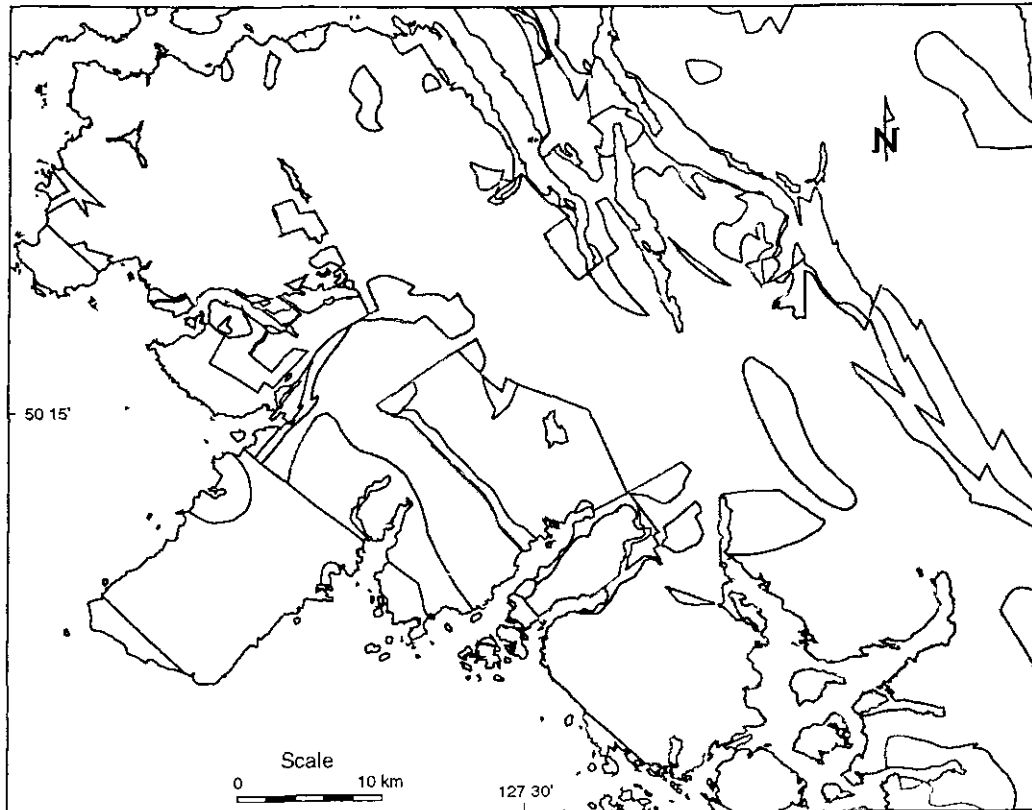


Figure 1. Distribution of Bonanza Group rocks (shaded pattern), 92L/SW.

from 294 first and second order drainages. The -80 mesh fraction of the sediment was analysed for a suite of 22 elements (Au, Cu, Zn, Pb, Ni, Co, Ag, Mn, Fe, Mo, U, Sn, W, Hg, As, Sb, Ba, Cd, V, F, Bi and Cr) and loss on ignition (LOI) using a variety of methods (see Matyssek *et al.*, 1989). Stream waters were analysed for uranium, fluoride and pH. Quality control procedures followed those established by the Geological Survey of Canada (Garrett *et al.*, 1980) and used for every RGS. Results from this survey were released to the public in 1989.

## METHODS

A catchment basin map of 92L/SW was produced from 1:50 000 scale topographic maps compiled and photo reduced to 1:100 000 scale. Catchment basins were delineated for 290 RGS sample sites by hand tracing the basin polygon onto a mylar overlay. Boundaries for catchment basins were defined by the topographic height of land which divided one drainage from another. Catchments which extended off the map sheet were truncated at the map edge.

The resulting polygons were then digitized at 1:100 000 scale, with each polygon labeled to correspond to its RGS sample number. On occasion, nested polygons were produced where two samples were taken from

successive sites on the same stream; in these cases the downstream polygon was defined to end at the upstream sample site. Areas of each polygon were calculated during the digitizing procedure. The corresponding RGS data were joined to each digital polygon record for interpretation.

## RESULTS AND DISCUSSION

### CATCHMENT BASIN AREAS

Figure 2 shows the distribution of RGS sites and their associated catchment basins. A histogram of the catchment basin area distribution is represented in Figure 3. Catchment basins range from 0.6 square kilometre to 20 square kilometres in area with a mean area on the order of 5 square kilometres. The modal area of the catchments falls within the 1 to 2 square kilometre range. Of the 290 RGS sites, 174 have drainage basins which cover an area of 5 square kilometres or less. Areal coverage of the RGS catchments totals 1417 square kilometres, or 54% of the 92L/SW land area. The remaining unsurveyed 46% of the map represents coastal areas lacking well defined drainages, broad valleys or, most importantly, drainages bounded by surveyed catchments which were intentionally excluded from the

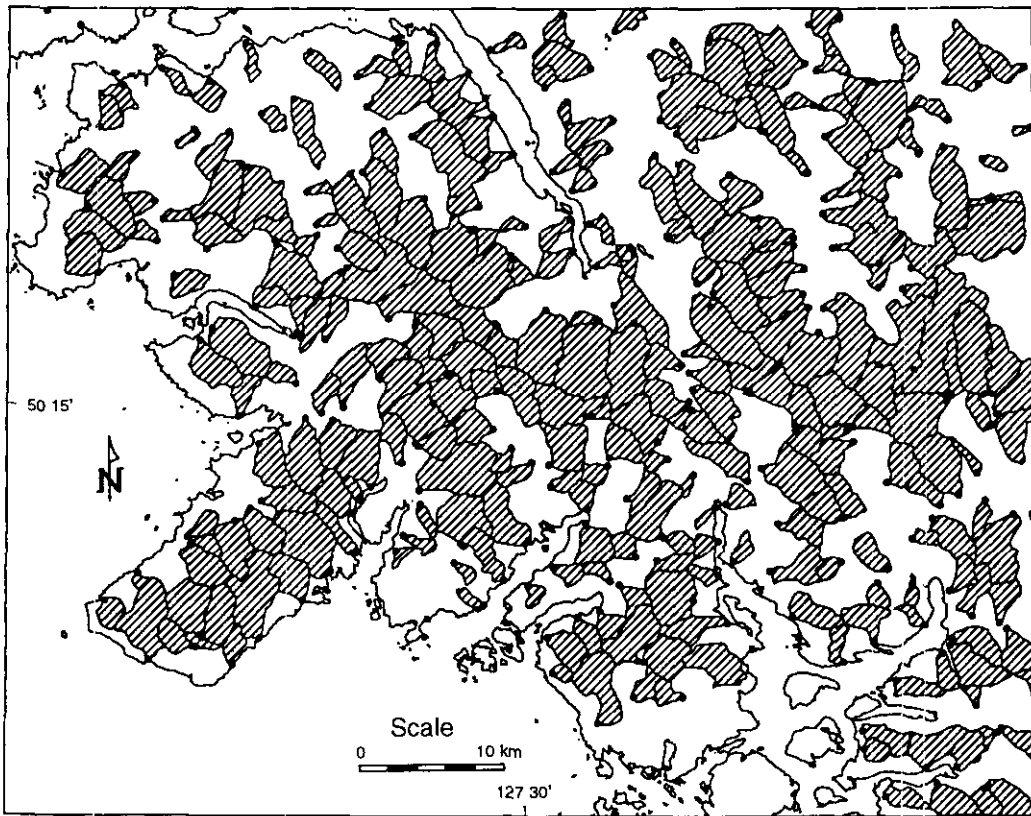


Figure 2. Distribution of RGS sites and associated catchment basins, 92L/SW.

sampling program. Exclusion of a catchment basin from the survey is a reflection of the intended sampling density of the RGS program. Designed to provide cost-efficient regional geochemical data, the RGS program does not define the geochemistry of every first and second order stream within a map area. It is entirely possible, therefore, that mineral occurrences in unsurveyed catchments may have been missed. Examination of regional anomalies or subtle geochemical patterns in drainages which bound these unsurveyed areas may help to identify prospective mineralized catchments.

Influence of catchment basin area on the sediment geochemistry appears to be minimal (Table 1). There are weak, yet statistically significant, correlations of catchment area with loss on ignition, manganese, fluoride, iron, chromium and vanadium (Figure 4). Negative correlations of catchment area with loss on ignition and manganese appear to be real. In general, there is an increase in the loss on ignition content of a sample with decreasing catchment area. Loss on ignition is a general measure of the organic content of moss-mat sediment whereas decreasing catchment area roughly corresponds to an increase in stream slope and stream energy. Increasing proportions of organic sediment imply that the amount of mineral sediment within a moss mat decreases with increasing stream energy.

Field observations confirm this finding, as moss mats in steep-gradient streams contain less than average mineral sediment and appear to have been washed clean

by high-energy stream flow (W. Jackamar, personal communication, 1993).

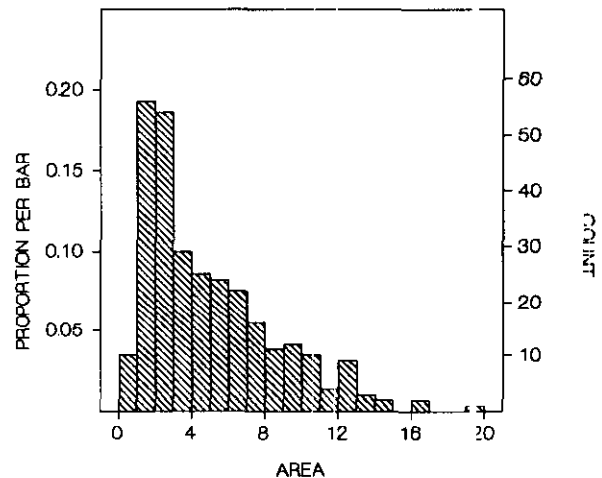


Figure 3. Distribution of catchment basin areas.

A negative correlation between manganese and catchment area and a high positive correlation between manganese and loss on ignition ( $r = 0.632$ ) indicates that the winnowing of mineral sediment from mosses in high-energy streams does not preferentially remove manganese from moss mats. Smith (1986), in a study of the geochemical response of moss-mat vegetation to mineralization, concluded that manganese accumulation occurs mainly by biochemical reactions which incorporate manganese into the plant material.

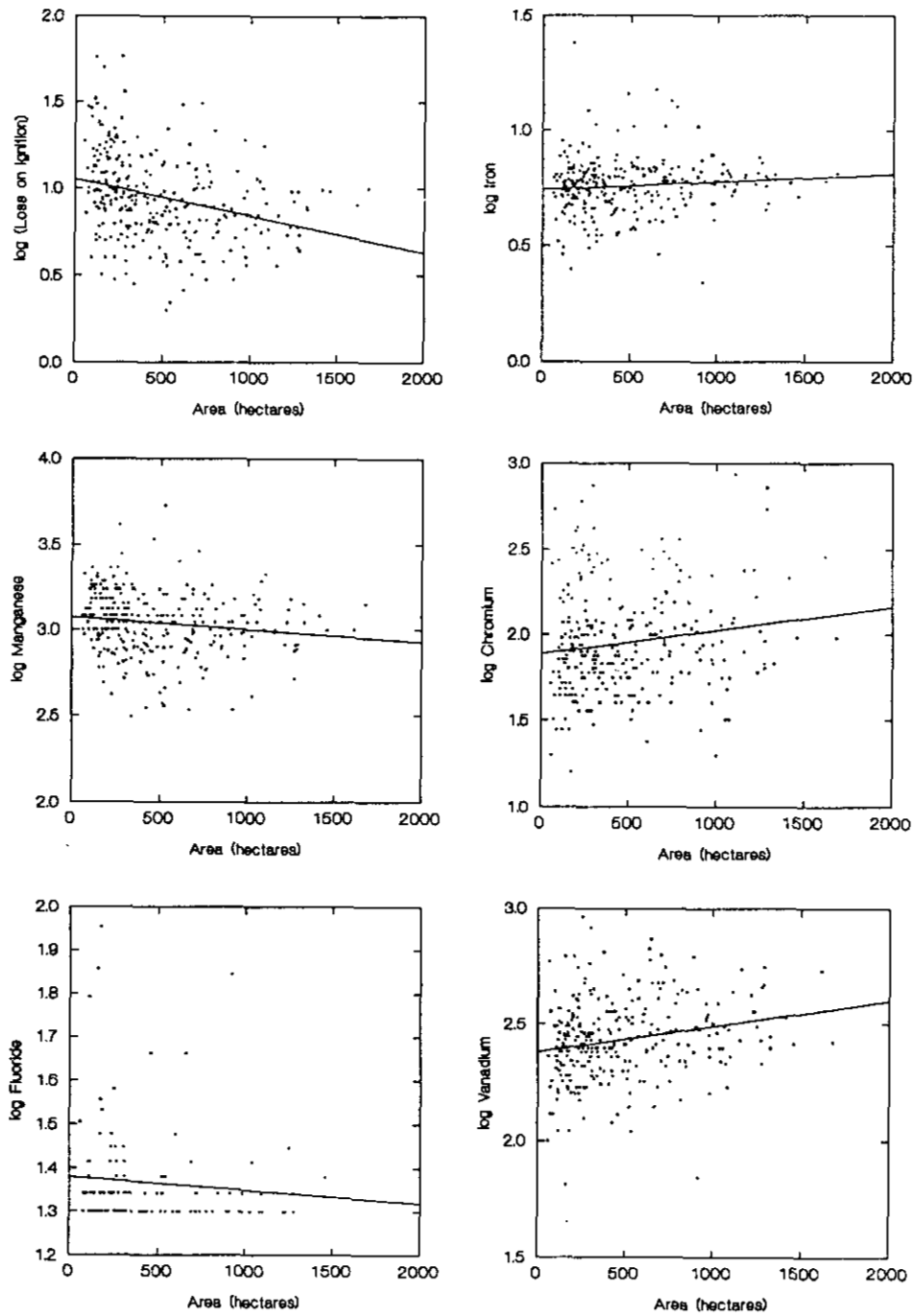


Figure 4. Scatterplots of significant correlations (>0.95) between RGS data and catchment area.

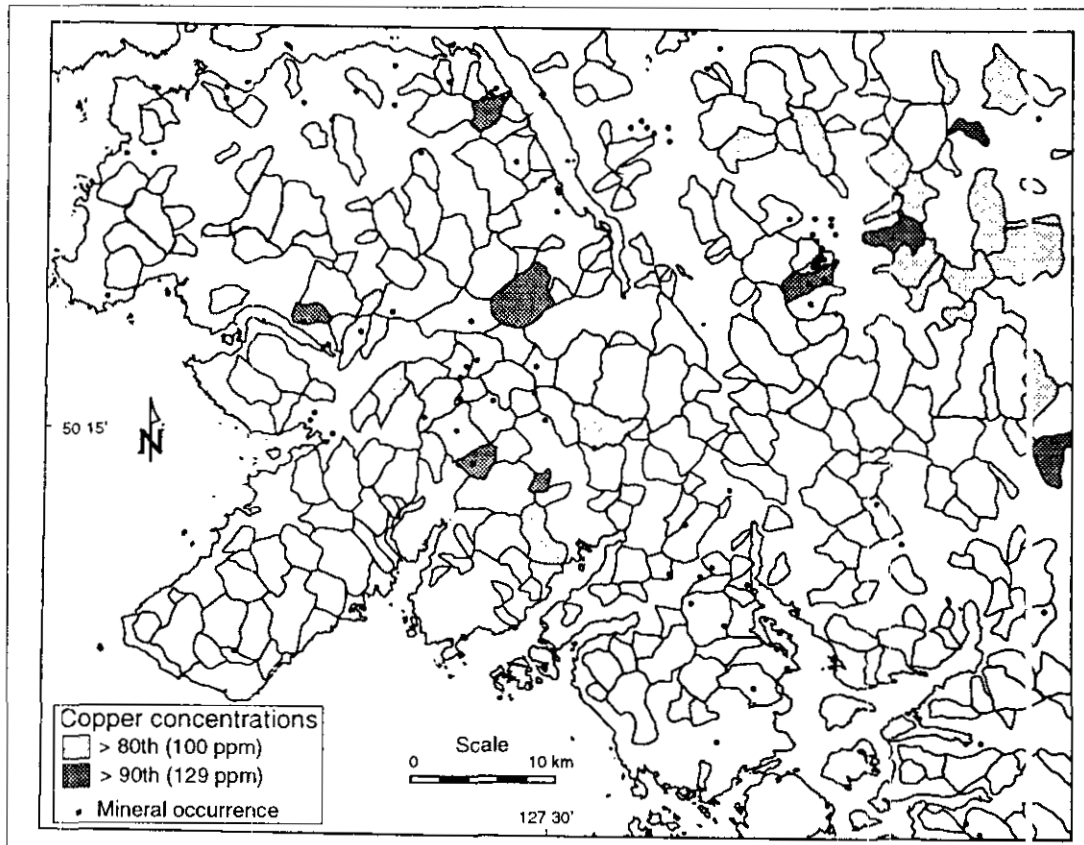


Figure 5. Location of mineral occurrences and catchment basins with copper concentrations above the 80th and 90th percentiles.

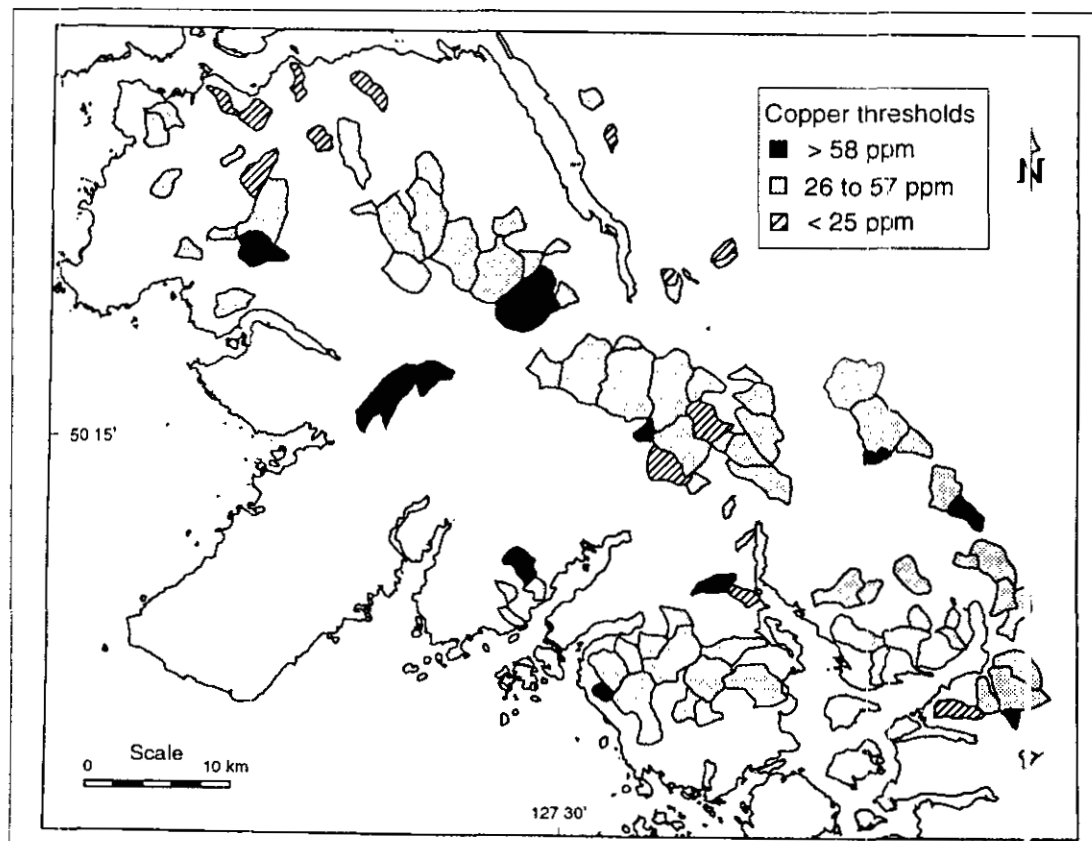


Figure 6. Redefined Bonanza Group copper thresholds for catchments underlain entirely by Bonanza Group rocks.

**TABLE 1. PEARSON CORRELATIONS  
BETWEEN CATCHMENT AREA  
AND RGS DATA**

	Area		Area
LOI	-0.289	Cd	0.010
Mn	-0.123	Au	0.015
F-w	-0.107	pH	0.025
Ba	-0.077	Co	0.026
Pb	-0.072	F	0.031
Bi	-0.061	U-w	0.033
W	-0.033	Cu	0.071
As	-0.030	Ni	0.079
Hg	-0.030	Fe	0.107
Sb	-0.027	Cr	0.137
Mo	-0.021	V	0.195
U	0.002		

N = 275      Rsig(.95) = 0.099

Positive correlations between iron, chromium and vanadium with catchment area suggest that the proportion of lithic fragments within each sample tends to decrease with decreasing catchment area (Figure 4). This hypothesis is in agreement with the negative correlations found for loss on ignition and manganese. The negative correlation between fluoride and catchment area can be attributed to the presence of outliers in the fluoride data set (Figure 4).

### CATCHMENT BASIN GEOCHEMISTRY

Figure 5 shows the distribution of catchment basins with copper concentrations above the 80th and 90th percentiles for the 92L/102I RGS data set. Source areas of these anomalous metal concentrations are readily visible, as are multiple-catchment anomalies in the northeast associated with the higher background copper concentrations of the Karmutsen volcanics. An overlay of mineral occurrences from the MINFILE database enables the rapid identification of anomalous catchments not associated with known mineralization (Figure 5). Roughly one-third of the mineral occurrences are located outside surveyed catchments. Less than 10% of the mineral occurrences are found in basins with copper concentrations above 100 ppm. As over 70% of the mineral occurrences in the 92L/SW map area contain significant copper-bearing mineralization (Hulme *et al.*, 1993), it is likely that either the geochemical response of these occurrences is not present or has been suppressed by the higher background copper concentrations in lithologies such as the Karmutsen volcanics.

In the 92L/SW map area, 99 catchments are underlain entirely by Bonanza Group rocks. Evaluation of these basins provides a more reliable estimate of background and threshold values due to the homogeneity

of the catchment lithology. Based upon these catchment basins, threshold values for copper of 26 and 58 ppm were estimated using a probability plot. Projection of the upper threshold (58 ppm) onto the catchment basin map (Figure 6) highlights twelve drainages with anomalous copper concentrations.

Presence of multiple lithologies within a catchment basin presents another challenge for establishing thresholds. Regression methods have been employed by Bonham-Carter and Goodfellow (1986) and Bonham-Carter *et al.* (1987) to correct for the areal proportions of geologic units within a map area. Future work will focus on developing this methodology on a completed catchment basin map of 92L/102I.

### CONCLUSIONS

Catchment basin maps provide an effective method of presenting regional geochemical stream sediment data. Influences of the catchment basin physiography on the geochemical response of a moss-mat sediment can be documented. Source areas for anomalous RGS sites can be easily discerned and their relationship to known mineralization or geological features quickly evaluated. Further, practical thresholds representing the actual geological distribution of a lithology can be estimated.

### ACKNOWLEDGMENTS

The author wishes to thank Wayne Jackaman, Wade Noble and Moira Smith for their assistance. John Newell provided insightful editorial comments.

### REFERENCES

- Bonham-Carter G.F. and Goodfellow W.D. (1986): Background Correction to Stream Geochemical Data Using Digitized Drainage and Geological Maps: Application to Selwyn Basin, Yukon and Northwest Territories; *Journal of Geochemical Exploration*, Volume 25, pages 139-155.
- Bonham-Carter, G.F., Rogers, P.J. and Ellwood, D.J. (1987): Catchment Basin Analysis Applied to Surficial Geochemical Data, Cobequid Highlands, Nova Scotia; *Journal of Geochemical Exploration*, Volume 29, pages 259-278.
- Garrett, R.G., Kane, V.E. and Zeigler, R.K. (1980): The Management, Analysis and Display of Regional Geochemical Data; *Journal of Geochemical Exploration*, Volume 13, pages 115-152.
- Gravel, J.L. and Matysek, P.F. (1989): 1988 Regional Geochemical Survey, Northern Vancouver Island and Adjacent Mainland (92E, 92K, 92L, 102I); in Geological Fieldwork 1988, B.C. Ministry of Energy, Mines and Petroleum Resources, Paper 1989-1, pages 585-591.

- Hulme, N.J., Vanderpoll, W. and Duffet, L.L. (1993): Alert Bay and Cape Scott Mineral Occurrence Map 092L/102I; *B.C. Ministry of Energy, Mines and Petroleum Resources*, MINFILE, released May, 1993.
- Matysek, P.F., Gravel, J.L. and Jackaman, W. (1989): 1988 Regional Geochemical Survey, Stream Sediment and Water Geochemical Data, NTS 92L/102I - Alert Bay - Cape Scott; *B.C. Ministry of Energy, Mines and Petroleum Resources*, RGS 23.
- Muller, J.E., Northcote, K.E. and Carlisle, D. (1974): Geology and Mineral Deposits of Alert Bay - Cape Scott Map- area, Vancouver Island, British Columbia; *Geological Survey of Canada*, Paper 74-8, 77 pages.
- Nixon, G.T., Hammack, J.L., Hamilton, J.V. and Jennings, H. (1993): Preliminary Geology of the Ma-iatta Creek Area, Northern Vancouver Island (92L/105); in *Geological Fieldwork 1992*, Grant, B. and Newell, J.M., Editors, *B.C. Ministry of Energy, Mines and Petroleum Resources*, Paper 1993-1, pages 17-35.
- Smith, S.C. (1986): Base Metals and Mercury in Bryophytes and Stream Sediments from a Geochemical Reconnaissance Survey of the Chandala Quadrangle, Alaska; *Journal of Geochemical Exploration*, Volume 25, pages 345-365.

## NOTES

## NATURAL ACID ROCK-DRAINAGE IN THE RED DOG - HUSHAMU - PEMBERTON HILLS AREA, NORTHERN VANCOUVER ISLAND (92L/12)

By Victor M. Koyanagi and Andre Panteleyev

**KEYWORDS:** Applied geochemistry, natural acid rock-drainage, porphyry copper-gold, advanced-argillic alteration, acid generation, sulphide weathering, Holberg Inlet, Nahwitti Lowland, Red Dog, Hushamu, Pemberton Hills, Northern Vancouver Island.

### INTRODUCTION

Northern Vancouver Island Upper Triassic sediments, Lower Jurassic Bonanza volcanics and related Jurassic Island Plutonic Suite intrusions host significant porphyry copper-gold, base metal skarns and advanced argillic acid-sulphate epithermal mineralization (Panteleyev and Koyanagi, 1993). This geological setting provides the focus for a study of natural acid rock-drainage.

The purpose of the study is to determine the source and demonstrate the extent of natural acid in waters draining areas of altered and mineralized rock. Over a 3-year period beginning in 1991, 248 water sites were sampled for pH, conductivity and total dissolved solids. Selected drainages were measured yearly to evaluate annual variations. Flushing effects after a major rainfall were determined by taking pH measurements before and after rainstorms. A total of twenty-one waters and nine silt samples from selected sites were collected and submitted for analysis of metal content. Data from 1991 and 1992 sampling are presented in Koyanagi and Panteleyev (1993). Analytical data from samples collected in the 1993 season are pending.

### LOCATION AND ACCESS

The study area in northern Vancouver Island is located between Nahwitti Lake and Holberg Inlet about 15 kilometres west of the Island Copper mine (Figure 1). The sample area in 1991 and 1992 was centred about Mount McIntosh and the Pemberton Hills. The survey expanded in 1993 to include waters draining the Red Dog deposit, the upper reaches of the Goodspeed River and its major tributaries, and parts of the Wanokana Creek and Nahwitti River drainage systems. Access from Coal Harbor in the south is primarily by well-maintained active logging roads and in the north along the Port Hardy - Holberg road.

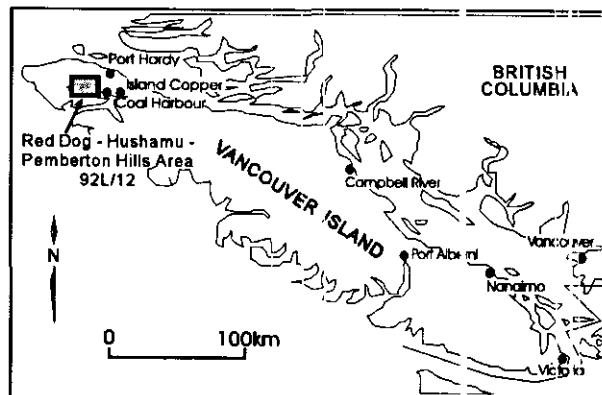


Figure 1. Location Map of the Red Dog - Hushamu - Pemberton Hills area, Northern Vancouver Island.

### PHYSIOGRAPHY

The study area falls within the Nahwitti Lowland which forms part of the Hecate Depression (Holland, 1976). The Nahwitti Lowland is characterized by low relief, rounded hills, narrow valleys and broad lowlands and valleys (Gravel and Matysek 1989). Elevations range from sea level up to 700 metres, generally diminishing toward the northwest.

Quaternary geology, as described by Kerr and Sibbick (1992), consists of widespread deposits of till common in both highland and lowland areas attaining tens of metres of thickness in valleys. Sand and gravel deposits of glaciofluvial outwash vary from 1 to 15 metres in thickness as valley-bottom fill. Colluvium derived from till and weathered bedrock occurs as a ubiquitous veneer (<1 m) or blanket (>1 m). A thin layer of ferricrete is widespread in the study area and is commonly exposed as resistant ledges overhanging stream banks and road cuts.

The most recent glaciation in the Nahwitti Lowlands (Wisconsinan) occurred 20 000 to 10 000 years ago. This glaciation is interpreted to have had a regional ice-flow direction generally to the northwest, originating from the Coast Mountains and crossing Queen Charlotte Strait (Kerr and Sibbick, 1992).

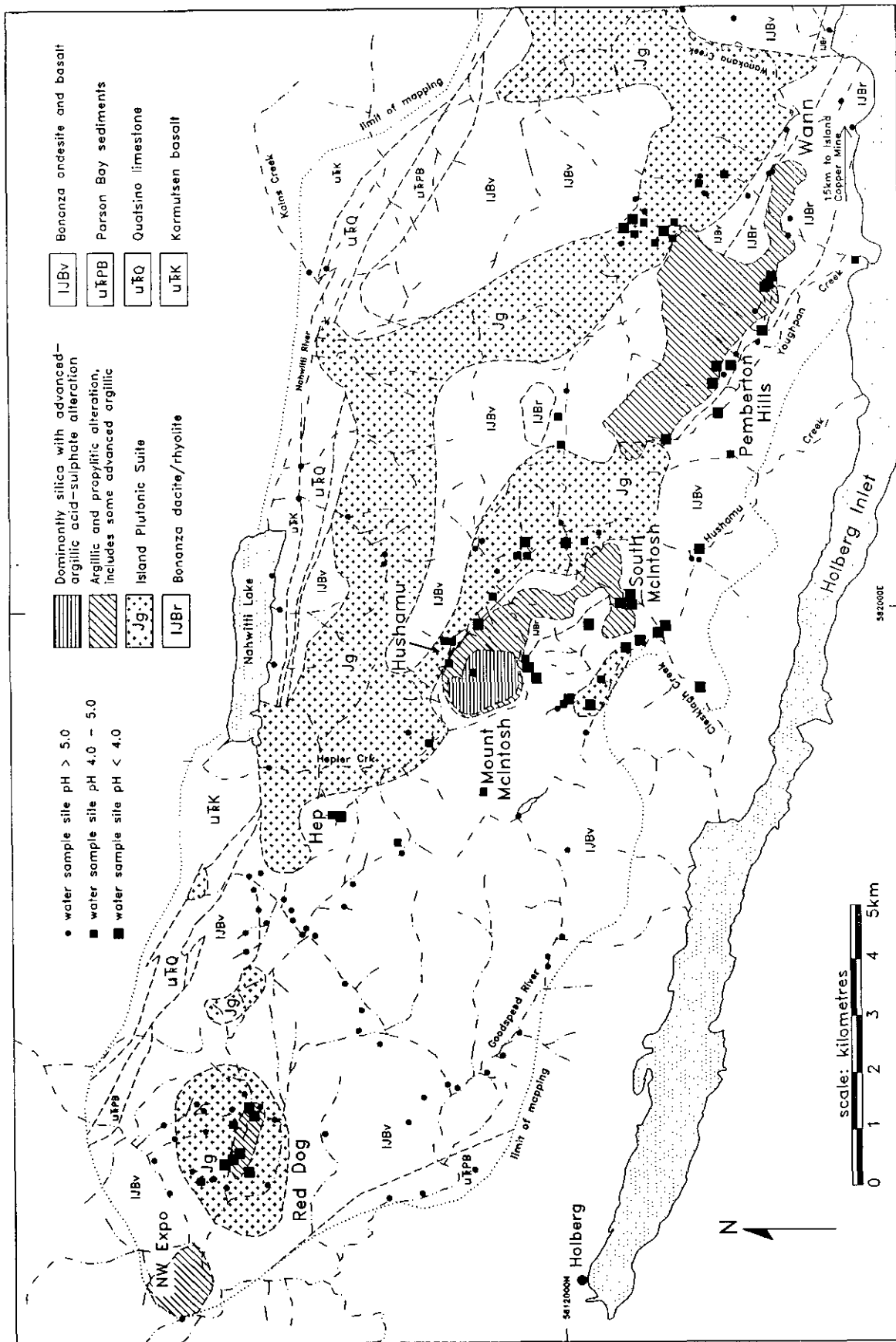


Figure 2. Sample location map illustrating spatial relationship of acidic waters within the study area; water sample data were collected from 1991 to 1993; note consistent trend of acid waters between the Red Dog and the Pemberton Hills correlating acid drainage to mineralization and alteration.

## GEOLOGICAL SETTING

The geology in the study area is dominated by Upper Triassic to Lower Jurassic volcanic and sedimentary rocks intruded by plutonic rocks of Jurassic, Island Plutonic Suite affinities (Figure 2). These rocks are unconformably overlain by Cretaceous sedimentary rocks along the north shore of Holberg Inlet. A detailed description of the regional geology is reported by Nixon *et al.* (1994, this volume).

Jurassic Bonanza Group units host porphyry copper-gold deposits (Island Copper mine, Hushamu, Hep, Red Dog) related to intrusion of the Island Plutonic Suite, as well as transitional to epithermal-type alteration and mineralization (NW Expo, Mount McIntosh, South McIntosh, Pemberton Hills, Wann). Advanced-argillic acid-sulphate mineralization transitional between porphyry and epithermal settings occurs in a belt of distinct alteration trending northwesterly from the Pemberton Hills to the Northwest Expo property (Figure 2). Descriptions of the transitional setting and associated alteration and mineralization are provided by Panteleyev (1992), and Panteleyev and Koyanagi (1993; 1994, this volume).

## FIELD STUDY AND ANALYTICAL PROCEDURE

Acid levels in waters were measured using a Corning CheckMate™ M90 portable microprocessor-based pH, conductivity and total dissolved solids meter. Readings were taken in the field by submersing the meter directly into waters.

During the 1993 sampling program, 171 waters were measured for pH, conductivity and total dissolved solids. Sampling included re-measuring sites tested in previous years, to determine annual variations. In the Wanokana, Youghpan and Hushamu Creek drainages measurements were taken before and after a major rainfall to determine the effects of short-term flushing.

Waters were surveyed during the month of August. Precipitation levels reported by Environment Canada indicate rainfall for July 1993 was below average with August 1993 rainfall slightly above average (Table 1). The below average rainfall in July resulted in small volumes of water flow in many drainages. In some smaller creeks levels were reduced to flow occurring only below the ground

surface. Background acid level, considered to be represented by the acid level in waters draining relatively unmineralized areas and the larger lakes, is about pH 5.6.

## RESULTS AND INTERPRETATIONS

A correlation between high acid levels in drainage waters and sulphide-bearing rocks, as reported by Koyanagi and Panteleyev (1993), was further substantiated by 1993 sampling. Acid levels measured in waters draining the Red Dog area provide evidence for this correlation (Figure 3). The Red Dog is a porphyry prospect with low-grade copper-gold-molybdenum mineralization hosted by a porphyritic intrusion of the Island Plutonic Suite. The surrounding country rocks are dominantly mafic to intermediate Bonanza flows with lesser Parson Bay sedimentary rocks cropping out to the north. A "bull's eye" pattern of pH measurements centred on the mineralized zone illustrates the source and

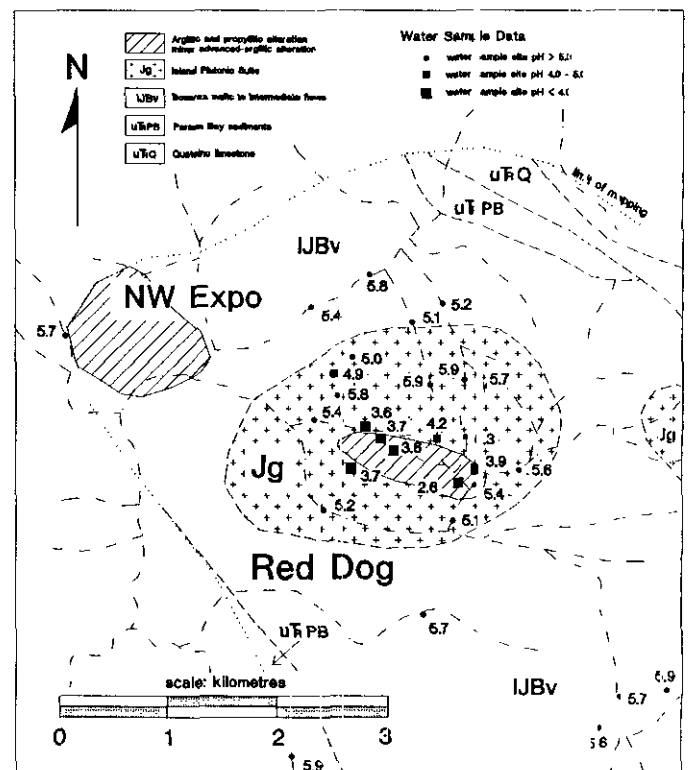


Figure 3. Sample location map of the Red Dog prospect illustrating the spatial relationship of acid waters in relation to alteration and lithologies.

TABLE 1. MONTHLY PRECIPITATION TOTALS FOR 1991 TO 1993.

	January	February	March	April	May	June	July	August
1991	185.8	184.2	104.0	95.0	52.6	61.6	78.6	186.6
1992	409.0	167.2	38.8	92.8	76.8	70.4	13.6	47.6
1993	-----	29.2	258.8	150.0	139.8	82.8	25.0	79.6
Average*	258.8	190.1	175.9	133.1	78.1	71.0	47.0	58.8

\* averages calculated for years 1961 to 1990. All measurements in millimetres

Reported by Atmospheric Environmental Service, Canada Climate Normals for British Columbia; station located at Coal Harbour 50°36'N 127°30'W, elevation 57 metres.

TABLE 2. WATER DATA FOR NEW 1993 SAMPLE SITES.

Sample Number	Main Drainage	pH	Cond.	TDS	Temp °C	Sample Number	Main Drainage	pH	Cond.	TDS	Temp °C
EC93VKO37	Goodspeed	5.7	49.0	24.4	14.0	EC93VKO20	Red Dog	5.4	86.9	43.6	13.0
EC93VKO38	Goodspeed	6.1	157.6	78.5	19.7	EC93VKO21	Red Dog	5.6	72.0	36.1	13.2
EC93VKO39	Goodspeed	5.9	142.7	71.4	21.3	EC93VKO22	Red Dog	3.9	205.0	102.0	14.9
EC93VKO40	Goodspeed	5.7	63.8	27.5	24.3	EC93VKO23	Red Dog	2.7	1503.0	753.0	14.2
EC93VKO41	Goodspeed	5.7	50.2	20.1	19.8	EC93VKO24	Red Dog	5.1	86.8	43.5	14.2
EC93VKO42	Goodspeed	6.3	160.4	86.2	23.8	EC93VKO25	Red Dog	5.7	46.4	22.7	12.3
EC93VKO43	Goodspeed	5.1	41.5	20.0	22.8	EC93VKO26	Red Dog	5.7	57.1	26.6	16.6
EC93VKO45	Goodspeed	5.9	91.0	45.7	15.6	EC93VKO27	Red Dog	5.6	88.8	47.7	14.2
EC93VKO46	Goodspeed	5.6	97.5	49.9	13.4	EC93VKO60	Clesclagh	4.3	179.0	90.0	14.4
EC93VKO47	Goodspeed	5.9	94.5	47.6	12.4	EC93VKO61	Clesclagh	5.9	93.7	38.6	12.0
EC93VKO48	Goodspeed	5.8	74.2	36.6	13.0	EC93VKO67	Clesclagh	5.5	67.8	34.1	14.1
EC93VKO49	Goodspeed	6.1	173.9	78.9	12.1	EC93VKO77	Hepler	5.8	72.4	43.5	12.2
EC93VKO50	Goodspeed	5.9	230.0	116.0	10.7	EC93VKO78	Hepler	5.5	64.7	31.9	14.8
EC93VKO51	Goodspeed	6.1	296.0	152.0	9.5	EC93VKO79	Hepler	5.8	42.3	20.0	14.7
EC93VKO52	Goodspeed	6.1	153.0	77.7	12.1	EC93VKO172	Hepler	5.5	---	---	11.7
EC93VKO54	Goodspeed	5.7	84.5	42.7	11.6	EC93VKO83	Hushamu	5.5	83.5	50.7	10.6
EC93VKO55	Goodspeed	5.7	68.2	34.1	12.5	EC93VKO87	Hushamu	4.3	137.0	69.6	16.4
EC93VKO56	Goodspeed	5.7	64.5	31.1	10.7	EC93VKO88	Hushamu	5.6	54.9	27.0	13.7
EC93VKO57	Goodspeed	5.6	84.5	41.6	10.9	EC93VKO95	Hushamu	5.3	53.8	26.6	14.1
EC93VKO58	Goodspeed	5.6	38.4	18.6	17.5	EC93VKO96	Hushamu	5.5	55.4	32.6	13.3
EC93VKO75	Goodspeed	5.2	85.5	38.5	8.9	EC93VKO168	Kains	5.6	---	---	12.5
EC93VKO76	Goodspeed	5.6	64.2	33.5	10.5	EC93VKO169	Nahwitti	5.7	---	---	13.6
EC93VKO170	Goodspeed	5.7	---	---	9.5	EC93VKO111	NW Expo	5.7	109.6	55.4	17.4
EC93VKO171	Goodspeed	5.6	---	---	15.5	EC93VKO135	Wakalish	6.4	189.1	95.4	13.2
EC93VKO16	Holberg	6.1	191.0	94.0	16.3	EC93VKO115	Wanokana	5.9	63.5	28.8	12.8
EC93VKO28	Holberg Rd	5.7	64.6	32.5	11.7	EC93VKO116	Wanokana	3.9	151.1	75.7	14.2
EC93VKO29	Holberg Rd	5.9	68.4	34.4	20.5	EC93VKO117	Wanokana	3.3	863.0	450.0	14.2
EC93VKO30	Holberg Rd	5.8	56.3	27.9	15.1	EC93VKO118	Wanokana	5.5	109.4	54.6	12.3
EC93VKO31	Holberg Rd	5.1	102.0	42.9	15.7	EC93VKO119	Wanokana	4.4	147.8	73.3	10.9
EC93VKO32	Holberg Rd	6.1	103.8	47.4	13.5	EC93VKO120	Wanokana	5.3	60.5	29.2	15.8
EC93VKO33	Holberg Rd	5.6	63.6	31.5	12.0	EC93VKO121	Wanokana	4.3	118.7	58.7	12.6
EC93VKO34	Holberg Rd	5.5	44.9	22.9	12.4	EC93VKO122	Wanokana	4.9	117.6	56.2	12.3
EC93VKO35	Holberg Rd	5.6	100.7	50.1	14.9	EC93VKO123	Wanokana	3.9	121.5	60.4	15.3
EC93VKO36	Holberg Rd	5.5	44.7	22.1	10.8	EC93VKO124	Wanokana	4.0	310.0	152.0	15.2
EC93VKO44	Holberg Rd	5.5	99.1	50.0	10.0	EC93VKO125	Wanokana	4.6	43.2	21.5	16.9
EC93VKO1	Red Dog	5.9	66.0	30.8	9.1	EC93VKO126	Wanokana	5.1	77.8	38.9	14.2
EC93VKO2	Red Dog	5.7	58.9	28.4	11.3	EC93VKO127	Wanokana	5.5	80.1	50.2	13.3
EC93VKO3	Red Dog	5.7	41.2	23.6	9.4	EC93VKO129	Wanokana	5.3	61.0	30.5	17.6
EC93VKO4	Red Dog	3.6	206.0	102.0	14.2	EC93VKO130	Wanokana	5.3	81.5	40.5	15.7
EC93VKO5	Red Dog	3.7	510.0	260.0	18.0	EC93VKO131	Wanokana	4.4	142.5	72.0	16.1
EC93VKO6	Red Dog	5.4	76.4	38.4	13.5	EC93VKO132	Wanokana	5.7	114.3	56.3	15.2
EC93VKO7	Red Dog	5.0	86.7	43.1	16.7	EC93VKO164	Wanokana	5.3	61.8	30.6	11.6
EC93VKO8	Red Dog	5.1	51.2	25.8	13.9	EC93VKO165	Wanokana	5.2	1078.0	535.0	11.8
EC93VKO9	Red Dog	5.2	52.4	26.4	13.5	EC93VKO166	Wanokana	5.5	---	---	11.9
EC93VKO10	Red Dog	4.9	50.4	17.7	23.5	EC93VKO167	Wanokana	5.9	---	---	12.0
EC93VKO11	Red Dog	5.8	77.3	38.5	19.6	EC93VKO99	Youghpan	5.9	64.8	31.9	15.1
EC93VKO12	Red Dog	5.4	23.0	10.9	20.3	EC93VKO101	Youghpan	5.3	30.8	15.4	16.7
EC93VKO13	Red Dog	5.8	58.3	27.0	22.1	EC93VKO102	Youghpan	5.3	57.5	28.2	21.2
EC93VKO14	Red Dog	3.7	157.6	75.3	16.2	EC93VKO103	Youghpan	3.5	149.6	70.2	20.5
EC93VKO15	Red Dog	5.2	87.5	42.9	13.6	EC93VKO104	Youghpan	4.2	94.3	44.0	17.9
EC93VKO17	Red Dog	4.2	103.8	44.9	13.6	EC93VKO105	Youghpan	4.0	46.7	23.6	14.2
EC93VKO18	Red Dog	5.3	84.1	41.8	10.6	EC93VKO107	Youghpan	3.4	353.0	157.0	20.9
EC93VKO19	Red Dog	3.6	340.0	170.0	14.2	EC93VKO133	Youghpan	3.7	868.0	433.0	26.3

extent of acid generation (Figure 3). The mineralized area is located on a topographic high which is coincident with the "bull's eye" centre. Acid levels of waters within the mineralized zone average pH 3.8. Within 500 to 1500 metres of the core of the prospect, waters returned neutral (near background) acid levels. The limited range of anomalous acidity in waters appears to reflect the dimensions of the prospect and the amount of sulphide mineralization.

The Goodspeed River watershed is located southwest of the Red Dog - Hushamu - Pemberton Hills mineralized belt. No significant mineral prospects are reported within this drainage system. The area is underlain by a thick package of Bonanza mafic to intermediate flows, Parson Bay sediments and Quatsino limestone. Sample results from this watershed demonstrate the low acid-generating capacity of the volcanic stratigraphy, the acid neutralizing ability of the calcareous sediments and the implicit absence of

significant acid-generating mineral deposits. Acid levels in waters measured in this area average pH 5.7, reflecting background to slightly above background levels (Table 2). Similar background levels were measured in the Nahwitti River - Kains Creek area in the northeast part of the study area. This watershed drains Karmutsen basalt, Quatsino limestone, Parson Bay calcareous shales and Bonanza volcaniclastic rocks. Disseminations of pyrite and pyrrhotite in Parson Bay siltstones and locally in calcisilicate-altered calcareous rocks are a potential source of acid generation. The buffering capacity of the calcareous stratigraphy is not exceeded by the acid generated, resulting in background acid levels.

Variations of acid levels in waters were tested over the short term (daily) and at 3-year intervals during the summer months of 1991-1993. Annual measurements revealed a consistency in levels of acid generated into streams over the 3-year period (Table 3). Acidic waters (pH <4.0) draining mineralized areas

TABLE 3. WATER DATA FOR SAMPLE SITES WITH REPEAT MEASUREMENTS.

Sample Number	Main Drainage	1993 Sampling				1993 Resampling				1992 Sampling				1991 Sampling			
		pH	Cond.	TDS	Temp	pH	Cond.	TDS	Temp	pH	Cond.	TDS	Temp	pH	Cond.	TDS	Temp
EC93VKO59	Clesclagh	5.7	52.8	27.2	12.8	5.5	55.5	28.0	11.0	5.4	55.0	27.4	15.6	---	---	---	---
EC93VKO62	Clesclagh	4.2	173.5	87.2	12.2	---	---	---	---	4.3	157.0	78.5	14.0	---	---	---	---
EC93VKO63	Clesclagh	4.9	75.7	37.6	11.6	---	---	---	---	5.3	71.1	35.5	12.0	---	---	---	---
EC93VKO64	Clesclagh	3.2	471.0	240.0	14.9	---	---	---	---	---	---	---	---	4.1	215.0	107.0	12.9
EC93VKO65	Clesclagh	4.0	140.0	68.0	18.4	3.4	360.0	182.0	11.9	---	---	---	---	---	---	---	---
EC93VKO66	Clesclagh	3.8	436.0	219.0	14.4	---	---	---	---	---	---	---	---	3.6	282.0	149.0	12.6
EC93VKO68	Clesclagh	3.4	458.0	233.0	15.7	---	---	---	---	---	---	---	---	3.1	442.0	219.0	14.3
EC93VKO69	Clesclagh	3.9	215.0	87.6	17.7	3.8	251.0	96.5	12.8	---	---	---	---	3.9	159.2	79.2	15.0
EC93VKO70	Clesclagh	4.0	189.3	93.0	17.5	---	---	---	---	---	---	---	---	3.5	255.0	128.0	13.9
EC93VKO71	Clesclagh	4.5	132.5	63.7	20.1	---	---	---	---	---	---	---	---	3.2	459.0	244.0	17.7
EC93VKO72	Clesclagh	4.1	230.0	120.0	14.3	---	---	---	---	3.9	184.2	92.9	14.9	---	---	---	---
EC93VKO80	Hepler	5.7	67.5	33.2	15.6	---	---	---	---	---	---	---	---	5.5	48.4	28.1	10.0
EC93VKO81	Hepler	5.6	72.8	35.1	13.5	3.8	325.0	161.0	12.3	---	---	---	---	4.1	100.0	50.0	11.2
EC93VKO81-1	Hepler	3.8	190.0	96.0	12.8	3.7	335.0	161.0	12.3	---	---	---	---	3.9	119.4	61.7	11.7
EC93VKO82	Hepler	2.9	1017.0	527.0	19.4	2.8	1566.0	781.0	14.9	---	---	---	---	---	---	---	---
EC93VKO112	Hushamu	5.7	64.5	31.9	17.7	5.5	81.7	37.3	12.0	4.8	53.1	25.4	13.7	---	---	---	---
EC93VKO73	Hushamu	5.7	78.5	37.9	18.0	5.6	67.1	33.2	13.3	---	---	---	---	6.0	61.3	36.9	10.6
EC93VKO74	Hushamu	3.4	157.9	79.7	16.5	4.1	131.4	65.5	12.0	---	---	---	---	3.9	163.2	81.8	13.1
EC93VKO84	Hushamu	5.2	105.7	52.3	19.0	---	---	---	---	4.5	92.4	44.9	19.5	---	---	---	---
EC93VKO85	Hushamu	4.4	153.9	72.5	12.8	4.2	180.1	89.4	16.8	---	---	---	---	4.3	141.2	70.8	15.8
EC93VKO86	Hushamu	3.7	509.0	249.0	12.8	3.7	687.0	357.0	11.0	---	---	---	---	3.7	53.9	27.3	9.1
EC93VKO89	Hushamu	5.4	48.7	24.7	13.5	---	---	---	---	---	---	---	---	5.8	48.1	24.2	14.1
EC93VKO90	Hushamu	5.3	58.1	29.1	14.4	5.0	50.0	25.2	11.1	4.7	51.2	25.6	19.1	---	---	---	---
EC93VKO91	Hushamu	3.7	125.6	63.4	13.8	4.1	135.2	63.8	12.3	---	---	---	---	4.3	120.0	61.1	13.7
EC93VKO92	Hushamu	3.7	181.0	90.2	11.9	3.8	129.6	64.9	10.9	---	---	---	---	3.8	176.5	92.0	14.6
EC93VKO93	Hushamu	4.4	70.6	35.2	13.4	---	---	---	---	---	---	---	---	4.0	---	---	11.2
EC93VKO94	Hushamu	3.8	219.0	110.0	11.9	---	---	---	---	---	---	---	---	5.4	---	---	12.2
EC93VKO53	Mt. McIntosh	2.9	420.0	195.0	16.9	---	---	---	---	3.2	259.0	128.0	23.4	3.6	88.0	44.7	12.2
EC93VKO114	Wanokana	5.6	60.9	33.3	16.8	4.8	48.9	22.8	13.0	---	---	---	---	---	---	---	---
EC93VKO128	Wanokana	4.5	117.8	58.9	15.3	4.3	114.3	57.0	11.4	---	---	---	---	---	---	---	---
EC93VKO100	Youghpan	5.4	55.6	27.6	17.9	---	---	---	---	5.3	89.9	28.3	12.6	---	---	---	---
EC93VKO106	Youghpan	3.5	408.0	203.0	17.1	3.4	469.0	234.0	11.0	3.4	347.0	175.0	11.5	---	---	---	---
EC93VKO108	Youghpan	3.4	449.0	232.0	21.9	3.2	298.0	147.0	12.5	2.9	311.0	157.0	15.4	---	---	---	---
EC93VKO109	Youghpan	3.7	250.0	130.0	16.6	---	---	---	---	3.1	252.0	124.0	12.4	---	---	---	---
EC93VKO110	Youghpan	2.9	1870.0	754.0	17.1	2.8	750.0	379.0	11.7	---	---	---	---	---	---	---	---
EC93VKO113	Youghpan	4.2	176.2	88.4	15.3	3.8	103.9	51.7	12.4	5.7	77.7	38.7	19.1	---	---	---	---
EC93VKO134	Youghpan	5.6	---	---	24.1	---	---	---	---	5.5	774.0	385.0	25.3	---	---	---	---
EC93VKO156	Youghpan	4.7	141.6	70.5	15.1	---	---	---	---	5.4	145.7	70.2	17.7	---	---	---	---
EC93VKO157	Youghpan	4.0	589.0	183.0	13.5	---	---	---	---	3.5	264.0	131.0	16.1	---	---	---	---
EC93VKO158	Youghpan	3.5	530.0	264.0	14.6	---	---	---	---	3.5	260.0	130.0	16.5	---	---	---	---
EC93VKO159	Youghpan	3.5	528.0	290.0	15.8	---	---	---	---	3.4	240.0	119.0	16.7	---	---	---	---
EC93VKO160	Youghpan	5.7	522.0	265.0	15.8	---	---	---	---	6.1	348.0	174.0	19.4	---	---	---	---
EC93VKO161	Youghpan	6.0	92.9	46.7	17.6	---	---	---	---	5.7	77.7	38.7	19.1	---	---	---	---
EC93VKO162	Youghpan	4.2	82.6	43.1	13.5	---	---	---	---	3.9	77.2	38.5	17.7	---	---	---	---
EC93VKO163	Youghpan	4.1	92.5	45.3	14.5	---	---	---	---	4.0	90.7	43.1	14.8	---	---	---	---
EC93VKO97	Youghpan	4.5	134.6	67.0	17.3	---	---	---	---	4.4	117.5	57.5	15.4	---	---	---	---
EC93VKO98	Youghpan	4.3	225.0	111.0	15.3	---	---	---	---	5.0	50.0	25.1	11.2	---	---	---	---

Measurements resampled in 1993 are utilized to determine short-term variations during a heavy rainfall, annual measurements are utilized to document long term variations.

invariably return similarly low pH levels in each of the 3 years. Minor fluctuations are commonly observed in weakly acid waters (pH 4.0-5.0). These fluctuations are attributed to flushing of trapped acid or dilution of acidity, either seasonally or daily. Because the pH scale is reverse logarithmic, the addition of small amounts of acid or the dilution of existing acidity in streams is more easily detected at pH levels of 5 to 4 than at pH levels of 4 to 3.

Short-term variations were recognized during a large rainfall in mid-August which lasted several days and resulted in the flushing of major watersheds. Acid in rocks and soils was flushed out concurrent with large scale mass wastage by erosion of stream bank outcrops. The result was a marked drop in pH levels in some creeks (Table 3). In other stream systems dilution effects during flushing by rainwater (pH ± 5.6) was indicated by a rise in pH levels. The rise or fall of acid levels in waters during rainfall is dominantly lithologically controlled.

Wanokana and Youghpan creeks were considerably swollen during the rainstorm. Water levels

rose from tens of centimetres to more than a metre near the mouths of these creeks. The Wanokana watershed drains an area of about 44 square kilometres. Water measured near the mouth of this relatively large drainage system returned pH levels of 5.6 before the rainstorm and 4.8 after flushing occurred. The drainage system is dominantly underlain by a monzodioritic pluton intruding Bonanza volcanics and volcaniclastics. Base metal bearing quartz veins, pyritic fault zones and advanced-argillic dumortierite-bearing hydrothermal alteration zones are reported to occur within the watershed. Although these mineral deposits are potentially acid generating, neutral acid levels (pH 5.6) measured prior to flushing indicate acid added to the system from these sources is negligible. The decrease in pH levels during rainfall is interpreted to be the result of flushing of organic and inorganic generated acid from rocks and soils. An influx of organic material and organic acid is visibly evident as increased turbidity of creek waters during flushing. The decrease in pH in Wanokana Creek reflects the influence of the addition of

small amounts of acid on waters with initially neutral pH levels (pH 5.6).

The Youghpan watershed drains an area of about 25 square kilometres and is dominantly underlain by altered and mineralized Bonanza volcanics and minor dioritic intrusions. Advanced-argillic acid-sulphate altered zones occupy a large portion of the drainage area and host massive to disseminated pyrite and marcasite mineralization (Panteleyev and Koyanagi, 1992). Evidence of sulphide dissolution in the Youghpan drainage system as the dominant source of acid generation is provided by high sulphate levels (Koyanagi and Panteleyev, 1992). Acid levels near the mouth of Youghpan Creek measured pH 4.2 prior to the rainstorm and pH 3.8 after flushing. Acidity generated by the strongly mineralized and altered rocks may be trapped within soils, joints, fractures and other open spaces. The heavy rainfall flushes trapped acid resulting in an influx of acid into the stream system. Substantial acid-generating sulphide mineralization throughout the Youghpan system accounts for the amount of flushed acid which exceeds the buffering effects of additional neutral waters such as rain and surface runoff, resulting in the net decrease in pH levels.

The Hushamu watershed drains an area of about 20 square kilometres. Heavy rainfall flushing the system resulted in a decrease in acidity with levels rising from pH 3.4 to 4.1. Tributaries on the west side of the Hushamu watershed drain the Mount McIntosh and South McIntosh areas. These areas comprise advanced-argillic acid-sulphate alteration zones with significant disseminated sulphide mineralization. Acid levels from these tributaries average pH levels of 3.8. A relatively unmineralized diorite intrusion underlies most of the eastern flanks of Hushamu Creek. Tributaries draining the diorite return dominantly background acid levels. The decrease in acid levels after flushing is the result of dilution by neutral waters draining unmineralized areas. Hushamu Lake, at the headwaters of the Hushamu watershed, has an average acid level of pH 4.3. During the heavy rainfall an influx of lake water into the more acidic waters of Hushamu Creek caused dilution and a subsequent rise in pH levels. This rise is reflected by measurements at a sample site located approximately 1 kilometre downstream from Hushamu Lake. Before the rainfall, waters at this site returned acid levels of pH 3.7. After lake waters overflowed into Hushamu Creek, acid levels measured pH 4.1. The overall increase in pH during flushing indicates the amount of acid flushed into the system is more than offset by the addition of less acidic and neutral waters.

## CONCLUSIONS

Natural acid rock-drainage is generated from altered and mineralized rocks into waters draining the Red Dog - Hushamu - Pemberton Hills area. The dominant source of acid is the dissolution of sulphides contained within advanced-argillic acid-sulphate alteration zones as well as porphyry copper-gold and

skarn-mineralized rocks. Within the study area, the amount of acid generated is proportional to the amount of sulphide mineralization. Detection of acidity several kilometres downstream from the acid-generating source is also a function of the size of the mineralized system. Acidic streams (pH <4.0) measured annually, returned consistently acidic levels over a 3-year period. Measurements of weakly acidic waters (pH 5-4) fluctuated from year to year. These fluctuations are attributed to flushing of trapped acid by seasonal runoff or during rainstorms. Due to the pH scale being reverse logarithmic, small changes in acid levels are more easily detected in less acid waters. Short term variations of acid levels in selected streams revealed fluctuations to be strongly lithologically controlled. Measurements before and after a large rainfall illustrate the effects of flushing of trapped acid. Acid levels increase or decrease depending on the abundance of acid-generating and acid-neutralizing rocks within the watershed.

## ACKNOWLEDGMENTS

The authors thank Steve Cook, Steve Sibbick and Wayne Jackaman for their assistance in providing background information and reference materials. Technical review by Jan Hammack is appreciated. This paper has benefited from final editorial comment by Brian Grant and John Newell.

## REFERENCES

- Gravel, J.L. and Matysek, P.F. (1989): 1988 Regional Geochemical Survey, Northern Vancouver Island and Adjacent Mainland (92E, 92K, 92L, 102I); in *Geological Fieldwork 1988, B.C. Ministry of Energy, Mines and Petroleum Resources*, Paper 1989-1, pages 585-591.
- Holland, S.S. (1976): Landforms of British Columbia: A Physiographic Outline. *B.C. Ministry of Energy, Mines and Petroleum Resources*, Bulletin 48, pages 32-35.
- Kerr, D.E. and Sibbick, S.J. (1992): Preliminary Results of Drift Exploration Studies in the Quatsino (92L/12) and the Mount Milligan (93O/4W) Areas; in *Geological Fieldwork 1991*, Grant, B. and Newell, J.M., Editors, *B.C. Ministry of Energy, Mines and Petroleum Resources*, Paper 1992-1, pages 341-347.
- Koyanagi, V.M. and Panteleyev, A. (1993): Natural Acid-Drainage in the Mount McIntosh - Pemberton Hills Area, Northern Vancouver Island (92L/12); in *Geological Fieldwork 1992*, Grant, B. and Newell, J.M., Editors, *B.C. Ministry of Energy, Mines and Petroleum Resources*, Paper 1993-1, pages 445-450.
- Nixon, G.T., Hammack, J.L., Koyanagi, V.M., Payie, G., Panteleyev, A., Massey, N.W.D., Hamilton, J.V. and Haggart, J. (1994): Preliminary Geology of the Quatsino - Port McNeil Map Area, Northern Vancouver Island, (92L/12, 11); in *Geological Fieldwork 1993*, Grant, B. and Newell, J.M., Editors, *B.C. Ministry of Energy, Mines and Petroleum Resources*, Paper 1994-1, this volume.

- Panteleyev, A (1992): Copper-Gold-Silver Deposits Transitional between Subvolcanic Porphyry and Epithermal Environments; *in* Geological Fieldwork 1991, Grant, B. and Newell, J.M., Editors, *B.C. Ministry of Energy, Mines and Petroleum Resources*, Paper 1992-1, pages 231-324.
- Panteleyev, A. and Koyanagi, V.M. (1993): Advanced Argillic Alteration in Bonanza Volcanic Rocks, Northern Vancouver Island - Transitions Between Porphyry Copper and Epithermal Environments (92L/12), *in* Geological Fieldwork 1992, Grant, B. and Newell, J.M., Editors, *B.C. Ministry of Energy, Mines and Petroleum Resources*, Paper 1993-1, pages 287-293.
- Panteleyev, A. and Koyanagi, V.M. (1994): Advanced Argillic Alteration in Bonanza Volcanic Rocks, Northern Vancouver Island, Lithologic and Structural Controls; *in* Geological Fieldwork 1993, Grant, B. and Newell, J.M., Editors, *B.C. Ministry of Energy, Mines and Petroleum Resources*, Paper 1994-1, this volume

## NOTES

# GEOLOGY AND MINERAL DEPOSITS OF PURCELL SUPERGROUP IN YAHK MAP AREA, SOUTHEASTERN BRITISH COLUMBIA (82F/1)

By D. A. Brown, J. A. Bradford, D. M. Melville, A. S. Legun,  
B.C. Geological Survey Branch  
and D. Anderson, Kootenay Exploration Ltd.

(Contribution No. 19, Sullivan-Aldridge Project)

**KEYWORDS:** Regional geology, Purcell Supergroup, Aldridge Formation, Creston Formation, Moyie sills, Moyie fault, Sullivan mine, Star, Iron Range.

## INTRODUCTION

The East Kootenay project was initiated to provide new 1:50 000-scale geological maps and stratigraphic studies for base metal exploration and land-use planning processes. The Yahk - Creston area has significant potential for undiscovered base metal deposits. It is underlain by Lower Purcell Supergroup rocks, a sedimentary rock succession that contains a number of significant deposits, including the Sullivan orebody, one of the world's largest massive sulphide deposits; the Troy mine (Spar Lake) and related copper-silver deposits in western Montana; and the Sheep Creek copper-cobalt deposit, also in Montana. In the last five years there have been a number of new discoveries in the Purcell Supergroup, including the Canam, Darlin, David, Dodge, Fors, and Star prospects. These new discoveries of Aldridge-hosted mineralization, coupled with established infrastructure, make this area in southern British Columbia attractive for exploration.

Geological mapping in the Creston area is dated; the most recent available maps were published for the Nelson East Half in 1941 by the Geological Survey of Canada (Rice, 1941). Farther east, the Fernie West Half map area was initially mapped by Daly (1912a), Schofield (1915) and Rice (1937), and later, Leech (1960) completed a 1:126 720-scale map (1" = 2 mile). More recent mapping has been published to the east and north by Höy (1993) and Reesor (1981, 1983, 1993) and south of the international boundary by Harrison *et al.* (1992) and Aadland and Bennett (1979; Figure 1).

Field work in 1993 focused on the Yahk map area (82F/01), where recent exploration activity has included diamond drilling on the Star, Eng and Goatfell properties. A six-week field season has generated a preliminary geological map of most of the Yahk sheet, with only limited coverage of the western third of the map area. Fill-in traverses and measured sections are

planned for the 1994 field season, in addition to extending the area of mapping to the west of Creston.

The Yahk map area is bisected by Highway 3, which follows the broad valleys of the Goat River, Kitchener Creek and the Moyie River. Access on logging roads and four-wheel-drive mineral exploration roads is good throughout the area. Topography is subdued, with the exception of the "Ramparts" east of Creston, where west-facing cliffs rise to peaks in excess of 2100 metres from the Creston valley floor at about 640 metres elevation. Extensive second and third-growth forest cover reflects widespread logging activity in the early 1900s. Outcrops are abundant on ridges above 1800 metre elevation, but are otherwise sparse in most of the map area. Lateral continuity of mappable units and only minor folding allows extrapolation based on widely spaced traverses.

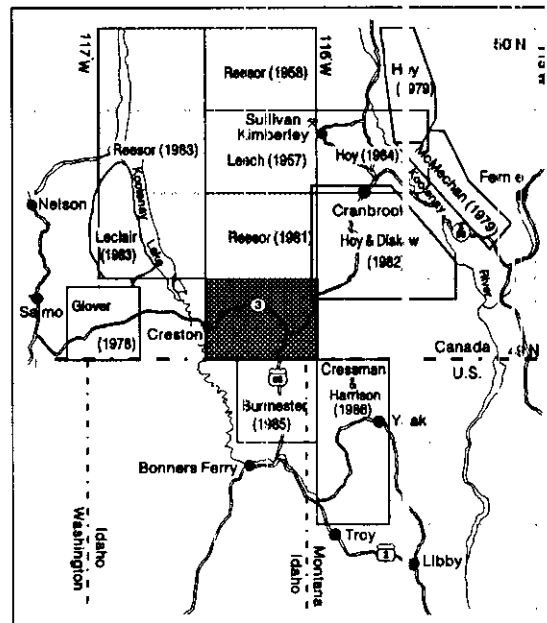


Figure 1. Location of the East Kootenay project map area (dark cross-hatched rectangle) relative to areas of previously published geologic maps. The 1:250 000 scale map coverage is not shown but includes: Fernie West-half (82F/west) -- Leech (1958, 1960), Höy and Carter (1988), Höy (1993); Nelson East-half (82G/east) -- Rice (1941), Reesor (1981, 1983); Sandpoint (82C) -- Aadland and Bennett (1979); Kalispell (82B) -- Harrison *et al.* (1992).

This project is designed to collaborate with and contribute to the Sullivan-Aldridge project -- a multidisciplinary research effort involving the Geological Survey of Canada, United States Geological Survey, Geological Survey Branch, four universities, Cominco Ltd. and other companies.

## GEOLOGICAL SETTING

Strata in the pericratonic Proterozoic Purcell (Belt in the United States) Supergroup basin are preserved in an area 750 kilometres long and 550 kilometres wide (130 000 km<sup>2</sup>). The rocks extend from southern British Columbia through eastern Washington, Idaho and western Montana (Figure 2). In British Columbia, the Middle Proterozoic strata of the Purcell Supergroup are exposed in the Purcell anticlinorium, a broad, northerly plunging structural culmination flanked by Paleozoic strata in the western part of the Foreland Belt (Figure 3). The stratigraphic nomenclature for the Purcell Supergroup varies across the basin. The East Kootenay project adopted divisions for the Nelson East Half based on Reesor (1983) and Höy (1993); correlative units in adjacent parts of the basin are illustrated in Figure 4.

Paleozoic and Mesozoic rocks of the Rocky Mountain fold and thrust belt lie mainly east of the Rocky Mountain Trench, while Late Proterozoic and younger rocks of the Kootenay Arc overlie the western extent of the exposed Purcell Supergroup rocks in Canada. Jurassic to Tertiary plutonic and gneissic rocks are exposed to the northwest (Bayonne batholith) and southwest (Kaniksu batholith, West Creston gneiss and Corn Creek gneiss) of the Creston area (Archibald *et al.*, 1984; Figure 3).

The Purcell (Belt) basin was the site of extension, crustal attenuation and possible intracratonic rifting in the Middle Proterozoic (*circa* 1500 Ma). This initiated the accumulation of 10 to 20 kilometres of sedimentary and mafic intrusive rocks in a confined basin. Paleotectonic reconstruction places the basin within a large land mass (Laurentia -- a part of Rodinia) at equatorial latitudes (Hoffman, 1991). Modern analogues could be the Black Sea, Red Sea and Gulf of California or fresh water Lake Baikal (Turner *et al.*, 1993).

The environment during the Proterozoic was significantly different than at present. The earth rotated faster which would have produced a stronger Coriolis force, and it had lower wind speeds, less precipitation and colder polar regions (Hunt, 1979). The atmosphere had less oxygen (about 1% of today's level) and more carbon dioxide (Cressman, 1989). The landscape was devoid of most forms of life including rooted plants that stabilize modern soils. The lack of living organisms to bioturbate sediment means exceptional preservation of primary sedimentary structures.

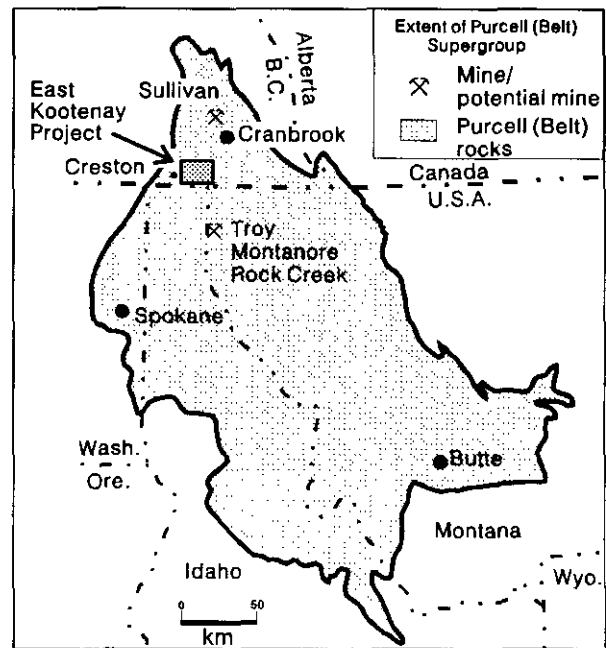


Figure 2. Extent of Purcell (Belt) strata relative to East Kootenay project area.

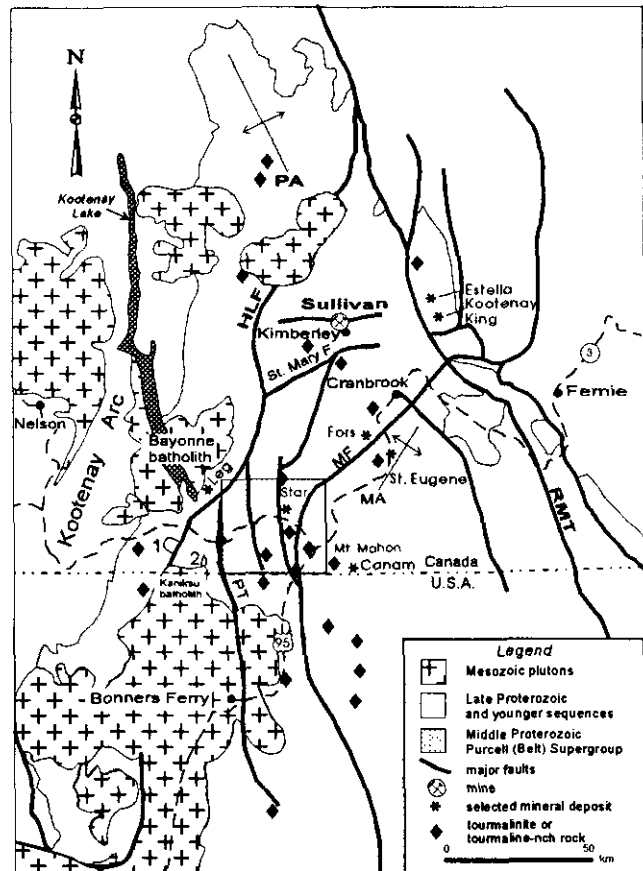


Figure 3. Purcell (Belt) Supergroup distribution and major faults in southern British Columbia and northern Washington, Idaho and Montana. Rectangle marks the project area. HLF = Hall Lake fault, MA = Moyie anticline, MF = Moyie fault, PA = Purcell anticlinorium, PT = Purcell Trench, RMT = Rocky Mountain Trench, 1 = Corn Creek gneiss, 2 = West Creston gneiss. Modified after Wheeler and McFeely, 1991. Tourmaline locations after Slack (1993).

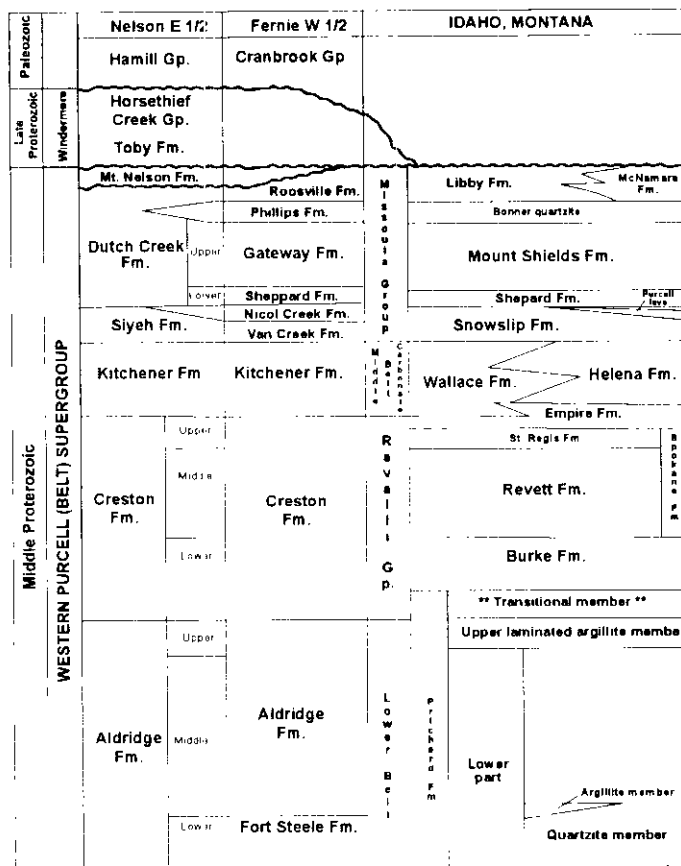


Figure 4. Table of formations for the Purcell Supergroup and their correlative units within the western Belt Supergroup of Idaho and Montana. Nelson East Half from Reesor (1981, 1983); Fernie West Half from Leech (1958); Idaho and Montana from Harrison *et al.* (1992) and Harrison and Cressman (1993). \*\* The *transitional member* of the Prichard Formation (Cressman, 1989) correlates with lower Creston of the Yahk map area.

Purcell sedimentation may have ended with the onset of the **East Kootenay orogeny**, a contractional tectonic event between 1350 and 1300 Ma (McMechan and Price, 1982). A Late Proterozoic extensional event, the **Goat River orogeny** (circa 800 Ma), resulted in continental rifting and initiation of the Cordilleran miogeocline with deposition of the Windermere Supergroup (Höy, 1993). The **Laramide orogeny** (100-70 Ma) produced the dominant folds and thrust faults in the map area. Strata of the Purcell anticlinorium were transported to the east on west-dipping imbricate thrust faults that extend into cratonic basement. Reactivation of some of these faults to form listric normal faults during an Eocene extension event is locally important, especially southwest of the map area (Newport fault and Priest River complex; Harms and Price, 1992).

## STRATIGRAPHY

The map area is underlain almost entirely by the Purcell Supergroup, a thick succession of siliciclastic and lesser carbonate rocks of Middle Proterozoic age (Figure 5). The Aldridge Formation (Schofield, 1915), the lowermost division of the Purcell Supergroup and the dominant unit in the map area, is more than 3500 metres thick. The correlative Prichard Formation in western Montana reaches a thickness of at least 6000 metres, including the gabbro sills (Cressman, 1983). The lower and middle Aldridge (Prichard) formations differ from the overlying Purcell Supergroup strata in that they were deposited in deeper water as turbidites, are intruded by numerous gabbro sills, contain extensive and distinctive marker units and have disseminated pyrrhotite throughout (Cressman, 1989). The Creston Formation (about 2300 metres thick; Reesor, 1983) gradually overlies the Aldridge Formation. It is exposed in the footwall of the Moyie fault in the eastern part of the Yahk map area, on the west side of the Carroll Creek/Kid fault in the central part, and in the northwest corner of the sheet. The overlying Kitchener Formation includes the lowermost significant carbonate accumulations in the Purcell succession. A small, possibly fault-bounded block of Kitchener Formation is exposed in the northeast part of the map area in the footwall of the Moyie fault.

## ALDRIDGE FORMATION

The Aldridge Formation comprises a thick succession of dominantly turbiditic siliciclastic rocks, including quartz wackes and arenites, siltstones and mudstones deposited in a middle to lower submarine fan setting. Although greenschist grade metamorphic mineral assemblages in these rocks are consistent with the use of metamorphic rock names (quartzite, siltite and argillite), sedimentary rock names are retained here because of the low level of deformation. East of the Yahk area, the Aldridge Formation has been subdivided into three units, the lower, middle and upper Aldridge, based on lithological characteristics and stratigraphic position. Mineralogic and chemical data for the Aldridge Formation are given by Edmunds (1977a). The lower and middle Aldridge are intruded by the Moyie sills, a suite of gabbroic sills which have been interpreted by Höy (1989) to be coeval with sedimentation in the Aldridge.

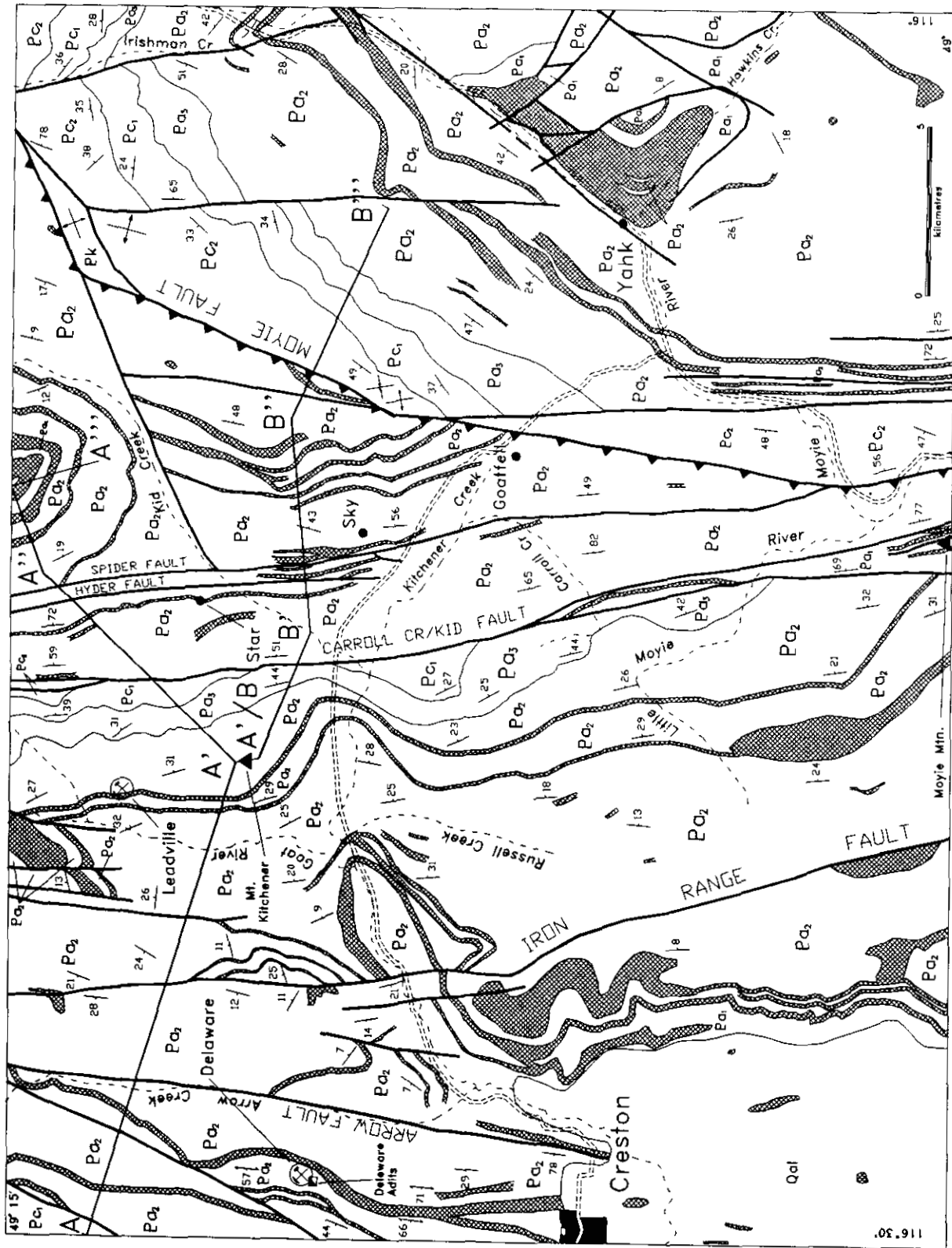


Figure 5. Simplified preliminary geology of the Yahk map area (82F/01), incorporating unpublished geology from Reesor and locations of selected mineral occurrences. Legend is included on Figure 8.

Total thickness of the Aldridge in the southern Purcell Mountains has been estimated to be over 4200 metres (Edmunds, 1977a, b; Höy and Diakow, 1981); its base is not exposed. Its age is constrained by the age of the Moyie sills (*circa* 1445-1480 Ma) and basement (1600 to 1700 Ma; Burwash *et al.*, 1962; Cressman, 1989). Recent zircon U-Pb dates of two Moyie sills in the Kimberley area are about 1480 Ma (Anderson and Parrish, 1993). A third sill in the same area yielded a zircon date of  $1468.0 \pm 1.5$  Ma (D. Davis, personal communication, 1993). The Cooper Lake granophyre, part of a gabbro sill 90 metres thick, located north of the present map area, yielded a 1425 to 1457 Ma zircon U-Pb date (Ross *et al.*, 1992). Slightly younger dates were reported for the Lumberton sill near Moyie Lake ( $1445 \pm 11$  Ma; Höy, 1989) and for the Crossport C sill in Idaho ( $1433 \pm 10$  Ma; Zartman *et al.*, 1982). Geochronometric and geochemical studies of the sills are ongoing by H.E. Anderson (GSC, Ottawa) and E. Schandl (University of Toronto) as part of the Sullivan-Aldridge project.

### LOWER ALDRIDGE (Pa<sub>1</sub>)

The upper part of the lower Aldridge in the Cranbrook-Kimberley area consists mainly of rusty weathering thinly bedded siltstone and argillite, interpreted as distal turbidites (Höy, 1993). The base of the middle Aldridge is placed below blocky, grey-weathering quartz wacke beds. The Sullivan deposit occurs at the transition from lower to middle Aldridge. This lithological transition is indistinct or is not seen in the Yahk-Creston map area. Possible lower Aldridge has been mapped in the southeast corner of 82F/01 by Höy (1993), where it occurs in the core of the Moyie anticline. Lower Aldridge has also been inferred in the hangingwall of the Carroll Creek/Kid fault in the south-central part of the map area (Figure 5). A thick succession of dominantly arenite and wacke, intruded by numerous thick sills and exposed in the Ramparts east of Creston, may also represent lower Aldridge, based on its structural position in the core of a regional anticline (Goat River anticline).

### RAMPART FACIES

Lithologically, rocks included in the upper lower Aldridge in the Yahk map area are distinct from the *thinly bedded, siltstone-dominated sequences* mapped by Höy (1993) to the northeast. They are informally referred to as the "Rampart facies" and consist primarily of distinct, light grey to buff, thick to medium-bedded quartz wacke with lesser green-grey siltstone. The thick beds form prominent cliffs or ribs along hillsides. Beds tend to weather with rounded edges. The sequence is notably non-rusty weathering, lacking pyrrhotite. Locally, the arenite is crossbedded, graded and/or laminated. Some beds are visibly lenticular in outcrop

and show cut-and-fill features at the base, suggestive of channel deposits. Beds tend to form amalgamated sets that fine upward. Between the sets are sequences of more thinly bedded quartzites with siltstones and wacke mudstone. Bedding is wavy and lenticular, showing features of current activity (ripple crosslamination) and loading (load ripples). Typical of the lower Aldridge, numerous Moyie intrusions are present in the Rampart sequence.

In most locales, the change from Rampart facies to middle Aldridge occurs approximately where the lower to middle Aldridge contact would be predicted on the basis of marker laminites (see below). The quartz wackes interbed upward into more quartzofeldspathic and locally calcareous beds of the middle Aldridge Formation. Lithologically the transition is subtle. Quartzitic beds of the Rampart facies and the middle Aldridge Formation are not distinguishable, if compared by individual bed.

### CORRELATION AND EXTENT

The Rampart facies thickens toward the U.S. border and thins eastward. At Creston the facies is estimated to be 700 metres thick. Eastward, Rampart facies can be recognized on the Canam property at America Creek and in drill core on the Eng property at Yahk (ddh E90-03, Stephenson, 1990a). Pale blue-grey quartzites dominate the cored interval at Yahk. The cored interval is believed to extend stratigraphically across Sullivan time, based on stratigraphic distance to marker laminites.

The facies has not been recognized on Mount Mahon immediately east of Yahk and north of America Creek. At Mount Mahon, an interbedded sequence of quartzites, sandstones, siltstones and argillites occupies approximately the same stratigraphic position as the Rampart facies. It is ascribed to a slightly quartzitic variation of typical lower Aldridge (Schiaffizza, 1984). Drilling by Chevron Minerals Limited between Mount Mahon and America Creek, intersected fine-grained sedimentary rocks in possible lower Aldridge (ddh MM87-1, Edmunds, 1988). Edmunds interpreted the features as indicating a rather quiet part of the basin. Drilling by Minnova Inc. on east Mount Mahon (ddh MM 91-02, Burge, 1992) intersected intervals dominated by quartz wackes in fining-upward sequences with cut-and-fill features. This may possibly be Rampart facies. Work needs to be done in this area to determine the eastern limit of the facies.

The Rampart facies in the Yahk area may correlate with a thickened middle Aldridge facies, or with the lower Aldridge footwall quartzite exposed in the Sullivan area. Both interpretations imply more proximal parts of turbidite fans in the Yahk area compared to the Sullivan area. Correlation with middle Aldridge facies implies that typical thin-bedded upper lower Aldridge sedimentary rocks occur at lower stratigraphic levels not exposed in the Yahk area. Correlation of the Rampart facies with footwall quartzite implies that the upper

siltstone of the Sullivan area, the more distal turbidites of the lower Aldridge, are replaced to the southwest by proximal middle fan turbidites of the Ramparts facies.

### MIDDLE ALDRIDGE (Pa<sub>2</sub>)

The middle Aldridge underlies most of the map area. It comprises a thick sequence of fine clastic rocks, dominantly planar-bedded, fine-grained quartzofeldspathic wacke to arenite, with lesser siltstone and mudstone. Medium-grained sandstone is uncommon, and coarse-grained sandstone and conglomerate are rare. Total thickness is at least 3000 metres, and may be as much as 4000 metres, based on estimates from map distribution. In contrast, the middle Aldridge in the Cranbrook area is about 2500 metres thick (Höy, 1993) and farther north at the Sullivan mine area, only 2100 metres thick.

Outcrop occurrences of "fragmentals" have been reported by D. Pighin and others. Sheet-like slumps and debris flows, as well as localized, crosscutting, dewatering-type fragmentals have been identified. One locality along the Goat River road is interesting because the fragmental unit forms a prominent, resistant knob just east of the road. Similar breccias in other parts of the Aldridge and Prichard formations are attributed to dewatering features (Höy, 1993; Cressman, 1989).

Typically, the middle Aldridge consists of rusty brown weathering quartzofeldspathic wacke beds, 0.2 to 1.0 metre thick, separated by thinner intervals (typically 0.05 - 0.3 m) of siltstone and argillaceous siltstone (Plate 1). Both thicker and thinner sandstone beds are less

common. The sandstone beds are even, planar and laterally continuous, massive to indistinctly graded, locally with coarse (<1 - 2 cm) dark and pale grey laminae. Flute casts, longitudinal and crescentic scour marks and load structures at the base of beds are ubiquitous but unfortunately best seen in talus blocks. Ripple marks and ball-and-pillow structures are rare.

Typical sandstones contain 40 to 60% quartz, 10 to 15% feldspar, 10 to 45% muscovite, up to 15% biotite and/or chlorite, and minor garnet, pyrrhotite, ilmenite, carbonate, titanite, tourmaline, epidote and zircon (J. Getsinger, Appendix III in Rebic, 1989). Siltstone intervals may include fine-grained wacke to mudstone, and are generally parallel laminated, sometimes with pale and dark grey laminae. Siltstone rip-ups are rare; crosslaminae may also be present. The interbedded sandstone and siltstone include variably developed A, AE and ACE Bouma turbidite sequences. Some sequences lack fine siltstone intervals and form thick sandstone units separated only by bedding planes, suggesting that fine material was either eroded or not deposited.

Rare facies variations within the middle Aldridge locally constitute mappable subunits within the thick turbidite succession. A relatively mudstone-rich facies contains numerous thin (<1-10 cm) mudstone beds interbedded with wacke and siltstone. This facies typically contains abundant soft-sediment deformation features, such as argillite rip-ups, mud-chip breccias (Plate 2) and load structures, and may contain wavy or lenticular bedding. Mudstone and siltstone beds are commonly platy, and may preserve excellent flutes and longitudinal scour marks. A second distinct facies

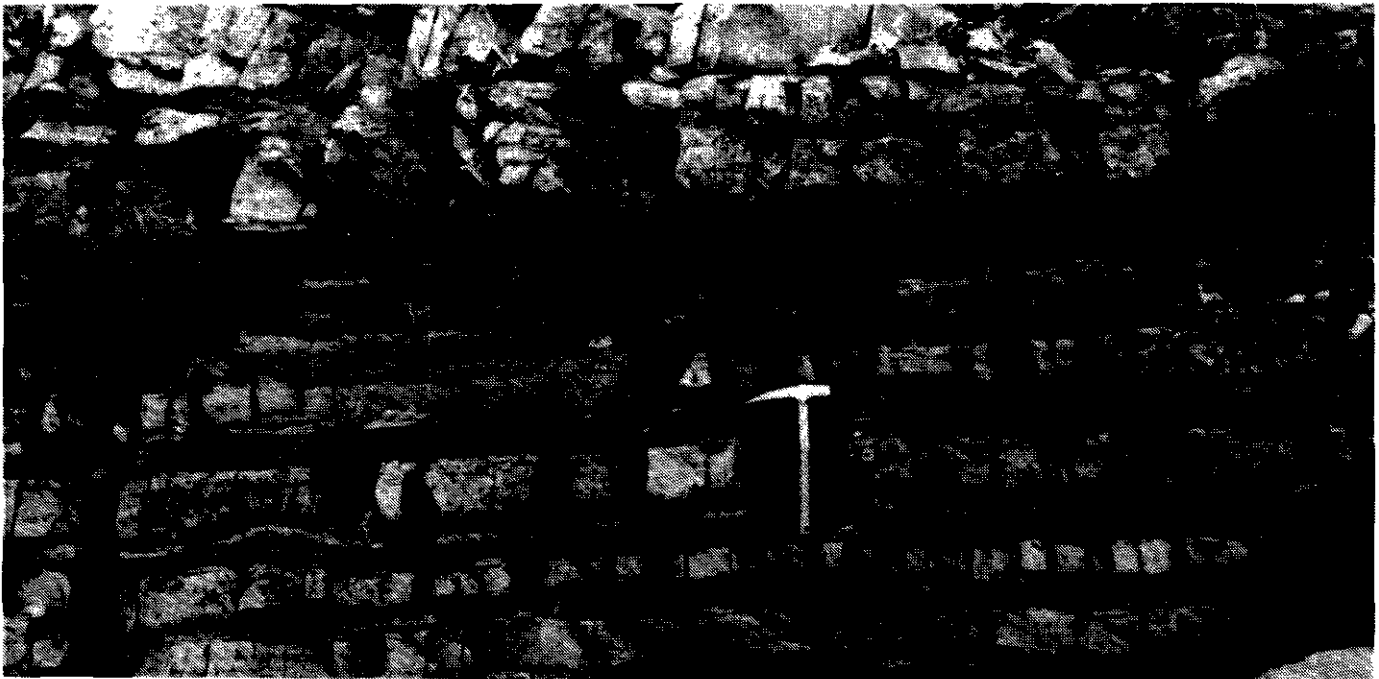


Plate 1. Typical outcrop of the middle Aldridge Formation displaying even, planar bedding (JBR93-78).



Plate 2. Sedimentary mudchip breccia within the middle Aldridge Formation on the Star Property (JBR93-26).

consists almost entirely of clean quartz arenite beds averaging 1.0 to 1.5 metres thick. Intervening siltstone intervals are absent or thin.

The upper part of the middle Aldridge is characterized by thinner wacke beds (0.05 - 0.5 m thick) which are more widely separated within grey to dark grey, thin-bedded to laminated siltstone and mudstone. Thin-bedded, argillaceous siltstone-dominated sequences in this part of the section can be easily interpreted as upper Aldridge in areas lacking good exposure. Sills are generally not found in the upper middle Aldridge. This distinct interbedded wacke and dark grey siltstone grades upward over about 100 metres into the upper Aldridge.

Limited paleocurrent data suggest northeasterly to northwesterly current directions (Figure 6). These trends are consistent in a general sense with those in the Fernie West-half area (82G W1/2; Höy, 1993), and in the central Belt basin in Montana (Finch and Baldwin, 1984), supporting a northwest-trending basin. A northwesterly trend probably parallels the topographic axis of the basin in middle Aldridge time (Winston *et al.*, 1984).

#### MARKER UNITS

Laminated siltstone marker units are present in numerous locations in the middle Aldridge. A stratigraphy comprising at least twenty markers developed by Cominco geologists and others has been found to be useful for stratigraphic control across the Purcell (Belt) basin (Edmunds, 1977b; Huebschman, 1972, 1973; D. Pighin, personal communication, 1993). South of the project area Cressman (1989, p. 30) refers to

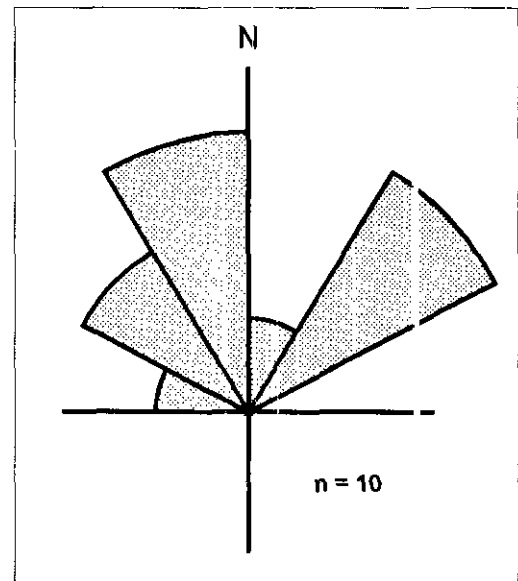


Figure 6. Paleocurrent rose diagram for the middle Aldridge Formation in the project area.

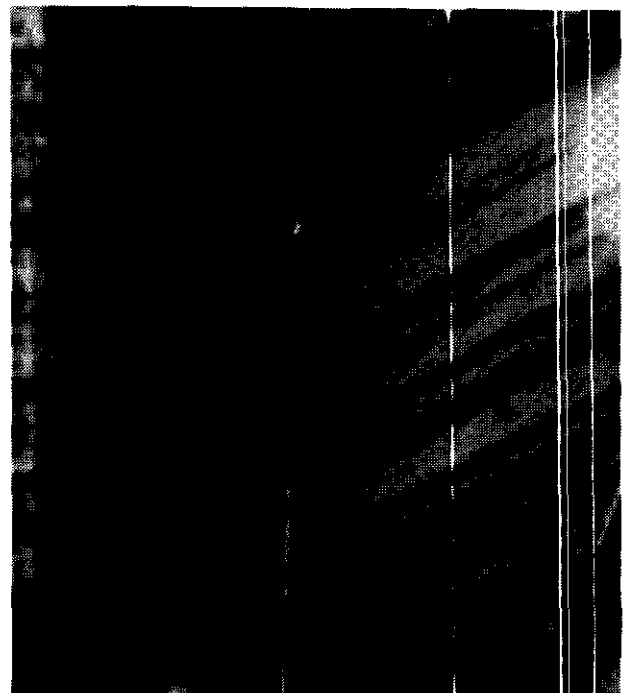


Plate 3. Marker unit from two localities 70 kilometres apart. Sample provided by D. Pighin, Consolidated Ramrod Gold Corporation.

a series of "key beds" (a through f on his Section 11) that may correlate in part with this marker stratigraphy.

Each marker unit comprises a distinct sequence of alternating light and dark grey, parallel siltite laminae that can be correlated over distances up to several hundred kilometres (Huebschman, 1973; Edmunds, 1977b; Plate 3). The layers consist of quartz and feldspar grains with disseminated biotite, muscovite and pyrrhotite (Huebschman, 1973). One to three % carbon provides the coloration difference between layers. The

marker units range in total thickness from a few centimetres to over 12 metres. Turbidite-derived wacke between markers varies from about 15 to 200 metres thick (Cominco Ltd., unpublished data). Intervals over which individual marker sequences occur can be greatly expanded or locally even partially eroded by wackes related to turbidite deposition.

The origin of these enigmatic units is a matter of debate. They may record episodic surface algal blooms producing the dark, organic-rich laminae with dust storms distributing silt over large areas of the basin (Huebschman, 1973). Alternatively, the pale laminae may record episodic sedimentation of terrigenous material from dust storms (Turner *et al.*, 1992) as has been recorded in the Gulf of California (Baumgartner *et al.*, 1991). The Black Sea may present a modern analogue of light and dark layered beds correlated across the entire basin. Although they are not directly comparable, because grain sizes vary between layers from silt to mud, unlike the Aldridge marker units. A third possible explanation for marker laminae could be that a large river supplied silt to the body of water and the silt was widely dispersed because density contrasts in the water column prevented rapid settling of the particles.

Individual laminae and sets of laminae within the marker intervals thicken slightly and proportionately over large areas. It is difficult to imagine a point sediment-source distributing sediment so uniformly and thinly, not only at one time but over a period of time represented by laminae sets. It seems necessary to invoke a feature fundamental to the body of water itself to explain the uniformity and continuity of the marker laminae. Individual pale laminae of the marker interval tend to have sharp bases and gradational tops. This suggests that the onset of deposition of the pale laminae is triggered by specific, basin-wide events. The pale laminae tend to be massive but the dark laminae are comprised of even finer microlaminae. Such fine laminations suggest a chemical control. Deposition of the marker laminites appears to have occurred in a bottom environment devoid of current activity. Perhaps physiochemical or biochemical changes in stagnant bottom waters controlled deposition from suspension. Further work is needed on the marker laminites.

### UPPER ALDRIDGE (Pa<sub>3</sub>)

The upper Aldridge Formation is distinguished by its rusty dark brown weathering, grey to dark grey, platy to fissile, thin and parallel-bedded to laminated siltstone and silty mudstone couplets. Ripple marks are rare. Characteristic white siltstone laminae are noted by Reesor (1981) and in the United States informally called "lined rock" (Cressman, 1989). Quartzofeldspathic wacke beds are very rare and thin (<10 cm). Commonly, the forest covered hillsides typical of the region turn to open grassy patches in areas underlain by upper Aldridge

argillite. Presumably this is due to disseminated sulphide in the argillaceous member that inhibits tree growth. Talus derived from the fissile upper Aldridge forms chip size fragments. Moyie sills are absent.

The contact between the middle Aldridge and upper Aldridge is transitional over at least 100 metres, as wacke beds become thinner and more widely separated up-section. The gradational contact leads to imprecise determination of thickness, but it is estimated to be about 400 to 500 metres in the Yahk map area. This is thicker than that suggested by Reesor (300 m, 1981) but comparable to that in the Fernie area (about 500 m; Höy, 1993). The gradational upper contact with the Creston Formation is placed where pale green colours, shrinkage (syneresis) cracks and other shallow-water sedimentary features first appear. Cressman (1985) uses similar features to divide the Prichard and Burke formations. A massive, thick bedded siltstone or wacke occurs at the base of the Creston Formation. It is also exposed in the Moyie Lake area.

The upper Aldridge reflects waning input of sandstone turbidites and final pelagic sedimentation prior to the shallowing of the Purcell (Belt) basin as represented by the Creston Formation.

### MOYIE INTRUSIONS (Pm)

The term Moyie sills was first used by Daly (1912a, b) to describe sills on "Moyie Mountain" along the International border 2 kilometres west of Kingsgate (Figure 5). Moyie intrusions, dominantly sills but also dikes, are more common west of the Rocky Mountain Trench, where they can comprise 30% of the section. There are two main episodes of sill emplacement important within the Aldridge Formation (Gorton *et al.*, in preparation; R. Turner, personal communication, 1993). No distinct features were recognized to differentiate the sills in the field. In the Lamb Creek area, west of Moyie Lake, the cumulative thickness of the sills is about 1300 metres (Höy, 1993).

The Moyie sills are widespread in the lower and middle Aldridge in the Yahk map area. They extend laterally over tens of kilometres, crosscutting bedding at small angles and, therefore, some can be used for gross stratigraphic correlation. Locally they are dikes cutting stratigraphy. The sills are fine to medium grained, and range in composition from hornblende ( $\pm$  pyroxene) gabbro to hornblende quartz diorite and hornblendite. Mafic phenocryst contents vary up to 70%. Some of the thicker sills (> 20 m) contain irregular patches of coarse pegmatitic hornblende and feldspar. Zones of granophyre, as described in the uppermost sill at the Sullivan mine, were not observed in the map area.

The sills vary greatly in thickness; typically they are 15 to 30 metres thick, although they reach up to 300 metres or more in thickness (Cressman, 1989, reports

sills up to 600 m thick). As in the Cranbrook area to the east, a conspicuous section in the middle part of the middle Aldridge contains from two to six prominent sills. Sills are absent in the underlying 1000 metres, and few if any occur above it. This upper sill succession is well exposed south of Kid Creek, where a sequence of four or five sills is repeated by faulting. To the west, on Mount Kitchener, the same stratigraphic section contains only two sills (Figures 5 and 8).

Sill margins are typically sharp and locally chilled. The variability in contact metamorphic effects, from a wide biotite hornfels to absent, has been attributed to differences in the level of emplacement that would have controlled the ambient temperature and pore water contents of the hostrocks (Cressman, 1989). Höy (1989, 1993) proposed that some of the sills intruded wet sediments coeval with deposition of the lower and middle Aldridge formations. Supportive evidence for this can be seen along Highway 3 near Kitchener, where a narrow zone of conglomerate with no bedding contains oblong, rounded quartz-sandstone cobbles and boulders in a matrix of the same composition (Turner *et al.*, 1992, Stop 1-7). This is interpreted as evidence of fluid streaming through wet sediments trapped between two sills, one exposed above the conglomerate in the outcrop and a lower sill exposed just to the east in a roadcut. An example of soft-sediment deformation along a Moyie sill margin occurs near trenches in the Iron Range. Bleached, albite-altered metasedimentary rocks occur locally, such as on the Goat River road near Highway 93 (Turner *et al.*, 1992; Stop 1-8), and may be due to sill emplacement.

The dark green to black sills look remarkably fresh and locally have planar, polygonal joints (Plate 4). Joint surfaces typically weather rusty brown. Sporadic white bull quartz veins, quartz-epidote veins and pods

containing minor chalcopyrite occur within some sills.

The chemistry of the Moyie sills has been reviewed by Höy (1993) and Gorton *et al.* (in preparation). They comprise two distinct populations: alkaline and transitional sills, only recognized in the Mount Mahon area just south of Yahk; and subalkaline tholeiitic sills elsewhere. Detailed petrography and geochemistry of correlative sills to the south, near Crossport, Idaho are presented by Bishop (1973). Continuing work on sill petrography, geochemistry and dating is in progress by H.E. Anderson as part of the Sullivan-Aldridge project.

### ***OTHER SILLS AND DIKES (Pb)***

Rare mafic sills and dikes, outwardly similar to the Moyie sills, intrude rocks as young as Kitchener Formation (Höy, 1993). In the Yahk map area, one such dike cuts lower Creston Formation on the ridge east of Leadville Creek. The dike is about 10 metres wide and intrudes Creston siltstone.

### ***CRESTON FORMATION***

The Creston Formation underlies about 10% of the Yahk map area. It crops out in four areas. The best exposures are on the northwest limb of the Moyie anticline and along a north-trending graben that extends southward into Idaho and Montana. Creston strata also underlie the eastern and western limbs of the Goat River anticline; the latter was not mapped in 1993 (Rice, 1941).

The Creston Formation in the Nelson East Hall map area is divided into a lower argillaceous member (~1000 m thick), a middle quartzitic member (~1000 m thick)

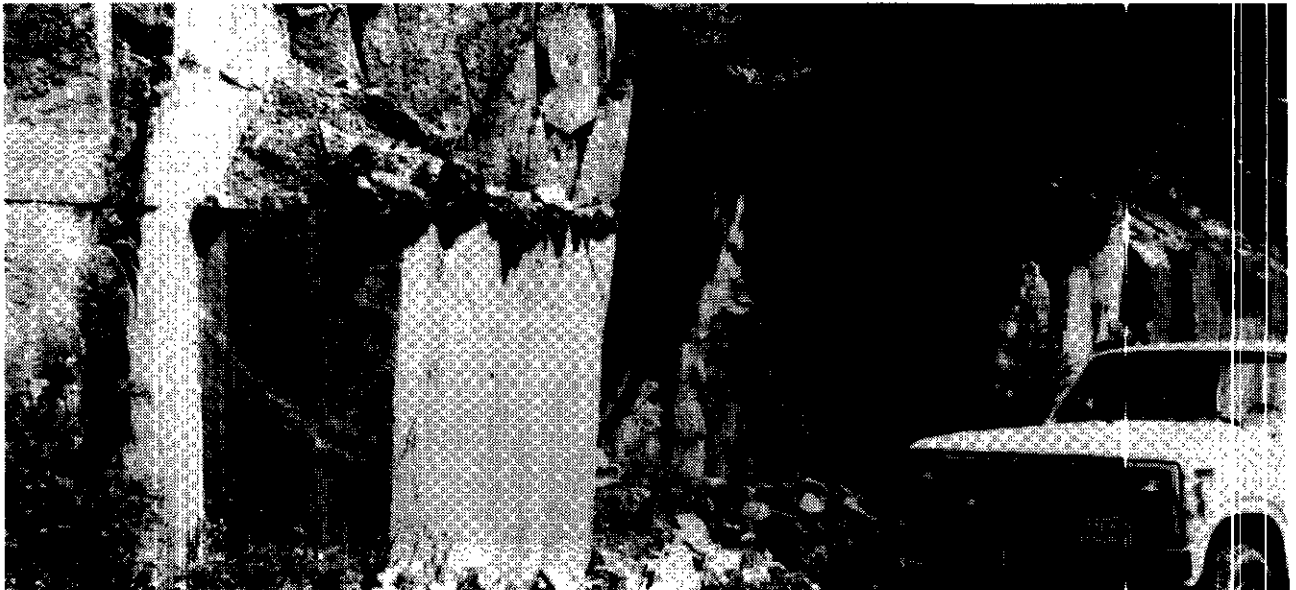


Plate 4. Moyie sill with prominent planar joints, on the Mount Thompson lookout road.

and an upper siltite and argillite (< 300 m thick). They correlate with the Burke, Revett, St. Regis and Empire formations of the Ravalli Group in the United States (Figure 4). The transitional member, in the upper part of the Prichard Formation of Cressman (1989) is correlative with lower Creston Formation in the Yahk area. The Creston Formation represents shallow-water, reworked deposits accumulated on prograding (from the south) deltas or fans (Hrabar, 1973), possibly in a tide-dominated delta as proposed by Kopp (1973). The Revett Formation hosts numerous important copper-silver deposits and occurrences in western Montana (see below).

Only the lower and middle Creston have been recognized in the Yahk map area. Disseminated magnetite and local veins within the Creston Formation produce prominent aeromagnetic anomalies which conform to the mapped distribution of the unit. Speckled argillite with small euhedral magnetite crystals is common in the Burke Formation.

### LOWER CRESTON (Pc<sub>1</sub>)

The lower Creston consists of thin-bedded, laminated siltstone, argillite and lesser fine-grained quartz wacke. Total thickness of the lower Creston in the Yahk map area is about 650 metres, best exposed northeast of Mount Kitchener. The contact with underlying upper Aldridge rocks is gradational, reflecting a gradual shallowing of the Purcell basin. Lower Creston Formation is distinguished from the Aldridge Formation by colour, bedforms and sedimentary structures. Lower Creston rocks are generally waxy pale green to olive, with tan weathered surfaces, although pale grey and mauve to purple siltstone and argillite are common. Wavy to lenticular bedding (Plate 5) and typically sub-phyllitic to phyllitic (sericitic, therefore soft) rocks are common, in contrast to planar, unfoliated Aldridge beds. Graded, fining-upward couplets of siltstone and mudstone are widespread. The most



Plate 5. Typical wavy bedding with flame structures developed in the Creston Formation (DBR93-102).

characteristic and diagnostic sedimentary structures are subaqueous shrinkage cracks (syneresis cracks) and asymmetric and symmetric ripples. The discontinuous cracks, developed in argillaceous beds, are a few centimetres long and consist of one to four irregular cracks. Unlike subaerial mudcracks, they do not form closed polygons. Other subaerial indicators, like raindrop imprints, are also lacking. Ripples have wavelengths of 3 to 10 centimetres and amplitudes of 3 to 10 millimetres, with about a 10:1 ratio (Plate 6); the ripple crests are commonly sinuous.

An intertidal to shallow subtidal mudflat setting is interpreted from these sedimentary structures and based on regional correlations. Winston (1986) has argued for a lacustrine setting for the upper Belt strata.

### MIDDLE CRESTON (Pc<sub>2</sub>)

The middle Creston overlies the lower Creston gradationally. It comprises at least 900 metres of thin to medium and less commonly thick-bedded, laminated quartz arenite to quartz wacke, siltstone and mudstone. Excellent exposures occur in the northeast corner of the map area, north of Leadville Creek and in the Kingsgate graben (Figure 5). In contrast to the lower Creston, it is characterized by mauve to purplish sequences which are interbedded with greenish sediments. Light grey to white medium-grained quartz arenite with commonly concordant but locally discordant mauve colour laminations or rings is a distinctive lithotype (Plate 7). Sandstone beds generally appear to be cleaner and more quartz rich than Aldridge sandstones. Bedding is planar to wavy; planar and trough crosslaminations, scour and fill, and graded fining-upward sequences are common. Bidirectional cross bedding, common in tidal flats (Davis, 1983), can be seen in places. Sedimentary structures are abundant, including load casts, ball-and-pillow structures and ripples (Plate 6). Desiccation cracks (mudcracks), which are not found in the lower Creston, indicate subaerial exposure, suggesting



Plate 6. View southwest to curve-crested, asymmetric ripples within maroon siltstone of the middle Creston Formation (DBR93-406).

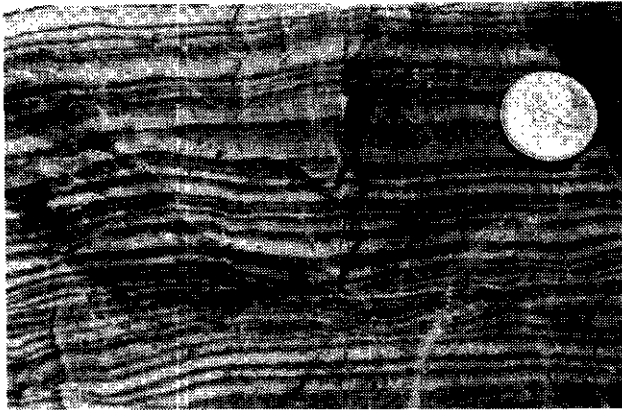


Plate 7. Distinctive mauve, laminated white quartz arenite of the middle Creston Formation (DBR93-102).



Plate 8. Middle Creston Formation mud-chip breccia consisting of maroon argillite chips within white quartz arenite (DBR93-184). The arenite beds are interpreted to represent repeated storm deposits across a mudflat.

continued shallowing during deposition of the Creston. Mud-chip breccia horizons with dark grey to brick-red mudstone fragments within white medium-grained quartz arenite are common; the bases of these beds are planar and the tops are rippled, perhaps indicating storm events in a shallow subtidal or intertidal environment (Plate 8).

The middle Creston is correlative, in part, with the deltaic facies of the Revett Formation in Montana, supporting a model of prograding fans from a southerly source.

### UPPER CRESTON ( $Pc_3$ )

The upper Creston Formation comprises green siltstone, light and dark, thinly laminated argillite and siltstone and purple argillite (Reesor, 1983). No definitive upper Creston was mapped in the project area.

### KITCHENER FORMATION ( $Pk$ )

The Kitchener Formation, defined by Daly (1905) and Schofield (1915), overlies the Creston Formation and

comprises green dolomitic siltite, argillite and carbonaceous dolomite and limestone. It forms a succession 1800 metres thick (in the Nelson East Half area where mapped by Reesor, 1983) of shallow-water deposits that correlate with the middle Belt carbonate, the Wallace Formation to the south and the Helena Formation to the southeast (Figure 4). Uncommon stromatolites are locally important.

The Kitchener Formation is poorly exposed in the northeast corner of the map area, in the foot wall of the Moyie fault. Farther northeast the formation outlines the northwest limb of the Moyie anticline. Prominent but thin, brown-weathering dolomitic siltstone beds distinguish Kitchener Formation from Creston Formation. They pit-out and produce rough and irregular weathered surfaces. Otherwise, the wavy bedded, pale green siltstone and argillaceous siltstone are similar to the Creston Formation. Isolated outcrops, faulting and tight folding preclude estimates of total thickness. Strata are phyllitic with local transposed bedding in this area.

### LAMPROPHYRE DIKES AND SILLS

Biotite lamprophyre intrusions outcrop in several areas, north of Kid Creek (Star property), near Goatfell and in the Iron Range. These are brown weathering, medium to coarse grained, and contain biotite, hornblende and possibly olivine. They occur as sills as well as steeply dipping dikes. Similar intrusions are found in the Cranbrook-Kimberley area, where they are inferred to be Early Cretaceous (Høy, 1993).

## STRUCTURE

### REGIONAL STRUCTURAL FEATURES

The map area lies on the western flank of the Purcell anticlinorium, the westernmost component of the Cordilleran fold and thrust belt. The anticlinorium itself allochthonous and transported eastward with respect to North American basement, is bounded on the east by the Rocky Mountain Trench. To the west, the Purcell Supergroup strata become progressively more deformed and metamorphosed within the Kootenay Arc (Figure 3). Southwest of Creston is the northern extension of the Purcell Trench, defined as a north-trending topographic depression and, in part, a graben in northern Idaho (Harrison *et al.*, 1972). Here, the Priest River Complex includes metamorphic rocks and Late Cretaceous granitic rocks (Kaniksu batholith) in the hanging wall of an inferred east-dipping normal fault (Purcell Trench fault, Yoos *et al.*, 1991). Farther east, the eastern margin of the Sylvanite anticline is the Libby thrust belt, a series of

west-dipping thrust faults that projects to a basal décollement 10 to 15 kilometres below the map area (Harrison *et al.*, 1992; Harrison and Cressman, 1993).

Much of the project area lies between the southwestern projections of the St. Mary and Moyie faults. These faults strike across the northern part of the Purcell (Belt) basin and have Proterozoic (St. Mary) and Paleozoic (Moyie) histories (Höy, 1979, 1993; McMechan, 1979, 1981). This transverse trend projects southwesterly toward the Yahk map area from a marked flexure in the eastern margin of the Purcell (Belt) basin. This flexure is reflected in isopachs of the middle Aldridge (Höy, 1993), and therefore is an original feature of the basin margin, and not a later tectonic feature. The transverse structures probably reflect structures and/or topography of the underlying continental basement.

### SEISMIC DATA

Moyie sills form prominent seismic reflectors on profiles acquired in southern British Columbia and the northern United States by LITHOPROBE, COCORP and industry (F.A. Cook, personal communication, 1993; Yoos *et al.*, 1991). The data also suggest that Aldridge Formation basement is involved in the folding and thrusting.

### FOLDING EVENTS

There are three ages of folding evident within the Purcell (Belt) strata: doubly plunging Late(?) Proterozoic folds, complex Cretaceous to Paleocene folds and thrusts (Laramide orogeny) and Eocene extension related folds (Benvenuto and Price, 1979; Harrison and Cressman, 1993). The broad to open Proterozoic folding was accompanied by greenschist grade metamorphism as indicated by metamorphic biotite cooling dates of  $1330 \pm 45$  Ma in Montana (Obradovich and Peterman, 1968). A

pegmatitic phase of the Hellroaring Creek stock, recently dated at  $1365 \pm 2$  Ma (U-Pb monazite; J. Mortenson, personal communication, 1992), provides a younger age constraint for this deformational event because the stock intrudes folded Aldridge Formation (Leech, 1962). A rapikivi granite of the same age (*ca.* 1365 Ma) intrudes greenschist-grade rocks of the Yellowjacket Formation (Aldridge Formation equivalent) in the Salmon River arch in east-central Idaho (Chamberlain and Doughty, 1993).

### PROJECT AREA STRUCTURAL FEATURES

The Yahk map area can be divided into three structural domains separated by high-angle faults. Bedding attitudes in the three domains are shown in Figure 7. The eastern and western domains are dominated by broad, north-trending and north-plunging folds, the Moyie and the Goat River anticlines (Figure 9). The southern extension of the Moyie anticline is called the Sylvanite anticline in western Montana (Harrison *et al.*, 1992). The Moyie fault and related structures truncate the western limb of the Moyie anticline in the east-central part of the map area, while the Carroll Creek/Kid fault cuts the eastern limb of the Goat River anticline (Figures 5 and 8).

Between the Moyie and Carroll Creek/Kid faults is a structurally complex, internally faulted horst-like panel, here called the central domain, which is entirely underlain by lower and middle Aldridge Formation. Tighter and more intense folding, with steeply plunging fold axes, is common adjacent to major faults like the Moyie and Carroll Creek. The lack of strata younger than Kitchener Formation precludes any definitive evidence for the timing of deformation in the map area; constraints from other regional studies are used.

Structural style of the Yahk map area is characterized by broad open folds and steep faults.

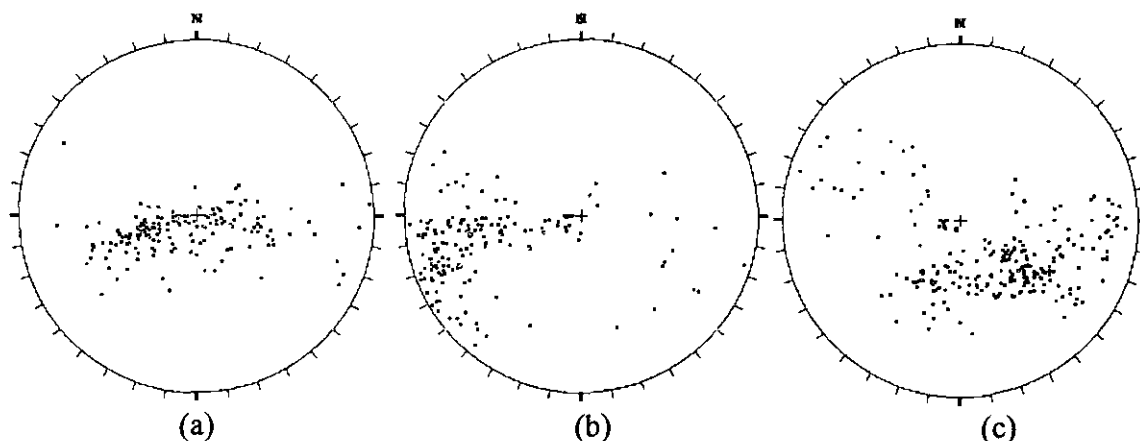


Figure 7: Stereonet plots of poles to bedding for (a) the Goat River antiform, west of the Carroll Creek/Kid fault (170 data points); (b) the central domain, between the Moyie and Carroll Creek/Kid faults (182 data points); (c) the Moyie antiform, east and south of the Moyie fault (236 data points). Equal area projection.

While a weak, spaced cleavage is present throughout the map area, penetrative fabrics are seen only within a broad zone adjacent to the Moyie fault and related structures, and within narrower zones along other faults.

An intense penetrative cleavage is present in the northwestern corner of the map area, in the west limb of the Goat River anticline. Gabbro sills are foliated with discrete shear zones (chlorite schist), west of Arrow Creek, that are possibly part of the St. Mary fault or related splays. Phyllitic (sericite-rich) siltite and foliated diorite are also present near the Delaware adits (Figure 5). The overall gradational increase in strain and metamorphism westward corresponds to the transition from the Purcell anticlinorium into the eastern fringe of the Kootenay Arc.

Metamorphic mineral assemblages in the metasedimentary rocks include muscovite-biotite-garnet-quartz-(k-spar-albite) and possibly muscovite-chloritoid-biotite-quartz-(k-spar-albite). Greenschist to lower amphibolite grade metamorphism accompanied Late Jurassic to Paleocene (Laramide) deformation, although this probably overprinted Proterozoic deformation and metamorphism during the East Kootenay orogeny (Höy, 1993).

## MOYIE FAULT

The Moyie and related faults extend from the east side of the Rocky Mountain Trench (Dibble Creek fault) through to the eastern part of the Yahk map area and into northern Idaho (Höy, 1993; Reesor, 1981; Harrison *et al.*, 1992). A complex history for the northwest-dipping Dibble Creek fault includes pre-Devonian north-side-down and younger oblique reverse movement (Lecch, 1958). Devonian gypsum served as the locus of movement in the footwalls of both the Dibble Creek and Moyie faults. In the Moyie Lake area, the fault cuts the western limb of the Moyie anticline (Höy and Diakow, 1982). The Moyie fault is also a right-lateral reverse fault with about 12 kilometres of displacement (Benvenuto and Price, 1979; Höy, 1993).

In the Yahk map area, the Moyie fault places middle Creston and possible Kitchener formations against middle Aldridge Formation (Figure 5). This requires an apparent vertical throw, with the west-side-up, on the order of 1.0 to 1.5 kilometres (similar to that estimated by Reesor, 1991). In the northeastern corner of the Yahk sheet, major displacement is transferred from a northeasterly trending segment to a north-trending segment, with an isolated block of Kitchener Formation occurring near the fault flexure. A possible extension of

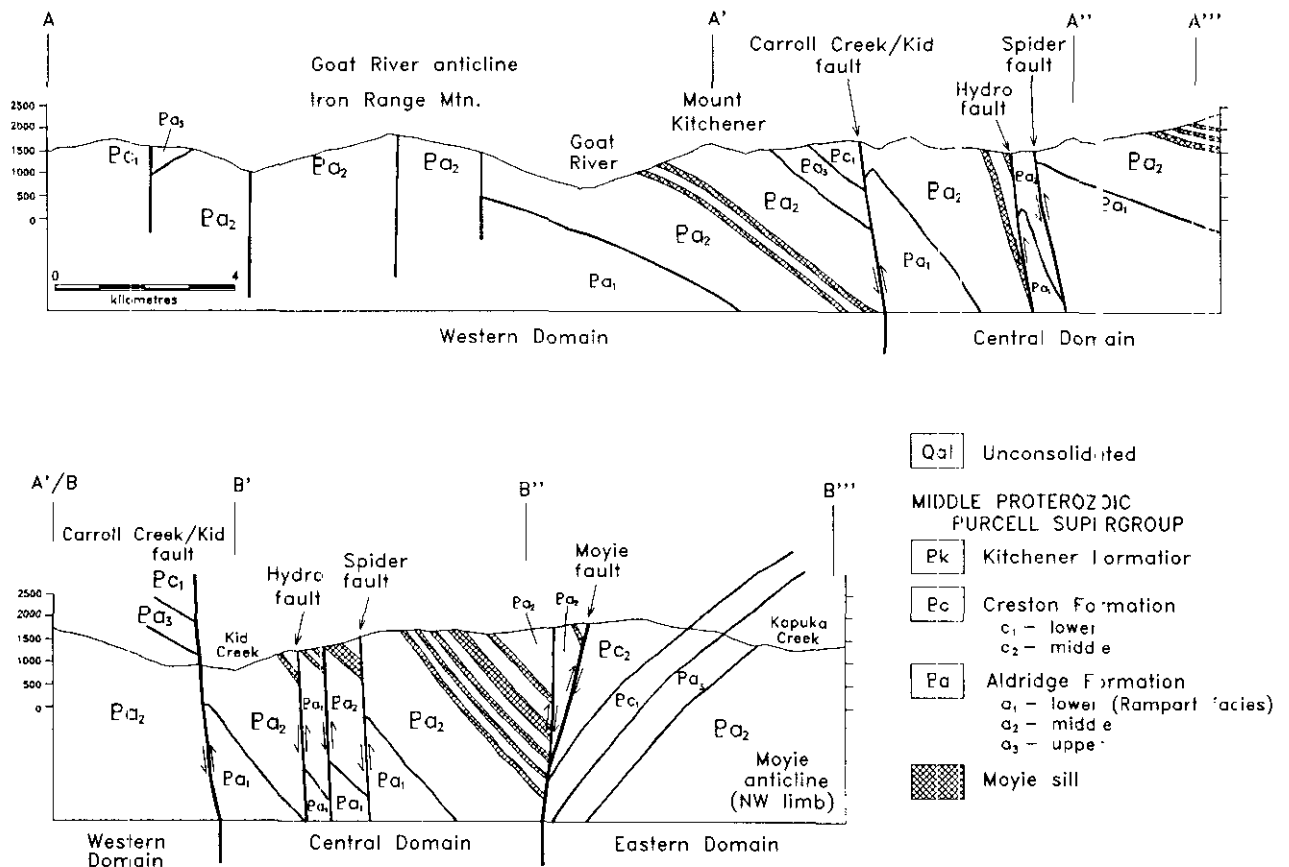


Figure 8(a). Cross-section A-A'-A''-A''', (b) Cross-section B-B'-B''-B'''. Vertical exaggeration 2x.

the northeasterly trending segment strikes southwest from this point along Kid Creek, separating a block of moderately to steeply dipping middle Aldridge Formation from a block of flat-lying rocks to the north. Both northeast-trending and north-trending fault segments are included as part of the Moyie fault system by Reesor (1993), although the relationship between them is unclear.

The Moyie fault dips steeply throughout the Yahk area. Tight folds and a penetrative cleavage are developed in thin-bedded footwall Creston and Kitchener Formation (Plate 9), while a weaker cleavage and broader folds occur in hangingwall middle Aldridge. The fault is a broad zone (up to 500 m wide) of intense brittle-ductile shearing.

## CENTRAL DOMAIN

The central domain is bounded by the Carroll Creek/Kid fault on the west and by the Moyie fault system on the east. Due to the southerly convergence of its bounding faults it is roughly funnel-shaped in map view, broadening from a width of about 3 kilometres at the Canada - U.S.A. border to over 12 kilometres north of Kid Creek. The central domain comprises a series of narrow, north-trending panels separated by steep faults, the most important of which are the Carroll Creek, Spider and Hydro faults. The latter two are east-dipping reverse faults which repeat a sequence of sills and marker laminates, the latter identified by detailed Cominco mapping. Dips within the block are moderate to steep, except for a flat-lying panel east of the Spider fault on the north side of Kid Creek. The Carroll Creek fault, juxtaposes lower Creston with middle Aldridge formation. It consists of a bleached, clay-altered mylonitic rock that was exposed across a zone 2 metres wide by road building on the Star Property (P. Ransom, personal communication, 1993). Minor folds are essentially absent and cleavage is poorly developed, except adjacent to the bounding faults.

## KINGSGATE GRABEN

The Kingsgate graben preserves middle Creston Formation in a north-trending belt that extends southward along the western flank of the Moyie-Sylvanite anticline. Bedding-cleavage intersections across the graben indicate most of it is on the east limb of a broad faulted syncline.

## IRON RANGE FAULT

The Iron Range fault zone, a series of faults across about a 1-kilometre width, trends subparallel to the axis of the Goat River anticline, and cuts gently dipping Aldridge Formation sedimentary rocks. A well-developed north-northeast-striking, steeply northwesterly



Plate 9. Open to close minor folds developed within thin-bedded to laminated, pale green phyllitic argillite, Kitchener Formation in the Moyie fault zone (DBR93-322).

dipping spaced to penetrative cleavage occurs within 100 metres of the fault zone. Individual faults consist of sheared rock 5 to 10 metres wide, with steeply dipping fault lineations representing latest motion. Bedding attitudes steepen within the fault zone and tight folds are common. Intense hematite-magnetite-quartz alteration zones occur along the fault zone, as discussed below.

Based on the correlation of marker laminates across the fault zone there is little vertical displacement at Iron Range Mountain. However, the fault zone is complex and it is interpreted to be deep-seated because of the abundant evidence of hydrothermal alteration along it. To the north, the fault projects into the St. Mary - Hall Lake system as mapped by Reesor (1981).

## MINERAL OCCURRENCES

The Sullivan-type scdex deposit has remained the prime exploration target throughout the Purcell (Belt) basin. The Sullivan deposit has been described by Hamilton *et al.* (1983) and Höy (1984). Recent studies by Leitch *et al.* (1991), Turner and Leitch (1992) and Leitch and Turner (1992) have refined the Sullivan model. Massive sulphide mineralization, tourmalinite, albite and muscovite alteration, manganese-rich garnet, sedimentary fragmental units and syndepositional sedimentary structures (slumps) and faults are characteristic features. Co-existing brown and black tourmalinite are considered to be an indication of high fluid to rock ratios and therefore may discriminate potentially mineralized from barren tourmalinite showings (Slack, 1993).

Characteristics of mineral occurrences in the Yahk map area are summarized in Table 1 and locations are

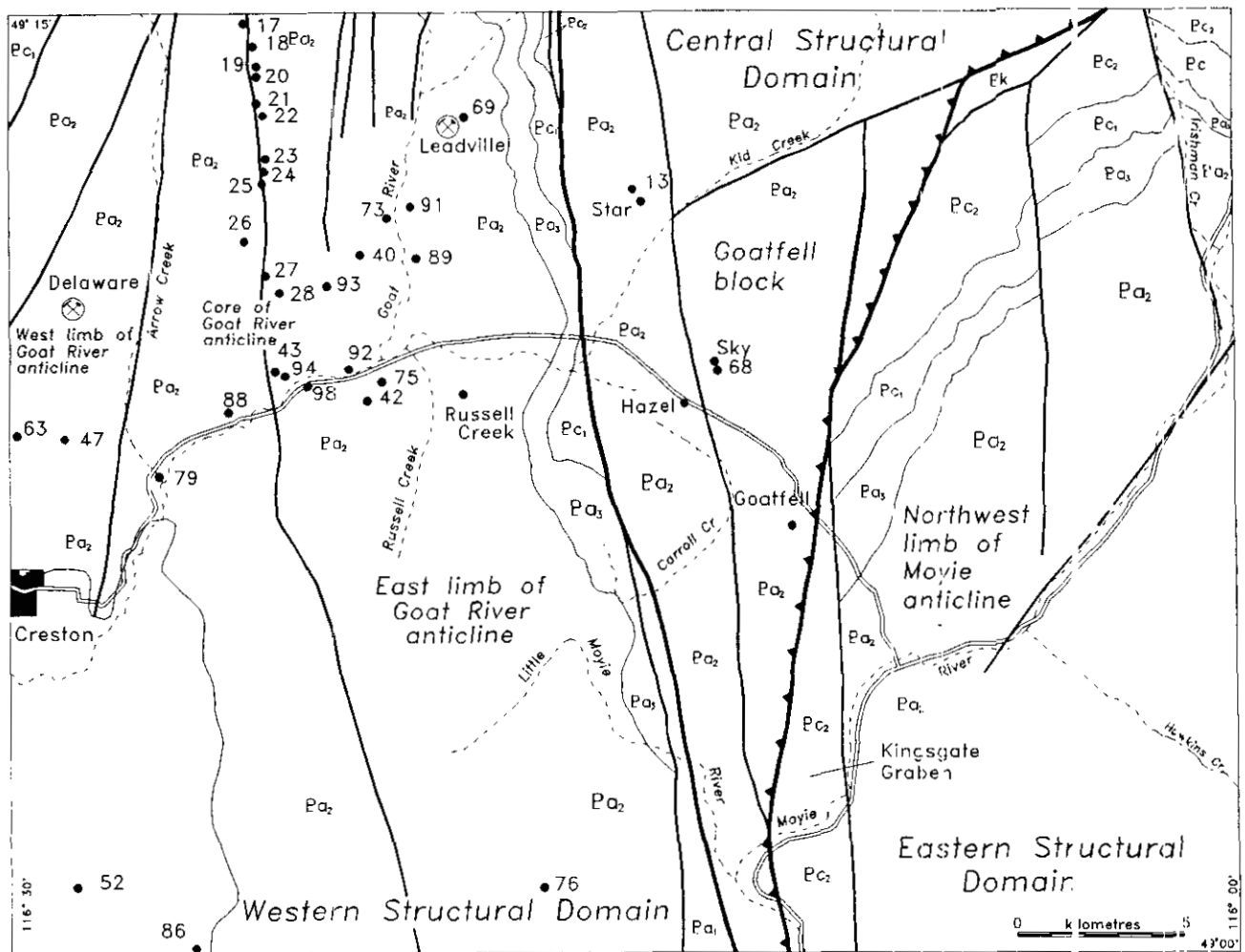


Figure 9. Mineral occurrence localities from MINFILE database and structural domains. Occurrences are described in Table 1. Central domain is shown by stippled pattern.

plotted on Figure 9. Lead-zinc mineralization is widespread in quartz veins in the middle Aldridge. Lead and silver production came from the Leadville and Delaware mines. Stratiform sedex mineralization has been discovered nearby at the Fors property west of Moyie lake. The lower-middle Aldridge contact, the stratigraphic position of the Sullivan deposit, is exposed at relatively shallow depth in the cores of the Moyie and Goat River anticlines, and in uplifted fault panels in the central domain.

The core of the Goat River anticline along the Iron Range fault zone is host to an unusual occurrence of iron oxide mineralization. The Iron Range occurrences, form a linear belt of discontinuous mineralization extending from south of the Goat River to the northern edge of the map sheet.

## SEDEX AND RELATED DEPOSITS

Occurrences of sedimentary fragments, tourmalinite, lead-zinc vein mineralization and soil anomalies within the central domain (Figure 9) were the target of exploration by Cominco and Chevron in 1987-1989, and by Kokanee Explorations Ltd. (now Consolidated Ramrod Gold Inc.) in 1990-1992. Although some exploration within this area focused on determining the location or depth to and testing of the lower-middle Aldridge contact, other work focused on anomalous lead-zinc within a metallogenic interval higher up in the middle Aldridge, near the stratigraphically lowest Moyie sill. This metallogenic event corresponds with a time of increased magmatic activity in the basin, represented by the second pulse of sill emplacement within the middle Aldridge.

**TABLE 1.**  
**DESCRIPTIONS OF MINERAL OCCURRENCES FOR THE YAHK MAP AREA (82F/01).**

Name(s)	MINFILE	UTM (Zone 11)	Description	References
Star, Kid	82FSE 002 82FSE 013	5450050 N 554650 E	ENE-striking and semi-concordant quartz veins with galena, sphalerite, pyrrhotite, chalcopyrite and arsenopyrite in muscovite-chlorite-altered middle Aldridge quartz wackes. Assays of up to 8.29% Pb, 0.71% Zn, 75.09 g/t Ag/ 6.2 m were obtained in drilling.	MacDonald (1978), Simpson (1984), Hagen (1990)
Leadville, Star	82FSE 006	5451550 N 549520 E	Galena with minor sphalerite and chalcopyrite in an ENE-striking quartz vein in middle Aldridge quartz wackes near a gabbro contact. About 9 tonnes of ore was hand cobbled and shipped in the 1920s.	Merrett (1958), Olson (1970)
Iron Range	82FSE 014 to 82FSE 028	5453750 N 543350 E	Hematite with lesser magnetite in steeply dipping veins, narrow stockworks, disseminations and breccia matrix in albitized and locally silicified gabbro and sericitized wackes and siltstones along a north-trending fault.	Young & Uglov (1928)
Empire State	82FSE 040	5447630 N 546885 E	Quartz-calcite veinlets in gabbro with disseminated pyrrhotite and chalcopyrite.	Rice (1941)
Delaware	82FSE 041	5446050 N 538300 E	Galena and minor sphalerite in a quartz vein striking 150/60-70 SW in middle Aldridge quartz wacke. Production from two main adits (1949-1950): 229 t containing 30.08 kg Ag, 21.23 t lead, 498 kg zinc.	Peck (1950), Peck (1951)
Creston Hill	82FSE 042	5443370 N 547160 E	Quartz-calcite veinlets in gabbro with disseminated pyrrhotite and chalcopyrite.	Curry (1953), Rice (1941)
May-Bee	82FSE 043	5444600 N 544360 E	Chalcopyrite in a quartz vein 0.3-1.5 m wide, striking 330/90, in a gabbro sill. Two adits were driven on the vein. Up to 1.81% Cu / 0.7 m.	Merrett (1958) Merrett (1959)
Otto Silver	82FSE 047	5442190 N 538055 E	Galena in a northeasterly striking, steeply dipping quartz vein.	Olson (1970)
Option	82FSE 068	5445450 N 556070 E	Several pits expose at least four quartz veins with pyrite and minor chalcopyrite and scheelite in silicified gabbro and quartz wacke.	McDonald (1960)
Goatfell	-	5441150 N 559250 E	An extensive zone of variably tourmalinized middle Aldridge quartz wacke and siltstone with quartz-muscovite veins with minor pyrite.	
Hazel	-	5443750 N 556700 E	Disseminated sphalerite in a narrow shear zone striking 180/90 in albitized middle Aldridge quartz wacke and siltstone.	
Sky	-	5445000 N 557600 E	Tourmalinized and silicified quartz wacke with pyrite, pyrrhotite, arsenopyrite and chalcopyrite.	Rebic (1989)
Sun	-	5444050 N 550100 E	Galena in east-striking, steeply south-dipping quartz veins up to 0.3 m wide.	

## STAR

The Star showing (also known as the Kid; MINFILE 82FSE-002 and 82FSE-013) is in middle Aldridge sedimentary rocks on the west side of Peterson Creek, a tributary of Kid Creek. The showing was discovered in 1967 following up a lead-zinc soil anomaly by surface trenching. The first drill hole by Cominco Ltd. targeted a UTEM anomaly in the late 1980s. Recent work by Kokanee Explorations, Ltd. (1990-1991) has included 5563 metres of diamond drilling in twelve holes.

Surface showings consist of steeply dipping, east to northeast-striking quartz veins with galena and minor sphalerite, in fine-grained quartz wacke. Mineralization intersected over wide intervals in drill core includes values of 4.08% zinc over 1.0 metre and 8.52% lead, 2.38% zinc over 2.0 metres (Stephenson, 1990b). Veins consist of quartz, galena, sphalerite and pyrrhotite, with minor pyrite, chalcopyrite and arsenopyrite. Bedding-parallel quartz-sulphide veins have also been intersected by drilling. Veins are commonly high-strain zones; locally quartz is broken into fragments surrounded by a deformed sulphide matrix of sphalerite and galena (Plate 10). Significant intervals (100 m true thickness) of strongly altered sedimentary rocks occur within the



Plate 10. Quartz-sulphide veins from the Star property illustrating typical textures from drill core of ddh S90-2: (a) quartz vein with intergranular pyrrhotite and galena, the left contact of the vein is brecciated quartz vein fragments within sheared pyrrhotite and galena (354.8 m depth) (b) angular sphalerite within sheared galena and pyrrhotite vein (351.3 m depth), and (c) brecciated chlorite-altered siltstone host and quartz vein fragments within galena, pyrrhotite and rare chalcopyrite vein (352.8 m depth). Abbreviations: C = chalcopyrite, H = hostrock, G = galena, S = sphalerite, Q = quartz.

mineralized zone. Patchy to pervasive chlorite and muscovite, locally associated with quartz-carbonate veining, overprints very fine grained biotite. Numerous lamprophyre sills, believed to be Cretaceous or Tertiary, intrude the mineralized zone.

A distinctive sedimentary facies is exposed in road outcrops and intersected in one drill-hole (ddh S90-5), 2 kilometres north and along strike from the mineralized zone. This facies comprises laminated black siltstone

and mudstone interbedded with dark grey quartz wackes. Wacke beds have rip-ups of black mudstone at their bases, while bedding in mudstone and siltsone is locally wispy to lenticular. A distinctive platy black siltstone, and thin mud-chip and wacke breccia horizons are common within this facies. Flutes and other scoured bedforms are abundant. Local tourmalinization of mudstone beds is evident. Diamond drilling down-dip from surface exposures intersected widespread tourmalinization of argillaceous intervals, as well as a chaotic breccia with quartzite clasts (Hage 1, 1990). Similar tourmalinization associated with mudstone beds and abundant sedimentary structures is exposed in roadcuts in the footwall west of the mineralized zone.

Mineralization occurs below the lowest of a group of sills which are repeated by reverse faulting south of Kid Creek. Only the two lowest sills are exposed in the fault block containing the mineralized zone. Dips between the lowermost sill and the Carroll Creek/Kid fault to the west are anomalously steep, averaging 65 to 70°. North-trending bedding is subparallel to the strike of the faults bounding the structural blocks; the faults cut bedding at a low angle both down dip and along strike. Anomalous southeasterly striking bedding crops out just south of the projected surface trace of the mineralized zone, suggesting the possibility of crossfaulting; however, exposures are insufficient to delineate these suspected faults.

## GOATFELL

The Goatfell tourmalinite occurrence (Ethier and Campbell, 1977) is in middle Aldridge sediments in the structural panel between the Spider and Moyie faults. The occurrence is exposed along the CPR railway about 1.5 kilometres east of Carroll Creek (Figure 9). The discordant zone crosscuts stratigraphy, and its shape as a resistant knob (less than 500 m in diameter) implies a pipe-like morphology. At the base of the zone thick-bedded, weakly altered quartzites are overlain by massive tourmalinized rock, with tourmalinization apparently having obscured bedding. Alteration appears to be *semiconcordant here*.

The degree of tourmalinization is variable and seems to reflect original lithologies. Quartz wacke beds tend to be darker grey and harder than unaltered equivalents, whereas argillaceous beds tend to be black, aphanitic and extremely hard, with a conchoidal fracture, reflecting more intense tourmaline replacement. Tourmalinized mud chips in quartzite are abundant. Presumably, the preferential replacement of clay-rich layers occurred because they provided the aluminum required to form tourmaline (Slack, 1993).

Only trace sulphide is associated with tourmaline alteration. Coarse-grained, east to south-east-trending clear to blue-grey quartz veins crosscut tourmalinized

rock, and locally contain pockets of fine to coarse-grained muscovite and 1 to 2% pyrite.

A zone of silicification and muscovite alteration is exposed west of the tourmalinite showing, along the railway tracks east of Carroll Creek. This alteration zone is in the hangingwall of the Spider fault, and may be unrelated to the tourmalinite zone.

Diamond drilling in the footwall of the Goatfell tourmalinite was carried out by Chevron Resources Limited in 1988-1989 (Hitzman, 1989; Rebic, 1989). Four holes were drilled to the Sullivan time horizon. Minor tourmalinite and fracture-controlled sphalerite-galena mineralization was intersected in these holes. No drill holes have been collared in the hangingwall of the Goatfell tourmalinite and its down-plunge extent is unknown.

## VEINS AND OTHER SHOWINGS

Several other showings occur within the central domain between the Star showing and the Goatfell tourmalinite:

The **Star South** property (Star 4 and 12 claims), owned by Cominco Ltd., covers an area on the ridge south of Kid Creek in the structural panel between the Spider and Carroll Creek/Kid faults (Figures 5 and 9). This panel contains typical middle Aldridge quartz wacke - siltstone turbidite sequences.

Work by Kootenay Exploration (Cominco Ltd.) in the late 1980s delineated two lead-zinc soil anomalies west of the Spider fault, with zinc analyses up to 637 ppm and lead to 130 ppm (McCartney, 1990). A small quartz-chlorite-albite alteration zone was mapped adjacent to the Spider fault in the northeast part of the claims (McCartney, 1990). Four sills can be traced across the ridge line within the claim block. The uppermost sill appears to thicken markedly in the area of the largest soil anomaly. It is possible that shearing, localized along the contacts of the upper two sills, provided permeability for fluid flow, remobilizing and concentrating lead and zinc from weakly metalliferous horizons in the sedimentary rocks. Brittle shears can be seen in outcrop along sill contacts in this area. Intersection of sill-sediment contacts with faults at depth would provide a locus for migrating hydrothermal fluids.

The **Hazel** showing is a narrow zone of albitization and silicification with minor pyrite, pyrrhotite and sphalerite along a north-trending fault on the west side of Hazel Creek. The showing is exposed by a small trench of uncertain vintage.

The **Sky** showing was discovered by F.R. Edmunds during a property mapping program for Chevron in 1989. A zone of tourmaline - sulphide and albite alteration 2 to 3 metres wide occurs in medium-bedded wackes and siltstones of the middle Aldridge. Petrographic observations suggest a multi-stage history of alteration

and shearing (Rebic, 1989). Sulphides include pyrite, pyrrhotite, arsenopyrite and chalcopyrite.

The **Option** showing occurs in and immediately adjacent to gabbro sills in the middle Aldridge. Numerous old pits and trenches expose quartz-pyrite vein mineralization in narrow silicified zones. The veins are reported to carry scheelite.

## TIMING OF VEIN MINERALIZATION

Galena lead isotope signatures of most veins fall in a cluster that includes stratiform deposits in the lower and middle Aldridge (Sullivan, North Star and Kootenay King: Table 2). The Sullivan orebody has the most radiogenic lead of this cluster and other deposits in the Sullivan corridor plot toward the radiogenic end (North Star, Stemwinder). The similarity of stratiform and vein-lead signatures suggests that the vein mineralization also occurred during the Middle Proterozoic (about Sullivan time). The only exception is the Midway deposit, in the middle Aldridge just east of the Yahk map area, which is distinctly more radiogenic. The Midway orebody also had higher gold grades (7.78 g/t; from Table 12 in Höy, 1993).

Although some of the veins with lead isotope ratios similar to the Sullivan deposit probably represent sedex feeder systems, some may be younger. There are two lines of evidence for this. First, several of the veins (e.g. St. Eugene, Star, Leadville) trend roughly orthogonal to regional fold axes. These could be interpreted as filling A-C joints developed during the Proterozoic (Goat River orogeny) or Jura-Cretaceous (Laramide orogeny; Höy, 1993). Second, the Society Girl vein (the eastern extension of the St. Eugene vein system) occurs in quartzite of the lower Creston Formation. Discordant Late Proterozoic K-Ar dates from alteration biotite along the margins of quartz veins at St. Eugene suggest a Proterozoic mineralizing event (Höy *et al.*, 1993).

## IRON RANGE

The Iron Range occurrences occur intermittently along the Iron Range fault zone for at least 20 kilometres. They comprise hematite and magnetite zones up to 200 metres wide. The main showings are located along the top of Iron Range Mountain, from about 6 kilometres north of the Goat River to the northern edge of the Yahk map area. Showings south of the Goat River were not visited during the 1993 field season. The northern showings are accessible by a poor four-wheel-drive road which leaves the Goat River road about 10 kilometres north of Highway 3.

The showings were explored in the early part of the century, and excellent detailed descriptions from that era have been published (Young and Uglow, 1928). Extensive trenching (more than 20 trenches) was carried out by Cominco in 1957 to evaluate the iron resource.

Mineralization occurs within the middle Aldridge Formation along a north-trending, subvertical fault zone (Iron Range fault, Figure 5). Aldridge Formation in the vicinity of the northern showings consists of well-bedded quartzofeldspathic wacke and laminated siltstone, which develop a phyllitic sericite foliation near the fault. Locally sericite alteration extends preferentially along specific bedding horizons, presumably due either to permeability or lithologic controls. Mineralization is primarily within sedimentary rocks and less commonly in altered gabbro. A fine-grained, dark green, foliated and mineralized mafic dike outcrops along the fault zone near the northern edge of the map area.

Mineralization consists of hematite and lesser magnetite in steeply dipping veins (0.3 to 0.6 m wide), broader stockworks of thin veinlets, breccia matrix and disseminated grains. Mineralization is sulphide-poor, except in the most northerly showings, where pyrite clots

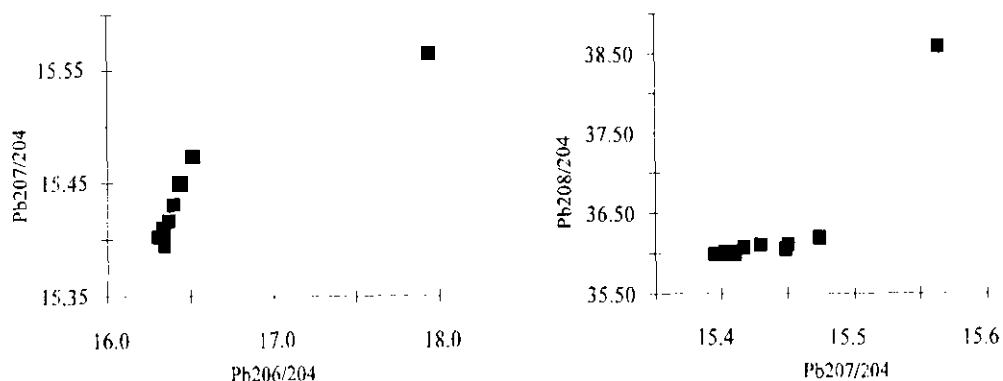
occur within the foliated mafic dike. Mineralized zones pinch and swell along strike, from narrow (0.5 m) veins within sheared rock, to broad (>100 m) zones of multiple veining and alteration.

Hostrocks are strongly albitized, sericized and/or silicified. Early quartz veins are commonly brecciated, with fragments enclosed in a hematite matrix. Early albitization is crosscut by hematite veining and angular albitized clasts float in a later hematite matrix in breccia zones. Late-stage white and colourless quartz veinlets commonly crosscut both albite alteration and hematite veining. Depth extent and down-dip variability of the system are unknown due to the lack of diamond drilling. Hematite at the north end of the system could be stratabound, associated with altered siliceous strata; at other exposures the mineralization is cross cutting and appears to be epigenetic.

**TABLE 2.**  
**LEAD ISOTOPE VALUES FOR DEPOSITS IN THE YAHK AND**  
**KIMBERLEY-CRANBROOK AREAS.**

Deposit	NTS	n	Type	Pb206/204	Pb207/204	Pb208/204
Sullivan	82F/09	8	sedex/ms	16.526	15.474	36.174
North Star	82F/09	1	sedex/ms	16.434	15.449	36.052
Stemwinder	82F/09	1	vein	16.444	15.450	36.087
Kootenay King	82G/12	2	sedex/ms	16.394	15.430	36.112
Fors	82G/05	3	vein	16.351	15.408	36.003
Society Girl	82G/05	2	vein	16.309	15.403	35.999
St. Eugene	82G/05	3	vein	16.339	15.395	35.974
Midway	82G/04	1	vein	17.940	15.564	38.593
Mt. Mahon	82G/04	2	vein	16.339	15.403	35.992
Alice	82F/02	1	vein	16.374	15.417	36.073
Kid Creek (Star)	82F/01	1	vein	16.332	15.406	35.985
Leadville	82F/01	1	vein	16.333	15.411	35.997

Data from Godwin *et al.* (1988).



## STRATABOUND Cu-Ag DEPOSITS IN MONTANA AND THEIR POTENTIAL IN CRESTON FORMATION

Stratabound copper-silver deposits occur in a narrow belt, the "Western Montana Copper Belt", about 70 kilometres south of Yahk. They include the Spar Lake (Troy), Montanore, and its western extension, the Rock Creek deposit. All three are significant deposits, but only Troy has been mined to date. The regional setting of these low-grade, high-tonnage deposits has been documented by Wells *et al.* (1981). The host Revett Formation, the central part of the Creston Formation, extends northward into the Yahk map area. The deposits formed when warm diagenetic ore solutions migrated laterally through permeable quartz arenite horizons and mixed with cooler pre-ore pore fluids (Hayes *et al.*, 1989). Vertical fluid ascent by water escape structures may also have played a role. Hayes *et al.* discuss the genesis of the Spar Lake deposit in detail.

The **Spar Lake (Troy) mine**, had start-up reserves of 58 million tonnes of 0.76% copper and 54 grams per tonne silver (Balla, 1982). The deposit, discovered in 1963, is hosted by grey-green to white, crosslaminated, well-sorted quartz arenites and siltstones of the Revett Formation, equivalent to the middle Creston. The orebody, 2250 metres long, 550 metres wide and about 20 metres thick, dips gently to the south-southwest (Hamilton and Balla, 1983). A fluviodeltaic environment has been inferred for this sequence. Stratiform and lesser discordant mineralization includes bornite, chalcocite, chalcopyrite, native silver and minor tetrahedrite (Balla, 1982). A pyrite halo surrounds the deposit. Detailed stratigraphy, mineral zonation and sulphur isotope geothermometry are reviewed by Hayes *et al.* (1989).

The continuation of Revett-equivalent stratigraphy north of the border into the Yahk map area indicates the potential for undiscovered deposits in the middle Creston. Although no copper mineralization was noted during the 1993 field season, two occurrences of disseminated hematite and magnetite were discovered. Careful prospecting and analysis of sedimentary facies may well lead to the discovery of significant copper-silver mineralization. Geochemically anomalous copper values are also reported in the eastern part of the basin in the Grinnell Formation, which is correlative with middle Creston Formation (Aitken and McMechan, 1991).

## CONCLUSIONS

In summary the study area has:

- atypical lower Aldridge, called Rampart facies, which is indistinct from the middle Aldridge
- deformation and metamorphism that increases to the west of the Arrow Creek fault, marking the transition from the Purcell anticlinorium into the Kootenay Arc
- scdex potential, for example, the nearby Fors occurrence
- a major but unusual iron ore deposit on Iron Range Mountain
- potential for discovery of a stratabound copper-silver deposit in middle Creston stratigraphy

## ACKNOWLEDGMENTS

Trygve Höy originally proposed the project and provided an excellent introductory field trip to the region. Our mapping was greatly assisted by an unpublished map of John Reesor's, kindly provided by the Geological Survey of Canada. Discussions and unpublished ideas and maps shared in the field by Trygve Höy, Peter Klewchuk, Dave Pighin, Paul Ransom and Dave Wiklund accelerated our apprenticeship into the Purcell Supergroup. Dave Lefebure's contributions to our mapping are appreciated. Drill core from the Star property was provided by Consolidated Ramrod Gold Corporation. Thorough reviews by Trygve Höy, John Newell and Dave Lefebure improved and amended the manuscript.

## REFERENCES

- Aadland, R.F. and Bennett, E.H. (1979): Geologic Map of the Sandpoint Quadrangle, Idaho and Washington; *Idaho Bureau of Mines and Geology*.
- Aitken, J.D. and McMechan, M.E. (1991): Middle Proterozoic Assemblages, Chapter 5; in *Geology of the Cordilleran Orogen in Canada*, Gabrielse, H. and Yorath, C.J., Editors; *Geological Survey of Canada, Geology of Canada*, No. 4, pages 97-124.
- Anderson, H.E. and Parrish, R.R. (1993): U-Pb Geochronology of the Middle Proterozoic Moyie Sills, Purcell Supergroup, Southeastern British Columbia; Belt III Symposium, poster session, Whitefish, Montana.
- Archibald, D.A., Krogh, T.E., Armstrong, R.L. and Farrar, E. (1984): Geochronology and Tectonic Implications of Magmatism and Metamorphism, Southern Kootenay Arc and Neighbouring Regions, Southeastern British Columbia, Part II: Mid-Cretaceous to Eocene; *Canadian Journal of Earth Sciences*, Volume 21, pages 567-583.
- Balla, J.C. (1982): Geology of the Troy Deposit, Northwestern Montana; Abstracts, Genesis of Rocky Mountain Ore Deposits, *Denver Regional Exploration Geological Society*.
- Baumgartner, T.R., Ferreira-Bartrina, V. and Moreno-Hentz, P. 1991: Varve Formation in the Central Gulf of California: A Reconsideration of the Origin of the Dark Laminae From the 20<sup>th</sup> Century Varve Record; in *The Gulf*

- Peninsular Province of the Californias, Dauphin, J.P. and Simmoneit, B.R.T., Editors, *American Association of Petroleum Geologists*, Memoir 47, pages 617-635.
- Benvenuto, G.L. and Price, R.A. (1979): Structural Evolution of the Hosmer Thrust Sheet, Southeastern British Columbia; *Bulletin of Canadian Petroleum Geologists*, Volume 27, pages 360-194.
- Bishop, D.T. (1973): Petrology and Geochemistry of the Purcell Sills in Boundary County, Idaho; in Belt Symposium, 1973, Volume II: *Idaho Bureau of Mines and Geology*, Special Publication, pages 15-66.
- Burge, C. (1992): Diamond Drilling Assessment Report on the Stoney Property, Fort Steele Mining Division; B.C. Ministry of Energy, Mines and Petroleum Resources, Assessment Report 22 233
- Burwash, R. A., Flaadsgaard, H. and Peterman, Z.E. (1962): Precambrian K-Ar Dates from the Western Canada Sedimentary Basin; *Journal of Geophysical Resources*, Volume 67, pages 1617-1625.
- Burmester, R.F. (1985): Preliminary Geological Map of the Eastport Area, Idaho and Montana; *U.S. Geological Survey*, Open-file Report 85-0517, scale 1:48 000.
- Chamberlain, K.R. and Doughty, P.T. (1993): Middle Proterozoic Mafic Magmatism, East Central Idaho: Implications for Age of Deposition of Belt Supergroup and Basin Subsidence Models; Abstracts with Programs, *The Geological Society of America*, Volume 25, Number 5, page 19.
- Cressman, E.R. (1985): The Prichard Formation in the Lower Part of the Belt Supergroup (Middle Proterozoic), near Plains, Sanders County, Montana; *U.S. Geological Survey*, Bulletin 1553.
- Cressman, E.R. (1989): Reconnaissance Stratigraphy of the Prichard Formation (Middle Proterozoic) and the Early Development of the Belt Basin, Washington, Idaho and Montana; *U.S. Geological Survey*, Professional Paper 1490.
- Cressman, E.R. and Harrison, J.E. (1986): Geologic Map of the Yaak River Area, Lincoln County, Northwestern Montana; *U.S. Geological Survey*, Miscellaneous Field Studies Map MF-1881, scale 1:48 000.
- Curry, H.N. (1953): Creston. B.C.; *Minister of Mines*, Annual Report 1952, page A 195.
- Daly, R.A. (1905): Summary Report 1904, Part A; *Geological Survey of Canada*, pages 91-100.
- Daly, R.A. (1912a): Geology of North American Cordillera at the Forty-ninth Parallel; *Geological Survey of Canada*, Memoir 38, Part 1.
- Daly, R.A. (1912b): Geology of the Forty-ninth Parallel; *Geological Survey of Canada*, Map 78A.
- Davis, R.A. (1983): Depositional Systems: A Genetic Approach to Sedimentary Geology; *Prentice-Hall, Inc.*, Englewood Cliff, N.J. 669 pages.
- Edmunds, F.R. (1977a): Multivariate Analysis of Petrographic and Chemical Data from the Aldridge Formation, Southern Purcell Mountain Range, British Columbia, Canada; unpublished Ph. D. dissertation, *Pennsylvania State University*, 385 pages.
- Edmunds, F.R. (1977b): Kimberley to Creston, Stratigraphy and Lithology of the Lower Belt Series in the Purcell Mountains, British Columbia; in Lead-Zinc Deposits of Southeastern British Columbia, Höy, T., Editor, *Geological Association of Canada*, Fieldtrip Guidebook 1, pages 22-32.
- Edmunds, F.R. (1988): Diamond Drill Hole, Top Claim - Top Claim Group, Fort Steele Mining Division; B.C. Ministry of Energy, Mines and Petroleum Resources, Assessment Report 17 078
- Ethier, V.G. and Campbell, F.A. (1977): Tourmaline Concentrations in Proterozoic Sediments of the Southern Cordillera of Canada and their Economic Significance; *Canadian Journal of Earth Sciences*, Volume 14, pages 2348-2363.
- Finch, J.C. and Baldwin, D.O. (1984): Stratigraphy of the Prichard Formation, Belt Supergroup (abstract); in Belt Symposium II, Proceedings, *Montana Bureau of Mines and Geology*, Butte, pages 5-7.
- Glover, J.K. (1978): Geology of the Summit Creek Area, Southern Kootenay Arc, British Columbia; unpublished Ph.D. thesis, *Queen's University*, 144 pages.
- Godwin, C.I., Gabites, J.E. and Andrew, A. (1988): Leadtable: A Galena Lead Isotope Data Base for the Canadian Cordillera; B.C. Ministry of Energy, Mines and Petroleum Resources, Paper 1988-4, 188 pages.
- Gorton, M.P., Schandl, E.S. and Höy, T. (In preparation): The Igneous and Metamorphic Evolution of the Moyie Sills in Southeastern British Columbia.
- Hagen, A.S. (1990): Star Property, *Kokanee Explorations, Ltd.*, internal report.
- Hamilton, J.M. and Balla, J. (1983): Belt-Purcell Supergroup; Troy (Spar Lake); in Stratatound Base Metal Deposits in Southeastern British Columbia and Northwestern Montana, *Geological Association of Canada*, Fieldtrip Guidebook No. 13, annual meeting, Victoria, pages 25-31.
- Hamilton, J.M., Delaney, G.D., Hauser, R.L. and Ransom, P.W. (1983): Geology of the Sullivan Deposit, Kimberley, B.C.; in Sedimentary-hosted Lead-Zinc Deposits, Sangster, D.F., Editor, *Mineralogical Association of Canada*, Short Course Notes, Chapter 2 pages 31-83.
- Harms, T.A. and Price, R.A. (1992): The Newport Fault: Eocene Listric Normal Faulting, Mylonitization, and Crustal Extension in Northeast Washington and Northern Idaho; *Geological Society of America*, Bulletin, Volume 104, pages 745-761.
- Harrison, J.E. and Cressman, E.R. (1993): Geology of the Libby Thrust Belt of Northwestern Montana and its Implications to Regional Tectonics; *U.S. Geological Survey*, Professional Paper 1524.
- Harrison, J.E., Cressman, E.R. and Whipple, J.W. (1992): Geologic and Structure Maps of the Kallipell 1° x 2° Quadrangle, Montana, and Alberta and British Columbia; *U.S. Geological Survey*, Miscellaneous Investigations Series, Map I-2267.
- Harrison, J.E., Kleinkopf, M.D. and Obradovich, J.D. (1972): Tectonic Events at the Intersection between the Hoppe Fault and the Purcell Trench, Northern Idaho; *U.S. Geological Survey*, Professional Paper 719, 24 pages.
- Hayes, T.S., Rye, R.O., Whelan, J.F. and Landis, G.P. (1989): Geology and Sulfur-isotope Geothermometry of the Spar Lake Cu-Ag Deposit in the Belt Supergroup, Montana; in Sediment-hosted Stratiform Copper Deposits; Boyle, R.W., Brown, A.C., Jefferson, C.W., Jowett, E.C. and Kirkham, R.V., Editors, *Geological Association of Canada*, Special Paper 36 pages 319-338.
- Hitzman, M.W. (1989): Geological, Geophysical and Diamond Drilling Work, Goatfell Group; B.C. Ministry of Energy Mines and Petroleum Resources, Assessment Report 18 633.
- Hoffman, P.F. (1991): Did the Breakout of Laurentia Turn Gondwanaland Inside-out?; *Science*, Volume 252, pages 1409-1412.
- Höy, T. (1979): Geology of the Estella - Kootenay King Area, Hughes Ranges, Southeastern British Columbia; B.C.

- Ministry of Energy, Mines and Petroleum Resources, Preliminary Map 36.
- Höy, T. (1984): Structural Setting, Mineral Deposits and Associated Alteration and Magmatism, Sullivan Camp, Southeastern British Columbia; in Geological Fieldwork 1983, *B.C. Ministry of Energy, Mines and Petroleum Resources*, Paper 1984-1, pages 24-35.
- Höy, T. (1989): The Age, Chemistry and Tectonic Setting of the Middle Proterozoic Moyie Sills, Purcell Supergroup, Southeastern British Columbia; *Canadian Journal of Earth Sciences*, Volume 26, pages 2305-2317.
- Höy, T. (1993): Geology of the Purcell Supergroup in the Fernie West-half Map Area, Southeastern British Columbia; *B.C. Ministry of Energy, Mines and Petroleum Resources*, Bulletin 84.
- Höy, T. and Carter, G. (1988): Geology of the Fernie West-half Map Sheet (and part of Nelson East-half); *B.C. Ministry of Energy, Mines and Petroleum Resources*, Open File 1988-14.
- Höy, T. and Diakow L. (1981): Geology of the Proterozoic Purcell Supergroup, Moyie Lake Area; in Geological Fieldwork 1980, *B.C. Ministry of Energy, Mines and Petroleum Resources*, Paper 1981-1, pages 9-14.
- Höy, T. and Diakow L. (1982): Geology of the Moyie Lake Area; *B.C. Ministry of Energy, Mines and Petroleum Resources*, Preliminary Map 49.
- Höy, T., Dunne, K. and Wilton, P. (1993): Massive Sulfide and Precious Metal Deposits in Southeastern British Columbia; *Geological Association of Canada, Mineralogical Association of Canada*, Annual Meeting, Field Trip A-7, Guidebook, 74 pages.
- Irbarr, S.V. (1973): Deep-water Sedimentation in the Ravalli Group (Late Precambrian Belt Megagroup), Northwestern Montana; in Belt Symposium, 1973: Department of Geology, *University of Idaho and Idaho Bureau of Mines and Geology*, Volume 2, pages 67-82.
- Huebschman, R.P. (1972): Correlation and Environment of a Key Interval within the Precambrian Prichard and Aldridge Formations, Idaho - Montana - British Columbia; unpublished M. Sc. thesis, *University of Montana*.
- Huebschman, R.P. (1973): Correlation of Fine Carbonaceous Bands Across a Precambrian Stagnant Basin; *Journal of Sedimentary Petrology*, Volume 43, pages 688-699.
- Hunt, B.G. (1979): The Effects of Past Variations of the Earth's Rotation Rate on Climate; *Nature*, Volume 281, pages 188-191.
- Kopp, (1973): Lithofacies and Depositional Environment of the Ravalli Group, Precambrian Belt-Purcell Supergroup; in Belt Symposium, Volume 2: *Idaho Bureau of Mines and Geology*, Special Paper, pages 83-111.
- Leclair, A.D. (1983): Stratigraphic and Structural Implications of Central Kootenay Arc Rocks, Southeastern British Columbia; in Current Research, Part A, *Geological Survey of Canada*, Paper 83-1A, pages 235-240.
- Leech, G.B. (1957): St. Mary Lake, Kootenay District, British Columbia (82F/9); *Geological Survey of Canada*, Map 15-1957.
- Leech, G.B. (1958): Fernie Map Area, West Half, British Columbia, 82G W1/2; *Geological Survey of Canada*, Paper 58-10.
- Leech, G.B. (1960): Geology Fernie (West Half), Kootenay District, British Columbia; *Geological Survey of Canada*, Map 11-1960.
- Leech, G.B. (1962): Metamorphism and Granitic Intrusions of Precambrian Age in Southeastern British Columbia; *Geological Survey of Canada*, Paper 62-13.
- Leitch, C.H.B. and Turner, R.J.W. (1992): Preliminary Field and Petrographic Studies of the Sulfide-bearing Network Underlying the Western Orebody, Sullivan Stratiform Sediment-hosted Zn-Pb Deposit, British Columbia; in Current Research, Part E, *Geological Survey of Canada*, Paper 92-1E, pages 71-82.
- Leitch, C.H.B., Turner, R.J.W. and Höy, T. (1991): The District-scale Sullivan - North Star Alteration Zone, Sullivan Mine Area, British Columbia; in Current Research, Part E, *Geological Survey of Canada*, Paper 91-1E, pages 45-57.
- MacDonald, J.G. (1978): Prospecting, Geochemical and Physical Work Report; *B.C. Ministry of Energy, Mines and Petroleum Resources*, Assessment Report 7481.
- McCartney, I.D. (1990): Report on Geological Mapping, Geophysical Surveys, and Soil Geochemical Surveys, Star 4 and Star 12 Claims; *B.C. Ministry of Energy, Mines and Petroleum Resources*, Assessment Report 21 230.
- McDonald, J.D. (1960): Creston; *B.C. Minister of Mines*, Annual Report 1959, page 73.
- McMechan, M.E. (1979): Geology of the Mount Fisher - Sand Creek Area; *B.C. Ministry of Energy, Mines and Petroleum Resources*, Preliminary Map 34.
- McMechan, M.E. (1981): The Middle Proterozoic Purcell Supergroup in the Southwestern Purcell Mountains, British Columbia, and the Initiation of the Cordilleran Miogeocline, Southern Canada and adjacent United States; *Bulletin of Canadian Petroleum Geology*, Volume 29, pages 583-641.
- McMechan, M.E. and Price, R.A. (1982): Superimposed Low-grade Metamorphism in the Mount Fisher Area, Southeastern British Columbia -- Implications for the East Kootenay Orogeny; *Canadian Journal of Earth Sciences*, Volume 19, pages 476-489.
- Merrett, J.E. (1958): Creston; *B.C. Minister of Mines*, Annual Report 1957, pages 60-62.
- Merrett, J.E. (1959): Creston; *B.C. Minister of Mines*, Annual Report 1958, page 50.
- Obradovich, J.D. and Peterman, Z.E. (1968): Geochronology of the Belt Series, Montana; *Canadian Journal of Earth Sciences*, Volume 5, pages 737-747.
- Olson, P.E. (1970): Otto Silver, Leadville; *B.C. Ministry of Mines and Petroleum Resources*, Annual Report 1969, page 322.
- Peck, J.W. (1950): Creston; *B.C. Minister of Mines*, Annual Report 1949, page A 194.
- Peck, J.W. (1951): Creston; *B.C. Minister of Mines*, Annual Report 1950, page A 152.
- Rebic, Z. (1989): Diamond Drilling, Geology and Geochemistry on Goatfell Property; *B.C. Ministry of Energy, Mines and Petroleum Resources*, Assessment Report 19 304.
- Reesor, J.E. (1958): Dewar Creek Map-area with special emphasis on the White Creek Batholith, British Columbia; *Geological Survey of Canada*, Memoir 292.
- Reesor, J.E. (1981): Grassy Mountain, Kootenay Land District, British Columbia (82F/8); *Geological Survey of Canada*, Open File 820.
- Reesor, J.E. (1983): Geology of the Nelson Map-area, East Half; *Geological Survey of Canada*, Open File 929.
- Reesor, J.E. (1993): Geology, Nelson (East Half; 82F/1,2,7-10,15,11); *Geological Survey of Canada*, Open File 2721.
- Rice, H.M.A. (1937): Cranbrook Map-area, British Columbia, *Geological Survey of Canada*, Memoir 207.
- Rice, H.M.A. (1941): Nelson Map Area, East Half; *Geological Survey of Canada*, Memoir 228.

- Ross, G.M., Parrish, R.R. and Winston, D. (1992): Provenance and U-Pb Geochronology of the Mesoproterozoic Belt Supergroup (Northwest United States): Implications for Age of Deposition and Pre-Panthalassa Plate Reconstruction; *Earth and Planetary Science Letters*, Volume 113, pages 57-76.
- Schiarizza, P. (1984): Kootenay/Mount Mahon 1983-84 Summary Report, Fort Steele Mining Division, B.C. Ministry of Energy, Mines and Petroleum Resources, Assessment Report 14 275
- Schofield, S.J. (1915): Geology of the Cranbrook Map-area; *Geological Survey of Canada*, Memoir 76.
- Simpson, R. (1984): A Preliminary Geochemical Survey on the Boo and Gobi Claims, Kid Creek Area, British Columbia; B.C. Ministry of Energy, Mines and Petroleum Resources, Assessment Report 12 856.
- Slack, J.F. (1993): Models for Tourmalinite Formation in the Middle Proterozoic Belt and Purcell Supergroups (Rocky Mountains) and their Exploration Significance; in Current Research, Part E, *Geological Survey of Canada*, Paper 93-1E, pages 33-46.
- Stephenson, L. (1990a) Report on Diamond Drill Hole E90-3, Eng Property, Yah 1 Claim, Fort Steele Mining Division, B.C. Ministry of Energy, Mines and Petroleum Resources, Assessment Report 20 829
- Stephenson, L. (1990b): Report on Diamond Drill Hole S90-1, Star Property, B.C. Ministry of Energy, Mines and Petroleum Resources, Assessment Report 20 571.
- Turner, R.J.W. and Leitch, C.H.B. (1992): Relationship of Albitic and Chloritic Alteration to Gabbro Dikes and Sills at the Sullivan Deposit and Nearby Area, Southeastern British Columbia; in Current Research, Part E, *Geological Survey of Canada*, Paper 92-1E, pages 95-106.
- Turner, R.J.W., Höy, T., Leitch, C.H.B. and Anderson, D. (1992): Guide to the Tectonic, Stratigraphic and Magmatic Setting of the Middle Proterozoic Stratiform Sediment-hosted Sullivan Zn-Pb Deposit, Southeastern British Columbia; B.C. Ministry of Energy, Mines and Petroleum Resources, Information Circular 1992-23.
- Turner, R.J.W., Höy, T., Leitch, C.H.B., Anderson, D. and Ransom, P. (1993): Guide to the Geological Setting of the Middle Proterozoic Sullivan Sediment-hosted Pb-Zn Deposit, Southeastern British Columbia; in Geologic Guidebook to the Belt-Purcell Supergroup, Glacier National Park and Vicinity, Montana and adjacent Canada; Link, P.K., Editor, Belt Symposium III Field Trip Guidebook, *Belt Association*, Spokane, Washington, pages 53-94.
- Wells, J.D., Lindsey, D.A. and Van Loenen, R.E. (1981): Geology of the Cabinet Mountains Wilderness, Lincoln and Sanders Counties, Montana; *U.S. Geological Survey*, Bulletin 1501-A, pages 9-21.
- Wheeler, J.O. and McFeely, P. (1991): Tectonic Assemblage: Map of the Canadian Cordillera and adjacent parts of the United States; *Geological Survey of Canada*, Map 1721A.
- Winston, D. (1986): Sedimentology of the Ravalli Group, Middle Belt Carbonate and Missoula Group, Middle Proterozoic Belt Supergroup, Montana, Idaho and Washington, in A Guide to the Proterozoic Rocks of Western Montana and Adjacent Areas, Roberts, S.M., Editor, *Montana Bureau of Mines and Geology*, Special Publication 94, pages 85-124.
- Winston, D., Woods, M. and Byer, G.B. (1984): The Case for an Intracratonic Belt - Purcell Basin: Tectonic, Stratigraphic and Stable Isotopic Considerations; *Montana Geological Society*, 1984 Field Conference, Northwestern Montana, Proceedings, pages 103-118.
- Yoos, T.R., Potter, C.J., Thigpen, J.L. and Brown, L.D. (1991): The Cordilleran Foreland Thrust Belt in Northwestern Montana and Northern Idaho from COCORP and Industry Seismic Reflection Data; *The American Association of Petroleum Geologists*, Bulletin, Volume 75, pages 1089-1106.
- Young, G.A. and Uglow, W.L. (1928): Iron Ores in Canada, Volume I, British Columbia and Yukon, *Geological Survey of Canada*, Economic Geology Series, No. 3, pages 132-142.
- Zartman, R.E., Peterman, Z.E., Obradovich, J.D., Gallego, M.D. and Bishop, D.T. (1982): Age of the Crossport C Sill near Eastport, Idaho; in Bulletin 24. Reid, R.R. and Williams, G.A., Editors, Society of Economic Geologists, Coeur d'Alene Field Conference, *Idaho Bureau of Mines and Geology*, pages 6-69.

## NOTES

## SUMMARY OF ACTIVITIES, NORTH SELKIRK PROJECT GOLDSTREAM RIVER AND DOWNIE CREEK MAP AREAS (82M/8, 9 AND PARTS OF 10)

By J. M. Logan and J. R. Drobe

**KEYWORDS:** Downie Creek, Goldstream River, Goldstream mine, Rain, Montgomery, Standard, volcanogenic massive sulphides, garnet zone, Lardeau Group, Badshot Formation.

### INTRODUCTION

The Goldstream area, east of the Columbia River in the northern Selkirk Mountains, contains a number of volcanogenic massive sulphide (VMS) deposits, including the operating Goldstream mine, in addition to carbonate replacement, vein and placer gold deposits. The Northern Selkirk project is a two-year study, undertaken to assess and promote the potential for VMS deposits in a 1500 square kilometre area centred 50 kilometres north of Revelstoke, British Columbia (Figure 1). Reconnaissance mapping and lithogeochemical sampling in 1993 will be used to further understand the tectonic setting and, in particular, the age and characteristics of the host succession. Detailed mineral occurrence descriptions will be the focus of the second year and correlating this succession regionally and, hence, evaluating VMS potential elsewhere in the Kootenay Terrane the ultimate goal.

The Northern Selkirk Mountains area is a complexly deformed and metamorphosed region situated between the Foreland fold and thrust belt of the southern Canadian Rockies on the east, and the Shuswap Metamorphic Complex in the west. The Goldstream area is underlain by strongly deformed Late Proterozoic to early Paleozoic metasedimentary and metavolcanic rocks of the Selkirk allochthon, as well as numerous large plutonic bodies, all part of the pericratonic Kootenay Terrane. The Selkirk allochthon consists of at least three tectonic slices (Figure 1). The Goldstream and Clachnacudain slices form the hangingwall of the Monashee décollement north of Revelstoke. The overlying Illecillewaet slice is the largest and possibly a composite slice making up the easternmost part of the allochthon (Read and Brown, 1981). The allochthon was displaced eastward along the Monashee décollement during Late Jurassic and Late Cretaceous orogenesis; regional extension in the Tertiary localized

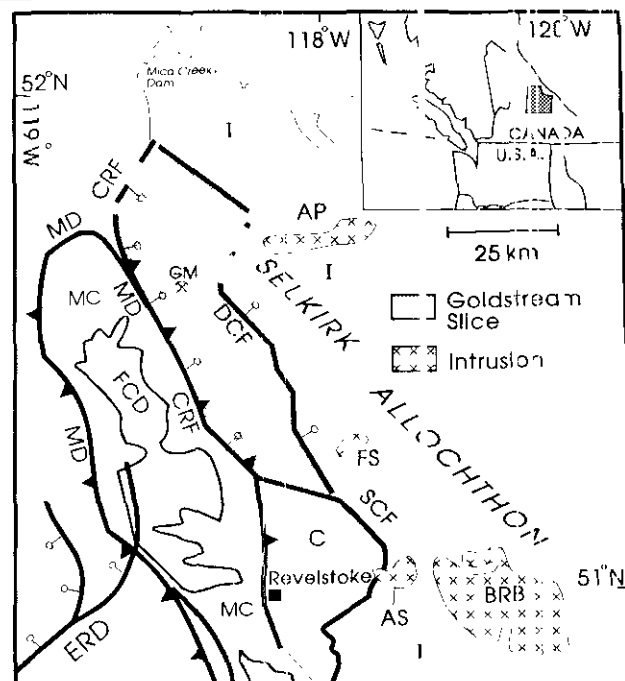


Figure 1. Location of the project area within the Goldstream slice of the Selkirk allochthon, after Brown and Lane (1988). I=Illecillewaet slice, C=Clachnacudain slice, CRF=Columbia River fault, DCF=Downie Creek fault, ERD=Eagle River detachment, SCF=Standfast Creek fault, MD=Monashee Décollement, MC=Monashee Complex, FCD=Frenchman's Cap dome, AP=Adamant pluton, FS=Fang stock, AS=Albert stock, BRB=Battle Range batholith, GM=Goldstream mine.

brittle normal faulting along this same structure (Brown and Lane, 1988).

The geology has been described by numerous authors beginning with Walker and Bincoft (1929), Gunning (1929) and Wheeler (1963, 1965). Read and Brown (1979, 1981), Trygve Høy (1979) of the Geological Survey Branch and R.L. Brown and his students at Carleton University (Brown *et al.*, 1977, 1978, 1983), notably Lane (1977, 1984), have done much work towards understanding the geology and tectonic setting.

### REGIONAL STRATIGRAPHY

The Selkirk allochthon is composed of the Upper Proterozoic Horsethief Creek Group, the Eocambrian Hamill Group, the Cambrian Badshot Formation, and

the lower Paleozoic Lardeau Group (Wheeler, 1965; Brown *et al.*, 1978). These divisions are broadly similar in lithology, and form the miogeoclinal wedge of ancestral North America, with rocks of the Lardeau Group as a more distal and possible marginal basin sequence to the wedge (Figure 2).

The Horsethief Creek Group consists mainly of phyllitic and slaty pelites, interbedded sandstone, conglomerate and minor carbonate rocks. In the Northern Selkirks, Brown *et al.* (1978) divided them into lower semipelite/amphibolite, middle marble and upper clastic divisions. Unconformably overlying these are Eocambrian Hamill Group rocks consisting mostly of feldspathic and quartzose arenites, which Devlin (1986) interprets as shallow-marine facies sandstones, and mafic metavolcanic rocks (Wheeler, 1963; 1965). Archeocyathid-bearing late Lower Cambrian limestones of the Badshot Formation conformably overlie the Hamill Group (Wheeler, 1963).

The Lardeau Group overlies the Badshot in stratigraphic conformity in the Illecillewact synclinorium (Colpron and Price, 1992) and in uncertain and possibly reverse stratigraphic order in the Trout Lake area (Smith and Gehrels, 1992a). In the Ferguson area, Fyles and Eastwood (1962) recognized six formations within the Lardeau Group

(Figure 2). The Index Formation is the lowest and consists of dark grey and green, rhythmically bedded phyllite, limestone, minor quartzite and, near the top, phyllitic volcanic rocks. Mafic and ultramafic intrusions (altered to talc schist) occur in the uppermost green phyllites. Above the Index are grey and black siliceous argillites of the Triune Formation, in turn overlain by grey quartz arenite with limy concretions of the Ajax Formation and dark grey siliceous argillite of the Sharon Creek Formation. Fritz *et al.* (1991) interpret these units as outer basinal sediment related to the margin of ancestral North America. Tholeiitic, pillowed and breccia flows, tuff and lesser limestone and phyllite of the Jowett Formation conformably overlie the Sharon Creek Formation. Grey quartz-feldspar grit, foliated micaceous quartzite and phyllite of the Broadview Formation form the uppermost part of the Lardeau Group. Fritz *et al.* (1991) propose a western source, outboard of ancestral North America, for the sands of the Broadview Formation.

Carboniferous Milford Group basal conglomerate, limestone, tholeiitic volcanics and siliceous argillite lie with angular unconformity on the Broadview Formation (Figure 2). Boulders of the Broadview Formation from the basal conglomerate of the Milford Group yield an Early to Middle Ordovician Rb-Sr

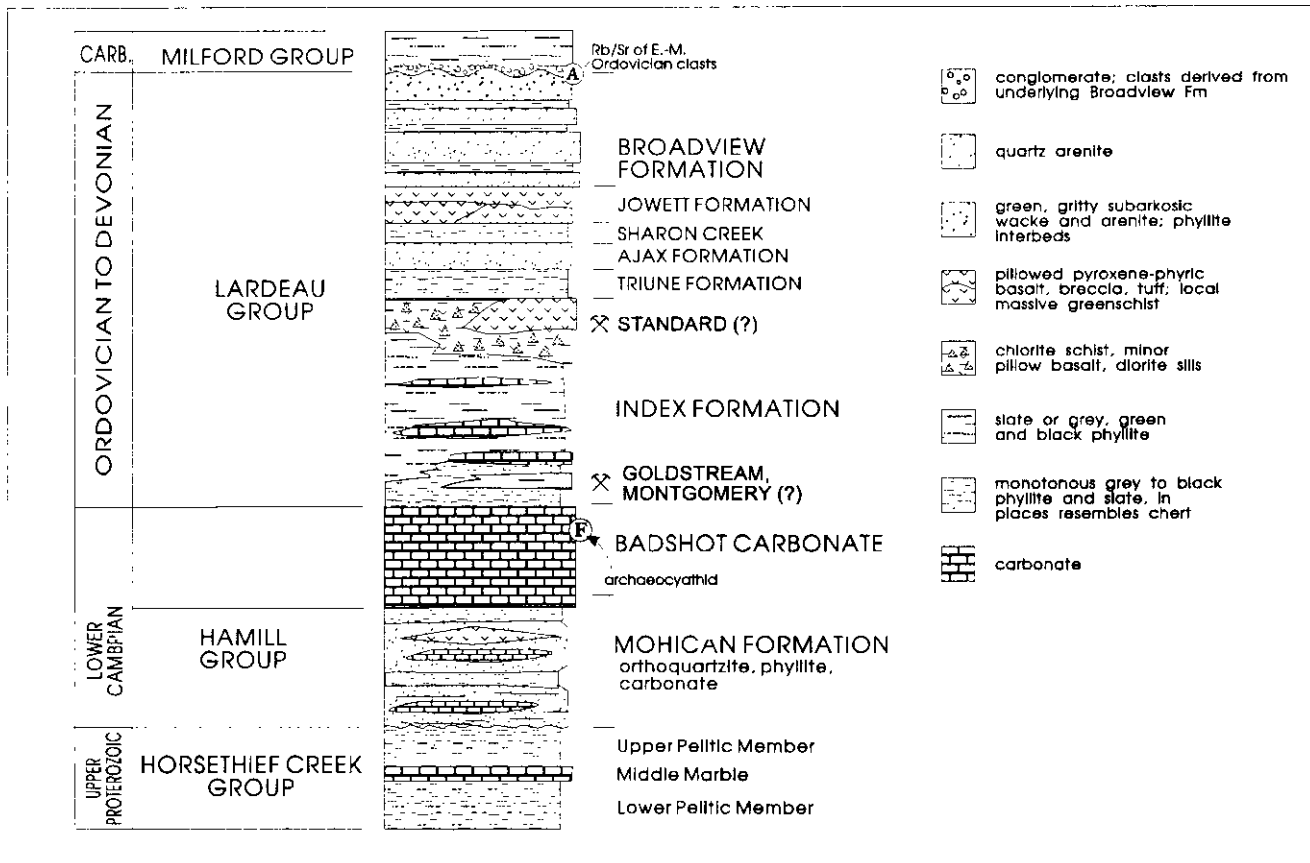


Figure 2. Schematic stratigraphic column of the Lardeau Group and underlying rocks, after Fyles and Eastwood (1962) and Brown *et al.* (1978). The Triune, Ajax, Sharon Creek and Jowett Formations of the Lardeau Group, and the Milford Group are not recognized in the study area. The relative thickness of the Lardeau Group is exaggerated for clarity.

whole-rock isochron date (Read and Wheeler, 1977).

## GOLDSTREAM SLICE LAYERED ROCKS

The stratigraphy of the Goldstream slice is dominated by pelitic rocks with interlayered carbonate horizons; quartzite and grit, carbonate, impure psammite and volcanic rocks. Wheeler (1965) showed much of the area to be underlain by Lardeau Group rocks, however specific correlations and stratigraphic definition within the slice are made difficult by the following problems:

- The Goldstream slice is entirely fault bounded.
- The absence of fossil-bearing strata.
- Lithological similarities between the Horsethief Creek, Hamill and Lardeau Groups
- Structural complexities resulting from repeated deformation.

Consequently, the stratigraphic nomenclature has evolved through many changes and stratigraphy is yet to be firmly established.

Wheeler assigned the rocks north of the Goldstream River to the Horsethief Group, which subsequent workers supported (Franzen, 1974; Brown *et al.*, 1977). More recent work by Gibson and Höy (1985) and Gibson (unpublished) suggest this area is underlain by younger rocks of the Hamill Group, Badshot Formation and Lardeau Group (Figure 3). Reconnaissance mapping this summer in the Groundhog Basin north of Goldstream River identified a package of well-sorted, graded beds of quartz-feldspar grits, quartzite and micaceous quartzite, black sericite schist and calcareous phyllite with lesser greenstone, talc schist and carbonate. Assigning these rocks to either stratigraphic sequence will require further work. Stratiform zinc-lead massive sulphide mineralization in possible equivalent at the Rift showing (12 km north of the map area) gives galena-lead model ages of Early Cambrian to Late Hadrynian (approximately 0.52 Ga; Hicks, 1982) supporting a younger age for the strata.

South of the Goldstream River, the westernmost Lardeau Group rocks were assigned to the Broadview Formation by Campbell (1972). Later, Brown *et al.* (1976), Lane (1977) and Höy (1979) considered the rocks to the east to belong to the upper Horsethief Creek and Hamill groups. On the basis of overturned stratigraphy, they proposed the following stratigraphic sequence: an older carbonate-pelitic schist unit, a middle mixed unit of impure psammite and pelite with metavolcanic rocks, and a younger carbonate-pelitic schist unit. These units were tentatively correlated with the Horsethief Creek Group, the Hamill Group and Badshot Formation - Lardeau Group, respectively. Höy (1979) further divided the middle mixed unit into a lower quartzite-schist division, a calcsilicate gneiss division and a metavolcanic-phyllite division,

correlating the latter with the Mohican Formation, the upper part of the Hamill Group in the Kootenay Arc.

Latest work by Brown *et al.* (1983), Höy *et al.* (1984), Brown and Lane (1988) and Brown (1991), show Hamill Group, Badshot Formation and Index, Jowett and Broadview formations of the Lardeau Group traceable north from Carnes Creek to Downie Creek (Figure 3). Gibson (1989) mapped Mohican and Marsh Adams formations of the Hamill, the Badshot Formation and Index Formation of the Lardeau Group in the area between Goldstream River and Downie Creek.

Using these most recent stratigraphic correlations we spent the summer measuring sections of apparently well constrained stratigraphy. The purpose of measuring sections was more to determine the relative proportion and distribution of lithologies than true thickness. Composite stratigraphic sections of the lower Lardeau Group rocks were measured in the area between the Goldstream River and the Goldstream mine and on the west and east limbs of the Downie Peak antiform (RS, DP and LC, Figures 4 and 5). In addition, stratigraphic sections were measured in four areas of known copper-zinc volcanogenic massive sulphide occurrences.

## SECTION RS

Three separate units comprise the stratigraphy measured northwest of the Goldstream pluton (RS). They include a structurally lowest micaceous quartzite-phyllite unit, chlorite schist and black phyllite, and an uppermost dolomitic marble. The quartzite-phyllite unit crops out along Highway 23 north of the Goldstream mine turn-off for 4.5 kilometres; at 5 kilometres from the turn-off the black phyllite crops out, followed by the marble unit at 6 kilometres. The stratigraphy is shown in Figure 4, and described in ascending structural order.

The quartzite-phyllite unit is comprised of rhythmic beds of greenish quartzite and green sericite-chlorite phyllite. Micaceous quartzite predominates and the proportion of quartzite to phyllite is greater than 1, generally on the order of 4. Bedding is planar, ungraded and varies from a centimetre to several metres thick. The unit is disrupted by folding and faulting and zones of argillic alteration. Thick metre-scale quartzite beds are thoroughly fractured, phyllite is crenulated and rusty weathering.

Structurally overlying the quartzite-phyllite is a succession of dark green, massive to phyllitic chlorite schist, interbedded sericite schist, quartzite and limestone, and dark phyllite exposed on secondary roads branching north from the Goldstream mine road, 5.5 kilometres from Highway 23. The chlorite schist is well foliated, contains carbonate partings and stringers and several percent euhedral pyritohedrons. It is overlain by a thinly bedded mixed unit of sericite-chlorite schist, marble and micaceous quartzite, which grades upwards into dark phyllite. Five metres of

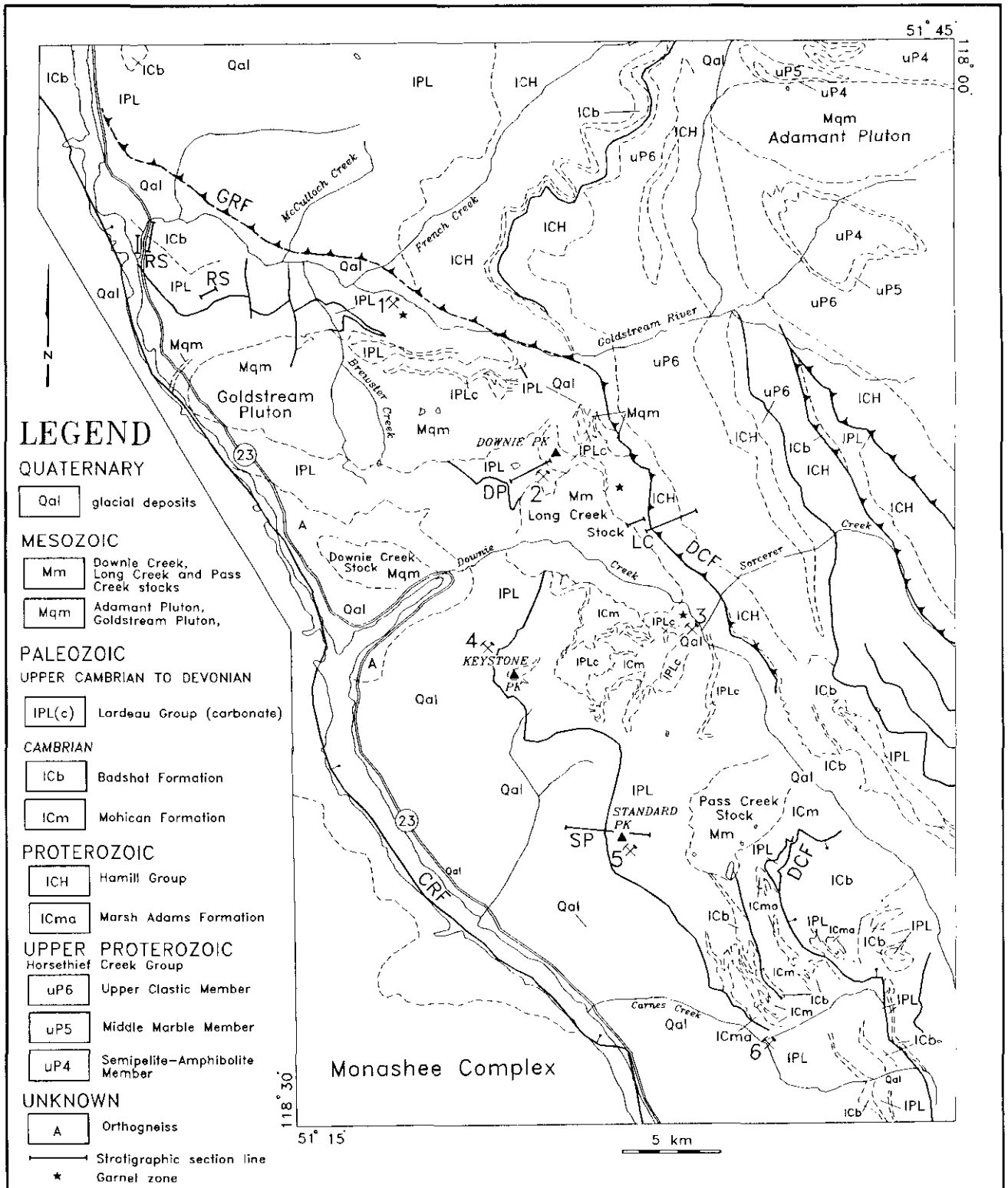


Figure 3. Geological map of the project area, modified from Gibson and Höy (in press). Mineral occurrences are shown by pick and hammer symbol: 1=Goldstream mine, 2=Montgomery, 3=Rain, 4=Keystone, 5=Standard, 6=J&L. Stratigraphic section lines: RS=Road and Goldstream River estuary outcrops (measured), DP=Downie Peak (measured), LC=Long Creek area, SP=Standard Peak. DCF=Downie Creek fault, CRF=Columbia River fault, GRF=Goldstream River fault.

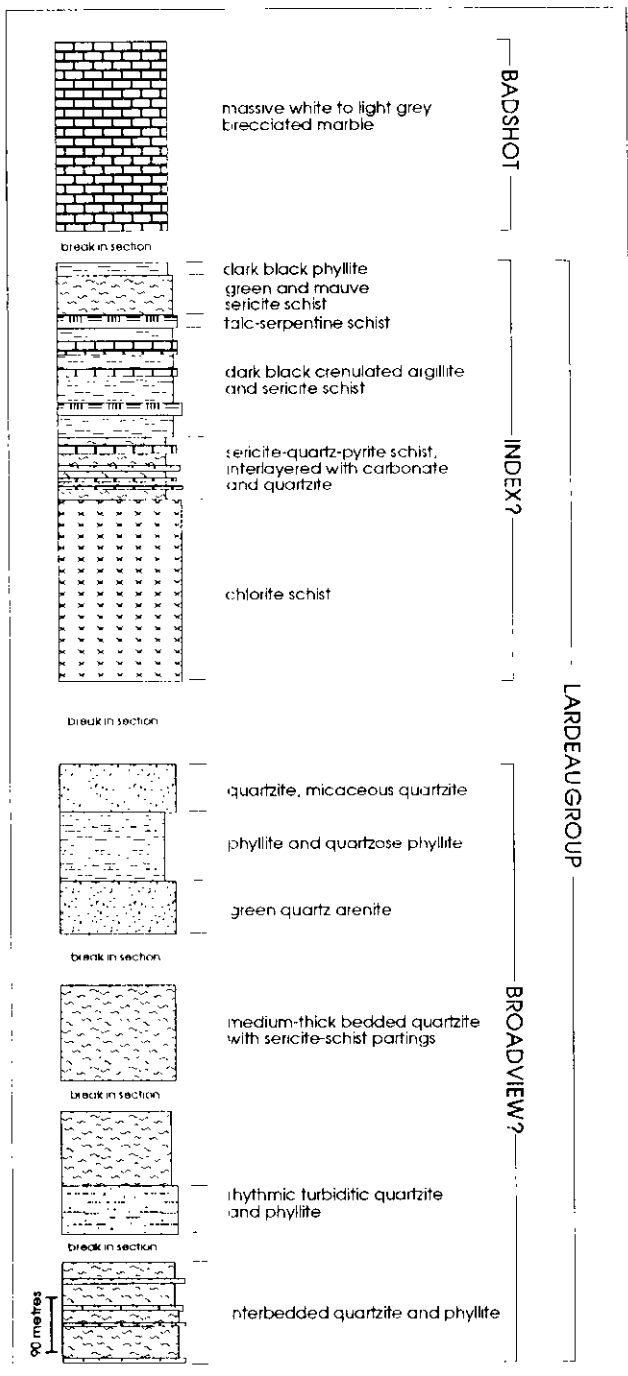


Figure 4. Schematic stratigraphic section compiled from measured outcrops along the Goldstream River estuary, Highway 23 and Goldstream mine road. The section is shown as structurally upright; stratigraphic correlations suggest this succession is inverted.

serpentine-antigorite schist within dark, banded phyllite are exposed in a soapstone quarry.

A structurally thickened package of dark, banded phyllite crops out along Highway 23, on strike with these phyllites. Talcose altered ultramafic rocks form the base of the section. The unit has been structurally interleaved with black calcareous and carbonaceous phyllite which contains brilliant green, coarsely

crystalline fuchsite adjacent to the ultramafites. Dark, thinly interbedded, silty argillite and phyllite comprise most of the road cut. The dark, banded phyllite is intruded by two, talc-antigorite-ankerite schist units, both approximately 3 metres wide. Ten metres of rhythmic bedded, dark and light brown marble are exposed near the top of the section. The marble is interbedded with, and overlain by, sericite schist and grey phyllite similar to those at the lower contact. Thinly bedded white carbonate with green and mauve sericitic schist partings overlies black graphitic sericite schists in the Goldstream River. To the east (up structure) are sericite schists, sericite psammites, micaceous quartzite horizons and lesser black graphitic phyllite. Black sericitic phyllite forms the uppermost unit below the massive marble of the Badshot Formation; the contact is not exposed. The marble is bright white to cream coloured and finely crystalline to amorphous. It is commonly dolomitic and, where not interbedded with phyllite or sericite schist, crops out as spectacular white carbonate massifs.

Lithologically the quartzite-phyllite, black phyllite and marble units (Figure 4) are similar to the Hamilton, Mohican and Badshot formations, an upright-facing succession. However, we agree with Gibson's (1989) correlation of these rocks with the Broadview, Index and Badshot formations, and the section therefore represents an inverted stratigraphic panel. More important is the correlation of black phyllite with the dark, banded phyllite which hosts the massive sulphide horizon at the Goldstream mine.

## SECTIONS DP AND LC

Lardeau Group stratigraphy was measured along the southwest flank of Downie Peak (DP). East of Long Creek a second section (LC) started in correlative units and continued eastward. Previous workers recognized Downie Peak as a second phase antiformal syncline cored by carbonate of the Badshot Formation (Brown *et al.*, 1977; Höy, 1979; Gibson, 1989); thus, a stratigraphic symmetry should be apparent across east and west limbs. However, our observations (Plate 1) and measured stratigraphic sections (Figures 3 and 5) suggest the stratigraphy is asymmetric on either side of Downie Peak, and we believe the carbonate may be of the Index Group.

The section west of Downie Peak began on the ridge east of Boulder Creek at an elevation of 1800 metres (6200 feet), ending 150 metres (500 feet) below the limestone which forms the summit at 2928 metres (9607 feet). It is a coarsening-upward sequence dominated by (1100 m) quartz-biotite and quartz-sericite schists interlayered with marble at lower elevations. This passes gradationally upwards through schist, quartzite and grit with lesser carbonate (650 m) to a micaceous quartzite unit (250 m) which is abruptly overlain by white marble forming the top of Downie Peak.

Stratigraphic Sections East and West of Downie Peak Antiform (?)

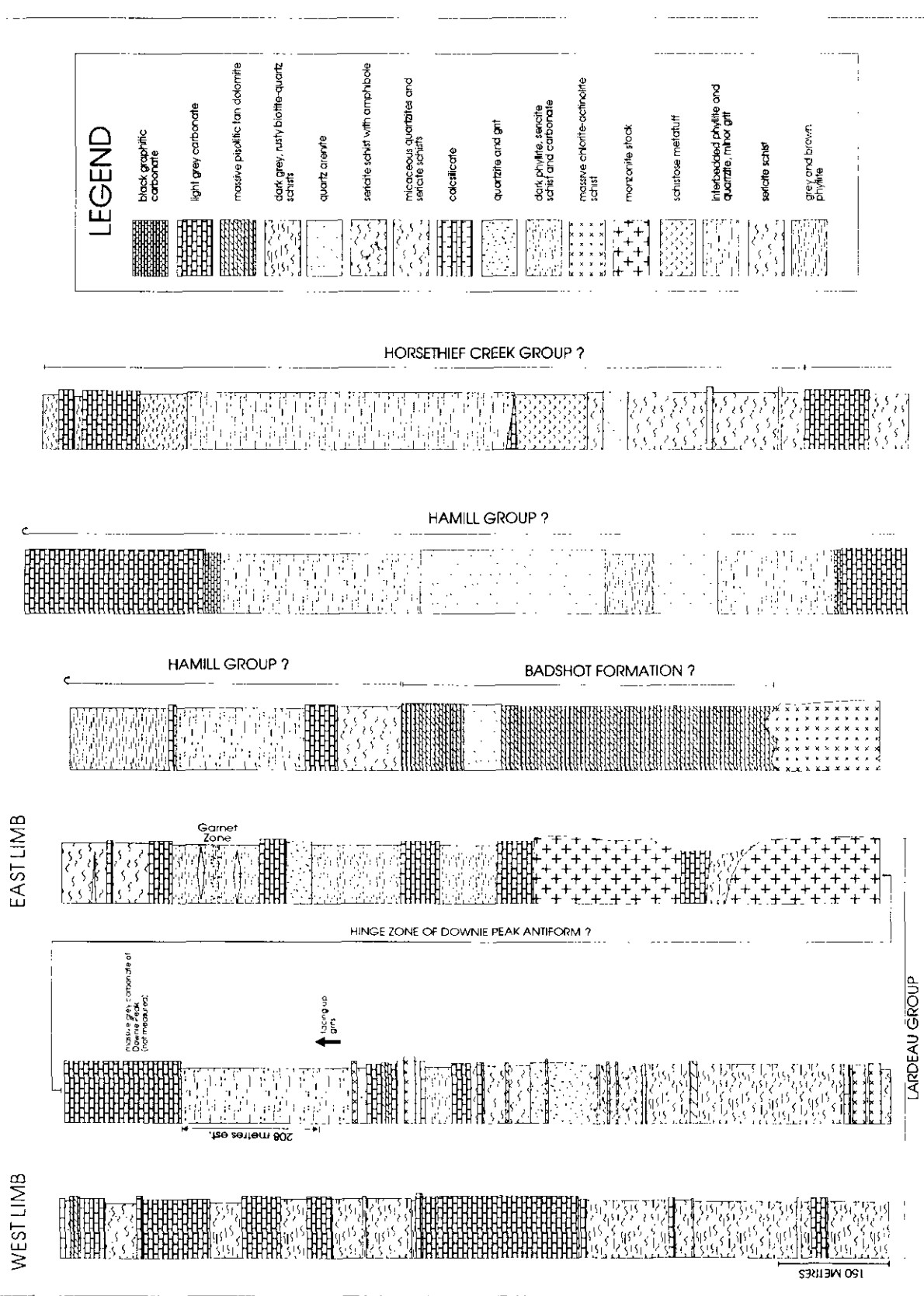


Figure 5. Schematic stratigraphic sections of rocks west of Downie Peak (measured) and east of Downie Peak (compiled from cross-sections). Note that the Long Creek pluton disrupts the stratigraphy east of Downie Peak, which is not easily correlated with stratigraphy west of the peak.



Plate 1. View of Downie Peak from the south. Note the gradational upper contact and sharp lower contact between the massive carbonate and adjacent quartzites and schists.

A thick carbonate unit (200 m) comprised mainly of grey marble and buff phyllitic carbonate separates the schist-carbonate package into lower biotite schist and upper sericite schist units. Pelitic schists of the lower package are mainly thinly foliated, dark grey to brown in colour. Carbonaceous schists are rare and calcareous schists are gradational to marble layers. Biotite-quartz schist contains numerous lenticular and sigmoidal augens of grey and yellow quartz. Quartz-rich layers contain trace amounts of disseminated pyrrhotite. Elongate metablasts (5 cm) of andalusite(?), now retrograded to muscovite and quartz, are common but bedding (composition) specific. Above the marble unit are roughly equal proportions of interlayered phyllitic carbonate and sericite-quartz schist which, near the top, contain interbeds of micaceous quartzite and metadiorite bodies. Lithologies are interbedded on a centimetre scale. Schists are pale green to silver and contain actinolite(?) porphyroblasts on  $S_2$  foliation planes. Carbonates include grey, black and brown marbles and phyllitic limestone. Coarse-grained, dark green metadiorite sills intrude the sediments near the top of the unit at low angles to foliation. These bodies are up to 20 metres thick; boudins less than a metre thick were noted within marble to the west of the section. Textures vary in the thicker sills from massive to

intersertal in the centre, to schistose and mylonitic near the margins.

A coarsening-upward package of clastic rocks overlies the carbonate-schist unit. It begins with interbedded quartzite and schist, followed by micaceous quartzite which grades upward into interbedded grit and quartzite. Gradual bedding at three locations indicates upright-facing units. Quartzites are pale grey, rarely pink and medium to fine grained. Schists contain matted clusters of centimetre-long amphibole porphyroblasts. A single dolomite layer occurs within micaceous quartzites low in the clastic sequence, while substantially more phyllitic carbonate is exposed near the top, where it is interbedded with quartz arenite, schist and grit. Grit beds commonly contain millimetre-size plagioclase and quartz grains in a finer grained, wacke matrix. The upper clastic unit consists of metre-scale interbedded quartzite, schist and grit and is distinctive due to its lack of carbonate. The unit coarsens upward, beginning with thin interbedded clean quartzite and schist, which become thicker bedded and interbedded with grit and micaceous quartzite. The section stopped 180 metres below the upper contact with the white marble of Downie Peak. Total thickness was calculated from airphotos.

The section east of Long Creek (LC) starts in quartz monzonite of the Long Creek stock and extends

east, up-structure but apparently down section, through approximately 4300 metres of rocks of the Lardeau Group, Badshot Formation (?), Hamill and possibly Horsethief groups. The section line crosses the Downie Creek fault which separates the Goldstream and Illecillewaet tectonic slices (Read and Brown, 1981).

Rocks of the Lardeau Group include a lower package of biotite-hornfelsed graphitic and pyrrhotitic phyllite, muscovite schist and interbedded marble (in part altered to calcisilicates), with lesser quartzose phyllite and micaceous quartzite. Sericite schist with lath-shaped porphyroblasts, micaceous quartzite and buff phyllitic carbonate comprise the structurally higher package. The garnet zone is projected into the section from 1 kilometre to the north, where it consists of thin-laminated siliceous spessartine-bearing graphitic phyllites, cherty and micaceous quartzites. The unit is fault bounded where it crops out (Figure 3). The structural top of the Lardeau schist-carbonate unit and the base of the Badshot Formation are intruded by dark green, massive to thinly foliated metadiorite sills (Figure 5). The greenstone is well cleaved and contains foliation-parallel patches of chloritic biotite crystal aggregates.

The structurally lowest carbonate of the Badshot Formation is a buff-weathering, fine-grained and thinly foliated dolomite. It is a pristine pisolitic dolomite above the metadiorite sill, where it mainly consists of concentric-layered, brown, ovoid pisoliths 5 millimetres in diameter within a white to buff cryptocrystalline dolomitic matrix (Plate 2). The excellent preservation of these primary sedimentary textures probably reflects a strain shadow developed adjacent to the massive diorite sill. The pisolites are good shallow-water paleoenvironmental indicators; pisoliths (pisolite-bearing carbonate) are currently believed to form by diagenesis in the vadose zone (Blatt *et al.*, 1980).

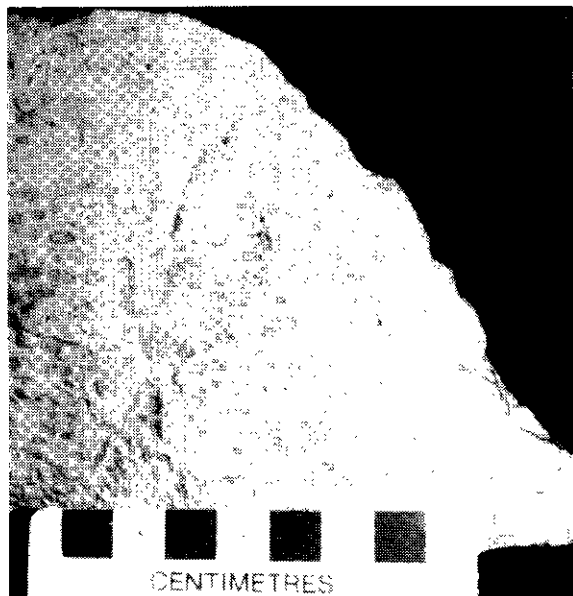


Plate 2. Well-preserved pisolitic dolomite from the section east of the Long Creek stock.

Quartz arenites, sericite schist and quartz-bearing dolomite are interbedded with the top of the dolomite. Thinly foliated, phyllitic dolomite, similar to the lowest dolomite, is gradational upwards into sericite schist, quartzite and phyllite, green-grey phyllite and light grey marble. We agree with Brown *et al.* (1978) that these rocks are probably Hamill Group, as shown on Figure 5. They are overlain, in turn, by a relatively thick unit of micaceous quartzite, quartz arenite, phyllite and grey marble, which may outline a synform, based on a repetition of stratigraphy (Figure 5). We also include this predominately quartzitic unit in the Hamill Group.

Overlying the grey marble (perhaps Mohican Formation of the Hamill Group), is a more heterogeneous package of sericite schist, quartzite, interbedded schist and quartzite, green metatuff and marble (Figure 5). Brown *et al.* (1978) assigned these rocks to the Horsethief Creek Group.

## INTRUSIONS

The Goldstream pluton is a complex of quartz monzonite sills and pendants of layered country rock. The intrusion consists of a mafic phase of hornblende-biotite quartz monzonite and a relatively younger, more felsic phase of biotite quartz monzonite. The margins of the intrusion are defined by east-west aligned hornfelsed or skarned pendants and inclusions of country rock. The inclusions show various stages of assimilation, but notably all are penetratively foliated. The age of the complex is unknown. A folded foliation in the quartz monzonite (Høy, 1979) has been interpreted to suggest a pre-phase 2 deformation, possible Devonian age for the intrusion. We feel that the presence of penetratively foliated country rock inclusions within the Goldstream intrusion suggests it postdated development of foliation and probably belongs to the Middle Jurassic suite of intrusive rocks.

The Adamant pluton, also east trending (Figure 3), is a composite body of hypersthene-augite monzonite with a hornblende-rich border (Fox, 1969). Foliation parallels enclosing Horsethief Creek metasediments and Fox suggests the body was emplaced prior to or during regional metamorphism and deformation. Concordant zircon ages (167-170 Ma; Shaw, 1980) have been interpreted to be synmetamorphic (Shaw, *op.cit.*); alternatively the ages may reflect a Middle Jurassic age for the pluton (Woodsworth *et al.*, 1991).

Younger(?), roughly circular stocks of mainly potassium feldspar porphyritic granite and quartz monzonite crosscut phase 2 structures and associated metamorphism. They are post-tectonic, undeformed intrusions of Middle Jurassic age and include the Fang pluton (168±2 Ma, Brown *et al.*, 1992), Pass Creek pluton (168±3 Ma, Brown *et al.*, 1992), the Downie Creek stock and Long Creek stock. Tungsten skarn mineralization occurs in calcareous country rocks adjacent to the Long Creek stock (Vanderpool, 1982).

## STRUCTURE

Earlier workers (Lane, 1977; Höy, 1979; Read and Brown, 1979) have suggested that second phase folds deform previously inverted stratigraphy and, in the Goldstream slice, strata occupy the inverted limb of an early nappe that has undergone two subsequent phases of deformation (Brown *et al.*, 1983). Phase 1 deformation has produced westerly verging kilometre-scale nappes and westerly directed thrust faults. The Scrip nappe (Raeside and Simony, 1983) and Carnes nappe (Brown and Lane, 1988) formed during this phase of pre-Middle Jurassic deformation. Upper age constraints on phase 1 deformation include a Middle Jurassic, 168 Ma date for the Pass Creek pluton which intrudes the upper limb of the Carnes nappe (Brown *et al.*, 1992). Map-scale phase 2 folds include the Downie Peak, Keystone and Standard antiformal west-verging structures. Phase 2 folds are tight to isoclinal, overturned to recumbent and characterized by axial plane schistosity which regionally dips either east, northeast or northerly. Axial surfaces plunge at moderate angles to the northeast. Phase 2 folding is synmetamorphic. Phase 3 folds are east-trending, open chevron and kink folds which deform  $S_2$  schistosity.

Major faults bound the study area and define the Goldstream slice. Along its western margin, the Monashee décollement and Columbia River fault zone separate the hangingwall Goldstream allochthon from the footwall rocks of the Monashee Complex. The eastern boundary of the allochthon is marked by the Downie Creek fault, a normal, east-side-down fault along its southern trace (Brown, 1991). North of Downie Creek, this structure curves west into the Goldstream valley and changes from an east-dipping to a north-dipping reverse fault (Goldstream River fault). East of the Long Creek stock, the bounding fault separates the Hamill Group from the Lardeau Group (Figure 3). However, we observed gradational contacts between these two groups, rather than a structural break, in section line LC, and question the location of the Downie Creek fault.

At Nichols Creek (north of the map area), the structure trends north again into the Columbia River fault zone (Read and Brown, 1981; Gibson and Höy, 1985). A less understood, sinuous north-trending structure divides the allochthon. Brown (1991) denotes it as the westerly directed Standard thrust fault. South of Goldstream River it is described as a pre- $S_2$  (?) slide fault (G. Gibson, personal communication, 1993).

## METAMORPHISM

Most of the Goldstream slice has undergone greenschist facies (chlorite zone) metamorphism, with local exceptions. Most significantly, rocks lying between Goldstream River and Downie Creek are

higher in grade, and range from the amphibolite facies to the biotite zone of greenschist facies. The elevated grade is probably related to intrusion of the late syn- $D_2$  to post- $D_2$  Goldstream pluton. Coarse, elongate porphyroblasts of fine-grained quartz and muscovite are a major constituent of many of pelitic schists in the Caribou Basin area. We interpret these as andalusite pseudomorphs, although Höy (1979) described them as possible kyanite pseudomorphs.

Pelitic schists around the Goldstream pluton are also characterized by coarse (up to 10 cm long), dark grey, flattened laths of an unknown mineral, thought to be either actinolite, andalusite or stibnomelane (Plate 3). It occurs with fine, millimetre-scale black actinolite randomly dispersed on  $S_2$  foliation planes. The crystal habit varies subtly from area to area and more than one mineral may be present.



Plate 3. Radiating clusters of elongate porphyroblasts on foliation surfaces of impure pelitic schist. These crystals may be actinolite.

## MASSIVE SULPHIDE DEPOSITS

Mineral deposits within the Goldstream allochthon include a wide spectrum of deposit types, from volcanogenic massive sulphide (the focus of this study) to lead-zinc carbonate replacement, tungsten-copper skarn, base and precious metal quartz veins, placer gold and placer concentrations of garnet. Although exploration on some of these deposits began before the turn of the century (e.g. Standard), the area remains under explored and highly prospective for volcanogenic massive sulphide targets.

Three copper-zinc massive sulphide deposits and one prospect occur within the study area (Figure 3, Table 1). To understand the setting of these deposits, stratigraphic sections were measured, or drill-core logged and samples collected for trace element geochemical analysis. Sections include the east wall of the Goldstream mine pit, the Standard Peak area

TABLE 1. MASSIVE SULPHIDE OCCURRENCES WITHIN THE STUDY AREA.

DEPOSIT (MINFILE)	TYPE	HOST	MINERALS	RESERVES
GOLDSTREAM (141)	Besshi VMS	dark graphitic sericite schists, green phyllite, chlorite schist (greenstone), serpentinite intrusions	po, sph, cp	1.436 mt @ 4.48% Cu, 3.03% Zn (News release, May 13, 1993)
MONTGOMERY (85)	Besshi VMS	calc-silicate, dark graphitic and cherty sericite schist	po, sph, cp	1 to 3.5 metres thick over 750 metre strike length (Campbell and Lewis, 1991)
RAIN (156)	Besshi VMS ?	black graphitic and cherty sericite schist	po, cpy	
STANDARD (166)	Besshi VMS	chlorite schist and talc-serpentine ultramafic rocks	py, po, cpy, sph	
C-1,2,3	stratabound	dark graphitic sericite schists, green phyllite	gl, sph	

VMS=volcanogenic massive sulphide,; cp=chalcopyrite, gl=galena, po=pyrrhotite, py=pyrite, sph=sphalerite

and drill core from the Rain property and Montgomery showing (1, 3, and SP, Figure 3).

### GOLDSTREAM MINE

Copper-zinc mineralization was discovered at Goldstream during construction of logging roads in 1972. Local prospectors Frank King, Gordon and Bruce Bried staked claims the following year and tested the showing with X-ray-drill holes and hand trenching. The Noranda Group acquired the property in 1975 and completed 8912 metres of diamond

drilling, outlining 3.175 million tonnes of ore grading 4.49 % copper, 3.24 % zinc and 20 grams per tonne silver. The portal was collared the next year and an adit driven south to the ore zone. Drifting proceeded east and west along the orebody and 40 underground diamond-drill holes were completed below the 700-metre level. The production decision was made in 1980 and the mine opened in 1983. Depressed metal prices forced closure less than a year later.

Bethlehem Resources Corporation and Goldnev Resources Incorporated acquired the Goldstream property from Noranda in 1989. Production began again in May 1991. The mine is currently producing

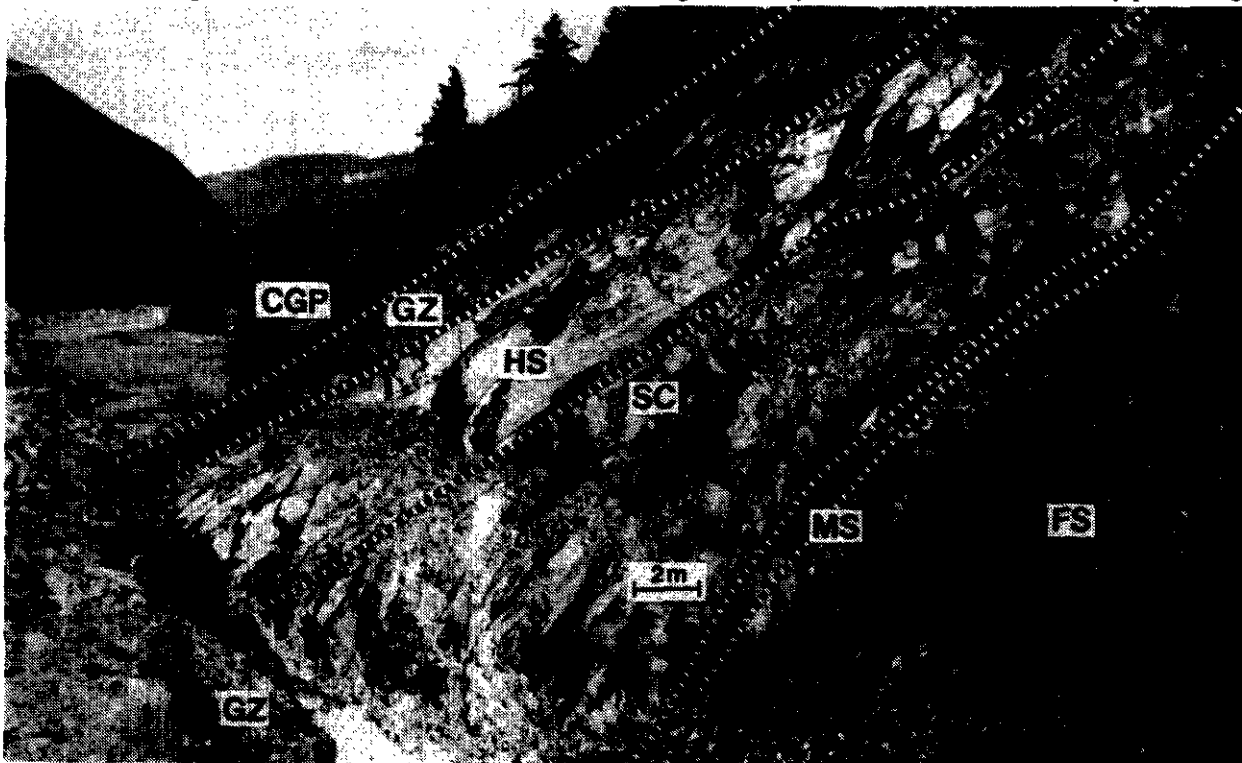


Plate 4. Goldstream mine open pit, viewed to the east. These rocks are described in the measured section of Figure 6. CGP=calcareous graphitic phyllite, GZ=garnet zone, HS=hangingwall schist, SC=silicified carbonate, MS=massive sulphides, FS=footwall schist.

at a rate of 1150 tonnes per day. Ore reserves are 1.436 million tonnes grading 4.48% copper and 3.03% zinc (News Release; Vancouver Stock Exchange, May 13, 1993).

The Goldstream deposit is within a mixed package of black graphitic and sericite schist, carbonate and less quartzite and greenstone. Approximately 50 metres of the mine sequence stratigraphy is exposed along the east wall of the open pit (Figure 6 and Plate 4). Strata dip moderately to steeply north into the east-trending pit; the sulphide horizon plunges gently northeast. Regional structures suggest the succession is inverted (Höy *et al.*, 1984), with the oldest rocks in the hangingwall.

The uppermost rocks in the open pit are tightly folded and faulted, black, thinly bedded, carbonaceous and quartzose phyllite, calcareous phyllite and phyllitic carbonate. Pyrrhotite is ubiquitous. The rocks are well indurated and contain quartz veinlets and augen. Five metres of dark green and mauve chlorite(?) -sericite schists underlie the dark, banded phyllite unit in gradational contact. The 'garnet zone' is a distinct brown-weathering, thin-bedded, but highly resistive siliceous unit. It contains rhythmic millimetre to centimetre-scale layers of graphitic, calcareous chert, chloritic phyllite and locally abundant spessartine garnet. Pyrrhotite occurs as wispy laminations and blebs and grunerite occurs in some dark siliceous layers (Höy *et al.*, 1984). The upper and lower contacts are gradational with quartzose phyllites and sericite-rich greenish and mauve schist. A 20-metre unit of mainly silver-weathering, mauve sericite-muscovite schist contains the massive sulphide layer. There is a 5-metre section of silicified interbedded marble, schist and quartzite, which contains disseminated pyrrhotite, chalcopyrite and sphalerite in the hangingwall of the massive sulphide layer. Sulphide concentration increases downwards toward the massive sulphide horizon, which is about 1.5 metres thick and consists of a disseminated sulphide zone (0.3 m), a quartz and chalcopyrite-rich zone (0.3 m) and a massive pyrrhotite, sphalerite and chalcopyrite zone. Footwall marble is a medium to dark grey, banded carbonate interbedded with rusty sericitic phyllite and quartz segregations. Massive to schistose fine-grained greenstone is exposed at the west end of the pit. The rock is composed of actinolite, chlorite, epidote and albite, and interpreted to be a basic volcanic unit (Höy *et al.*, 1984). It correlates with chlorite schist farther northwest, which may represent a thick intrusive body.

## **RAIN**

The Rain property is located between Standard and Murder creeks south of Downie Creek. It is underlain by Lardeau Group graphitic phyllite, sericite

schist and carbonate similar to the host stratigraphy at the Goldstream mine. Diamond drilling has intersected manganese-enriched, garnetiferous and sulphide-bearing zones that may correlate with the garnet zone at the Goldstream mine (C. Wild, personal communication, 1993). Two drill holes were logged from the 1992 drilling and limited surface mapping was completed.

Figure 7 illustrates the stratigraphy of drill holes 92RN-1 and 92RN-3. In hole 92RN-1 175 metres of dark and light grey, banded marble, graphitic marble and lesser calcisilicate structurally overlie 30 metres of dark calcareous phyllite and cherty phyllite. The calcareous rocks can be divided into an upper, relatively clean marble and lower graphitic marble and calcareous phyllite. The underlying dark phyllitic units contain massive sulphide lenses and disseminated sulphides, and a graphitic zone containing a few percent pink spessartine garnets to 2 millimetres diameter. Light brown to grey, biotite-quartz-sericite schist, metadiorite sills, and lesser calcisilicate layers and quartzite occupy the bottom of the section.

Light grey, banded marble also overlies graphitic dark phyllites in hole 92RN-3. The transition from marble to the graphitic phyllite is abrupt and marked by pyrrhotite lenses and a garnet zone in cherty, graphitic phyllite immediately below the contact. Rhythmic-layered centimetre-scale beds of graphitic phyllite and carbonate (calcareous phyllite), light grey, banded marble, and green sericite schist separate the upper garnet zone from another black, cherty graphitic phyllite which contains two narrow garnet zones. The remainder of the hole cuts a monotonous package of calcareous phyllite with layers of banded marble and minor dark phyllite. These carbonates contrast with the biotite-sericite schists which underlie the dark phyllite and garnet zone in hole 92RN-1 and make correlation of the two holes difficult. Attitudes of compositional layering relative to the core axis change frequently and probably reflect significant folding.

Dark calcareous and graphitic phyllite and sericite schist underlie the area of Murder Creek. Massive, light grey, banded marble forms the ridge to the west and structurally underlies the dark phyllites exposed in the creek. Thinly interbedded phyllite and carbonate correspond to the calcareous phyllite in the drill holes. Coarse disseminated, stratabound pyrite is common in some graphitic units and Wild (1990) describes a garnet zone within these rocks. The dark phyllite/sericite schist is strongly contorted adjacent to the contact with underlying marble and overprinted by a quartz vein stockwork. The contact appears to be faulted; if it is not, then the strata is opposite to that in the drill holes, and stratigraphy must turn over in an unrecognized fold between the creek and the holes. Massive quartzite appears to underlie the marble on the ridge west of Murder Creek.

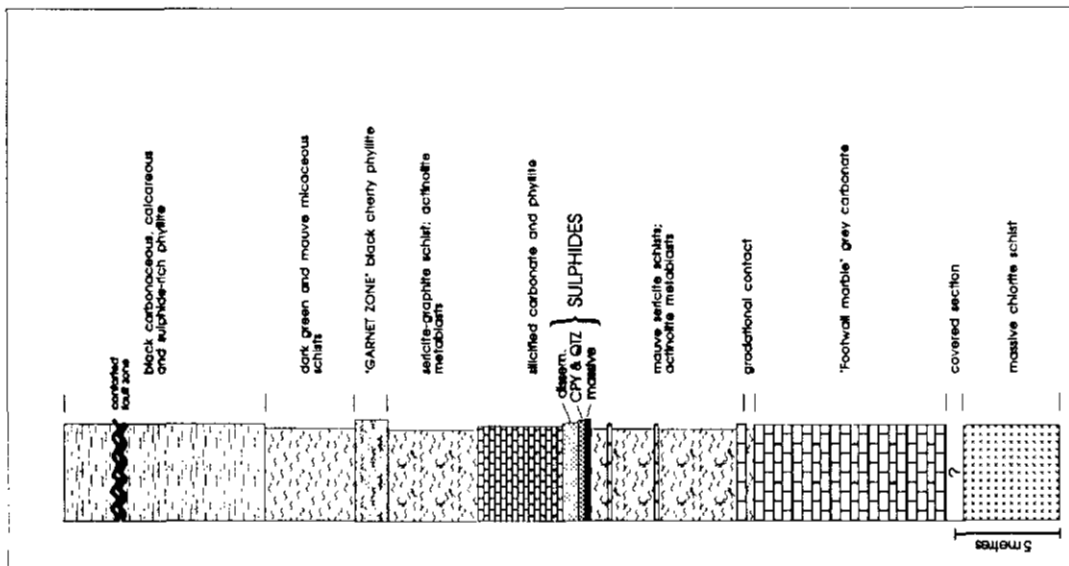


Figure 6. Measured stratigraphic section of the east wall of the Goldstream mine open pit

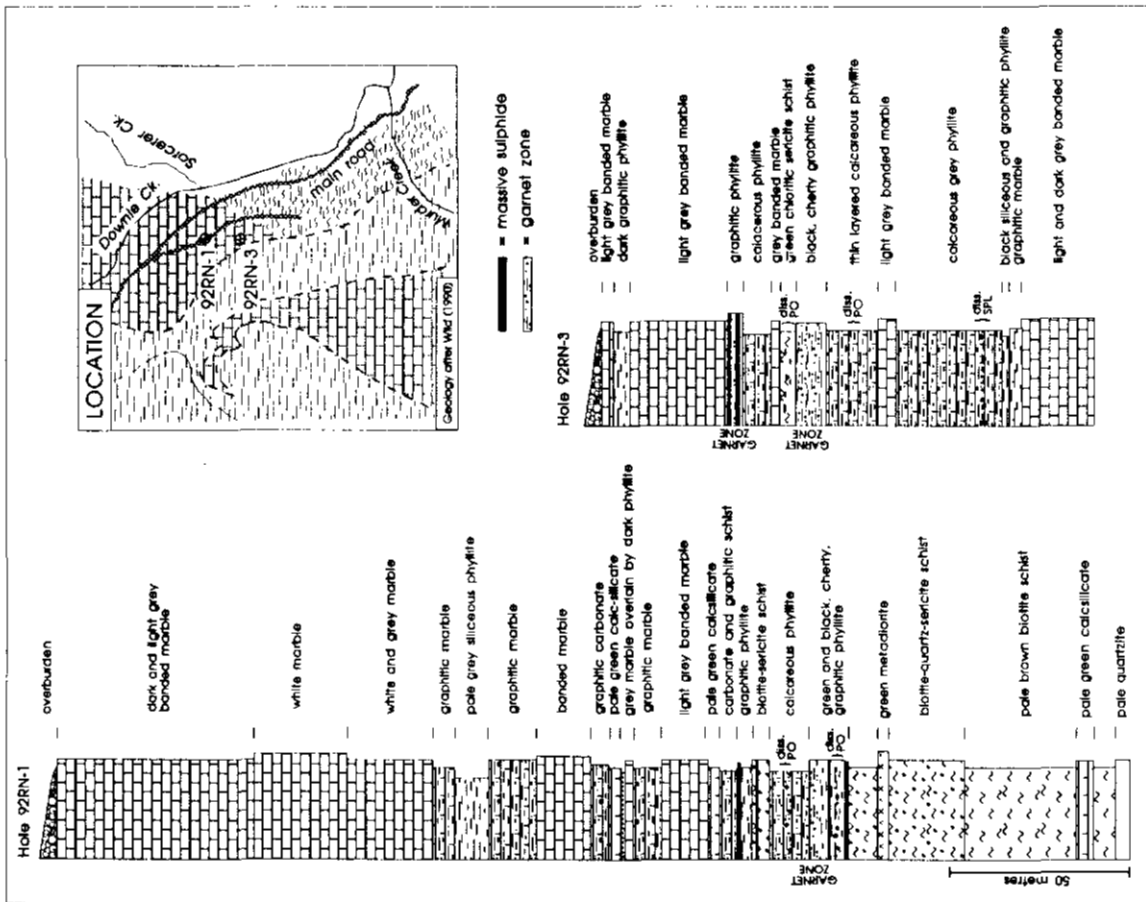


Figure 7. Stratigraphy of drill holes 92RN-1 and 92RN-3 on the Rain property between Standard and Murder creeks. PO=pyrrhotite, SPL=sphalerite.

## MONTGOMERY

The Montgomery property is located approximately 12 kilometres southeast of the Goldstream mine (Figure 3). The showings comprise a series of massive and disseminated sulphide lenses in micaceous quartzose schist and carbonaceous sericite-chlorite phyllite interlayered with carbonates. Felsite apophyses from the Long Creek stock crosscut the succession and skarn calcareous units. Sulphides have been traced intermittently by trenching for 770 metres (Schindler, 1982). The sulphides consist of several lenses of massive pyrrhotite up to 3 metres thick, with minor amounts of chalcopyrite, sphalerite and trace galena. The massive sulphide horizon contains clear, rounded fragments of quartz and dark green chlorite inclusions identical to Goldstream ore. Hangingwall rocks are quartz-rich graphitic and rusty weathering biotite-sericite schist that contain coarse stringers of chalcopyrite and pyrrhotite. The footwall to the sulphides is mafic chlorite-biotite-quartz schist and calcisilicate. Two diamond-drill holes were completed in October of 1990 (Campbell and Lewis, 1991) to test the down-dip extension of the massive sulphides exposed at the adit. The drill core was logged after visiting the adit and tracing out the sulphide horizons on surface (Figure 8). The holes penetrated a series of calcisilicate units within biotite-quartz-sericite schist. Massive sulphide horizons occur between felsite sills

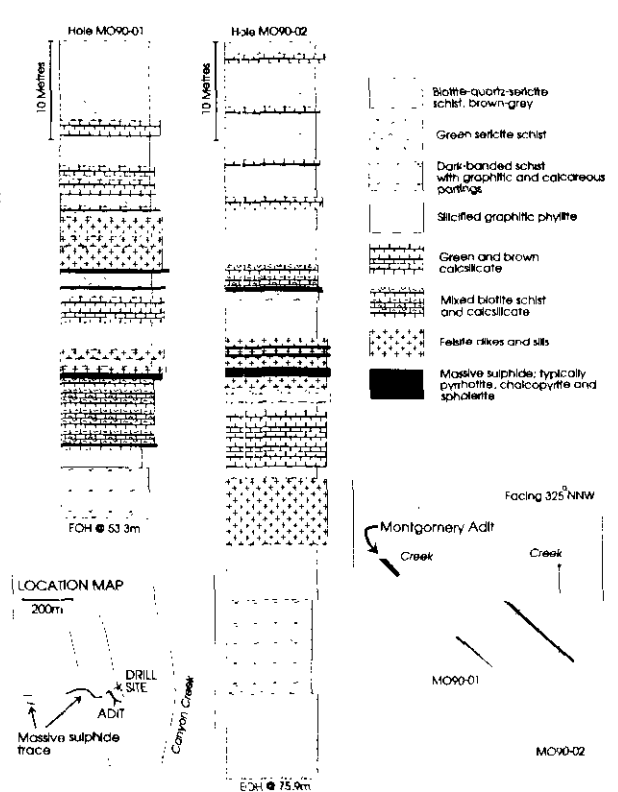


Figure 8. Stratigraphy of drill holes MO-90-01 and MO-90-02 on the Montgomery property between Canyon and Boulder creeks.

or within thinly intercalated biotite-schist and calcisilicate.

The host rocks are higher metamorphic-grade equivalent rocks to those at the Goldstream mine and Rain occurrence. They represent another mineralized horizon in the stratigraphy. Reconnaissance mapping in the Montgomery area identified a number of rusty horizons with pyrite-pyrrhotite and occasional chalcopyrite.

## STANDARD

The Standard showings are located on the east side of Standard Peak and consist of a series of discontinuous pyrrhotite-pyrite-chalcopyrite-sphalerite lenses in green volcanic-derived feldspathic sandstone and black graphitic phyllite. Sill-like bodies of serpentinite and talc schist intrude along the contacts of these units and are spatially associated with sulphide occurrences. The structure in the area consists of a north-plunging, east-dipping overturned antiform which repeats strata and sulphide lenses (Höy *et al.*, 1984). The sulphides are traceable intermittently for 1500 metres along strike. The stratigraphic position of several adits is shown on Figure 9. The rocks are correlated with basic metavolcanic rocks and phyllite of the upper Indus Formation (Brown *et al.*, 1983). Two stratigraphic sections containing sulphide occurrences, were measured on the east limb of the anticline. Figure 9 is a composite section of the west limb and structurally underlying rocks.

The symmetrical distribution of grey foliated carbonate, dark phyllite and chlorite schist around a 10-metre hinge zone of dark phyllite defines the Standard Peak antiform. The east limb is apparently thinned relative to the west. The west limb consists of 10 to 15 metres of grey foliated carbonate and about 5 metres of buff-weathering dolomite structurally underlain by 20 to 30 metres of dark phyllite. The dark phyllite is identical to black sericite schists interlayered with carbonate units at Keystone Peak, Downie Creek and Goldstream River. The most common unit at Standard Peak is massive chlorite schist, which underlies the dark phyllites on the west limb and overlies them on the east limb. In places the schist contains flattened gneissic fragments that may represent relict flow breccia. The chlorite schist contains thick intervals of black and green phyllite, feldspathic sandstone and volcanic wacke and rare medium-grained, foliated metadiorite bodies. It is structurally underlain to the west by grits and dark phyllites, followed by thinly bedded calcareous green-grey tuff and quartzofeldspathic psammitic schist. At least 5 metres of pink quartzite overlies the chlorite schist on the east limb.

Sill-like, boudinaged sheets of serpentinite and talc schist up to 30 metres thick intrude along or near the contacts of dark phyllite and massive chlorite schist and dark phyllite and carbonate. On the west

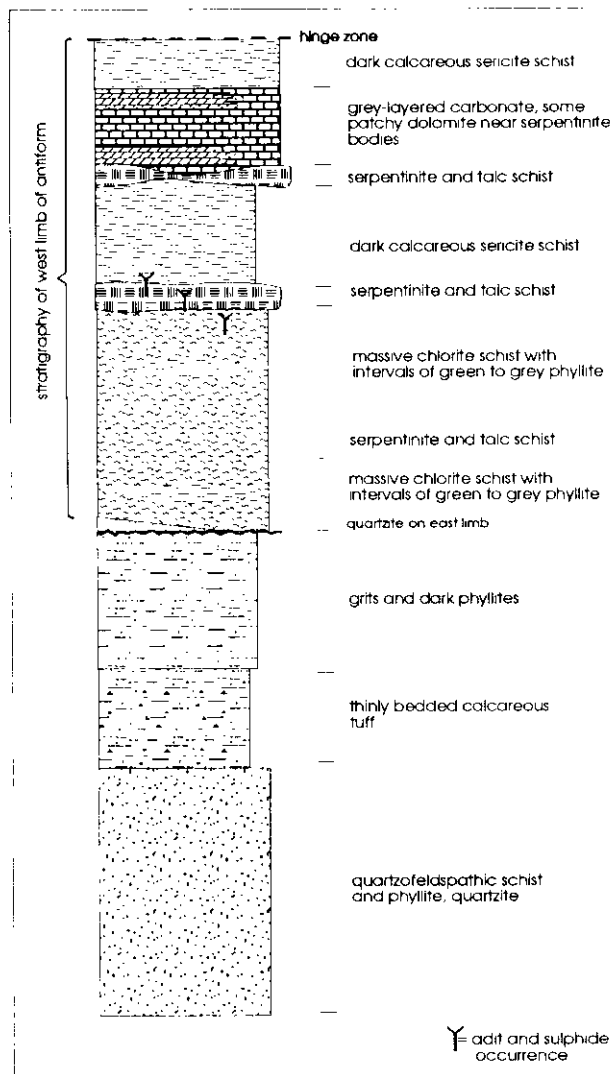


Figure 9. Schematic stratigraphy at Standard Peak. The succession above the Standard Peak thrust fault (heavy undulating line) forms the western limb of the north-trending and plunging Standard antiform.

limb of the antiform, the thickest and most continuous sill crosscuts foliation and stratigraphy. The other ultramafic bodies appear to be conformable. Similar ultramafic rocks occur in the Keystone area along the contact of chlorite schist and dark phyllite.

## OTHER MINERAL OCCURRENCES

North of the Goldstream River, three active placer gold mining operations were conducted, one on French Creek and two on McCulloch Creek. Gold-tungsten and base metal quartz veins that crosscut regional penetrative foliation occur in the headwaters of these two creeks. Stratabound mineralization was not encountered.

## EXPLORATION GUIDELINES

The copper-zinc deposits of the Goldstream area occur in dark graphitic schists, sericite schists and calcareous phyllites associated with actinolite schists (Table 2). They are interpreted to have formed in a rifted marginal or back-arc basin, in contrast with the numerous lead-zinc deposits which occur in platformal rocks of southeastern British Columbia (Höy, 1982). The copper-zinc deposits are similar to the Besshi-type deposits in Japan (Höy *et al.*, 1984; Höy 1991), which characteristically occur within either mafic volcanic rocks (typically tholeiitic) or terrigenous clastic rocks interlayered with flows or sills.

A number of diagnostic features characterize Besshi-type deposits (Slack, in press). Table 2 compares these features with those of massive sulphide deposits in the area. The features include: a generally sheet-like morphology within clastic marine sediments and minor mafic volcanic rocks; a sulphide mineralogy consisting of mainly pyrite and/or pyrrhotite, minor chalcopyrite and sphalerite and very little galena; relatively high contents of cobalt and Co/Ni ratios. In addition, distinctive wallrock lithologies including metachert, magnetite iron formation, coticule (fine-grained spessartine-quartz rock), tourmalinite, albitite and chlorite and sericite-rich schist are common (Slack, in press). These lithologies result from alteration by, or direct precipitation from, hydrothermal fluids related to ore deposition and therefore provide useful exploration targets.

In the Goldstream area, a distinctive spessartine-bearing, pyrrhotite-rich, thin-laminated graphitic coticule unit termed the 'garnet-zone' is associated with the massive sulphide layer. The garnet zone is interpreted to be a manganese-iron-rich seafloor hydrothermal precipitate; an exhalite (Höy *et al.*, 1984). Garnet zone also occurs at the Rain property and west of the Long Creek stock. No garnet zone has been recognized at the Standard or Montgomery showings. Chlorite and sericite-rich phyllites enclose the massive sulphide layer, and schists are common to all occurrences in the study area. Extrusive volcanic rocks, with the exception of the Standard area, are rare. Sparse, but ubiquitous greenstones are actinolite metadiorite dikes or sills, common features in Besshi deposits. Sulphide mineralogies are consistent but there is little data on cobalt and nickel contents for the ores.

Current stratigraphic correlations indicate the mineral deposits are hosted at three different horizons in the Index Formation. The Goldstream and Rain occur lowest and the Montgomery higher in a mainly sedimentary sequence. The Standard is hosted in a volcanic dominated sequence higher in the formation.

Tourmalinites are closely associated with coticules (garnet zone) in sequences containing clastic metasedimentary and mafic metavolcanic rock (Slack, 1993). The preservation of iron-manganese-boron

**TABLE 2. COMPARISON OF THE CHARACTERISTICS OF BESSHI TYPE DEPOSITS WITH MASSIVE SULPHIDE OCCURRENCES IN THE STUDY AREA.**

<b>BESSHI TYPE DEPOSITS (after Slack, in press)</b>	<b>GOLDSTREAM</b>	<b>MONTGOMERY</b>	<b>STANDARD</b>	<b>RAIN</b>
Sheet-like morphology, within clastic marine sediments, minor mafic volcanic rocks, or metadiorite sills	yes ? yes	yes no yes	yes yes yes	yes ? yes
Sulphide mineralogy of mainly pyrite and/or pyrrhotite, with minor chalcopyrite and sphalerite	yes	yes	yes	yes
High Co content, high Co/Ni ratio	no	?	?	?
Distinctive wall rocks:				
• metachert	yes	?	?	yes
• coticule (garnet zone)	yes	no	no	yes
• albite	?	?	?	?
• chlorite and sericite schist	yes	yes	yes	yes

exhalites may require venting into a thermally and chemically isolated brine pool (Slack *et al.*, 1993), conditions also necessary for sulphide accumulation. These garnet zones are important viable exploration targets. Work this summer measuring sections resulted in the discovery of a new garnet zone located midway between the Rain property and the Goldstream mine emphasizing the fact that the area is under explored and incompletely mapped.

The relationship of ultramafic rocks with the apparently stratabound, volcanogenic mineralization at Goldstream and Standard is not known. Both may be indicative of crustal-scale faults capable of tapping deep circulating hydrothermal fluids and ultramafic intrusive melts.

## **CORRELATIONS AND CONUNDRUMS**

The stratigraphy of the Goldstream slice of the Selkirk allochthon correlates well with lower and middle packages of the Eagle Bay assemblage in the Adams Lake-Clearwater area (Schiarizza and Preto, 1987). Correlations are based on the archaeocyathid-bearing limestones of the Tshinakin (Eagle Bay assemblage) and the Badshot limestone of the Kootenay Arc. Associated with the Tshinakin limestone are mainly calcareous chlorite schists derived from mafic volcanic rocks. Structurally below the limestone are siliceous and graphitic phyllite, limestone and quartzite (unit EBGs of Schiarizza and Preto, 1987) similar to the section exposed northwest of the Goldstream mine. The metasedimentary rocks of unit EBGs host lead-zinc-silver mineralization on Adams Plateau and similar stratabound showings (C-1, C-2 and C-3) have recently been discovered by

Bethlehem Resources Corporation in the above mentioned section. Polymetallic precious and base metal massive sulphide deposits (*e.g.* Homestake, Rea) are associated with Devonian-Mississippian intermediate to felsic volcanism in the Eagle Bay assemblage. These Kuroko-type deposits could be outboard, arc-equivalent deposits of the marginal basin Besshi-type Goldstream deposit and, if so, suggest the Goldstream deposit is Devonian in age as the preliminary lead-isotope model ages infer (Höy *et al.*, 1984).

The stratigraphy of the Lardeau Group has been studied in the type area by Smith and Gehrels (1992a) and correlated with Cordova Group and Bradeen Hill assemblage to the south, in northeastern Washington (Smith and Gehrels, 1992b). Their correlation suggests that the established stratigraphy of the Lardeau Group as defined by Fyles and Eastwood (1962) is inverted and suggest the Broadview Formation is the oldest and the Index Formation the youngest unit of the Lardeau Group. Devonian age fossils from the Bradeen Hill assemblage, correlative with the Index Formation, and the Early to Middle Ordovician Rb-Sr whole-rock isochron date from boulders of the Broadview Formation (Read and Wheeler, 1977) support this contention. Neither fossils nor contact relations which would permit addressing this aspect of the stratigraphy were recognized this year.

## **ACKNOWLEDGEMENTS**

The authors appreciate the invaluable logistical and geological assistance provided by Pat McAndless and Chris Wild of Bethlehem Resources Corporation.

Chris was particularly helpful in leading our frequent underground tours of the Goldstream mine. Gordon Gibson is thanked for his geological introduction to the area, tours and informative discussions. Field visits by Trygve Höy and Dave Lefebure contributed to our understanding of the geology and the depositional environments of volcanogenic deposits. Jim Patrick provided useful information on the mineralogy and history of the Groundhog Basin. The safe and friendly flying of Gerry Richard of Selkirk Mountain Helicopters is greatly appreciated. Reviews by Trygve Höy, John Newell and Brian Grant improved the manuscript.

## REFERENCES

- Blatt, H., Middleton, G. and Murray, R. (1980): Origin of Sedimentary Rocks; Prentice-Hall, New Jersey.
- Brown, R.L. (1991): Geological Map and Cross Section, Downie Creek Map Area (82 M/8) British Columbia; Geological Survey of Canada, Open File 2414.
- Brown, R.L. and Lane, L.S. (1988): Tectonic Interpretation of West-verging Folds in the Selkirk Allochthon of the Southern Canadian Cordillera; *Canadian Journal of Earth Sciences*, Volume 25, pages 292-300.
- Brown, R.L., Höy, T. and Lane L.S. (1976): Stratigraphy and Structure South of Goldstream River, Selkirk Mountains; in *Geological Fieldwork, 1976*, B.C. Ministry of Energy, Mines and Petroleum Resources, pages 17-22.
- Brown, R.L., Perkins, M.J. and Tippet, C.R. (1977): Structure and Stratigraphy of the Big Bend Area, British Columbia; in *Current Research, Part A, Geological Survey of Canada*, Paper 77-1A, pages 273-275.
- Brown, R.L., Tippet, C.R. and Lane, L.S. (1978): Stratigraphy, Facies Changes, and Correlations in the Northern Selkirk Mountains, Southern Canadian Cordillera; *Canadian Journal of Earth Sciences*, Volume 15, pages 1129-1140.
- Brown, R.L., Lane, L.S., Psutka, J.F. and Read, P.B. (1983): Stratigraphy and Structure of the Western Margin of the Northern Selkirk Mountains: Downie Creek Map Area; in *Current Research, Part A, Geological Survey of Canada*, Paper 83-1A, pages 203-206.
- Brown, R.L., McNicoll, V.J., Parrish, R.R. and Scammell, R.J. (1992): Middle Jurassic Plutonism in the Kootenay Terrane, Northern Selkirk Mountains, British Columbia; in *Radiogenic Age and Isotopic Studies: Report 5; Geological Survey of Canada*, Paper 91-2, pages 135-141.
- Campbell, R.B. (1972): Geological Map of part of the Southeastern Canadian Cordillera; in *Structural Styles of the Southern Canadian Cordillera, XXIV International Geological Congress, Field Excursion X01-A01, Figure 2*.
- Campbell, I. and Lewis, L. (1991): Assessment Report on the R and W Claim, Revelstoke, British Columbia; *B.C. Ministry of Energy, Mines and Petroleum Resources*, Assessment Report 20 997.
- Colpron M. and Price, R.A. (1992): Preliminary Results on the Stratigraphy and Structure of the Lardeau Group in the Illecillewaet Synclinorium, Western Selkirk Mountains, British Columbia; in *Current Research, Part A, Geological Survey of Canada*, Paper 92-1A, pages 157-162.
- Devlin, W.J. (1986): Geologic and Isotopic Studies related to Latest Proterozoic - Early Cambrian Rifting and Initiation of a Passive Continental Margin, Southeastern British Columbia and Northeastern Washington, U.S.A.; unpublished Ph.D. thesis, *Columbia University*, New York.
- Fox, P.E. (1969): Petrology of the Adamant Pluton, British Columbia; *Geological Survey of Canada*, Paper 67-61.
- Franzen, J.P. (1974): Structural Analysis in the Selkirk Fan Axis near Argonaut Mountain, Southeastern British Columbia; unpublished M.Sc. thesis, *Carleton University*, Ottawa, 55 pages.
- Fritz, W.H., Cecile, M.P., Norford, B.S., Morrow, D. and Geldseltzer, H.H.J. (1991): Cambrian to Middle Devonian Assemblages; in *Geology of the Cordilleran Orogen in Canada*, Gabrielse, H. and Yorath C.J., Editors, *Geological Survey of Canada*, Geology of Canada, No. 4, pages 152-218.
- Fyles, J.T. and Eastwood, G.E.P. (1962): Geology of the Ferguson Area, Lardeau District, British Columbia; *B.C. Ministry of Energy, Mines and Petroleum Resources*, Bulletin 45.
- Gibson, G. (1989): Geological and Geochemical Report on the Brew Property; *B.C. Ministry of Energy, Mines and Petroleum Resources*, Assessment Report 19 580.
- Gibson, G. and Höy, T. (1985): Rift, a Zinc-Lead Massive Sulphide Deposit in Southeastern British Columbia, (82M/15); in *Geological Fieldwork 1984*, *B.C. Ministry of Energy, Mines and Petroleum Resources*, Paper 1985-1, pages 105-119.
- Gibson, G. and Höy, T. (in press): Geology of the Columbia River - Big Bend area, NTS 82M; *B.C. Ministry of Energy, Mines and Petroleum Resources*, Mineral Potential Map 82 M.
- Gunning, H.C. (1929): Lardeau Map-area, British Columbia, Mineral Deposits; *Geological Survey of Canada*, Memoir 161.
- Hicks, K.E. (1982): Geology and Mineralogy of the "Rift" Zinc-Lead Massive Sulphide Deposit, Southeastern British Columbia; unpublished B.Sc. thesis, *The University of British Columbia*, 55 pages.
- Höy, T. (1979): Geology of the Goldstream Area; *B.C. Ministry of Energy, Mines and Petroleum Resources*, Bulletin 71.
- Höy, T. (1982): Stratigraphic and Structural Setting of Stratabound Lead-Zinc Deposits in Southeastern B.C.; *Canadian Mining and Metallurgical Bulletin*, Volume 75, pages 114-134.
- Höy, T. (1991): Volcanogenic Massive Sulphide Deposits in British Columbia; in *Ore Deposits, Tectonics and Metallogeny in the Canadian Cordillera*, *B.C. Ministry of Energy, Mines and Petroleum Resources*, Paper 1991-4, pages 89-123.
- Höy, T., Gibson, G. and Berg, N.W. (1984): Copper-Zinc Deposits Associated with Basic Volcanism, Goldstream Area, Southeastern British Columbia; *Economic Geology*, Volume 79, pages 789-814.
- Lane, L.S. (1977): Structure and Stratigraphy, Goldstream River - Downie Creek Area, Selkirk Mountains, British Columbia; unpublished M.Sc. thesis, *Carleton University*, Ottawa, 140 pages.
- Lane, L.S. (1984): Deformation history of the Monashee Décollement and Columbia River fault zone, British Columbia; unpublished Ph.D. thesis, *Carleton University*, Ottawa.
- Raeside, R.P. and Simony, P.S. (1983): Stratigraphy and Deformational History of the Scrip Nappe, Monashee Mountains, British Columbia; *Canadian Journal of Earth Sciences*, Volume 20, pages 639-650.
- Read, P.B. and Brown, R.L. (1979): Inverted Stratigraphy and Structures, Downie Creek, Southern British Columbia; in *Current Research, Part A, Geological Survey of Canada*, Paper 79-1A, pages 33-34.

- Read, P.B. and Brown, R.L. (1981): Columbia River Fault Zone: Southeastern Margin of the Shushwap and Monashee Complexes, Southern British Columbia; *Canadian Journal of Earth Sciences*, Volume 18, pages 1127-1145.
- Read, P.B. and Wheeler, J.O. (1977): Geology Lardeau, West-half Map Area and Marginal Notes, Revised Edition; *Geological Survey of Canada*, Open File 432, 1:125 000 map.
- Schiarizza, P. and Preto, V.A. (1987): Geology of the Adams Plateau - Clearwater - Vavenby Area; *B.C. Ministry of Energy, Mines and Petroleum Resources*, Paper 1987-2.
- Schindler, J.N. (1982): Geological and Geochemical Report on the Peak Claims, Goldstream River Area, Revelstoke Mining Division, *B.C. Ministry of Energy, Mines and Petroleum Resources*, Assessment Report 10 180.
- Shaw, D. (1980): A Concordant Uranium-Lead Age for Zircons in the Adamant Pluton, British Columbia; in Rubidium-Strontium and Uranium-Lead Isotopic Age Studies, Report 3; *Edited by W.D. Loveridge in Current Research, Part C, Geological Survey of Canada*, Paper 80-1C, pages 243-246.
- Slack, J.F. (in press): Descriptive and Grade-Tonnage Models for Besshi-Type Massive Sulphide Deposits; in Mineral Deposit Models, *Geological Association of Canada*.
- Slack, J.F. (1993): Models for Tourmaline Formation in the Middle Proterozoic and Purcell Supergroups (Rocky Mountains) and their Exploration Significance; in Current Research, Part E; *Geological Survey of Canada*, Paper 93-1E, pages 33-40.
- Slack, J.F., Palmer, M.R., Stevens, B.P.J. and Barnes, R.G. (1993): Origin and Significance of Tourmaline-rich Rocks in the Eroken Hill District, Australia; *Economic Geology*, Volume 88, pages 505-542.
- Smith, M.T. and Gehrels, G.E. (1992a): Structural Geology of the Lardeau Group near Trout Lake, British Columbia: Implications for the Structural Evolution of the Kootenay Arc; *Canadian Journal of Earth Sciences*, Volume 29, pages 1305-1319.
- Smith, M.T. and Gehrels, G.E. (1992b): Stratigraphic Comparison of the Lardeau and Cordova Groups: Implications for the Structural Evolution of the Kootenay Arc; *Canadian Journal of Earth Sciences*, Volume 29, pages 1320-1329.
- Vanderpool, W. (1982): Downie Creek Property; *B.C. Ministry of Energy, Mines and Petroleum Resources*, Assessment Report 11164.
- Walker, J.F. and Bancroft, M.F. (1929): Lardeau Map-area, British Columbia, General Geology; *Geological Survey of Canada*, Memoir 161, pages 17-142.
- Wheeler, J.O. (1963) Rogers Pass Map-area, British Columbia and Alberta (82 N West Half); *Geological Survey of Canada*, Paper 62-32.
- Wheeler, J.O. (1965): Big Bend Map-area, British Columbia (82 M East Half); *Geological Survey of Canada*, Paper 64-32.
- Woodsworth, G.J., Anderson, R.G. and Armstrong, R.L. (1991): Plutonic regimes; in Geology of the Cordilleran Orogen in Canada, Gabrielse, H. and Yorath C.J., Editors, *Geological Survey of Canada*, Geology of Canada, No. 4, pages 491-531.
- Wild, C.J. (1990): Geological and Geochemical Report on the Rain 1-17 Mineral Claims; *B.C. Ministry of Energy, Mines and Petroleum Resources*, Assessment Report 20 628.

## NOTES

## REGIONAL AND ECONOMIC GEOLOGY OF THE TULSEQUAH RIVER AND GLACIER AREAS (104K/12 & 13)

By M. G. Mihalynuk, M. T. Smith, K.D. Hancock and S. Dudka

**KEYWORDS:** Regional geology, Stikine assemblage, Whitewater metamorphic suite, Boundary Ranges metamorphic suite, Stuhini, Laberge, Sloko, Llewellyn fault, Tulsequah Chief, Polaris-Taku, Big Bull, volcanogenic massive sulphide, skarn, copper, zinc, gold

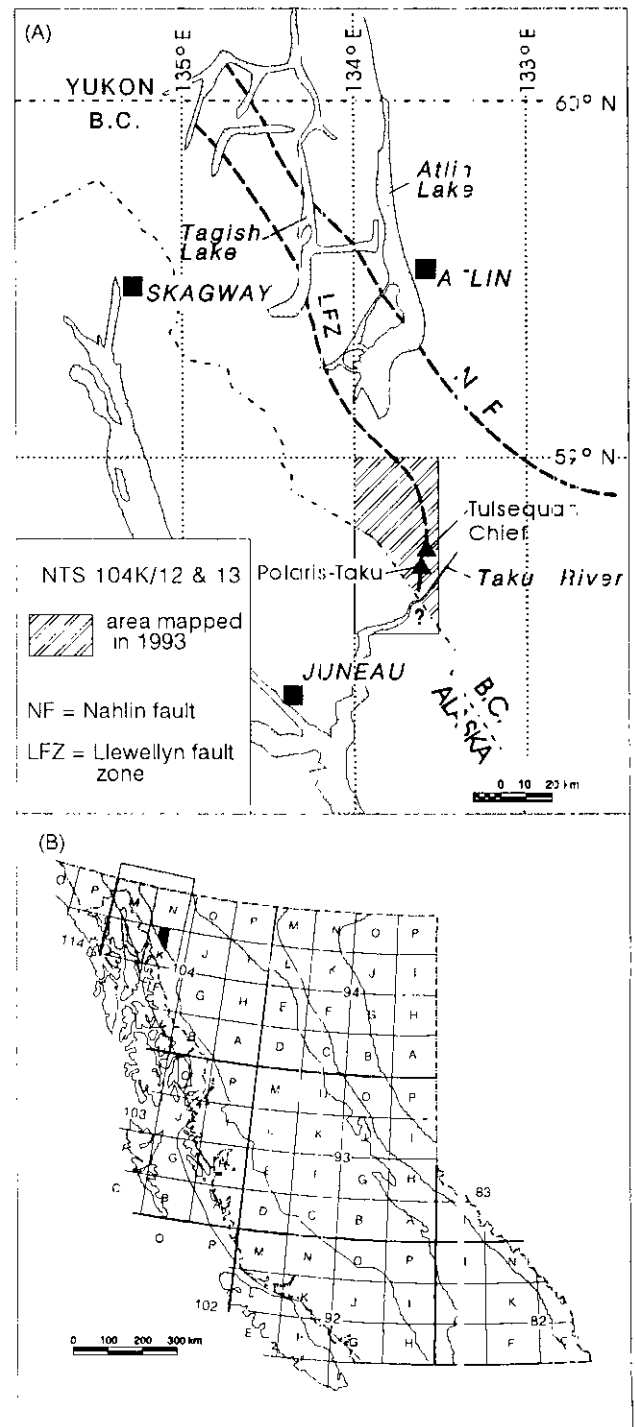
### INTRODUCTION

Geological mapping in 1993 expanded 1991 reconnaissance surveys of NTS map sheets 104K/12 and 13 (Smith and Mihalynuk, 1992; Figure 1). Mapping of both quadrangles was completed at 1:50 000 scale during a 2-week field season in 1992 and a 7-week field season in 1993, aided by compilation of previous industry work in 104K/12. Objectives of 1993 fieldwork included:

- Determination of the age(s), regional extent and stratigraphy of the Paleozoic northern Stikine assemblage, with identification and correlation of key mineralized intervals.
- Identification of a southern continuation of the Llewellyn gold province at the transition between Stikinian and metamorphosed rocks to the west.
- Determination of mesothermal gold potential in veins associated with metamorphosed tuff and ultramafic pods, analogous to the Polaris-Taku deposit, and of the age and nature of such mineralization.
- Investigation of associations between samples collected in 1991 yielding anomalous gold analyses and their apparent association with east-west cross-faults, age of motion on these faults, and identification of other examples elsewhere in the map area.
- Evaluation of the mineral potential of widespread Sloko Group volcanic strata and structures which may focus hydrothermal mineralization.

Maps produced during this study are designed to aid exploration, guide future land use and resource management decisions and address public questions. This paper focuses on: lithological packages not previously recognized or fully described, or which differ significantly from correlative strata elsewhere; structures that affect them; and their mineral potential.

Figure 1. A) Location of map area with respect to major geographic and geological features in northwest British Columbia and adjacent Alaska. B) location in NTS coordinate system.



## PREVIOUS WORK

Mineral exploration in the area dates back to at least 1924 with the discovery of the Tulsequah Chief deposit. However, systematic regional mapping was not begun until Kerr's investigations in 1930 and 1932 (Kerr, 1931a,b, 1948). In 1958 to 1960 Souther (1971) completed 1:250 000-scale mapping of the Tulsequah area. Geological mapping since that time has been primarily restricted to company reports with limited distribution. Maps produced by Cominco Ltd. (Payne and Sisson, 1988) cover a large part of 104K/12. This work was based in part on regional surveys by Anglo Canadian Mining Corporation (Payne *et al.*, 1981), a compiled version of which was published by Nelson and Payne (1984).

Recent advancements in understanding of the Stikine assemblage have arisen from regional mapping studies to the south, in the Tatsamenic Lake and Forest Kerr areas by Brown *et al.* (1991), Bradford and Brown (1993, and references therein) and Logan and Drobe (1993).

## LOCATION, PHYSIOGRAPHY AND ACCESS

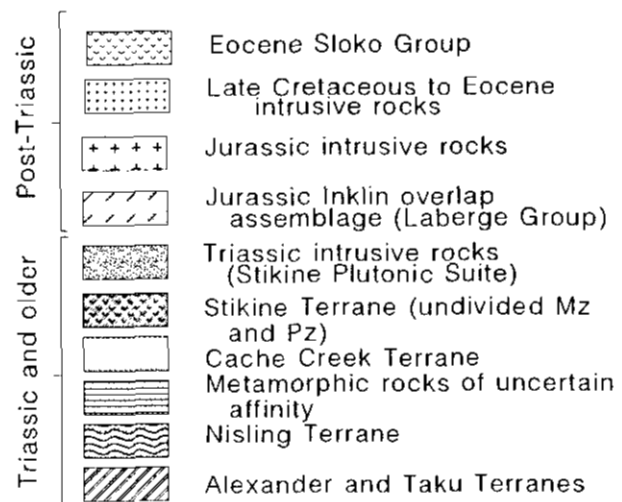
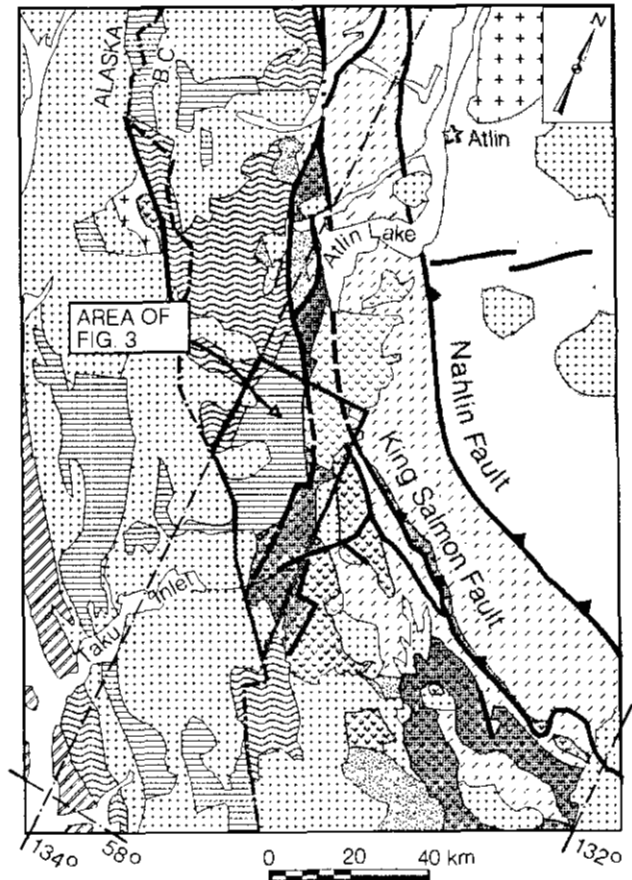
The Tulsequah River (104K/12) and Tulsequah Glacier (104K/13) map areas cover about 1300 square kilometres of the Coast Mountains, centred 90 kilometres east of Juneau, Alaska and 100 kilometres south-southwest of Atlin, British Columbia (Figure 1). The map area lies mainly north of the steep-sided Taku River valley. More gentle and drier Stikine Plateau uplands flank the area to the east. Most of the area is rock or forest, with roughly 5% outcrop in forested areas. Large covered areas are restricted to ice cover, river bottoms and swamp which collectively amount to about 30% of the area. Fieldwork in general is hampered by steep topography, snow and ice cover and poor weather, but the summer of 1993 was unusually hot and dry, resulting in a low snow pack and better exposure than usual.

Access is easiest by fixed-wing aircraft from Atlin or Juneau. Two airstrips are serviceable. A gravel strip is located northwest of the confluence of the Taku and Tulsequah rivers, and will accommodate a DC-3 or Caribou aircraft, but is subject to flooding two or more times each summer. A shorter strip at the Polaris-Taku minesite is less flood prone, but has a difficult approach and will accommodate only small aircraft. A few short road segments were built during development and production years of the Tulsequah Chief and Polaris-Taku mines, but all are at least in part washed out and overgrown, and none are linked to the provincial road network. Travel from the airstrips to other parts of the map area is by helicopter. Helicopters are intermittently based in the Tulsequah valley, but otherwise must be chartered from Atlin or Juneau.

Figure 2. Simplified geologic map of the Atlin and Tulsequah area after Wheeler *et al.* (1989), showing major faults and lithotectonic elements. The Tulsequah map area straddles parts of the Jurassic Inklin overlap assemblage, Stikine Terrane, and metamorphic rocks of mixed arc and siliciclastic affinity and uncertain (possibly Yukon-Tanana) terrane assignment.

## GENERAL GEOLOGIC AND TECTONIC SETTING

The Tulsequah River and Tulsequah Glacier area is one of extreme geological diversity and structural complexity resulting from the juxtaposition and deformation of several Mesozoic to Paleozoic and older tectonostratigraphic terranes (Figure 2). Subsequent intrusion by Cretaceous-Tertiary Coast plutons and burial by Tertiary volcanic rocks complicate investigations into the nature of terranes and their plate tectonic contexts. In northwestern British Columbia and Yukon these studies are further hampered by a proliferation of nomenclature.



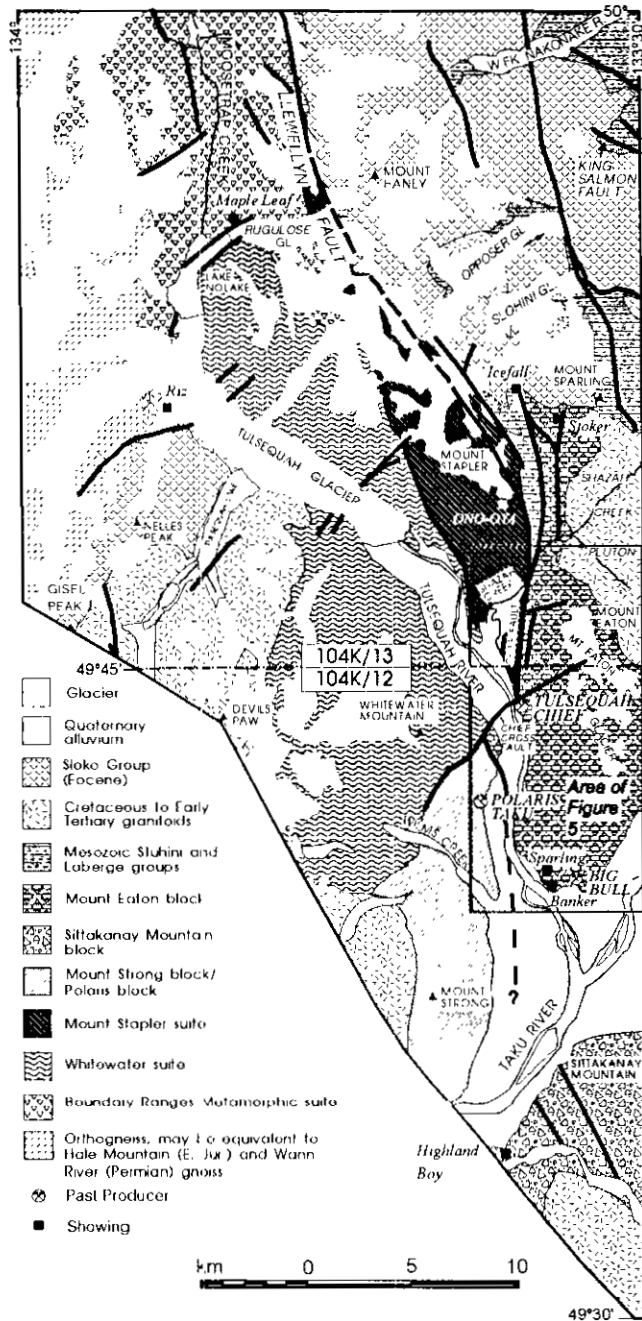


Figure 3. Simplified geological map of the Tulsequah area, showing major Mesozoic and Paleozoic lithotectonic assemblages, Late Cretaceous and Tertiary volcanic and intrusive rocks, faults (thick lines) and the locations of past-producing mines and significant showings. Geology simplified from 1993 British Columbia Geological Survey mapping, Nelson and Payne (1984), and Smith and Mihalyuk (1992).

Nevertheless, recognition of terrane affiliation and context are important keys to understanding regional metallogenesis, and terrane assignments are made here.

A thorough treatment of the subject is, however, beyond the scope of this paper. Interested readers are referred to a pragmatic view of terranes in the Yukon by Mortensen (1992). Terranes shown on Figure 2 are modified from Wheeler *et al.* (1991) and Mortensen (1992).

The southern extension of the Llewellyn fault (known locally as the Chief fault), a major tectonic boundary in northern British Columbia, divides pre-Tertiary rocks in the map area into metamorphosed rocks of presumed Paleozoic and older age, which underlie the southern and western half of the area, and weakly metamorphosed upper Paleozoic and Mesozoic rocks, which underlie the eastern half (Figure 3). West of the fault, three suites of rocks are recognized, divided on the basis of lithologic associations and degree of deformation (Figure 4). From west to east, corresponding with decreasing metamorphic grade and degree of deformation and variation from predominantly basinal to predominantly arc character, they are: the **Whitewater suite** (or metamorphic suite, informal) which refers to a distinctive package of amphibolite-grade quartz-rich graphitic schist, quartzite, metabasite and ultramafite, that may be correlative with parts of the Yukon-Tanana Terrane having continental margin affinity; the **Boundary Ranges suite** (or metamorphic suite; Mihalyuk and Rouse, 1988), consisting of schists of volcanic and sedimentary origin; and the **Mount Stapler suite**, a low-grade package which shares some characteristics with both the Whitewater and Boundary Ranges suites and locally can be demonstrated to be gradational into both.

East of the Llewellyn fault, Paleozoic rocks are assigned to the **Stikine assemblage** (Monger, 1977), a low-grade package of middle to upper Paleozoic volcanic arc rocks which form the basement to the Stikine arc and host the Tulsequah Chief and other volcanogenic massive sulphide deposits in the area (Figures 3 and 4). Building on the work of Nelson and Payne (1984), the Stikine assemblage is further divided into three structural-stratigraphic blocks. These are separated by large valleys (and known or suspected faults), but share important lithologic elements. **Mount Eaton block** lithologies are most clearly correlative with *bona fide* Stikine assemblage to the south (Brown *et al.*, 1991). More deformed, but obviously equivalent strata comprise the **Sittakanay block**. While Nelson and Payne did not include the rocks on Sittakanay Mountain with those in the Mount Eaton block, they did acknowledge their lithologic similarities; we believe them to be correlative on this basis. **Mount Strong block** rocks are of more questionable affinity. They are dominantly sedimentary in character and are here interpreted to be a distal equivalent of the other blocks, but with uncertainty as to the position of the Mount Strong block with respect to the trace of the Llewellyn fault, this correlation is tentative.

Mesozoic rocks include volcanic and volcanogenic rocks of the Upper Triassic Stuhini Group, an arc assemblage of the Stikine Terrane, and Lower to Middle Jurassic sedimentary rocks of the Laberge Group, an overlap assemblage that straddles the Stikine and other inboard terranes (Figures 2 and 3).

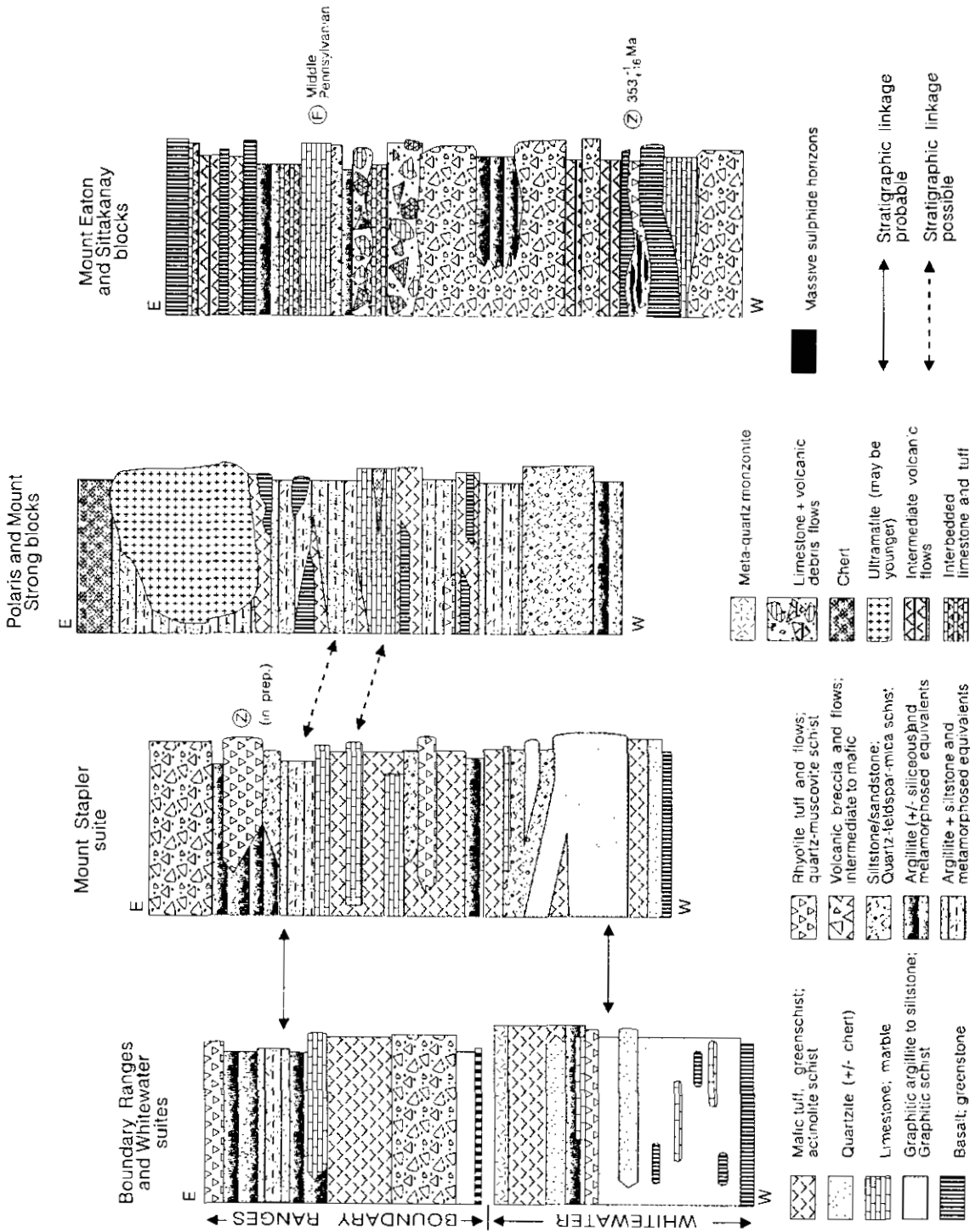


Figure 4. Pseudo-stratigraphic columns for the major Paleozoic lithologic suites in the Tulsequah area. With regard to columns 1-3, age and facies are uncertain and structural disruption and metamorphic recrystallization are significant, thus the columns are intended only to give the reader an estimate of the relative proportions of lithologic types. Column 4 (Mount Eaton formation) is a more accurate representation of the stratigraphic section. Section thicknesses are on the order of a few kilometres.

## METAMORPHIC SUITES

Metamorphic suites described here grossly conform to a west to east progression from higher grade, lower structural and stratigraphic(?) position to structurally higher and lower grade rocks interpreted to be some of the youngest metamorphic units. Emphasis is placed on units that have not been described previously; detailed descriptions of the Boundary Ranges suite can be found in Mihalynuk *et al.* (1989).

### WHITEWATER METAMORPHIC SUITE

The name "Whitewater suite" is given to a distinctive lithologic association formerly mapped by Souther (1971) as "undifferentiated schist and gneiss of pre-Triassic age". It consists of a belt of regionally metamorphosed rocks which extends from Rugulose glacier (104K/13) to Wilms Creek (104K/12), composed of quartz-rich graphitic schist with intercalated quartzite and metabasite, with minor marble, quartzofeldspathic schist (metarhyolite?), monzonitic orthogneiss and variably serpentized ultramafite. The Whitewater suite is exposed in a north-plunging anticlinorium and generally increases in metamorphic grade and degree of recrystallization to the south. Regional metamorphism is overprinted by contact metamorphism near large plutons.

#### GRAPHITIC SCHIST

Most characteristic of the Whitewater suite is an extensive unit consisting of bright orange-weathering, quartz-rich graphitic schist. In most places the unit contains conspicuous, black spessartine garnet (manganiferous) porphyroblasts which display a pronounced {110} parting, and locally feldspar porphyroblasts, which may reach 2 to 3 centimetres in diameter. More than 60% of the rock is composed of ribbon quartz. Biotite and muscovite occur in subequal amounts up to 30% combined. Plagioclase and graphite are the remaining major components. Pyrrhotite is a significant accessory in quantities of 1 to 3%; sparse tourmaline prisms are also typical. At a few localities fibrolite has been tentatively identified in hand samples. Minor bands of dark grey to tan, banded carbonate are common, but rarely exceed 3 metres in thickness and comprise less than 1% of the section. These are associated with talc-tremolite schist and serpentinite (see below).

Widespread hornfelsing of the unit tends to destroy its schistose fabric, producing a finer grained, gneissic rock with a graphite component that is much less apparent.

#### METABASITE

Metabasite is second in abundance to graphitic schists within the Whitewater suite. It is generally gneissic to massive, dark green and commonly mottled

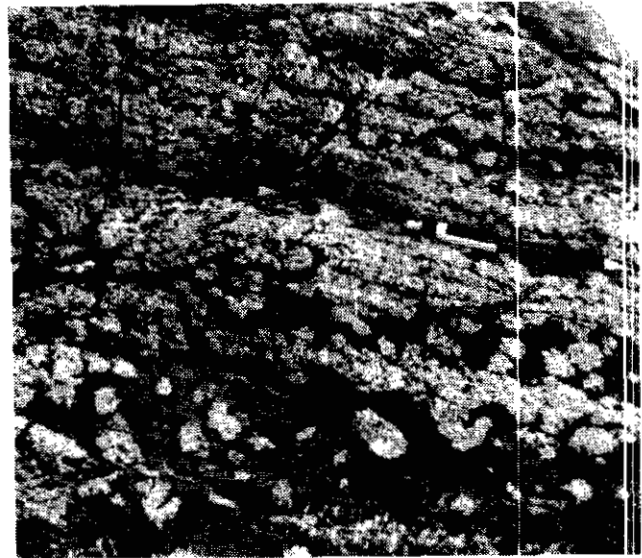


Plate 1. Conspicuous feldspar poikiloblasts developed in metabasite unit of the Whitewater suite.

with white-weathering plagioclase poikiloblasts up to 5 centimetres across (Plate 1). Metamorphism varies from transitional greenschist-amphibolite grade to amphibolite grade. Respective metamorphic mineral assemblages, in decreasing order of abundance are: actinolite-biotite±chlorite-feldspar-quartz-epidote±garnet and hornblende-biotite-plagioclase-quartz-diopside-garnet-epidote. Ferromagnesian minerals comprise 40 to 60% of the rock. Except for feldspar poikiloblasts, these rocks are generally medium grained. Locally, contact metamorphism has resulted in coarsely recrystallized rocks with plumose actinolite commonly up to 10 centimetres long.

#### QUARTZITE TO QUARTZ-FELDSPAR-MUSCOVITE-GARNET SCHIST

Quartzite and quartz-feldspar-muscovite-garnet schist and gneiss occur as bands up to 100 metres thick within the graphitic schist unit. Quartz content is typically greater than 90% with some layers of nearly pure, medium-grained quartz. Feldspar poikiloblasts may comprise over 10%, and in places they take the form of remnant granules or pebbles, but no unequivocal conglomeratic facies have been found. Muscovite is common in abundances of 5 to 10%; tourmaline and clear, red garnet are common accessories up to 1 centimetre in size. Most quartzite bands are discrete units, while others have gradational contacts with enclosing graphitic schist. In thin section the quartz and micas are highly strained, lacking any annealed texture. Garnets are xenoblastic and commonly fractured.

Quartzite layers are most abundant near the contact with the metabasite division, suggesting some common genesis. Gradational contacts with graphitic schist point to remnant depositional contacts. Relict feldspathic "granules" and consistent occurrence of tourmaline, probably as recrystallized detrital grains, points to a clastic protolith with a quartz-rich provenance.

## **TALC-TREMOLITE-MAGNESITE(?) SCHIST AND SERPENTINIZED ULTRAMAFITE**

Bright green and white-weathering talc-tremolite±magnesite schist and associated, variably serpentinitized, dark green and red-weathering ultramafite are conspicuous, but relatively minor components of the Whitewater suite. Together they comprise less than 0.1% of the suite, normally as lenses and pods less than a metre thick, although rarely to 20 metres thick, within the graphitic schist unit. Bright green tremolite-actinolite commonly occurs as very coarse intergrown prisms randomly aligned within foliation planes. Talc and minor magnesite(?) comprise the matrix of the rock, commonly with sparse, but well-crystallized chromium mica.

Podiform serpentinite bodies occur in zones of intense structural disruption within the graphitic schist unit. They pinch and swell, attaining mappable thicknesses of over 20 metres, and are semicontinuous for a kilometre or more. Generally, few primary igneous textures have survived. In a few localities serpentinitization appears to have been at the expense of pyroxenite, but thin section analysis reveals a hornfels texture in which quartz flooding has produced very dark clinzoisite porphyroblasts, poikiloblastic feldspar-garnet and finely intergrown actinolite. All of these minerals have grown statically on a remnant "lizard skin" texture outlined by dustings of fine mafic grains. The serpentinite protolith remains in question.

## **METARHYOLITE**

White-weathering metarhyolite is best exposed on the ridges a few kilometres east of the Devil's Paw (Figure 3). It is well foliated and composed of alternating centimetre to decimetre-thick feldspar and quartz-rich layers. On this basis it is easily distinguished from the metaquartzite unit. It also lacks tourmaline, garnet and muscovite±biotite±chlorite layers, contains much less quartz, and has sharp contacts with the graphitic schist unit.

## **FELSIC ORTHOGNEISS**

Pinkish grey, slabby weathering, medium-grained orthogneiss underlies a few square kilometres west of Whitewater Mountain. It mainly occurs as part of a single, large tabular body, with several nearby smaller, related(?) bodies. At one locality protolith textures are preserved, but generally the rock is strongly foliated, commonly presenting a second fabric. Composition varies from place to place with an average of quartz monzonite. Pink to yellowish grey feldspar comprises 55%, ribboned quartz 35%, muscovite 6%, and biotite 2%.

## **BOUNDARY RANGES METAMORPHIC SUITE**

Rocks assigned to the Boundary Ranges metamorphic suite (Mihalynuk and Rouse, 1988) primarily underlie the northwestern part of 104K/13 near Moosetrap Creek (Figure 3). They consist of schists of variable composition, reflecting a wide variety of protolith types, cut by several phases of igneous rocks. Based on a Late Mississippian U-Pb age on crosscutting intrusive rocks 100 kilometres to the north (Currie, 1992), some or all of the Boundary Ranges metamorphic suite in the Tulsequah area may be early Paleozoic or older. The suite appears to be gradational to the southeast into the Mount Stapler suite, where probable protoliths are similar but metamorphic grade and degree of recrystallization are lower.

## **SCHISTOSE ROCKS**

Interlayered schists of highly variable composition are characteristic of the Boundary Ranges metamorphic suite (BRM). They are interlayered on a scale ranging from decimetres to several tens or rarely hundreds of metres. Medium-grained, schistose to gneissic amphibole-chlorite-plagioclase schist and gneiss (metabasalt, diorite or gabbro) is volumetrically the most significant unit. It ranges from dark green actinolite or hornblende schist to gneissic rocks with equal parts actinolite (or hornblende) and plagioclase. This lithology dominates the western and central Moosetrap Creek area, where it ranges from layers more than 100 metres thick to interlayered with other units on a metre scale. Light green chlorite and muscovite-rich schist and phyllite (metatuff of intermediate composition?), typically displaying a strong second foliation and tight crenulations, is the most important lithologic element in the eastern Moosetrap Creek area, and appears to be gradational into the Mount Stapler assemblage. Quartz-biotite-muscovite-feldspar±garnet schist (metapelite and related metasedimentary rocks) is present throughout the section. It is characterized by the presence of garnets that range from nearly fresh to completely replaced by chlorite, suggesting a retrograde low greenschist facies overprint of formerly high greenschist to low amphibolite facies rocks. This effect is more pronounced east of Moosetrap Creek, and less pronounced west of the creek, where amphibolite facies rocks are still locally preserved. Quartzofeldspathic schist (metamorphosed clastic sediments), and quartz-rich schist or quartzite (metarhyolite or metaquartzite) are minor but significant constituents of the BRM. They are typically white to tan or brown weathering and form lenses rarely more than several metres thick. They are particularly abundant in the area immediately northeast of Lake Nolake, where they are interlayered with minor impure marble and biotite schist. Dark grey graphitic schist forms thin (generally <2 m) layers within schists of metasedimentary protolith.

## **GNEISSIC ROCKS OF IGNEOUS ORIGIN**

Two orthogneiss units of regional extent and significance, and numerous units of restricted extent,

occur within, or along the margin of the Boundary Ranges metamorphic suite.

Orthogneiss of intrusive and possible extrusive origin underlies parts of the extreme western 104K/13 map area (Figure 3). It is banded on a centimetre to metre scale with coarse, sill-like quartz-feldspar segregations. Individual bands consist of interlayered hornblende and plagioclase; biotite, hornblende and plagioclase; and biotite, plagioclase and quartz. Bands are medium grained and poorly foliated. There are similarities between this unit and the Permian Wann River Gneiss (Currie, 1992).

immediately west of the north end of Lake Nolake. The other units are poorly foliated and barely metamorphosed, suggesting a relatively young age.

### **MOUNT STAPLER/POLARIS STRUCTURAL SUITES**

Variable arc lithologies, probably reflecting original rapid facies changes, are preserved within the Mount Stapler suite (Figure 4). It includes metavolcanic and



Plate 2. Late, east-trending kink folds in the rhyolite tuff unit of the Mount Stapler suite.

A unit of strongly to weakly foliated hornblende quartz diorite to granodiorite intrudes the banded gneiss. An identical unit was previously described in the Tagish Lake area where it is mapped as the Hale Mountain granodiorite (Mihalynuk and Mountjoy, 1990; Mihalynuk *et al.*, 1990). It is correlated region-wide with the Aishihik magmatic episode, which forms an intrusive belt extending from the map area to west-central Yukon. The suite is distinguished from similar protoliths by the common occurrence of plagioclase porphyroblasts and epidote (Johnston, 1993). Recent U-Pb dating (Currie, 1992; Johnston, 1993) suggests a crystallization age of approximately 186 Ma.

Of limited regional extent are variably foliated and lineated pink potassium feldspar megacrystic granodiorite and granite, gabbro, and pyroxenite, which form layers and lenses rarely exceeding a few tens of metres in thickness. The former is an augen gneiss that is strongly deformed, metamorphosed to greenschist facies and interlayered with marble and greenstone

metasedimentary rocks that lie immediately west of the northern extension of the Llewellyn fault system north of Shazah Creek, and east of the Whitewater suite.

Pronounced strain gradients over areas of several metres to several tens of metres are characteristic, resulting in juxtaposition of rocks with strained, but recognizable protolith textures with phyllite and semischist. Original thicknesses of most of the units are thus unknown. Fine-grained actinolite in greenstone samples suggests low greenschist facies metamorphic conditions. Biotite in metagreywacke from near the contact with the Boundary Ranges metamorphic suite suggests conditions of at least middle greenschist facies. The age of this sequence is unknown, but presumed to be in part middle or late Paleozoic. The age is presently under investigation using U-Pb isotopic techniques (Sherlock *et al.*, 1994, this volume).

Major protolith types in the Mount Stapler suite include: rhyolite, limestone, siliciclastic rocks, intermediate to mafic tuff, and augite-phyric volcanic

rocks. The first three units are typically interlayered with the fourth on a scale of several to tens of metres; the latter two units tend to form sections up to several hundred metres thick.

### **RHYOLITE FLOWS AND TUFF**

Metarhyolite and metarhyolite tuff are white to tan weathering, and range from quartz-feldspar-muscovite schist to meta-lapilli and ash tuff (Plate 2) and flows with relict lapilli, bedding, flow banding, and feldspar and quartz phenocrysts. Rhyolitic rocks forms lenses rarely more than 30 metres thick, and make up approximately 5% of the total section.

### **LIMESTONE**

Limestone is recrystallized, light grey to white, massive to banded, isoclinally folded, and forms lenses up to a few kilometres long but rarely more than 20 metres thick. Several limestone lenses, interbedded with siliciclastic rocks, chert, and andesitic and rhyolitic tuff, are exposed northwest of Shazah Creek, west of the Chief fault. One limestone layer in this interval hosts a metre-thick exhalative massive sulphide horizon (Ono-Oya showing; Figure 3).

### **SILICICLASTIC ROCKS**

Quartz-rich siliciclastic rocks can be subdivided on the basis of the predominance of various platy minerals or relict sedimentary structures. These include dark grey graphitic to quartz-rich phyllite and medium grey muscovite schist; brown to medium to dark grey, thin-bedded siliceous metasiltstone; greenish brown, thin to medium-bedded metagreywacke with thin slate interbeds (volcanogenic turbidites?); meta-argillite; dark to light grey metachert; and rare lithic conglomerate with clasts derived from all protoliths represented in the Mount Stapler suite. All sedimentary rock types are interlayered with metarhyolite flows and tuff, meta-andesite tuff, and limestone, on scales ranging from centimetres to several metres. On the lower part of the ridge separating the Tulsequah River from Shazah Creek, a section composed mainly of dark grey siliceous to graphitic argillite and phyllite is gradational westward into quartz-rich graphitic schist of the Whitewater suite.

### **INTERMEDIATE TO MAFIC METATUFFS**

Intermediate to mafic metatuffs are volumetrically the most significant unit in the Mount Stapler assemblage. They range from metamorphosed light to dark green ash to lapilli tuff and rare breccia with flattened clasts, to greenstone with millimetre-scale light and dark green compositional layers or spaced chloritic partings, to crenulated chlorite phyllite and rare schist. A thick section is exposed west of the summit of Mount Stapler, with rare interbeds of rhyolite and metasedimentary rocks.

### **BASALT**

An eastern unit up to 1 kilometre thick of augite-phyric, amygdaloidal basalt with relict pillows and breccia fragments is only tentatively assigned to the Mount Stapler suite. It is largely in fault contact with the other units in the suite across a strand of the Llewellyn fault, is less deformed than most of the rest of the suite, and strongly resembles parts of the Stuhini Group, to which it may be related. However, this unit is also occasionally found interlayered on a metre scale with other rock types of the Mount Stapler suite.

Along the northern edge of the Rugulose Glacier, interbedded greywacke, argillite, phyllite, rhyolite and andesitic tuff of the Mount Stapler suite grade westward with no apparent major breaks into chlorite-actinolite schist and garnet metapelite of the Boundary Ranges metamorphic suite. A boundary is roughly drawn between the two where protolith textures are no longer visible and garnet grade rocks are in evidence.

### **POLARIS BLOCK STRATIGRAPHY**

A suite dominated by weakly to strongly foliated green basaltic lapilli and ash tuff hosts the Polaris-Taku deposit. Subordinate lithologies include gabbro, marble, altered ultramafite and rare intermediate to felsic lapilli tuff layers. Serpentinite and gabbro intrusive bodies mapped along north-trending faults in the north part of the block are similar to the geology hosting the Polaris-Taku deposit in the southern part of the block. Metamorphic grade is lower to middle greenschist and stratigraphic relationships are complicated by tight folding with extreme limb attenuation producing rootless hinges (J. Moors, personal communication, 1993). Resultant strain partitioning is similar to that seen in the Mount Eaton block, but more severe.

Rocks most resembling those of the Polaris block are unmetamorphosed strata of the Mount Eaton block, an association suggested by Souther (1971; at that time both were believed to be part of the Upper Triassic Stuhini Group). So far, our attempts to date this package have been unsuccessful as all samples collected for conodont separates have been barren.

### **STRATIGRAPHY WITH WELL-PRESERVED PROTOLITH TEXTURES**

Lithologic packages of Paleozoic age in which pristine protolith textures are commonly preserved and the maximum metamorphic grade is lower greenschist, include the Mount Eaton and Sittakanay blocks. Both rock packages are typical of the Stikine assemblage, the upper Paleozoic basement to the Mesozoic Stikine arc. Mesozoic strata are dominated by Upper Triassic Stuhini Group arc rocks and Lower Jurassic fore-arc(?) and successor basin strata of the Laberge Group. Conventional wisdom places the former in the Stikine Terrane and the latter as part of an overlap assemblage

(Wheeler *et al.*, 1991).

## STIKINE TERRANE

Distribution of the Stikine Terrane has historically been considered coextensive with regionally correlated Upper Triassic and Lower Jurassic volcanic successions of probable arc origin. These arcs were, in turn, built upon Paleozoic arc and sedimentary successions collectively known as the Stikine assemblage (Monger, 1977). Gross aspects of a stratigraphy originally thought restricted to Permian and locally late Mississippian in age, can be correlated from place to place, but details differ greatly. Oldest Stikine assemblage rocks are now known to predate Late Devonian intrusions (Logan *et al.*, 1993). Thick limestones, at one time lumped by default with "Permian limestone", then considered the Stikine assemblage hallmark, are now known to span ages ranging from Devonian to Permian (Brown *et al.* 1991). Similarly, Stikine assemblage strata in the Tulsequah area are known to range in age from early Mississippian (Sherlock *et al.*, 1994, this volume) to middle Pennsylvanian (Nelson and Payne, 1984), and are suspected to range in age from Devonian to Permian. New fossil collections and samples for isotopic age determination now being processed will help to further constrain ages. Meanwhile, the stratigraphic interpretation here remains necessarily simplistic, with treatment of physiographic "blocks" and only preliminary correlations within and between them.

## PALEOZOIC MOUNT EATON BLOCK

The Mount Eaton block is bounded on the north and south by Shazah Creek and Taku River, and on the east and west by a Tertiary pluton and the Tulsequah River, respectively (Figure 5). South and north of the Mount Eaton block, similar rocks also underlie the eastern part of Sittakanay block and the southern part of Mount Sparling (Figure 3).

Paleozoic strata of the Mount Eaton block, referred to by previous workers as the Mount Eaton group (informal; Payne and Sisson, 1988), display radical lateral facies changes, intraformational unconformities and synsedimentary deformation. In the absence of detailed age control, the group is tentatively subdivided here into lower, middle and upper divisions. The **lower division** is distinguished by the relatively common occurrence of felsic tuff, and near the Tulsequah Chief deposit has been informally subdivided into the hangingwall, footwall and mine series (McGuigan *et al.*, 1993). They are at least in part early Mississippian in age on the basis of U-Pb zircon dating (Sherlock *et al.*, 1994, this volume).

Overlying hangingwall series rocks are here subdivided into a **middle division** of massive pyroxene-phyric volcanic tuff, agglomerate and volcanogenic turbidite, succeeded by a sediment-dominated **upper division** which marks the influx of bioclastic limestone. Middle division rocks are undated, whereas upper

division rocks at one locality have returned middle Pennsylvanian fossils (Nelson and Payne, 1984).

### *Lower Division (Early Mississippian to Late Devonian?)*

Stratigraphically and structurally lowest recognized strata within the Mount Eaton block are mafic volcanics overlain by bimodal volcanic and sedimentary rocks which host the Tulsequah Chief and Big Bull deposits (Figures 4, 5). Based on correlation of an enveloping limestone marker bed, the rocks probably extend to the north and south ends of the Mount Eaton block. In the vicinity of the orebodies these rocks have been subdivided into more than three dozen units, but on a regional scale they can be represented by only a few (for a more detailed description of Tulsequah Chief and Big Bull stratigraphy, readers are referred Sherlock *et al.*, 1994, this volume).

Bounding the mine succession to the west is a **massive limestone** unit, consisting of a north-trending series of limestone lenses that separate the mine series (see below) to the east from the augite-phyric, chlorite-quartz amygdaloidal unit to the west (Figure 5). The limestone is light grey on weathered and fresh surfaces, fine grained (to coarse grained where hornfelsed by the Shazah Creek pluton) and massive to banded. It is not clear whether the limestone is in stratigraphic contact with the mine succession, or part of a fault panel that is juxtaposed against the mine succession.

In the valley bottom east of the massive limestone unit is a dark green to black, **indurated augite-phyric, chlorite-quartz amygdaloidal basalt breccia** and lesser flows and fine-grained sediments. It forms the eastern bank of the Tulsequah River immediately south of the Tulsequah Chief deposit where it is known as the **footwall series**. Finely disseminated sulphides, including chalcopyrite, are common. Near the mine site, pervasive silicification and pyritization of this unit produce totally bleached, rusty and white-weathering outcrops such that contacts with overlying felsic units are difficult to distinguish.

**Dacitic to andesitic tuffs** overlie the basalt breccia and are best developed, and probably coarsest where they host the Tulsequah Chief deposit. Fine-grained felsic tuff at the Big Bull deposit and intervening dacitic tuff and flows may be distal equivalents, but the possibility of a distinct felsic package has not been ruled out. They are typically white weathering, locally epidotized, sericitic or spherulitic. Similar rocks also occur within the Sittakanay block.

### *Middle Division (Mississippian to Pennsylvanian)*

Interfingering, fine mafic and felsic buffaceous and sedimentary strata form a diffuse contact between the lower division and distinctive, **pyroxene-alagloclase-phyric volcanic breccia and agglomerate** of the middle division. This is the single most abundant lithology within the upper Mount Eaton block, but is locally subordinate to volcanogenic turbidite and waterlain ash tuff. From a distance, this cliff-forming unit is massive and dark green, but in detail it is bright green, with dark green to black, xenomorphic, medium-grained pyroxene phenocrysts and 1 to 5-millimetre chlorite amygdaloids.



## LEGEND

### MOUNT EATON SUITE; Devonian to Permian arc succession of the STIKINE ASSEMBLAGE

#### Pennsylvanian to Permian

PESC	Medium-bedded, creamy white, tan, light grey or greenish chert. Commonly interbedded with tan limestone or fusulinid packstone; Rarely black and rusty weathering; Permian?
Pese	Sedimentary exhalative horizon. Siliceous, with disseminated to semimassive fine-grained pyrite; minor quartz-sericite schist.
PEst	Tuffaceous shale to siltstone. Tan and dark grey weathering, laminated to medium bedded; AE turbidites, locally with cross-stratified ACE.
PEsd	Debris flow - fossiliferous carbonate > volcanic fragments and tuffaceous shale. Matrix green volcanic sandstone to (rarely) limestone. Clasts up to several metres in diameter.
PEsl	Brown bioclastic packstone. Tuffaceous; well bedded; interbeds of shale, greywacke, massive limestone.
PEvt	Finely laminated maroon lapilli-ash tuff; locally massive tuff breccia, some green fragments; intervals of tan, siliceous tuff.
PEvb	Dark green, abundantly vesicular and sparsely K-feldspar megacrystic pillow basalt and breccia.
PEvd	Subophitic dike and sill complex. Dark green, medium to fine crystalline with chilled margins, massive, dioritic to gabbroic.
PEvc	Volcanogenic conglomerate. Light to medium green weathering, epidotized, massive to crudely bedded, rare sand intervals.
PEstm	Tuffaceous mudstone/greywacke. Distinctive white to pea-green weathering unit is thin to thick bedded, with locally common bioclastic limestone/debris flows and purple weathering massive limestone intervals; Characteristic red and white striped appearance where hornfelsed; may also weather dark green to maroon.

#### Mississippian or Pennsylvanian

MPEva	Agglomerate. Pyroxene > feldspar porphyritic, mainly monomict, commonly strongly epidotized, light to medium green weathering, some clasts weather maroon.
MPEv	Undifferentiated andesite to basalt flows, breccia, and minor lapilli and ash tuff. Dark green, generally pyroxene phyric, chlorite amygdaloidal, tuff typically well bedded. As mapped, does not represent a single stratigraphic interval.
MPEvt	Finely laminated maroon lapilli-ash tuff, locally massive tuff breccia, some green fragments; intervals of tan, siliceous tuff.
MPEvit	Medium to dark green lapilli tuff. As mapped, includes intervals of ash tuff and breccia.
MPEvb	Mainly dark green pillow basalt and massive basalt. Pyroxene phyric.
MPEst	Tuffaceous shale to siltstone. Tan and dark grey weathering, laminated to medium bedded; AE turbidites, locally with cross-stratified ACE.
MPEstm	Tuffaceous mudstone/greywacke. White to pea-green weathering; dark grey to dark green fresh; thin to thick-bedded.
MPEsm	Massive marble/limestone. Hackley, light grey weathering; recrystallized; may be sparsely fossiliferous at margins.
MPEvbb	Massive basaltic tuff breccia and lesser flows. Dark green to maroon, massive; relatively undeformed; generally pyroxene > tabular feldspar porphyritic.

#### Early Mississippian

eMEM	Massive limestone or marble. Light grey to white; banded; fine to medium grained.
eMEMS	Massive sulphide mineralization. Most commonly pyrite±gypsum or sphalente>galena> chalcopyrite>tetrahedrite. Adjacent rocks sericitized.
eMER	Rhyolite breccia; minor flows. Light grey to light green; may include bleached quartz amygdaloidal basalt in part.
eMED	Dacite to andesite tuff, breccia and flows; light grey to mauve. Tuff may be foliated and sericitic; flows may be spherulitic.
eMEb	Basalt breccia. Quartz and chlorite vesicular; pyroxene and lesser feldspar-phyric; well indurated; traces of chalcopyrite in the matrix; black to dark green weathering.
eMEv	Undifferentiated andesite to basalt flows, breccia, and minor lapilli and ash tuff. Dark green, generally pyroxene phyric, ± chlorite vesicular, tuff typically well bedded. As mapped, does not represent a single stratigraphic interval.

Pyroxene is commonly subequal or subordinate to medium or coarse tabular plagioclase phenocrysts. Clasts are round to subangular and most may have formed as pillow breccia, particularly where enclosing sparse pillowed flows. Associated sediments including mafic ash tuff and pyroxene-feldspar crystal tuff, tuffite and green to grey turbidite occur throughout the succession. Overlying polymictic debris-flows and conglomerate mark a transition to the upper division.

#### *Upper Division (Middle Pennsylvanian to ?Permian)*

Upper division rocks of known Permo-Pennsylvanian age are the structurally highest and youngest dated unit in the Mount Eaton block. They outline a large east-verging, north-northwest-plunging anticline, with the axis near the west side of the Mount Eaton Glacier (Figure 5) and are distinguished by the presence of interbedded brown-weathering bioclastic rudite debris flows. Calcareous micrite, shale, siltstone, chert, variegated tuff and sparse pillow basalt flows locally dominate parts of the section.

Conspicuous bioclastic rudite debris flow lenses, generally less than 2 metres thick, characterize the division. Fossil debris is silicified and often very well preserved, and consists of a diverse assemblage of

solitary and colonial corals, brachiopods, bryozoans, crinoid stems, pelecypods and fusulinids of middle Pennsylvanian age (Nelson and Payne, 1984). All are re-sedimented and thus fossil ages reflect the maximum age of the rock. Bedding ranges from laminated in the shale and micrite intervals to medium and thick bedded in the coarser lithologies. Sedimentary features, including grading, crossbedding and flame structures, are spectacularly displayed. A slight tuffaceous component may impart a pink or greenish tinge to these rocks which are normally light brown to tan or white.

A polymictic, mainly volcanic conglomerate and sandstone unit marks the base of the upper division; it is particularly well developed north of Roger Lake where it is over 500 metres thick. These rocks are green, and massive to rarely bedded. Beds are medium to thick, with rare grading and thin-bedded intervals. Clasts are subangular to rounded pebbles to boulders up to 2 metres in diameter, of dark to light green, aphanitic to feldspar or augite-phyric volcanics, lesser limestone, siliciclastics, felsic tuff and rare pyritic tuff with copper staining.

Thick sheet to lens-like coarse debris flow deposits are exposed at the base of the bioclastic limestone unit in many locations. They consist principally of clasts of fossiliferous to massive limestone and intermediate to mafic volcanic breccia fragments in a matrix ranging

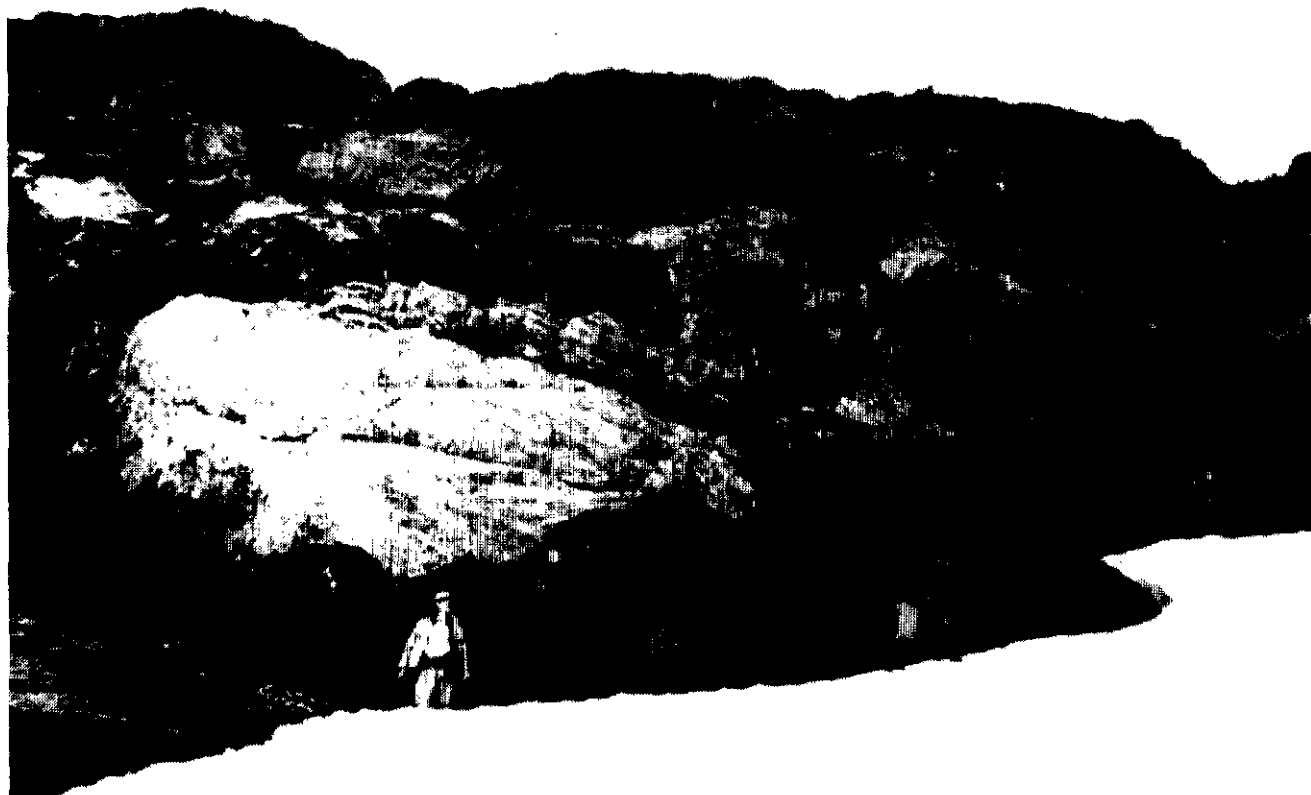


Plate 3. Outcrop in the limestone debris flow unit. Note extremely poor sorting, blocks up to several metres in diameter, and dark volcanogenic matrix.

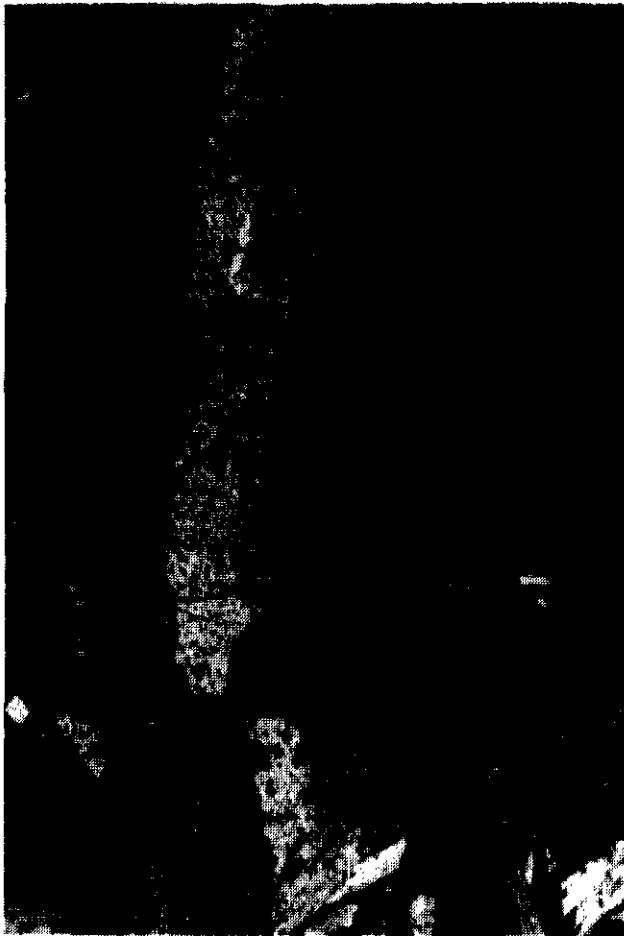


Plate 4. Hyaloclastite unit in the Mount Eaton sequence. Note angular volcanic fragments and boundary between cooling units (white layer).

from limestone to fine-grained volcanic material. Lenses are massive and poorly sorted, with clasts ranging from granule to house-size, (Plate 3) and may be up to 50 metres thick. Some limestone blocks appear to have been subjected to subaerial weathering or karsting.

Brightly coloured, green and maroon lapilli ash tuff is a very distinctive unit within the upper division (Plate 4). It is mainly comprised of lapilli and ash, but blocks are not uncommon. Fragment composition is fairly consistently intermediate and ranges from aphanitic to fine feldspar and pyroxene porphyritic. Ash and dust matrix is commonly calcareous. Individual beds may show grading and are typically less than a metre thick forming sets ten or more metres thick. They are interlayered with bioclastic debris flows and turbiditic units, but are mainly concentrated in two or three parts of the section.

Pea-green volcanogenic turbidites (Plate 5) are thin to medium bedded and well graded. Coarse bases are mainly composed of volcanic lithic grains, feldspar crystals and sparse bioclasts grading upward into dark grey argillite. Scours, and syndimentary flame and slump structures are common. Locally the unit is intimately interbedded with thin micrite, bioclastic limestone, grey-black turbidites and debris-flow layers on

a centimetre to metre scale; however, sets of green volcanogenic turbidite beds several metres up to tens of metres thick are typical.

Intervals of black (shale/argillite) and tan-weathering (sandstone) AE ( $\pm$  D) turbidites are most commonly interlayered with volcanic breccia and conglomerate. Most beds are thinly laminated to medium bedded, but rare thick beds are observed. Thicker intervals of the turbidite unit exceed 250 metres. Thinner intervals lie within and interfinger with the bioclastic limestone unit. The unit differs from the volcanogenic turbidites in its colour, composition and commonly associated lithologies. Like the volcanogenic turbidites, however, it is locally interlayered with most other lithologies in the upper division, including pea-green volcanogenic turbidites.

Beautifully pillowed units of dark green, highly vesicular, potassium feldspar megacrystic basalt are exposed in the Mount Manville area. Potassium feldspar megacrysts are white to pink, iron oxide stained and commonly up to 4 centimetres in diameter (Plate 6). Megacrysts and vesicles form concentric layers mimicking the shape of pillows. Distribution of this unit



Plate 5. Well-preserved, thin to medium-bedded intermediate ash tuffs in the Mount Eaton sequence near Mount Manville. These rocks are interbedded with massive to pillowed basalt.

is limited to two areas separated by several kilometres, providing a distinctive marker. It is uncertain whether these flows are related to much more common basalt flows that lack potassium feldspar megacrysts.

Intermediate to mafic volcanic breccia and flows are dark green to black, grey or purplish, and poorly bedded. Angular lapilli are mainly finely feldspar porphyritic. This unit is best developed in the Mount Manville area on the far eastern limb of the Mount Eaton antiform, and thus is one of the structurally highest and

possibly youngest units in the area.

**Subophitic hypabyssal sills** are relatively abundant locally within the upper division, particularly in volcanogenic turbidites of the Mount Manville area. Sills are grey to dark green and range from aphanitic, particularly near sill margins, to medium grained in the cores. Peperite textures and fluid escape features in overlying strata are locally well developed and point to injection penecontemporaneous with sedimentation, probably coincident with pillow basalt outpourings. One sill more than 300 metres thick crops out on both sides of the Mount Eaton glacier near its terminus, although most are only decimetres thick.

An accumulation of light brown, tan and white-weathering bioclastic rudite, micrite and sets of thin calcareous turbidite layers marks the top of the division. One mappable unit within this package is a **massive bioclastic limestone** unit 90 metres or more thick.

On the north end of Mount Eaton, a distinctive medium **interbedded limestone and chert** unit crops out to the southeast of the massive limestone described above. Composition ranges from medium-bedded chert to massive limestone which are both light grey to buff weathering, rarely darker. At least two fusulinid packstone marker beds are present within the section. Another distinctive bed of siliceous pyritic, exhalative black chert and minor sericite schist is continuous for at least 200 metres within this sequence. The chert-limestone unit is exposed in a series of tight, complex folds, and it grades from limestone breccia into andesitic to basaltic lapilli tuff and minor flows and thin to medium-bedded tuff and siltstone, perhaps correlative with the middle division. To the north of these outcrops, there is a very thick section of massive limestone. It is interbedded with andesitic ash to lapilli tuff and tuffite to the north and siliceous mudstone to the south. Both margins are fossiliferous, which may help to tightly constrain the age.

## **SITTAKANAY BLOCK**

Rocks on the west ridge of Sittakanay Mountain, in the extreme southern part of 104K/12 (Figure 3) are here called the Sittakanay Mountain block. Many rock types in the Mount Eaton block are represented in the Sittakanay Mountain block, and the rocks are interpreted as correlative. However, the overall degree of ductile deformation of the Sittakanay Mountain block, particularly the western half, is more pronounced. Rock types represented in the eastern half of the block include (from most to least abundant) andesitic lapilli tuff, breccia and ash tuff; brown to grey-weathering, thin to medium-bedded turbiditic shale, siltstone, sandstone and rare conglomerate; augite-phyric flows; limestone, ranging from massive grey to brown bioclastic; chert and siliceous argillite; maroon hyaloclastite and lapilli tuff; felsic tuff, and dioritic to gabbroic hypabyssal intrusive bodies. The western part of the ridge may be a more deformed and recrystallized equivalent of the units to the east. It consists primarily of alternating panels of quartz-



Plate 6. Potassium feldspar megacryst in vesicular pillow basalt. This distinctive unit crops out at several locations in the upper Mount Eaton sequence.

rich phyllite and semischist (shale, argillite, siltstone and sandstone), and chlorite phyllite and greenstone (tuff and flows of intermediate composition) with rare quartz-rich intervals (felsic tuff or clastics).

## **MOUNT STRONG BLOCK**

The Mount Strong block underlies the area bounded on the east by the Tulsequah and Taku rivers, on the west by a large granitic pluton, and on the north is separated from the Polaris block by Wilms Creek (Figure 3). Six lithologic units or associations are mapped in the block. In order of decreasing volumetric significance they are: siliceous greywacke, siltstone and shale; basaltic tuff and flows; limestone; pyroxenite; argillaceous chert; and andesitic(?) tuff. South and west of Mount Strong, rocks are strongly foliated but barely recrystallized and show effects of later hornfelsing, but to the north, protolith textures are still preserved.

## **SILICICLASTIC ROCKS**

Most of the Mount Strong block is underlain by metamorphosed siliceous argillite, siltstone, sandstone, and phyllite. Siltstone and sandstone are quartz rich, light to dark brown or grey with compositional bands that

resemble thin beds and laminations. Thick sections are present on the south ridge of Mount Strong, alternating with sections of dark grey phyllite and siliceous argillite. Where protolith textures are preserved north of Mount Strong, siltstone and sandstone are medium to thin bedded and rarely graded.

### MARBLE

A single, large body of light grey to white, medium to coarse-grained, banded to massive, foliated marble crops out on the upper slopes of Mount Strong. It is phyllitic along the margins and contains layers of cherty argillite, mafic tuff and phyllite. It pinches out to the south and splits into two distinct bands to the north, suggesting that it may represent a very attenuated, rootless isoclinal fold. The layer is over 300 metres thick (perhaps representing a double thickness if the fold interpretation is correct), but its original depositional thickness may have been substantially greater.

### BASALT

Basalt flows and tuffs are locally interlayered with argillite and siltstone units described above, primarily along the east flank of the north-trending ridge north of Mount Strong. The unit is characteristically featureless, only rarely displaying ghosts of a primary fabric. Relict lapilli and stretched white feldspar phenocrysts and amygdules distinguish these volcanic rocks from the argillites. Near Mount Strong, rocks are dark green to black and very fine grained due to hornfelsing.

### ULTRAMAFITE

A nearly circular, polyphase pyroxenite to hornblende ultramafite body approximately 2 kilometres in diameter is exposed 1.5 kilometres south of the confluence of Wilms and Bacon creeks. Pyroxenite is dark green to black, fine to coarse grained, weakly foliated, and dominantly composed of pyroxene with minor biotite (or phlogopite? up to 7%), opaque spinel (up to 10%) and secondary serpentine and carbonate. Hornblende to gabbro is very coarse with crystals up to 10 centimetres long with interstitial feldspar, locally partly altered to epidote. Contacts with the enclosing sedimentary rocks are sheared and, where best exposed, the ultramafite is thoroughly serpentinized, thus contact relations and relative age are uncertain.

### ANDESITIC TUFF

Metatuff of probable intermediate composition is exposed 1 kilometre southwest of the summit of Mount Strong, where a section approximately 50 metres thick is interlayered with younger intrusive rocks and hornfelsed basalt and siltstone. It is light to medium green, locally phyllitic, and fine grained, with compositional bands suggestive of thin beds and laminations.

## STUHINI GROUP

Regionally extensive, arc and arc-derived rocks of the Upper Triassic Stuhini Group underlie much of the Stikine Terrane. Region-wide, it consists largely of green, augite-phyric pillowed flows, breccia, tuff, hyaloclastite, feldspar-phyric flows and massive Norian limestone, with other minor sedimentary rocks. The Stuhini Group was originally thought to underlie much of the map area (Souther, 1971). However, more recent workers (Nelson and Payne, 1984; J. Mortensen, personal communication, 1992) established that much of the section mapped as Stuhini Group belongs to the upper Paleozoic Stikine assemblage which it strongly resembles. Stuhini rocks are also difficult to distinguish in some areas from intermediate volcanics of the Sloko Group. In the map area, rocks definitely identified as Stuhini Group are only slightly deformed, contain a sub-greenschist or low greenschist facies mineral assemblage, and consist mainly of breccias and sedimentary rocks. A relatively extensive unit of penetratively deformed augite-phyric flows that bounds the east side of the Llewellyn-Chief fault system in many areas may belong either to the Stuhini Group or one of the Paleozoic units.

In general, the units here can be correlated with units at the southern end of Atlin Lake where they have been described in detail (Bultman, 1979; Mihalynuk and Mountjoy, 1990).

A **basal conglomerate** mapped immediately east of the Llewellyn fault in the extreme northern part of 104K/13 includes mainly clasts of Mount Stapler-type lithologies and intrusive cobbles (from a body dated c. 220 Ma). Immediately overlying(?) strata are indurated, poorly bedded, black, cherty and pyritic argillite. However, contact relationships are obscured by intense brittle deformation along the Llewellyn fault which is well exposed at this locality.

Volcanic lithologies dominate the succession. They include: maroon and green feldspar-phyric breccia, **heterolithic lapilli tuff** and derived volcaniclastics; variegated, locally quartz-bearing intermediate tuff; **augite-phyric tuff and flows**, hyaloclastite(?) breccia and pillowed flows; and bright green, picritic, augite-phyric, hyaloclastite(?) breccia.

Carbonate near the top of the succession forms discontinuous layers, pods and olistoliths. It is tentatively correlated with the upper Norian Sinwa Formation which is best exposed several kilometres outside the eastern edge of the map area, at Sinwa Mountain. Within the map area the Sinwa Formation is mainly covered, eroded away or faulted out of the section. Exposed remnants are strongly veining and brecciated. The unit may grade laterally into pyroxene-phyric tuffs with a matrix of carbonate.

A succession of fine-grained, dark grey to black, thin-bedded to laminated **graphitic shale and argillite** is exposed several kilometres north of Mount Sparling. It is tentatively assigned to the Stuhini Group on the basis of preliminary identification of *Halobia* of Late Triassic age, and the presence of layers of similar lithologies several metres thick, interbedded with conglomerates and

breccias of the Stuhini Group immediately to the south. The section is several tens of metres thick, and is overlain by coarse, medium to thick-bedded feldspathic wackes.

**Cobble to boulder conglomerate and sandstone** are exposed below the Sloko unconformity along both sides of the lower Opposer Glacier and the unnamed glacier to the southeast. It is generally light green to white or salmon-pink weathering, massive to rarely crudely bedded, and epidotized. It contains rare thin to medium-bedded, green sandstone and siltstone intervals. Clasts are subangular to well rounded, and typically composed of augite or feldspar-phyric to aphanitic light green (epidotized) volcanics. At its easternmost mapped occurrence, the conglomerate is interlayered with green to maroon volcanic breccias assigned to the Stuhini Group, and is thus correlated. Similar rocks in northwest 104K/13 are, however, suspected to be of late Pliensbachian age based on association with finer grained sediments of that age, and are correlated with the Laberge Group.

## LABERGE GROUP

Marine turbidites and fan deposits of the Laberge Group are best exposed in the northeasternmost part of 104K/13. Mapping of deep glacial valleys incising the Sloko Group reveals several occurrences of Laberge Group, extending its known distribution much farther to the west. Several new macrofossil localities discovered at new and previously known Laberge Group localities should help to further constrain the age of these rocks.

Laberge Group lithologies in the Tulsequah area include indurated, finely bedded siliciclastics: dark, fissile argillite; coarse feldspathic wacke; intrusive cobble conglomerate; and tuffite. With the exception of the tuffite and the enormous thickness of some conglomerate lenses, the lithologies present in the Tulsequah area are much the same as those near Atlin Lake to the north where the Laberge Group has been thoroughly described (Bultman, 1979; Mihalynuk *et al.*, 1989; Johannson, 1993).

**Siliciclastics** are grey-brown to red-brown, fine turbiditic greywacke and siliceous shale. Beds are thin to thick, AE to nearly complete Bouma sequences. A slight cleavage is locally developed in fine-grained layers.

**Distinctive cobble to boulder conglomerate** forms the southeasternmost Laberge Group exposures. It is characterized by the presence of very well rounded, high sphericity granitic clasts, which make up 20 to 30% of the total clast population. Clasts which are more abundant include: fine-grained green-grey intermediate volcanic; grey feldspar porphyry; maroon ash tuff; and silt and sandstone. Intrusive cobbles are predominantly orange-yellow, biotite granite with euhedral potassium feldspars, and white granodiorite with pink potassium feldspars, hornblende and subordinate biotite. Clasts of lesser abundance include: green lapilli tuff, coarse pyroxene porphyry, rare white chert or rhyolite, and very rare hornblende-feldspar gneiss. In two locations this

unit appears to directly overlie volcanic breccias of the Stuhini Group. Thus, it may represent the basal unit in the Laberge Group in the Tulsequah area.

Intervals of buff-weathering **greywacke and granule conglomerate** are enclosed by argillite. The greywackes are quartz and feldspar rich; clasts in the conglomerate are much like those in the lower conglomerate unit including volcanic (pyroxene and hornblende feldspar porphyries, feldspar porphyries, aphanitic mafic to felsic); sedimentary (light and dark grey, rarely fossiliferous carbonates with lesser wackes and argillite); and intrusive (syenites through leucogranites) rocks. The rocks are generally medium to thick bedded with thin silty interbeds. This unit includes lithologies mapped by Souther (1971) as "Takwahoni Formation".

**Green tuffite**, bisected by the interpreted northern extension of the King Salmon fault, underlies the Sloko unconformity in the extreme northeast corner of 104K/13 (Figure 3). East of the fault, it consists of alternating layers of thin-bedded green to maroon and chocolate-brown tuffaceous siltstone and shale, thin to thick-bedded sandstone and massive conglomerate lenses. Sandstone and conglomerate clasts are almost wholly volcanic in composition. This unit appears to grade northeastward into tan-weathering, thick-bedded sandstone, then brown to grey, thin-bedded siltstone and shale typical of the Laberge Group. The contact area is poorly exposed and contains numerous small faults. Ammonites collected from this unit are probably upper Pliensbachian, thus correlation with the Laberge Group seems likely. Strata west of the King Salmon fault consist of massive, green, volcanogenic sandstone intervals up to 100 metres thick interlayered with intervals of fossiliferous, black, graphitic argillite and siltstone 2 to 5 metres thick. Although very similar in nature to the Upper Triassic section, these rocks also contain upper Pliensbachian ammonites.

## SLOKO GROUP

Mafic to felsic Sloko Group volcanic strata rest with profound and irregular unconformity above Mesozoic and older strata. Sloko Group rocks were originally mapped as covering most of the northeast part of the map area and many of the higher peaks in the western part of the map area. This distribution is borne out by our mapping, but with important exceptions. Several windows through the Sloko expose Mesozoic strata, diminishing the expansive blanket of Sloko Group rocks.

Numerous volcanic centres, rapid facies changes, and synvolcanic high-angle faulting characterize the Sloko Group, yet it is easily subdivided into regionally mappable volcanic units. On the basis of 1993 fieldwork, the group is divided into six map units not previously reported in the area: basal conglomerate; massive, well-indurated, black pyroclastics (Opposer formation); massive, tan-weathering breccias (Mount Haney formation); distinctive interlayered flows and volcanoclastic rocks (Nakonake formation); rhyolite

domes and tuffs, and trachyte flow succession(s).

### **BASAL CONGLOMERATE**

Sloko Group strata were deposited on a paltosurface of considerable relief, as evidenced by irregular, sloping contacts, slump deposits and a wide variety of volcanic types overlying the unconformity. In some areas, a basal conglomerate is developed over the erosional surface. It is characterized by subangular to well-rounded, poorly sorted, crudely bedded polymictic cobble conglomerate, composed of intraformational clasts (porphyritic andesite, rhyolite) and clasts derived from underlying rocks (schist, gneiss, argillite, granitoid rocks). The basal conglomerate is generally poorly indurated, and may grade laterally and/or up-section into volcanic breccia and tuff. Deposition of the conglomerate is clearly diachronous.

### **OPPOSER FORMATION (INFORMAL)**

Very well indurated, cliff-forming vitrophyric tuff and flows of the Opposer formation are characteristically massive, dark green to dark grey or black. On outcrop scale, Opposer rocks typically consist of sparse breccia fragments ranging from a few centimetres to about 20 centimetres across in a massive, black, fine-grained matrix. Matrix material often exhibits conchoidal fracture, suggesting relatively high silica content. Breccia fragments are light grey to green, often epidote altered with diffuse margins. Fragments of granitoid rocks are not uncommon. Opposer formation underlying Nelles Peak and many of the other high peaks in the region is nearly 2000 metres thick. In at least three locations (Nelles Peak, the Devil's Paw, and an unnamed peak southeast of Mount Hancy), the Opposer formation is intruded by granitic plutons, suggesting that its distribution coincides with regional magmatic centres.

### **MOUNT HANEY FORMATION (INFORMAL)**

Poorly indurated, epidote or clay-altered, tan to light green weathering Mount Hancy formation is massively bedded, dacitic to andesitic volcanic breccia and lapilli tuff up to several hundred metres thick. Breccia fragments range from a few centimetres in diameter to house sized, but are typically 10 to 20 centimetres across; they are feldspar porphyritic and maroon to green in relatively unaltered sections. Vent facies are recognized locally, and in several localities pyroclastic dikes of the same composition are proof of a pyroclastic origin. Elsewhere, laharc facies predominate, and in at least one locality growth faults and highly chaotic layering indicate infill of a collapse feature.

### **NAKONAKE FORMATION (INFORMAL)**

Alternating recessive volcaniclastic and resistant flows create the distinctive light and dark ribbed appearance of the Nakonake formation (Plate 7).

Volcaniclastic layers are poorly consolidated, tan weathering lahar, breccia and tuff in layers from metres to tens of metres thick. Maroon to dark brown-weathering, white feldspar porphyritic flows, range from 5 to over 50 metres in thickness. Nakonake formation both grades laterally into and overlies the proximal facies Opposer and Mount Hancy formations, and probably represents both distal facies and the waning, more quiescent phases of Sloko volcanism. This is well illustrated in the north-central part of 10-K/13, where Opposer formation rocks that underlie Mount Hancy grade laterally eastward into the Nakonake formation, and southeast of Mount Hancy, where the Nakonake formation overlies the Opposer formation.

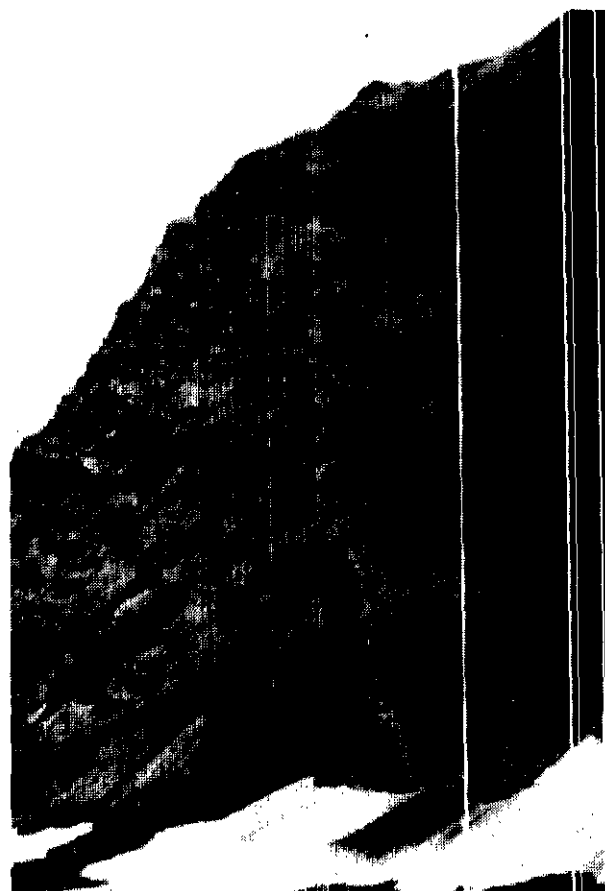


Plate 7. Volcanic rocks of the Nakonake formation of the Sloko Group. Approximately 300 metres of section are illustrated in this photo.

### **RHYOLITE**

Mappable units of rhyolitic flows and tuff crop out in a few localities, typically near or at the base of the section. Tuff is generally well indurated, light green to grey weathering, and characterized by lapilli sized fragments of feldspar±quartz-phyric rhyolite in an ash matrix. A basal rhyolite tuff and breccia unit is exposed south and west of Mount Sparling for several kilometres along strike. Rhyolite flow-domes are mapped in a few localities within the Mount Hancy formation. They are irregular lenses of flow-banded, aphanitic to sparsely

feldspar and quartz-phyric rhyolite and welded rhyolite tuff. Flow banding is often steeply inclined.

## TRACHYTE FLOW SUCCESSION

Thick, locally columnar jointed trachyte flow successions can be mapped in northeastern 104K/13. Here they are in gradational contact with Mount Haney formation laharic strata near the toe of the "Slohini Glacier" (informal name) and are deposited with angular discordance on the Nakonake formation north of the "Opposer Glacier" terminus. Immediately underlying Mount Haney formation strata are somewhat distinctive in that they contain up to 3% pebble-sized rusty weathering and strongly pyritized clasts of uncertain protolith.

Trachyte flows may be flow banded and form cooling units up to several tens of metres thick. They weather bluish or greenish grey to tan or brown, containing 10% pinkish, glomeroporphyritic sanidine(?) and plagioclase partly altered to chlorite. Rarely fine-grained quartz phenocrysts are present. Chlorite and calcite-filled vesicles are locally common, perhaps outlining the tops of individual cooling units. Matrix material is very fine grained to aphanitic.

## DIKE AND SILL SWARMS

Dikes believed to be coeval with Sloko volcanism are of four types: white, flow-banded rhyolite, grey to maroon banded trachyte, green to grey aphanitic to hornblende-phyric and pyroclastic Mount Haney formation feeders.

White rhyolite dikes are most conspicuous and are thus the best mapped of Sloko dikes. They attain thicknesses of metres to tens of metres and commonly follow or form topographic linears which, in at least some cases, are related to zones of structural weakness. Such relationships are well documented at the Tulsequah Chief deposit (G. Dawson, personal communication, 1993). Trachyte dikes are conspicuous where they cut darker volcanic strata of the Nakonake formation, but have generally not been mapped on an individual basis. Pyroclastic dikes are recognized in only a couple localities, but are clearly related to the Sloko volcanic episode. Darker coloured dikes are at least as common as rhyolitic lithologies, although they lack the contrasting colour which enables the former to be mapped from a distance.

Dikes form swarms with two predominant orientations: north and northeast; although individual dikes are observed with almost any orientation. Rhyolite dikes following linears in the Mount Eaton block are invariably oriented north-south.

## PLUTONIC ROCKS

With the possible exception of the early Jurassic Hale Mountain intrusion correlation described under **Gneissic Rocks of Igneous Origin** above, no Mesozoic

plutons have yet been clearly documented in the area. One intrusion near Sittakanay Mountain is interpreted to be Late Cretaceous based solely on its relatively high degree of alteration. Elsewhere in the map area, deeply incised valleys have exposed the roofs of several discrete plutons which vary compositionally from granodiorite to monzodiorite. Most are undeformed and cut Sloko volcanics with which they are probably comagmatic, and on this basis are assigned an Eocene age. A similar relationship is displayed near Tutshi Lake to the north. Here good age control dates both the volcanics and crosscutting intrusion as 55 Ma (M.G. Mihalynuk, unpublished data).

## LATE CRETACEOUS?

A medium-grained, epidote-chlorite-altered hornblende and lesser biotite granodiorite to quartz diorite forms the northwestern ridge of Mount Sittakanay. From a distance it appears black and massive with irregular jointing. Local foliation is probably igneous in origin. A Cretaceous age assignment will be tested using K-Ar isotopic dating techniques.

## EOCENE

Plutons of known Sloko or younger age underlie Shazah Creek, and the unnamed ridge southeast of Mount Haney, Devil's Paw, east Gisel Peak, and the north cirque of Nelles Peak (Figure 3). They generally range in composition from hornblende-biotite quartz monzonite to biotite granite, and are medium crystalline, homogeneous, light weathering, and exhibit pronounced exfoliation features and/or one or more prominent joint sets.

On the basis of these features, a granite pluton with granodioritic margins centred on Bacon Creek is also suspected to be of Eocene age. Contacts with country rocks are generally sharp and relatively unaltered, with the exception of the southwest contact of the Shazah Creek pluton, which has a very irregular contact and a wide contact aureole with associated brecciation of the country rocks up to 2 kilometres from the contact. The plutons are generally fresh and unaltered, but one body near Tulsequah Lake is cut by a myriad of chlorite-lined fractures. A cataclasite is produced where fracture density is greatest, but no sense of offset has been ascertained.

Sparse pea sized blebs of molybdenum and traces of disseminated chalcopyrite and pyrite occur in otherwise unaltered granite east of Gisel Peak.

## DEFORMATION

All Mesozoic and older rocks in the map area were affected to various degrees by post-Early Jurassic, north to northwest-trending, polyphase folding, faulting and metamorphism. The degree of ductile deformation and

metamorphism generally increases westward from relatively undeformed Mesozoic strata to amphibolite grade gneisses of the Boundary Ranges and Whitewater suites. Possibly long-lived northwest-trending faults have been reactivated into the Early Tertiary. Late easterly to northeasterly crossfaults and crenulation cleavage are locally developed. Deformational styles differ between lithotectonic suites. These are described briefly below, grouped where appropriate.

## MESOZOIC ROCKS

Deformation in the Stuhini and Laberge Groups is characterized by open to tight, mainly upright, north-northwest-trending, gently plunging folds. Rocks only locally possess a weak cleavage, typically in fold hinges in fine-grained strata. Volcanic rocks contain the assemblage chlorite+epidote+albite+quartz, indicative of subgreenschist facies metamorphism. Several small, northwest-striking, northeast-dipping thrust faults imbricate the section. The largest of these, apparently a continuation of the King Salmon thrust mapped by Souther (1971) to the east, is marked by a breccia zone up to a few metres wide and a zone of reddish alteration up to 50 metres wide. Rocks on both sides appear to be the same age and lithology (see above under lithologic descriptions), so total motion is probably not great. Movement on the King Salmon fault is thought to be Bajocian (Middle Jurassic) in age, related to emplacement of the Cache Creek Terrane over the Stikine Terrane (Thorstad and Gabrielse, 1986).

## STIKINE ASSEMBLAGE

The Mount Eaton block and the more strongly deformed Sittakanay and Mount Strong blocks that make up the Stikine Terrane in the Tulsequah area are characterized by a single dominant phase of folding, subgreenschist to middle greenschist facies deformation, weakly to locally strongly developed penetrative foliation and lineation, and steeply dipping, north-trending structural grain. This is overprinted locally by a non-pervasive second phase of east-trending folds that generally have wavelengths of less than 1 kilometre.

Deformation in the Mount Strong block is characterized by upright, tight to isoclinal, north or south-trending, gently plunging folds on a scale of centimetres to metres. In an otherwise monotonous sequence, panels of consistently west or east-vergent folds, as well as an apparently duplicated marble layer, suggest the presence of isoclinal folding on a kilometre scale. Rocks range from intensely flattened and strongly lineated parallel to fold axes south of Mount Strong to relatively undeformed several kilometres north of Mount Strong.

A similar structural style is exhibited by rocks in the western Sittakanay block (Plate 8). Although folds are not abundant on an outcrop scale, repetitions of strata suggest that the section may be folded on a kilometre

scale. Rocks are phyllitic and generally lack primary depositional features.

Rocks in the eastern part of the Sittakanay block are openly to tightly folded on a metre to kilometre (locally centimetre) scale. Folds are generally upright, north-trending and gently plunging. Rocks show primary depositional features but (with the exception of massive flow rocks) display a pronounced flattening fabric, stretching lineation parallel to fold axes, and locally, a second, subparallel axial planar fabric.



Plate 8. Tight folds in thin bedded tuffs of the Sittakanay Mountain block showing intense deformation of units that still retain protolith textures. Note refolded isoclinal, upper right of ice axe head.

Rocks in the Mount Eaton block are only weakly penetratively deformed, except in the cores of appressed folds where intense and chaotic folding produces a phyllitic fabric. Several large, open to appressed folds with sheared axial regions divide the Mount Eaton block into eastern, central and western structural panels (Figure 5). The eastern panel includes rocks east of the Mount Eaton glacier (Mount Manville area) which strike north-northwest, are steeply dipping to overturned, mainly east facing, and represent the eastern limb of a large, north-plunging anticline (Mount Eaton anticline). Minor folds are most commonly gently plunging and parallel to the strike direction.

The central panel exhibits the most complex deformation and includes the hinge and immediate western limb of the Mount Eaton anticline. It covers the area west of the Mount Eaton glacier in the vicinity of Roger and Wendy lakes, and extends along strike to the north and south. The hinge zone is mostly ice covered, but in at least two locations, where outlined by relatively competent massive volcanic breccia (e.g., northeast of Roger Lake), it is ruptured with shortening accommodated by several faults. Exact lithologic correlations cannot be made across the hinge zone, suggesting either significant facies changes or significant

motion on faults within the hinge. A northward continuation of the anticlinal hinge is represented by a very complex series of refolded anticlines and synclines at the northwest end of the Mount Eaton glacier.

Abundant east-verging folds on the immediate western limb of the Mount Eaton anticline are outlined well by the bioclastic unit, and to a lesser extent units below it, which are tightly folded around north trending fold axes, (Plate 9). Near Wendy Lake, folds axes trend southwest and axial planes dip northwest. Rocks are locally phyllitic and coarse tuff units have a pronounced flattening fabric. Locally an orthogonal set of folds produces a steep, second fabric oriented southwest to west. These folds have been clearly outlined through detailed mapping by Dawson *et al.* (1993) in the vicinity of the Big Bull mine. A north-trending zone of relatively intense ductile deformation, well developed west of Wendy Lake (the "Wendy Lake shear zone") separates the central and western structural panels.

The western structural panel includes rocks on the eastern bank of the Tulsequah River. Structural trends in this area are difficult to decipher due to thick vegetative cover, massiveness and rapid facies changes in the dominantly volcanic section. On a regional scale, bedding is steep and north to northwest trending, possibly representing another large fold. Minor folds also trend in the same direction. A set of fairly tight, north-plunging folds which are cut by numerous north-

imparted compositional layering, layer-parallel foliation and intrafolial isoclinal folds of variable orientation (Plate 10). It is locally difficult to recognize because it is largely coaxial to second phase deformation. The latter is characterized by greenschist to amphibolite facies metamorphism, schistose to phyllitic foliation with regional north-northwest strike and moderate to steep east dip, and millimetre to possibly regional scale appressed to isoclinal folds with axes that plunge gently and trend roughly 015°. Fold styles are highly variable, with competent units displaying metre-scale cylindrical to disharmonic folds and nearby phyllitic units tightly crenulated, sheared and refolded (Plate 10). Peak metamorphism of middle amphibolite grade is associated with second phase deformation. It is thought to be mid-Jurassic, as evidence by an  $^{40}\text{Ar}/^{39}\text{Ar}$ -sericite plateau age of 172 Ma in the Moosetrap Creek area (Smith and Mihalynuk, 1992) and by reference to mapping and geochronology in other areas to the north (*e.g.* Currie, 1992). Foliated orthogneiss units do not reach amphibolite grade and may be late synkinematic with respect to second phase deformation.

Manifestations of third phase deformation include millimetre to decimetre-scale kink and crenulation folds with steep axial planes (locally forming a strong cleavage), and open to tight chevron folds, developed on a metre to kilometre scale. Cleavage and axial planes in both types strike 050° to 090° with steep dips, similar to



Plate 9. East-verging chevron folds in the bioclastic limestone unit west of Mount Eaton. View to the northwest.

trending high-angle faults, has been well delineated by drilling at the Tulsequah Chief mine (G. Dawson and T. Chandler, personal communication, 1993).

### **BOUNDARY RANGES AND MOUNT STAPLER SUITES**

At least three phases of deformation are evident in the Boundary Ranges metamorphic suite. Phase 1

the second fabric developed in the Mount Eaton block. The effects of third phase deformation are variable, locally quite strong, and are accompanied by a retrograde, greenschist (chlorite grade) facies metamorphic overprint.

Deformation in the Mount Stapler suite is similar, but apparently represents higher crustal levels than the BRM. The highest grade rocks of this suite are middle greenschist facies.

## **POLARIS BLOCK**

Variably developed foliation in the Polaris block probably corresponds to structural position whereby more intensely foliated rocks occur in the cores of tight north-trending folds. The eastern limbs of these folds are attenuated and locally cut off, at one locality sinistral offset is indicated. En echelon repetition of such structures on the outcrop scale produces a distribution of units with hook-like outlines (J. Moors, personal communication, 1993).

## **WHITEWATER SUITE, FOLIATED ORTHOGNEISS UNITS**

Rocks of the Whitewater suite are relatively coarsely recrystallized upper greenschist to amphibolite facies rocks. Rocks tend to possess a relatively weak schistosity and strong gneissic compositional banding. As in the Boundary Ranges suite, first phase intrafolial isoclinal folds are locally well developed and manifest by folded compositional bands. Second phase effects include open to tight folds, developed on a metre to kilometre scale in competent units (Plate 11), to tight folds and a crenulation or transposition fabric in graphitic schist. Latest folding produces the dominant structural style



Plate 10. Detail of outcrop in the western Boundary Ranges metamorphic suite, showing various generations and styles of folding. Photo illustrates: an early, first phase, intrafolial isoclinal fold (left centre of photo); a tight, upright, second phase fold, with both cylindrical (top) and kink (bottom) fold characteristics; and a late synkinematic quartz vein. Long dimension of photo represents about 0.6 m.

where minor folds with amplitudes of metres to tens of metres cascade down the limbs of folds with kilometre-scale wavelengths. Faults associated with fold limbs are common. In contrast to the Boundary Ranges suite, retrograde effects are generally not in evidence, except near plutons.

The banded gneiss unit (Wann River gneiss?) has a weak foliation and strong compositional banding, which generally strikes northeast and dips gently to moderately southeast. Folds are uncommon. The younger orthogneiss unit (Hale Mountain granodiorite?) is only weakly foliated.

## **FAULTS**

### **NORTH TO NORTHWEST-TRENDING FAULTS**

North to northwest-trending high-angle faults with complex movement histories are common in the map area. The largest is the regionally significant Llewellyn fault, which is mapped as far north as the southern Yukon, where it merges with the Tally Ho shear zone (Doherty and Hart, 1988), and continues southward into the map area, where it merges with the Chief fault (Payne and Sisson, 1988) south of Shazah Creek (Figure 2). Early movement on the Llewellyn fault zone is manifested by zones of ductile sinistral shear, which to the north, are largely pre-180 Ma. Sinistral shear zones, generally less than a few metres wide, are present in the Mount Stapler, Boundary Ranges and Mount Strong units up to several kilometres west of the main strand of the Llewellyn fault zone (Plate 12). Small dextral shear zones are relatively common throughout the map area, particularly in the vicinity of the Llewellyn fault; to the north these zones postdate sinistral motion on the fault (Mihalynuk and Mountjoy, 1990). The main strand of the Llewellyn fault is a ductile to brittle mylonite zone up to several metres wide, which is well exposed in the extreme northern part of 104K/13 and the adjoining map sheet to the north (104N/4; unpublished BCGRS mapping, 1991; Plate 13) and north of Shazah creek. In both locations, the fault zone contains sheared and comminuted intrusive rocks ranging from granodiorite to leucogabbro in composition. In some areas, the intrusive rocks form flower structures - west-verge thrust fans that root to the east in the near-vertical main fault. Brittle faulting postdates ductile shear, but largely predates Sloko volcanism, and may be coeval with middle Jurassic movement on other regionally significant thrust faults to the east (Nahlin and King Salmon faults). Minor Eocene reactivation of the fault is indicated by areas where the Sloko Group is offset by up to several hundred metres.

A few kilometres north of Shazah Creek, the fault bends southwestward and splays into several strands. It is offset by the Chief crossfault (see below and Figures 4 and 5) to west of the Tulsequah River. The trace of the Llewellyn-Chief fault south of the Polaris-Taku mines is uncertain. The dramatic contrast in metamorphic grade



Plate 11. Outcrop-scale tight fold in interlayered quartz-rich and graphitic schist of the Whitewater suite. View to the northwest. Fold verges southwest. Thick resistant layer to right is amphibolite gneiss.

across the fault zone to the north is not present in the vicinity of Mount Strong and Sittakanay Mountain, where the westward increase in metamorphic grade and deformation is relatively gradual. This may be explained by several alternatives: distributed shear along numerous small fault strands; as yet unrecognized overthrusting of the fault by higher grade rocks from the west; or gradual southward dying out of the Llewellyn fault zone. Existing data do not permit evaluation of these alternatives.

Other north to northwest-trending brittle faults and ductile shear zones are common in the map area. Most are minor and located in fold hinge areas or bounding units of differing competency. West of the Tulsequah River, several such faults contain sheared serpentinite. Two relatively significant faults include the Whitewater fault, which separates the Whitewater suite from the Polaris suite, and an unnamed brittle fault in the northeastern corner of the map sheet that, to the south, down-drops Sloko Group breccias against Mesozoic rocks, perhaps representing at least a few kilometres of syn-Sloko movement. This fault crosscuts a section of Laberge and Stuhini rocks imbricated along older northwest-trending faults.

Thrust faults are recognized in the Mount Eaton block (Plate 14) where offset is thought to be relatively

minor, but the true extent and significance of this type of faulting is largely unknown.

#### EAST TO NORTHEAST-TRENDING CROSSFAULTS

East to northeast-trending, high-angle, brittle crossfaults with limited displacement are common in the map area. Faults with offsets significant on a 1:50,000 scale are spaced every few kilometres, and may be even more common. Both dextral and sinistral offsets are displayed. Assay samples taken in 1991 from quartz veins close to these faults returned gold values well above background values (Smith and Mihalyuk, 1992). Additional examples were not positively identified in 1993.

The most significant crossfault in the Tulsequah area is the Chief crossfault, a structure that is interpreted to offset the Llewellyn-Chief fault system about 2 kilometres in a dextral sense (Figure 5). The fault is located immediately north of the Tulsequah Chief mine, and cuts off the mine sequence to the north (Plate 15). It is well displayed in the bioclastic limestone unit more than 1000 metres above the mine, where it is marked by a steeply north-dipping zone of brecciation and ductile deformation. On the west bank of the Tulsequah River it

juxtaposes virtually undeformed augite porphyry, tuff and breccia with graphitic schist of the Whitewater suite. The Chief crossfault is important for two reasons. It increases the width of the Mount Eaton block and the area prospective for volcanogenic massive sulphide deposits by several kilometres and determination of the amount of motion on this fault may help to constrain the location of the northern continuation of the Tulsequah Chief orebody, if one exists.

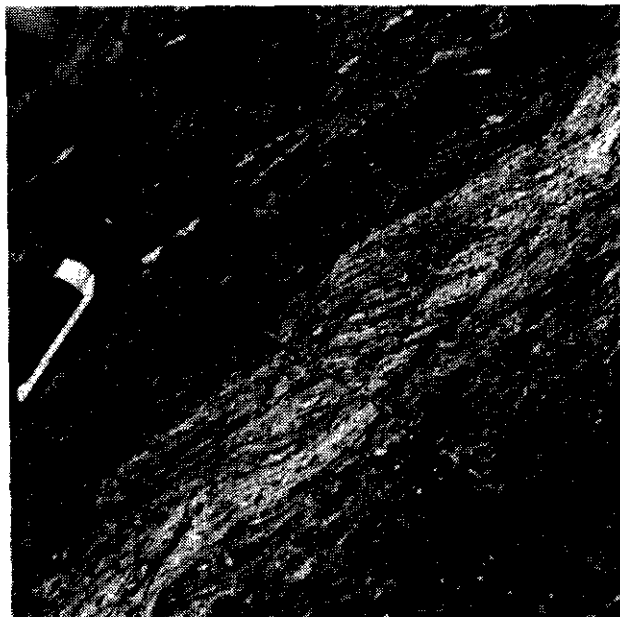


Plate 12. Shear fabric in siliceous argillite, south of the summit of Mount Strong. This fabric is indicative of sinistral shear. View to the north.

## MINERAL DEPOSITS AND REGIONAL POTENTIAL

Within the Tulsequah map area are three significant past-producing mines: the Tulsequah Chief and Big Bull volcanogenic massive sulphide accumulations, and the Polaris Taku mesothermal vein-hosted gold deposit. Several prospects, including the Banker and Sparling, are located near these mines and have been included in property-scale geophysical surveys and mapping, but have not been explored in detail in recent years. Other showings that have been the target of exploration activity in the last few years include the Maple Leaf, Riz, and Highland Girl. British Columbia Geological Survey crews investigated the Maple Leaf showing in 1991 (Smith and Mihalynuk, 1992). The Riz and Highland Girl, prospects, visited in 1993, are described below, as are newly discovered showings of potential economic significance. These new showings, named the Stoker and Icefall, are located several kilometres north and west of Shazah Creek.

Plate 14. Small thrust faults (dashed) in the Mount Eaton block. Note hangingwall cut-offs (highlighted by solid lines).

## TULSEQUAH CHIEF AND BIG BULL

Redfern Resources Ltd. conducted an aggressive exploration program on its significant claim holdings which include the Tulsequah Chief and Big Bull deposits as well as all intervening ground. A comprehensive

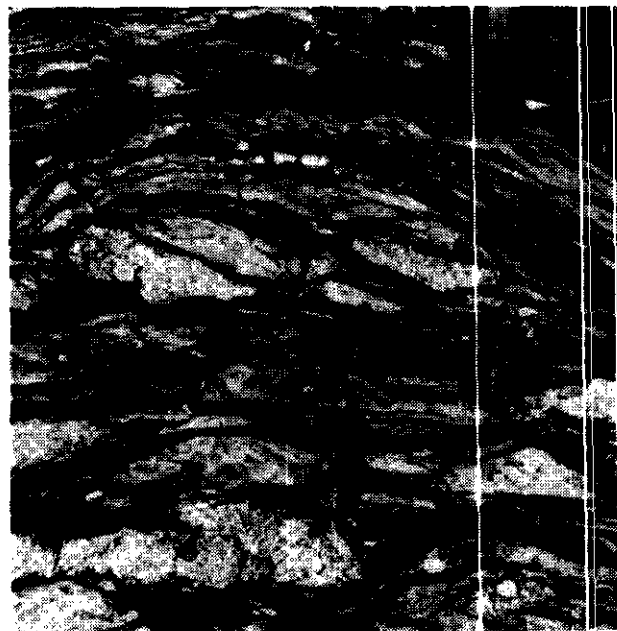


Plate 13. Sheared volcanic breccia along the Lowellyn fault zone.



geophysical survey helped to guide exploration drilling. In all, 32 holes totaling 11,200 metres were drilled on the property. At the Tulsequah Chief deposit, six surface and fourteen underground fill-in and exploration holes were drilled. Successes include more detailed delineation of the main AB zones and increased grade and tonnage of the G zone.

At the Big Bull deposit, twelve drill holes helped to greatly extend the known dimensions of the alteration zone. Base metal sulphides were intersected at depth, but new zones of economic accumulations remain elusive. Redfern plans to continue exploration on both the Tulsequah Chief and Big Bull deposits in 1994.

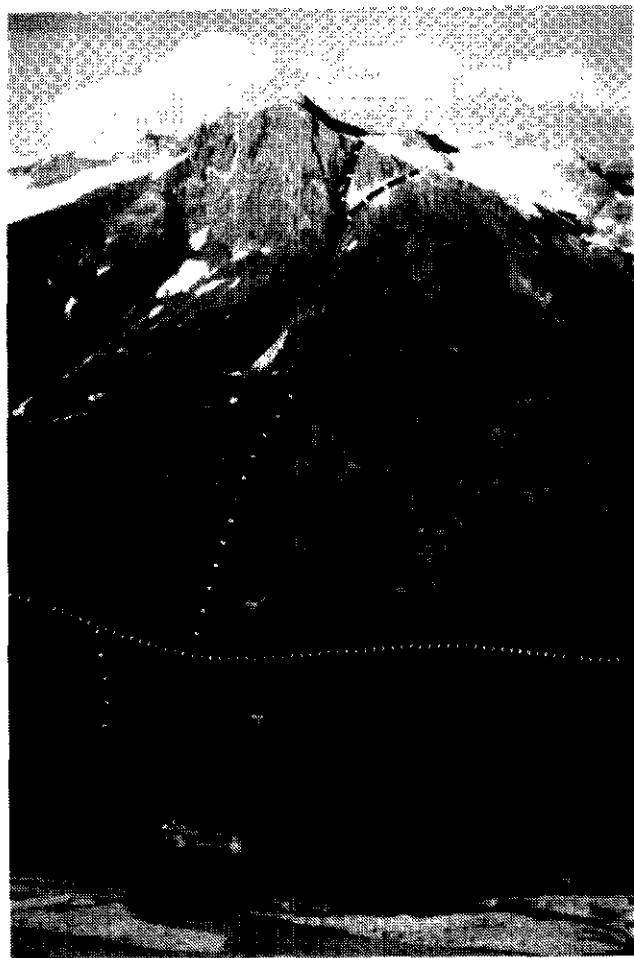


Plate 15. Aerial view to the northeast showing: the Tulsequah Chief mine portals at the 5200 (near river level), 5400 (camp level), 5900, 6300 and 6500 levels; trace of the Chief crossfault where known (solid) and suspected (dash); and the 4400 fault (fine dash). Gross stratigraphy on southern Mount Eaton is shown with felsic units beneath the heavily treed lower slopes; dark, mafic volcanics underlying the higher, sparsely vegetated slopes; and light-coloured bioclastic limestone capping the peak in the centre of the photo.

## STOKER AND ICEFALL SHOWINGS

Two showings of potential economic significance were discovered approximately 8 kilometres north of the Tulsequah Chief deposit in the course of 1993 mapping.

The Stoker showing is located west of the head of a south-flowing creek, and the Icefall showing is approximately 2 kilometres to the west-northwest in steep, red-weathering cirque walls on both sides of an icefall.

The Stoker showing displays two styles of mineralization. Massive chalcopyrite and minor sphalerite and galena occur as bands up to 40 centimetres thick on the margin of a deformed limestone body several metres thick. Limy tuffaceous(?) strata topographically below the first occurrence host a zone about 60 metres by 10 metres minimum dimensions in which disseminated sphalerite and galena comprise up to 15% combined, but generally less than 1% of the rock. Nearby, greasy grey chalcedonic quartz cements brecciated country rocks.

The Icefall prospect consists of two mineralized areas separated by an inaccessible icefall, which, on the basis of mineralized float, probably masks continuity between the two showings. On the west side of the icefall mineralization consists of pyrite±quartz veins hosted by argillites of the Laberge or Stuhini Group. This style of mineralization grades eastward into a zone of green to white (bleached) weathering rocks, apparently of volcanic origin. Float from this relatively inaccessible area contains abundant disseminated sulphides, primarily pyrite, and several zones of copper staining were observed in the cliff face. Boulder trains on the glacier approximately 1 kilometre south of the cliff contain abundant mineralized detritus, including bleached lapilli tuff, felsic intrusive, quartz-eye porphyry and rocks of uncertain protolith, containing disseminated and semimassive pyrite and sphalerite, with minor galena and chalcopyrite. A regional stream sediment sampling program reported anomalous lead and zinc values from creeks draining both the Icefall and Stoker showings (Matysek *et al.*, 1988).

The lithologies and styles of mineralization are suggestive of a high-level porphyry system involving rocks of Sloko age, or possible remobilization of a deeper volcanogenic massive sulphide accumulation. Lead isotope data might help to further constrain the source of mineralization.

## RIZ SHOWING

The Riz showing, discovered and prospected by American Bullion Minerals, Limited in 1990 (American Bullion Minerals Limited, 1990), is located where the north-facing Nelles Peak cirque intersects the Tulsequah Glacier. It was visited in 1991 as part of our reconnaissance survey. It consists of a red-weathering, ice-cored medial moraine or landslide deposit consisting of boulders of relatively fine grained quartz monzonite that hosts sulphide mineralization, both disseminated and in veinlets. Primary sulphide minerals include pyrite, pyrrhotite, sphalerite and minor galena. Most of the Nelles Peak cirque is underlain by the Opposer formation, except for minor gneissic rocks. These are intruded by quartz monzonite stocks that are the probable source of the mineralized boulders. The source has not

been pinpointed; however, an east-trending high-angle fault with altered wallrocks cuts through the cirque. Adjacent gneissic rocks contain up to several percent disseminated pyrrhotite, and are possible targets for further investigation.

### **HIGHLAND BOY**

The Highland Boy mineral showing is located on the north side of the Sittakanay River 3.5 kilometres east of its confluence with the Taku River (Figure 3). Gold, silver, lead and arsenic mineralization is hosted by fine-grained quartz-mica schist and dark grey to black, strongly folded, slates and phyllites. Foliation in rocks around the showing trends  $345^{\circ}$  and most commonly dips moderately to the east. The rocks contain abundant, barren, 5 to 6 centimetre wide, concordant quartz veins. Mineralization occurs within a discontinuous, vertical, mineralized shear over a metre in width and trending  $035^{\circ}$ . It cuts a quartz vein 60 metres long and up to 10 metres wide (oriented  $210^{\circ}/37^{\circ}W$ ).

Galena, pyrite and arsenopyrite mineralization is reported over a 60-metre strike length and has been tested by an adit 23 metres long, a shaft 4 to 6 metres deep and six old hand trenches (Aspinall, 1991). Our assay data were not available as this paper went to press. However, Aspinall reports on analysis of samples from a trench and from the shaft. They returned 8.05 and 10.4 grams per tonne gold, 475.2 and 35.3 grams per tonne silver, 6.88% and 0.10% lead and 24.27% and 22.69% arsenic respectively.

### **OTHER OCCURRENCES**

One new occurrence found in the Mount Sittakanay area remains unnamed. At this locality hornfelsed boulders up to 4 metres in diameter are mineralized with several percent pyrrhotite, about 1% chalcopyrite and minor sphalerite. The boulders are in moraine which was derived from the cirque wall less than 1.5 kilometres away.

Near the east end of Wendy Lake a pyrite-sericite alteration zone was discovered in a synclinal keel at the contact between dominantly sedimentary and volcanic packages. It is on strike with, and about 3 kilometres north of the Big Bull deposit. Mapping indicates that this horizon trends down towards the Big Bull open pit (K. Curtis, personal communication, 1993). Intervening rocks at the same stratigraphic level together with those along trend to the north, warrant further investigation.

### **REGIONAL MINERAL POTENTIAL**

The Tulsequah region is prospective for several types of mineral deposits, including volcanogenic massive sulphides, vein and shear-hosted gold deposits, porphyry copper-gold-molybdenum deposits, and skarns.

Significant **Kuroko-type volcanogenic massive**

**sulphide deposits** in the Mount Eaton block include the Tulsequah Chief and Big Bull orebodies. Exhalite mineralization is also recognized in the chert and limestone sequence on the north end of Mount Eaton, and perhaps in the Sittakanay Mountain block. On the basis of these known occurrences, regional potential for additional deposits of this type is high. The presence of other showings of this type in the Stikine assemblage north of Telegraph Creek underscores the need for additional mapping and exploration in intervening areas underlain by known and suspected Stikine assemblage rocks.

The massive sulphide potential of the Mount Stapler and Boundary Ranges suites may also be significant. Unusual mineralization at the Ono and Oya showings north of Shazah Creek includes several layers of massive sphalerite-galena-pyrite-arsenopyrite up to 30 centimetres thick and 30 metres long (Nelson, 1981). They are hosted in limestone, and according to Nelson (1981), in chert exhalite(?) and rhyolite. To the north, at the Maple Leaf showing, mineralized moraine boulders with semimassive pyrite, sphalerite and galena associated with areas of quartz-sericite-pyrite-altered schist may also be primary and exhalative in origin. Sediment from streams that drain the area yield regionally anomalous lead, zinc and copper values (Matysek *et al.*, 1988).

The area adjacent to the Llewellyn fault zone north of the map area contains numerous small **shear-related quartz veins** with anomalous precious, base metal and arsenic concentrations. The fault zone as a whole corresponds with pronounced regional geochemical anomalies. A similar style of mineralization apparently continues into the Tulsequah area, where numerous shear-related quartz-sulphide veins are in evidence, including the Banker, Sparling and Highland Girl showings, as well as several others in the Mount Sittakanay area. The Polaris-Taku mesothermal gold vein system may be genetically related to these smaller occurrences. Younger crossfaults also host quartz veins with minor sulphides and anomalous gold values (Smith and Mihalyuk, 1992).

**Skarn, porphyry and other intrusive-related deposit types** have not been previously identified in the Tulsequah River or Glacier map areas, despite the abundance of intrusive rocks and the presence of porphyry copper and molybdenum showings in the Mount Ogden area to the south. A possible candidate for this type of mineralization is the combined Stoker-Loeffel showing area, where chalcidonic quartz veins, skarn and porphyry-style(?) mineralization are all present. Pea-sized blebs of molybdenum and chalcopyrite in granites near Gisel Peak point to additional potential for porphyry-style mineralization, albeit in a restricted and inaccessible area.

### **SUMMARY AND DISCUSSION**

The Tulsequah region is underlain by Jurassic rocks of the Inklin overlap sequence (Laberge Group), the upper Palaeozoic Stikine assemblage (Mount Eaton and

Sittakanay blocks) and Upper Triassic Stuhini Group of the Stikine Terrane, metamorphic rocks of dominantly volcanic affinity (Polaris block, Boundary Ranges and Mount Stapler suites) and dominantly sedimentary affinity (Mount Strong block and Whitewater suite). Low grade Mesozoic and Paleozoic rocks are separated from high grade rocks along the Llewellyn fault and its southern continuation, the Chief fault.

A tentative geological/metallogenic evolution of the Tulsequah area is as follows:

- **Early to Late Paleozoic:** deposition of the Boundary Ranges and Mount Stapler suites, perhaps in part coeval with and/or overlying the Whitewater suite. Felsic to mafic volcanism and the abundance of associated sedimentary rocks suggests an arc-flank environment.
- **Pre-Pennsylvanian(?):** first phase deformation and development of intrafolial isoclinal folds in units west of the Llewellyn fault.
- **Devonian to Permian:** Stikine assemblage arc volcanism in the Late Devonian(?) to Mississippian, waning by late Pennsylvanian time. The Boundary Ranges and Mount Stapler suites may be in part lateral facies equivalents or basement to the lower part of the Stikine assemblage. Early Mississippian felsic volcanism and associated volcanogenic massive sulphide deposition.
- **Late Triassic:** Construction of the Stuhini arc over Stikine assemblage basement.
- **Early Jurassic:** deposition of the Inklin overlap assemblage above the Stuhini Group. Magmatism possibly correlative with the Hale Mountain granodiorite to the north. Major, mainly sinistral, offset on the Llewellyn fault
- **Early to Middle Jurassic.** Deformation and metamorphism of all older units; imbrication of units along west-directed thrust faults and the Llewellyn fault. Possible timing of precious metal mineralization along the dominantly dextral Llewellyn fault.
- **Late Cretaceous:** emplacement of scattered plutons.
- **Early Tertiary:** a major magmatic event producing the Sloko Group and formation of caldera complexes cored by high-level plutons. Easterly trending cross-faulting and associated base and precious metal vein mineralization. Porphyry-style and related skarn mineralization associated with some intrusions.

## ACKNOWLEDGMENTS

Our understanding of Stikine assemblage nuances has been greatly enhanced by discussions with other officers of the Geological Survey Branch, particularly Derek Brown, Jim Logan and John Drobe. Tulsequah emeritus JoAnne Nelson provided on-the-rocks geological orientation in the Stikine assemblage, dredging up all that she could remember of a mapping frenzy more than a decade ago. Data from Anglo Canadian Mining Corporation files were generously contributed to the project by Ron Stokes. Cominco

Limited provided company maps thanks to Bill Wolfe. Our job was made easier and safer through the expertise of Norm Graham of Discovery Helicopters. Terry Chandler, Garnett Dawson, Kerry Curtis, John Greig and other Redfern Resources Ltd. employees were gracious hosts at the Tulsequah Chief camp, who shared with us their hot showers, premium office space, and an extensive knowledge of the deposits.

## REFERENCES CITED

- Aspinall, N.C. (1991): Geological and Geochemical Assessment Report on the Denver - Rocky Gold - Juneau - Niagara #8 and Highland Girl Group of Claims, Tulsequah; *B.C. Ministry of Energy, Mines and Petroleum Resources*, Assessment Report 21 121.
- American Bullion Minerals, Limited (1990): Maple Leaf Property, A New Volcanogenic Sulphide Discovery; press release.
- Bradford, J.A. and Brown, D.A. (1993): Geology of the Bearskin Lake and Tatsamenie Lake Map Areas, Northwestern British Columbia (104K/1 and 8); in *Geological Fieldwork 1992*, Grant, B. and Newell, J.M., Editors, *B.C. Ministry of Energy, Mines and Petroleum Resources*, Paper 1993-1, pages 159-176.
- Brown, D.A., Logan, J.M., Gunning, M.H., Orchard, M.J. and Bamber, W.E. (1991): Stratigraphic Evolution of the Paleozoic Stikine Assemblage in the Stikine and Iskut Rivers Area, Northwestern British Columbia; *Canadian Journal of Earth Sciences*, Volume 28, pages 958-972.
- Bultman, T.R. (1979): Geology and Tectonic History of the Whitehorse Trough West of Atlin, British Columbia; unpublished Ph.D. thesis, *Yale University*, 284 pages.
- Currie, L.D. (1993): Metamorphic Rocks in the Tagish Lake Area, Northern Coast Mountains, British Columbia: A Possible Link Between Stikinia and Parts of the Yukon-Tanana Terrane; in *Current Research, Part A, Geological Survey of Canada*, Paper 92-1A, pages 199-208.
- Dawson, G.L., Harrison, D.J. and McGuigan, P.J. (1993): Big Bull Mine, Northwestern B.C., Tulsequah Chief Project 1992 Geological Program; *B.C. Ministry of Energy, Mines and Petroleum Resources*, Assessment Report 22 939.
- Doherty, R.A. and Hart, C.J.R. (1988): Preliminary Geology of the Fenwick Creek (105D/3) and Alligator Lake (105D/6) Map Areas; *Indian and Northern Affairs Canada*, Open File 1988-2, 87 pages.
- Johansson, G.G. (1993): Preliminary Report on the Stratigraphy, Sedimentology and Biochronology of the Inklin Formation in the Atlin Lake Area, Northern British Columbia; in *Current Research, Part A, Geological Survey of Canada*, Paper 93-1A, pages 37-42.
- Johnston, S.T. (1993): Emplacement Foliations in Aishihik Batholith (186 Ma), Southwest Yukon: Implications for Northern Stikinia; *Geological Association of Canada/Mineralogical Association of Canada*,

- Kerr, F.A. (1931a): Some of the Mineral Properties of the Taku District, British Columbia; *Geological Survey of Canada*, Summary Report 1930, Part A, pages 17-40.
- Kerr, F.A. (1931b): Explorations between Stikine and Taku Rivers, B.C.; *Geological Survey of Canada*, Summary Report 1930, Part A, pages 41-55.
- Kerr, F.A. (1948): Taku River Map-area; *Geological Survey of Canada*, Memoir 248.
- Logan, J.M. and Drobe, J.R. (1993): Geology and Mineral Occurrences of the Mess Lake Area (104G/7W); in *Geological Fieldwork 1992*, Grant, B. and Newell, J.M., Editors, *B.C. Ministry of Energy, Mines and Petroleum Resources*, Paper 1993-1, pages 135-148.
- Logan, J.M., Drobe, J.R. and McClelland, W.C. (1993): Devonian Intraoceanic Arc Magmatism in Northwestern Stikinia; *Geological Association of Canada/Mineralogical Association of Canada*, Programs and Abstracts, Edmonton, page A-60.
- McGuigan, P.J., Dawson, G.L. and Melnyk, W.D. (1993): Tulsequah Chief Mine, Northwestern B.C. 1992 Exploration Program: Diamond Drilling, Geology and Reserve Estimation; *B.C. Ministry of Energy, Mines and Petroleum Resources*, Assessment Report 22 939.
- Matysek, P.F., Day, S.J., Gravel, J.L. and Jackaman, W. (1988): Tulsequah Area, NTS 104K; *B.C. Ministry of Energy, Mines and Petroleum Resources*, BC RGS 20/GSC OF 1647 Regional Geochemical Survey release.
- Mihalynuk, M.G. and Rouse, J.N. (1988): Preliminary Geology of the Tutshi Lake Area, Northwestern British Columbia (104M/15); in *Geological Fieldwork 1987*, *B.C. Ministry of Energy, Mines and Petroleum Resources*, Paper 1988-1, pages 217-231.
- Mihalynuk, M.G., Currie, L.D., and Arksey, R.L. (1989): Geology of the Tagish Lake Area (Fantail Lake and Warm Creek); in *Geological Fieldwork 1988*, *B.C. Ministry of Energy, Mines and Petroleum Resources*, Paper 1989-1, pages 293-310.
- Mihalynuk, M.G. and Mountjoy, K.J. (1990): Geology of the Tagish Lake Area (104M/8, 9E); in *Geological Fieldwork 1989*, *B.C. Ministry of Energy, Mines and Petroleum Resources*, Paper 1990-1, pages 181-196.
- Mihalynuk, M.G., Mountjoy, K.J., Currie, L.D., Lofthouse, D.L. and Winder, N. (1990): Geology and Geochemistry of the Edgar Lake and Fantail Lake Map Area; *B.C. Ministry of Energy, Mines and Petroleum Resources*, Open File 1990-4.
- Monger, J.W.H. (1977): Upper Paleozoic Rocks of the Western Canadian Cordillera and their Bearing on Cordilleran Evolution; *Canadian Journal of Earth Sciences*, Volume 14, pages 1832-1859.
- Mortensen, J.K. (1992) Pre-mid-Mesozoic Evolution of the Yukon-Tanana Terrane, Yukon and Alaska; *Tectonics*, Volume 11, pages 836-854.
- Nelson, J. (1981): Ono-Oya Claims, Geology and Geochemical Results; *B.C. Ministry of Energy, Mines and Petroleum Resources*, Assessment Report 9007.
- Nelson J. and Payne, J.G. (1984): Paleozoic Volcanic Assemblages and Volcanogenic Massive Sulphide Deposits near Tulsequah, British Columbia; *Canadian Journal of Earth Sciences*, Volume 21, pages 379-381
- Payne, J.G. and Sisson, J.G. (1988): Geological Report on the Tulsequah Property; *B.C. Ministry of Energy, Mines and Petroleum Resources*, Assessment Report 17 054.
- Payne, J.G., Nelson, J.L. and Gosson, G. (1981): Taku-Tulsequah Regional Geology and Mineral Deposits; unpublished report, *Anglo Canadian Mining Corporation*.
- Sherlock, R., Childe, F., Barrett, T.J., Mortenson, J., Chandler, T., McGuigan, P., Dawson, G.L., Allen, R. and Lewis, P. (1994): Geological Investigations of the Tulsequah Chief Massive Sulphide Deposit, Northwestern British Columbia; in *Geological Fieldwork 1993*, Grant, B. and Newell, J.M., Editors, *B.C. Ministry of Energy, Mines and Petroleum Resources*, Paper 1994-1 this volume.
- Smith, M.T. and Mihalynuk, M.G. (1992): Tulsequah Glacier: Maple Leaf (104K); in *Exploration in British Columbia 1991*, *B.C. Ministry of Energy, Mines and Petroleum Resources*, pages 133-142.
- Souther, J.G. (1971): Geology and Mineral Deposits of Tulsequah Map-area, British Columbia; *Geological Survey of Canada*, Memoir 362.
- Thorstad, L.E. and Gabrielse, H. (1986): The Upper Triassic Kutcho Formation, Cassiar Mountains, North-central British Columbia; *Geological Survey of Canada*, Paper 86-16.
- Wheeler, J.O., Brookfield, A.J., Gabrielse, H. Monger, J.W.H., Tipper, H.W. and Woodsworth, G.J. (1971): Terrane: Map of the Canadian Cordillera; *Geological Survey of Canada*, Map 1713A.

## NOTES



**B.C. REGIONAL GEOCHEMICAL SURVEY PROGRAM:  
HIGHLIGHTS FROM THE 1993 RELEASE  
(104M)**

**By Wayne Jackaman**

*(Contribution to the Corporate Resources Inventory Initiative)*

**KEYWORDS:** Regional Geochemical Survey, reconnaissance, multi-element, stream sediment, stream water, Skagway.

**INTRODUCTION**

During the 1992 field season the British Columbia Ministry of Energy, Mines and Petroleum Resources conducted reconnaissance-scale stream sediment and water geochemical surveys in the northwest corner of the province (Figure 1). As part of the Ministry contribution to the Corporate Resources Inventory Initiative (CRII), the 1992 Regional Geochemical Survey (RGS) program contributed to the development of a detailed geoscience database. This database is vital to the evaluation of the mineral potential of this under-explored region and has stimulated further exploration and development of the local mineral resources. Prior to the 1992 RGS program, publicly available regional geochemical data for this area was limited to several small-scale surveys conducted by the Ministry as part of a 1:50 000 geological mapping project concentrated in areas adjacent to the Llewellyn fault (Mihalynuk and Rouse, 1988b; Mihalynuk, 1989; Mihalynuk *et al.*, 1990).

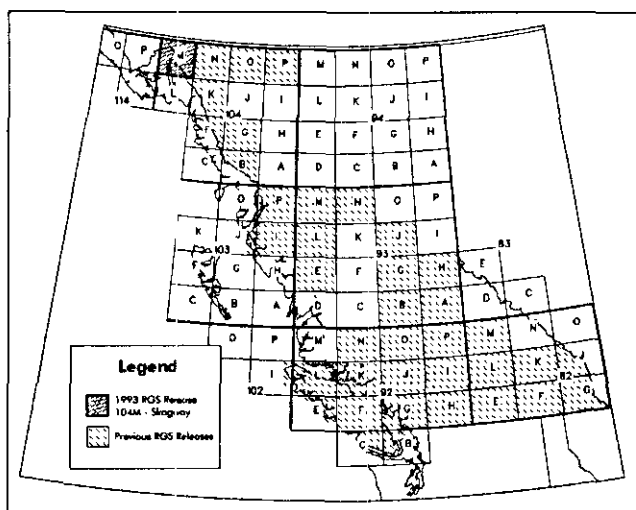


Figure 1. Current status of RGS program.

Results of the RGS program conducted in the Skagway map area (NTS 104M) were released as BC RGS 37 on August 4, 1993. The data package presented

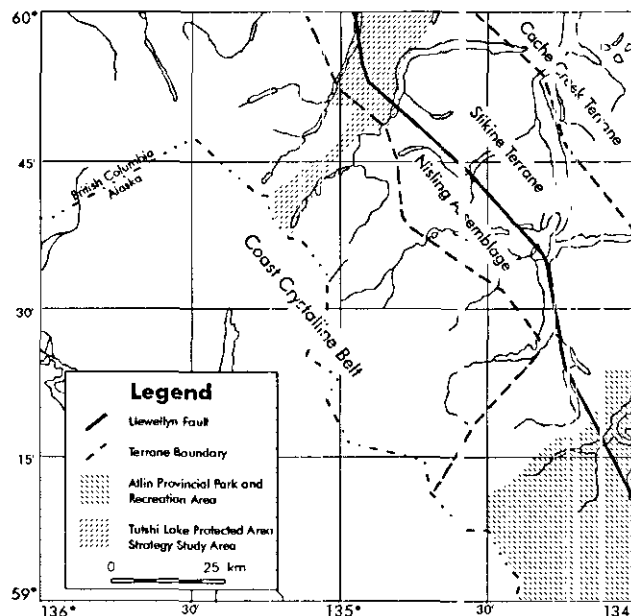


Figure 2. Skagway map sheet (NTS 104M).

field and analytical results for 785 samples located at an average density of 1 sample site every 10 square kilometres. Samples were also collected in the Allin Provincial Park and Recreation Area as well as in the Tutshi Lake Protected Area Strategy (PAS) study area (Figure 2). Survey results identified high concentrations of both base and precious metals in regions of known mineral potential as well as a number of new areas with little or no recorded exploration activity (Jackaman and Matysek, 1993). This paper will review survey results and highlight exploration opportunities by outlining regions of high mineral potential and identifying top-rated RGS sample sites.

**REGIONAL SETTING**

Situated in the northwest corner of British Columbia, the Skagway map sheet covers about 750 square kilometres and includes the Coast Mountain and Tachish Highland physiographic subdivisions (Holland, 1976). Trending southeast to northwest, the Coast Mountains extend along the western edge of the map area and are characterized by rugged mountain peaks separated by numerous glaciers and snowfields. Bordering this range

to the northeast are the Tagish Highlands which form a transition zone between the Coast Mountains and the Yukon plateaus. This region contains relatively smooth and gently sloping mountains separated by wide, U-shaped valleys.

The Skagway map area straddles the boundary between the Coast and Intermontane tectonic belts (Figure 2). In the west, the Coast crystalline belt is comprised of Late Cretaceous to Tertiary, undifferentiated granitoid rocks. To the east, Permian to Devonian Boundary Range metamorphic rocks and Paleozoic to Late Proterozoic Florence Range metamorphic rocks of the Nisling assemblage (Nisling Terrane?) mark the transition between the major tectonic belts (Mihalynuk and Mountjoy, 1990; Currie, 1990). The Intermontane Belt is dominated by rocks of the Whitehorse trough and includes Lower Jurassic Laberge Group sediments, younger volcanics of the Inklin overlap assemblage, rocks of the Upper Triassic Stuhini Group as well as Boundary Range metamorphic rocks (Mihalynuk and Rouse, 1988a; Mihalynuk *et al.*, 1989; Mihalynuk and Mountjoy, 1990). Mississippian to Upper Triassic Cache Creek Complex and Middle to Upper Triassic Peninsula Mountain volcano-sedimentary rocks are found in the northeast corner of the map area (Mihalynuk and Rouse, 1988a). Cretaceous to Tertiary granitic rocks of the Coast Plutonic Complex intrude rock units throughout the Intermontane Belt (Mihalynuk and Rouse, 1988a). The Llewellyn fault cuts the map sheet from southeast to northwest and marks the western extent of the Whitehorse trough. The Nahlin fault system separates the Whitehorse trough from the Cache Creek Terrane.

Historically, exploration activity has been concentrated in areas adjacent to the Llewellyn fault. This region extends from the Venus mine in the Yukon to the Engineer mine in the southeast corner of the Skagway map sheet. The zone is recognized for its anomalous antimony-arsenic provinces and scattered high gold and silver values (Mihalynuk and Mountjoy, 1990). Known mineral prospects in the region include precious and base metal quartz and quartz-carbonate veins, gold-copper skarns, massive sulphide pods and gold associated with listwanite-altered ultramafic rocks.

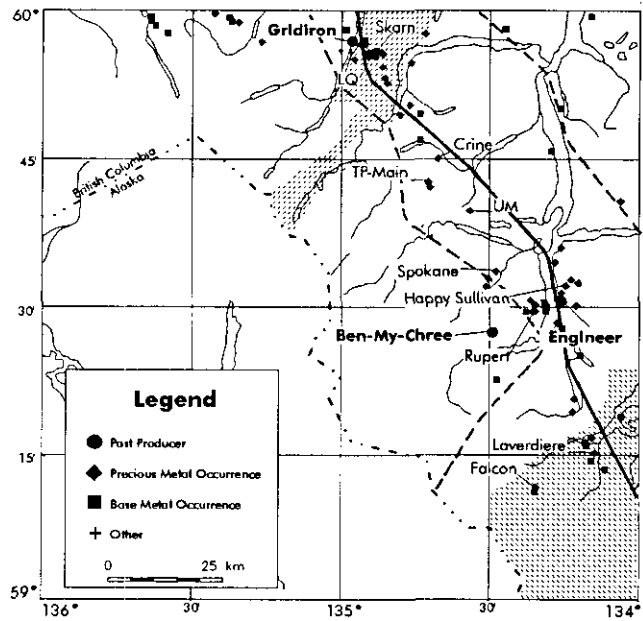


Figure 3. Recorded mineral occurrences.

A total of 87 mineral occurrences have been recorded in the Skagway map area (Jakobsen, 1993). Table 1 details existing past-producers, developed prospects and prospects as recorded in the British Columbia mineral deposits database (MINFILE). Figure 3 illustrates the distribution of these occurrences.

### GEOCHEMICAL TRENDS

Several regional trends have been identified utilizing the 104M data set. Figure 4 highlights selected geological units which show elevated mean concentrations for key ore and pathfinder elements relative to the 104M data set as well as to the current RGS provincial data set. These units are primarily located adjacent to the Llewellyn fault zone and the mineralization found in this region is often associated with this structure. Rocks of the Laberge Group (IJL, IJLg), Stuhini Group (uTsv) and the Boundary Range Metamorphic Suite (PPmb) provide mean concentrations

TABLE 1  
SELECTED MINERAL OCCURRENCES

Name	MINFILE id	Commodities	Status	Type	Geology	Rock Type
Gridiron	104M 001	Ag-Au-Pb-As-Zn	Past Producer	Vein	Boundary Range Metamorphic Suite	gneiss
Spokane	104M 006	Au-Ag-Zn-Pb-Cu	Dev. Prospect	Vein	Boundary Range Metamorphic Suite	schistose gneiss
Rupert	104M 008	Ag-Au-Pb-Zn-Cu	Prospect	Vein	Boundary Range Metamorphic Suite	gneiss
Ben-My-Chree	104M 011	Ag-Au-Cu-Pb-Zn	Past Producer	Vein	unknown	diorite
Happy Sullivan	104M 013	Au-Ag	Prospect	Vein	Laberge Group	greywacke
Engineer Mine	104M 014	Au-Ag-Sb-Te	Past Producer	Vein	Laberge Group	greywacke
Laverdiere	104M 022	Cu-Ag-Au-Mo	Prospect	Skarn	Stuhini Group	limestone
LQ	104M 044	Au-Ag-Zn-Cu-Pb	Prospect	Vein	Boundary Range Metamorphic Suite	gneiss
TP - Main	104M 048	Au-Ag-Co-Cu-Fe	Prospect	Skarn	Boundary Range Metamorphic Suite	marble
Crine	104M 081	Au-Ag-Pb-Zn-As	Prospect	Vein	Boundary Range Metamorphic Suite	schist
UM	104M 084	Au-Ag	Prospect	Vein	unknown	listwanite-altered peridotite
Skarn	104M 085	Au-Cu	Prospect	Skarn	Stuhini Group	porphyritic volcanoclastics
Falcon	104M 087	Ag-Au-Zn-Pb-Cu	Prospect	Vein	Nisling Assemblage	schist

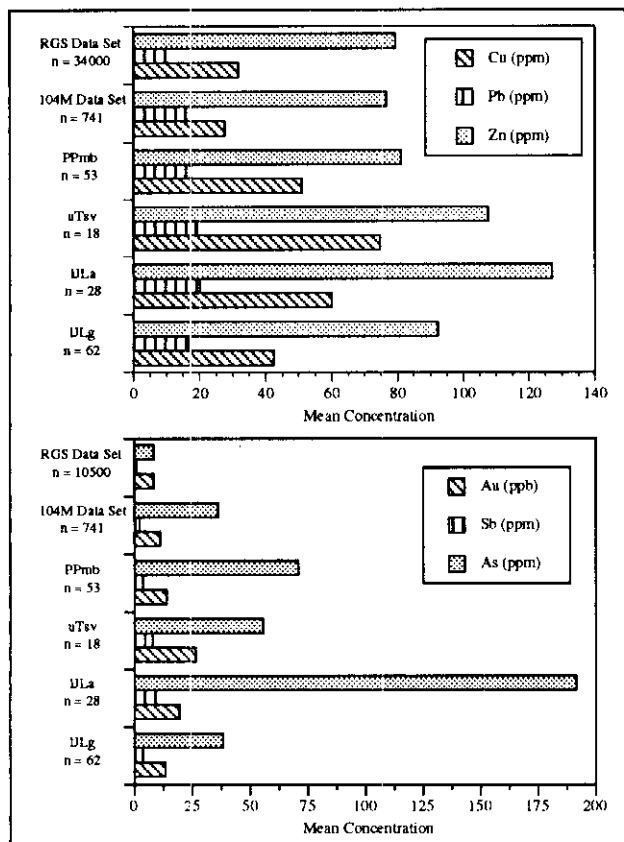


Figure 4. Average concentrations for key elements.

for gold, antimony and arsenic which are significantly higher than both the survey and provincial averages. Average values for copper, lead and zinc show similar results. Lead also returns high average concentrations for several units associated with the Coast Plutonic Complex. These general patterns further define lithological units adjacent to the Llewellyn fault system which have previously been identified as having potential for hosting mineralization (Mihalynuk and Rouse, 1988a; Mihalynuk *et al.*, 1989; Mihalynuk and Mountjoy, 1990).

### TOP-RATED RGS ANOMALIES

Utilizing an interpretive technique described in detail by Jackaman and Matyssek (1993), samples from the 104M survey which are characterized by anomalous, multi-element signatures have been identified. In general, the technique attempts to distinguish samples which are most likely to reflect mineralized sources from samples affected by lithological units characterized by high background values. Each sample is coded with the predominant lithology found within the drainage basin boundaries upstream from the sample site. The geology base map used to code sample sites is an unpublished compilation by Mihalynuk and Smith (1993). Percentile or threshold values for every element are calculated for each identified lithology. Ratings of 1, 2 or 3 are assigned to each element based on the calculated 90th, 95th and 98th percentile values, respectively. Multi-

element anomalies for a base metal suite of elements (Cu-Pb-Zn-Ag) and a precious metal suite (Au-Sb-As-Hg-Ag) are determined by summing the element ratings for each sample. The top 25% of the anomalies determined by this technique are ranked in Table 2 and Table 3. The distribution of these sites is illustrated on Figure 5. The table includes the relationship of the sites to known mineral occurrences and mineral tenure as well as the location relative to the Atlin Provincial Park and Recreation Area and the Tutshi Lake PAS study area.

As expected, a large number of the base and precious metal anomalies are concentrated within a zone 10 to 50 kilometres wide adjacent to the Llewellyn fault. This trend extends from Bennett Lake to Willisson Bay and into the Atlin Provincial Park and Recreation Area. Several base metal anomalies are also clustered in the Primrose River region. With reference to Table 2 and Table 3, about half of the listed sample sites are associated with intrusive rocks of the Coast Plutonic Complex (eTg, KTg, IKg, Kg). Stuhini Group (uTsv) and Boundary Range metamorphic rocks (PPmb) are represented by over 10% of the sample sites. Five sites list Laberge Group rocks (JLa, JLg) as the predominant drainage basin lithology upstream from the sample site. Known mineral occurrences are located within drainage basin boundaries upstream from eleven of the top-rated sample sites. Also identified are a large number of anomalies associated with existing mineral claims, including seven of the top-rated anomalies which were staked in August as a direct result of the 1992 survey. Detailed follow-up work will be conducted on several of these new mineral claims during 1994 (R.H. McMillan, personal communication, 1993). Of the remaining sites open to staking, the most notable are several base metal anomalies including four sites (923200, 923111, 925233 and 921112) which also returned significant precious metal values.

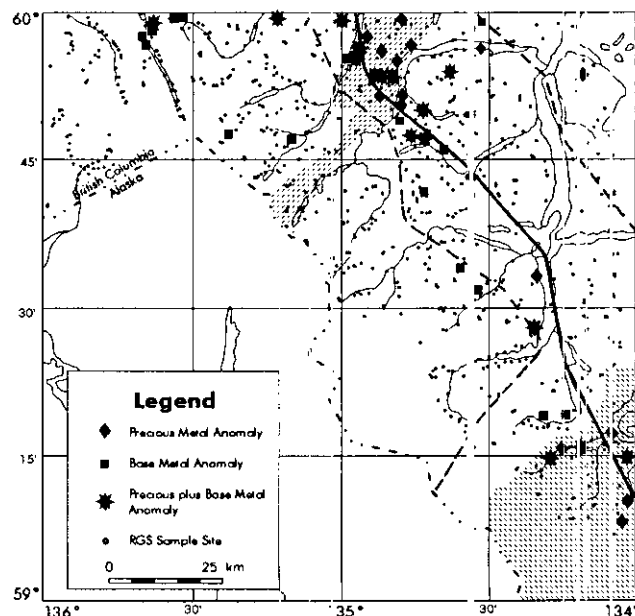


Figure 5. Top-rated multi-element anomalies.

TABLE 2  
TOP-RATED BASE METAL ANOMALIES

MAP	ID	FORM	Cu ppm	Pb ppm	Zn ppm	Ag ppm	Anomaly Rating					Total	Status (September, 1993)	Recorded Mineral Occurrences
							Cu	Pb	Zn	Ag				
104M08	925191	eJgd	114	65	268	0.7	3	3	3	3	12	staked (Ice Claims)	none	
104M15	923200	IJLa	140	74	498	0.8	3	3	3	3	12	open, PAS	none	
104M15	925271	Kg	83	165	129	3.0	3	3	3	3	12	staked August, 1993 (Pen Claims)	none	
104M15	925363	IKg	94	65	135	1.4	3	3	2	3	11	staked (Pavey Claims), PAS	Silver Queen (002) - Au,Cu,Ag	
104M15	925111	IJLg	132	51	160	0.9	3	3	2	3	11	open	none	
104M14	925162	eTg	52	107	386	1.0	2	3	3	3	11	open	none	
104M15	923119	IKg	104	35	166	0.7	3	2	3	2	10	open, forfeited tenure	none	
104M15	925350	Qal	130	76	286	1.3	1	3	2	3	9	partially staked (Ben Claims), PAS	none	
104M15	925349	Qal	230	39	227	1.2	3	2	1	3	9	partially staked (Catfish Claims), PAS	none	
104M15	925122	uTsv	100	46	301	0.7	1	2	3	3	9	staked (Tut Claims)	none	
104M15	925348	Qal	180	62	178	1.2	2	3	1	3	9	staked (Catfish Claims), PAS	Catfish (074) - Au,Ag,Cu,Pb,Zn,As	
104M01	923044	PPgn	82	20	357	0.7	3				3	mineral and placer reserve	none	
104M10	925230	PPmb	76	40	152	0.8	1	2	2	3	8	staked (TP Claims)	none	
104M10	925056	eKt	131	18	72	0.2	3	2	3		8	open	none	
104M15	923226	IKg	9	127	133	5.0		3	2	3	8	open, PAS	Net 3 (059) - Ag,U,Th,Mo,W	
104M13	925138	eTg	33	175	199	1.2	1	3	1	3	8	open	none	
104M13	925470	eTg	43	186	407	0.5	1	3	3		7	open	Silt (054) - Mo	
104M13	923086	eTg	27	72	252	1.6	1	1	2	3	7	open	none	
104M01	925095	Kg	118	28	134	0.5	3	1	3		7	mineral and placer reserve	none	
104M08	923010	PPgn	78	75	234	0.6	1	3	1	2	7	open	none	
104M15	925365	ImJv	29	115	136	2.3		3	1	3	7	staked (Pavey Claims), PAS	Gaug-West (038) - Au,Ag,Pb,Sb,As	
104M08	925004	PPgn	80	9	349	0.6	2	3	2	7	7	open, forfeited tenure	none	
104M15	923208	TP	47	8	113	0.2	3				6	open	none	
104M15	923196	PPmb	60	43	145	0.6		3	1	2	6	staked August, 1993 (Tutshi Claims)	Jessie (027) - Ag,Au,Cu,Pb,Zn	
104M01	925088	ITgd	78	9	59	5.2	3				3	Atlin Provincial Park	none	
104M14	925127	Es	18	33	106	0.3	3	3			6	staked August, 1993 (Part Claims)	none	
104M15	925233	PPmb	82	22	197	0.6	1		3	2	6	open	none	
104M15	925362	IKg	43	18	158	0.7	1		3	2	6	staked (Pavey Claims), PAS	Net 6 (058) - U,Th	
104M13	925468	KTg	15	33	104	0.7		3	3	6	6	open	none	
104M10	925335	PPmb	74	36	167	0.6	1	3	2	6	6	staked (TP Claims)	TP (048,049,050) - Au,Ag,Co,Cu,Ma	
104M13	921110	KTg	31	38	164	0.4		3	3	6	6	open	none	
104M14	925242	eTg	18	92	165	1.0	2	1	3	6	6	open	none	
104M10	923024	PPmb	103	43	105	0.3	3	3			6	staked August, 1993 (Horn Claims)	none	
104M13	921112	eTg	18	120	203	0.8	3	1	2	6	6	open	Pit Creek (055) - Mo	

TABLE 3  
TOP-RATED PRECIOUS METAL ANOMALIES

MAP	ID	FORM	Au ppb	Sb ppm	As ppm	Hg ppm	Ag ppm	Anomaly Rating					Total	Status (September, 1993)	Recorded Mineral Occurrences
								Au	Sb	As	Hg	Ag			
104M15	925348	Qal	72	18	1000	960	1.2	3	2	3	3	3	14	staked (Catfish Claims), PAS	Catfish (074) - Au,Ag,Cu,Pb,Zn,As
104M08	925191	eJgd	30	11	190	70	0.7	2	3	3	3	3	14	staked (Ice Claims)	none
104M15	925365	ImJv	287	140	390	20	2.3	3	3	3	3	12	staked (Pavey Claims), PAS	Gaug-West (038) - Au,Ag,Pb,Sb,As	
104M15	925271	Kg	217	15	160	20	3	3	3	3	3	12	staked August, 1993 (Pen Claims)	none	
104M15	925350	Qal	61	27	670	30	1.3	2	3	3	3	11	partially staked (Ben Claims), PAS	none	
104M01	923043	IThg	26	18	32	600	0.3	2	3	2	3	10	Atlin Provincial Park	none	
104M15	925363	IKg	41	69	910	50	1.4	1	3	3	3	10	staked (Pavey Claims), PAS	Silver Queen (002) - Au,Cu,Ag	
104M15	923200	IJLa	81	71	3200	80	0.8	1	3	3	3	10	open, PAS	none	
104M01	925095	Kg	2	31	150	170	0.5		3	3		9	mineral and placer reserve	none	
104M15	925349	Qal	27	24	320	40	1.2	2	2	2	3	9	partially staked (Catfish Claims), PAS	none	
104M15	925362	IKg	41	22	1100	50	0.7	1	3	3	2	9	staked (Pavey Claims), PAS	Net 6 (058) - U,Th	
104M15	923119	IKg	32	34	740	50	0.7	1	3	3	2	9	open, forfeited tenure	none	
104M01	925088	ITgd	18	4.8	31	40	5.2	1	3	2	3	9	Atlin Provincial Park	none	
104M15	925366	PTgd	317	4.3	48	20	0.2	3	3	3	3	9	staked (Pavey Claims), PAS	none	
104M14	925127	Es	170	2.2	36	10	0.3	3	3	3	3	9	staked August, 1993 (Part Claims)	none	
104M15	921004	ITg	363	7.5	160	40	0.2	3	3	3	3	9	staked August, 1993 (Pad Claims), PAS	none	
104M15	925391	eTg	150	1.7	24	20	0.2	3	3	3	3	9	staked August, 1993 (Pat Claims)	none	
104M01	925090	PPgn	4	4.3	34	170	1.4	3			3	9	mineral and placer reserve	none	
104M15	921006	ITg	94	10	170	30	0.2	3	3	3	3	9	staked (Catfish Claims), PAS	none	
104M15	925122	uTsv	25	16	200	30	0.7	3	2	3	2	8	staked (Tut Claims)	none	
104M15	921005	ITg	30	10	140	30	0.2	2	3	3	3	8	staked (Catfish Claims), PAS	none	
104M15	923240	uTsv	67	12	220	70	0.4	2	1	3	2	8	staked August, 1993 (Wyn Claims), PAS	none	
104M15	925233	PPmb	33	19	770	50	0.6	3	3	3	2	8	open	none	
104M15	925384	IJLg	22	18	170	30	0.6	1	3	3	1	8	staked (Willard Claims), PAS	Ben (045,046) - Au,Ag,Pb,Cu	
104M15	925364	ImJv	41	13	1100	40	0.5	2	3	3	3	8	staked (Pavey Claims), PAS	none	
104M08	921019	ITgd	5	27	28	340	0.2	3	2	3	3	8	mineral and placer reserve	none	
104M18	921058	MTCI	15	5.8	28	210	0.2	1	3	2	2	8	open	none	
104M15	923205	ImJv	34	35	510	40	0.5	2	3	3	3	8	staked (L-B Claims), PAS	Skarn (088) - Au,Cu	
104M10	925227	uTs	12	8.3	79	40	0.3	1	3	3	3	7	open, forfeited tenure	none	
104M15	923242	IKg	208	9.6	200	30	0.5	3	2	2	2	7	open, PAS	none	
104M15	925345	IKg	44	8.3	260	20	0.6	2	2	2	1	7	open, forfeited tenure	none	
104M01	923044	PPgn	22	3.4	42	50	0.7	3	1		3	7	mineral and placer reserve	none	
104M09	925318	PPmb	39	11	45	70	0.2	2	2		3	7	open	none	
104M01	925084	IThg	36	11	20	130	0.3	2	3	1	1	7	Atlin Provincial Park	none	
104M15	925103	Qal	27	5.3	81	30	0.6	2	1	2	2	7	open	none	
104M15	925111	IJLg	25	3.7	92	50	0.9	2	2	2	3	7	open	none	
104M15	925352	IJLa	46	6.2	260	20	0.7	1	3	3	3	7	open, PAS	none	
104M13	921112	eTg	35	0.6	18	20	0.8	3	2	2	2	7	open	Pit Creek (055) - Mo	

Although this evaluation of the 104M data set has identified many of the top-rated anomalies, some significant results are overlooked. For example, single-element highs for both base and precious metal results are not highlighted by this technique. In terms of precious metal values this includes five unstaked sites returning gold values greater than 100 ppb, three that produced gold values in excess of 50 ppb and one that returned a silver value of 12 ppm. A second limitation of this method is the small number of elements considered. The 104M data set includes analytical determinations for a total of 35 metals in stream sediments and four element determinations in stream waters. Finally, the identification of subtle multi-element highs would also benefit from a more rigorous statistical interpretation which includes detailed background modeling techniques.

## CONCLUSIONS

Results of this survey have defined new zones of high mineral potential adjacent to the Llewellyn fault. Anomalous values for gold, antimony, arsenic, copper, lead and zinc are associated with several key geological units including rocks of the Laberge Group, Stuhini Group and the Boundary Range Metamorphic Suite. These units are noted to have potential for precious metal vein deposits, gold-quartz veins, gold-stibnite veins, auriferous quartz-carbonate zones and gold skarns. Although many top-rated RGS anomalies have been staked, several sample sites with significant base and precious metal values remain open to new exploration. In addition, regions previously explored deserve new attention in response to the results of this survey.

## ACKNOWLEDGMENTS

Acknowledgments are extended to Paul Matysek for his critical review of this paper. The manuscript also benefited from editorial comments by John Newell.

## REFERENCES

- Currie, L.D. (1990): Metamorphic Rocks in the Florence Range, Coast Mountains, Northwestern British Columbia; in Geological Fieldwork 1989, *B.C. Ministry of Energy, Mines and Petroleum Resources*, Paper 1990-1, pages 197-203.
- Holland, S.S. (1976): Landforms of British Columbia, A Physiographic Outline; *B.C. Ministry of Energy, Mines and Petroleum Resources*, Bulletin 48.
- Jackaman, W. and Matysek, P.F. (1993): British Columbia Regional Geochemical Survey - Skagway (NTS 104M); *B.C. Ministry of Energy, Mines and Petroleum Resources*, BC RGS 37.
- Jakobsen, D.E. (1993): Skagway Mineral Occurrence Map; *B.C. Ministry of Energy, Mines and Petroleum Resources*, MINFILE, revised August 1993.
- Mihalynuk, M. (1989): Geology and Geochemistry of the Warm Creek (East Half) and Fantail Lake (West Half) Map Area; *B.C. Ministry of Energy, Mines and Petroleum Resources*, Open File 1989-13.
- Mihalynuk, M.G. and Mountjoy, K.J. (1990): Geology of the Tagish Lake Area; in Geological Fieldwork 1989, *B.C. Ministry of Energy, Mines and Petroleum Resources*, Paper 1990-1, pages 181-196.
- Mihalynuk, M.G. and Rouse, J.N. (1988a): Preliminary Geology of the Tutshi Lake Area, Northwestern British Columbia; in Geological Fieldwork 1988, *B.C. Ministry of Energy, Mines and Petroleum Resources*, Paper 1988-1, pages 217-232.
- Mihalynuk, M.G. and Rouse, J.N. (1988b): Geology and Regional Geochemistry Survey of the Tutshi Lake Map Area; *B.C. Ministry of Energy, Mines and Petroleum Resources*, Open File 1988-5.
- Mihalynuk, M.G. and Smith, M. (1993): Geology Compilation of NTS Map Sheet 104M - Skagway; *B.C. Ministry of Energy, Mines and Petroleum Resources*, unpublished map.
- Mihalynuk, M.G., Currie, L.D. and Arksey, R.J. (1989): The Geology of the Tagish Lake Area; in Geological Fieldwork 1988, *B.C. Ministry of Energy, Mines and Petroleum Resources*, Paper 1989-1, pages 293-310.
- Mihalynuk, M.G., Mountjoy, K.J., Currie, L.D., Lofthouse, D.L. and Winder, N. (1990): Geology and Geochemistry of the Edgar Lake and Fantail Lake Map Area; *B.C. Ministry of Energy, Mines and Petroleum Resources*, Open File 1990-4.

## NOTES

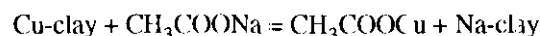


**THE SEQUENTIAL EXTRACTION OF COPPER, SILVER, MOLYBDENUM,  
IRON AND MANGANESE FROM GEOCHEMICAL STANDARDS AND  
SELECTED SAMPLES**

By **B.Bhagwanani and R.E.Lett**

**KEYWORDS:** Applied geochemistry, sequential extraction, copper, molybdenum, iron, manganese, silver, lake sediments, glaciolacustrine sediments.

surface of clay minerals and metal in the form of carbonates. An example of the exchange of copper from clay with sodium acetate is:



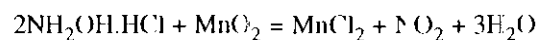
**INTRODUCTION**

The sequential, selective extraction of elements from geochemical samples using different chemicals is becoming a routine procedure for determining the distribution of metals in mineral phases which commonly constitute weathered materials. Several sequential extraction techniques have been developed to aid in the interpretation geochemical data by measuring the relative mobility of the elements in the near-surface environment (Tessier *et al.*, 1979; Hoffman and Fletcher, 1979; Gatehouse *et al.*, 1977). Sequential extraction analysis has been applied to assessing environmental problems by determining the bio-availability of potentially toxic metals such as chromium, lead, mercury and cadmium in contaminated sediments and soils (Campbell *et al.*, 1988). The efficiency of the extraction procedure to selectively remove all of the metal from samples and the quality of the data produced are important for reliably interpreting the results of sequential analysis.

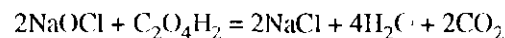
Research has focused on establishing the most suitable sequence of extraction for treating different sample types and for improving the efficiency of the extraction method (Rose, 1975; Chao and Sanzalone, 1992; Papp *et al.*, 1991; Hall *et al.*, 1993). This paper describes the extraction of copper, silver, molybdenum, iron and manganese from geochemical reference materials and selected samples using a sequence of sodium acetate solution, hydroxylamine hydrochloride solution, sodium hypochlorite solution and Lafort aqua regia.

The method used in this study is modified from a procedure developed by Hall *et al.* (1993). Sodium acetate solution (pH 5) removes metal adsorbed on colloidal iron and manganese oxides, metal adsorbed on organic particles, metal held in exchange sites on the

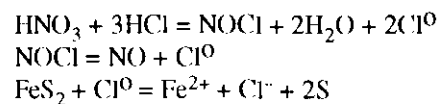
Hydroxylamine hydrochloride (NH<sub>2</sub>OH.HCl) solution reduces amorphous manganese and iron oxides and releases absorbed trace metals in the process. The reaction between manganese dioxide and hydroxylamine hydrochloride is:



Alkaline sodium hypochlorite (NaOCl) solution oxidizes organic matter to release absorbed and complexed metals. Mineral sulphides are not oxidized by this reagent (Papp *et al.*, 1991). An example of the oxidation reaction for a simple organic compound such as oxalic acid is:



Lafort aqua regia (3 volumes concentrated nitric acid mixed with 1 volume concentrated hydrochloric acid) oxidizes sulphide minerals and dissolves noble metals such as gold and platinum. The initial reaction between nitric acid and hydrochloric acid produces nascent chlorine which dissolves metals and oxidizes sulphides. An example of the reaction for the oxidation of pyrite is:



The Lafort digestion was chosen for the final stage of the sequential extraction because this acid mixture is a powerful oxidizing agent, especially for sulphides, and is commonly used in the analysis of regional geochemical samples collected in British Columbia.

In addition to the sequential extraction, the reference materials and samples were also analysed separately for the same elements, using a concentrated hydrofluoric-perchloric-nitric-hydrochloric acid digestion. This

mixture will dissolve most of the silicate, oxide and sulphide minerals found in weathered materials. Certain aluminosilicate and oxide minerals, however, are resistant to the attack by this acid mixture and are only partially dissolved (Chao and Sanzalone, 1992).

## ANALYTICAL METHODS

### QUALITY CONTROL AND SAMPLES

The CANMET reference materials LKSD 1 and 3, and the United States Geological Survey reference material GXR3 were used to monitor the analytical precision of the extraction data. Each batch of 24 samples contained a replicate sample, LKSD1 and LKSD3 standards and a solution blank. In one batch, GXR1 was substituted for LKSD 1. A description of each reference material, the recommended mean value, the uncertainty range for each element and the loss on ignition are shown in Table 1. The information is taken from compilations by Lynch, 1990 and by Gladney and Roelandts, 1990.

**Table 1. Mean values and uncertainty range ( $\pm 2$  standard deviation) for elements in reference samples**

Description	Silver (ppm)	Copper (ppm)	Iron (%)	Manganese (ppm)	Molybdenum (ppm)	LOI (%)
LKSD 1 Lake bottom sediment	0.6 $\pm$ 0.1	44 $\pm$ 10	2.8 $\pm$ 0.2	700 $\pm$ 60	10 $\pm$ 4	23.5 $\pm$ 1.0
LKSD 3 Lake bottom sediment	2.7 $\pm$ 0.2	35 $\pm$ 6	4.0 $\pm$ 0.4	1440 $\pm$ 160	<0.5	11.8 $\pm$ 1.2
GXR1 Igneous rock sample	31 $\pm$ 4	1110 $\pm$ 115	25 $\pm$ 1.2	880 $\pm$ 70	18 $\pm$ 6	5.3 $\pm$ 0.7

Other samples analysed were pulverised lake bottom sediments (Cook, 1993) and the -63 micron fraction of glaciolacustrine sediments (Bobrowsky *et al.*, 1993). All of the samples were collected in central British Columbia.

### SEQUENTIAL EXTRACTIONS

Standards and samples were analysed for copper, silver, molybdenum, iron and manganese by the following sequence of extraction reagents.

#### SODIUM ACETATE SOLUTION

A 2.00-gram sample was weighed into a 25 by 100 millimetre Pyrex test tube (calibrated at 20 mL) and mixed with 20 mL of 1.00 M sodium acetate solution (136.00 g anhydrous sodium acetate dissolved in 800 mL of distilled water and 20 mL glacial acetic acid. The pH

was adjusted to  $5.0 \pm 0.1$  with acid and the solution diluted to 1 L with distilled water). Each tube was stoppered and the contents carefully mixed to avoid loss of material (due to frothing) using a Vortex mixer every 20 minutes for 6 hours. The samples were then centrifuged for 10 minutes at approximately 3000 rpm. Turbid solutions were centrifuged again for another 5 minutes. Clear solutions were decanted into clean 25 by 150 millimetre glass test tubes (calibrated at 30 mL). Residues were mixed thoroughly with 5 millilitres of distilled water, centrifuged for 10 minutes and the washings added to the extracts. The washing was repeated with another 5 millilitres of distilled water and combined washings and extracts diluted to 30 millilitres with distilled water. Samples were stored in the dark to limit loss of silver by precipitation. Residues were digested in hydroxylamine hydrochloride.

#### HYDROXYLAMINE HYDROCHLORIDE SOLUTION

The residue from the sodium acetate extraction was added to 20 millilitres of 0.25 M hydroxylamine hydrochloride (17.36 g of hydroxylamine hydrochloride dissolved in 500 mL of distilled water, mixed with 21 mL of concentrated hydrochloric acid and diluted to 1 L) in stoppered tubes and mixed thoroughly using a Vortex mixer every 5 to 10 minutes until frothing subsided. The samples were heated at 60°C for 2 hours in a water-bath with shaking and vortexing every 30 minutes. After extraction the residues were washed twice with distilled water using the same procedure as in the sodium acetate extraction. Hydroxylamine hydrochloride extracts and distilled water washings were combined and solutions diluted to 30 millilitres. The residues were digested in sodium hypochlorite solution.

#### SODIUM HYPOCHLORITE SOLUTION

Twenty millilitres of 5% sodium hypochlorite solution (pH 9.5) was mixed with the hydroxylamine hydrochloride extraction residue. If frothing occurred the samples were carefully mixed every 5 to 10 minutes until the frothing subsided. The samples were heated at 100°C for 1 hour in a water-bath with shaking and vortexing of each sample every 20 minutes. After the extraction stage was completed the residue was washed twice with distilled water using the same procedure as in the sodium acetate extraction. Sodium hypochlorite extracts and distilled water washings were combined and solutions diluted to 30 millilitres. The residues were digested in Lefort aqua regia

#### LEFORT AQUA REGIA

Five millilitres of concentrated nitric acid (ACS grade) were mixed thoroughly with the sodium

hypochlorite residues and the samples allowed to stand overnight. The sample tubes were then heated at 90°C for 30 minutes in a water-bath, the contents mixed, 1.5 millilitres of concentrated hydrochloric acid added and the mixing repeated. The samples were then heated at 90°C for a further 90 minutes in the water-bath, the contents cooled and then diluted to 20 millilitres with distilled water. The solutions were mixed, centrifuged and the residue discarded.

### HYDROFLUORIC-PERCHLORIC-NITRIC-HYDROCHLORIC ACIDS

One gram of sample was mixed with 5 millilitres concentrated hydrochloric acid, 5 millilitres of a nitric-perchloric acid mixture (3:1 v/v) and 5 millilitres hydrofluoric acid in a teflon beaker and reduced to dryness on a hotplate. Residues were heated for 10 to 15 minutes with 4 millilitres concentrated hydrochloric acid and 1.5 millilitres concentrated nitric acid, cooled and the contents of the beaker transferred to calibrated test tubes. The solutions were made up to 15 millilitres with distilled water, mixed thoroughly and centrifuged.

### ANALYSIS OF EXTRACTS FOR METALS

The extracted solutions and hydrofluoric-perchloric-nitric-hydrochloric acid digests were analyzed for copper, silver, molybdenum, iron and manganese using a Perkin Elmer 2280 atomic absorption spectrometer. Background correction was applied for silver which was analysed first (preferably on same day as the extraction), to avoid silver loss from solution by precipitation. Approximately 10 milligrams of aluminum chloride was added to a 2-millilitre aliquot of the solutions for the molybdenum analysis. The calibration standards were made with a similar concentration of aluminum chloride.

### DISCUSSION OF RESULTS

Copper, silver, molybdenum, iron and manganese precision expressed as relative standard deviations (%RSD) for the reference materials LKSD 1 and LKSD 3 are shown in Tables 2 and 3.

Table 2. Precision for LKSD 1 (mean of 7 analyses)

	Sodium	Hydroxylamine	Sodium	Aqua	Hydrofluoric
	Acetate	Hydrochloride	Hypochlorite	Regia	Acid
Cu-Mean (ppm)	1	8	18	18	44
Cu (%RSD)	28	17	16	15	3
Mo-Mean (ppm)	0.5	0.5	3	2	10
Mo (%RSD)	31	53	48	51	7
Mn-Mean (ppm)	230	86	37	64	686
Mn (%RSD)	7	8	205	18	5
Fe-Mean (%)	0.039	0.043	0.044	1.36	2.79
Fe (%RSD)	48	22	57	22	7

Table 3. Precision for LKSD 3 (mean of 7 analyses)

	Sodium	Hydroxylamine	Sodium	Aqua	Hydrofluoric
	Acetate	Hydrochloride	Hypochlorite	Regia	Acid
Ag-Mean (ppm)	0.5	1.4	1.4	11	2.8
Ag (%RSD)	0	21	21	7	5
Cu-Mean (ppm)	3	8	9	11	25
Cu (%RSD)	19	15	34	0	2
Mn-Mean (ppm)	647	435	101	137	1276
Mn (%RSD)	3	6	255	3	3
Fe-Mean (%)	0.029	1.32	0.01	1.83	3.86
Fe (%RSD)	4	20	46	5	5

The mean and RSD values for each element were calculated from seven repeat determination: of the reference materials analysed by the sequential extractions and by the hydrofluoric-perchloric-nitric-hydrochloric acid digestion. Table 4 shows the copper, molybdenum, iron and manganese precision calculated from sequential extraction data for ten replicate samples inserted in batches during routine analysis. Silver precision for LKSD 1 and for the replicates samples and molybdenum precision for LKSD 3 are not reported because values are below or just above detection limits.

Table 4. Precision calculated from ten replicate samples

	Sodium	Hydroxylamine	Sodium	Aqua
	Acetate	Hydrochloride	Hypochlorite	Regia
Replicate Mean Cu	100	117	13	90
RSD Cu (%)	9	3	14	3
Replicate Mean Mo	8	3	14	2
RSD Mo (%)	7	17	11	16
Replicate Mean Mn	154	433	11	129
RSD Mn (%)	149	5	5	3
Replicate Mean Fe	0.132	1.04	0.03	1.73
RSD Fe (%)	160	3	21	3

Most precise silver, copper, molybdenum, iron and manganese determinations (< 8% RSD) are for the reference samples analysed with the hydrofluoric-perchloric-nitric-hydrochloric acid digestion. Good precision (< 8% RSD) is also revealed for manganese extracted from the reference samples with sodium acetate and hydroxylamine hydrochloride. The manganese precision for the sodium hypochlorite extraction of the reference samples (Tables 2 and 3) and the sodium acetate extraction of the replicate samples is poor (>14% RSD) reflecting large differences between repeat determinations (Table 4). However, precision calculated from replicate analyses, improves for the sodium hypochlorite extractable manganese.

Copper precision (RSD) ranges from 34% for the sodium hypochlorite extraction of LKSD 1 (Table 2) to 15% for Lefort aqua regia digestion of LKSD 3 (Table 3). The variation of iron and manganese precision for the different extractions resembles copper in that the largest RSD is for the sodium hypochlorite extraction (Table 3). The relatively poor precision for the sodium hypochlorite

extractable copper, iron and manganese may be due to variations in the amount of organic matter oxidized from the reference sample and precipitation of colloidal hydroxides in the alkaline solution. Replicate sample analysis for iron reveals that RSD values are greater 100% for the sodium acetate extraction. This precision reflects a large difference between the iron values for one of the replicate samples. Molybdenum replicate data reveal improved precision due to the higher concentrations of molybdenum in the replicates compared to the reference samples.

Metal concentrations extracted by each reagent from the reference materials LKSD 1, LKSD 3 and GXR 1 are shown in Table 5. Values are expressed in parts per million and as a percentage of the reported mean concentration for the element in the reference material. Silver distribution in LKSD 1 and molybdenum distribution in LKSD 3 have not been included in Table 5 because many of the element concentrations are below detection limits. Sums of the percentage copper, silver, molybdenum, iron and manganese, extracted at each stage from GXR 1, range from 90 to 110% indicating that the sequential extraction process has removed the bulk of the metals from the reference sample. The sums of percentage silver extracted at each stage from LKSD 3, copper from LKSD 1 and manganese from LKSD 3 are also close to 100%, compared to values obtained using the hydrofluoric-perchloric-nitric-hydrochloric acid digestion. This range shows that the sequential extraction process effectively removes the bulk of these metals in the reference samples. However, the sum of percentage metal extracted for other elements, especially manganese in LKSD 1 and copper in LKSD 3, are much lower or significantly higher than 100%. The analytical error determined in each extract and the depletion of the sample during the extraction process may be contributing factors responsible for excessively large or small sums of percentage extracted metal.

*Progressive loss of sample during the extraction process through oxidation or organic matter and transfer of material from stage to stage can also give misleading values because the metal concentration is calculated from the original sample weight rather than the actual weight of the residue from each extraction.* The low percentage sums for molybdenum and manganese relate to the more highly organic reference material LKSD 1. Precipitation of metal hydroxides in the alkaline sodium hypochlorite extract, despite the neutralizing effect of the weakly acid distilled water, may be one reason for the low total sums of the extracted iron and manganese. However, this factor does not appear to have influenced the extraction of manganese from LKSD 3 which contains a higher manganese content than LKSD 1.

**Table 5. Extraction of metals from GXR 1, LKSD 1 and LKSD 3**

	Sodium Acetate	Hydroxylamine Hydrochloride	Sodium Hypochlorite	Aqua Regia	Hydrofluoric Acid	Sum of extracts (%)
Ag in GXR1	0.5	23	3	1	31	
% Ag extracted	2	74	10	3	100	89
Mean Ag in LKSD 3	0.5	1.4	1.4	0.1	2.8	
% Ag extracted	1	50	50	3		103
Cu in GXR1	184	520	2	360	1160	
% Cu extracted	17	47	0.5	32	100	96
Mean Cu in LKSD 1	3	8	18	18	44	
% Cu extracted	5	18	41	41	100	106
Mean Cu in LKSD 3	3	8	9	21	35	
% Cu extracted	9	23	26	60	100	118
Mo in GXR1	0.5	0.5	4	15	19	
% Mo extracted	1	1	22	83	100	105
Mean Mo in LKSD 1	0.5	0.5	3	2	10	
% Mo extracted	10	10	30	20	100	70
Mn in GXR1	143	591	3	88	880	
% Mn extracted	16	67	0.5	10	100	93
Mean Mn in LKSD 1	230	86	37	64	686	
% Cu extracted	33	12	6	10	98	61
Mean Mn in LKSD 3	647	435	101	187	1270	
% Mn extracted	45	30	7	13	88	95
Fe in GXR1	0.99	3.86	0.001	23	Not	
% Fe extracted	0.5	15	0.5	92	determined	107
Mean Fe in LKSD 1	0.039	0.043	0.044	1.36	2.79	
% Fe extracted	2	15	2	50	100	69
Mean Fe in LKSD 3	0.029	1.32	0.01	1.83	3.86	
% Fe extracted	1	33	0.5	46	97	80

Data represents 1 determination of GXR1 and the mean of 7 analyses of LKSD 1 and LKSD 3.

The extraction of metals from two different sample types is shown in Table 6.

**Table 6. Mean percent metal extracted from eight lake sediments and twelve glaciolacustrine sediments**

	Sodium Acetate	Hydroxylamine Hydrochloride	Sodium Hypochlorite	Aqua Regia	Sum of Extracts
	% Extracted	% Extracted	% Extracted	% Extracted	(%)
Cu-A	4	11	49	48	113
Cu-B	35	40	1	21	97
Mo-A	22	22	42	49	135
Mo-B	9	17	38	13	77
Mn-A	44	30	3	22	98
Mn-B	25	47	0	20	93
Fe-A	1	25	4	58	87
Fe-B	1	30	0.01	43	75

Both groups were analysed as part of the same sample batch. Group A comprises eight pulverised lake-sediment samples (mean LOI of 29%) and group B consists of twelve glaciolacustrine sediment samples (mean LOI of 4%). The stronger association of the copper with organic matter in the lake sediments is clearly revealed by the greater abundance (49%) of sodium hypochlorite extracted copper compared to the much smaller amount (1%) liberated from group B samples. The mean sum of the manganese extracted at each stage from both groups ranges from 90 to 100%. However the mean sum of iron extracted at each stage ranges from 75% in group B to 87% in group A. Precipitation of iron hydroxide in the alkaline sodium hypochlorite may be responsible for the low mean sum of extracted iron.

Extraction of copper and manganese from individual lake sediment and glaciolacustrine sediment samples is shown in Figures 1 and 2.

**Figure 1. Copper extracted from lake sediments (Lk.Sed.) and glaciolacustrine sediments (Glac.)**

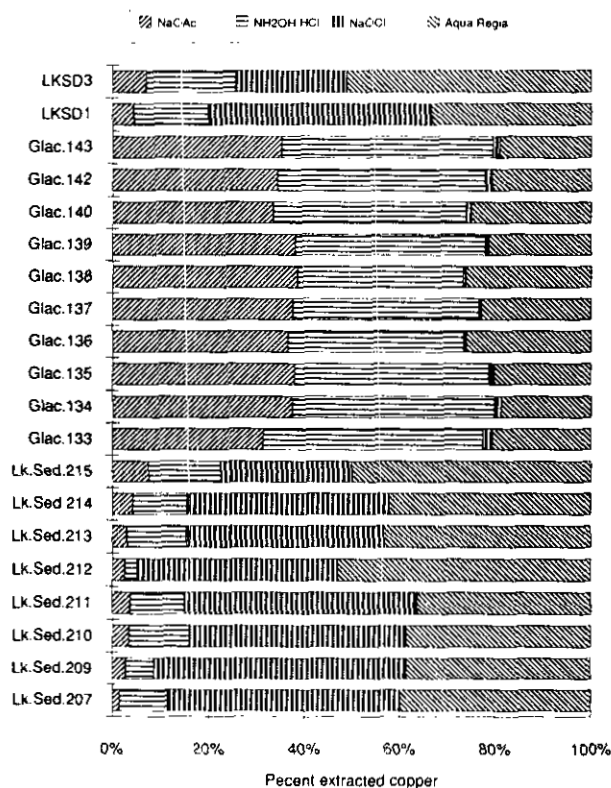
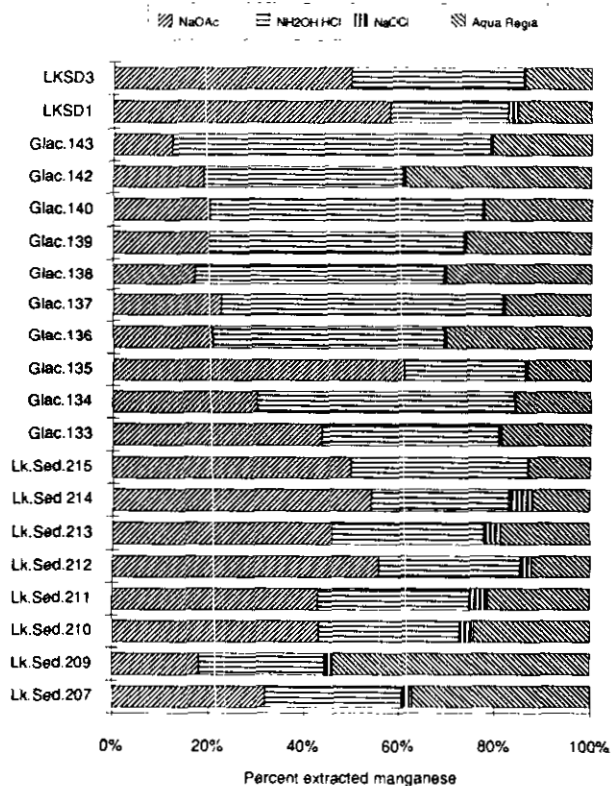


**Figure 2. Manganese extracted from lake sediments (Lk.Sed.) and glaciolacustrine sediments (Glac.)**



All of the extraction sums have been normalized to 100% for ease of comparison. A greater amount of the copper is extracted by the sodium hypochlorite and aqua regia from the lake-sediment samples and the reference materials LKSD 1 and LKSD 3 than from the glaciolacustrine samples. However, more of the copper is extracted by sodium acetate and hydroxylamine hydrochloride from the glaciolacustrine samples. More manganese is extracted by the hydroxylamine hydrochloride from the glaciolacustrine sediments than from the lake sediments (Figure 2). Unlike copper, manganese distribution in the extractions from the two sample groups is less uniform.

## CONCLUSIONS

Results of sequential extraction analysis of geochemical reference samples, lake-sediment samples and glaciolacustrine sediment samples reveals the following features.

- Copper and manganese precision (expressed as relative standard deviation) is less than 20% for the majority of extracts. Sodium hypochlorite extracted copper and manganese determinations are less precise and the larger error may be due incomplete extraction of metals from reference materials. Relatively poor precision for silver and molybdenum extracted from the reference materials LKSD1 and LKSD 3 reflects low element concentrations in the samples. Data for sodium hypochlorite extracted iron for the reference samples reveals a large error and especially for the more organic rich LKSD 1. Precipitation of iron hydroxide during the sodium hypochlorite extraction stage and variation in the amount of organic matter oxidized may be responsible for the poor precision.
- The extraction process removes more than 90% of all metals from the jasperoid reference sample GXR1. The high total of extracted copper for the reference materials LKSD 1 and 3 may reflect loss of sample during the extraction process and analytical error. The low total of extracted iron and manganese for the more organic rich LKSD 1 sample may be due to precipitation of elements as hydroxides during the sodium hypochlorite oxidation.
- Accumulation of copper by organic matter in lake-bottom sediments is clearly revealed by the high concentration of metal in the sodium hypochlorite extract. In glaciolacustrine samples the greater abundance of copper and manganese in the hydroxylamine hydrochloride

and Lefort aqua regia extracts indicate that more of the metals are associated with secondary minerals formed during weathering.

Exploration; pages 691-706 in *Geochemical Exploration 1974, Proceedings of the Fifth International Geochemical Exploration Symposium*, Vancouver, Elliott, I.L and Fletcher, W.K., Editors, *Association of Exploration Geochemists Special Publication No. 2*.

## ACKNOWLEDGMENTS

The authors would like to thank G.E.M.Hall, Geological Survey of Canada for her helpful advice on the analytical method used. Constructive criticism by P.F.Matysek, S.J.Sibbick and J. Newell is very much appreciated.

Tessier, A., Campbell, P.G.C. and Bisson, M. (1979): Sequential Extraction Procedure for the Speciation of Particulate Trace Metals; *Analytical Chemistry*, Volume 51, No.7, pages 844-850.

## REFERENCES

- Campbell, P.G.C., Lewis, A.G., Chapman, P.M., Crowder, A.A., Fletcher, W.K., Imber, B., Luomer, S.N., Stokes, P.M and Winfrey, M (1988): Biologically Available Metals in Sediments; *National Research Council Canada*, NRCC Number 27694, 298 pages.
- Chao, T.T and Sanzofone, R.F. (1992): Decomposition Techniques; *Journal of Geochemical Exploration*, Volume 44, pages 65-106.
- Cook S.J. (1993): Preliminary Report on Lake Sediment Studies in the Northern Interior Plateau, Central British Columbia; in *Geological Fieldwork 1992*, Grant, B. and Newell, J.M., Editors, *BC Ministry of Energy, Mines and Petroleum Resources*, Paper 1993-1, pages 475-482.
- Gatehouse, S., Russell, D.W and Van Moort, J.C. (1977): Sequential Soil Analysis in Exploration Geochemistry; *Journal of Geochemical Exploration*, Volume 8, pages 483-494.
- Gladney E. S. and Roelandts, I. (1990): 1988 Compilation of Element Concentration Data for U.S.G.S. Geochemical Exploration Reference Material GXR-1 to GXR-6; *Geostandards Newsletter*, Volume 14, No.1, pages 21-118.
- Hall, G.E.M., Vaive, J.E. and Kaszycki, C. (1993): The Diagnostic Capabilities of Selective Leaching; *Explore*, No. 80, pages 3-9.
- Hoffman, S. J. and Fletcher, W.K. (1979): Selective Sequential Extraction of Cu, Zn, Fe, Mn and Mo from Soils and Sediments; in *Proceedings of the 7th International Geochemical Exploration Symposium*, J. Waterson, Editor, *Association of Exploration Geochemists*, Denver, pages 289-299.
- Lynch, J. (1990): Provisional Element Values for Eight New Geochemical Lake Sediment and Stream Sediment Reference Materials LKSD-1, LKSD-2, LKSD-3, LKSD-4, STSD-1, STSD-2, STSD-3 and STSD-4; *Geostandards Newsletter*, Volume 14, No.1, pages 153-167.
- Papp, C.S.E., Filipek, L.H. and Smith, K.H. (1991): Selectivity and Effectiveness of Extractions Used to Release Metals Associated with Organic Matter; *Applied Geochemistry*, Volume 6, pages 349-353.
- Rose, A.W. (1975): The Mode of Occurrence of Trace Elements in Soils and Stream Sediments Applied to Geochemical



# COALBED METHANE DESORPTION RESULTS FROM THE QUINSAM COAL MINE AND COALBED METHANE RESOURCE OF THE QUINSAM COALFIELD, BRITISH COLUMBIA.

(92F/13,14)

By Barry D. Ryan, British Columbia Geological Survey Branch.

and

Michael F. Dawson, Institute of Sedimentary and Petroleum Geology.

**KEYWORDS:** Quinsam mine, coalbed methane, desorption, mine ventilation, coal quality, coalbed-methane resources, Comox Formation.

## INTRODUCTION

Coalbed methane is potentially a valuable resource in British Columbia. Resource development is in its early stages and it is important for government agencies to acquire the data now that companies will need in the future when they plan exploration programs. Gathering coalbed methane (CBM) desorption data from drill-core samples is an important first step in assessing the resource potential of an area. Companies undertaking coal exploration may not at present incorporate a CBM component, to the program but are willing to provide samples to government agencies for CBM desorption tests. The provincial and federal geological surveys are cooperating to ensure that desorption data are obtained wherever possible and the results used in an assessment of the CBM resource of the province.

This paper discusses the results of desorption tests on drill-core samples from the Quinsam coal mine. A separate paper (Ryan and Dawson, 1994) discusses the method of desorption data collection in detail and the background to the corrections applied to the data.

## QUINSAM COAL MINE

The Quinsam coal mine is located 20 kilometres west of the town of Campbell River on Vancouver Island.

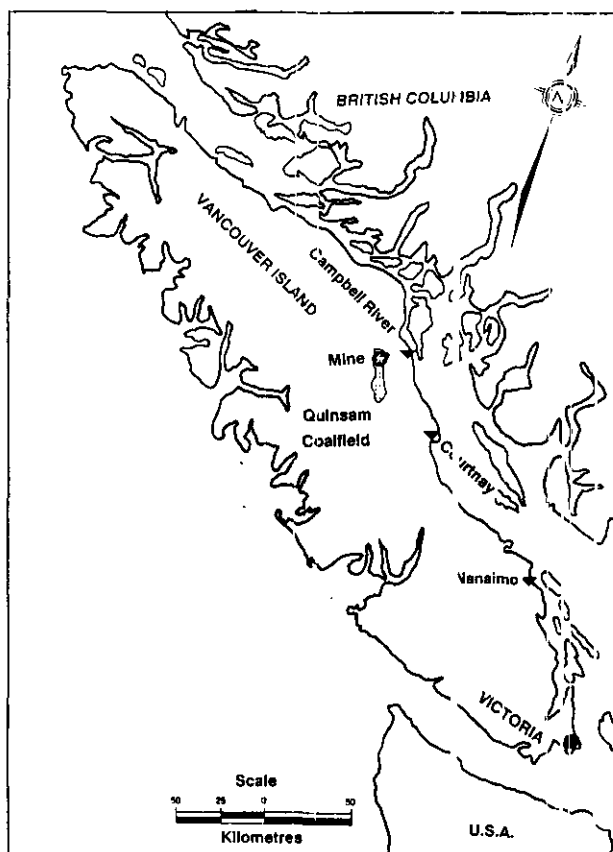


Figure 1. Location map, Vancouver Island and the Quinsam coal mine.

Access is by an all-weather gravel road that joins Highway 28 at kilometre 20 west of Campbell River (Figure 1). The mine opened in 1987, initially as a small surface mine and now as a combined surface and underground operation. Present annual raw-coal production is 500 000 tonnes; this is planned to increase to 1 000 000 tonnes by 1995.

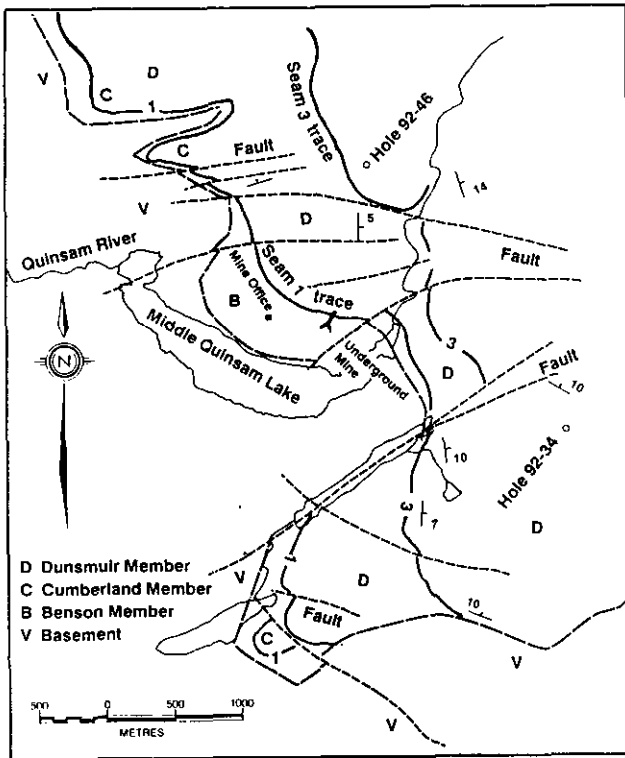


Figure 2. Simplified geology of the Quinsam mine area from Kenyon *et al.* (1991).

The coal seams at Quinsam are in the Comox Formation of the Upper Cretaceous Nanaimo Group (Kenyon *et al.*, 1991). The Comox Formation is divided into the basal conglomeratic Benson Member, which is overlain by the Cumberland and Dunsmuir members. Two seams outcrop in the Cumberland Member and two seams in the Dunsmuir Member. Most of the reserves are in the lowermost seam 1 in the Cumberland Member. Seam 1 averages 2.3 metres in thickness and is sometimes accompanied by a rider which averages 0.40 metre. Seam 1 is mined underground and in surface pits. The overlying seam 2 ranges from 0.30 to 0.55 metre in thickness and is mined at surface in some pits. Seam 3 in the Dunsmuir Member ranges from 2.4 to 3.4 metres thick and is mined in surface pits. Seam 4 is thin and is not mined. The stratigraphic separation of seams 1 and 3 is 30 to 60 metres.

Quinsam management elected to drill two holes for CBM testing because of the expansion in the underground mining activity and the renewed interest in using CBM as an energy resource to support the mining activity. The locations of the two holes with reference to the present mine operations are indicated in Figure 2. Five samples from seam 3 and four samples from seam 1 were desorbed initially at the mine site and then in Victoria.

## CANISTER DESORPTION TECHNIQUES

The techniques used to collect and correct the methane desorption data are described in detail in Ryan and Dawson (1994, this volume).

The samples in this study were recovered from shallow depth where the rock temperature is probably less than 25°C. For this reason the canisters were not put in a temperature controlled box. The lost-gas corrections applied in this study were calculated using the U.S. Bureau of Mines method (Diamond and Levine, 1981) applied to cumulative gas volumes corrected to standard temperature and pressure (STP). The U.S. Bureau of Mines method was used because the down-hole lost-time component was so small that a more complicated method of correcting for lost gas was not justified. The drilling times used to calculate the lost-time are reported in Table 1. Two estimates of lost time for each sample are recorded in the table. In the first case it was assumed that the hole was dry and the gas started to desorb as soon as the seam was drilled, and in the second case it was assumed that the hole was filled with water and that gas started to desorb when the core sample was half-way up the hole.

Hole 92-34 was not making water when drilled and it was assumed to be dry to the sampling depth, whereas hole 92-46 was making some water and was assumed to be filled with water to the collar. The lost-gas calculations for samples from hole 92-34 were made using both dry and wet lost-time estimates. The longer, dry lost-time estimates increased the lost-gas calculation by about 15% (excluding sample 92-34-6). The lost-gas estimate for sample 92-34-6 was made using a modified plot described in Ryan and Dawson (1993, this volume) and appears to be about 641 cubic centimetres. The other samples from hole 92-34 have dry lost-gas estimates ranging from 126 to 132 cubic centimetres.

All samples with the exception of 92-34-6 produced reasonable cumulative gas (STP) *versus* square-root time linear plots.

Dead space corrections are necessary because of the effect of changing pressure and temperature on the empty space in the canister. This correction is referred to as the canister dead space correction and is described in Ryan and Dawson (1994, this volume). Obviously it is important to minimize the dead space in the canister and to be able to measure it. The canisters used in this study have spacer rings to fill in space if the core diameter is much less than the inside diameter of the canister.

The dead space in the canister was measured in the following way: after making a measurement the manometer is used to pressure the canister with the methane just expelled or with air. This is done by raising the water reservoir bulb above the water level in the burette while the manometer is still attached to the

canister. Measure the difference in water levels (h in cm). This value represents the pressure above atmosphere forcing methane or air back into the canister. Measure the volume of gas (M) returned to the manometer at atmospheric pressure (PA). Calculate the dead space (DS) using

$$DS \times (P_a + P_h) = (DS + M) \times P_a$$

$$DS = M \times P_a / P_h$$

$P_h$  (millibars) =  $980.62 \times 0.998 \times h / 1000$  where 0.998 corrects for the density of water at room temperature.

TABLE 1  
QUINSAM SAMPLE COLLECTION DATA

HOLE	DATE	SEAM	METRES		ELEVATION	
			EASTING	NORTHING		
H92-34	1/10/92	3	324284	5532297	336	
H92-46	16/10/92	1	322854	5534322	317	
METRES FROM-TO	CUT	TIMES TRIP	SURFACE	SEAL	LOST TIME DRY WET	T <sub>25%</sub>
<b>HOLE 92-34 SEAM 3 SAMPLES 92-34-2 (TOP) TO 92-34-6 (BOTTOM)</b>						
141.5-141.9	14.46	14.50	14.51	14.56	10 6	
141.9-142.3	14.46	14.50	14.51	14.57	11 6	4.13
142.3-142.7	14.46	14.50	14.51	14.58	12 7	8.92
142.7-143.1	14.46	14.50	14.51	14.59	13 8	8.48
143.1-143.5	14.46	14.50	14.51	14.00	14 9	8.93
145.3-145.7	15.02	14.09	14.11	14.15	13 6	0.98
<b>HOLE 92-46 SEAM 1 SAMPLES 92-46-1 (TOP) TO 92-46-4 (BOTTOM)</b>						
108.5-108.9	14.57	15.01	15.02	15.10	13 9	7.16
109.4-109.8	14.57	15.01	15.02	15.08	11 7	15.2
111.5-111.9	14.09	15.14	15.15	15.19	10 5	3.95
111.9-112.3	14.09	15.14	15.15	15.20	11 6	3.75

LOST TIME DRY = Lost-time minutes assuming dry hole.  
LOST TIME WET = Lost time minutes assuming water-filled hole.  
CUT TIME = Time (hours.minutes) drill cuts coal.  
TRIP TIME = Time (hours.minutes) core starts to surface.  
SURFACE TIME = Time (hours.minutes) coal reaches surface.  
SEAL TIME = Time (hours.minutes) sealed in canister

SMITH AND WILLIAMS TERMS

T<sub>s</sub> = Cut time to seal time.  
T<sub>d</sub> = Cut time to surface time.  
T<sub>25%</sub> = Time from cut time to time for 25% desorption into canister  
Note this is not time for 25% total desorption loss because it does not consider the lost gas component  
SURFACE-TIME RATIO = (T<sub>s</sub> - T<sub>d</sub>)/T<sub>s</sub>  
LOST-TIME RATIO = T<sub>s</sub>/T<sub>25%</sub>

This method of calculating the dead space has a number of advantages. Calculations can be made after each desorbed gas measurement and a number of measurements averaged. The method requires no additional equipment and is direct. Lastly, it measures the same volume as the desorbing gas occupies, not a liquid filled volume or a theoretical volume.

The desorption data were corrected for the effect of water vapour in the canister. The vapour pressure of water is temperature dependent and ranges from 0.5 to 7.5 Kilopascals (5 to 75 millibars) in the temperature range of 0 to 40°C. The desorbed gas volumes were calculated using atmospheric pressure minus partial pressure of water. Applying a water vapour correction reduces the measured gas volume at STP by about 2.5%. The resultant gas volume is dry gas at STP.

Finally the desorbed gas volumes were converted to the equivalent volume at STP using the general relationship for ideal gases:

$$P_1 \times V_1 / T_1 = P_2 \times V_2 / T_2$$

## DESORPTION AND COAL QUALITY DATA

Samples from two holes were desorbed at room temperature which is assumed to be similar to *in situ* rock temperature. Canister sample data, coal quality and desorption results are recorded in Tables 2 and 3. Samples were analyzed for as-received moisture, air-dried moisture, volatile matter (VM), ash and fixed carbon content (FC). Some samples were also analyzed for equilibrium moisture and Hardgrove Index (HGI). The mean maximum reflectance values (R<sub>max</sub>) of all samples were measured.

TABLE 2  
SUMMARY CANISTER AND SAMPLE ANALYTICAL DATA

SAMPLE No	CANISTER VOLUME	CANISTER DATA IN cm <sup>3</sup>			SPECIFIC GRAVITY		
		DEAD SPACE	SAMPLE VOLUME	SAMPLI WEIGH gram			
<b>SEAM 3</b>							
92-34-2	2975	990	1985	2854	1.4		
92-34-3	2936	876	2060	2560	1.4		
92-34-4	3002	986	2016	2398	1.39		
92-34-5	2874	1050	1824	2241	1.35		
92-34-6	2947	1100	1847	2179	1.38		
<b>SEAM 1</b>							
92-46-1	2975	1248	1727	2192	1.37		
92-46-2	2936	1220	1716	2204	1.38		
92-46-3	3002	1645	1357	1642	1.31		
92-46-4	2874	1313	1561	2194	1.31		
SAMPLE	R <sub>max</sub>	COAL QUALITY DATA				EQUIL H <sub>2</sub> O	HGI
		% H <sub>2</sub> O ar	% VM	% ASH	% FC		
<b>SEAM 3</b>							
92-34-1		2.83	38.63	11.85	46.69		
92-34-2	0.64	1.87	22.15	54.61	21.37	3.8	61
92-34-3	0.67	3.25	33.92	15.24	47.59	4.7	
92-34-4	0.67	3.13	35.83	11.92	49.12		
92-34-5	0.66	3.28	36.91	5.97	53.84		
92-34-6	0.64	5.38	31.07	27.59	35.96	4.3	63
<b>SEAM 1</b>							
92-46-1	0.70	6.28	36.03	8.12	49.57		
92-46-2	0.65	6.62	35.5	7.99	49.88	5.3	53
92-46-3	0.63	7.96	36.03	9.51	46.50		
92-46-4	0.66	8.69	30.99	19.05	41.27		

data reported on an as-received basis  
R<sub>max</sub> = Mean maximum reflectance  
ar = As-received VM = Volatile matter  
FC = Fixed carbon EQUIL H<sub>2</sub>O = Equilibrium moisture  
HGI = Hardgrove Index

Hole 92-34 intersected seam 3 at 141.5 metres where it has a vertical thickness of 4.3 metres. Six samples, each being 40 centimetres of core, were collected and sealed into canisters. The ash contents of the samples range from 5.97 to 54.61% (arb). The samples spanned the seam from hangingwall to footwall and Figure 3 presents the density and gamma geophysical log traces of the seam. Unfortunately the hangingwall canister

(sample 92-34-1) leaked. The samples of seam 3 were desorbed at room temperature for 15 days, at which time the canisters were re-used for the seam 1 samples. At this time only one sample had finished desorbing and the last increment of desorbed gas from the other seam 3 samples was estimated by projecting the cumulative desorption curves. In all cases the correction was less than 250 cubic centimetres.

TABLE 3  
SUMMARY DESORPTION DATA CORRECTED FOR CANISTER DEAD SPACE AND CONVERTED TO STP DRY GAS

SAMPLE	L GAS cm <sup>3</sup> /g	D GAS cm <sup>3</sup> /g	S GAS cm <sup>3</sup> /g	T GAS cm <sup>3</sup> /g	T GAS daf/g
<b>HOLE 34 SEAM 3</b>					
92-34-2	0.0441	0.3919	0.0053	0.441	1.014
92-34-3	0.0516	0.7127	0.0332	0.797	0.978
92-34-4	0.0551	0.7239	0.0676	0.847	0.997
92-34-5	0.0562	0.8694	0.0919	1.018	1.121
92-34-6	0.1482	0.9456	0.0000	1.094	1.632
<b>HOLE 46 SEAM 1</b>					
92-46-1	0.0402	0.7906	0.0000	0.8308	0.971
92-46-2	0.0436	0.8685	0.0000	0.9121	1.068
92-46-3	0.0633	0.8091	0.0000	0.8724	1.057
92-46-4	0.0574	0.9046	0.0000	0.9620	1.331

ABBREVIATIONS

- L GAS = Gas lost prior to sealing sample in canister.
- D GAS = Gas desorbed into canister.
- S GAS = Estimate of gas desorbed after samples removed from canister.
- T GAS = Total estimated gas desorbed from samples.
- T GAS daf = Total gas on a dry, ash-free basis per dry gram.

Hole 92-46 intersected seam 1 at 108.5 metres where it has a vertical thickness of 3.80 metres. Four samples 40 centimetres long, including hangingwall and footwall were sealed into canisters (Figure 3). The ash contents of the samples range from 7.99 to 19.05% (arb). Samples were desorbed at room temperature for periods ranging from 44 to 54 days. At this time the gas being desorbed (after correcting for variations of pressure and temperature between readings) was less than 5.0 cubic centimetres per day.

ADSORPTION DATA

An adsorption isotherm (Table 4 and Figure 4) was measured for sample 92-34-3 at a temperature of 22°C per 1000 metres and an equilibrium moisture of 4.72%. At a geothermal gradient of 18°C per 1000 metres a temperature of 22°C is equivalent to a depth of about 500 metres. Above 500 metres the adsorption data probably predict an unrealistically low gas capacity and below 500 metres they probably predict an unrealistically high gas capacity.

The results fit the Langmuir equation well (Langmuir, 1918). The data plotted on a linearized Langmuir plot scatters about a straight line with an R<sup>2</sup> value of 0.994. The Langmuir volume (VI) which is the predicted gas content of the sample at infinite pressure, is

18.6 cubic centimetres per gram and the Langmuir pressure (PI) is 1335.6 psia or 947 metres based on hydrostatic pressure. The VI value is similar to the values obtained for coals of similar rank by Olszewski and Schraufnagel (1992), who fitted Langmuir curves to U.S. Bureau of Mines desorption data reported by Kim (1977).

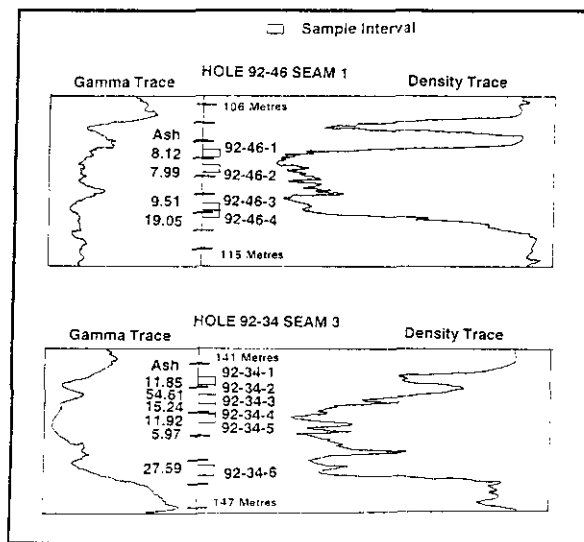


Figure 3. Geophysical logs for Quinsam coal mine holes 92-34 and 92-46.

The Langmuir pressure for the Quinsam sample (1335.6 psia or 947 metres hydrostatic) is approximately seven times greater than PI values obtained by Olszewski and Schraufnagel on coals of similar rank. They modelled data obtained from air-dried samples. The Quinsam isotherm was measured on a sample with equilibrium moisture of 4.72%. Olszewski and Schraufnagel mention the effect of moisture but do not quantify its effect in the Langmuir rank equation that they derive. Moisture decreases the adsorption ability of coal (Joubert *et al.*, 1973) up to a critical content above which increase in moisture content has no effect on adsorption ability. The critical moisture for a particular coal is similar to its equilibrium moisture. Data from Joubert *et al.* indicate that, decrease in moisture content below the critical moisture value increases VI but has a much more pronounced effect on PI, increasing it markedly. This means that the adsorption curve is flattened and adsorption contents at low pressures are decreased.

The retention ability of high-volatile bituminous and sub-bituminous coals at low pressures may vary below predicted values, based on changes in the high and variable equilibrium moisture contents.

A number of curves predicting adsorption capacity are plotted on Figure 4. These curves are derived from the work of Kim (1977), Eddy *et al.* (1982) and Olszewski and Schraufnagel (1992; Langmuir rank equation). The equations used to derive these curves used data from desorbed samples which, for the low-rank coals may not have been saturated, consequently the curves for low-rank coals may not match experimental adsorption curves measured on saturated low-rank coals. It is therefore not surprising that two of these curves plot below the adsorption curve (Figure 4).

TABLE 4  
ADSORPTION DATA FOR SAMPLE 92-34-3

Coal quality					
Equilibrium moisture = 4.72 %					
Ash db = 15.75 %					
Volatile matter db = 35.06 %					
R <sub>max</sub> = 0.67 %					
Adsorption data run at 22 °C					
Pressure psia	Depth metres	scf/ ton	cm <sup>3</sup> / gram	psia/ (scf/ton)	kPa/ (cm <sup>3</sup> /g)
232	164.5	83.6	2.61	2.78	597.7
423	300.0	137.7	4.30	3.07	510.9
633	448.9	174.8	5.46	3.623	799.5
937	664.4	241.3	7.53	3.882	858.0
1270	900.6	274.3	8.56	4.631	1023
1553	1101.2	302.1	9.43	5.141	1135
1919	1360.8	333.0	10.4	5.763	1272
Adsorption data dry ash free basis					
Pressure psia	Depth metres	scf/ ton	cm <sup>3</sup> / gram	psia/ (scf/ton)	kPa/ (cm <sup>3</sup> /g)
232	164.5	99.2	3.10	2.342	503.2
423	300.0	163.4	5.10	2.587	430.8
633	448.9	207.5	6.48	3.052	673.6
937	664.4	286.4	8.94	3.270	722.7
1270	900.6	325.5	10.16	3.902	861.9
1553	1101.2	358.6	11.19	4.332	956.9
1919	1360.8	395.3	12.34	4.855	1072.3
Langmuir Constants					
As-received			Dry ash-free basis		
V <sub>L</sub>	P <sub>L</sub>		V <sub>L</sub>	P <sub>L</sub>	
scf/ton	cm <sup>3</sup> /g	psia	kPa	scf/ton	cm <sup>3</sup> /g
564.8	17.6	1335.6	9209	670.3	20.9
				1335.6	9209

1335.6 psia = 947 metres hydrostatic pressure

There is some evidence that the adsorption capacity of high-volatile B rank coals may actually be higher than that for high-volatile bituminous A rank coals. The Langmuir volume for the Quinsam coal with a reflectance of about 0.65% is 20.9 cubic centimetres per gram (daf basis) whereas the Langmuir volumes of three samples from the Telkwa coalfield with reflectances ranging from 0.9 to 0.99% are 14.6, 12.3 and 11.1 cubic centimetres per gram daf basis (Ryan and Dawson, this volume).

## RESULTS AND INTERPRETATION

The gas contents of the five samples from seam 3 in hole 92-34 range from 0.44 cubic centimetres per gram at the hangingwall of the seam to 1.09 cubic centimetres per gram at the footwall of the seam. On a dry, ash-free basis the values range from 1.014 to 1.632 cubic centimetres per gram (Table 3). The R<sub>max</sub> values of the samples vary from 0.64 to 0.67% (Table 2) which is characteristic of high-volatile bituminous coal.

The gas contents of the four samples from seam 1 in hole 92-46 range from 0.97 cubic centimetres per gram at the top of the seam to 1.331 cubic centimetres per gram at the bottom and from 0.97 to 1.33 on a dry, ash-free basis (Table 3). The R<sub>max</sub> values of the samples range from 0.63 to 0.70% (Table 2).

The rank of the Quinsam coal is low and its adsorption capacity is probably greater than the cumulative gas it has generated. Karweil in Meissener, (1984) suggests that methane generation starts after the coal has achieved a rank equivalent to a volatile matter (VM) (daf) content of about 37.8%. Dow (1977) indicates that wet gas generation starts after the rank of the samples exceeds an R<sub>max</sub> of 0.8%. Models of other workers indicate initiation of methane generation at VM (daf) values ranging from 35 to 46% (Meissener, 1984). Some data (Snowden and Powell, 1982) indicate that methane generation may start at ranks below a R<sub>max</sub> value of 0.6%.

The R<sub>max</sub> of Quinsam coal is below Dow's threshold for methane generation. Before using the Karweil equation the VM (daf) value for the coal must be determined. The Quinsam coal contains calcite which dissociates to CaO and CO<sub>2</sub> during VM determinations; consequently the determinations are influenced by a variable addition of CO<sub>2</sub>, depending on the amount of ash. An estimate of the true VM (daf) can be obtained by plotting individual VM (daf) determinations (Y axis) versus the individual ash contents dry-basis (X axis). The Y intercept is then VM (daf) at zero ash, and without addition of CO<sub>2</sub> from the ash. A plot of this type for the nine Quinsam samples provided an average VM (daf) at zero ash of 40.33%. Obviously the various methane generation models would indicate very little or no methane generation by the coal.

There is another result of the higher than normal concentration of carbonate in the coal. Generally it is more useful to report gas contents on a mineral-free basis rather than an ash-free basis. The weight of mineral matter is usually approximated from the weight of ash using the Parr equation (Parr, 1932). This equation does not take variations in ash chemistry into account. The line of VM (daf) versus ash (db) has a negative slope of 0.19%. If this is caused by release of volatile components, including CO<sub>2</sub>, from the ash then the

original mineral-matter weighed 1.19 times the weight of ash.

The gas contents of the coal on a mineral matter free (mmf) basis will be higher than the concentrations on a dry ash-free basis. For low ash contents the increase is probably about 2.5% and at high ash contents it is about 23%. For most of the samples the effect is not significant, but the gas contents (mmf basis) for samples 92-34-2 (55% ash) and 92-34-6 (29% ash) would increase significantly.

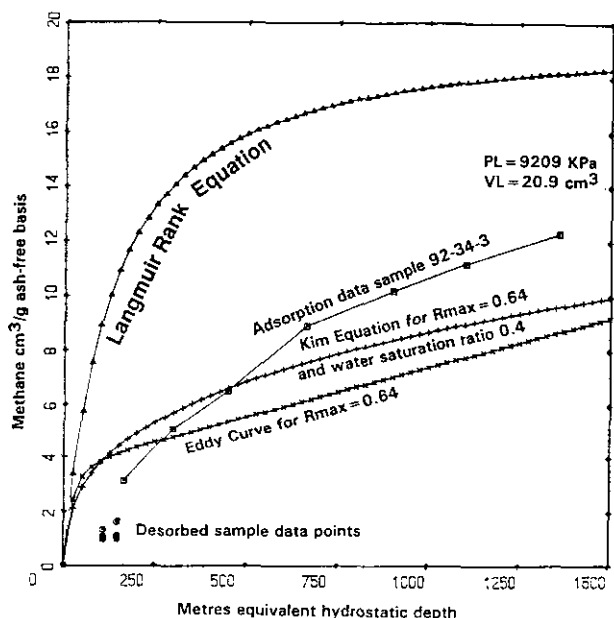


Figure 4. Desorption data, adsorption curve for sample 92-34-3 and theoretical adsorption curves predicting the adsorption capacity of low-rank coals.

The only way of doing the mineral matter correction accurately is to weigh a low-temperature ash sample (true mineral matter sample). The mineral matter can then be subjected to a standard ash analysis to provide a mineral matter to ash weight ratio to correct the ash content measurements of other samples to equivalent mineral matter contents.

The Quinsam samples are under saturated with respect to their adsorption capacities and much of the gas adsorbed on the samples may have been scavenged from elsewhere. The scavenged gas could be methane generated by, and released from higher rank coals, carbon dioxide generated by low-rank coal or biogenic methane. Carbon dioxide is strongly adsorbed by coal.

The seam 3 samples were intersected at about 140 metres. If the hydrostatic head was also 140 metres then the adsorption capacity of these samples should be about 2.7 cubic centimetres per gram (daf basis). The hydrostatic head is probably less than 140 metres. For example, if the water table is 20 metres below surface

then the adsorption capacity is 2.2 cubic centimetres per gram (daf) basis. The actual desorbed gas contents range from 1.0 to 1.6 cubic centimetres per gram and the samples are therefore undersaturated, containing between 40 and 70% of the maximum possible adsorbed gas.

The seam 1 samples were intersected at about 110 metres. If the hydrostatic head is 110 metres, then the coal can adsorb 2.2 cubic centimetres per gram, or if the hydrostatic head is only 90 metres, the adsorption capacity drops to 1.8 cubic centimetres per gram. Consequently seam 1 samples contain between 50 and 70% of the maximum possible adsorbed gas.

Under ideal conditions, if the coal is saturated, the gas contents on a dry, ash-free basis of samples from throughout the seam should be similar, assuming that the petrography of the samples is similar. Seam 3 sample 92-34-6, which contains the most gas on a dry ash-free basis, is also the most crushed seam 3 sample. It probably contains the most gas because its smaller size range allowed it to scavenge gas more easily. It is also the sample that desorbed the quickest because of its finer size range. The situation is the same for the seam 1 samples; the footwall sample (92-46-4) which was the most crushed also contained the most gas and desorbed the quickest.

The samples from holes 92-34 and 92-46 were collected from similar depths and one would expect the gas contents on a dry ash-free basis to be similar. Ignoring the two footwall samples, which definitely contain higher than average gas contents (Figure 5) there is still a considerable spread of gas contents on a daf basis (Table 3). This spread may indicate that the method of correcting to an ash free or mineral matter free basis is incorrect. It is suggested in some literature that finely dispersed ash can damage the adsorption capacity of coal by blocking the microporosity (Gamson *et al.*, 1993). If this is the case then the ash content of a sample may have two components. One may act as a dilutant and be composed of easily removed rock splits and the other may consist of more difficult to remove inherent ash which has a more damaging effect on adsorption capacity. The finely dispersed inherent ash which makes up the last component to be removed by washing may cause a large decrease in gas capacity per 1% ash whereas ash additions above a critical value act as a dilutant to the gas capacity. In Figure 5 the gas contents on an as-received basis are plotted against the ash content. A correction line is plotted that, above 10% ash, has a dilution-effect slope and below 10% ash the slope is increased by a factor of 3 implying that a 1% increase in ash will decrease gas content by 3%.

There is some suggestion that the data may plot on a steeper line at lower ash contents. There are indications of this in other data sets (Dawson 1993; Faiz and Cook, 1991). If this is the case it has a number of important implications for predicting gas contents. Generally gas

contents on a dry ash-free basis will be underestimated. The relationship between depth and gas content on a dry ash-free basis will be obscured. Predictions of gas contents at different ash contents from samples with measured gas contents will be in error.

The specific gravity (S.G.) of the samples was calculated using the sample weight, canister volume and the dead-space volume. This approach is interesting because it comes close to estimating *in situ* bulk density which is an elusive property to measure. Sample 92-34-2 has a high ash content and S.G. whereas the other four samples average 14% ash on a dry basis and a S.G. of 1.25. This value could be useful for calculating *in situ* tonnages from coal seam volumes.

The HGI values for samples from holes 92-34-2, 92-34-6 and 92-46-2 average 59. Sample 92-46-2, which has the lowest ash content has the lowest HGI and is therefore the hardest sample. The sample with the highest HGI is visibly the most crushed sample and has the highest gas content on a daf basis.

The HGI values correlate with the rate of desorption. The time required for half the gas to desorb is inversely correlated to HGI, thus the sample with an HGI of 63 required only 7 hours to lose half its gas, whereas the sample with an HGI of 53 required 90 hours. This relationship, which is related to the degree of crushing of the coal, may be useful in rating the coals for their safety when mined underground. In a situation where coal pillars start to crush there could be an increase in the rate of methane desorption.

The equilibrium moisture increases as the ash content decreases. The data indicate that the equilibrium moisture of the pure coal is greater than 6.0%.

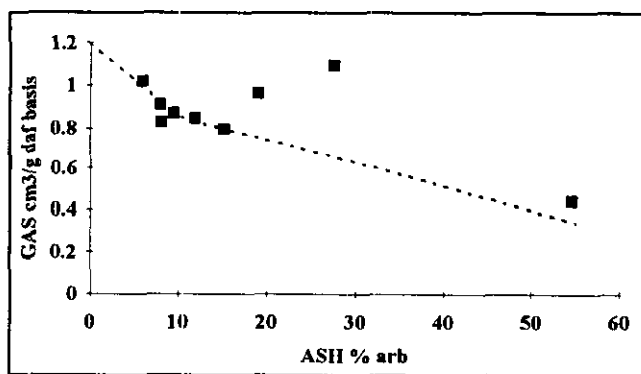


Figure 5: Gas contents on an as-received basis versus ash contents

## RESOURCE POTENTIAL

The potential coalbed methane resource of the Quinsam coalfield is limited by the low rank, shallow depth of burial and apparent under saturation of the coal.

A number of estimates of the resource have been made. Kenyon *et al.* (1991) estimate a resource of 90 billion cubic feet or 2.55 billion cubic metres (BCM) using a methane content of about 4.7 cubic centimetres per gram in the coal. This study uses a lower gas content of 1.5 cubic centimetres per gram based on a somewhat lower estimate of the average  $R_{max}$  value for the coalfield. The mine reports total coal reserves of about 50 million tonnes. If this coal has an average gas content of 1.5 cubic centimetres per gram (or 1.5 cubic metres per tonne) then a minimum resource of 0.075 BCM exists at the mine. The area of the Quinsam coalfield is about 200 square kilometres and the cumulative coal thickness in the Comox Formation in the mine area is estimated at 7.5 metres (Bickford and Kenyon, 1988). It is unlikely that this thickness of coal exists over all the coalfield. If it is present over half the coalfield and the average gas content is 1.5 cubic metres per tonne then the resource of the coalfield is 1.4 BCM.

Over fifty  $R_{max}$  measurements have been made from 24 sites in the Quinsam coalfield (Kenyon *et al.* 1991; A. Matheson, personal communication, 1993) and this study. A variogram of the data indicates that there is no coherent contour pattern and consequently the data are not contoured. Regressions of  $R_{max}$  versus easting or  $R_{max}$  versus northing provided very low  $R^2$  values, confirming the lack of any systematic regional trends in the data. A numeric average for the data is  $0.70 \pm 0.07\%$ ; the highest and lowest values recorded are 0.85 and 0.52%. There is no evidence that seam 1 is of higher rank than seam 3. It appears that the samples desorbed had ranks similar to but slightly lower than the average for the coalfield.

The Langmuir rank equation (Olszewski and Schraufnagel, 1992) can be used to predict the adsorption capacity of Quinsam coal at different ranks and depths. Based on Figure 4, the equation seems to predict values that are high for Quinsam coal but probably the increments between samples of different rank are more accurate. At 150 metres and a temperature of 22 °C the adsorption capacity increases 0.34 cubic centimetres per gram over a rank increase of 0.52 to 0.85%  $R_{max}$ .

There is the possibility of using methane to meet some of the on-site energy requirements of the mine. The Quinsam mine does not have a coal drier so the main opportunities for using CBM are for heating buildings or fueling light trucks. As an example, a hypothetical well is considered which utilizes 60% of the gas in 1 square kilometre times 5 metres of coal. The coal has a methane content of 1.0 cubic metres per tonne. If the well has a life of 5 years then it will provide 2000 cubic metres of methane per day (order of magnitude estimate). One litre of gasoline has the same calorific value as about 1 cubic metre of gas. The well therefore could provide the equivalent of over 2000 litres of gasoline per day. This would meet the daily fuel

requirements for several light vehicles if they were adapted to burn natural gas. A small office complex using 300 kilowatt hours per day of electricity for heating, if converted to natural gas, would use about 30 cubic metres of gas. Even at low productivity rates, a single well can provide sufficient methane to fuel light vehicles and heat mine buildings. The cost of converting to natural gas and drilling the well has to be compared to the cost savings in gasoline and electricity over the life of the well.

The value of natural gas on a Btu basis is about \$1 to \$2 dollars per million Btu. The cost of gasoline on the same basis is \$10 to \$20, about the same as electricity. The replacement value of natural gas can therefore be surprisingly high and the imaginary well has a gasoline replacement reserve value of \$2 to \$4 million undiscounted. These numbers are order of magnitude, but it is apparent from the discussion that if coalbed methane can be used as a replacement for on-site gasoline or electricity, then the feasibility of drilling single wells should be carefully investigated.

The cost of on-site coal, if the mining costs are \$25 per tonne, is about \$1 per million Btu. The general advantages of replacing on-site coal use with gas are not obvious, and if there are advantages, they would derive from the specific details of a mining operation.

## IMPLICATIONS FOR METHANE IN UNDERGROUND MINES

Some general comments can be made about methane released from low-rank coals in underground mines. The data cannot be used to draw specific conclusions about methane in the Quinsam underground mine.

Methane is an explosive hazard underground if the concentration in the mine air is between 5 and 15%. Mine safety regulations in British Columbia require that the concentration be maintained below 1.0% for normal mine operation. In order to maintain sufficient ventilation it is important to know the rate of methane release per tonne of coal mined. It is also important to know if this value is going to fluctuate over short periods of time, or, as the mining face geometry changes. McCulloch *et al.* (1975) provide a plot for estimating the methane released per ton of coal mined based on the desorbed methane content of fresh coal. They indicate that the methane released is usually between 6 and 9 times the amount desorbed per ton.

Based on the present desorption data, coal from the Quinsam underground mine probably contains between 0.5 and 2.0 cubic metres per tonne, depending on rank, depth and ash content. Using the relationship of McCulloch *et al.* (1975), the methane released into the underground workings would be between 3 and 18 cubic

centimetres per gram (100 to 575 standard cubic feet) per ton of coal mined. McCulloch *et al.* indicate that the relationship only provides an estimate for mature mines that have constant production. An estimate of ventilation requirements can be obtained by multiplying daily coal production recalculated to an average of tons produced per minute by a methane release per ton value by 100. The 100 is to reduce the methane concentration to 1.0%. A million tonnes per year raw coal production averages out at about 2 tonnes per minute for 24-hour shifts. At this production rate ventilation requirements for methane extraction would range from 550 to 3250 cubic metres (20 000 to 115 000 cubic feet) per minute if the desorbed gas content is between 0.5 and 2.0 cubic centimetres per gram.

These ventilation requirements are calculated using data from low-rank samples that are undersaturated based on their predicted adsorption capacity (Figure 4). If coal is encountered that is of higher rank or is saturated, then the gas content could increase significantly and so would ventilation requirements.

The rate of desorption increases as the grain size of the coal decreases. If coal pillars are subjected to high strain-rates causing crushing, then this might cause an increase in the rate of methane desorption. Ongoing desorption tests, as the mine progresses, could help track any changes in rank or the degree of methane saturation of the coal. The rapid desorption of the footwall samples indicates that gas concentrations may be higher at the base of the seams. An increase in the amount of crushed coal in the lower part of the seam may signal increased gas desorption.

Methane desorbed from coal may collect in porous sandstones adjacent to the coal seams. A coal desorbing 1.0 cubic centimetre per gram at surface effectively has as much gas as a sandstone with 13.0% porosity at 100 metres, but the sandstone may expel its gas into the mine workings faster. The hangingwall of the seam 1 is a mudstone overlain by the seam 1 rider which is about 0.35 metre thick. The footwall is a soft, light grey mudstone seat earth. Undisturbed the hangingwall and footwall lithologies of seam 1 are probably relatively impermeable and will tend to contain the methane in the seam so that it will migrate up dip. Seam 3 often has a sandstone roof and a moderately strong mudstone or siltstone floor.

Specific comments on the methane ventilation requirements, or the need for methane drainage holes cannot be made based on this limited database.

## CONCLUSIONS

- Coal from the Quinsam coal mine does not contain high concentrations of methane. This is partly because of the low rank but also because the coal at depths of 100 and 150 metres is at least 30% under-saturated.
- When coals with low gas contents are desorbed it is important to accurately correct the data to standard temperature and pressure conditions, otherwise large percentage errors are introduced into the data.
- The methane resource potential of the Quinsam coalfield is low, but a single well could be an economic alternative to electricity for heating and gasoline for light vehicles.
- The desorbable methane content is higher in footwall coal than for the rest of the seam. This may be because footwall coal is more crushed and has scavenged methane. The broken nature of the footwall coal and its resulting high HGI correlate with faster methane release.

## ACKNOWLEDGMENTS

This study was made possible by the initiative of Steve Gardner, Mine Manager at the Quinsam coal mine. Multifaceted field assistance was provided by Jim Lehtinen who was managing the drilling program for Quinsam. David Grieve, with his usual patience, worked at improving my English.

## REFERENCES

- Bickford, C.G.C. and Kenyon, C. (1988): Coalfield Geology of Eastern Vancouver Island (92F), in Geological Fieldwork 1987, B.C. Ministry of Energy, Mines and Petroleum Resources, Paper 88-1, pages 441-450.
- Dawson, F.M. (1993): Geological Survey of Canada Coalbed Methane Research Joint Venture Project, Fording Coal Limited, Summary Report; internal report, *Institute of Sedimentary and Petroleum Geology*, Calgary.
- Diamond, W.P. and Levine, J.R. (1981): Direct Method Determination of the Gas Content of Coal, Procedures and Results; *U.S. Bureau of Mines, Report of Investigations 8515*, pages 1-36.
- Dow, W.G. (1977): Kerogen Studies and Geological Interpretations; *Journal of Geochemical Exploration* Volume 7, pages 79-99.
- Eddy, G.E., Rightmire, T.T. and Byrer, C. (1982): Content of Coal Rank and Depth: Relationship of Methane; in *SPE/Department of the Interior, Proceedings to the Unconventional Gas Recovery Symposium*, Pittsburgh, Pennsylvania, *SPE/Department of the Interior SPE/OOE 10800*, pages 117-122.
- Faiz, M.M. and Cook, A.C. (1991): Influence of Coal Type Rank and Depth on the Gas Retention Capacity of Coals in the Southern Coalfield, N.S.W. in *Gas in Australian Coals*, Bamberry, W.J. and Depers, A.M., Editors; *Geological Society of Australia, Symposium Proceedings 2*, pages 19-29.
- Gamson, P.D., Beamish, B.B. and Johnson, D.P. (1993): Coal Microstructure and Micropermeability and their Effects on Natural Gas Recovery; *Fuel*, Volume 73, pages 57-71.
- Joubert, J.I., Grein, C.T. and Beinstock, D. (1973): Sorption of Methane in Moist Coal; *Fuel*, Volume 52, pages 181-185.
- Kenyon, C., Cathyl-Bickford, C.G. and Hoffman, G. (1991): Quinsam and Chute Creek Coal Deposits (NTS) (92/13,14); *B.C. Ministry of Energy, Mines and Petroleum Resources*, Paper 1991-3.
- Kim, A.G. (1977): Estimating Methane Content of Bituminous Coalbeds from Adsorption Data; *U.S. Bureau of Mines, Report of Investigations 8245*, pages 1-22.
- Kissell, F.N. McCulloch, C.M. and Elder, C. I. (1973): The Direct Method of Determining Methane Content of Coalbeds for Ventilation Design; *U.S. Bureau of Mines, Report of investigations 7767*.
- Langmuir, L. (1918): The Adsorption of Gases on Plane Surfaces of Glass, Mica and Platinum; *Journal of the American Chemical Society*, Volume 40, pages 1361-1402.
- McCulloch, C.M., Levine, J.R., Kissell, F.N. and Duell, M. (1975): Measuring the Methane Content of Bituminous Coalbeds; *U.S. Bureau of Mines, Report of Investigations 8043*.
- Meissener, F.F. (1984): Cretaceous and Lower Tertiary Coals as Sources for Gas Accumulations in the Rocky Mountain Area; in *Hydrocarbon Source Rocks of the Greater Rocky Mountain Region*; Woodward, J. Meissener, F.F. and Clayton, J.L., Editors; *Rocky Mountain Association of Geologists*, 1984 Symposium, pages 401-431.
- Olszewicki, A.J. and Schraufnagel, R.A. (1992): Development of Formation Evaluation Technology for Coalbed Methane Development; *Quarterly Review of Methane From Coal Seams Technology*; Volume 10, Number 2, pages 27-35.
- Parr, S.W. (1932): The Analysis of Fuel, Gas, Water and Lubricants; *McGraw-Hill*, New York.

- Ryan, B.D. and Dawson, M.T. (1994): Coalbed Methane Canister Desorption Techniques; *in Geological Fieldwork 1993*, Grant, B. and Newell, J.M., Editors, *B.C. Ministry of Energy, Mines and Petroleum Resources*, paper 1994-1, this volume.
- Snowden, L.R and Powell, T.G. (1982): Immature Oil and Condensate-modification of Hydrocarbon Generation Model for Terrestrial Organic Matter; *American Association of Petroleum Geologists, Bulletin*, Volume 66, pages 775-788.



# POTENTIAL COAL AND COALBED METHANE RESOURCE OF THE TELKWA COALFIELD, CENTRAL BRITISH COLUMBIA (93L/11)

By Barry D. Ryan, British Columbia Geological Survey Branch.

and

Michael F. Dawson, Institute of Sedimentary and Petroleum Geology.

**KEYWORDS:** Telkwa coalfield, coal resource, coalbed methane, coalbed methane reserve, regional permeability, coal rank.

## INTRODUCTION

The British Columbia Geological Survey Branch and the Geological Survey of Canada have initiated a joint project to assess the coalbed methane (CBM) potential of the coalfields of British Columbia. The project includes sampling and desorption testing of fresh coal samples obtained from companies conducting exploration throughout the province. In addition methane adsorption isotherm tests are performed on some samples.

During the summer of 1992 a project was undertaken to test coal seams intersected in the ongoing Manalta Coal Limited drilling program in the Telkwa coalfield. On-site activities consisted of the collection and desorption of five samples. This report presents the desorption results and coal quality data for the five samples and three adsorption isotherms. The coal resource, the potential coalbed methane resource and reserve for the Telkwa coalfield are also discussed.

The Telkwa coalfield in central British Columbia (Figure 1) extends for about 50 kilometres along the Bulkley River from north of the town of Smithers to south of the village of Telkwa (Figure 2). The coalfield

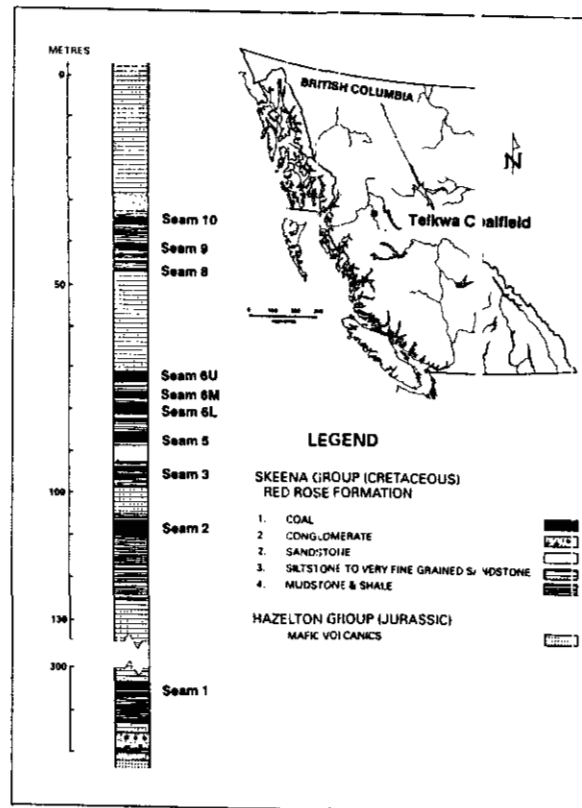


Figure 1: Location map for the Telkwa coalfield and a generalized stratigraphic column for the coalbed methane sampling area.

contains a potential coal resource of approximately 850 million tonnes. South of Telkwa, 20 to 50 million *in situ* tonnes have been identified as potentially surface mineable. The rank of the coal ranges from high-volatile bituminous A to anthracite. Most of the coal is in the range high-volatile to medium-volatile bituminous. The coalfield has historically been explored as a source of thermal coal but the wide range in rank means that there is potential for metallurgical coal.

south of Smithers near the Bulkley River, north of the Telkwa River in the vicinity of Pine Creek, east and west of Goathorne Creek and at the headwaters of Tenas and Cabinet creeks (Figures 2 and 3). Cretaceous rocks of Hauterivian age outcrop along the northeast edge of the coalfield. These rocks contain traces of coal but no coal seams have been found.

## EXPLORATION HISTORY

Thermal coal and small quantities of anthracite were mined in the coalfield in the early part of the century. More recently, near Telkwa, the coalfield has been intensively explored by a number of companies with the intention of developing an open-pit thermal-coal mine. This area, referred to as the Telkwa coal property, is about 100 square kilometres and is centred on the confluence of the Telkwa River and Goathorne Creek (Figure 3). Measured coal resources have been outlined in this area and probable coal resources outlined in the Cabinet Creek area.

The Telkwa coal property was intensively explored in the period 1978 to 1990 by Crowsnest Resources Limited when over 350 exploration holes were drilled and a large test pit excavated. The exploration activity is recorded in a number of geological assessment reports submitted to the B.C. Ministry of Energy, Mines and Petroleum Resources and in Prospectus, Stage 1 and Stage 2 Reports submitted to the Ministry as part of the approval process for mine development. The Ministry drilled six short holes in the Goathorne Creek area in 1989 (Matheson and Van Den Bussche, 1990).

Manalta Coal Limited acquired the property in 1991 and drilled more holes in 1992 and 1993. At the time of writing it plans to continue exploration.

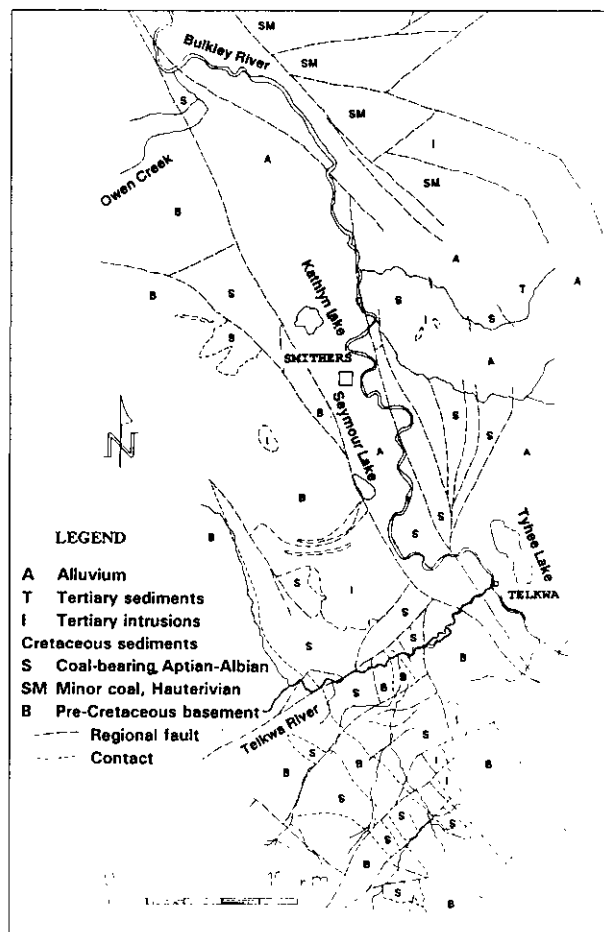


Figure 2: Regional geological map of the Telkwa coalfield.

The geology of the Telkwa coalfield is discussed in a number of papers (e.g. Koo, 1983; Palsgrove and Bustin, 1989) and is covered by regional geology maps, Tipper (1976), MacIntyre *et al.* and Ryan (1993). Coal-bearing rocks in the coalfield belong to the Skeena Group of Early Cretaceous age and are assigned to the Red Rose Formation of late Aptian to Albian age.

Much of the basin is covered by alluvium but coal-bearing rocks outcrop north of Owen Creek, west and

## REGIONAL GEOLOGY

The Cretaceous Aptian to Albian sediments on the Telkwa coal property were divided into four units by Palsgrove and Bustin (1989; Figure 3). The lowest unit, which is 20 to 100 metres thick, rests unconformably on Lower Jurassic volcanic rocks of the Telkwa Formation, Hazelton Group. It is a non-marine coarse clastic unit which contains a single coal zone with up to six component seams that are together referred to as seam 1. The cumulative vertical coal thickness varies up to 7 metres, based on drill hole information in the Goathorne Creek area (Figure 3).

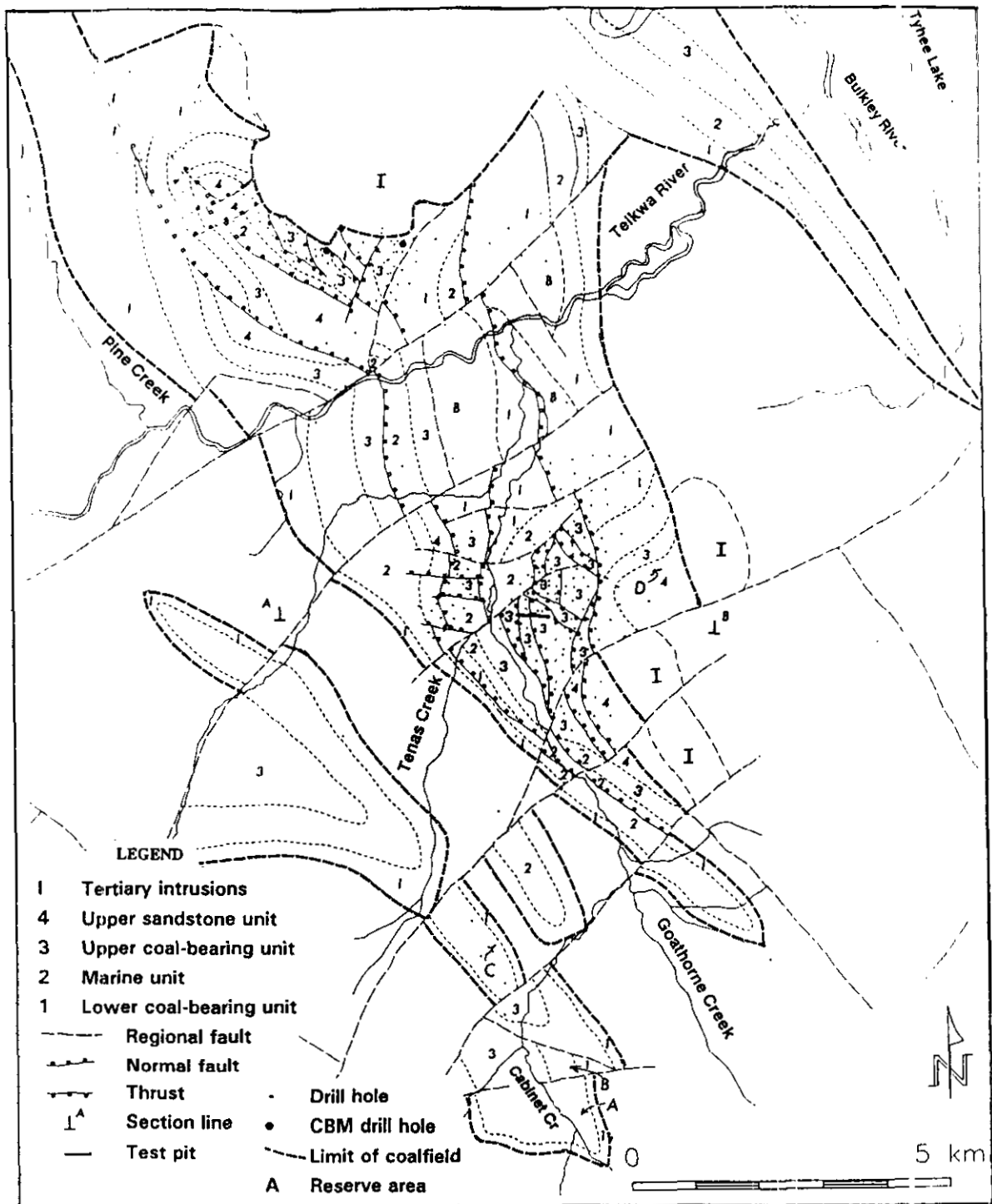


Figure 3: Detailed geology of the Goathorne Creek area in the Southern part of the Telkwa coalfield

Unit 2 is composed of from 60 to 170 metres of shallow-marine mudstones and siltstones and does not contain coal.

The major coal-bearing zone, comprising seams 2 to 10, is within unit 3 which averages 90 metres in thickness. The cumulative coal thickness ranges from 6 to 14 metres in the area covered by Figure 3. Unit 3 is overlain by the sandstone-rich unit 4 of unknown thickness.

Outcrop is sparse on the Telkwa coal property. An understanding of the structural geology has evolved as information from drilling and a number of geophysical surveys has become available. Bedding generally dips gently southeast or east and is disrupted by at least two generations of faulting. Early faults are east-dipping thrusts that, east of Goathorne Creek, offset the effect of the east dip of the sediments. Late steep-dipping faults trend northwest or northeast.

## COALBED METHANE DESORPTION TESTS

Two exploration boreholes, drilled in September, 1992, provided five samples for CBM desorption tests. The holes are located on Figure 3 and the coordinates provided in Table 1. Rotary borehole T92R-17 was drilled to a depth of 125 metres and chip samples GSC92-1 (seam 4) and GSC92-2 (seam 2) were collected from depths of 105 to 106 metres and 117.6 to 119.0 metres, respectively. Chip samples were collected off a screen in front of the drill discharge pipe. They were immediately placed into canisters and sealed for desorption measurements. Proximate analyses of the chip samples indicate that some of the sample collected included rock material from elsewhere in the hole.

TABLE 1  
DRILL HOLE LOCATION AND SAMPLE IDENTIFICATION DATA  
SUMMARY DESORPTION DATA

SAMPLE		SAMPLE LOCATIONS METRES			COLLAR COORDINATES		SAMPLE INTERVAL	
ID	SEAM	HOLE	EAST	NORTH	ELEV	FROM	TO	
GSC92-1	S4	T92R-17	617644	6059906	931	105	106	
GSC92-2	S2	T92R-17	617644	6059906	931	117.6	119	
GSC92-3	S3U	T92D-22	618906	6059980	799	64	64.4	
GSC92-4	S2R	T92D-22	618906	6059980	799	83	83.4	
GSC92-5	S2L	T92D-22	618906	6059980	799	90.8	91.2	
GSB82-6	S1	TW224	620653	6054054	773	231.7	231.8	

ID / SEAM	WT adb	COALBED METHANE DATA			GAS CONTENT PER GRAM			
		DESORB GAS cm <sup>3</sup>	LOST GAS cm <sup>3</sup>	TOTAL GAS cm <sup>3</sup>	adb	INSITU	daf	mmfb
1 / S4	629.9	1632.3	60.7	1693	2.69	2.58	3.94	4.45
2 / S2	692.5	223.2	147	370.2	0.53	0.51	0.72	0.79
3 / S3U	724.8	2330.7	170	2500.7	3.45	3.31	3.75	3.82
4 / S2R	671.9	2023.5	38	2061.5	3.07	2.94	4.25	4.69
5 / S2L	758.2	2621	77	2698	3.56	3.41	4.49	4.79

adb = Air-dried basis  
INSITU = *In situ* moisture; assumed to be 5 %  
daf = Dry ash-free data  
mmfb = Corrected for mineral matter using the Parr equation  
(see text for explanation)

The second borehole (T92D-22), a diamond-drill hole, provided three NQ core samples 4.7 centimetres in diameter and a maximum of 40 centimetres long. Samples were placed in canisters and sealed at the drill site after being described. Sample GSC92-3 (seam 3 upper) is from a depth of 64. to 64.4 metres, sample GSC92-4 (seam 2 rider) is from a depth of 83.0 to 83.4 metres and sample GSC92-5 (seam 2 lower) is from a depth of 90.8 to 91.2 metres. Holes were geophysically logged when completed. Figure 4 illustrates the log response through the coal-bearing interval for boreholes T92R-17 and T92D-22, respectively. A generalized stratigraphic column for the area is presented on Figure 1.

Desorption measurements were undertaken in Smithers, approximately 20 minutes drive from the drill

sites. Samples were desorbed at a temperature of approximately 20°C for a period of about 3 days before being transported to Calgary where desorption measurements continued until less than 5 cubic centimetres of gas were evolved over a 24-hour period. Sample weights were estimated by weighing the canisters with and without samples. Dead-space corrections were applied to adjust for variations in barometric pressure and desorption temperature. Lost-gas calculations for each canister were made based upon the U.S. Bureau of Mines method (McCulloch *et al.*, 1975).

After desorption samples were submitted to Core Laboratories, Calgary for laboratory analysis. Based on the results of these analyses two samples were chosen for adsorption isotherms. An additional sample was selected from drill-core samples originally collected by J. Koo in 1982 and stored in Victoria. This provided a sample of seam 1 from a location distant from the intrusions. The sample is from hole TW224 which was collared approximately 100 metres southwest of the western end of the test pit (Figure 3).

## DESORPTION RESULTS

Total measured gas volumes, estimated lost-gas volumes and gas contents for the samples are summarized in Table 1. Excluding sample 2, the gas contents range from 3.75 to 4.49 cubic centimetres per gram on a dry ash-free (daf) basis and do not increase with increasing depth. The low desorption value for sample 2 may be due to a failure in the canister seal. The gas contents of the samples are also expressed on an *in situ* basis assuming a 5.0% *in situ* moisture (Ryan 1991).

Before data are corrected to a dry mineral-matter free basis (dmmf) the weight loss experienced by the mineral matter when it is converted to ash must be known. The Parr equation (Rees, 1966) predicts values ranging from 1.1 to 1.25 for the ratio (mineral matter/ash) depending on the sulphur content. Five calculations of the ratio for coals from Telkwa average 1.16 as reported in Ryan (1991 b). These values are derived by plasma ashing the samples and subjecting the mineral matter residue to an ash analysis. An alternative method of estimating the weight loss experienced by ash is to plot volatile content (daf) versus ash. As the ash content increases the volatile matter (daf) values increase because of addition of volatiles from the ash. The slope of the plot provides an estimate of the ratio (mineral matter/ash). In the case of the five samples here the ratio is 1.25.

The dmmf gas contents reported in Table 1 are calculated using the Parr equation and are probably low, based on the above discussion. As most measured and theoretical adsorption curves are expressed on an as-

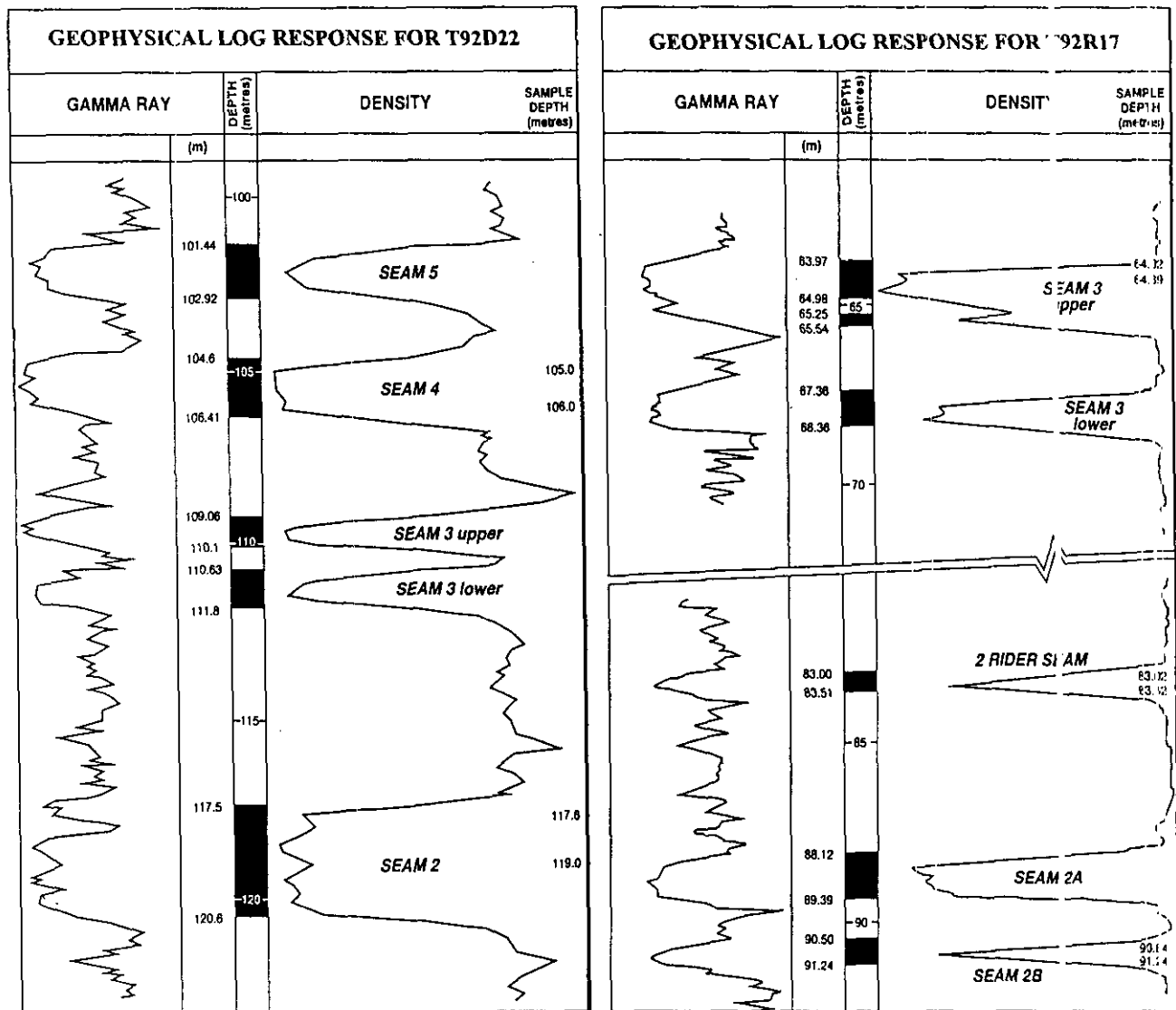


Figure 4: Geophysical log responses over sample intervals in holes T92D22 and T92D17 which provided the CBM desorption samples.

received or daf basis the dmmf calculation is not critical. Normally, for a coal with 20% ash a concentration expressed on a dmmf basis will be less than 10% higher than the same concentration expressed on a daf basis.

## COAL QUALITY

Following completion of desorption experiments, the coal samples were analyzed for ash, moisture, volatile, carbon and sulphur contents. Hardgrove Index determinations were made on two samples and equilibrium moisture contents determined on three samples. Analytical data are presented in Table 2.

Samples were sealed in canisters as soon as they reached the surface and there was not always time to pick

the most appropriate sample interval for testing. Consequently the ash contents of the samples range from 7.98 to 31.05%. Geophysical logs were not available at the time of sampling. As a result, samples 4 and 5 were collected from thinner seams with ash contents uncharacteristically high for seams at Telkwa. Samples 1 and 2 are chip samples and may contain high-ash contaminants from outside the sample interval.

Sulphur contents vary widely, ranging from 0.53 to 5.87% on an air-dried basis. The intrusion which outcrops less than 150 metres from both holes (Figure 3) may be responsible for the high and variable sulphur contents of samples 4 and 5.

Volatile matter and fixed carbon contents are consistent with coals of high-volatile A bituminous rank.

Mean maximum reflectance measurements ( $R_{max}$  values) for samples 3, 4 and 5, are 0.94, 0.99 and 0.92%,

respectively, indicating a rank of high-volatile bituminous A. The values are somewhat higher than average  $R_{max}$  values north of the Telkwa River calculated by contouring all available data, probably because of the proximity of the drill holes to the intrusion. The values do not correlate with depth and average 0.95%.

### ADSORPTION ISOTHERM DATA

Following completion of sample desorption, three samples were selected for testing to provide methane adsorption isotherms. Isotherms were measured on samples at equilibrium moisture and at a temperature of 22° C. Analyses were performed by Core Laboratories Limited, Calgary. Gas adsorption capacity was measured at seven pressures using standard techniques established for this experiment. Adsorption data including Langmuir volumes and pressures, are presented in Table 3 and the curves are plotted on Figure 5.

The adsorption curve for sample 5 is distinctly different from those of samples 3 and 6, even when the

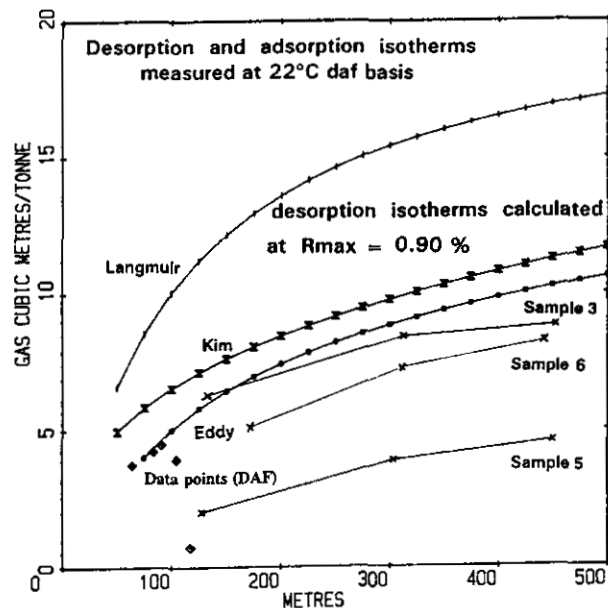


Figure 5: Desorption and adsorption data with theoretical curves from Kim (1977), Langmuir (1918) and Eddy *et al.* (1982)

TABLE 2  
COAL QUALITY DATA FOR DESORPTION SAMPLES

ID / SM	BASIS	H <sub>2</sub> O%	ASH%	VM %	FC %	S %	R <sub>max</sub>	HGI
1 / S4	ar	20.24						
	ad	0.75	31.05	24.06	44.14	1.11		
	db	0	31.28					
2 / S2	ar	29.79						
	ad	0.68	25.93	24.58	48.81	0.55		
	db	0	26.11					
3 / S3U	ar	8.6						
	ad	1	6.98	25.12	66.9	0.54	0.94	68
	db	0	7.05					
	eq	3.6						
4 / S2R	ar	21.78						
	ad	0.68	27.13	21.99	50.2	5.87	0.99	
	db	0	27.32					
5 / S2L	ar	10.1						
	ad	0.82	19.92	29.3	49.96	3.69	0.92	69
	db	0	20.08					
	eq	2.95						
6 / S1	eq	4.5	33.83			0.5	0.9	

ar = As-received moisture as measured at laboratory  
ad = air-dried moisture  
db = dry basis calculated data  
eq = equilibrium moisture  
HGI = Hardgrove Index

Note Samples 1 and 2 chip samples  
Samples 3, 4 and 5 NQ core samples  
Sample 6 small core fragment retrieved from archives  
Sulphur and R<sub>max</sub> values estimated from measurements on adjacent core

data are normalized to a daf basis. The isotherms for samples 3 and 6 project close to the desorption values for samples 1, 3, 4 and 5 (Figure 5). Samples 3 and 6 have  $R_{max}$  values 0.94 and 0.90% respectively, and equilibrium moistures of 3.6 and 4.6%.

The isotherm for sample 5 is low, and if real, implies that most of the samples are over saturated. The  $R_{max}$  value for sample 5 is 0.92%; this decrease in rank from sample 3 is not large enough to explain the difference in the two isotherms, especially considering that the equilibrium moisture of sample 5 (2.95%) is lower than for sample 3. Adsorption increases as equilibrium moisture decreases.

It is difficult to explain the fact that sample 5 appears to have desorbed more gas than it was capable of adsorbing in a later experiment. If the sample was over saturated with gas at 91 metres then one would expect the lost-gas correction (Table 1) on the desorption test to be noticeably higher than the lost-gas corrections for samples definitely not over saturated (e.g. sample 3). This is not the case. Another possibility is that the sample is slightly oxidized and that the oxidation has increased the desorbed volume of carbon dioxide but decreased the adsorption ability for methane. Whatever the explanation, it appears that the lower isotherm is not representative of Telkwa coal.

TABLE 3  
ADSORPTION ISOTHERM DATA  
SAMPLE GSC92-3

3.6 % MOISTURE		7.05 % ASH(db)		DRY ASH-FREE BASIS	
PRESSURE		VOLUME		VOLUME	
psia	H <sub>2</sub> O	scf/ton	cm <sup>3</sup> /g	scf/ton	cm <sup>3</sup> /g
180	127	187.3	5.85	201.5	6.29
442	311	250.9	7.83	270	8.43
638	449	262.8	8.2	282.8	8.83
921	648	281	8.77	302.3	9.44
1317	926	296.2	9.25	318.6	9.94
1543	1085	295	9.21	317.4	9.91
1948	1370	305.9	9.55	329.1	10.27

SAMPLE GSC92-5

2.95 % MOISTURE		20.1 % ASH(db)		DRY ASH-FREE BASIS	
PRESSURE		VOLUME		VOLUME	
psia	H <sub>2</sub> O	scf/ton	cm <sup>3</sup> /g	scf/ton	cm <sup>3</sup> /g
180	128	50.5	1.58	63.2	1.97
428	304	100.6	3.14	125.8	3.96
634	450	117.4	3.66	146.8	4.58
1006	713	154.7	4.83	193.6	6.04
1221	806	172.6	5.39	216	6.74
1602	1136	199.6	6.23	249.8	7.8
1971	1398	211.4	6.6	264.5	8.26

SAMPLE GSB82-6

4.5 % MOISTURE AND 35.43 % ASH (db)		DRY ASH-FREE BASIS		DRY ASH-FREE BASIS	
PRESSURE		VOLUME		VOLUME	
psia	H <sub>2</sub> O	scf/ton	cm <sup>3</sup> /g	scf/ton	cm <sup>3</sup> /g
240	168.8	106	3.31	164.1	5.12
440	309.4	150.9	4.71	233.7	7.29
626	440.2	170.9	5.33	264.7	8.26
912	641.4	199.4	6.22	308.8	9.64
1210	850.5	225.5	7.04	349.2	10.9
1513	1064	234.8	7.33	363.7	11.35
1984	1395	244.6	7.63	378.8	11.82

CONSTANTS

	GSC92-3	GSC92-5	GSB82-6
Sample depth (metres)	64.0-65.0	91.5-91.9	231.7
Langmuir Volume (cm <sup>3</sup> /g) adb	10.38	9.856	9.46
Langmuir Pressure (psia)	171.6	982.7	451.8
Equivalent water column in metres	120.7	691.1	317.7
daf volume (cm <sup>3</sup> /g)	11.17	12.331	14.63
Predicted volume adb (cm <sup>3</sup> /g)	4.8	1.08	3.98
(from adsorption isotherm)			
Measured volume adb (cm <sup>3</sup> /g)	3.45	3.56	
(from desorption data)			
Note H <sub>2</sub> O is the height in metres of a water column equivalent to psia pressure			

## DATA SOURCES AND ANALYSIS TECHNIQUES FOR RESOURCE ASSESSMENT

A coalbed methane resource analysis requires information about the thickness, depth and rank of the coal, as well data on its gas content. Data for cumulative coal-seam thicknesses, depth of seams and thicknesses of

stratigraphic units are available from geophysical logs of 350 holes drilled in the Telkwa area. This information has been entered into a computer database which makes it possible to grid and contour various parameters.

A number of  $R_{max}$  values of Telkwa coal are available (Ryan, 1992a). The  $R_{max}$  data are analyzed with help of a number of computer programs. Files of  $R_{max}$  data by seam with UTM locations were entered into GEOEAS, a variogram, kriging and contouring computer program distributed in the public domain by the Environmental Protection Agency (1988). This software was used to grid the data. Programs generated in-house were then used to calculate area-weighted averages for the data, construct Autocad DXF files and generate contour files compatible with QUIKMAP, a simple GIS software package (Environmental Sciences Limited, 1990). The series of programs allows for geostatistical analysis, resource evaluation and display of results.

Use was also made of a database of Telkwa coal quality which consists of over 3000 lines, each line representing a set of up to seven different analyses of a single sample. Data are derived from all ten seams sampled from over 350 holes, many of which were corec-

## COAL RESOURCE IN THE TELKWA COALFIELD

The intensive exploration from 1978 to 1993 in the area west of Goathorne Creek and north of the Telkwa River has outlined a proven open-pit mineable reserve in the range of 20 to 50 million *in situ* tonnes. It is difficult to assess the resource of the whole basin, which extends from Cabinet Creek in the south to north of Owen Creek in the north (Figure 2) because information is scarce or lacking in many areas. The regional geology is compiled on two 20 000-scale map sheets and a set of geological sections (Ryan, 1993). These maps and sections are used extensively to outline coal-bearing areas, as a base to plot the distribution of cumulative coal thickness in units 1 and 3 and as a base to plot the regional distribution of  $R_{max}$  values.

There is substantial information available for the area south of the village of Telkwa (sheet 1, Ryan, 1993). North of Telkwa and south of Smithers there is some information (Sheet 2, Ryan, 1993). North of Smithers there is little information except for the Owen Creek area which was sampled by the senior author in 1991.

An attempt is made to apply the informal four-unit stratigraphic classification of Palsgrove and Bustin (1989) to the whole basin and assess the resources in terms of cumulative coal in units 1 and 3. Unit 1 is

recognized south of Smithers and possibly near Owen Creek. Unit 3 outcrops extensively south of the Telkwa River, adjacent to the Bulkley River and near Kathlyn Lake.

The coal resources are calculated in ten areas (Figure 6), and assigned to either unit 1 or 3. They are also classified as proven, probable or inferred (Table 4). These terms are used informally; proven refers to areas where there are numerous drill holes; probable refers to areas where there is some outcrop data and/or a few drill holes and inferred refers to areas where unit 1 or 3 are inferred to outcrop and a cumulative coal thickness is assumed.

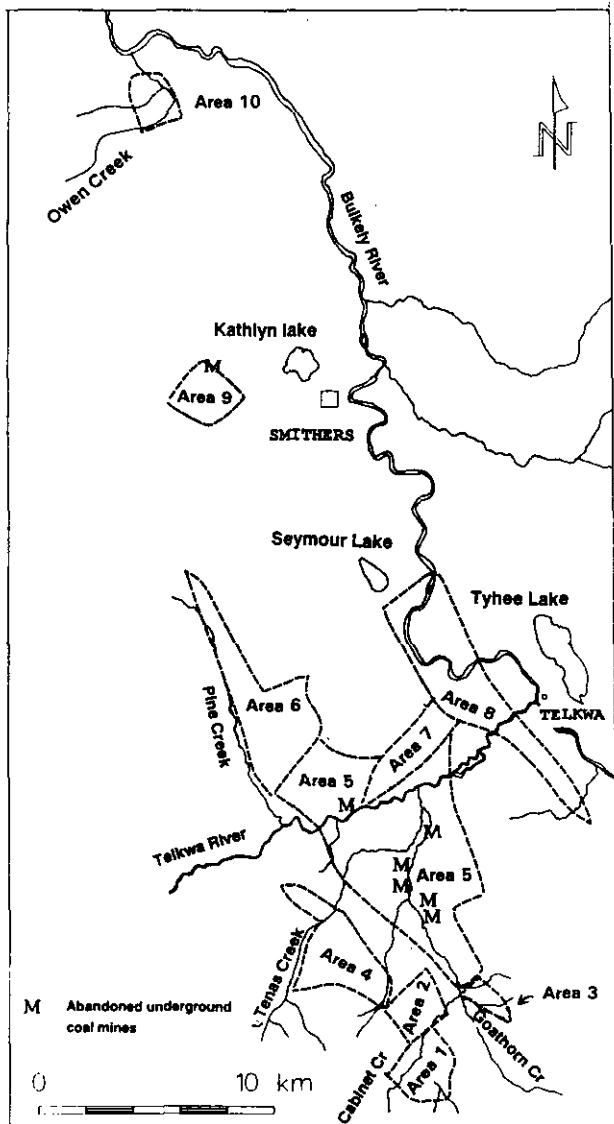


Figure 6: Resource calculation areas; southern Telkwa coalfield.

The average ash content for seams in unit 3 is assumed to be 21% at 1% air-dried moisture. The average ash content of seam 1 (unit 1) is assumed to be 30% at an air-dried moisture of 1%. These values are the average values extracted from the Telkwa Stage 2 report (1984) which covers only area 5. As area 5 contains over 70% of the coal resource in the coalfield, these values are applied to all other areas. The *in situ* moisture for Telkwa coal is estimated to be about 5% (Ryan, 1991a). Based on these data an average specific gravity of 1.26 is used for *in situ* unit 3 coal and 1.45 for *in situ* unit 1 coal.

TABLE 4  
COAL RESOURCE IN THE TELKWA COALFIELD

AREA	UNIT 1			UNIT 3			TOTAL
	proven	probable	inferred	proven	probable	inferred	
1							
2	0	25	0	0	14.6	0	39.6
3	0	9.7	5.2	0	0	0	14.9
4	0	0	6.6	0	0	0	6.6
5	0	0	49.6	0	0	19	68.6
6	353.7	0	0	316.1	0	0	669.8
7	0	21.6	5.8	0	0.7	0	28.1
8	0	0	3.1	0	0	2	5.1
9	0	0	6.5	0	0	13.9	20.4
10	0	0	0	0	5	0	5
	0	4	0	0	0	0	4
<b>TOTAL</b>	<b>353.7</b>	<b>60.3</b>	<b>76.8</b>	<b>316.1</b>	<b>20.3</b>	<b>34.9</b>	<b>862.1</b>

SUMMARY million tonnes	values used to calculate tonnage in%		
		Unit 1	Unit 3
PROVEN	669.8		
PROBABLE	80.6	average <i>in situ</i> ash	29
INFERRED	111.7	average <i>in situ</i> moisture	5
TOTAL	862.1	average <i>in situ</i> S.G.	1.45
			1.26

The resources in areas 1, 2, 3 and 4 (Figure 6) are calculated by planimetry of the areal extent of units 1 and 3 and multiplying by an average cumulative coal thickness obtained by averaging drill-hole and outcrop data in the area.

The probable resource of area 1, which covers the synclinal remnants of units 1 and 3 in the Cabinet Creek area, is 39.6 million tonnes. There is one drill hole in this area and a number of coal outcrops that were mapped and sampled by the senior author in 1990.

The probable and inferred resource of area 2 is 14.9 million tonnes. This area covers two postulated synclinal remnants of coal-bearing sediments in which there are three drill holes. Area 3 is similar to area 2 and also covers a postulated synclinal remnant of sediments with an inferred resource of 6.6 million tonnes.

There is not much public information available for area 4 which is assigned an inferred resource of 68.6 million tonnes. Manalta Coal Limited drilled here this area in 1992 and 1993 and intersected coal, so that a more confident assessment of the resource will be available in the future.

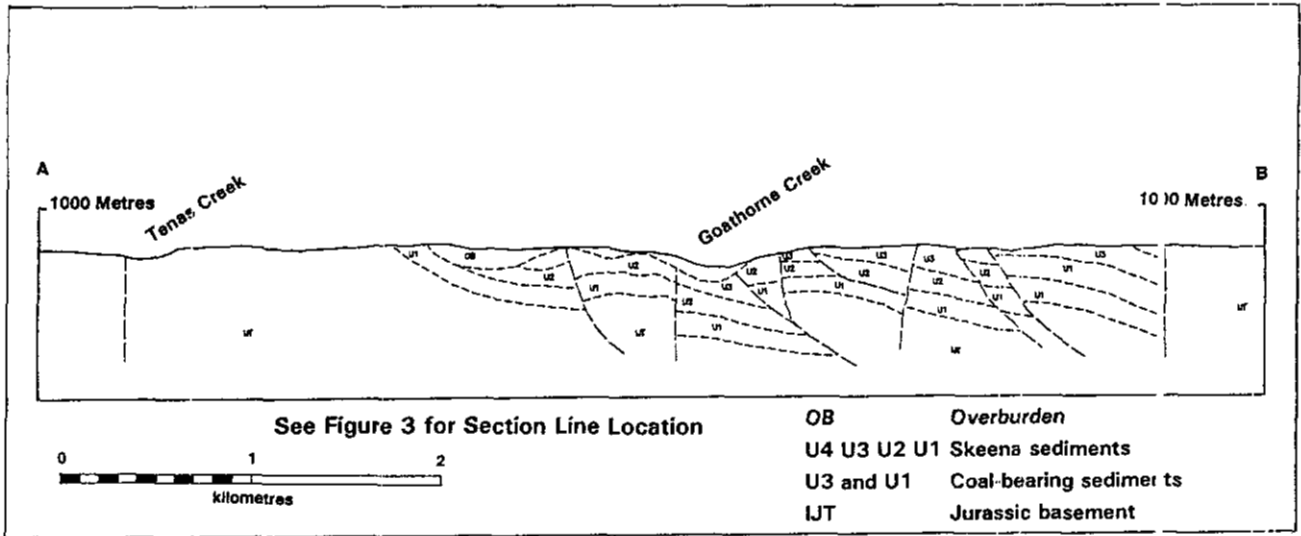


Figure 7: Geological section of the Goathorne Creek area.

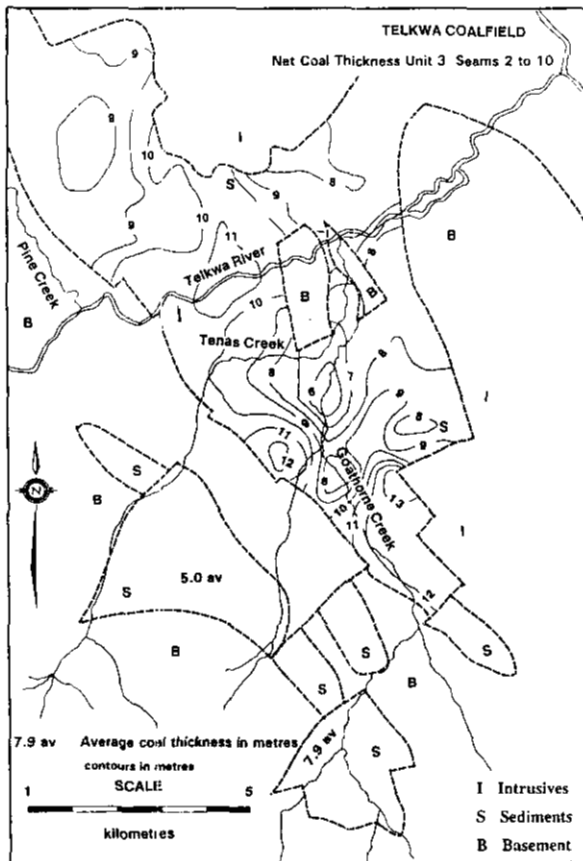


Figure 8: Cumulative coal intersected in unit 3

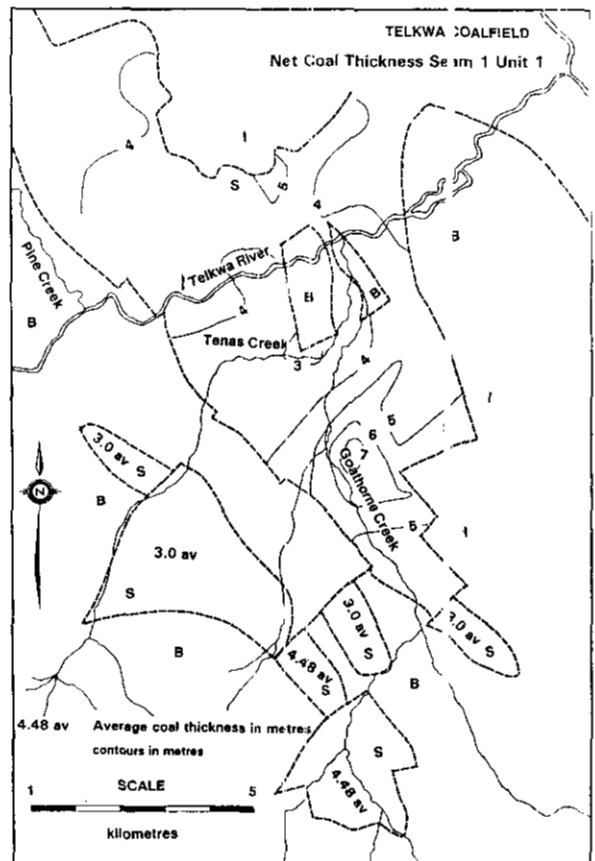


Figure 9: Cumulative coal intersected in unit 1

Much of the exploration in the Telkwa coalfield was in area 5 where most of the 171 holes that intersect unit 3 and the 100 holes that intersect unit 1 were drilled. A test pit in area 5 excavated 5000 tonnes of coal (Figure 3). Five detailed geological sections (Ryan, 1993) outline the distribution of the units in the area. One of these sections (Figure 7) is located on Figure 3.

Cumulative coal data for units 1 and 3 were gridded and the data contoured in Figures 8 and 9. Cumulative coal thicknesses do not indicate the total cumulative coal in the units because few holes penetrated the total thickness of either unit. The grid cells were constructed so that they match the section lines. This allows average coal thicknesses to be located on the sections at 500-metre spacings. Average coal thicknesses were multiplied by the length of coal-bearing unit in each fault block outlined on the sections. Summing the resulting coal area increments provides a volume of coal for each section line. These values were multiplied by an appropriate lateral distance and a specific gravity of 1.26 or 1.45, to provide the appropriate tonnage.

This method of evaluation provides only an estimate of the total resource in area 5. The resource classified as proven is 670 million tonnes. A more complete approach would require constructing isopach and structural contour maps for units 1 and 3 in each fault block. There is sufficient information available to do this in area 5, but it was not considered warranted for this study.

Thirteen holes have been drilled in area 6 but it is not currently included in any mining reserve estimation. A resource of 28.1 million tonnes is outlined. Area 7, to the east, is similar but does not contain any drill holes so the 5.1 million tonne resource is classified as inferred.

In area 8, postulated to contain unit 3 and 1, thin seams outcrop adjacent to the Bulkley River, south of Smithers. Area 8 is assigned an inferred resource of 20.4 million tonnes.

Multiple thin seams outcrop west of Kathlyn Lake (area 9) where there was some mining from 1932 to 1936. All these outcrops are assigned to unit 3 and an inferred resource of 5 million tonnes is estimated.

The Telkwa coalfield extends north of Smithers for about 17 kilometres. The valley floor is covered by alluvium and it is not known if the Skeena Group sediments (unit 1?) which outcrop north of Owen Creek (area 10) are continuous at depth with outcrops at Kathlyn Lake. There are very little data available to assess the potential coal resource in this area. Mapping in 1991 by the senior author located 2.55 metres of

cumulative coal in seven thin seams. A probable resource of 4 million tonnes is assigned to the area.

## COAL RANK

The rank of coal in the Telkwa coalfield is discussed by Ryan (1992a). Some new analyses are now available for areas in the northern part of the coalfield. This paper presents the new  $R_{\max}$  data and discusses the lateral and vertical variations of  $R_{\max}$  values in area 5.

Generally the rank of coal in the Goathorne Creek area of the coalfield (area 5) is high-volatile bituminous A. The rank increases to the south and north away from area 5. In the Cabinet Creek area measurements on outcrop coal provide an average  $R_{\max}$  value of 2.3%. The coal adjacent to the Bulkley River in area 8 has an average  $R_{\max}$  value of 1.27% and further to the north a sample has an  $R_{\max}$  value 1.97%. The Lake Kathlyn deposit is anthracite and  $R_{\max}$  values of coal north of Owen Creek (area 10) are variable but average 1.6%.

For areas other than area 5 single average  $R_{\max}$  values are assigned to the area. There are sufficient data in area 5 to produce a contour map of  $R_{\max}$  values for unit 1 (seam 1) and unit 3 (seam 2). This is done in part using  $R_{\max}$  measurements and in part using  $R_{\max}$  values estimated from volatile measurements (Ryan, 1992a). The procedure used is similar to that employed by Stevens *et al.* (1993). A number of papers discuss the relationship between volatile matter (VM) on a dry ash-free basis (daf) or dry mineral-matter-free basis (dmmf) and  $R_{\max}$  values (Bustin *et al.*, 1983; Meissener, 1986).

Volatile matter data can be corrected to an ash-free or mineral-matter-free basis by first plotting all VM data against ash data on a seam by seam basis to derive the best-fit linear relationships and then using the slope of the lines to correct individual VM measurements to an equivalent VM ash-free value. The slope of the line will equal the Y intercept (VM af) if the ash acts only as a dilutant. If the mineral matter and any sulphides add inorganic volatile matter to the VM measurement then the slope will be decreased by a component equal to the gassiness of the mineral matter.

Based on the data in Table 5 the mineral matter in seam 2 is gassier than in seam 1. Non-gassy mineral matter is often associated with a reactive rich coal (Slaghuis *et al.*, 1990) and probably also indicates less pyrite.

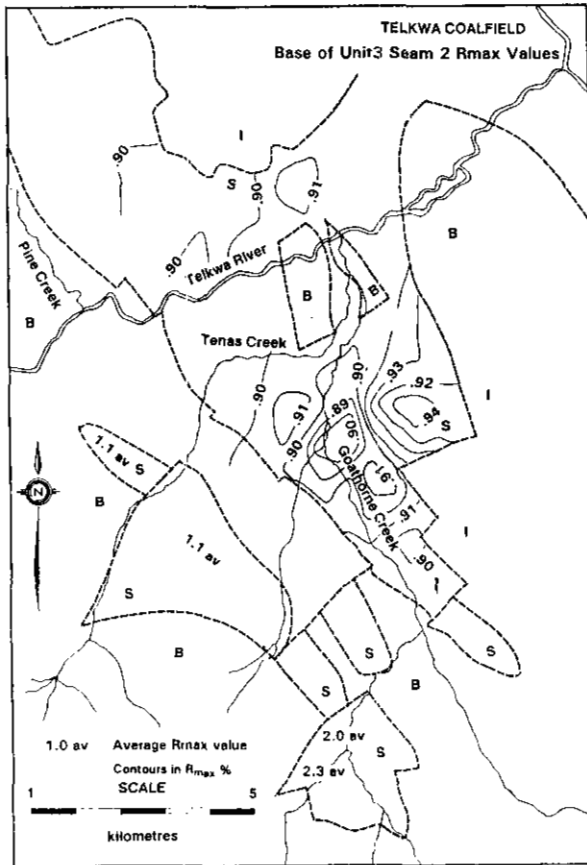


Figure 10: Seam 2  $R_{max}$  contours

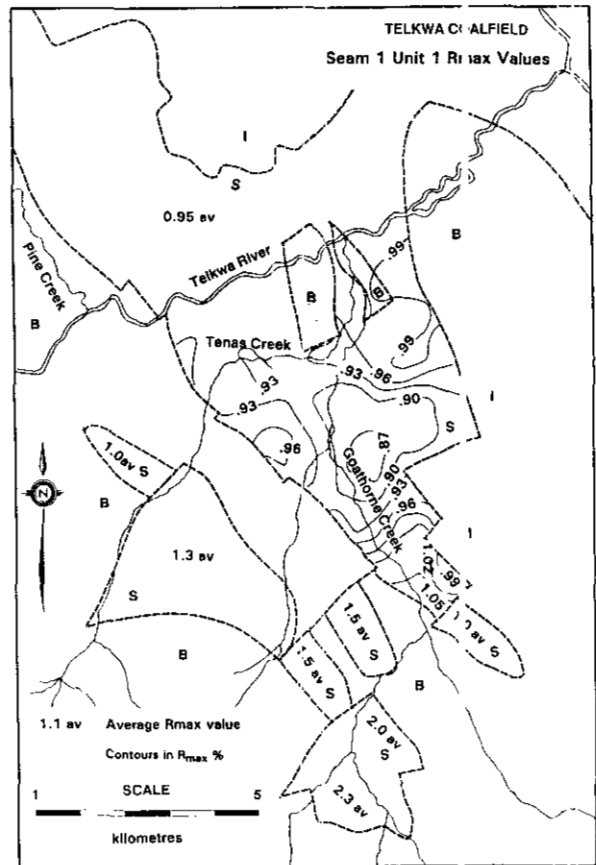


Figure 11: Seam 1  $R_{max}$  contours

Once a method is developed to provide volatile matter ash-free values (VM af%) it is possible to investigate the relationship of VM% (af) versus  $R_{max}$  values on a seam by seam basis using the existing  $R_{max}$  measurements. There are eight VM% (af) versus  $R_{max}$  pairs for seam 1, and sixteen pairs for seam 2. Lines are fitted through each data suite (Table 5). It is now possible to convert any VM% measurement to an estimated  $R_{max}$  value using the VM% versus ash% relationships and the VM% (af) versus  $R_{max}$  value relationships for each seam. Using this technique 128 data points for seam 2 (unit 3) and 56 data points for seam 1 (unit 1) were generated and the data used to generate contour plots (Figures 10 and 11). The calculated  $R_{max}$  values were also gridded on grids that matched the geological section base lines. This permitted  $R_{max}$  values to be posted onto the sections at 500-metre spacing.

TABLE 5  
RELATIONSHIP OF  
VOLATILE MATTER ASH-FREE BASIS TO REFLECTANCE ( $R_{Tmax}$ )

EQUATION	count	$R^2$
<b>SEAM 6</b>		
$VM = 29.6 - 0.176 \times ash$	134	-0.59
$VM af = VM + 0.176 \times ash$		
$R_{max} = 1.53 - 0.022 \times VM af$	12	-0.82
<b>SEAM 2</b>		
$VM = 29.3 - 0.168 \times ash$	167	-0.54
$VM af = VM + 1.68 \times ash$		
$R_{max} = 1.31 - 0.014 \times VM af$	16	-0.54
<b>SEAM 1</b>		
$VM = 30.9 - 0.304 \times ash$	84	-0.46
$VM af = VM + 0.304 \times ash$		
$R_{max} = 2.46 - 0.0479 \times VM af$	8	-0.88

af = ash-free basis

## METHANE CAPACITY OF TELKWA COAL

The best way to calculate the methane resource of an area is to measure the desorbed gas from a number of samples of varying rank and from different depths and to use the results to provide gas content per tonne values for coal tonnages in each sub-area. In the absence of sufficient data there are three alternative approaches.

- Adsorption isotherms provide information on the maximum adsorption gas capacity at increasing pressure and constant temperature (in this case 22°C). The adsorbed gas capacity is not necessarily the actual gas capacity. It does not consider the free-gas component which is probably not measured in the desorption test.
- There are a number of empirical curves that illustrate the actual averaged lost plus desorbed gas contents of coals of different ranks at different depths (Eddy *et al.*, 1982).
- There are equations, derived in part from empirical relationships and in part from theoretical considerations, that predict the maximum adsorption capacity of coal of different ranks and at different depths (Langmuir, 1918; Kim, 1977; Olszewicki and Shraufnagel, 1992).

The five desorption tests performed on Telkwa coal are plotted on an ash-free basis on Figure 5 with the three adsorption isotherms for samples 3, 5 and 6. The adsorption isotherms were measured at a constant temperature of 22°C which may not be the reservoir temperature. Increasing temperature decreases the adsorption capacity of the coal. Most of the coal considered in this study is shallow and at depths ranging up to 500 metres. If the average surface temperature is 11°C and the geothermal gradient is assumed to be 20°C per 1000 metres then a temperature of 22°C corresponds to a depth of 550 metres.

The adsorption isotherms for samples 3 and 6 project close to the plotted positions of samples 1, 3, 4 and 5 (Figure 5). All data are calculated to a dry-ash-free basis. It appears that these samples are saturated and that the isotherms for samples 3 and 6 provide a reasonably accurate method of predicting their gas capacity at increasing pressure and constant temperature.

Eddy *et al.* (1982) provide five curves of lost plus desorbed gas contents for coals of constant rank at varying depths. These are empirical curves based on numerous desorption results. To some extent they provide a static picture, in that the coal rank generally increases with depth.

Ryan (1992b) fitted an empirical equation which contains the additional variable of  $R_{\max}$  to Eddy's curves. It permits curves to be constructed for intermediate ranks that still conform to the general form of the five original Eddy curves or to illustrate the effect of increasing rank with depth.

A modified Eddy curve for a  $R_{\max}$  of 0.90% projects close to the desorption data and isotherm for sample 3 (Figure 5). The average  $R_{\max}$  value of three of the samples (3, 4, and 5) is 0.95%. A similar Eddy curve for  $R_{\max}$  of 0.95 predicts desorbed gas contents about 16% higher for the depths of 60 to 120 metres than the 0.90%. If this discrepancy is real then it means that Telkwa coal, as represented by samples 3, 4 and 5, even when saturated, contains about 16% less gas than coals of similar rank from the U.S. database used to establish the original Eddy curves.

Kim (1977), using in part desorption data and in part theoretical predictions of the relationships of adsorption *versus* temperature and pressure, produced a set of equations that predict the adsorption capacity of coal. Kim's equations predict a maximum capacity for coals of different ranks at various temperatures and pressures. This maximum capacity is then decreased by an amount based upon the critical moisture content of the coal. This term is rank dependent and is approximated by the equilibrium moisture of the coal and is also dependent on the oxygen content of the coal.

Oxygen data are not always available for coal samples. Because of the partial rank dependency of the oxygen content of coal it is possible to establish a relationship of critical moisture to volatile matter (daf) using data in Kim's paper and a relationship of VM (daf) *versus*  $R_{\max}$  using relationships in Meissener (1984). Using these relationships it is possible to calculate the critical moisture corresponding to a specific  $R_{\max}$  value.

There are no oxygen data available for the desorption samples but some averaged data from north of the Telkwa River provide a value of 9.3% and similar data from south of the Telkwa River provide an average of 7.6%. The average  $R_{\max}$  value of the desorption samples is 0.95% and their average equilibrium moisture is 3.28%.

These data provide four ways of estimating the critical moisture and therefore four different adsorption values at a constant depth. At a depth of 100 metres the four predicted gas contents are 6.73, 5.85, 4.95 and 5.99 grams per cubic centimetre for critical moistures calculated using 1/ an  $R_{\max}$  value of 0.95%, 2/ an oxygen content of 7.6 3/ an oxygen content of 9.3% and 4/ an equilibrium moisture of 3.28%. This compares to an adsorption content of 5.04 grams per cubic centimetre measured by the adsorption isotherm for sample 3 at a depth of 100 metres.

Kim's equations provide only an estimate of predicted maximum adsorption capacity and no estimate

TABLE 6  
PREDICTED GAS CONTENTS OF UNIT 1 AND UNIT 3 COALS WITH  
INCREASING RANK AND DEPTH OF BURIAL  
calculated using Equation A (Ryan, 1992b)  
values adjusted by 16% (see text)

Depth m	R <sub>max</sub>	UNIT 1		in situ ash 29% in situ moisture 5%					
		0.86	0.88	0.9	0.92	0.94	0.96	0.98	I
50	1.14	1.3	1.45	1.6	1.74	1.86	2	2.12	
100	2.48	2.64	2.79	2.93	3.07	3.2	3.33	3.45	
150	3.26	3.41	3.56	3.7	3.85	3.98	4.11	4.23	
200	3.81	3.96	4.12	4.26	4.4	4.53	4.66	4.78	
250	4.23	4.39	4.54	4.69	4.83	4.96	5.09	5.21	
300	4.59	4.75	4.9	5.04	5.17	5.31	5.43	5.56	
350	4.88	5.04	5.14	5.33	5.58	5.6	5.74	5.85	
400	5.14	5.3	5.45	5.59	5.73	5.86	5.99	6.12	

Depth m	R <sub>max</sub>	UNIT 3		in situ ash 20% in situ moisture 5%					
		0.86	0.88	0.9	0.92	0.94	0.96	0.98	I
50	1.3	1.48	1.66	1.81	1.97	2.13	2.27	2.41	
100	2.81	2.99	3.17	3.33	3.49	3.64	3.78	3.92	
150	3.7	3.88	4.05	4.22	4.37	4.52	4.67	4.8	
200	4.33	4.51	4.68	4.84	5	5.15	5.29	5.44	
250	4.81	5	5.17	5.33	5.49	5.64	5.78	5.92	
300	5.22	5.39	5.56	5.73	5.88	6.03	6.18	6.32	
350	5.55	5.73	5.9	6.07	6.22	6.37	6.52	6.65	
400	5.84	6.02	6.19	6.35	6.51	6.66	6.8	6.95	

Equation A  
 $K = 0.98$      $R = R_{max} \times K$      $C = \text{Depth in metres} \times R^{2.5} - 0.3$   
 $B = (L \ln(C) / (2.30259 - 1.095) / 0.03913)$      $\text{Gas cm}^3/\text{g} = B \times (100 - M - A) / 100 / 32.037$   
M = moisture content    A = Ash content

of the free gas component. Based on the data above, Kim's equations provide predictions that range from good agreement with isotherms 3 and 6 to 35% higher than the isotherms. The apparent over estimate of the gas capacity of the samples may be because Kim's equations were developed using coals with a generally higher vitrinite content than Telkwa coals. She used a database of 22 samples collected from Appalachia and the Black Warrior coal basin. Some papers appear to indicate that vitrinite has a higher adsorption capacity than other coal macerals (Lamberson and Bustin, 1992). Work by the present authors may indicate that small amounts of inherent ash can damage the adsorption capacity and confuse the maceral *versus* adsorption capacity relationship. Also Kim's equations use proximate data to estimate coal rank which influences gas adsorption capacity. Because of the lower vitrinite and therefore lower volatile content of Telkwa coals, Kim's equations will over estimate ranks and gas contents for the coal.

Olszewicki and Shraufnagel (1992) used the same database as Kim but used the Langmuir equation (Langmuir, 1918) to produce another model of gas content *versus* depth. Their model has been adapted to allow for construction of gas content *versus* depth tracts that illustrate the effect of increasing rank and temperature with depth. The modified Langmuir curve for a R<sub>max</sub> of 0.90 and a geothermal gradient of 18°C per 1000 metres (Figure 5) plots much higher than the data. No explanation for the large discrepancy could be found in the data or in the original paper.

The difference in the three methods of predicting desorption curves (Eddy *et al.*, Langmuir, and Kim)

indicates the level of uncertainty in trying to predict gas contents. Gas capacities cannot be predicted accurately based only on proximate data, depth and temperature. The various approaches serve mainly to illustrate relative trends as coal quality, rank, depth and temperature change.

The modified Eddy curve appears to provide the best way to model the gas content of Telkwa coal for changing ranks and depths. However predicted gas contents must be decreased by 16% to account for the fact that an Eddy curve of R<sub>max</sub> = 0.95% is 16% higher than the 4 data points which average a R<sub>max</sub> of 0.95%.

The desorption samples were collected from within 150 metres of a Tertiary intrusion (Figure 3). The R<sub>THIX</sub> values do not appear to have been increased by the intrusion, but intrusions probably cause movement of heated geothermal water outside any identifiable metamorphic halo. This water could easily remove methane from the coal and at the same time deposit finely dispersed mineral matter in the microporosity of the coal which could damage its adsorption ability.

## METHANE RESOURCE

Gas contents for different ranks and depths are calculated using modified Eddy curves generated by Ryan, (1992b) and the ranks and depths established for each block or sub-block of the coal resource. The gas contents are all decreased by 16%. This factor could be explained as an adjustment to account for the moderately low vitrinite content of Telkwa coals as compared to the database used to establish the original Eddy curves. Average *in situ* ash and moisture contents are used for all unit 1 coals (29% and 5%) and unit 3 coals (20% and 5%). Table 6 provides a matrix of gas concentrations per tonne calculated using equation A for unit 1 and 3 coals, for varying depth and rank.

In most areas an average depth and rank is assigned to the coal tonnage reported in Table 4. The tonnages are multiplied by the appropriate gas-content value (Table 6). The procedure is not accurate because there is very little coal-depth information in many of the areas. A more accurate assessment of the resource is possible in area 5. Depths are assigned to each block of coal between faults on the sections and individual gas content values used. The methane resource is classified based on an estimate of the degree of assurance (Table 7). Level 1 indicates a high level of assurance and level 3 a low level. The informal level terms were used to avoid using terms such as proven resource which might carry implied definitions from the oil and gas industry that would not be appropriate in this study.

The total coalbed methane resource of the Telkwa coalfield is 3.7 billion cubic metres (Table 7). This is not

large when compared to the resources in the major coalfields such as the southeast British Columbia coalfield which has a resource of 565 billion cubic metres (Johnson and Smith, 1991). On the other hand, the Telkwa coalfield is close to the towns of Smithers and Telkwa which may offer ready markets for small quantities of gas.

Any discussion of the potential for recoverable reserves requires an understanding of the regional structure and its influence on regional permeability.

## REGIONAL STRUCTURE

Beds in the Telkwa coalfield generally strike northwesterly, dip to the east and are segmented into numerous fault blocks by northwest-striking east-dipping reverse and thrust faults. There are at least two episodes of later normal faulting. Older normal faults trend northerly. A few outcrops of andesite dikes, striking northwest, are apparently associated with these faults. Younger normal faults trend east-west. The regional fault pattern is well documented in the Goathorne Creek area by extensive exploration drilling. In other areas only the major block faults have been identified (MacIntyre *et al.*, 1989).

Mesoscopic faults and folds seen in outcrop support this geometry and sequence. Small-scale thrusts and reverse faults, striking northwest, break the beds and in places are associated with folds which generally are not found elsewhere. In some places early thrusts and reverse faults are broken by younger northwest-striking normal faults. Occasionally easterly striking vertical faults, assumed to be the youngest structures, are seen. They are often associated with brecciation.

Fold trends in some areas are estimated from stereonet plots of poles to bedding. In the Cabinet Creek area folds trend 320° and plunge 20°. To the north, in the Goathorne Creek area the average fold-axis trend is azimuth 135° and plunge 25°. In the Telkwa and Bulkley River areas the fold axes appear to trend 180° with a zero plunge. The orientations of minor fold axes, compressional faults and normal faults are plotted on Figure 12. The data are mostly from the area south of Telkwa. The vector average fold-axis orientation is 143° trend with a plunge of 13°.

Some joint and minor fault data have been collected from drill holes and these are discussed in the context of their effect on permeability.

## PERMEABILITY

Favourable regional permeability within the coal seams is one of the most important parameters required for an economic CBM well. Permeability measurements were made as part of the Telkwa Stage 2 study (Crowsnest Resources Limited, 1984). The data are included in two geotechnical reports, one by Klohn Leonof Limited and one by Piteau Limited.

The Klohn Leonof study was undertaken to aid pit design in the area east of Goathorne Creek. As part of the study, packer tests were performed over coal intersections in diamond-drill holes. The Piteau study in 1990 was part of an amended Telkwa Stage Two submission and included data on the permeability of interburden rocks north of the Telkwa River.

Permeability data from these two reports are collected in Table 8. Permeabilities of coal seams, numbers 2 to 8 in three drill holes in the east Goathorne area were measured at depths ranging from 29 to 158 metres. Permeabilities do not correlate with depth and values range from 0.5 to 50 millidarcies. Measurements were made as drilling commenced, using packers to isolate individual seams. Data were reported as hydraulic conductivity (metres per second) and an approximate conversion to millidarcies is made by multiplying by 105.

TABLE 7  
COALBED METHANE RESOURCE IN THE TELKWA COALFIELD

AREA	UNIT 1			UNIT 3			TOTAL
	level 1	Level 2	Level 3	Level 1	Level 2	Level 3	
1	0	229.1	0	0	131	0	360.1
2	0	75.6	40.9	0	0	0	116.5
3	0	0	3.7	0	0	0	3.7
4	0	0	336	0	0	103.6	439.6
5	1836.9	0	0	735.8	0	0	2572.7
6	0	98.8	0	0	2.9	0	101.7
7	0	0	13.9	0	0	10.3	24.2
8	0	0	0	0	0	0	0
9	0	0	0	0	61.1	0	61.1
10	0	31.4	0	0	0	0	31.4
<b>TOTAL</b>	<b>1836.9</b>	<b>434.9</b>	<b>394.6</b>	<b>735.8</b>	<b>195</b>	<b>113.8</b>	<b>3711</b>

SUMMARY	million m <sup>3</sup>
LEVEL 1	2572.8
LEVEL 2	629.8
LEVEL 3	508.4
<b>TOTAL</b>	<b>3711</b>

The CBM content per tonne values were derived using average ash and moisture contents and varying rank and depth values as indicated in Table 6.

Depth and  $R_{max}$  data estimated from regional geology as described in text

Levels are informal indications of assurance 1 = high 3 = low.

Permeabilities of 0.5 to 50 millidarcies cover the range from low to excellent for coal, considering the depth of the measurements. In the Black Warrior basin, Alabama, permeabilities range from 0.5 to 14 millidarcies at depths of approximately 350 metres (Ellard and Roark, 1992). Generally a permeability of 5

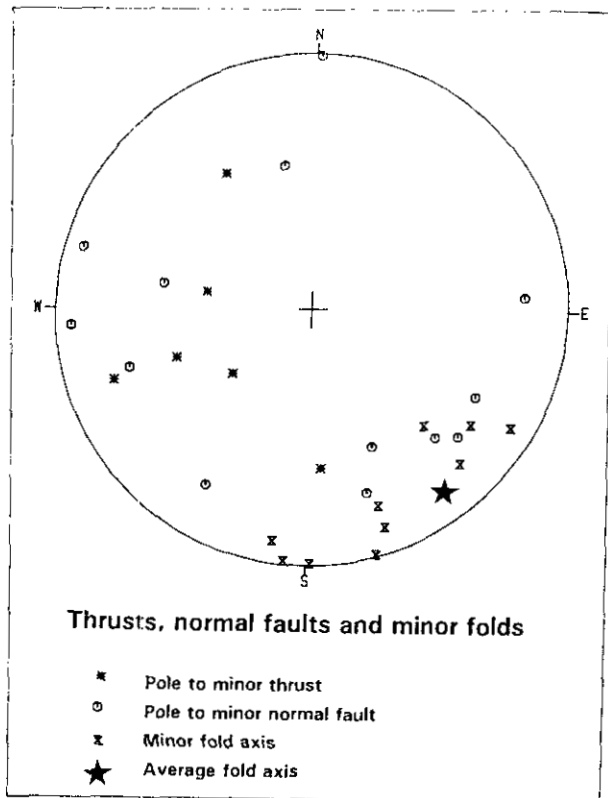


Figure 12: Minor fold axes and minor faults

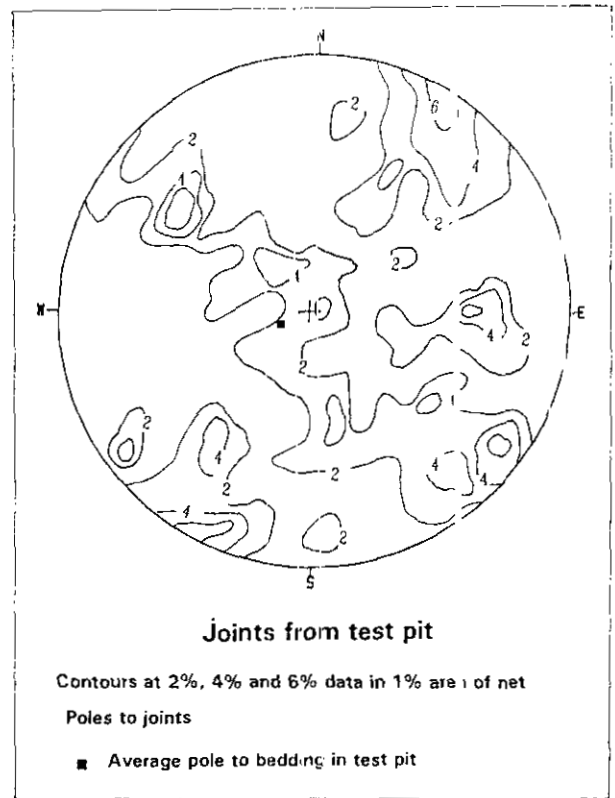


Figure 13: 46 bedding measurements and 198 joints from the test pit east of Goathorne Creek

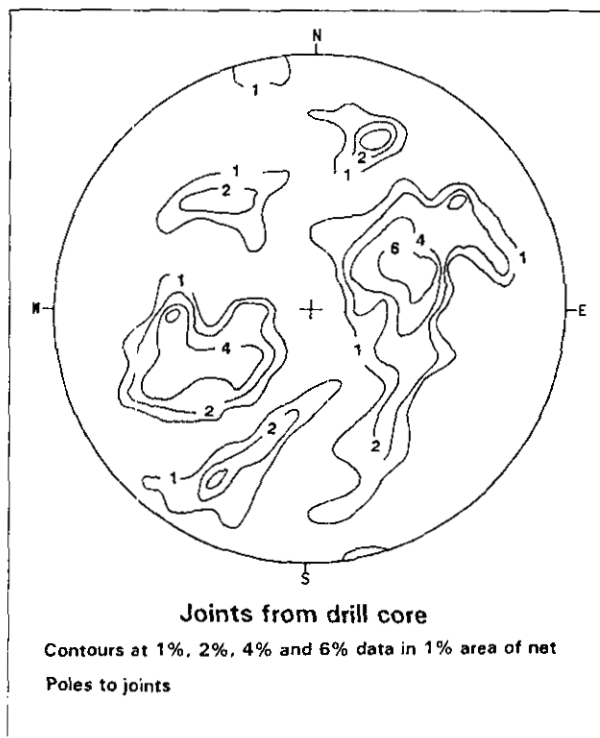


Figure 14: Joint sets from 22 diamond-drill holes

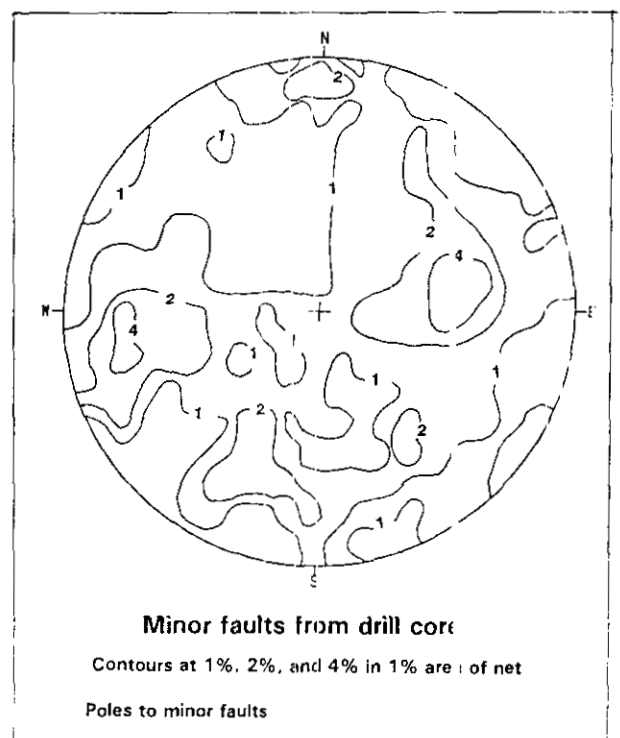


Figure 15: Minor faults from 16 diamond-drill holes

millidarcies is considered to be the minimum required for an economic well (Yee *et al.*, 1992)

The permeability of sections of mudstone, siltstone and sandstone interburden varying in thickness from 14 to 27 metres was measured in drill holes north of the Telkwa River. Permeabilities range from 13 to 35 millidarcies. At the depths of less than 200 metres permeabilities of interburden rock and coal are moderate. The permeability of the interburden is on average greater than that of the coal. In order to be able to drain water from the seams it will be important to have impermeable hangingwall and footwall material. This information is available in the core descriptions and geophysical logs included in the assessment reports submitted to the provincial government.

TABLE 8  
PERMEABILITY TEST RESULTS

HOLE	LOCATION		METRES
	Easting	Northing	Elevation
DR255	6.00E+05	6.00E+06	802
DR256	6.00E+05	6.00E+06	890
DR257	6.00E+05	6.00E+06	729
DR258	6.00E+05	6.00E+06	747
DR604A	6.00E+05	6.00E+06	813
DR905S	6.00E+05	6.00E+06	803
DR905D	6.00E+05	6.00E+06	803
DR906A	6.00E+05	6.00E+06	806
DR913	6.00E+05	6.00E+06	923

HOLE	DRILL SECTION	TEST	HEAD	ROCK OR SM	MILLI DARCIES
DR255	91.7-93.9	PACKER	NA	COAL S8	50
DR255	107.9-110.3	PACKER	NA	SMS8	60
DR255	114.9-121.0	PACKER	NA	SM S6	2
DR255	138.4-139.9	PIEZO	138M	SMS3	3
DR256	157.9-159.4	PIEZO	158M	SL	1
DR257	28.8-31.1	PIEZO	27.6M	SM S2	3
DR258	44.5-46.3	PIEZO	44M	SM S7	1
DR258	45.7-48.0	PACKER	NA	SM S7	6
DR258	50.6-52.9	PACKER	NA	SM S6	1
DR258	64.3-69.2	PACKER	NA	SM S5	2
DR258	114.9-121.0	PACKER	NA	SM S2L	2
DR604A	24.8-32.6	PIEZO	23.4M	MD+CL	24
DR905S	17.9-26.1	PIEZO	25.6M	SL+CL	NA
DR905D	48.9-58.3	PIEZO	24.4M	RK+CL	25
DR906A	55.2-67.7	PIEZO	26.5M	MD+CL	22
DR913	24.9-32.5	PIEZO	14.2M	SL+CL	13

Section = depth range in metres  
 Test = Packer test or piezometer  
 Head = height of water column above test zone in metres  
 Rock = Rock type or seam number  
 RK= rock, MD=mudstone, SL=siltstone, ST=sandstone, CL=coal

Permeability is strongly influenced by the regional geometry of folds, faults and cleats or joints. Outcrop is sparse but joints were measured in the test pit in the Goathorne Creek area. The pit which yielded over 5000 tonnes of coal for testing was mapped and 46 bedding and 198 joints measured (Figure 13). Beds dip 13° to the northeast and strike 157°. The joints tend to intersect bedding at large angles along a line of intersection trending northwest (fold-axis trend) or along a line

perpendicular to the fold-axis trend. This is a common geometry for tectonic joints.

Subsurface bed orientations are available from dipmeter logs measured during a number of exploration programs. Subsurface joint measurements were made in 1982 during a geotechnical program and the results reported in the Telkwa Stage 2 submission. Joints were measured in core by recording the joint surface to drill-core angle and the clockwise rotation around the circumference of the core of the joint surface dip-line from the bedding surface dip-line. The technique requires good core in which bedding surfaces and joint surfaces are both well developed. Using the dipmeter logs to provide an average true orientation of the bedding for the hole, it is possible to rotate the joints into their "true orientation" using astereonet. The technique is approximate because only a single average bed orientation is used to rotate all the joints in a hole.

Measurements of joints from 22 holes were tabulated and the four best-developed joint concentrations identified for each hole. These concentrations were ranked (1 to 4) based upon degree of development and then plotted separately on astereonet and the distribution analyzed. There was no difference in the plots of the first ranking through to the fourth ranking joint

TABLE 9  
MEAN UNIAXIAL COMPRESSIVE STRENGTHS  
FROM POINT LOAD TESTS

LITHOLOGY	FORM/FAILURE	COUNT	STRENGTH (MPa)
COAL	massive	2	14
	joints/bedding	12	2
SILTSTONE	massive	15	50
	bedding or joints	60	7
SILTY	massive	9	16
MUDSTONE	bedded	15	2
TUFFACEOUS	massive	3	35
MUDSTONE	bedded	9	6
COALY	massive	3	7
MUDSTONE	bedded	5	2
SANDSTONE	massive	11	65
	bedded	22	13

MPa = megapascals (1 MPa = 145 psia)

concentrations. All the concentrations are contoured on Figure 14.

A vertical hole will not intersect a vertical joint and the frequency of intersection of a joint set increases as the dip of the joint set decreases. This means that the data plotted on Figure 14 are not representative of the true joint frequency; despite this, it appears that the joints tend to form a great circle girdle about the northwest-trending fold direction. Eigen vectors provide a pole to the great circle girdle trending 316° with a plunge of 1°. This means that the joints intersect the bedding surface along a line parallel to the northwest-trending foldaxis.

A similar stereonet plot was made for 218 minor faults identified in sixteen drill holes (Figure 15). The

pattern is more dispersed but a southwest to northeast girdle is still discernible. The pole to the girdle trends 331° with a plunge of 3°.

Based on the joint data from surface and drill holes and the minor fault data from drill holes, it is probable that the face cleats in the coal seams strike northwest and dip steeply east or west. The surface joint pattern identifies a northeast-trending joint set which is perpendicular to the fold trend. This may be the orientation of butt cleats in the coal.

Permeability will be improved in a direction trending 315° to 360° (face cleats) and probably to a lesser extent in a direction trending 30° to 60° (butt cleats). Generally permeability in the direction of the face cleats is three times better than in the direction of the butt cleats.

Faults mapped in the test pit are generally tight and will block the flow of methane along the seam but probably will also not discharge much water into the coal seam reservoir as it is drained. The area in each coal seam available to be drained will be limited in a northeast to southwest direction, but may extend farther in a northwest-southeast direction because of the improved permeability and the absence of crosscutting faults.

The presence of joints or cleats does not guarantee good permeability. The coal must have sufficient strength to resist overburden stresses and maintain some porosity along the joint surfaces. Generally coal is not as strong as the surrounding rock and it is more difficult to maintain interconnected pathways along the joint surfaces.

The Klohn Leonof report contains data on the uniaxial compressive strength of rock types used in an assessment of ripability of rocks east of Goathorne Creek (Table 9). The coal is as strong as the mudstone and weaker than other rock types. Compared to many coals from other areas in British Columbia, Telkwa coal is strong. This is substantiated by the Hardgrove index of Telkwa coal which ranges from 45 to 65 compared to values on coal from southeast of the province that range from 80 to 110. Hardgrove index is a measure of the friability of coal. It is probably also a measure of coal's ability to resist compaction pressure (overburden pressure minus hydrostatic pressure). A coal with a low HGI is more likely to withstand overburden pressure and maintain joint sets with an interconnected permeability than a friable coal.

Hardgrove index data exist for many seams in the major coalfields in British Columbia. The data may be very useful in provisionally screening coal seams for their potential regional permeability.

## GROUNDWATER CHEMISTRY

Coalbed methane wells usually produce formation water before and during methane production. The water can be pumped back into formations or disposed of on the surface, either in evaporation ponds or directly into rivers. The last method of disposal is the cheapest but is permitted only if the formation water meets certain standards.

Water samples were taken from the piezometers in holes 604A, 905S, 905D, 906A and 913 described in Table 8. The samples are from formation intervals that include coal and other rock types. The water is soft with carbonate loadings ranging from 6.4 to 52.3 milligrams per litre (with one exception of 86.8). Total filterable residue concentrations range from 397 to 1045 milligrams per litre. The accepted concentration for drinking water is 500 milligrams per litre. Concentrations of iron, sulphate, chlorine and fluoride are all within drinking water standards. Based on these data it appears that formation water can be disposed of into existing rivers via a series of settling ponds.

## POTENTIAL METHANE RESERVES

Two important points must be made before any discussion of potential CBM reserves in the Telkwa coalfield can proceed. Firstly, in a ranking of potential CBM targets in British Columbia Telkwa would not rank high. At present there appear to be much better prospects in the southeast and northeast of the province. Secondly, any plan to develop the CBM potential at Telkwa must come to terms with any ongoing surface coal mining operations.

Cech *et al.* (1992) model the economics of hypothetical wells recovering from 50 to 160 million cubic metres of gas. These wells were projected to depths in excess of 600 metres. Any well at Telkwa would be considerably shallower. To put these numbers in perspective, an area of 1 square kilometre (100 hectares) underlain by 10 metres of coal with a gas content of 5 cubic metres per tonne contains 50 million cubic metres of gas. In the Telkwa coalfield unit 3 contains the most coal, with cumulative thicknesses averaging 9.6 metres, but this unit is generally shallow. The deeper unit 1 contains 4.3 metres of coal on average but is 100 to 200 metres below unit 3. There is a trade-off between 4.3 metres of deeper coal with higher gas contents and 9.6 metres of shallower coal with lower gas contents. Seam 1 in unit 1 generally has higher ash and is more difficult to wash than seams in unit 3. Some data appear to indicate that finely disseminated ash can damage the

adsorption ability of coal. Consequently there is some concern that the gas contents of seam 1 in unit 1 may be lower than expected.

Permeability in the coal seams is average. In this case a well has a better chance of being economic if it extracts methane from numerous seams over a small surface area than if it extracts gas from fewer coal seams over a larger surface area. The piezometer data indicate that the coal seams are not under pressured. The water level in the piezometers in most cases was at or close to ground surface. Shallow coal seams are therefore likely to have retained the expected amount of gas based on depth and rank.

A number of potential targets are located on Figure 3 by letter. The synclinal remnants of unit 1 in the south (areas A, B and C) each may contain sufficient gas to support one to three wells. The wells would target a projected 4 to 5 metres of coal with a  $R_{\max}$  value 2.0% or higher.

The area east of Goathorne Creek is being studied for its open-pit potential. Unit 3 coal may be open-pit mined but wells could still recover methane from unit 1 coal which is 100 to 150 metres below unit 3. Unit 3 dips eastward east of areas presently proposed for open-pit mining and could contain sufficient methane for a single well in area D (Figure 3).

Coal has been mined underground at Telkwa since the 1900s. The mines were small room-and-pillar operations mining down the full dip of the seams. The underground workings located on Figure 6 are probably now flooded but there is some chance that they have been sealed by caving and now act as gas reservoirs.

The potential CBM resource in the Telkwa coalfield is 3.7 billion cubic metres. If only five wells are developed for a total recoverable gas of 0.25 billion cubic metres over 10 years, this is sufficient gas to meet the heating requirements for over 10 000 houses in the area.

The Pacific Northern Gas Limited natural gas pipeline crosses the Telkwa coalfield south of Telkwa. This pipeline connects Prince Rupert and Kitimat with pipelines from northeast and southwest British Columbia. It is unlikely that it would be economic to build the infrastructure to collect and compress Telkwa gas prior to putting it into the provincial pipeline network.

## CONCLUSIONS

Five desorption results indicate that coal in the Telkwa coalfield retains methane at shallow depths. Four of the five samples collected over a depth range of 64 to 120 metres have gas contents that range from 3.75 to 4.49 cubic centimetres per gram on a dry ash-free basis. Most of the samples appear to be saturated based on the results of adsorption isotherms. The maximum

adsorption capacity of Telkwa coal appears to be less than that predicted by models based on vitrinite-rich U.S. coals by an amount of 16% or more.

The Telkwa coalfield contains a potential coal resource of 862 million tonnes. The rank of this coal varies from high-volatile A bituminous to semi-anthracite.

An assessment of the CBM potential requires information on the coal distribution, coal rank and on gas content. Recent work provides a good database of information on the geology and rank distribution.

In the Goathorne Creek area cumulative coal thicknesses intersected in unit 3 range from 6.4 to 14.3 metres and average 9.6 metres. The coal thickness in unit 1 ranges from 2.8 to 7.7 metres and averages 4.3 metres.

The  $R_{\max}$  values of seam 2 at the base of unit 3 range from 0.859 to 0.946% and average 0.905%. Values for seam 1 range from 0.855 to 1.11% and average 0.954%.

The CBM resource is estimated at 3.7 billion cubic metres. This is small in comparison to the possible resources elsewhere in the province. Much of the resource may be contained in thin seams, with low gas contents and at shallow depths, making it difficult to recover the gas economically. Despite this, there are areas which appear to be favourable for wells. If there are only five successful wells recovering 250 million cubic metres over 10 years, they could provide sufficient gas to meet the energy requirements for over 10 000 houses.

Drilling wells in the Telkwa coalfield, especially south of the Telkwa River, will be cheap if the proposed open-pit mine is developed, because of the established infrastructure.

## ACKNOWLEDGMENTS

Manalta Coal Limited provided the samples for desorption tests. The adsorption isotherms were measured by John Clow of Western Core Laboratories Limited, Calgary.

## REFERENCES

- Bustin, R.M., Cameron, A.R., Grieve, D.A. and Kalkreuth, W.D. (1983): Coal Petrology, Its Principles, Methods, and Applications; *Geological Association of Canada*, Short Course Notes, Volume 3.
- Cech, R., Carlson, J.D. and MacLeod, R.K. (1992): Economics of Coalbed Methane Projects in the Western Canadian Basin; *Canadian Coal and Coalbed Methane Geoscience Forum*, Proceedings, pages 39-55.

- Crownsnest Resources Limited (1984): Telkwa Stage 2 Submission; submitted to the *B.C. Ministry of Energy, Mines and Petroleum Resources*.
- Eddy, G.E., Rightmire, C.T. and Byren, C.W. (1982): Relationship of Methane Content of Coal Rank and Depth: Theoretical vs. Observed; *Society of Petroleum Engineers, Department of the Interior, Proceedings of the Unconventional Gas Recovery Symposium*, Pittsburg, Pennsylvania, SPE/DOE 10800, pages 117-122.
- Ellard, J. and Roark, R. (1992): Coalbed Methane Production from the Pottsville Formation at Cedar Cove Field, Black Warrior Basin, Alabama, U.S.A., *Canadian Coal and Coalbed Methane Geoscience Forum*, Proceedings, pages 73-84.
- Environmental Protection Agency (1988): GEOEAS; Geostatistical Environmental Assessment Software; *U.S. Environmental Protection Agency, Environmental Monitoring Systems Laboratory*, Las Vegas, Nevada.
- Environmental Sciences Limited (1990): QUIKMAP; *ESL Environmental Sciences Limited*, Sidney, B.C.
- Johnson, D.G.S. and Smith, L.A. (1991): Coalbed Methane in Southeast British Columbia; *B.C. Ministry of Energy, Mines and Petroleum Resources*, Petroleum Geology, Special Paper 1991-1.
- Kim, A.G. (1977): Estimating Methane Content of Bituminous Coalbeds from Adsorption Data; *U.S. Bureau of Mines*, Report of Investigations, Number 8245.
- Koo, J. (1983): The Telkwa, Red Rose and Klappan Coal Measures in Northwestern British Columbia; in *Geological Fieldwork 1983, B.C. Ministry of Energy, Mines and Petroleum Resources*, Paper 1984-1 pages 81-90.
- Lamberson, M.N. and Bustin, R.M. (1992): Coalbed Methane Characteristics of the Gates Formation Lithotypes, Northeastern British Columbia; *The Canadian Coal and Coalbed Methane Forum*, Proceedings, pages 87-101.
- Langmuir, L. (1918): The Adsorption of Gases on Plane Surfaces of Glass, Mica and Platinum; *Journal of the American Chemical Society*, Volume 40, pages 1361-1402.
- McCartney, J.T. and Ergun, S. (1967): Optical Properties of Coals and Graphite; *U.S. Bureau of Mines United States Department of the Interior*, Bulletin 641.
- MacIntyre, D., Desjardins, P., Tercier, P. and Koo, J. (1989): Geology of the Telkwa River Area NTS 93L/11; *B.C. Ministry of Energy, Mines and Petroleum Resources*, Open File 1989-16.
- Matheson, A. and Van Den Bussche, B. (1990): Subsurface Coal Sampling Survey; Central British Columbia; in *Geological Fieldwork 1989, B.C. Ministry of Energy, Mines and Petroleum Resources*, Paper 1990-1, pages 445-448.
- McCulloch, C.M., Levine, J.R., Kissell, F.N. and Duel, M. (1975): *Measuring the Methane Content of Bituminous Coalbeds*; *U.S. Bureau of Mines*, Report of Investigations 8043.
- Meissener, F.F. (1984): Cretaceous and Lower Tertiary Coals as Sources for Gas Accumulations in the Rocky Mountain Area; in *Hydrocarbon Source Rocks of the Greater Rocky Mountain Region*, Woodward J., Meissener F.F. and Clayton, J.L., Editors, *Rocky Mountain Association of Geologists*, 1984 Symposium, pages 401-431.
- Olszewicki, A.J. and Schraufnagel, R.A. (1992): Development of Formation Evaluation Technology for Coalbed Methane Development; *Quarterly Review of Methane from Coal Seams Technology*, Volume 10, No. 2, pages 27-35.
- Palsgrove, R.J. and Bustin, R.M. (1989): Stratigraphy and Sedimentology of the Lower Skeena Group, Telkwa Coalfield, Central British Columbia (93L/11); in *Geological Fieldwork 1989, B.C. Ministry of Energy, Mines and Petroleum Resources*, Paper 1990-1 pages 449-454.
- Rees, O.W. (1966): Chemistry, Uses and Limitations of Coal Analyses; *Illinois State Geological Survey*, Report INV 220, page 55.
- Ryan, B.D. (1991): Density of Coals from the Telkwa Coal Property, Northwestern British Columbia; (93L/11); in *Geological Fieldwork 1990, B.C. Ministry of Energy, Mines and Petroleum Resources*, Paper 1991-1 pages 399-406.
- Ryan, B.D. (1992a): Coal Rank Variations in the Telkwa Coalfield, Central British Columbia (93L/11); in *Geological Fieldwork 1991*, Grant, B. and Newell, J.M., Editors, *B.C. Ministry of Energy, Mines and Petroleum Resources*, Paper 1992-1, pages 451-460.
- Ryan, B.D. (1992b): An Equation for Estimation of Maximum Coalbed-Methane Resource Potential; in *Geological Fieldwork 1991*, Grant, B. and Newell, J.M., Editors, *B.C. Ministry of Energy, Mines and Petroleum Resources*, Paper 1992-1, pages 393-396.
- Ryan, B.D. (1993): Geology of the Telkwa Coalfield, British Columbia; *B.C. Ministry of Energy, Mines and Petroleum Resources*, Open File 1993-21.
- Slaghuis, J.H., Ferreira, L.C. and Judd, M.R. (1990): Volatile Matter in Coal: Effect of Inherent Mineral Matter; *Fuel*, Volume 70, pages 468-470.
- Stevens, S.H., Kelso, B.S., Lombardi, T.E. and Coates, J.M. (1993): Raton Basin, Assessment of Coalbed Methane Resources; *Quarterly Review of Methane from Coal Seams Technology*, Volume 10, No. 3 pages 7-13.
- Tipper, H.W. (1976): Smithers Map Area 93L; *Geological Survey of Canada*, Open File Map 351.
- Yee, D., Seidle, J.P. and Hanson, W.B. (1992): Gas Adsorption on Coal; Abstract, *American Association of Petroleum Geologists*, Annual Meeting, Calgary, 1992.

## NOTES



## COALBED METHANE CANISTER DESORPTION TECHNIQUES

By **B.D. Ryan, British Columbia Geological Survey Branch.**

and

**F.M. Dawson, Institute of Sedimentary and Petroleum Geology.**

**KEYWORDS:** Methane desorption, lost-gas corrections, dead-space corrections, moisture corrections, desorption curve fitting, diffusion constants, Quinsam mine.

### INTRODUCTION

The British Columbia Geological Survey Branch and the Geological Survey of Canada have initiated a joint project to assess the coalbed-methane potential of coal deposits in British Columbia. This project entails participation with private industry to obtain fresh coal samples for desorption from exploration projects throughout the province. Samples are collected from the drill site and undergo a series of desorption measurements that allow an assessment of the *in situ* coalbed methane (CBM) content.

There is a great deal of interest in documenting and exploiting the CBM resource of western Canada both by government agencies and industry. Much of the work involves desorption tests of fresh coal recovered from drill holes. Data from the desorption tests are used to generate resource values that are the starting point for an appraisal of the CBM economic potential of an area. The tests measure the amount of methane released from a coal sample and therefore represent a point estimate of the CBM resource.

The coal sample to be desorbed is sealed in a canister and the incremental desorbed gas is bled off and measured over time. A cumulative gas volume is calculated from the incremental data. In general the procedure is simple and fairly well standardized. There are, however, a number of corrections that must be applied to the measurements and it is not always clear in the literature if they are uniformly applied.

This paper outlines some of the methodologies adopted by the authors for data collection. The paper also presents desorption data from drill-core samples collected from the Quinsam coal mine, 20 kilometres

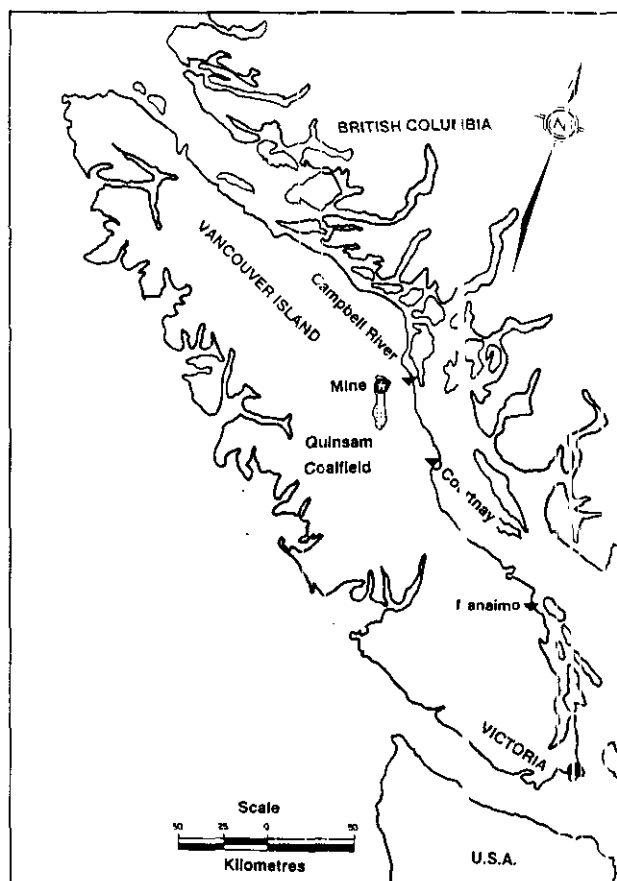


Figure 1: Location map for the Quinsam coal mine on Vancouver Island, British Columbia.

west of the town of Campbell River on Vancouver Island (Figure 1). The data are used to illustrate in more detail the various correction factors that must be applied to the measured data to derive true total desorbed gas contents.

The Quinsam mine has been in operation since 1987, initially as a small surface mine and now as a combined surface and underground operation. It mines high-volatile C bituminous coal for export as a thermal coal. The coal seams are in the Comox Formation of the Upper Cretaceous Nanaimo Group (Kenyon, *et al.*, 1971).

Four seams outcrop in the coal-bearing section. Most of the reserves are in the lowermost seam 1 which averages 2.3 metres in thickness and is mined underground and in surface pits. The overlying seam 2 ranges from 0.30 to 0.55 metre in thickness and is mined at surface only. Seam 3 ranges from 2.4 to 3.4 metres thick and is mined at surface. Seam 4 is thin and is not mined. The stratigraphic separation of seams 1 and 3 is 30 to 60 metres.

Two holes were drilled in 1992 for CBM testing. The first hole (92-34) intersected seam 3 at 141.5 metres and the second hole (92-46) intersected seam 1 at 108.5 metres. Five samples from seam 3 and four samples from seam 1 were desorbed, initially at the mine site and then in Victoria.

## FIELD PROCEDURES

The direct method of measuring methane desorbed from coal samples was first described by Bertard *et al.* (1970) and was later adapted by Kissell *et al.* (1973) and Diamond and Levine (1981). The method requires a fresh coal sample to be sealed in a canister. At measured time intervals the gas desorbing into the empty space in the sample canister is released into a manometer and the volume measured at ambient temperature and pressure. The canister is resealed and more gas allowed to desorb. A series of measurements that may span months provides data for a gas desorption *versus* time plot and an estimate of the total desorbed gas in the coal. Samples are usually drill core or drill chips. Both types of samples can be used for gas content determination, although the collection techniques are different.

## CORE SAMPLE COLLECTION

Core samples provide the best samples for desorption testing. In order to determine the volume of gas lost prior to sealing the sample in the canister it is important to record five critical times:

- Time of intersection of coal seam with core bit.
- Time of completion of coring of coal seam.
- Time of tripping off bottom of borehole with core barrel.
- Time of core barrel reaching surface.
- Time of coal being sealed in canister.

These times are used in the various procedures for correcting for the lost gas. Details of these correction procedures are presented later in the paper.

When the core is brought to surface the depth of the coal sample should be accurately determined using geophysical logs, core descriptions and driller's logs.

Before putting the core into canisters, broken and fractured core should be reconstructed to represent as best as possible the true core length. The core is striped using a felt marker to provide a record of core piece position. A lithological description of the core is quickly completed to determine sample intervals and to delineate obvious rock partings.

A problem often associated with core samples from conventional oil and gas drilling rigs is the long trip time, which may be up to 2 to 3 hours, required to bring the core barrel to surface. In some coals with fast diffusion rates the lost gas may equal or exceed the cumulative amount of gas desorbed into the canister. Wireline drilling allows the core to be brought to surface much quicker and decreases the impact of the lost-gas correction on the total desorbed gas measurement. Field programs in western Canada using wireline systems have yielded trip times of less than 10 minutes for depths of 600 metres.

## CHIP SAMPLE COLLECTION

Chip samples can be used for CBM testing when core samples are not available. This may be because the borehole is being drilled to test a deep conventional hydrocarbon target and coal core samples from shallow horizons are not required. The collection of the chips does not incur additional drilling cost and can provide information about the CBM potential of the seams penetrated by the borehole.

It is difficult to obtain representative chip samples. Chip samples are often contaminated with extraneous non-coal material which can increase as-received ash contents to over 45%. Unrepresentative and high ash contents will lower the measured gas contents. Even when the data are corrected to the accepted *in situ* ash content the gas contents may be too low. This is because inherent ash often appears to decrease gas contents more than would be expected based on dilution effect.

Extraneous rock material can be removed from the sample by floating it in a 1.6 S.G. liquid. The sample can then be air-dried and weighed to determine the true sample weight that theoretically provided the methane gas measured during desorption. This correction takes into account the extraneous non-coal diluant material but it assumes that no material with a specific gravity greater than 1.6 contributed methane to the total gas content of the sample. Current work by the authors addresses the adsorptive capability of coal and coaly material at differing specific gravities, to determine a specific gravity threshold that may be used for chip samples.

Another problem associated with chip samples is the small and variable grain size of the sample. Drilling

processes often produce chip samples that are less than 20 mesh in size. In order to collect a representative sample all the coaly material, including the fine particles, must be collected. The fine particles are often held in suspension in the drilling fluids and do not arrive at the surface at the same time as the chips. Collection of drilling fluids and the suspended fine-coal produces a sample with a high water content. Excess water in the sample tends to inhibit the desorption process.

Corrections for "as-received" sample weight versus "air-dried" sample weight can be made to correct for the excess moisture, but the significance of the presence of excessive amounts of water in the canister on the desorption rates and overall desorption volumes has yet to be quantified. Because chip samples as collected may contain excess water, it is critical that an accurate air-dried weight is obtained after desorption by carefully removing all the sample from the canister.

Determination of sample depth for chip samples is often difficult. Although the depth of penetration of the coal seam can usually be determined accurately using drilling breaks or marker horizons, the actual source of the coal chips may be unknown. If parts of the coal seam are friable or sheared, then these parts may cave into the hole increasing the proportion of coal collected from the intervals, consequently the sample may not be representative of the whole seam. Similarly, if multiple seams are drilled, caving from upper seams can contaminate lower seam samples. These effects can be minimized by drilling fixed short intervals and cleaning the hole of cuttings between each interval. These techniques have been successful in ensuring less contamination of the sample recovered from the shale shaker. Selecting the proper drill bit to maximize the chip size may improve the grain size of the sample but the cost of tripping in and out of the hole to change bits may be costly.

### **DATA COLLECTION TIME INTERVALS**

It is important to make sufficient measurements in the early stages of desorption in the canister in order to accurately determine lost-gas volumes and to define the shape of the desorption curve. The optimum time increments used by the authors to measure desorbed gas are:

- Initially every 2 minutes for the first 30 minutes;
- every 5 minutes from 30 to 60 minutes;
- every 10 minutes from 60 to 120 minutes;
- every 30 minutes from 120 to 360 minutes;
- every 60 minutes from 360 to 720 minutes;
- further times are defined by desorption rate.

These measurement increments are defined for coals from the Mist Mountain Formation, which have high

diffusion rates. For coals from other formations the time increments may be adjusted to reflect the amount of gas being desorbed; *i.e.* if less than 10 cubic centimetres of gas are desorbed for any time increment, the interval between readings can be lengthened.

### **DATA PROCESSING**

There are a number of important corrections and estimations that have to be made during and after data collection in order to estimate the true amount of gas desorbed from the coal.

### **LOST-GAS CORRECTION**

The first correction estimates the amount of gas that escapes from the coal sample by desorption prior to sealing it in the canister. Generally samples are freshly drilled core or chips that are placed in the canister as soon as they reach surface. Unfortunately some gas desorbs from the coal as it is brought up the hole and more desorbs at surface before it is sealed.

There is also gas in the macroporosity and fractures in the coal. This is the free gas component which exists either as a gas or as gas in solution in water. Free gas is compressed by an amount dependent on the hydrostatic pressure in the coal seam. The amount of gas in solution increases with pressure but the solubility of methane in water is generally low. The volume of free gas at surface can be estimated using the universal gas law. Free gas is released into the drilling fluid as the pressure decreases. It is usually a minor component of the total gas. Rightmire (1984) provides some data referred to as free-gas estimates that range from 5 to 17% of the total gas in the samples. Generally the amount of free gas, which will increase with hydrostatic pressure and void porosity and decrease with increasing temperature, can only be estimated from production wells. If the gas-filled porosity is 2% then at 1000 metres the free gas is about 1 cubic centimetre per gram.

There is an important distinction between free gas and lost gas. Lost gas is estimated using desorption theory applied to desorption data measured on the coal after it is placed in the canister. Measurements of lost gas may be influenced by the amount of free gas in the *in situ* coal but generally they do not include an estimate of the amount of free gas. The presence of evolving free gas in the coal as it is brought to surface will have minimal effect on the pressure acting on the coal. It will therefore have minimal effect on the desorption that is also occurring as the coal is brought to surface

Diamond and Levine (1981) provide an empirical method for estimating the amount of lost gas, now generally referred to as the U.S. Bureau of Mines method. They plot the square-root of time ( $X$  axis) against cumulative gas desorbed ( $Y$  axis) for the first few measurements. The data usually plot on a straight line, implying that a linear projection backward in time for the appropriate time prior to sealing the sample (lost time) will provide an estimate of the lost gas. This method is most applicable for short holes recovering core samples that tend to desorb more slowly than chip samples. In this situation the lost time is generally less than 30 minutes and the lost gas makes up a small percentage of the total desorbed gas volume (<20%).

It is an assumption of the U.S. Bureau of Mines method that the desorption behavior of the coal is similar before and after sealing it in the canister. This may be true for the period, "coal at surface to coal in canister", but is unlikely to be true for the period, "coal cut by drill bit to coal reaching surface".

A more complicated method of measuring the lost gas was introduced by Smith and Williams (1984). They used the unipore diffusion model originally derived by Wheeler (1951), which is applicable to the early stages of desorption, and adapted it to take account of a range of depths (pressures). This model predicts that for the initial stages of desorption the gas desorbed is proportional to the square-root of time. Obviously the unipore model is assumed to apply in the U.S. Bureau of Mines method though it is not emphasized in its reports. Smith and Williams integrate the unipore model over the range of decreasing pressures affecting the sample as it comes up the hole. They do not consider the effect of the temperature change that the coal experiences as it is brought from *in situ* temperature to surface temperature.

The final calculation of lost gas is made with the help of graphs that use the total lost time and the time at surface prior to sealing as components. It should be understood that if the data do not plot on a straight line on a cumulative "gas" *versus* "square-root time" plot then the unipore model is not describing the desorption process and neither the U.S. Bureau of Mines nor the Smith and Williams method is likely to give an accurate estimate of the lost gas. Even if the data obtained after the coal is sealed in the canister plot on a straight line, indicating that desorption in the canister can be modelled by the unipore model, this still does not mean that diffusion before entering the canister obeyed the unipore model.

The Smith and Williams and U.S. Bureau of Mines methods both appear to under-estimate the amount of lost gas based on laboratory experiments (Olszewicki and McLennan, 1992). The Smith and Williams method provided the best predictions, but the predicted lost-gas values had to be multiplied by factors ranging from 1.2 to 1.7 to bring them up to the actual lost-gas values.

Desorption is faster at higher temperatures, therefore a sample that cools as it is brought to surface will lose less gas than one that arrives at surface without cooling. Neither of the two lost-gas estimation methods considers varying temperatures and it is not clear if varying temperature will cause them to over or under-predict the amount of lost gas.

Once the sample is in the canister it should be desorbed at reservoir temperature to simulate the conditions of a production well. This means keeping the canister in a temperature controlled box which may be difficult if the canisters have to be moved sometime during the weeks or months that they take to desorb.

In general it appears that any lost-gas measurement is an under-estimation of the sum of the gas desorbed from the sample and free gas lost from the macroporosity in the sample prior to sealing it in the canister.

The cumulative gas values used for predicting the lost-gas component should be corrected back to standard temperature and pressure conditions (STP) as described in a subsequent section. This may not be as simple as it seems for the first few measurements. If the canister is moved from the drill site to a base camp then there may be significant changes in temperature and pressure. The interior of the canister equilibrates to atmospheric pressure quickly once the canister is opened for a measurement. The same is not true for temperature. It may take tens of minutes before the temperature of the coal in the canister and of the gas bled from the canister are the same as room temperature (or heat controlled box temperature), which is the temperature recorded. Yet measurements are being made at intervals of a few minutes. Ideally the manometer used to measure the gas and the canister should be at the same temperature, otherwise it is difficult to report a true gas volume at STP.

Desorption is an endothermic process which will cool the coal below ambient temperature. When the methane is released into the manometer it expands adiabatically, causing a further drop in temperature. For samples containing a lot of gas desorbing into a canister with very little empty space, care should be taken to ensure that the methane volume released into the manometer is at ambient temperature. In some cases non-linear lost-gas plots may be the result of inappropriate temperature corrections to the initial measurements and not problems with the diffusion model.

Preliminary checks appear to indicate that the internal temperature of the Quinsam coal sample canisters equilibrated quite quickly with the external temperature. The samples were recovered from shallow depth where the rock temperature is probably less than 25°C. For this reason the canisters were not put in a temperature controlled box. The lost-gas corrections for the Quinsam coal samples were calculated using the U.S.

TABLE 1  
QUINSAM DATA LOST-GAS CALCULATION AND DESORPTION CURVE-FITTING CONSTANTS

Sample	Initial desorption		Lg(Na)		DX10 <sup>-4</sup>		desorption curve		T(.5)
	To	Na	Lg(Na)	Lg(2)	To	Na	R <sup>2</sup>		
92-34-2	48	2.4	156	126	66	2.1	2.0	0.85	11.3
92-34-3	82	3.2	163	132	19	5.3	1.9	0.92	29.8
92-34-4	67	3.2	207	132	21	3.4	2.0	0.95	25.2
92-34-5	65	2.0	176	126	14	6.1	2.0	0.94	30.3
92-34-6	23	4.0	641	N/A	610	7	2.3	0.87	1.7
92-46-1	58	1.3	61	88	2	145	1.9	0.73	82.3
92-46-2	52	1.3	56	96	2	119	2.0	0.83	55.8
92-46-3	35	1.9	120	104	31	36	3.1	0.86	14.7
92-46-4	43	2.2	194	116	36	26	2.3	0.79	12.3

Initial desorption: constants To and Na calculated from linear TNa versus cumulated desorbed gas at STP plot for first few hours

Lg(2) = lost gas calculated using Na=2

T(.5) = total time in hours for half of the gas to be desorbed; calculated using desorption data.

Desorption curve: constants To and Na calculated by fitting Airey equation to desorption curve except for first two and last two points

Airey equation: is  $V = V_t \times (1 - \exp\{-T/To\}^{1/Na})$

derivation

$$\text{if } dV/dT = Vr \times \lambda$$

$$\text{where } \lambda = (A \times Tn)$$

Vr = gas remaining at time T where T is time in hours from cutting coal

$$\text{Then } \log_e((dV/dT)/Vr) = \log_e(A) + n \times \log_e(T)$$

intercept of line is  $\log_e(A)$  and slope is n

integration gives  $V = V_t \times (1 - \exp\{-(A/(1+n)) \times T^{(1+n)}\})$

Airey constants are calculated from  $Na = 1/(1 - \text{slope})$

$$To = ((1 + \text{slope}) / (2.718 \log_e(A)))^{Na}$$

Bureau of Mines and Smith and Williams methods applied to cumulative gas volumes corrected to STP.

Most of the data produce reasonably good linear plots of square-root time versus cumulative gas for the first 10 to 15 measurements extending over 2 to 4 hours.

The U.S. Bureau of Mines method predicted lost-gas values ranging from 88 to 132 cubic centimetres with one exception (Table 1). The drilling times used to calculate the lost time are reported in Table 2. Two estimates of lost time are possible for each sample. If the hole is dry then it is assumed that the gas starts to desorb as soon as the coal is cut. If the hole is filled with water then it is assumed that the gas starts to desorb when the core is half way up the hole.

Hole 92-34 was dry and the lost gas was estimated using the dry lost-time estimate (Table 2). Hole 92-46 was water filled and lost gas was estimated using the wet lost-time estimates (Table 2). For comparison purposes the lost-gas calculations for samples from hole 92-34 were made using both dry and wet lost-time estimates. The longer dry lost-time estimates increased the lost-gas calculation by about 15%.

All samples with the exception of 92-34-6 produced reasonably linear cumulative gas (STP) versus square-root time plots. To check the U.S. Bureau of Mines method more closely plots were made where the Y intercept is the projected lost gas and the X axis is the number of points used to define the line (Figures 2 and 3). All predictions started with the first three measurements and then incorporated additional measurements up to a maximum of fourteen. The plots illustrate that for samples 92-34-6 and 92-34-2, the lost-

gas prediction increases as the number of points decreases and for most other samples it decreases as the number of points decreases; only sample 92-34-4 seems to fit the unipore diffusion model closely.

TABLE 2  
QUINSAM SAMPLE COLLECTION DATA

HOLE	DATE	SEAM	METRES		ELEVATION
			EASTING	NORTHING	
H92-34	1/10/92	3	32-284	5532297	335
H92-46	16/10/92	1	32-854	5534322	317

HOLE	SEAM	TIMES		LOST TIME	T <sub>25%</sub>
		FROM-TO	CUT TRIP SURFACE SEAL		

HOLE 92-34 SEAM 3 SAMPLES 92-34-2 (TOP) TO 92-34-4 (BOTTOM)

141.9-142.3	14.46	14.50	14.51	14.57	11	4.13
142.3-142.7	14.46	14.50	14.51	14.58	12	8.92
142.7-143.1	14.46	14.50	14.51	14.59	13	8.48
143.1-143.5	14.46	14.50	14.51	14.00	14	8.93
145.3-145.7	15.02	14.09	14.11	14.15	13	0.98

HOLE 92-46 SEAM 1 SAMPLES 92-46-1 (TOP) TO 92-46-4 (BOTTOM)

108.5-108.9	14.57	15.01	15.02	15.10	13	7.16
109.4-109.8	14.57	15.01	15.02	15.08	11	15.2
111.5-111.9	14.09	15.14	15.15	15.19	10	3.95
111.9-112.3	14.09	15.14	15.15	15.20	11	3.75

LOST TIME DRY = Lost-time minutes assuming dry hole

LOST TIME WET = Lost-time minutes assuming water-filled hole

CUT TIME = Time (hours.minutes) drill cuts coal

TRIP TIME = Time (hours.minutes) core starts to surface

SURFACE TIME = Time (hours.minutes) coal reaches surface

SEAL TIME = Time (hours.minutes) sealed in canister

SMITH AND WILLIAMS TERMS

Ts = Cut time to seal time

Td = Cut time to surface time

T<sub>25%</sub> = Time from cut time to time for 25% desorption into canister

Note this is not time for 25% desorption because it does not

consider the lost-gas component

SURFACE-TIME RATIO = (Ts - Td) / Ts

LOST-TIME RATIO = Ts / T<sub>25%</sub>

The Smith and Williams method is difficult to apply when the lost time is short. The correction curves in Smith and Williams paper are linear at low values of lost-time ratio and the volume correction factor can be estimated from

$$VCF = (LTR) \times [(STR) \times .127 + .107]$$

where

VCF = volume correction factor

LTR = lost-time ratio

STR = surface-time ratio

These terms are defined in Table 2. In all cases Smith and Williams predicted very low lost-gas volumes.

Another approach to estimating the volume of lost gas is investigated in this paper. Airey (1958) fitted an empirical curve to desorption data. Feng and Lu (1981) fitted the Airey equation to desorption data from coal samples from southeast British Columbia and achieved a good fit. The equation proposed by Airey has the form;

$$V = V_t \times (1 - \exp\{-T/To\}^{1/Na})$$

where V is the gas desorbed up to time T, Vt is the total gas available for desorption, To is a constant with the units of time and Na is a dimensionless constant. This equation has the general form of a radioactive

exponential decay equation in which the decay constant is a time dependent term. Decay equations are based on the premise that the amount of daughter generated in any given time interval is proportional to the amount of parent remaining. The equivalent for desorption data is;

$$dV/dT = D \times V_r \text{ where } D \text{ is a desorption constant at time } T.$$

$dV/dT$  is incremental desorbed gas.

$V_r$  is gas remaining at time  $T$ .

If  $D = A \times T^n$  then a plot of

$\log_e[(V/dT)/(V_r)]$  versus  $\log_e(T)$  will provide a straight line having a slope ( $sl$ ) whose value is  $n$  and  $Y$  intercept ( $in$ ) whose value is  $\text{Log}(A)$ . This plot can be generated without knowing the lost-gas component because it requires only knowledge of the gas left to desorb.

Integration of  $dV/dT = A \times T^n \times V_r$  provides

$$V = V_t \times [(1 - \exp[-K \times T^{(1-n)}])] \text{ where } K = A/(1+n).$$

This is similar to the Airey equation but is developed in a way that makes it easier to derive the constants  $A$  and  $n$  which can easily be changed to the Airey constants,  $N_a$  and  $T_o$ .

$$N_a = 1/(1+sl) \text{ and } T_o = [(1+sl)/(2.718^{in})]^{N_a}$$

Figure 4 is a  $\log$  (time) versus  $\log [(dV/dT)/V_r]$  plot of data from sample 34-6 used to calculate the Airey constants  $T_o$  and  $N_a$ . The first and last two points were not used in the regression analysis. The constants derived from Figure 4 were used to fit the predicted desorption curve through the measured desorption data for sample 34-6 as illustrated by Figure 5.

Airey states that  $V_t$  is proportional to  $T^{1/N_a}$  for values of  $T$  much less than  $T_o$  ( $T \ll T_o$ ). The relationship is

$$V = V_t \times (T/T_o)^{1/N_a}$$

This is based on his empirical equation that fits desorption curves to data from experimental samples with no lost-gas component. The constant  $T_o$  is proportional to the square of particle size and inversely proportional to initial methane pressure (depth of burial) (Airey, 1968, Figure 3). Values of  $T_o$  in this paper are in the range from 7 to 145 hours (Table 1) and indicate effective particle sizes ranging from about 1 to 5 millimetres. Lost-gas projections are made over the first 7 hours or less to ensure that the condition of  $T \ll T_o$  is met.

The fact that  $V_t$  is proportional to  $T^{1/N_a}$  is important because it means that desorption data will plot on a straight line if the  $X$  axis is  $(\text{time})^{1/N_a}$ . The conventional procedure using the unipore model plots  $(\text{time})^{1/2}$  on the  $X$  axis for lost-gas estimates. Empirical data indicate

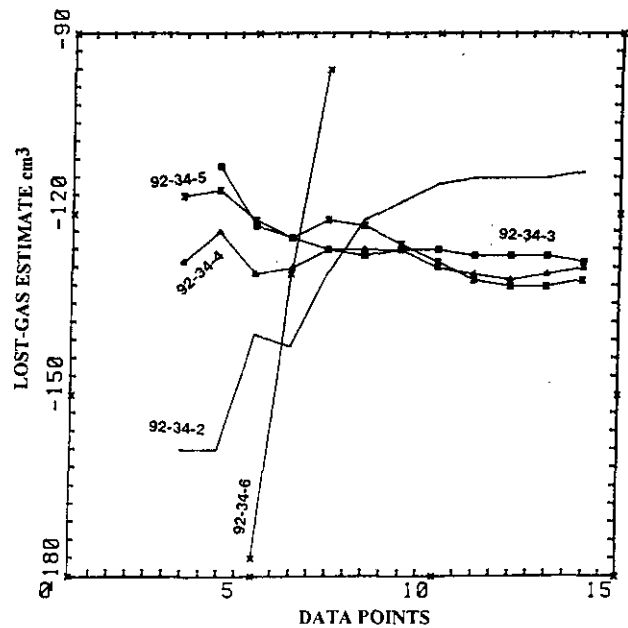


Figure 2: Lost-gas estimate versus number of data points, hole 92-34.

that the power term varies based on the coal. Airey found no relationship between  $N_a$  and size, moisture or initial pressure. In this study values of  $N_a$  range from 1.3 to 4 (Table 1) and in the study by Feng and Lu (1981)  $N_a$  values range from 2.4 to 2.8. Higher values of  $N_a$  seem to correlate with shearing and rapid initial desorption.

Figures 2 and 3 indicate that a value of 2 for  $N_a$  may not provide the best linear plot. It is easy to adjust values of  $N_a$  until the sample tracks in Figures 2 and 3 are horizontal. If the lost-gas predictions decrease as the number of points decreases then the value of  $N_a$  is less than 2 and if they increase as the number of points decreases then the value of  $N_a$  should be greater than 2. Values of  $N_a$  were calculated to achieve this are presented in Table 1 and new lost-gas estimates made. The values of  $T_o$  (Table 1) were then calculated using  $V_t$  (lost plus desorbed gas) and the slope of the line  $V$  versus  $T^{1/N_a}$ .

Using values of  $N_a$  greater than 2 increases the predicted amount of lost gas and could result in the lost-gas predictions of Olszewicki and McLennan (1992) agreeing more closely with their measured data. A change of  $N_a$  from 2 to 3 approximately doubles the lost-gas prediction.

Values of  $N_a$  and  $T_o$  can also be calculated using plots of  $\log(dV/V_r)$  versus  $\log(\text{time})$  which exclude the first and last few points. This method provides an easy way of checking the fit of the desorption data to an Airey equation.

For the Quinsam data the linear plots have  $R^2$  values ranging from 0.83 to 0.95 (Table 1). Values of  $N_a$  and  $T_o$  calculated by this method differ somewhat from

values calculated using the initial part of the desorption curve and  $V$  versus  $T^{1/N_a}$  plots. This may indicate that a single Airey equation cannot explain the complete desorption curve or that for this particular dataset, the composition of the gas is changing over time and different diffusion constants are coming into play.

An alternate method of predicting lost gas using the Airey equation was tried on the Quinsam data. This method attempts to use the shape of the mid-part of the desorption curve. The total desorbed gas ( $V_t$ ) is not known because it includes the lost gas but  $V_t$  can be calculated by using pairs of data points thus:

$$\begin{aligned} \text{point 1 } & V_1 + L_g = V_t \times (\exp^{-(T_1/T_0)^{1/N_a}}) \\ \text{point 2 } & V_2 + L_g = V_t \times (\exp^{-(T_2/T_0)^{1/N_a}}) \end{aligned}$$

where  $L_g$  is the unknown lost-gas component. Subtracting gives:

$$V_t = (V_2 - V_1) / (\exp^{-(T_1/T_0)^{1/N_a}} - \exp^{-(T_2/T_0)^{1/N_a}})$$

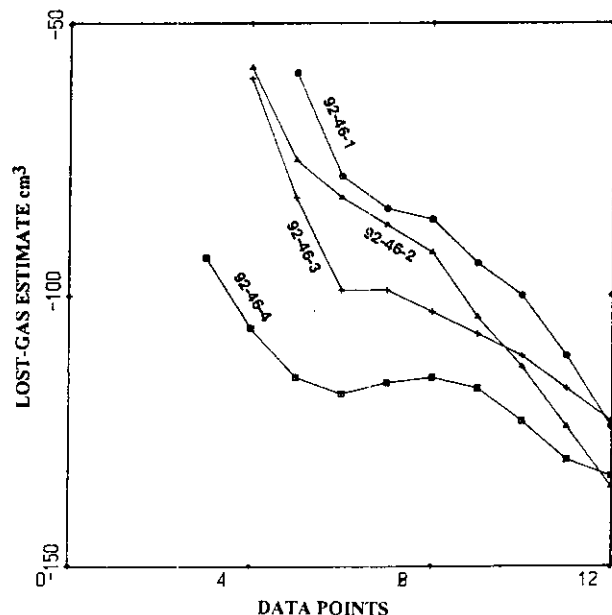


Figure 3: Lost-gas estimate *versus* number of data points, hole 92-46.

Numerous data pairs can be used to calculate values of  $V_t$  and the results averaged. The values of  $T_0$  and  $N_a$  are determined from a  $\log_e((dV/dT)/(V_t))$  *versus*  $\log_e(T)$  plot. This approach provides an averaged estimation of the total gas desorbed based on the shape of the desorption curve and the amount of gas remaining. The lost-gas component is the difference between  $V_t$  calculated and the cumulated desorbed gas measured.

Applying this approach to the Quinsam data, the calculated  $V_t$  values were generally greater than the cumulative desorbed gas by an amount similar to the previously calculated lost-gas value. However, the errors associated with the calculated  $V_t$  values were large.

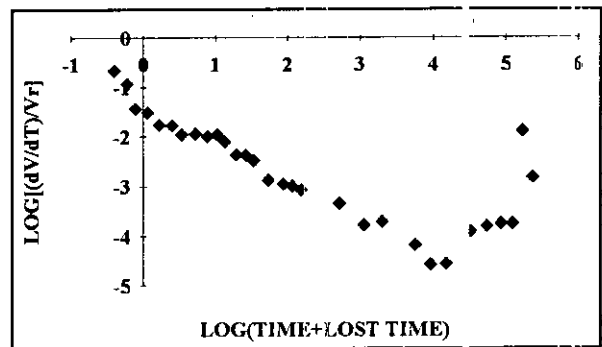


Figure 4: Plot of  $\log(\text{time})$  *versus*  $\log$  desorption data for Quinsam sample 34-6 used to calculate Airey constants.

It is not clear if this approach is theoretically sound but it does seem that in some cases the Airey equation may provide a rough estimate of the maximum possible lost-gas component. The approach needs to be tried on a larger data set to see if it will be useful. It is interesting because it may estimate the maximum lost-gas component based on the form of the desorption curve and not on the conditions that existed prior to sealing the sample in the canister. Obviously the sample must be desorbed at a constant temperature.

Fresh coal adsorbs oxygen and this process may influence the initial desorbed methane measurements. When the coal is brought to surface the coal adsorbs oxygen from the empty space in the canister, causing a reduction in pressure. The coal sample is moving towards a new equilibrium based upon the new pressure regime and a more complex mixture of gasses. Methane, oxygen, carbon dioxide and nitrogen all have different adsorption constants on the coal and different distribution coefficients for the gas to solid phases. Methane desorption, in part stimulated by adsorption of oxygen, counters the reduction in pressure. But when the volume of methane is measured in a manometer at atmospheric pressure it will be under-estimated. This problem can be countered by flooding the canister with nitrogen to remove the oxygen, but nitrogen inhibits desorption of methane and may also confuse the results. The Quinsam samples were not flooded with nitrogen because it was felt that all the implications were not understood.

## DEAD-SPACE CORECTION

Desorbed gas volumes are usually reported at standard temperature and pressure (288° K and 101.325 kilopascals pressure). The correction from ambient conditions to STP uses standard relationships (Table 3) and the correction is easy if ambient conditions do not

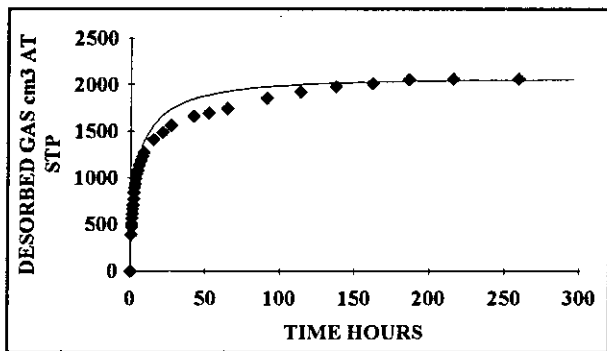


Figure 5: Desorption data for Quinsam sample 34-6 with predicted desorption curve using Airey equation.

change from measurement to measurement. However if conditions change because of change in elevation, weather or temperature, an additional correction must be applied based on the empty space in the canister and the magnitude of the change in ambient conditions. This is referred to as the canister dead-space correction.

It is not clear if all published desorption data are corrected for canister dead space. In simple terms the empty space in the canister is occupied by pre-existing gas and gas desorbed since the last measurement when the canister was opened. If ambient conditions change then the existing gas will occupy a different volume at the new ambient conditions. The change in volume must be added to or subtracted from the volume of new gas measured.

An equation for calculating the dead-space correction is outlined in Table 3. A simple graph to estimate the dead-space correction at ambient conditions, once the dead-space volume is known, is presented on Figure 6. Obviously it is important to minimize and measure the dead space in the canister. The canisters used by the authors have spacer rings to fill in space if the core sample diameter is much less than the inside diameter of the canister.

A number of ways of calculating the dead-space volume (DS) are described here:

1. Weigh the coal sample and use an estimate of specific gravity to calculate its volume. Find the dead-space by subtracting coal-sample volume from canister volume

2. Use a sensitive pressure gauge attached to the canister to measure the pressure (P1) prior to releasing the gas then use the relationship:

$$P1 \times DS = Pa \times (M+DS);$$

where Pa = atmospheric pressure, M = manometer volume displaced by the gas.

3. When the sample has finished desorbing open the canister to the atmosphere; seal it and then cool it in a refrigerator. When cool attach the canister to the

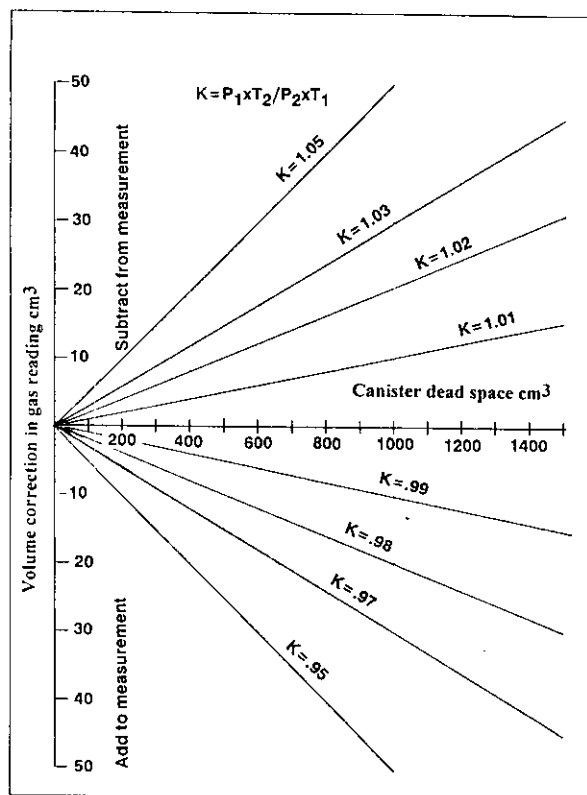


Figure 6: Dead-space correction based on changes in temperature, pressure and volume of dead-space in canister

manometer and measure the decrease in volume at atmospheric pressure. Use the relationship;  
 $(DS)/(273 + \text{room temperature}) = (DS-M)/(273 + \text{fridge temperature})$   
to calculate the dead-space volume.

4. After making a measurement use the manometer to pressure the canister with methane or air. Raise the water reservoir bulb above the water level in the burette while the manometer is still attached to the canister. This forces the methane or air back into the canister. Measure the difference in water levels (h in cm). This value represents the pressure above atmosphere forcing the methane or air back into the canister. Measure the volume of gas (M) returned to the manometer at atmospheric pressure (Pa). Calculate the dead space using:

$$DS \times (Pa + Ph) = [(DS + M) \times Pa]$$

$$DS = M \times Pa / Ph$$

$$Ph \text{ (millibars)} = 980.62 \times 0.998 \times h / 1000,$$

where 0.998 corrects for the density of water at room temperature.

Method four has a number of advantages. Dead-space calculations can be made after each desorbed gas measurement and a number of measurements averaged. The method requires no additional equipment and is direct. Lastly it measures the same volume as the desorbing gas occupies; rather than measure a liquid-

filled volume or a theoretical volume. The method was used on the Quinsam samples and appeared to work well. If oxygen adsorption is a problem the procedure can be carried out after the coal has finished desorbing and before it is removed from the canister.

### WATER VAPOUR CORRECTION

The water vapour correction is required to correct for the presence of water vapour in the canister. In most cases the dead space in the canister is saturated with water vapour because there is excess water in the coal sample. The vapour pressure of water is temperature dependent and ranges from 0.5 to 7.5 kilopascals in the temperature range 0 to 40°C. The volume of gas should be calculated using atmospheric pressure minus partial pressure of water vapour times manometer reading. Applying a water vapour correction reduces the measured gas volume at STP by about 2.5%. The resultant gas volume is dry gas at STP.

TABLE 3  
PROCEDURE FOR CORRECTING MEASURED GAS VOLUMES TO DRY GAS AT STP

Conditions
Vc = Canister volume
DS = empty space in canister not occupied by sample (dead-space)
Canister opened to atmosphere at time Tm1
Conditions at Tm1
Atmospheric pressure = Pa1    Temperature = T1
Desorbed gas measured at time Tm2 and canister equilibrated with existing atmospheric conditions Conditions at Tm2
Atmospheric pressure = Pa2    Temperature = T2
Apparent volume of desorbed gas at existing atmospheric conditions = Vg
<b>Dead-Space Correction</b>
$(DS \times Pa1) / T1 = (DS - Vc) \times Pa2 / T2$
This equation expresses the apparent change in volume (Vc) of the pre-existing gas in the canister. This change will affect the value of Vg, the apparent volume of new gas desorbed from Tm1 to Tm2, measured at ambient conditions existing at Tm2.
$DS = (DS - Vc) \times (Pa2 \times T1) / (Pa1 \times T2)$
$DS = (DS - Vc) / K$ Where $K = (Pa1 \times T2) / (Pa2 \times T1)$
$Vc = DS \times (K - 1)$
Vc can be calculated using a simple nomograph (Figure 6)
The actual volume of gas desorbed at Tm2 is $Vgc = Vg - Vc$
<b>STP Correction</b>
Volume Vgc must be corrected to STP conditions
$Vgc(STP) \times P(STP) / T(STP) = Vgc \times Pa2 / T2$
$Vgc(STP) = (Vg - Vc) \times Pa2 \times T(STP) / (T2 \times P(STP))$
P(STP) = 1013.25 millibars    T(STP) = 273 + 15 °C
<b>Moisture Correction</b>
If DS in the canister has 100% humidity then a further correction to dry gas at STP must be made
Pw2 = the partial pressure of water vapour at T2    Actual pressure of dry methane at T2 = Pd2
Pd2 = Pa2 - Pw2
$Vgc(STP \text{ dry}) = (Vg - Vc) \times Pd2 \times T(STP) / (T2 \times P(STP))$

### CORRECTION TO STP

Finally, the measured gas volume must be converted to the equivalent volume at standard temperature and pressure using the general relationship for ideal gases:

$$P_1 \times V_1 / T_1 = P_2 \times V_2 / T_2$$

The accuracy of the STP correction can be monitored by checking the apparent volume of gas evolved from an empty canister as weather conditions change from day to day. After all corrections are applied the desorbed volume should be zero. If it is not, the corrected gas volumes desorbed from the samples are probably also in error.

### SAMPLE WEIGHT AND BASIS FOR REPORTING DATA

The gas contents are expressed in terms of: as-received sample, air-dried sample, dry ash-free sample *in situ* sample or mineral-matter free sample. Data cannot be calculated to any of these bases without using a measurement of sample weight and corresponding moisture content as a starting point.

It is possible to estimate the sample weight by weighing the canister with and without the sample, but without knowing the moisture content of the sample the weight cannot be converted to a dry weight. The as-received moisture reported by an analytical laboratory subsequent to desorption may be similar to the moisture existing in the canister during desorption, when the canister plus sample was weighed, if all the moisture was removed from the canister and the sample did not dry while being shipped to the laboratory. In this case the gas content is calculated on an as-received basis and then adjusted to other bases. The best methods to ensure that all the sample is removed from the canister and shipped to the laboratory and that the laboratory reports a sample weight on an air-dried basis. Gas content can be recalculated to a dry ash-free basis by using the appropriate moisture and the ash content expressed at that moisture.

If the data are to be used for resource calculations, the gas content should be recalculated to an *in situ* base using an estimate of the *in situ* moisture which will be similar to but a little higher than the equilibrium moisture content of the sample.

Often data are reported on a mineral-matter free basis (dmmf). Whereas calculations to the other bases are exact, a calculation to a dmmf basis requires assumptions. Before the data can be corrected the weight loss when the mineral-matter is converted to ash, must be known. Often the weight of mineral matter in the sample

is estimated from the weight of ash using the Parr equation, (Parr, 1932). The equation  $[(1.08 \times \text{ash} + 0.55 \times \text{total sulphur})]$  predicts values ranging from 1.08 to 1.25 for the weight ratio (mineral matter/ash) depending on the ash and sulphur content. The Parr equation assumes that all sulphur is present as pyrite and is converted to iron oxide, and that the ash chemistry is constant. The mineral matter to ash ratio can be measured directly using plasma ashing. The results of plasma ashing five samples from Telkwa (Ryan, 1991) indicated that the mineral matter/ash ratio is about 1.16 which is higher than that predicted using the Parr equation.

An alternative method of estimating the ratio is to plot volatile content (daf) versus ash (db). As the ash content increases, VM (daf) values increase because of the addition of volatiles from the ash ( $\text{H}_2\text{O}$ ,  $\text{CO}_2$  and  $\text{SO}_2$ ). The slope of the plot provides an estimate of the mineral matter/ash ratio. For Quinsam data the slope is 0.18, indicating a mineral matter/ash ratio of 1.18.

The the dmmf gas contents reported in Table 1 are calculated using the Parr equation and are probably low based on the above discussion. As most measured and theoretical adsorption curves are expressed on an as-received or daf basis the dmmf calculation is not critical. Normally, for a coal with 20% ash, a concentration expressed on a dmmf basis will be less than 5% higher than the same concentration expressed on a daf basis. The difference will be greater for samples with a higher ash content. If it is necessary to quote data on a dmmf basis then the method of making the correction should be justified in terms of the chemistry of the particular coal being studied.

## DESORPTION CURVES

Nine samples from Quinsam, each consisting of 40 centimetres of core, were desorbed at room temperature. The desorption curves for the samples from hole 92-34 are on Figure 7 and the curves for samples from hole 92-46 are on Figure 8. The gas contents are expressed as cubic centimetres per gram daf and at STP with a water vapour correction applied. The cumulative gas content totals are provided in Table 4. Coal quality information for the samples is in Ryan and Dawson (1994, this volume).

The samples of seam 3 (hole 92-34) were desorbed for 15 days, at which time the canisters were re-used for the seam 1 samples (hole 92-46). At this time only one seam 3 sample had finished desorbing and the last increment of desorbed gas from the other seam 3 samples had to be estimated by projecting the cumulative desorption curves. In all cases the correction was less than 250 cubic centimetres. Seam 1 samples were

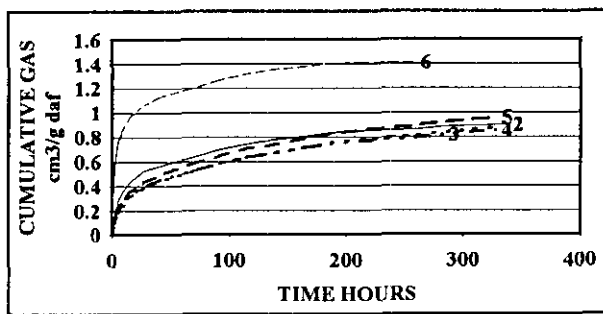


Figure 7: Desorption curves for samples from hole 92-34 (dry ash-free basis).

desorbed for periods ranging from 44 to 54 days. At this time the gas being desorbed after correcting for variations of pressure and temperature between readings was less than 5.0 cubic centimetres per day.

Under ideal conditions, if the coal is saturated, the gas contents of samples on a dry ash-free basis from throughout the seam should be similar. This assumes that the petrography of the samples is similar. Gas contents are similar except for the footwall samples from each seam. These samples contain more gas and are noticeably more crushed than the other samples. Their smaller size-consist probably allowed them to scavenge gas more easily.

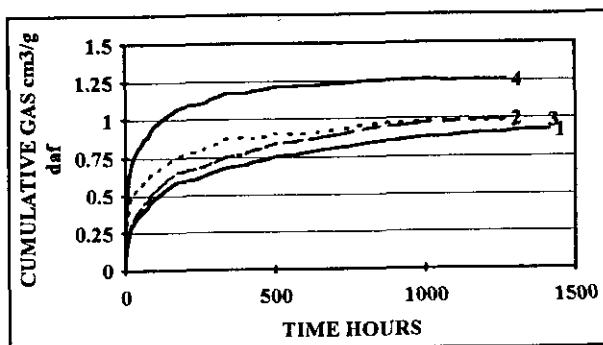


Figure 8: Desorption curves for samples from hole 92-46 (dry ash-free basis).

## IN SITU SPECIFIC GRAVITY

Desorption data are often collected as one component of a resource evaluation and the data will probably eventually be expressed as gas content per *in situ* tonne of coal. It is therefore useful to be able to estimate the *in situ* specific gravity versus ash

TABLE 4  
SUMMARY DESORPTION DATA CORRECTED FOR CANISTER DEAD SPACE  
AND CONVERTED TO STP DRY GAS

SAMPLE	L GAS cm <sup>3</sup> /g	D GAS cm <sup>3</sup> /g	S GAS cm <sup>3</sup> /g	T GAS cm <sup>3</sup> /g	T GAS daf/g
<b>HOLE 34 SEAM 3</b>					
92-34-2	0.0441	0.3919	0.0053	0.441	1.014
92-34-3	0.0516	0.7127	0.0332	0.797	0.978
92-34-4	0.0551	0.7239	0.0676	0.847	0.997
92-34-5	0.0562	0.8694	0.0919	1.018	1.121
92-34-6	0.1482	0.9456	0.0000	1.094	1.632
<b>HOLE 46 SEAM 1</b>					
92-46-1	0.0402	0.7906	0.0000	0.8308	0.971
92-46-2	0.0436	0.8685	0.0000	0.9121	1.068
92-46-3	0.0633	0.8091	0.0000	0.8724	1.057
92-46-4	0.0574	0.9046	0.0000	0.9620	1.331

**ABBREVIATIONS**

- L GAS = Gas lost prior to sealing sample in canister
- D GAS = Gas desorbed into canister.
- S GAS = Estimate of gas desorbed after samples removed from canister.
- T GAS = Total estimated gas desorbed from samples.
- T GAS daf = Total gas on a dry, ash-free basis per dry gram.

relationship of the coal. The *in situ* specific gravity of core samples can be estimated using the dead-space volume, canister volume, and weight of sample in the canister. If there is not much excess water in the canister this provides sufficient information to calculate a specific gravity for the sample which will be a reasonable estimate of the *in situ* specific gravity. If the samples have a range of ash contents then an ash *versus in situ* specific gravity calibration curve can be constructed.

The specific gravities of the Quinsam samples were calculated using this method and they varied from 1.44 for a 54% ash to 1.2 for an 8% ash sample.

**DIFFUSION RATES**

The desorption curves provide information on the diffusion characteristics of the coal. Quantifying the rate of desorption is important as one of the parameters used to estimate the productivity of a potential coalbed methane well.

Airey introduced the constants  $T_0$  and  $N_a$ . Smith and Williams (1983) quantify the rate of desorption using the effective diffusivity constant ( $D_f$ ) calculated from the slope of the lost-gas plot using:

$$D_f = (\text{slope}^2 \times \pi) / (Vt^2 \times 36)$$

The effective diffusivity constant of Smith and Williams is derived from the diffusion equation of Barrier and Brook (1953) in which  $D_f = D/R_0^2$ ;  $D$  is the diffusion constant in Ficks equation and  $R_0$  is a particle size term that does not necessarily correspond with the visual particle size.

Values of  $T_0$ ,  $N_a$  and  $D_f$  are reported in Table 1 for the Quinsam data set. The  $T_0$  and  $D_f$  values decrease

and the  $N_a$  values increase as the amount of shearing in the coal increases. There is also an increase in Hardgrove index with shearing.

Another measure of diffusion is the time taken for the coal to diffuse half or one quarter of its methane, including the lost-gas component. This value can be derived from the desorption data or estimated from the Airey equation fitted to the data using:

$$T_{1/2} = -T_0 \times \log_e(.5^{N_a}) \text{ or } T_{1/4} = -T_0 \times \log_e(.25^{N_a})$$

The values in Table 1 were calculated from the desorption data. Values of  $T_{1/2}$  decrease as the Hardgrove index and amount of shearing increase.

**CONCLUSIONS**

There are a number of corrections that must be made to the desorbed gas measurements before a true total desorbed gas content can be calculated.

- There is no foolproof way of making lost-gas corrections, but there are ways of checking the appropriateness of the correction method.
- The Airey equation indicates that it might not always be appropriate to estimate lost gas using a cumulative gas *versus* (time)<sup>1/2</sup> plot. The value 2 should be replaced by the Airey constant calculated from the desorption data. A limited data set indicates that the value  $N_a$  may vary from 1.3 to 4. The Airey equation may also provide a way of estimating the maximum possible lost gas based on the shape of the desorption curve.
- The distinction between free gas and lost gas is important. Free gas occupies the macro-pores in the coal. The term lost gas generally refers to gas that desorbs prior to sealing the sample in the canister.
- Cumulative gas volumes should be reported as dry methane at standard temperature and pressure conditions. The concentrations can be expressed in terms of dry coal, dry ash-free coal *in situ* coal or dry mineral-matter free coal based on a knowledge of the weight of the sample and its corresponding moisture content.
- Useful information on *in situ* specific gravity can be obtained at the same time that the desorption data are collected.

## REFERENCES

- Airey, E.M. (1968): Gas Emission from Broken Coal. An Experimental and Theoretical Investigation; *International Journal of Rock Mechanics and Mineral Science*, Volume 5, pages 475-494.
- Barrier, R.M. and Brook, D.W. (1953): Methane Desorption; *Faraday Society Transactions*, Volume 49, pages 1049-1059.
- Bertard, D., Bruyet, B. and Gunther, J. (1970): Determination of Desorbable Gas Concentration of Coal (Direct Method); *International Journal of Rock Mechanics and Mineral Science*, Volume 7, pages 43-65.
- Diamond, W.P. and Levine, J.R. (1981): Direct Method Determination of the Gas Content of Coal, Procedures and Results; *U.S. Bureau of Mines Report of Investigations 8515*, pages 1-36.
- Feng, K.K. and Lu, B.C.Y. (1981): Desorption of Gases from Canadian Coals; *Energy, Mines and Resources Canada, Canmet Report 81-20*.
- Kenyon, C., Cathyl-Bickford, C.G. and Hoffman, G. (1991): Quinsam and Chute Creek Coal Deposits (NTS (92/13,14); *B.C. Ministry of Energy, Mines and Petroleum Resources*, Paper 1991-3.
- Kissell, F.N. McCulloch, C.M and Elder, C.H. (1973): The Direct Method of Determining Methane Content of Coalbeds for Ventilation Design; *U.S. Bureau of Mines, Report of Investigations 7767*.
- Olszewicki, A.J. and McLennan, J.D. (1992): Development of Formation Evaluation Technology For Coalbed Methane Development; *Quarterly Review of Methane from Coal Seams Technolog*, Volume 6, No. 1, pages 25-29.
- Parr, S.W. (1932): The Analysis of Fuel, Gas, Water and Lubricants; *McGaw-Hill, New York*.
- Rightmire, C.T. (1984): Coalbed Methane Resource; Rightmire, C.T., Eddy, G. and Kirr, J., Editors, *American Association of Petroleum Geologists Studies in Geology, Series 17*, pages 1-15.
- Ryan, B.D. (1991): Density of Coals from the Telkwa Coal Property, Northwestern British Columbia; *in Geological Fieldwork 1990, B.C. Ministry of Energy, Mines and Petroleum Resources*, Paper 1991-1, pages 399-406.
- Ryan, B.D. and Dawson, F.M. (1993): Coalbed Methane Desorption Results from the Quinsam Coal Mine and Coalbed Methane Resource of the Quinsam Coalfield, British Columbia, Canada (92F/13,14); *in Geological Fieldwork 1993*, Grant, B. and Newell, J.M., Editors, *B.C. Ministry of Energy, Mines and Petroleum Resources*, Paper 1994-1, this volume.
- Smith, D.M. and Williams, F.L. (1984): Diffusion Models for Gas Production from Coals: Application of Methane Content Determination; *Fuel*, Volume 63, pages 251-255.
- Wheeler, A. (1951): *Advances in Catalysis*; Volume 3, *Academic Press*, page 250.



## HYDROTHERMAL BRECCIAS AND ASSOCIATED ALTERATION OF THE MOUNT POLLEY COPPER-GOLD DEPOSIT (93 A/12)

Theresa M. Fraser  
Mineral Deposit Research Unit, U.B.C.  
(MDRU Contribution 039)

**KEYWORDS:** Economic geology, porphyry Cu-Au, Mount Polley, hydrothermal breccia, alteration, skarn, magnetite, albite, garnet, actinolite.

### INTRODUCTION

The Mount Polley alkalic porphyry copper-gold deposit in south-central British Columbia (52°30'N, 121°35'W) is located 56 kilometres northeast of Williams Lake. The current owner of the property, Imperial Metals Corporation, has estimated geological reserves at 2.8 million ounces of gold and 1.5 billion pounds of copper, using a copper equivalent cut-off grade of 0.2%, and mineable reserves at 48.8 million tonnes grading 0.383% copper and 0.556 gram gold per tonne, using a copper equivalent cut-off grade of 0.39% (Gorc *et al.*, 1992).

The deposit is hosted by a diorite stock that intrudes compositionally similar volcanic rocks in the central part of the Quesnel Terrane. The diorite consists of several intrusive phases and a number of breccia bodies.

Fieldwork was undertaken in June, 1993, to map the area surrounding the proposed S19 open pit at a scale of 1:2000. The objective was to subdivide the breccias on the basis of mineralogy, textural differences, type of matrix, alteration of clasts, timing and distribution. Alteration minerals and their modes of occurrence were noted on surface and combined with drill-log information to outline the distribution of potassic (subdivided into biotite, actinolite and potassium feldspar), propylitic and pyritic assemblages. Nomenclature of the alteration zones has changed slightly from last season (Fraser *et al.*, 1993) in that the calc-potassic zone has been subdivided into areas corresponding to the dominant alteration mineral, for example, actinolite. Finally, vein assemblages that were recognized previously were mapped to determine the relative timing of vein-filling and brecciation.

### DEPOSIT GEOLOGY

The Mount Polley deposit is hosted by a moderate sized diorite intrusion (Figure 1) that is crosscut by several breccia types, including intrusion and hydrothermal breccias (Fraser *et al.*, 1993). Most of the ore is contained within hydrothermal breccias. The deposit is dissected by

a prominent north-trending fault. The type of breccia changes across the fault; an albite-rich breccia is present in the west zone while actinolite and biotite-rich breccias characterize the east zone (Figure 1). The breccias are intruded by a variety of late to post-mineral dikes, the most abundant of which are augite porphyry dike swarms.

Lithologies, including distinct types of breccia, are described from oldest to youngest:

**Volcanics** (unit 1) do not outcrop in the area mapped. In the region, however, volcanic rocks consist of diverse maroon polymictic volcanic breccias, augite-phyric basalts, trachybasalts and tuffs. Volcanic xenoliths are commonly found in the diorite unit. Drill-hole logging on cross-section 3460 N identified a block of green crystal lapilli tuff contained within a plagioclase porphyry intrusion breccia.

**Diorite** (unit 2) forms a stock-like intrusion and is the dominant host for the mineralized breccia bodies at Mount Polley. Most commonly, the diorite is dark grey, fine grained, and equigranular to weakly porphyritic (plagioclase and clinopyroxene phenocrysts). Euhedral plagioclase laths are andesine in composition and are moderately sericitized. The most prominent mafics are biotite and clinopyroxene; the latter occasionally has altered rims of hornblende. The diorite is relatively fresh away from the breccias but the intensity of alteration increases towards the core of the system (where the unit is cut by several vein types, including magnetite, actinolite and potassium feldspar).

**Plagioclase porphyry** (unit 3) forms a massive intrusive unit and the matrix of locally extensive intrusion breccias. For mapping purposes, the two textural types have been grouped together and are identified on the map as unit 3a (plagioclase porphyry) and unit 3b (intrusion breccia) based on the predominant textural characteristic.

The plagioclase porphyry is crowded with plagioclase phenocrysts (up to 70%), and locally seriate in texture. The feldspars are euhedral and moderately sericitized. Accessory minerals include biotite, magnetite, hornblende and trace apatite. Most of the unit has suffered moderate to intense potassium feldspar alteration. Plagioclase porphyry forms the matrix of the intrusion breccia that is dominated by subangular fragments of diorite, normally more than 3 centimetres across. The

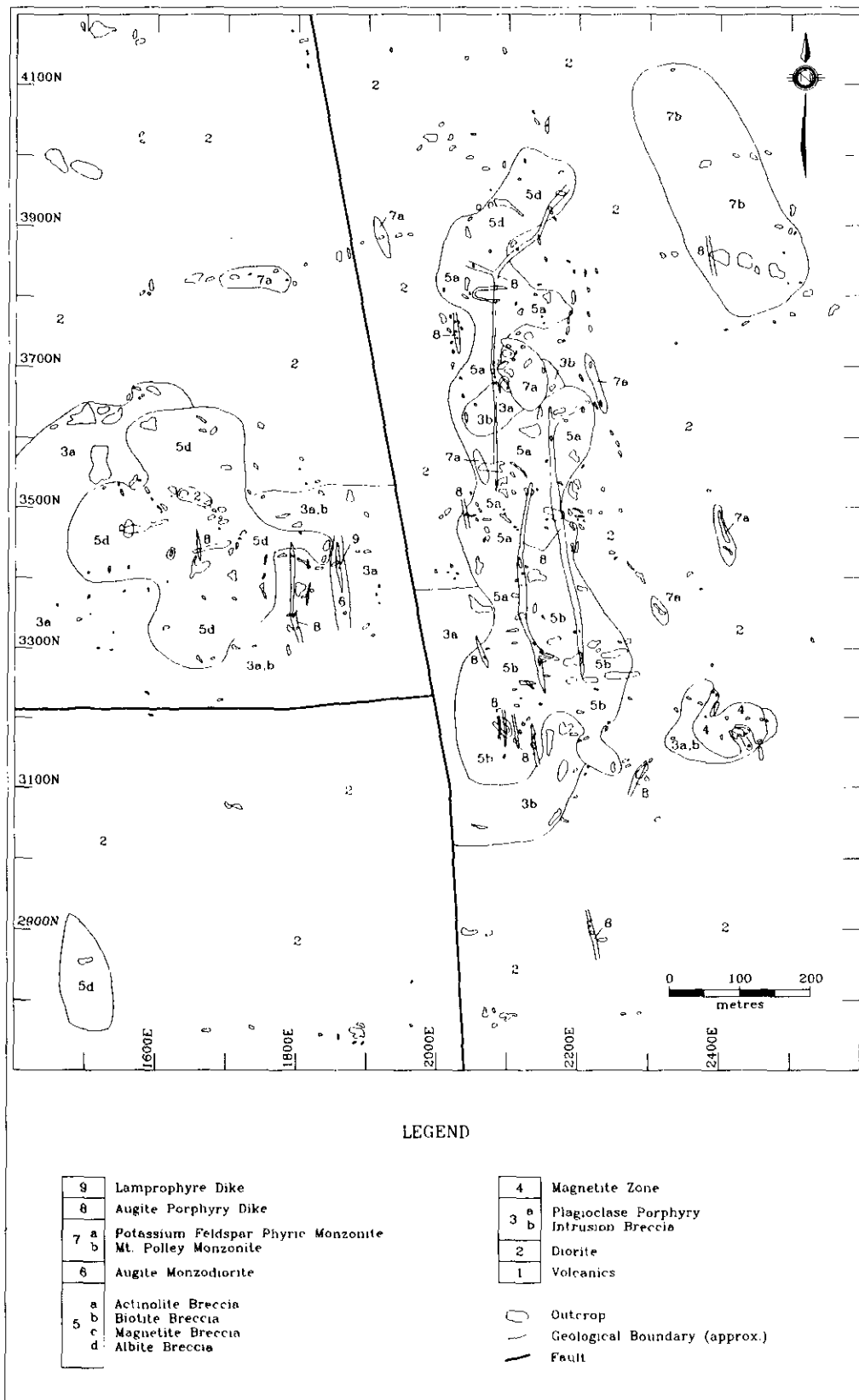


Figure 1. Surface geology map of the Mount Polley deposit using the Imperial Metals Corporation grid.

breccia is matrix supported and locally contains up to 35% clasts. The unit has undergone intense alteration, with strongly sericitized feldspar phenocrysts and the development of secondary potassium feldspar that has destroyed primary textures in many areas.

**Magnetite-Garnet** (unit 4) forms a "replacement zone" in an area roughly 100 by 100 metres in the southeastern portion of the proposed S19 open pit. The zone lies at the contact between diorite to the north and plagioclase porphyry to the south (Figure 1). The margin of the zone is not well exposed but appears to interfinger and have sharp contacts with the plagioclase porphyry unit. Plagioclase porphyry has a narrow, bleached alteration envelope adjacent to the contact and this is accompanied by the destruction of primary texture.

The magnetite zone consists of 40 to 70% magnetite; the remainder is strongly weathered brown garnet (Plate 1A). Garnet-rich areas form irregular elongate patches with diffuse margins that are crosscut by magnetite veins and microfractures along which garnet has been replaced by magnetite. Epidote veins cut the magnetite-garnet replacement zone and small voids within the unit have been partially filled with zeolites and calcite.

**Hydrothermal breccias** (unit 5) are prominent in the map area and have been subdivided on the basis of texture and mineralogy. Four breccia types have been identified, each with its own characteristic matrix mineralogy: actinolite breccia, biotite breccia, magnetite breccia and albite breccia. Clasts are dominated by the local country rock to the breccia, typically diorite and occasionally plagioclase porphyry. Crosscutting relationships between the various hydrothermal breccias are difficult to identify due to poor exposure on surface. A more detailed description of the breccia types will follow in a separate section entitled "Hydrothermal breccias and veins".

**Porphyritic augite monzodiorite** (unit 6) only outcrops in the western zone and is present at depth, for example on cross-section 3460 N. Generally it forms dike-like bodies with a northerly strike and moderate to shallow easterly dip. Macroscopically, this unit is very distinctive, having 10% prominent rounded green clinopyroxene phenocrysts in an intensely sericitized plagioclase groundmass. Accessory minerals include magnetite, apatite and biotite. This unit is unmineralized and unaltered.

**Potassium feldspar phyric monzonite** (unit 7) occurs in two distinct locations, the core of the deposit and the summit of Mount Polley (Figure 1).

The monzonite unit (unit 7a) occurs as dikes and pods in the centre of the deposit and extends to undefined depths. Euhedral, zoned potassium feldspar phenocrysts (20%) form a trachytic texture with individual phenocrysts up to 2 centimetres long. Most of the groundmass has weakly aligned tabular plagioclase grains. Accessory minerals include clinopyroxene, sphene, apatite and

magnetite. Clasts of diorite occur in the monzonite intrusion. Diamond-drill hole MP89-125 cut a 15-metre interval of intrusion breccia in which 20 to 30% angular fragments of hornblende pyroxenite and diorite were identified. The pyroxenite may be derived from a larger body at depth.

The Mount Polley summit monzonite (unit 7b) was mapped in the 1993 field season. It has been previously described by Hodgson *et al.* (1976) as an intrusion breccia, but on surface no fragments were visible and drill core was unavailable. The rock resembles unit 7a, having a moderate alignment of feldspars and containing 5% large megacrysts of potassium feldspar. The extent of the unit is unknown and it may be much larger than shown on Figure 1; it is bounded on the south by diorite. The monzonite is unmineralized, but is partially altered to epidote, albite and minor pyrite.

**Augite porphyry dikes** (unit 8) occur as swarms throughout the deposit, striking northerly and dipping moderately to the east. Dikes are continuous along strike and have an average thickness of 4 metres. Most have an aphanitic chilled margin with occasional augite or plagioclase phenocrysts. Clinopyroxene (35-55%) forms optically zoned, euhedral phenocrysts and plagioclase forms the bulk of the groundmass, together with disseminated magnetite.

**Biotite lamprophyre dikes** (unit 9) crosscut all rock units and are possibly Tertiary in age. They have been mapped throughout the deposit, have a maximum thickness of 2 metres, and are oriented roughly north-south (similar to other post-mineral dikes). The dikes are fine grained, friable and weather rapidly on surface to a dark green sand. Euhedral biotite forms 40% of the unit, imparting a foliation, with lesser moderately to weakly aligned plagioclase laths and sparse pyroxene phenocrysts.

## HYDROTHERMAL BRECCIAS AND VEINS

The features of each breccia type intersected in drill holes were systematically noted by using the Geolog system (Blanchet and Godwin, 1972) for porphyry deposits. Representative sections, corresponding to assay intervals, were logged. Where diamond-drill core was unavailable, surface material was described. Hydrothermal breccia characteristics are summarized in Table 1.

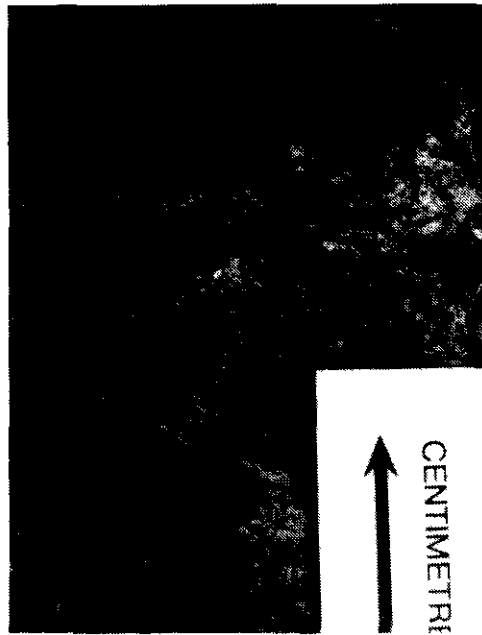
**Actinolite breccia** (unit 5a) is only present east of the fault; no actinolite has been identified in the west zone. This unit is hosted by diorite. Diorite blocks show minor rotation with small triangular vugs between blocks. The vugs are filled with fibrous dark green actinolite and are surrounded by envelopes of potassium feldspar. Diorite clasts are subangular and 2 to 3 centimetres across on average. The clasts commonly have unaltered interiors but



**A**



**B**



**C**



**D**

Plate 1. **A** An outcrop photograph of massive magnetite (black) and elongate garnet patches (white). **B** A cut slab of biotite breccia from the central zone of Mount Polley. The breccia has coarse hydrothermal biotite in the matrix (black) and subangular diorite clasts. **C** Magnetite breccia from the west zone with strongly altered angular clasts and matrix of magnetite, accessory sulphides and diopside. **D** Texture of weathered albitic breccia from the west zone is evident. The albitic matrix is recessive (black) and clasts are strongly altered to potassium feldspar.

TYPICAL HYDROTHERMAL BRECCIA FEATURES

Breccia Type	Ave. Matrix Size (mm)	Ave. Clast Size (cm)	% Clasts	Max. Clast Size (cm)	Sorting	Clast Roundness	Clast Sphericity	Open vs Closed
Actinolite	1.0	4.5	85	200	3	3	7	C
Biotite	6.0	3.0	85	100	2	5	9	C (O)
Magnetite	2.0	3.0	90	5	2	5	9	C
Albite	0.5	4.5	75	10	5	7	9	C

Table 1. Biotite, magnetite and albite breccias were estimated using representative drill holes over intervals up to 30 metres. Information about the actinolite breccia was accumulated on a large stripped outcrop in the central zone. Scales are as follows: Sorting - 2 = very poorly sorted and 5 = moderately sorted, Roundness - 3 = subangular and 7 = moderately rounded, Sphericity - 9 = most spherical (refer to Blanchet and Godwin's (1972) L-scale definitions). Open versus closed refers to matrix-supported and clast-supported breccias, respectively.

become increasingly altered by potassium feldspar toward their margins where primary texture has been destroyed. The matrix consists entirely of actinolite with traces of disseminated chalcopyrite. The breccia is generally cut by abundant actinolite (±chalcopyrite, diopside) veins with potassium feldspar envelopes. Similar veins occur throughout the central zone of the Mount Polley deposit. Actinolite breccia appears to grade into the biotite breccia to the south and into actinolite-albite breccia to the north. In the latter, 1 to 3-centimetre vugs have been partially filled by prismatic albitic crystals (3 x 3 x 10 mm). Their margins are albitically altered and locally overprint potassium feldspar alteration.

**Biotite breccia** (unit 5b, Plate 1B) is exposed on surface in the southern part of the central zone, where it is extensively oxidized and outcrops are weathered and friable. Clasts are pervasively altered to potassium feldspar and the original rock type is difficult to identify; remnant textures suggest that the clasts are dominantly diorite and plagioclase porphyry. The majority of clasts are in the 2-centimetre range, but locally are up to a metre across. The breccia is largely clast supported but locally there are zones of matrix-supported breccia.

The matrix contains coarse-grained hydrothermal biotite flakes up to 2 centimetres in diameter, with patchy development of secondary chlorite (Plate 1B). The matrix assemblage has an average composition of 60% biotite, 25% chrysocolla (with trace malachite) and 15% zeolites. Chrysocolla is intimately intergrown with biotite and also has impregnated clasts, suggesting extensive mobility during the oxidation of sulphides. The zeolites are late in the formation of the breccia and have filled void space around biotite and chrysocolla.

**Magnetite breccia** (unit 5c, Plate 1C) is not abundant, but is developed locally throughout the Mount

Polley deposit; it rarely forms areas large enough to illustrate at the scale of mapping. Diorite and plagioclase porphyry host zones of magnetite breccia. Clasts are predominantly 2 to 3 centimetres across and are pervasively altered to potassium feldspar. The matrix consists of massive to euhedral grains of magnetite (2 to 3 mm) locally accompanied by accessory sulphides and pyroxene. This variety of hydrothermal breccia is always clast supported, with an average of 10% matrix.

**Albite breccia** (unit 5d, Plate 1D) is a distinctive variety found in the west zone. It is typified by variably altered clasts with interiors that retain some primary texture, including albitic twinning in plagioclase, and margins that have remnant sericitized plagioclase and relict primary clinopyroxene. Fragment boundaries are irregular and undulating. Albite alteration has caused extensive recrystallization and replacement along margins of clasts, clouding the distinction between fragments and matrix. In many cases, the matrix is only identified on the basis of secondary biotite in small vugs. The unit is largely clast supported, containing small vugs partially filled with pristine, zoned prismatic albite crystals or alternatively the matrix may consist of fine-grained albite with accessory biotite, magnetite and disseminated sulphides.

To constrain the timing of veins, crosscutting relationships among vein sets were identified. Most of the data were collected from split drill-core with lesser amounts from available outcrop. Veins are almost always weathered at surface to such an extent that positive identification of minerals is difficult and much ambiguity results. Vein assemblages and the location and relative timing of distinct veins are summarized in Table 2. Field relationships suggest the following:

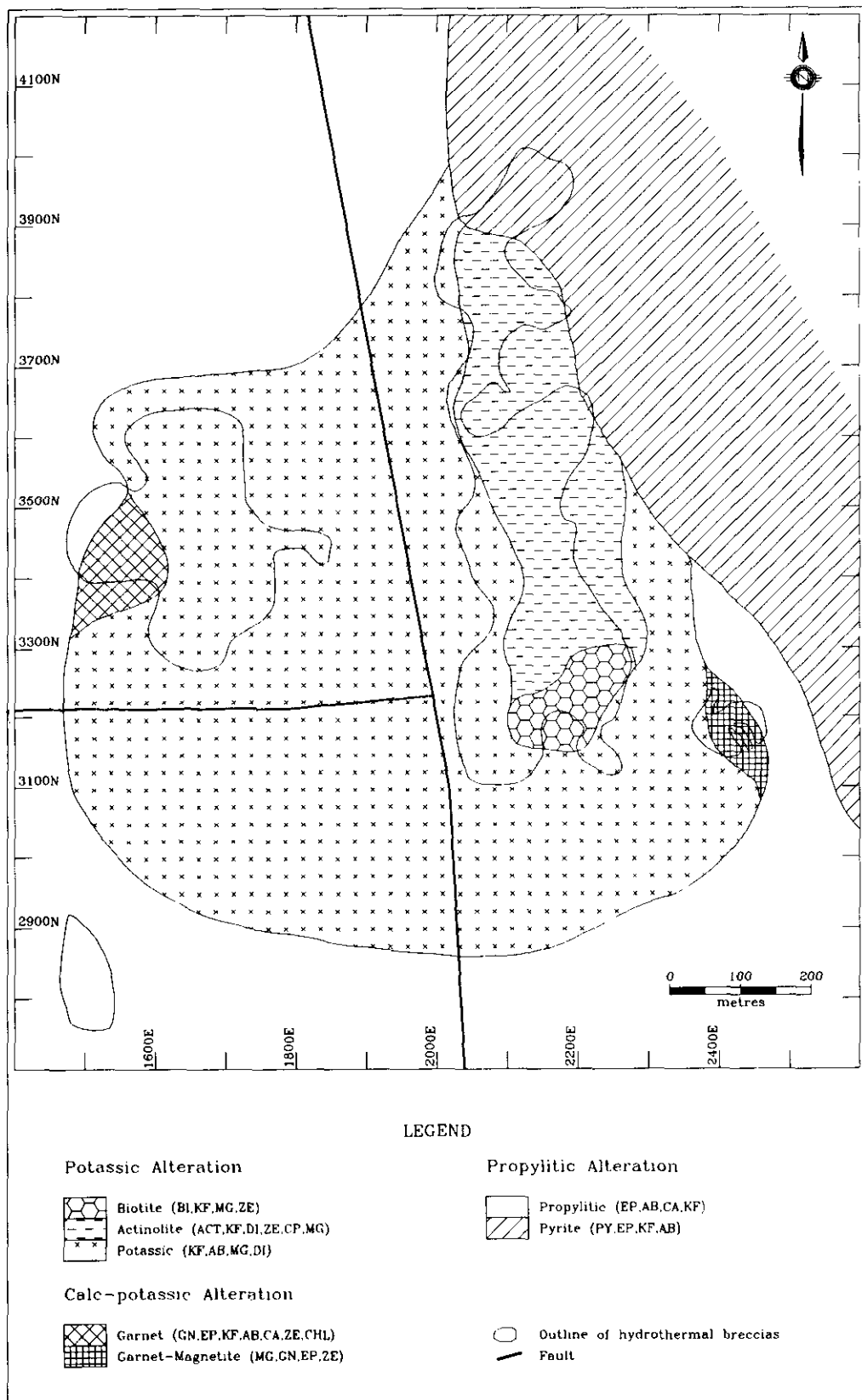


Figure 2. Alteration map of Mount Polley. Modes of occurrence of alteration minerals are: vein (actinolite, chalcopyrite, pyrite, epidote, magnetite, diopside, albite, potassium feldspar), pervasive (epidote, potassium feldspar) and vug-fill (biotite).

## SUMMARY OF VEIN ASSEMBLAGES AT MOUNT POLLEY

Vein Type	Name	West Zone	Central Zone	Fringe	Relative Timing
1	actinolite		AC+DI+CP (KF)		early
2	magnetite	MG+DI+CP+PY (KF)	MG+DI+CP+PY (KF)		early
3a	chalcopyrite	CP+BO+MG	CP+BO+MG		intermediate
3b	pyrite			PY+MG+CP	intermediate
4	epidote			EP+PY+CC	intermediate
5	albite			AB	intermediate
6	quartz		QZ		late to post-mineral
7	calcite	CC+ZE	CC+ZE	CC+ZE	post-mineral

Table 2. The abbreviations are as follows: AC = actinolite, DI = diopside, CP = chalcopyrite, KF = potassium feldspar, MG = magnetite, PY = pyrite, BO = bornite, EP = epidote, CC = calcite, AB = albite, QZ = quartz and ZE = zeolites.

- Actinolite veins crosscut a variety of breccia units and intrusives east of the fault. The veins are present in a narrow zone elongated north-south and superimposed on the actinolite breccia zone. The veins are mineralized and have accessory diopside. Potassium feldspar envelopes occur around the veins and similar alteration envelopes are associated with microfractures that contain no vein-fill.
- Magnetite veins are widespread throughout the deposit. Most veins contain chalcopyrite, trace diopside and pyrite. Locally, narrow potassium feldspar envelopes are developed, similar to those around actinolite veins.
- Chalcopyrite-bornite-magnetite veins (3a) occur in the core of the system and grade outward to pyrite-magnetite-chalcopyrite veins (3b). Veins 3a and 3b may have been produced by the same hydrothermal fluid but at different temperatures or sulphur fugacities.
- Epidote veins are found on the fringe of the breccia complex and mark the propylitic zone. Most veins contain considerable coarse-grained euhedral pyrite and accessory calcite.
- Albite veins crosscut pre-existing potassium feldspar envelopes and actinolite veins. Almost all veins examined are strongly weathered and the presence of other minerals is obscured. The association of albite with hydrothermal breccias in the west zone may indicate that the veins are related to mineralization and the peripheral propylitic zone.
- Rare, late quartz veins cut the plagioclase porphyry unit in drill hole MP89-126 and on

surface, east of the fault in the core of the system. These veins truncate actinolite and chalcopyrite-bearing veinlets. The unmineralized quartz veins may be unrelated to the Mount Polley system.

- Calcite and zeolite veins cut all lithologies and vein types. They are widespread throughout the deposit and occur in all alteration zones. These are post-mineral veins, and like quartz, may be unrelated to the main mineralizing event.

All of the distinct vein assemblages are summarized in Table 2. Distribution of assemblages is noted, as well as an estimate of the timing of vein formation. Both early and intermediate veins are mineralized, and are separated on the basis of mineralogy and suspected time of deposition. Intermediate veins were formed during the main hydrothermal event in the core of the system and are probably contemporaneous with epidote and pyrite on the fringe.

### DISTRIBUTION OF ALTERATION

Previous authors, Hodgson *et al.* (1976) and Bailey and Hodgson (1979), identified three concentrically zoned alteration assemblages: a potassic core surrounded by a garnet-epidote zone, and an outer propylitic rim. An extensive pyrite halo was mapped on the eastern portion of the Mount Polley deposit. A combination of detailed mapping and drill-hole logging during the past two field seasons generally supports this interpretation but, in addition, the potassic core is now divided into three distinct units based on the dominant mineral assemblage (Figure 2).

## POTASSIC ALTERATION

A potassic core (Figure 2) coincident with the hydrothermal and intrusion breccias can be subdivided into three major subtypes:

- A biotite zone characterized by the development of coarse, secondary black biotite within vugs of the hydrothermal breccia (unit 5b), with pervasive secondary potassium feldspar in clasts.
- An actinolite zone characterized by abundant actinolite-chalcopyrite-diopside-magnetite veins that crosscut breccias, diorite and plagioclase porphyry and by the presence of actinolite in vugs within hydrothermal breccias. The zone is elongate in a north-south direction within the core of the system on the east side of the fault. Actinolite veins and breccias have not been noted in the west zone. Associated with the veins are quite extensive potassium feldspar envelopes which tend to obliterate primary textures adjacent to the vein.
- A potassium feldspar - albite zone is arcuate around the biotite and actinolite zones. Almost all of the rock units in this area have undergone varying degrees of pervasive potassium feldspar alteration or veining. In the western part of the deposit, albite occurs as envelopes around microfractures and vuggy regions of the breccias, in addition to or in place of potassium feldspar.

## CALC-POTASSIC ALTERATION

Garnet alteration occurs in two areas (Figure 2), and does not have a uniformly concentric distribution as previously described (Hodgson *et al.*, 1976). Its occurrence is confined to the perimeter of the S19 pit, generally in areas of intense albitic and potassic alteration. In the western area, two drill holes contain brown, zoned, euhedral to massive garnet in hydrothermal veins or vugs within the albitic breccia at the 150 to 180-metre level. Primary textures of clasts have been overprinted by secondary potassium feldspar and vugs in the matrix are partially or wholly filled with an assemblage of albite, magnetite, garnet, calcite, epidote, zeolites, chlorite, pyrite and chalcopyrite.

The eastern area contains a body of massive brown garnet overprinted by magnetite and diopside, with abundant epidote veins and retrograde alteration minerals (unit 4). The timing of this replacement body is ambiguous and may not correspond with the garnet-epidote assemblage found elsewhere in the deposit.

## PROPYLITIC ALTERATION

A peripheral propylitic zone is generally developed outside the proposed pit (Figure 2). The rock units are weakly altered and commonly contain epidote-pyrite veins and disseminated epidote which may replace mafic minerals. Albite veining is diffuse and crosscuts all lithologies. Calcite-zeolite veins are also prominent but are post-mineral.

A pyrite zone is present in the north-east section of the Mount Polley property. It is characterized by abundant pyrite veins crosscutting the breccias and diorite. Veins sometimes contain accessory magnetite and chalcopyrite. The zone has undefined lateral extents and reaches beyond the mapped area. It has a potential length of more than 1.4 kilometres and minimum width of 200 metres. Most of the lithologies are pervasively altered to potassium feldspar and are crosscut by pyrite, epidote and albite veins.

## CONCLUSIONS

The Mount Polley alkalic porphyry deposit is part of a complex system involving a variety of intrusive bodies and hydrothermal breccias. It is further complicated by the overprinting of several alteration zones and related sets of veins.

Detailed mapping on a property-wide basis and extensive drill-core logging has yielded the following picture of Mount Polley summarized in Figure 3. The deposit is hosted by a diorite stock that contains volcanic xenoliths and screens. Plagioclase porphyry intrudes the diorite and forms the matrix to intrusion breccias. A series of four distinct hydrothermal breccias (actinolite, biotite, magnetite and albite) formed in the core of the system and provide the host to much of the mineralization. A zone of magnetite-garnet in the south-eastern part of the deposit may replace intrusive and/or volcanic rocks by skarn-type reactions, as suggested by Sutherland Brown (1967) and Simpson and Saleken (1990). Late to post-mineral dikes were intruded, following these main events.

During the main hydrothermal event, the core of the system was potassically altered. The most characteristic minerals of this zone are biotite, actinolite, diopside and magnetite. Numerous mineralized veins crosscut the breccias, with actinolite-diopside-chalcopyrite and chalcopyrite-magnetite-bornite veins being the most important. A discontinuous garnet-epidote zone, with lesser chlorite, zeolites and pyrite separates the potassic and propylitic zones. A propylitic assemblage of epidote, pyrite and albite fringes the entire deposit. A laterally extensive pyrite zone lies to the north-east.

Time	Intrusions	Brecciation	Alteration	Mineralization
	Lamprophyre Dike		none	
	Augite Porphyry Dike		none	
	KF Phyric Monzonite		KF (SR)	
	Augite Monzodiorite		SR (KF)	
	Plagioclase Porphyry		KF - MG - AC - CP DI - PY - SR	
Diorite	Potassic - Propylitic			

Figure 3. Summary diagram for the sequence of intrusive, breccia and alteration events at Mount Polley. The abbreviations are as follows: KF = potassium feldspar, SR = sericite, MG = magnetite, AC = actinolite, CP = chalcopyrite, DI = diopside and PY = pyrite.

## ACKNOWLEDGMENTS

I wish to thank Imperial Metals Corporation for access to the Mount Polley property and invaluable drill-log information. John Thompson is thanked for comments in the field and insightful ideas on the genesis of albitic alteration and skarn processes. The company of my field assistants, Jennifer Garrett and Julie Kadar, and their hard work was greatly appreciated over the last two summers. The following colleagues at the Mineral Deposit Research Unit are gratefully acknowledged for their help using the AUTOCAD program: A. Toma, R. Bartsch, P. Metcalfe and P. Lewis.

Fieldwork for this study was supported financially by the Mineral Deposit Research Unit at the University of British Columbia and it forms part of the project "Porphyry Copper-Gold Systems of British Columbia".

## REFERENCES

- Bailey, D.G. and Hodgson, C.J. (1979): Transported Altered Wall Rock in Laharic Breccias at the Cariboo-Bell Cu-Au Porphyry Deposit, British Columbia, *Economic Geology*, Volume 74, pages 125 - 128.
- Blanchet, P.H. and Godwin, C.I. (1972): Geolog System for Computer and Manual Analysis of Geologic Data from Porphyry and Other Deposits; *Economic Geology*, Volume 67, pages 796 - 813.
- Fraser, T.M., Godwin, C.I., Thompson, J.F.H. and Stanley, C.R. (1993): Geology and Alteration of the Mount Polley Alkalic Porphyry Copper-Gold Deposit, British Columbia (93A/12); in *Geological Fieldwork 1992*, Grant, B. and Newell, J.M., Editors, *B.C. Ministry of Energy, Mines and Petroleum Resources*, Paper 1993-1, pages 295 - 300.
- Gore, D., Nikic, Z.T. and Pesalj, R. (1992): Mount Polley; *Imperial Metals Corporation*, unpublished report, 11 pages.
- Hodgson, C.J., Bailes, R.J. and Verzosa, R.S. (1976): Cariboo-Bell; in *Porphyry Deposits of the Canadian Cordillera*, Sutherland Brown, A., Editor, *Canadian Institute of Mining and Metallurgy*, Special Volume 15, pages 388 - 396.
- Simpson, R. and Saleken, L.W. (1990): Cariboo-Bell Deposit; *Geological Association of Canada - Mineralogical Association of Canada - Canadian Geophysical Union*, Joint Annual Meeting, Volume 1, Trips 1 - 8, pages 13 - 21.
- Sutherland Brown, A. (1967): Cariboo-Bell; *B.C. Ministry of Energy, Mines and Petroleum Resources*, Annual Report 1966, pages 126 - 131.

## NOTES

**GEOLOGY AND MINERALIZATION IN THE  
NORTHERN PART OF THE IRON MASK BATHOLITH,  
KAMLOOPS, BRITISH COLUMBIA  
(92I/9, 10)**

**Clifford R. Stanley, James R. Lang and Lori D. Snyder,  
Mineral Deposit Research Unit, U.B.C**

*(MDRU Contribution # 037)*

**KEYWORDS:** Economic geology, porphyry, copper, gold, alkalic, Nicola volcanics, Pothook diorite, Sugarloaf diorite, Cherry Creek monzonite, Iron Mask, Quesnellia, hydrothermal alteration.

**INTRODUCTION**

The Iron Mask batholith is an earliest Jurassic (207±3 Ma; Ghosh 1993), composite alkalic intrusion located approximately 10 kilometres southwest of Kamloops, British Columbia (Figure 1). It lies in the southern part of the Quesnel Terrane, a volcanic arc that lay somewhere offshore of North America during the Late Triassic (Souther, 1992). The batholith is an elongate, northwest-trending body approximately 22 kilometres long and 5 kilometres wide, and intrudes volcanic and sedimentary rocks of the Upper Triassic Nicola Group (Preto, 1968). The batholith is exposed in the Iron Mask pluton to the

southeast and in the smaller Cherry Creek pluton to the northwest which are separated by a graben of down-faulted Eocene Kamloops Group volcanic and sedimentary rocks (Kwong, 1987).

The Iron Mask batholith is host to a number of alkalic porphyry copper-gold deposits. These include the Afton, Crescent, Pothook, Ajax East, Ajax West and Iron Mask deposits, all of which have been mined, and the Galaxy, Big Onion, DM and Python zones, all of which have published reserve figures (Kwong, 1987). With the exception of the Iron Mask underground mine, production in the district occurred between 1977 through 1991.

Previous authors (Preto, 1968; Northcote, 1974, 1976, 1977) have identified five principal intrusive units that form the Iron Mask batholith. Their interpretation of age relationships among the units was, from oldest to youngest, Iron Mask hybrid, Pothook diorite, serpentinized picrite, Sugarloaf diorite, and Cherry Creek diorite-

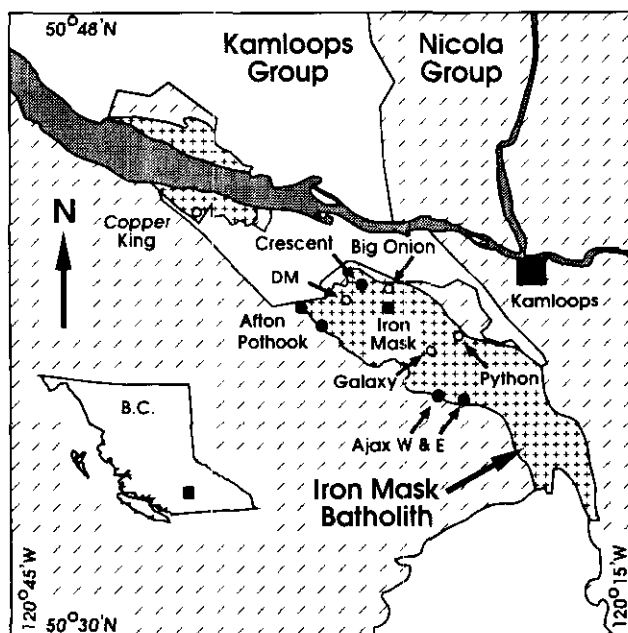


Figure 1. Generalized geological map of the Iron Mask batholith, showing locations of the principle mineral deposits (simplified from Kwong, 1977).

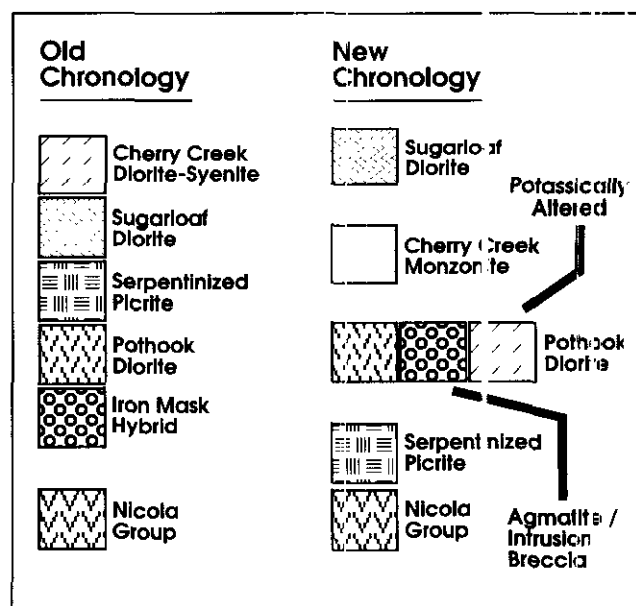


Figure 2. Chronology of the old and new interpretations of the volcanic and intrusive history of the Iron Mask batholith.

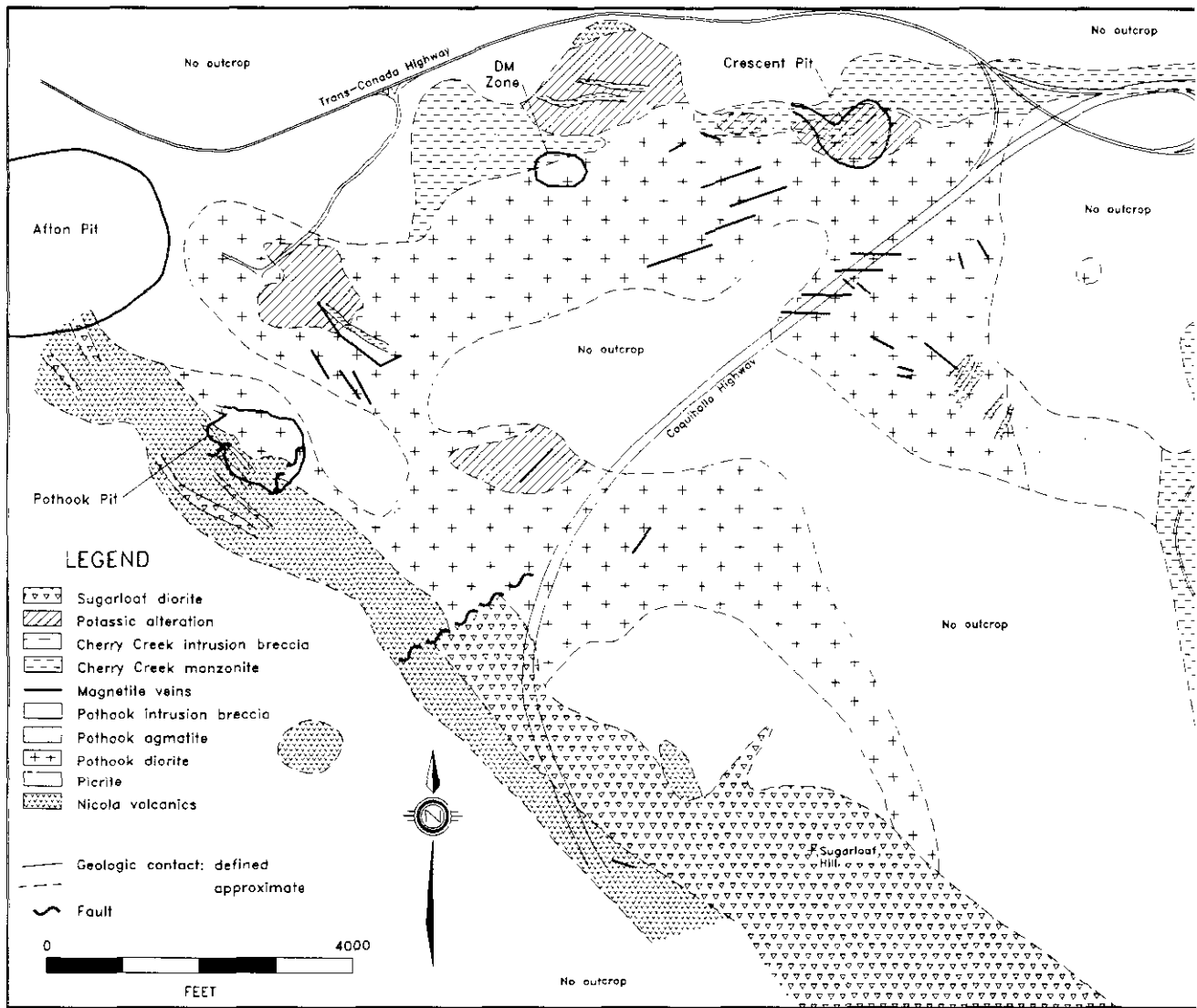


Figure 3. Geological map of the northern part of the Iron Mask pluton, Iron Mask batholith (map is continued on opposite page).

syenite (Figure 2). All of these units, except the serpentinized picrite, were considered to be comagmatic.

Snyder and Russell (1993a), based on mapping during the 1992 field season, suggested a revised chronological order for these intrusions (Figure 2) and more thoroughly described the relationships between them. Snyder and Russell (1994, this volume) do not consider the serpentinized picrite unit to be part of the intrusive suite of the batholith but rather interpret its occurrences as megaxenoliths of extrusive picrite entrained in the batholith. The new chronological order of intrusive phases of the batholith is, from oldest to youngest, Pothook diorite, Cherry Creek monzonite and Sugarloaf diorite (Figure 2). The Iron Mask hybrid is not recognized as a separate intrusive phase because it is now interpreted to be intrusion breccia and agmatite with a Pothook diorite matrix and Nicola volcanic clasts.

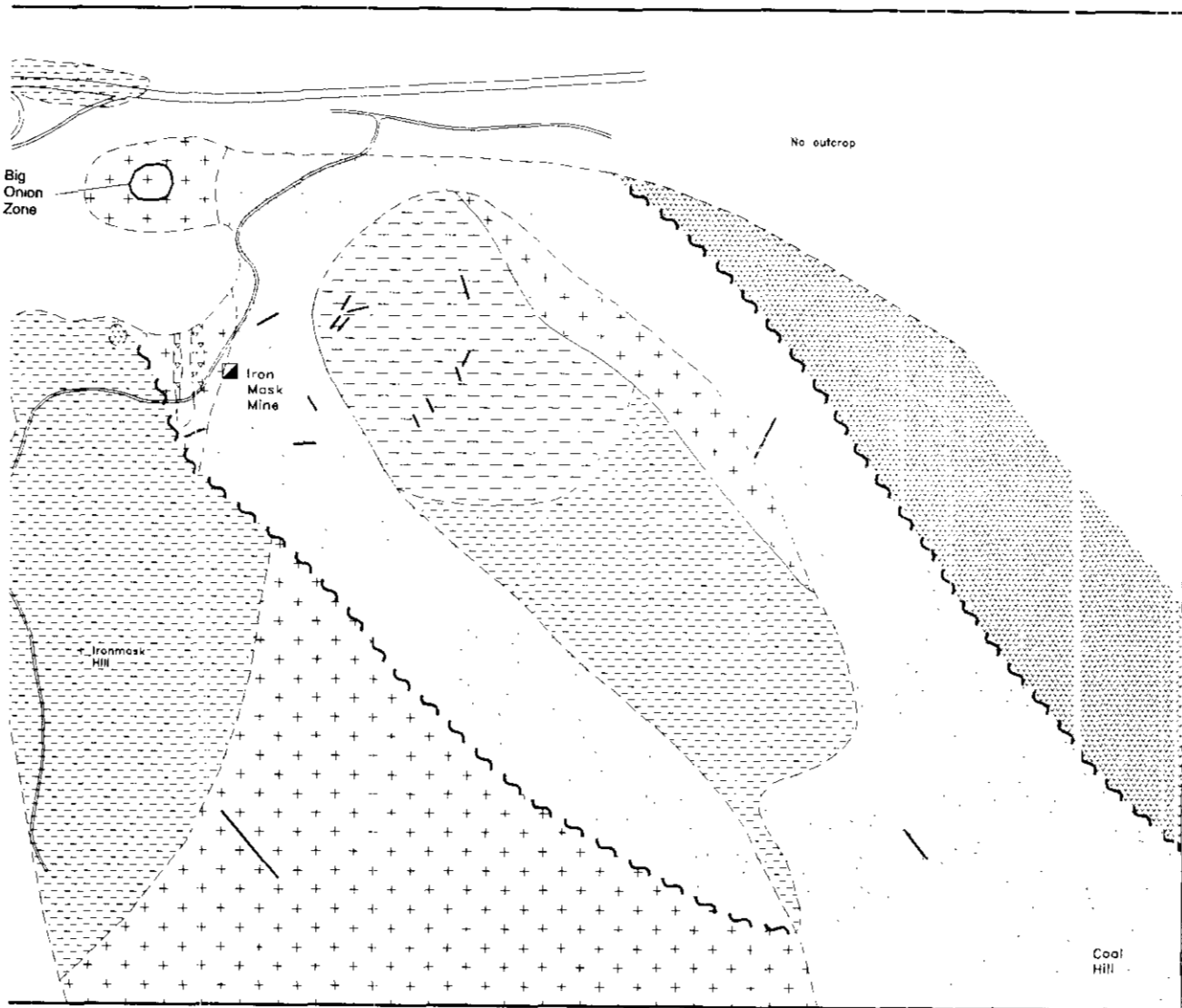
The following detailed description of the intrusive and volcanic units in and around the Iron Mask batholith is based on: 1:20 000-scale mapping of the batholith by Snyder during the summer of 1992, 1:2400-scale map-

ping of the north portion of the Iron Mask pluton by Stanley and Lang during the summer of 1993, 1:600-scale mapping of the Pothook and Crescent open pits by Stanley and Lang, respectively, during the summer of 1993, detailed logging of the Pothook and Crescent exploration drill-core by Stanley and Lang, also during the summer of 1993, and thin section petrography and other studies on samples collected by all three authors. A compilation map is presented in Figure 3.

## NICOLA GROUP

In the Iron Mask area, the Carnian to Norian Nicola group is comprised of six principle rock types. These units are interlayered and consist of:

- dark green to black, aphyric to plagioclase-phyric, massive basalt flows,
- maroon to dark grey, aphyric to sparsely plagioclase or augite-phyric, poorly bedded, ash to lapilli mafic tuffs and lesser blocky agglomerates,
- black, augite-phyric, massive basalt flows,



	Early	Late
Plagioclase (30 %)	—————	—————
Apatite (1 %)	—————	
Pyroxene (40 %)	—————	
Magnetite (15 %)	—————	—————
Biotite (10 %)		—————
K-feldspar (4 %)		—————
Hornblende (0 %)		

Figure 4. Igneous mineral paragenesis of the Pothook diorite.

- dark grey, crowded plagioclase-phyric andesite flows and feeder dikes,
- light green, well-bedded and sorted, ash to lapilli, andesite to dacite tuffs, and
- reddish, fine-grained, hematitic, poorly bedded to massive cherts up to 1 metre thick, and

Picritic basalts with olivine and clinopyroxene phenocrysts outcrop near the top of the Nicola succession

(Snyder and Russell, 1993b). Outside the batholith picrites are relatively fresh, are not serpentinized, and have cumulate and fragmental textures. Within the batholith, picrite occurs as large serpentinized ultramafic screens. A more detailed description of this unit is presented in Snyder and Russell (1994, this volume).

## POTHOOK DIORITE

Snyder and Russell (1993a) consider the Pothook diorite to be the oldest intrusive phase of the Iron Mask batholith. It is predominantly an equigranular, slightly foliated, plagioclase-augite diorite with late potassic biotite which encloses both plagioclase and augite inclusions. Up to 15% disseminated magnetite, accessory potassium feldspar, and minor disseminated apatite and titanite are also present (Figure 4). Toward the centre of the batholith, Pothook diorite is medium grained, near the margins of the intrusion it is fine to medium grained, and at intrusive contacts with Nicola Group it is chilled. Agophyses of Pothook diorite also intrude along faults and

steeply dipping depositional contacts within the volcanic host. Nicola volcanic rocks within 50 metres of the Pothook diorite have been contact metamorphosed to a biotite hornfels with up to 5% disseminated magnetite and less than 1% disseminated pyrite cubes.

Pothook diorite incorporated numerous xenoliths of volcanic and intrusive rocks. In places, especially near the margins of the diorite, the xenoliths are sufficiently abundant to form an intrusion breccia. A typical traverse toward these breccias begins in uncontaminated, fine or medium-grained

Pothook diorite, which becomes gradually more magnetite rich, and which then acquires a patchy textural variation which ranges from fine to medium grained. The proportion of xenoliths of Nicola volcanic rocks gradually increases until an intrusion breccia designation is required. These intrusion breccias continue to be magnetite rich and have significant textural variability in the matrix. The transition from normal Pothook diorite to intrusion breccia has been observed across distances of 50 to 250 metres.

The clasts in some of these breccias have reacted with and partially assimilated into the diorite matrix, forming agmatite. On the outcrop scale, these agmatites exhibit great textural variability from fine to very coarse grained, and consist predominantly of interlocking, randomly oriented grains of hornblende, biotite, plagioclase and magnetite. Commonly, fine, medium and coarse-grained varieties of agmatite are mutually crosscutting. Within zones of agmatite, Nicola clasts commonly have undergone different degrees of reaction with, and assimilation into, Pothook diorite.

Previous authors (Preto, 1968; Northcote, 1974, 1976, 1977) have included both the intrusion breccia and agmatite within the Iron Mask hybrid unit. Recognizing that both the intrusion breccia and the agmatite have a matrix consisting of Pothook diorite, the Iron Mask hybrid and Pothook diorite units are now thought to be coeval, and are here considered two different facies of a single intrusive phase.

The Pothook diorite contains abundant magnetite-apatite-actinolite veins, blebs, schleiren and breccias. These structures occur at millimetre to metre scales and may contain epidote, chlorite, pyrite and chalcopyrite,

both within the structures and in envelopes about them. Blebs and schleiren usually occur in large envelopes about major magnetite veins. The Magnet showing and similar major magnetite veins in the Iron Mask batholith are representative of these structures (Cann, 1979). These veins have strong structural controls trending northwest and east-northeast (*cf.* Stanley, 1994, this volume; Lang, 1994, this volume). The magnetite-bearing structures are hosted by fine to medium-grained Pothook diorite or by intrusion breccia with a fine or medium-grained Pothook diorite matrix; they probably formed from coalescing orthomagmatic fluids evolved from the Pothook diorite during late stage crystallization.

## CHERRY CREEK MONZONITE

The next intrusive phase is the Cherry Creek monzonite. This unit intrudes only Pothook diorite and agmatite, has no foliation, and occurs both as grey, very fine to fine-grained dikes which commonly have an aplitic texture, and as pink, medium-grained stocks. It is generally an equigranular, biotite monzonite with minor augite, accessory magnetite and apatite, and trace quartz (Figure 5; Snyder and Russell, 1993b). It also locally contains small miarolitic cavities filled with quartz. Where intruded as dikes, emplacement of Cherry Creek monzonite was controlled by structures oriented northwest and east-northeast within the Pothook diorite. No visible contact metamorphic effects were imposed upon the Pothook diorite by the Cherry Creek monzonite.

Snyder and Russell (1993a) recognized that, although some of the outcrops originally mapped (Kwong, 1977) as Cherry Creek diorite-syenite do, in fact, belong to the Cherry Creek monzonite, many are actually potassically altered Pothook diorite. Although some of these rocks are mineralogically equivalent to syenite, they probably never existed as syenite melts. The potassic alteration is pervasive and not substantially controlled by fractures. It selectively replaces plagioclase with potassium feldspar, but poikilitic biotite remains stable. Disseminated magnetite in the Pothook diorite was at least partially destroyed by this alteration, and augite was commonly replaced by epidote.

The intensity of pervasive potassic alteration varies across the batholith; in altered Pothook diorite it generates a wide, apparent compositional variation from diorite to syenite. In some cases, zones of pervasive alteration grade outward into fractures with 'potassic' alteration envelopes, demonstrating that locally the outer parts of these alteration zones formed from coalescing alteration envelopes. In other cases, fracture-controlled potassium metasomatism is a later, separate event (Lang, 1994, this volume).

Pervasive potassium metasomatism is spatially associated with the contacts between true Cherry Creek monzonite and Pothook diorite, and often obscures their precise locations. Whereas the margins of Cherry Creek monzonite intrusions tend to be strongly altered, the cores of the intrusions remain relatively fresh. Therefore,

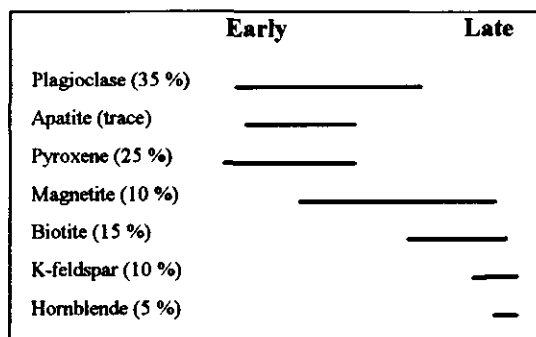


Figure 5. Igneous mineral paragenesis of the Cherry Creek monzonite.

this pervasive alteration style is thought to result from deuteric reaction of orthomagmatic fluids emanating from the Cherry Creek monzonite during the later stages of crystallization. This redefinition of the Cherry Creek unit indicates that it is substantially over-represented in previous maps of the batholith; Pothook diorite affected by pervasive potassium metasomatism should be considered an alteration facies of the Pothook diorite unit.

## SUGARLOAF DIORITE

The youngest intrusive phase of the Iron Mask batholith is the Sugarloaf diorite unit. This diorite has a sparsely to strongly crowded porphyritic texture with a phenocryst population which includes stubby hornblende, smaller augite, and plagioclase that commonly displays trachytic alignment. Phenocrysts are set in an aphanitic groundmass of plagioclase, potassium feldspar and disseminated magnetite, with locally significant pyrite and chalcopyrite (Figure 6; Snyder and Russell, 1993a). The Sugarloaf diorite was emplaced predominantly as a set of northwest-trending, steeply dipping dikes along the southwestern edge of the batholith and as lenticular bodies along northwesterly striking structures within the central part of the batholith. These dikes intrude Nicola Group more commonly than Pothook diorite, do not intrude the Cherry Creek monzonite, and are widest, most abundant, and, in some cases radially oriented, around Sugarloaf Hill, which is thought to be a volcanic neck and intrusive centre (Snyder and Russell, 1993b). The intrusive form of the Sugarloaf diorite resembles the classic hypabyssal volcanic neck at Shiprock, New Mexico (Press and Siever, 1978).

Sugarloaf diorite produced contact metamorphism in adjacent volcanic country rocks. This involved the wholesale recrystallization of mafic volcanic rocks to actinolite and plagioclase with abundant disseminated magnetite; total destruction of textures commonly precludes recognition of the volcanic protolith immediately adjacent to the intrusion. Contact metamorphic effects were not observed in Pothook diorite where it is intruded by dikes of Sugarloaf diorite. The more extensive recrystallization of volcanic rocks associated with emplacement of the small Sugarloaf diorite dikes may suggest that these dikes were intruded at higher temperatures than the Pothook diorite.

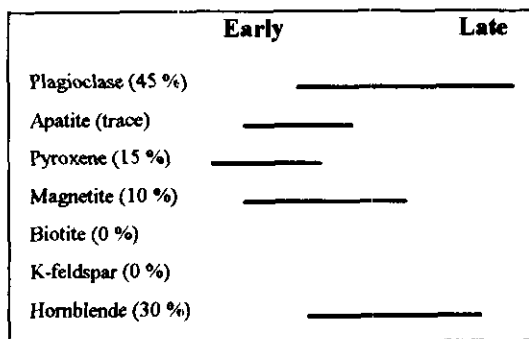


Figure 6. Igneous mineral paragenesis of the Sugarloaf diorite.

Alternatively, the probably higher volatile fugacity of the Sugarloaf phase, as indicated by its more porphyritic texture, may have more efficiently catalyzed recrystallization and metasomatism in texturally destructive hornfels.

After the Sugarloaf diorite was emplaced, another episode of hydrothermal alteration took place. This took the form of weakly to totally pervasive 'albitic' alteration. Albitization occurs only in intrusive rocks and, where less intense, fracture control was nominal. Where intense, alteration envelopes about fractures coalesce, producing a pervasive style of alteration. In the Pothook diorite, albite replaced plagioclase, augite and potassium feldspar, and chlorite replaced biotite. Where less intense, Pothook diorite is incompletely albitized in zones which are commonly restricted to fracture envelopes and in which plagioclase has suffered selective replacement by albite but biotite, augite and potassium feldspar remained stable. The Sugarloaf diorite has experienced only selective albitization. Albite replaced plagioclase and potassium feldspar, but hornblende generally remained stable. Sugarloaf diorite also contains blebs of epidote which may be related to this alteration event. Significant albitic alteration is restricted to the Pothook copper-gold deposit, the Big Onion zone, and to a few structurally controlled zones close to exposures of Sugarloaf diorite. Albitic alteration probably resulted from deuteric reaction of orthomagmatic fluid emanating from dikes of Sugarloaf diorite during their later stages of cooling.

## CONTRASTING STYLES OF COPPER-GOLD MINERALIZATION

The northern part of the Iron Mask pluton hosts the majority of porphyry copper-gold deposits in the Iron Mask batholith. Although the Afton and Iron Mask deposits were not physically accessible to study, two contrasting styles of mineralization have been recognized among the remaining deposits (Stanley, 1994, this volume; Lar g, 1994, this volume).

The Pothook and Big Onion deposits occur near contacts between Nicola volcanic units (including picrite) and the Pothook diorite. Dikes of Sugarloaf diorite intrude along and adjacent to this contact, and were probably the cause of the pervasive albitic alteration associated with these deposits. The deposits themselves are hosted by zones of high fracture and fault density, possibly due to the brittle behaviour of albitically altered rocks. These fractures control a through-going, vein-related potassic alteration that crosscuts earlier albitic alteration. Mineralization is hosted by Pothook diorite, Sugarloaf diorite and Nicola Group. It is predominantly associated with planar, crosscutting chlorite-magnetite (specular) hematite veins without significant envelopes, and hydrothermal breccias with a variety of millid volcanic and intrusive fragment types. Mineralization consists of pyrite, chalcopyrite and bornite, in order of decreasing abundance. In the Pothook zone, copper/gold ratios vary considerably across the deposit. A more

thorough description of the geology of the Pothook zone is presented in Stanley (1994, this volume).

The Crescent and DM deposits, and the smaller, intervening Audra zone, represent a different style of mineralization (Lang, 1994, this volume). These deposits are located near contacts between the Pothook diorite and Cherry Creek monzonite. Furthermore, the deposits have experienced pervasive potassic alteration and have high fracture and fault densities. Mineralization is hosted by biotite+potassium feldspar±quartz±epidote±magnetite veins, with chalcopyrite greater than pyrite. Biotite is commonly altered to chlorite. These sinuous veins occur in irregular stockworks and their biotite - potassium feldspar - magnetite envelopes form pseudobreccias of strongly altered and less altered Pothook diorite. Later quartz-calcite-matrix fault breccias and veins also host some mineralization, especially in the DM zone. In the Crescent zone copper/gold ratios are very constant. A more thorough description of the geology of the Crescent deposit is presented in Lang (1994, this volume).

## CONCLUDING STATEMENT

A revised intrusion history of the Iron Mask batholith, together with remapping of the northern part of the Iron Mask pluton, has provided significant new insight regarding the style of intrusion of the batholith, its cooling history, and its relationship to the country rocks. A more complete understanding of the styles and causes of mineralization in the field area has also been achieved. Improved insights into the nature of porphyry copper-gold deposits in the batholith have significant implications for both regional and local exploration.

## REFERENCES

Cann, R.M. (1979): Geochemistry of Magnetite and the Genesis of Magnetite-Apatite Lodes in the Iron Mask Batholith, British Columbia; unpublished M.Sc. thesis, *The University of British Columbia*, 196 pages.

Ghosh, D. (1993): Uranium-Lead Geochronology; in Porphyry Cu-Au Systems of British Columbia, Mineral Deposit Research Unit, *The University of British Columbia*, Annual Technical Report, pages 11.1-11.26.

Kwong, Y.T.J. (1987): Evolution of the Iron Mask Batholith and Associated Copper Mineralization; *B.C. Ministry of Energy, Mines and Petroleum Resources*, Bulletin 77.

Lang, J.R. (1994): Geology of the Crescent Alkalic Porphyry Cu-Au Deposit, Afton Mining Camp, Kamloops, British Columbia (92 I/9, 10); in *Geological Fieldwork 1993*, Grant, B. and Newell J.M., Editors, *B.C. Ministry of Energy, Mines and Petroleum Resources*, Paper 1994-1, this volume.

Northcote, K.E. (1974): Geology of the Northwest Half of the Iron Mask Batholith; in *Geological Fieldwork 1974*, *B.C. Ministry of Energy, Mines and Petroleum Resources*, Paper 1975-1, pages 22-26.

Northcote, K.E. (1976): Geology of the Southeast Half of the Iron Mask Batholith; in *Geological Fieldwork 1976*, *B.C. Ministry of Energy, Mines and Petroleum Resources*, Paper 1977-1, pages 41-46.

Northcote, K.E. (1977): Geological Map of the Iron Mask Batholith (92I/9W and 10E); *B.C. Ministry of Energy, Mines and Petroleum Resources*, Preliminary Map No. 26 and accompanying notes, 8 pages.

Press, F. and Siever, R. (1978): *Earth*; *W.H. Freeman and Company*, San Francisco, 649 pages.

Preto, V.A.G. (1968): Geology of the Eastern Part of the Iron Mask Batholith, *B.C. Ministry of Mine and Petroleum Resources*, *Annual Report 1967*, pages 137-147.

Snyder, L.D. and Russell, J.K. (1993a): Field Constraints on Diverse Igneous Processes in the Iron Mask Batholith (92I/9,10); in *Geological Fieldwork 1992*, Grant, B. and Newell J.M., Editors, *B.C. Ministry of Energy, Mines and Petroleum Resources*, Paper 1993-1, pages 281-286.

Snyder, L.D. and Russell, J.K. (1993b): Petrology and Geochemical Aspects of Rocks in the Iron Mask Batholith; in *Porphyry Cu-Au Systems of British Columbia*, *Mineral Deposit Research Unit, The University of British Columbia*, Annual Technical Report, pages 5.0.0-5.2.15.

Snyder, L.D. and Russell, J.K. (1994): Petrology and Stratigraphic Setting of the Kamloops Lake Picritic Basalts, Quesnellia Terrane, South-central B.C.; in *Geological Fieldwork 1993*, Grant, B. and Newell J.M., Editors, *B.C. Ministry of Energy, Mines and Petroleum Resources*, Paper 1994-1, this volume.

Souther, J.G. (1992): Volcanic Regimes; in *Geology of the Cordilleran Orogen in Canada*, Gabrielse, H. and Yorath, C.J., Editors, *Geological Survey of Canada*, Decade of North American Geology Project, Paper No. 4, pages 457-490.

Stanley, C.R. (1994): Geology of the Pothook Alkalic Porphyry Cu-Au Deposit, Afton Mining Camp, British Columbia (92 I/9, 10); in *Geological Fieldwork 1993*, Grant, B. and Newell J.M., Editors, *B.C. Ministry of Energy, Mines and Petroleum Resources*, Paper 1994-1, this volume.



**GEOLOGY OF THE POTHOOK  
ALKALIC COPPER-GOLD PORPHYRY DEPOSIT,  
AFTON MINING CAMP, BRITISH COLUMBIA  
(92I/9, 10)**

**Clifford R. Stanley, Mineral Deposit Research Unit, U.B.C.**  
(MDRU Contribution # 035)

**KEYWORDS:** Economic geology, porphyry, copper, gold, supergene, alkalic, Nicola, Pothook, Sugarloaf, Cherry Creek, diorite, monzonite, Iron Mask, Quesnellia.

**INTRODUCTION**

The Pothook deposit is one of several alkalic porphyry copper-gold deposits (Afton, Crescent, Ajax East, Ajax West) developed in the Afton mining camp, located 10 kilometres west of Kamloops, British Columbia. These deposits are all hosted by the Iron Mask batholith, a large composite alkalic intrusion of earliest Jurassic age that intrudes latest Triassic Nicola volcanic rocks of the Quesnellia oceanic island arc terrain (Souther, 1992). The Pothook deposit is located on the southwestern edge of the Iron Mask batholith, approximately 750 metres south-east of the much larger Afton copper-gold deposit (Figure 1). It contained a geological reserve of 3.26 million tonnes grading 0.40% copper and 0.16 gram per tonne gold (\$0.40 copper equivalent cut-off; Bond, 1985).

Between October 1986 and September 1988, Afton Operating Corporation, a division of Teck Corporation, mined 2.60 million tonnes of ore with an average grade of 0.35% copper and 0.21 gram of gold per tonne from an open-pit, with a stripping ratio of 1:1.9 (L. Tsang, personal communication, 1993).

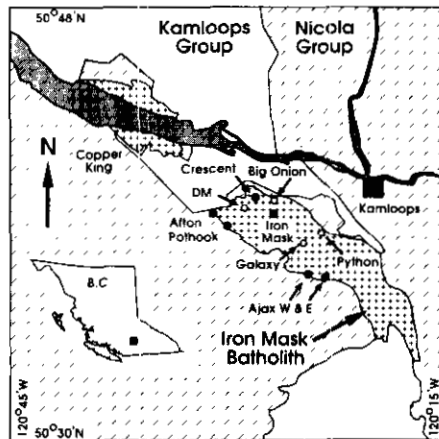


Figure 1. Generalized geological map of the Iron Mask batholith, showing locations of the principle mineral deposits (after Kwong, 1977).

Detailed open-pit mapping at 1:300 scale, more regional mapping of the area around the Pothook deposit at 1:2400 scale, and drill-core logging carried out during the summer of 1993 have documented the complicated geological history of the deposit. An open-pit map of the Pothook deposit is presented in Figure 2.

**GEOLOGICAL HISTORY**

The geological history of the Pothook zone is summarized in Table 1 and a full description of the geological units and events is presented in chronological order below.

**LATE TRIASSIC**

Several different volcanic lithologies act as host-rocks for the Iron Mask batholith in the deposit area. These consist of: dark green to black, aphyric to plagioclase-phyric, massive basalt flows; maroon to dark grey, aphyric to sparsely plagioclase or augite-phyric, poorly bedded, ash to lapilli mafic tuffs and lesser blocky agglomerates; black, crowded, augite-phyric, massive basalt flows; dark grey, crowded plagioclase-phyric andesite flows and feeder dikes; and dark green to black, crowded augite-phyric picrite flows (Snyder and Russell, 1993b). These units comprise the Carnian to Norian (latest Triassic) Nicola Group on the southwestern edge of the Iron Mask batholith (Preto, 1977).

**EARLY JURASSIC**

The Nicola Group was intruded during the earliest Jurassic (at approximately 2073 Ma; Ghosh, 1993) by the Iron Mask batholith. Several intrusive bodies comprise the batholith; all are exposed in the Pothook open pit.

**POTHOOK DIORITE**

The first to intrude was the Pothook diorite phase, a predominantly fine to medium-grained, equigranular, plagioclase-augite diorite with late poikilitic biotite containing both plagioclase and augite inclusions (Snyder and Russell, 1993a). Disseminated magnetite in variable concentrations up to 10%, and accessory potassic feldspar and apatite also occur. The Pothook diorite incorporated

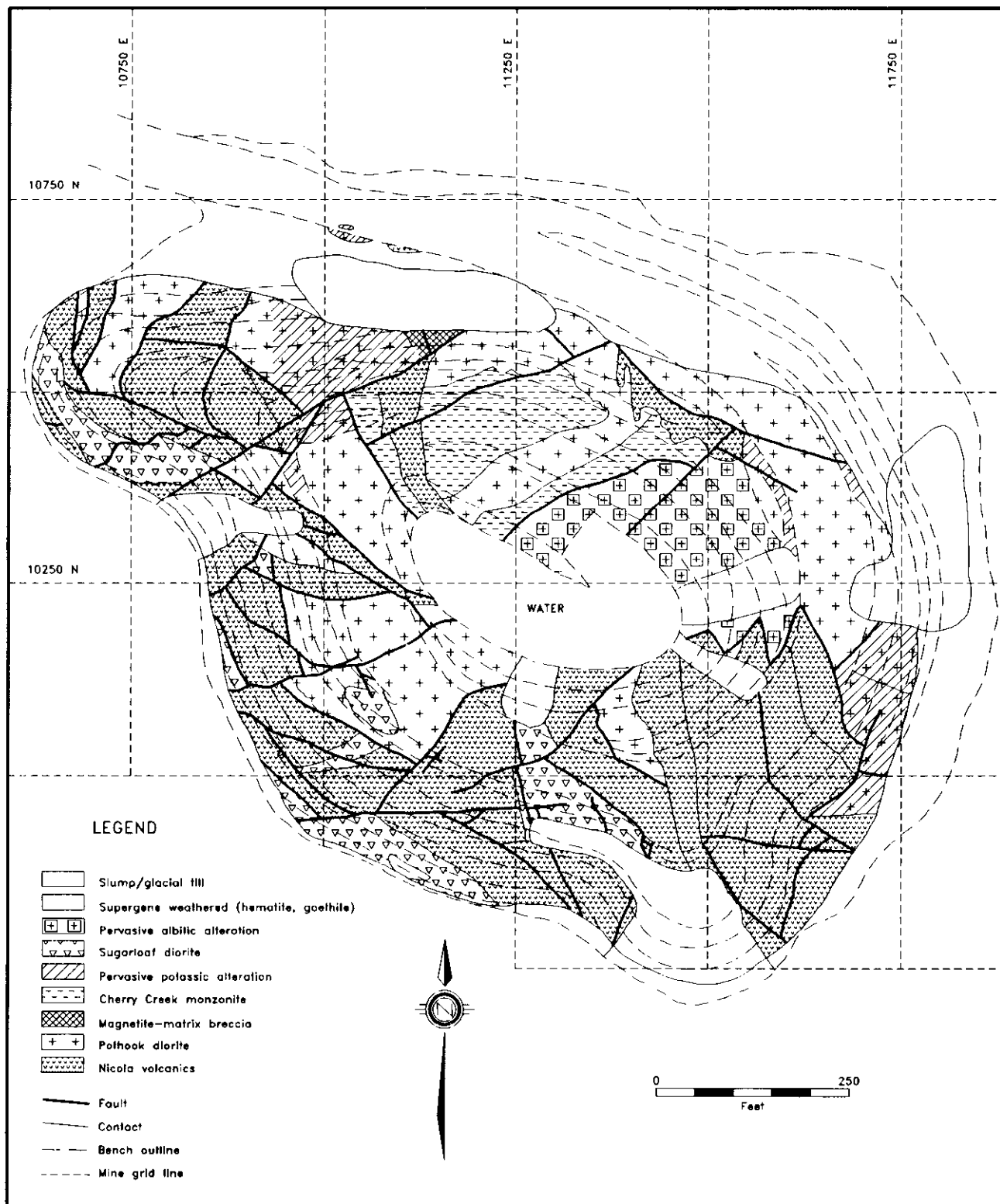


Figure 2. Geological map of the Pothook alkalic porphyry copper-gold deposit open pit.

**TABLE 1**  
**SUMMARY OF CHRONOLOGY OF INTRUSIVE, STRUCTURAL,**  
**ALTERATION/METAMORPHISM/WEATHERING EVENTS IN THE POTHOOK ALKALIC PORPHYRY**  
**COPPER-GOLD DEPOSIT**

Event	Age	Intrusion	Faulting	Alteration / Metamorphism / Weathering
1	earliest Jurassic	Fine to medium-grained Pothook diorite intrudes Nicola volcanics		Hornfels in adjacent Nicola volcanics
2	earliest Jurassic	Medium-grained Pothook diorite intrudes fine to medium-grained Pothook diorite		
3	earliest Jurassic		Steep NNW and ENE faulting disrupts intrusive contacts	
4	earliest Jurassic			Magnetite-apatite-actinolite blebs, veins and breccias cut Pothook diorite
5	earliest Jurassic	Cherry Creek monzonite intrudes earlier Pothook diorite phase		
6	earliest Jurassic			Pervasive potassic alteration - K-spar replacement / mag destruction in Pothook diorite
7	earliest Jurassic		Steep NNW and ENE faulting disrupts intrusive contacts	
8	earliest Jurassic	Sugarloaf diorite dikes intrude volcanics and fine to medium-grained Pothook diorite		act-plag hornfels contact metamorphic replacement of Nicola volcanics
9	earliest Jurassic			Pervasive albitic alteration - alb replacement of feldspar and aug. chl replacement of biot
10	earliest Jurassic			K-feldspar-epidote veins cut Pothook diorite and Cherry Creek monzonite
11	earliest Jurassic		Steep NNW and ENE faulting disrupts intrusive contacts	
12	earliest Jurassic			Iron-oxide-Cu-sulphide (chlorite-epidote) veins and breccias cut all lithologies
13	earliest Jurassic			Chlorite / kaolinite veins fill joints and microfractures in all lithologies
14	earliest Jurassic			Calcite veins and crackle zones cut all lithologies
15	Eocene		Shallow NW faulting throws tops to SW	
16	Eocene	Aphyric mafic dikes associated with Kamloops Group volcanics cut Pothook diorite		
17	Eocene			Quartz veins cut all lithologies
18	Eocene to Pleistocene			Supergene weathering dissolves cpy, precipitates native Cu, chal and earthy hematite
19	Eocene to Pleistocene		Steep NW reverse faulting down drops supergene-weathered zones into grabens	
20	Pleistocene			Glacial erosion produces current exposure level

mag=magnetite; act= actinolite; plag-plagioclase; alb-albite; aug-augite; chl-chlorite; biot-biotite; cpy-chalcocite; chal=chalcocite

numerous blocks of volcanic rocks as xenoliths within the intrusion. In places, especially near the margins of the diorite, these xenoliths are sufficiently abundant to comprise an intrusion breccia. Apophyses of Pothook diorite also intruded along faults and steeply dipping depositional contacts in the volcanic hostrocks. A fine-grained chilled margin of the diorite occurs at the intrusive contacts with these volcanics. Volcanic rocks adjacent to the diorite contact recrystallized to a biotite hornfels containing less than 1% disseminated pyrite cubes and disseminated magnetite.

A medium-grained variety of Pothook diorite was intersected at depth in exploration drill-holes. This later variety intrudes the fine to medium-grained Pothook diorite variety, but is otherwise petrologically similar. It is not observed to intrude, nor contain xenoliths of, Nicola volcanic rocks.

After the Pothook diorite intrusion had cooled sufficiently to allow brittle fracture, an episode of largely steep faulting disrupted the diorite-volcanic contact and juxtaposed volcanic rocks, without contact metamorphic recrystallization effects, and diorite. Displacements along these numerous, steeply dipping faults (most have dips >70) are probably vertical, appear to be generally less than 100 metres, and several sets of fault orientations were observed (NNW and ENE; Figure 3). This faulting appears to predate the pervasive potassic alteration described below.

After and probably during this steep faulting, magnetite-apatite-actinolite veins, blebs, schleiren and breccias formed along dilatant fractures. These fractures also occasionally contain epidote and chlorite, both within the structures and in alteration envelopes surrounding them.

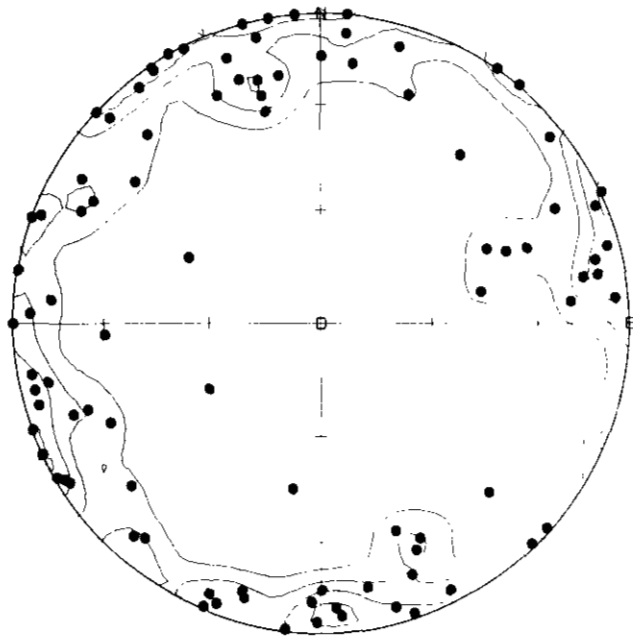


Figure 3. Stereonet of poles to steeply dipping faults cutting Pothook diorite and Nicola volcanics ( $n = 97$ ).

Blebs and schleiren tend to occur in large envelopes about major magnetite veins. The Magnet showing, and probably other magnetite veins in the Iron Mask batholith, formed at this time (Cann, 1979). In the Pothook deposit area, all of these magnetite-bearing structures are hosted by the fine to medium-grained Pothook diorite or by intrusion breccia with a fine to medium-grained Pothook diorite matrix. These magnetite-bearing structures may have formed from coalescing orthomagmatic hydrothermal fluids evolved from other, still molten, parts of the Pothook diorite during late stage crystallization.

### CHERRY CREEK MONZONITE

The Cherry Creek monzonite phase of the Iron Mask batholith was next to intrude. In the Pothook area, it intruded only Pothook diorite (Stanley *et al.*, 1994, this volume). This intrusion is generally a very fine grained, equigranular, potassium feldspar-plagioclase-biotite-augite monzonite with accessory magnetite and apatite, and trace quartz (Snyder and Russell, 1993a). It also contains small miarolitic cavities filled with quartz, and locally exhibits an aplitic texture. Its emplacement was apparently controlled by pre-existing structures within the Pothook diorite; it does not intrude Nicola volcanic rocks in the Pothook area (Stanley *et al.*, 1994). No contact metamorphic effects were observed in Pothook diorite adjacent to the Cherry Creek monzonite.

A generally pervasive potassic alteration occurs within but near the margins of the Cherry Creek monzonite and in Pothook diorite adjacent to exposures of Cherry Creek monzonite in the open pit. This alteration involved the 'selective pervasive' replacement of plagioclase by potassium feldspar in both phases, and the partial destruction of disseminated magnetite in the Pothook diorite. Biotite remained stable, but augite was commonly replaced by epidote. At the margins, this 'selective pervasive' alteration grades outward into fractures with potassic alteration envelopes, indicating that at least the outer parts of these alteration zones formed from coalescing alteration envelopes. The close spatial association between this alteration and the monzonite suggests that the alteration is probably deuteric and was related to and occurred during the late stages of cooling of the monzonite. The widespread nature of this alteration, and the pink colour imparted by the potassium feldspar, have caused pervasive, potassically altered fine to medium-grained Pothook diorite to be confused with the fine-grained Cherry Creek monzonite in the past (Stanley *et al.*, 1994, this volume). In the Pothook open-pit, this early pervasive potassic alteration is restricted to the north wall, adjacent to and above the exposure of Cherry Creek monzonite.

After intrusion of the Cherry Creek monzonite, additional steep faulting took place. Displacements occurred largely along pre-existing structures, and this further disrupted intrusive contacts along the southwest edge of the batholith.

## SUGARLOAF DIORITE

The second period of faulting was followed by the intrusion of the Sugarloaf diorite into earlier phases of the Iron Mask batholith and surrounding rocks. This diorite contains large, sparse to crowded, stubby hornblende phenocrysts, generally smaller augite and commonly trachytically aligned plagioclase phenocrysts. These are set in an aphanitic groundmass of plagioclase and potassium feldspar with disseminated magnetite (Snyder and Russell, 1993a). The Sugarloaf diorite was emplaced as a set of northwest-trending, steeply dipping dikes along the southwestern edge of the batholith. These intrude Nicola volcanics more commonly than Pothook diorite, do not intrude the Cherry Creek monzonite, and are widest, most abundant, and, in some cases radially oriented, around Sugarloaf Hill, which is thought to be a volcanic neck and intrusive centre (Snyder and Russell, 1993b). As such, the intrusive form of the Sugarloaf diorite resembles the classic hypabyssal volcanic neck at Shiprock, New Mexico (Press and Siever, 1978).

Sugarloaf diorite produced contact metamorphism in adjacent volcanic rocks. This involved the complete recrystallization of mafic volcanic rocks to an actinolite-plagioclase hornfels with abundant disseminated magnetite. This contact metamorphism was texturally destructive so the protoliths of amphibolitized Nicola volcanic rocks cannot be ascertained. No contact metamorphic effects are apparent in Pothook diorite where it is intruded by the Sugarloaf diorite dikes, probably because of the low hydration state of the Pothook diorite and the stabilities of the minerals comprising it under those metamorphic conditions. The more extensive recrystallization of volcanic hostrocks associated with emplacement of the small Sugarloaf diorite dikes may suggest that these dikes were intruded at higher temperatures than the Pothook diorite. Alternatively, the probably higher volatile fugacity of the Sugarloaf phase, as indicated by its more porphyritic texture, may have more efficiently catalyzed recrystallization and metasomatism, forming the higher grade hornfels.

Another stage of hydrothermal alteration took place after intrusion of the Sugarloaf diorite. This took the form of partial to pervasive albitic alteration and was confined to the intrusive rocks. This alteration becomes pervasive where envelopes surrounding fractures coalesce. It probably occurred during cooling of the Sugarloaf diorite, and may also have been deuteric. In the Pothook diorite, albite replaced plagioclase, augite and potassium feldspar, and chlorite replaced biotite. Moderate but subequal amounts of chalcopyrite and pyrite precipitation accompanied this alteration. This albitic alteration is most intense (pervasive) on the southeast wall of the open pit, below the ramp, where the Pothook diorite consists almost completely of albite. Elsewhere, Pothook diorite is incompletely albitized, occasionally in fracture envelopes, where plagioclase is selectively but pervasively replaced by albite but chlorite has not replaced biotite, and augite and potassium feldspar remained stable. The Sugarloaf diorite is only 'selective pervasively' albitized. Al-

bite replaced plagioclase and potassium feldspar, but hornblende generally remained stable. Sugarloaf diorite also contains blebs of epidote thought to be related to this alteration event.

The pervasive albitic alteration is overprinted by fracture-controlled potassic alteration represented by through-going potassium feldspar-biotite-epidote veins. These were strongly controlled by steeply dipping, north-northwest-striking fractures (Figure 4) and are restricted to the Pothook diorite and Cherry Creek monzonite intrusions. These veins are not significantly dilatant but are continuous across 20 vertical and 30 horizontal metres and in many places constitute 'sheeted' vein sets. During this hydrothermal alteration, different vein and envelope alteration mineral assemblages were produced in different lithologies. Specifically, in unaltered to moderately albitized Pothook diorite and Cherry Creek monzonite, the veins are primarily filled by potassium feldspar and biotite and have epidote envelopes. In pervasively albitized Pothook diorite, the veins are commonly filled by epidote and have potassium feldspar and biotite envelopes. In pervasively potassically altered Pothook diorite, the veins are generally filled only by epidote. All of these potassium feldspar - epidote veins contain small but subequal amounts of chalcopyrite and pyrite, and are well developed on the southeast wall of the open pit above the ramp, and along the north wall of the open pit just above the ramp on the lower benches. This structurally controlled potassic alteration introduced a small amount of copper and gold mineralization, as chalcopyrite and bornite, in the veins.

Following the episode of fracture-controlled potassic alteration, further steep faulting dissected many of the Sugarloaf diorite dikes and through-going potassium feld-

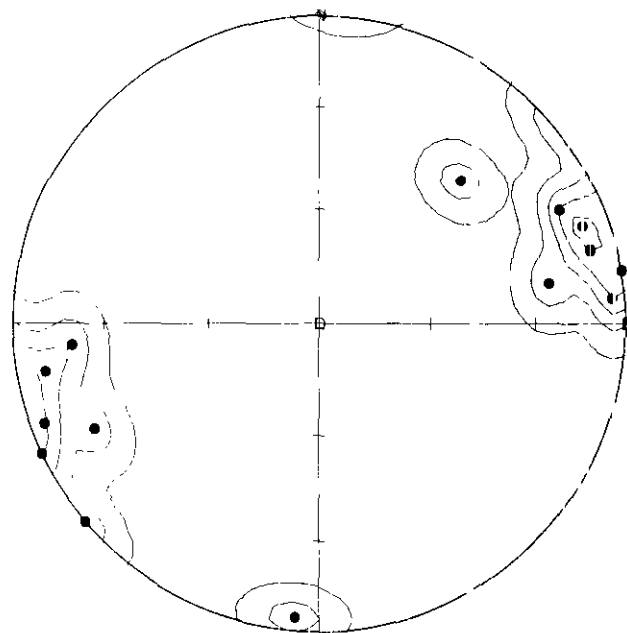


Figure 4. Stereonet of poles to structurally controlled potassium feldspar - epidote veins ( $n = 10$ ).

spar-epidote veins, and further disrupted the margin of the Iron Mask batholith. Much of this movement took place along pre-existing structures.

### COPPER-GOLD MINERALIZATION

None of the previously described pervasive or fracture-controlled hydrothermal alteration events is characterized by the introduction of significant amounts of copper to the Pothook area. The copper ore-forming event is represented by iron oxide - sulphide veins. On the southwest side of the open-pit, these veins are characterized by a chlorite-pyrite-chalcopyrite-magnetite-(specular) hematite mineral assemblage, whereas on the northeast side they contain chalcopyrite, bornite and magnetite. These veins, like the potassium feldspar-epidote veins that they cut, were not significantly dilatant. Similarly, they also have a preferred orientation approximately perpendicular to the orientation of the potassium feldspar - epidote veins, ranging from west-southwest to northwest with dips generally greater than 45 (Figure 5). The density of these mineralized veins appears to control ore grade, and produced some very significant copper and gold concentrations (occasionally up to 2% Cu and 2 g/t Au in exploration drilling samples). Where these veins cut Nicola volcanic rocks or their metamorphosed equivalents, significant chlorite selvages and envelopes are developed. Where they cut intrusive rocks, epidote envelopes and selvages predominate on the vein margins. These veins are not through-going and tend to dissipate into micro-fractures with epidote or chlorite envelopes. Previously existing fault zones are also at least partially filled by these iron oxide - sulphide veins.

In the centre of the open pit, and seen only in drill core, there is a large body of hydrothermal breccia that contains rotated and clasts of Pothook diorite, Cherry

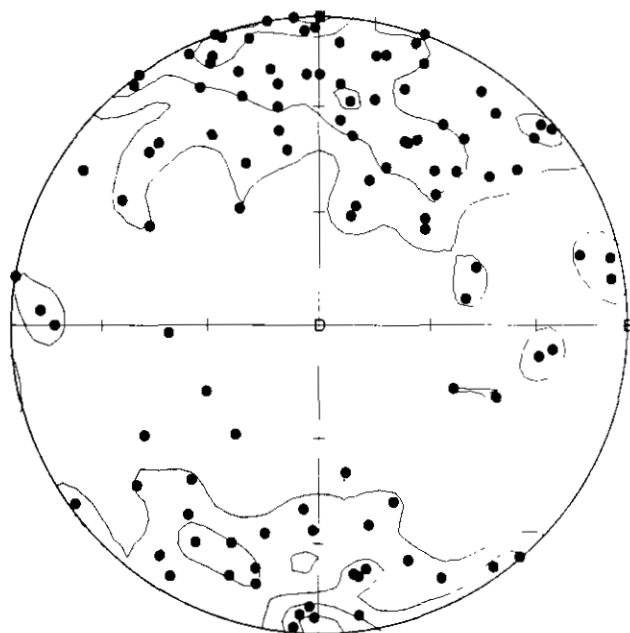


Figure 5. Stereonet of poles to iron oxide - sulphide veins (n = 112).

Creek monzonite, Sugarloaf diorite, and Nicola volcanics in a matrix of rock flour, chlorite and pyrite, with subordinate amounts of magnetite, chalcopyrite and bornite. In places, especially toward the centre of the breccia, these clasts are well rounded due to milling, range in size from 5 to 100 millimetres, and are clast supported. Toward the margins of the breccia, fragments are larger and more angular, and the breccia grades into a crackle zone with unrotated fragments in a disrupted stockwork of iron oxide - sulphide veins. As such, the hydrothermal breccia and veins are interpreted to be genetically related.

The mineralizing episode that produced the sulphide-bearing veins and breccia was followed by, or possibly evolved into, a propylitic episode of chlorite veining without significant amounts of associated copper or gold mineralization. Chlorite veinlets fill narrow fractures at all scales, from large through-going joints down to microfractures, in both volcanic and intrusive rocks. They are responsible for the predominantly dark colour of rock exposures in the open pit because blasting has broken the rocks along these veins, exposing dark green chlorite. This chlorite veining event involved no other alteration minerals, except for minor amounts of calcite and disseminated pyrite intergrown with the chlorite. Chlorite veins do not occur in pervasive albittically altered Pothook diorite. Rather, late kaolinite-calcite-filled microfractures are prevalent (Bond, 1985). These veins may be the equivalent to the chlorite veins, but contain no chlorite because of the lack of iron and magnesium in intensely albittized Pothook diorite.

Calcite veins crosscut the propylitic chlorite veins. In the intrusive units, these veins consist solely of calcite with no associated alteration envelopes. In the Nicola volcanic rocks, they are commonly associated with talc and serpentine, and have chlorite selvages. Calcite veins have no preferred orientation, and are not through-going. In general, wider calcite veins tend to be truncated by smaller, crosscutting calcite veins. Wider calcite veins are generally isolated from each other, and thus are rarely widespread and abundant enough to form crackle zones. Nevertheless, the overall distribution of these calcite veins suggest that the rocks have been intensively shattered, in spite of the relative absence of large crackle zones. The calcite veins postdate the sulphide-bearing veins and probably formed from lower temperature fluids. They also partially fill pre-existing fault zones.

### EOCENE

Another episode of faulting followed the mineralizing and alteration events. Unlike the earlier episodes of faulting, movement occurred along relatively shallow planes with southeasterly strikes and dips generally less than 30 to the southwest (Figure 6). Numerous faults with this orientation cut the upper southwest wall of the open pit, and display spoon-like, concave-upward (listric) forms. The displacement direction is generally to the southwest, and movements of up to 50 metres are indicated on individual fault planes. Given the number of these faults, the main mass of Pothook diorite and Sugar-

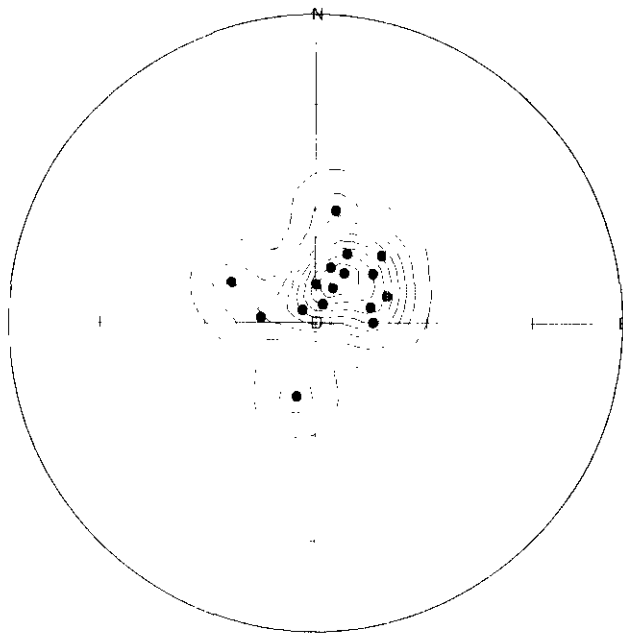


Figure 6. Stereonet of poles to shallow listric faults with southwesterly directed throw (n = 16).

loaf diorite dikes above these faults may have been displaced significant distances from the margin of the batholith (up to or exceeding 250 m) onto unmetamorphosed Nicola volcanics. This stage of faulting may reflect unroofing of the batholith, possibly during a period of extensional tectonics that affected the region during the Eocene (Souther, 1992).

Late, relatively rare mafic dikes intruded the Pothook area during the Eocene. These are aphyric to sparsely plagioclase phyrlic and are unaltered. They may be feeder dikes to the mafic volcanic rocks in the Eocene Kamloops Group, which fills grabens formed during extension (Souther, 1992).

Rare, late quartz-calcite-chlorite veins cut through all lithologies in the open pit. They partially fill all faults, including those with shallow dips, and previously formed veins with open spaces. They also fill shallow-dipping fractures oriented parallel to the shallow-dipping 'detachment' faults. These veins contain amethystine quartz and may be related to hydrothermal activity associated with Kamloops Group mafic volcanic feeder dikes.

During a period of late Tertiary supergene weathering, some of the chalcopyrite and bornite was destroyed and replaced by native copper, chalcocite and earthy hematite. Pyrite was also partially destroyed and replaced by earthy hematite and goethite during this supergene event. This weathering appears to have occurred without significant supergene enrichment, but local movements into adjacent fractures undoubtedly occurred. This relative lack of copper mobility was probably due to the high calcite and low pyrite abundances in the deposit. The relative absence of pyrite limited the amount of acid that could be produced during weathering, and the calcite neutralized any acid that was produced. This prevented descending meteoric fluids becoming sufficiently acidic to transport copper downward to form a supergene enrichment

blanket. Instead, the meteoric fluids caused the destruction of primary copper sulphide mineralization and the formation of secondary native copper and chalcocite. This produced a supergene blanket without copper enrichment (*cf.* Kwong, 1987). This weathering is predominantly fracture controlled, often occurring in open spaces thought to be originally filled by calcite, and penetrates to depths of up to 50 metres below the bedrock surface in unfractured rocks and to depths greater than 200 metres along faults.

Finally, further movement on pre-existing, northwest-striking faults down-dropped supergene weathered material into grabens where they were protected from subsequent Pleistocene glacial erosion.

## ORE DISTRIBUTION

Copper and gold grades in both exploration drill-holes and production blast-holes were examined to assess lithological and structural controls on mineralization. Scatterplots of copper and gold concentrations are presented in Figure 7. This demonstrates that copper and gold concentrations are not well correlated, and that, in general, high copper concentrations occur in samples with relatively low gold grades, and *vice versa*. This lack of correlation between copper and gold grade is different from most other alkalic porphyry copper-gold deposits, which commonly exhibit strongly correlated copper and gold concentrations, and relatively constant copper/gold ratios within individual deposits (average ratios in individual deposits range from 10 000 to 25 000 Stanley, 1993).

Figures 8 and 9 are bubble plots of copper and gold blast-hole assays from the 2340-foot bench in the Pothook open pit. Higher copper grades exhibit a strong structural control and define trends with variable strikes. Many of these trends can be traced directly into fault zones mapped on the 2340-foot bench (Figure 2). These

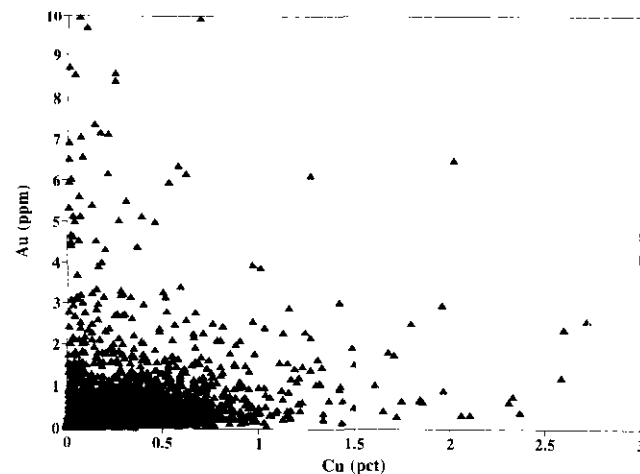


Figure 7. Scatterplot of exploration drill-hole and production blast-hole copper and gold assays from the 2100, 2160, 2220, 2280, 2340 and 2400-foot benches in the Pothook open pit (n = 3992).

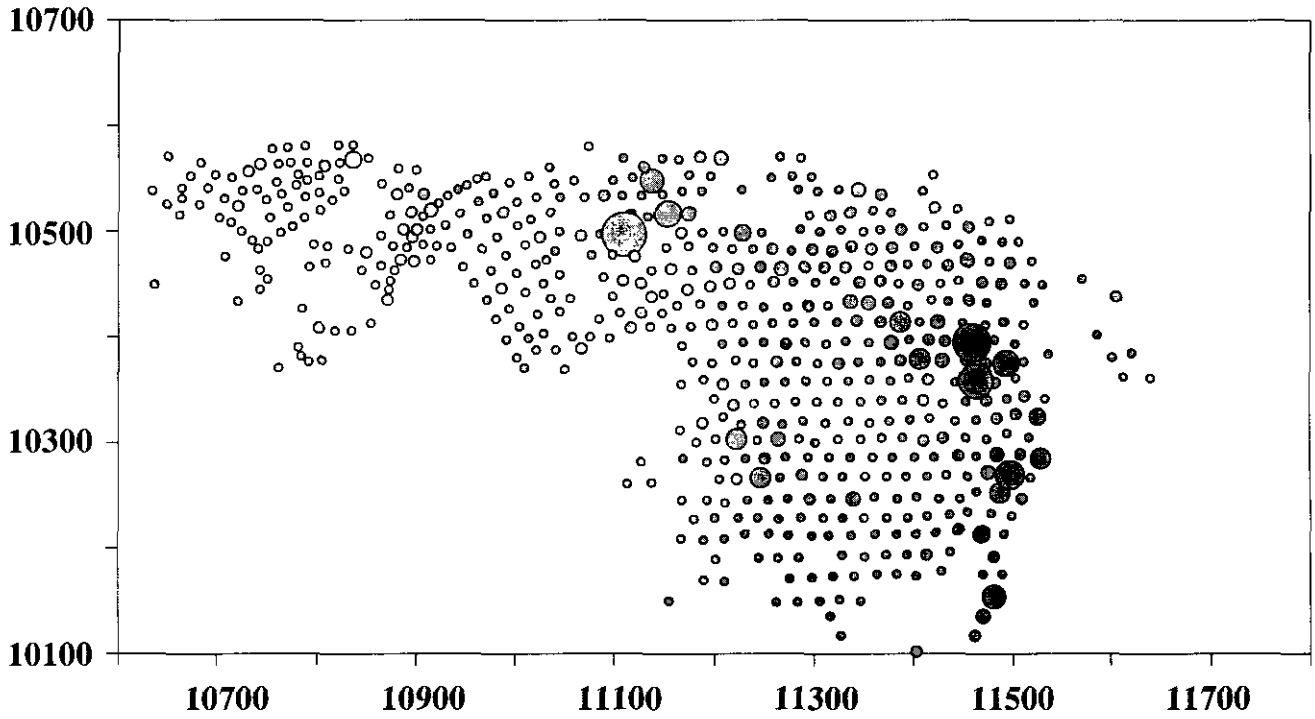


Figure 8. Bubble plot of production blast-hole copper assays from the 2340-foot bench of the Pothook open pit. Assays have been transformed and scaled to enhance geochemical contrast. The smallest and largest bubbles corresponds to copper grades of 0.01% and 2.60%, respectively (n = 635).

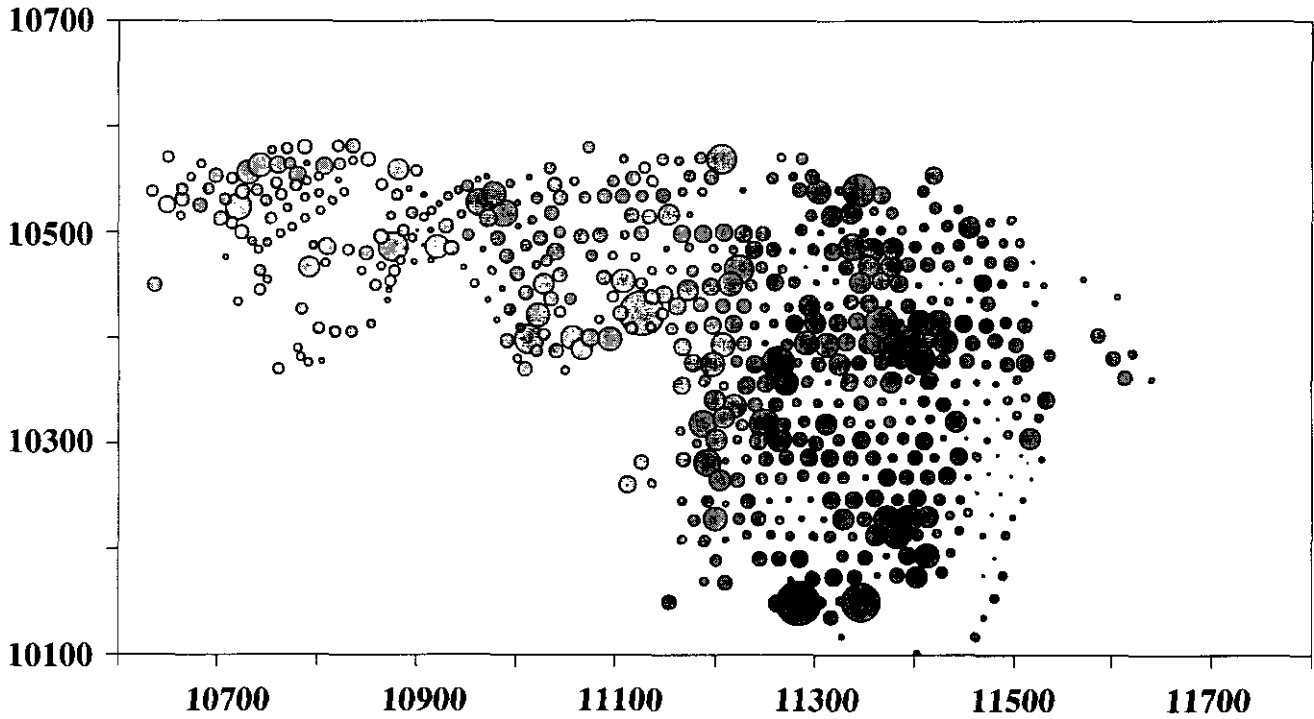


Figure 9. Bubble plot of production blast-hole gold assays from the 2340-foot bench of the Pothook open pit. Assays have been transformed and scaled to enhance geochemical contrast. The smallest and largest bubbles correspond to gold grades of 0.034 and 28.972 grams per tonne, respectively (n = 635).

fault zones are steeply dipping and were active before, during and after mineralization in the Pothook deposit.

The distribution of higher gold concentrations, however, suggests that the gold and copper mineralization in the Pothook deposit is not identically controlled (Figure 9). In fact, there is little correspondence between the locations of high gold and high copper concentrations in blast holes. The lack of correlation between copper and gold, in terms of both magnitude and space, may be due in part to local mobility during supergene weathering, or to inaccuracies produced by nugget effects. However, given the relatively high density of blast-holes (approximately 20-foot spacing), the spacing of assays in exploration drill-core samples (continuous, immediately adjacent intervals), and the masses of these samples (>2 kg), it is more likely that copper and gold do not share an identical mineral paragenesis. Whereas the timing of copper mineralization can be determined because the copper minerals are visible, the timing of gold mineralization remains unclear. Copper and gold may have been introduced at different times, or by the different means, during the hydrothermal history of the deposit.

## CONCLUSIONS

In the Pothook area, the Pothook diorite, Cherry Creek monzonite and Sugarloaf diorite all intruded latest Triassic Nicola volcanics during the earliest Jurassic. These intrusions and their host-rocks have been affected by several, largely pre-mineral, stages of hydrothermal alteration: magnetite veins and breccias controlled by fractures in the Pothook diorite; pervasive potassic alteration associated with the Cherry Creek monzonite; pervasive albitic alteration associated with the Sugarloaf diorite; and late, potassium feldspar - epidote veins.

Copper-gold mineralization in the Pothook area appears to be most closely related to Sugarloaf diorite dikes that cut Nicola volcanics along the southwest margin of the Iron Mask batholith. Mineralization occurs predominantly in hydrothermal breccia and steeply dipping, east-striking veins that cut all three phases of the batholith and the surrounding Nicola volcanics. The Pothook orebody is characterized by abundant pyrite, magnetite, chlorite and minor (specular) hematite gangue and chalcopyrite, bornite and native copper ore minerals.

Ore-stage mineral zoning is spatially consistent with both the predominant orientation of the veins and a hydrothermal fluid source in the Sugarloaf diorite dikes. The zoning of pyrite-chalcopyrite and chalcopyrite-bornite mineral assemblages across the deposit suggests that copper and gold mineralization may have precipitated under variable temperature and/or fluid sulphidation conditions (Einaudi, 1993) encountered as fluids migrated away from the Sugarloaf diorite dikes.

Precipitation of copper and gold occurred after the pervasive albitic alteration event that affected all intrusive rock types, and contact metamorphism of volcanics adjacent to Sugarloaf diorite dikes. The hostrocks to mineralization appear to have been made more competent by

these pre-mineral alteration events such that they fractured more brittlely and acted as ready hosts for mineralization.

Late, post-mineral chlorite veins cut unalbitized rocks, whereas kaolinite veinlets cut albitized rocks. Later calcite veins cut all lithologies.

During the Eocene, low-angle 'detachment' faulting, mafic dike emplacement and graben formation reflect the extensional tectonic episode that affected the Pothook area. Late quartz-bearing veins are associated with this tectonic and intrusive episode.

## REFERENCES

- Bond, L. (1985): Geology and Mineralization of the Pothook Zone; *Afton Operating Corporation*, internal company report, 99 pages.
- Cann, R.M. (1979): Geochemistry of Magnetite and the Genesis of Magnetite-Apatite Lodes in the Iron Mask Batholith, British Columbia; unpublished M.Sc. thesis, *The University of British Columbia*, 196 pages.
- Einaudi, M.T. (1993): Anatomy of Porphyry Copper Systems, in Volcanoes and Ore Deposits, *Mineral Deposit Research Unit, The University of British Columbia*, Short Course No. 14, April.
- Ghosh, D. (1993): Uranium-Lead Geochronology, in Porphyry Copper-Gold Systems of British Columbia; *Mineral Deposit Research Unit, The University of British Columbia*, Annual Technical Report, pages 11.1-11.25.
- Kwong, Y.T.J. (1987): Evolution of the Iron Mask Batholith and its Associated Copper Mineralization; *B.C. Ministry of Energy, Mines and Petroleum Resources*, Bulletin 77.
- Press, F. and Siever, R. (1978): *Earth*; *W.H. Freeman and Company*, San Francisco, 649 pages.
- Preto, V.A. (1977): The Nicola Group: Mesozoic Volcanism Related to Rifting in Southern British Columbia; in Volcanic Regimes in Canada, Baragar, W.R.A., Coleman, L.C. and Hall, J.M., Editors, *Geological Association of Canada, Special Paper No. 16*, pages 39-57.
- Snyder, L.D. and Russell, J.K. (1993a): Field Constraints on Diverse Igneous Processes in the Iron Mask Batholith (9219,10); in *Geological Fieldwork 1992*, Grant, B. and Newell, J.M., Editors, *B.C. Ministry of Energy, Mines and Petroleum Resources*, Paper 1993-1, pages 281-286.
- Snyder, L.D. and Russell, J.K. (1993b): Petrology and Geochemical Aspects of Rocks in the Iron Mask Batholith; in Porphyry Cu-Au Systems of British Columbia, *Mineral Deposit Research Unit, The University of British Columbia*, Annual Technical Report, pages 5.0.0-5.2.15.
- Souther, J.G. (1992): Volcanic Regimes; in Geology of the Cordilleran Orogen in Canada, Gabrielse, H. and Yorath, C.J., Editors, *Geological Survey of Canada, Decade of North American Geology Project*, Paper No. 4, pages 457-490.
- Stanley, C.R. (1993): A Thermodynamic Geochemical Model for the Co-precipitation of Gold and Chalcopyrite in Alkaline Porphyry Cu-Au Deposits; in Porphyry Cu-Au Systems of British Columbia, *Mineral Deposit Research Unit, The University of British Columbia*, Annual Technical Report, pages 12.1-12.17.
- Stanley, C.R., Lang, J.R. and Snyder, L.D. (1994): Geology and Mineralization in the Northern Part of the Iron Mask Pluton,

Kamloops British Columbia (92I/9, 10); *in* Geological Fieldwork 1993, Grant, B. and Newell, J.M., Editors, *B.C.*

*Ministry of Energy, Mines and Petroleum Resources*, Paper 1994-1, this volume.

## GEOLOGY OF THE CRESCENT ALKALIC PORPHYRY COPPER-GOLD DEPOSIT, AFTON MINING CAMP, BRITISH COLUMBIA (92/1/9)

By James R. Lang  
Mineral Deposit Research Unit, University of British Columbia

(MDRU Contribution 036)

**KEYWORDS:** Economic Geology, Porphyry, Copper, Gold, Iron Mask Batholith, Pothook Diorite, Cherry Creek Monzonite, Alkalic, Quesnellia

### INTRODUCTION

The Crescent deposit is one of several porphyry-style deposits located within the Iron Mask batholith. Other mined deposits in the district include the Afton, Ajax East and West, and Pothook deposits; the Big Onion, DM, and Python zones have published reserves but have had no production (Figure 1; Kwong, 1977). The Iron Mask is a composite intrusion of alkalic affinity which was emplaced at about  $207 \pm 3$  Ma (Ghosh, 1993) into coeval volcanic rocks of the Nicola Group which is part of the Quesnellia oceanic island-arc terrane (Souther, 1992). The copper-gold deposits within the batholith

have been classified within the silica-saturated group of alkalic porphyry deposits (Lang *et al.*, 1992). The Crescent deposit is located 3 kilometres due east of the Afton deposit, the largest orebody in the district (Figure 1), and yielded 1.36 million tonnes of ore with an average grade of 0.46% copper and 0.2 gram per tonne gold during production in 1989 and 1990.

The work reported here is based on a map of the open pit prepared at a scale of 1:600 (Figure 2), an outcrop map at 1:2400 scale for areas outside the pit (see Stanley *et al.*, 1994), and examination of diamond drill core. Only preliminary thin section work has been conducted as of this writing, and geochemical data are not yet available. This report summarizes the geology within the open pit, the characteristics of hydrothermal alteration and mineralization, and the currently recognized controls on the distribution of mineralization.

### GEOLOGY

The geology of the open pit (Figure 2) is dominated by Pothook diorite and a finer grained, porphyritic monzodiorite to diorite which intrudes the Pothook and is tentatively assigned to the Cherry Creek phase of the Iron Mask batholith (Snyder and Russell, 1993). Minor rock types include andesite dikes and plagioclase diorite porphyry dikes. The contact zone between the diorite and monzodiorite is afforded special treatment because it is the locus for development of economic copper-gold mineralization.

### POTHOOK DIORITE

The Pothook diorite is the oldest unit and dominates the south and west portions of the pit (Figure 2). Least altered samples of the diorite are greenish grey and equigranular, with a mineral assemblage comprising euhedral to subhedral plagioclase and pyroxene, poikilitic biotite, anhedral magnetite and potassium feldspar, and accessory euhedral apatite (Table 1); subhedral titanite was observed in one sample. Grain size is typically 1.5 to 3 millimetres, but more fine-grained areas have been recognized, particularly close to the contact with the Cherry Creek monzodiorite. Within the batholith as a whole, the Pothook diorite is notable for a magnetite

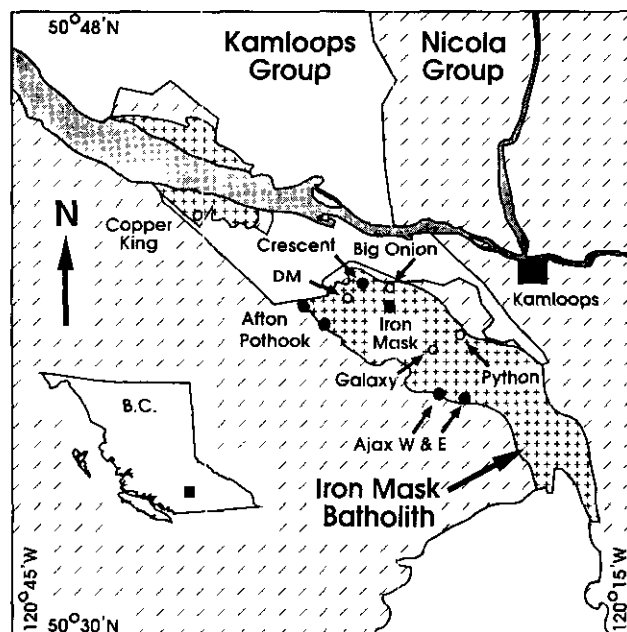


Figure 1. Location of the Iron Mask batholith and associated mineral deposits. Closed and open symbols respectively distinguish deposits with production from those that have not been mined. Dark grey is Kamloops Lake.

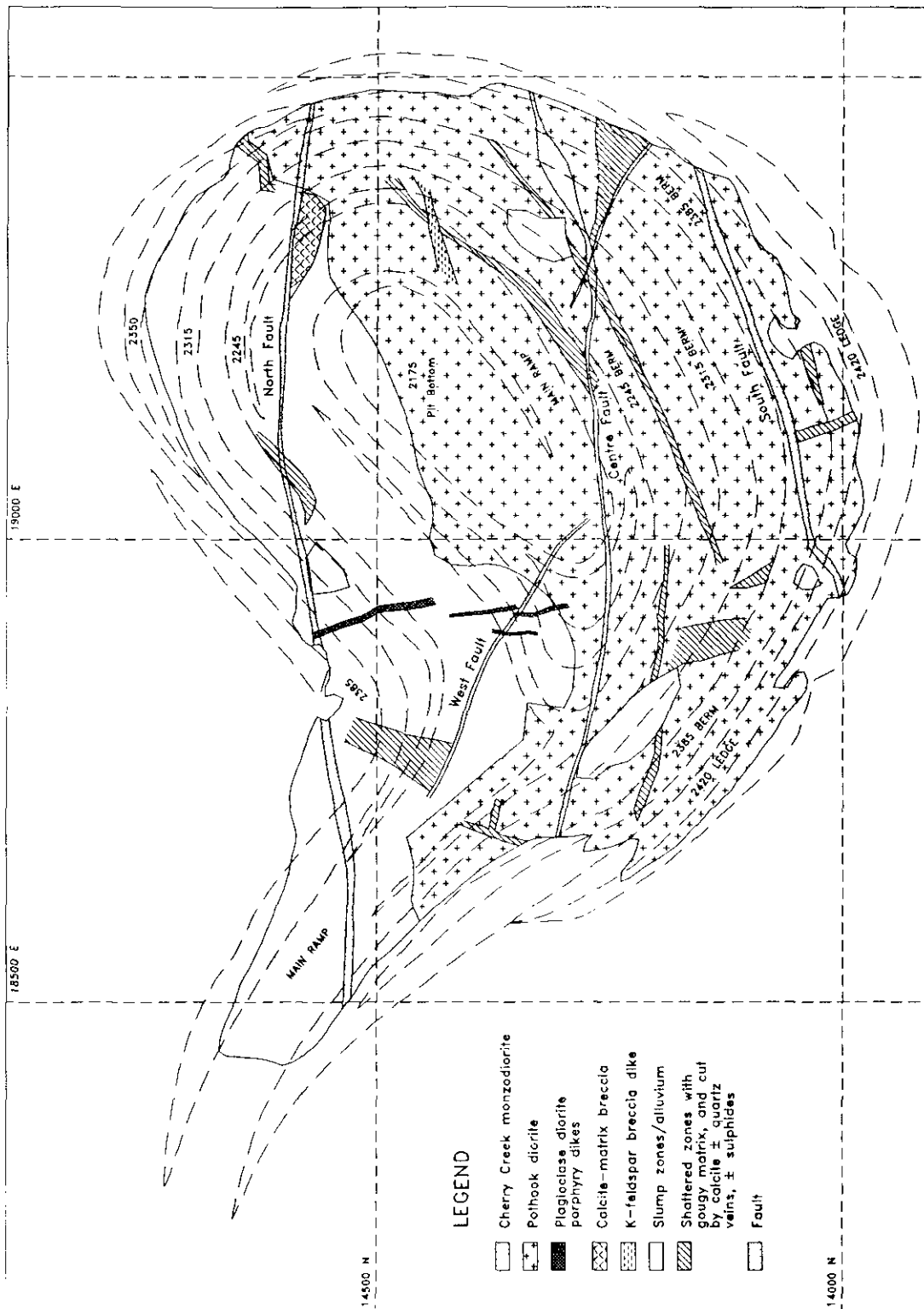


Figure 2. Geologic map of the Crescent open pit.

content which locally exceeds 15%, large poikilitic biotite grains which enclose plagioclase and augite (Snyder and Russell, 1993), and magnetite veins and segregations which may reach several metres in width (Stanley *et al.*, 1994; Cann, 1979); these features are also present in and adjacent to the Crescent deposit. Near its contact with the Cherry Creek monzodiorite, Pothook diorite has been affected by strong potassium metasomatism which has locally given it a pseudoporphyritic texture as a result of conversion of the margins of plagioclase grains to massive, pink potassium feldspar. Subangular to rounded xenoliths of an amphibolized mafic rock, interpreted as a Nicola volcanic unit, are only rarely present.

### CHERRY CREEK MONZODIORITE

The northern part of the pit (Figure 2) is dominated by a monzodioritic to microdioritic intrusion that is assigned to the Cherry Creek phase of the batholith (Stanley *et al.*, 1994). Although it is treated as a single intrusive phase, substantial variation in texture, and possibly in mineralogy, do not preclude the presence of several discrete units. In general, Cherry Creek monzodiorite is more fine grained than Pothook diorite, is variably porphyritic, and ranges from light pinkish grey to greenish grey in colour. Phenocrysts include euhedral plagioclase laths and less abundant, more equant, subhedral to euhedral pyroxene. Strongly altered, subhedral amphibole was observed in trace to minor amounts in a few samples. The aphanitic to fine-grained groundmass comprises potassium feldspar, magnetite, biotite, plagioclase, and sporadic occurrences of apatite (Table 1). Locally, and particularly near intrusive contacts, the plagioclase phenocrysts have a trachytic texture. Strong to intense potassium metasomatism has locally obliterated the porphyritic texture and has converted the rock to a dense, maroon-coloured, nearly aphanitic rock with few visible grains.

### MINOR ROCK TYPES

#### ANDESITE DIKES

Andesite dikes are rare in the Crescent pit and are typically less than a metre wide, black to dark green in colour, aphanitic, and commonly discontinuous. Larger examples observed elsewhere in the northern part of the Iron Mask batholith have pyroxene phenocrysts to 3 millimetres and may also contain equant plagioclase phenocrysts less than 2 millimetres in size. The groundmass is always macroscopically aphanitic. These rocks have not been affected by alteration or mineralization events, and may be related to the Eocene

**TABLE 1. PETROGRAPHIC CHARACTERISTICS OF THE POTHOOK DIORITE AND CHERRY CREEK MONZODIORITE.**

	Pothook Diorite	Cherry Creek Monzodiorite
N	8	5
Pyroxene	17 to 22	11 to 15*
Amphibole		0 to 5*
Biotite	5 to 15	2 to 10*
Magnetite	7 to 10	2.5 to 7
Plagioclase	50 to 55	51 to 65*
K-Feldspar	<5 to 10	1 to 15
Apatite	trace to 0.5	0 to low 0.5
Quartz		15 in one spl
Grain Size	1.25 to 3mm	Matrix: 10-40 microns; Pheno: 0.2-1.5mm
Phenocryst %	0	0 to 80
Texture	equigranular to seriate	equigranular to porphyritic

\* Observed as a phenocryst phase

mafic volcanism of the Kamloops Group. In the pit, andesite dikes are cut by flat fractures and faults but offsets in excess of 2 metres were not observed.

#### PLAGIOCLASE DIORITE PORPHYRY DIKES

Plagioclase diorite porphyry dikes are common throughout the northern end of the batholith but are rare and of very minor volume in the Crescent pit. As a group, they are typically dark green in colour, and range from less than 1 metre to about 5 metres in width. Narrow examples are commonly aphyric or have only very small plagioclase phenocrysts. Wider dikes have cores characterized by subhedral plagioclase, and more rarely pyroxene phenocrysts, in a fine-grained to aphanitic, dark grey-green groundmass, and chilled, dark grey, aphanitic margins up to 1 metre in width. Contacts with the hostrock are typically sharp but are commonly irregular. Xenoliths, where present, are limited to the immediate wallrock and are volumetrically minor. These dikes intruded during the waning stages of the pervasive potassium metasomatism event described below; in the Crescent pit, however, they are cut by later mineralized veins.

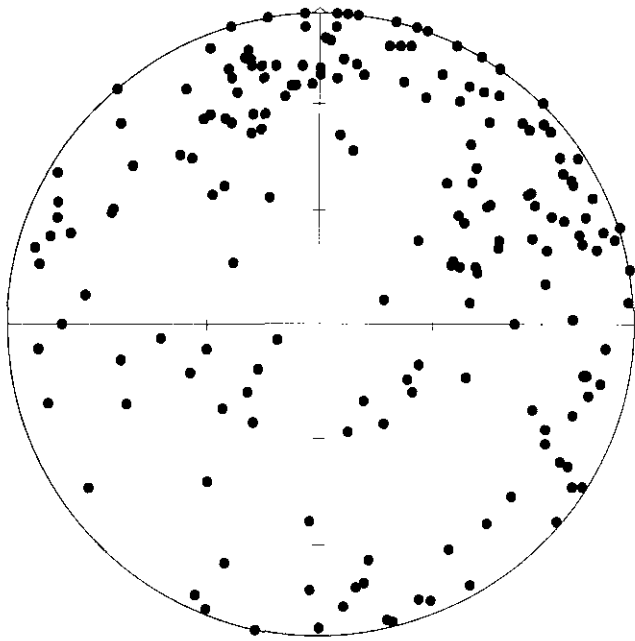


Figure 3. Lower hemisphere projection of poles to faults and fractures, Crescent deposit. Only those fractures continuous over at least one full bench face are included.

## STRUCTURES

Major faults which could be traced visually across the pit include the North, Centre, South and West faults (Figure 2). The absence of marker units has, however, severely limited assessment of offset. The North fault is the largest break and varies in width from 1 to about 5 metres along its easterly trace. It may be offset slightly by the West fault. The North fault cuts the plagioclase diorite porphyry dike but does so right at the bedrock surface on the 2385 bench (Figure 2) and offset cannot be determined. The Centre fault is parallel to the North fault but less prominent. On the southernmost margin of the pit, the South fault forms a major fracture zone of unknown offset with a trend of  $070^{\circ}$ . The West fault is visible in the south wall of the pit as a major structure, but it disappears beneath the flooded pit bottom and projects beneath the main ramp; displacement of the plagioclase diorite porphyry dikes between benches 2245 and 2315 suggests a maximum offset of a few metres. The Centre fault may have effected left-lateral offset of the West fault by up to 35 metres. These major fault zones are dominated by gougy or strongly shattered material with abundant calcite and chlorite; locally they contain calcite-quartz±pyrite veins, very rarely with trace chalcopyrite.

All rocks exposed in the open pit are intensely fractured. Typically these fractures are planar and many can be traced over more than one bench. The fractures are filled with strongly shattered rock which is usually cut by veins and vein swarms comprising calcite-chlorite-quartz±pyrite±epidote±trace chalcopyrite. The width of the broken material is usually less than 10 centimetres, but may range up to several metres. Hydrothermal veins may be the dominant fill in narrower fractures but form only a small portion of the filling of larger structures. Most of the fractures dip more steeply than  $60^{\circ}$  and have orientation modes of roughly  $350^{\circ}$ ,  $060^{\circ}$  and  $120^{\circ}$  (Figure 3). Fractures with relatively shallow dip were also noted. Steeply dipping fractures almost invariably host hydrothermal veins but veins are largely absent from flatter fractures. The preferred orientations are roughly parallel to the major faults, the contact zone between the Pothook and Cherry Creek intrusions, and the zone of mineralization.

## CONTACT BETWEEN POTHOOK AND CHERRY CREEK INTRUSIONS

The contact zone between the two major intrusive phases provided the locus for hydrothermal alteration and mineralization in the Crescent deposit. Vein density and alteration are most intense immediately adjacent to the contact zone. The most important features along this contact are development of intrusion breccias, pervasive potassium metasomatism, and the formation of pseudobreccia textures as a consequence of hydrothermal veining. The intensity of the metasomatism commonly obscures the nature and exact location of the contact itself.

Near its contact with the Pothook diorite, the Cherry Creek monzodiorite contains exotic inclusions which increase in abundance as the contact zone is approached and which become sufficiently abundant locally for the rock to be called an intrusion breccia. The fragments are mostly angular, but range to subrounded. They are dominated by Pothook diorite which displays various degrees of development of potassium metasomatism. Less common xenoliths include fragments of amphibolitized Nicola volcanic units, and fragments of massive magnetite veins which are similar to the magnetite segregations common in the Pothook diorite. Even more rarely, fragments macroscopically similar to the Cherry Creek intrusion itself are present; these are either ripped up margins of the Cherry Creek intrusion or strongly metasomatized Pothook diorite which has assumed a pseudoporphyritic texture, as described above.

To the south of the contact lies what may be an intrusion breccia in the form of a dike (Figure 2). The matrix is similar to the Cherry Creek phase but is not macroscopically porphyritic. Fragments include Pothook diorite with various degrees of potassium metasomatism,

finer grained porphyries similar to the Cherry Creek unit and, more rarely, fragments of a mafic rock now converted to amphibolite. The fragments are typically angular, but some are milled to a subrounded form. The dike has a constant thickness of about 2 metres in the single exposure on the main ramp. It is not mapped on the overlying bench, but may widen to the west where it is exposed in a narrow rill on the floor of the main ramp.

The main contact is typically obscured by intense potassium metasomatism. This alteration event was contemporaneous with intrusion of the Cherry Creek monzodiorite, and affects both the Pothook and Cherry Creek intrusions. Typically, primary igneous plagioclase and white potassium feldspar are selectively replaced by salmon-pink potassium feldspar. Magnetite is destroyed in strongly altered areas. The alteration is centred on the contact and strong effects extend up to 75 metres into the Pothook diorite, at which point the intensity of alteration decreases gradationally but rapidly, although local effects are visible well beyond the pit boundary to the southeast. In many places near the contact the Pothook diorite acquires a 'spotted' texture resulting from formation of ovoid clots up to 7 millimetres across, comprising chlorite with lesser calcite; this texture reliably indicates proximity to the contact both within the Crescent deposit and elsewhere in the northern end of the batholith. Nearly identical occurrences of potassium metasomatism are present in many exposures of Pothook diorite in the northern end of the batholith and these have commonly been mapped as Cherry Creek monzonite and syenite. This alteration is best described as deuteritic. It preceded the introduction of sulphides into the Crescent deposit; later mineralizing fluids overprinted the early deuteritic alteration but apparently followed similar flow paths.

## ALTERATION AND MINERALIZATION

### SEQUENCE OF VEIN TYPES

Six vein types have been recognized in the pit. Crosscutting relationships are well defined and permit a paragenetic sequence to be established (Table 2).

### MAGNETITE VEINLETS

Magnetite veinlets have irregular forms and are most common near the main intrusive contact. They are usually less than 1 millimetre wide but may exceed 1 centimetre. They have narrow, distinct alteration envelopes of pink potassium feldspar. Although minor chalcopyrite has been observed, these veins are not abundant and did not carry significant copper.

## POTASSIUM FELDSPAR VEINS/DIKELETS

Throughout the deposit, veins of pink potassium feldspar with minor biotite have the appearance of syenite dikelets. In the pit, most of these veins formed as replacements of wallrock along tight fractures, but an intrusive origin cannot be ruled out for larger examples with very sharp contacts with their host. An intrusive origin is not inconsistent with observation: in other parts of the northern end of the batholith where similar dikelets have been noted near the contact between Pothook diorite and Cherry Creek intrusions. Sulphide is rare in these veins and they did not contribute substantially to ore grade.

## CHLORITE-SULPHIDE VEINS

Chlorite-sulphide veining is best developed within the tabular ore zone and its hangingwall in the Pothook diorite. The altered and mineralized rocks have a distinct mottled colour in shades of pink, black and green. Individual veinlets are narrow and discontinuous and may impart a brecciated appearance to the rock. The dominant minerals are chlorite and magnetite. Chlorite may be a replacement of biotite, which has been observed locally. Magnetite either coexists with or is replaced by hematite. Calcite is common, potassium feldspar is usually present as a trace mineral, and epidote was observed in one case. Quartz is minor and sporadically present and pyrite is absent to minor. Several percent chalcopyrite may be present within veinlets of calcite, chlorite and minor quartz, or in their alteration envelopes. Hostrock between the veinlets is usually altered by potassium feldspar, chlorite, magnetite/hematite and calcite. In the most intensely veined rocks, magnetite is often destroyed, but may be preserved only millimetres away from veins. This alteration type is largely coincident with the ore zone, and the high abundance of chalcopyrite in these veins suggests that they carry most of the copper.

## EPIDOTE VEINS

Epidote veins are abundant and widespread but are most common peripheral to the tabular ore zone. They vary from planar structures to more irregular, diffuse veins and, more rarely, they form the matrix to small breccia zones. They range from less than a millimetre to several centimetres in width. Epidote and calcite are the major minerals but pyrite and chalcopyrite locally constitute up to 10%. Minor potassium feldspar and albite(?) were observed, together with rare quartz. Distinct alteration envelopes were not observed, but the veins are often associated with clots of alteration minerals similar to those found in the veins themselves. Chlorite is common in the alteration clots and in the wallrocks to the veins, and is associated with

**TABLE 2. PETROGRAPHIC CHARACTERISTICS AND SEQUENCE OF HYDROTHERMAL VEINS.**

Vein/Alteration Stage	Major Minerals	Minor Minerals	Envelopes	Morphology
<i>Early</i>				
Magnetite	mag	cpy	K-spar	sinuous
K-spar-dominated	K-spar	bio-cpy-mag-hem	K-spar	irregular
Chlorite-Sulfide	chl-mag-hem-calc-cpy	K-spar-ep-qtz-py	mag?	irregular
Calcite-Quartz	calc-qtz	hem-py-cpy-K-spar-ep	K-spar-mag-cpy	planar
Epidote-dominated	ep-cac-py-cpy	K-spar-qtz	K-spar-chl	planar
Calcite Only	calc	py-chl	none	planar
<i>Late</i>				

Abbreviations: chl, chlorite; calc, calcite; ep, epidote; qtz, quartz; py, pyrite; cpy, chalcopyrite; mag, magnetite; hem, hematite; K-spar, potassium feldspar

disseminated chalcopyrite. Beyond the pit boundary these veins carry magnetite, hematite, epidote and minor calcite, in some cases with alteration envelopes of albite and/or epidote.

#### **CALCITE-QUARTZ VEINS**

Calcite-quartz veins are broadly distributed through the deposit. They range from 2 millimetres to several centimetres in width, have sharp contacts with their host, and are usually planar. Calcite usually, but not always, exceeds quartz in abundance. Hematite, pyrite, chalcopyrite, and potassium feldspar are present, and epidote was observed in one sample. Envelopes of pink potassium feldspar similar in width to the veins themselves are almost always developed. In one sample an alteration envelope grades from an inner zone comprising potassium feldspar with minor magnetite and chalcopyrite to an outer zone of magnetite with minor chalcopyrite. Commonly, the grain size of calcite and the abundance of quartz increase toward the core of these veins; the reverse is rare.

#### **CALCITE VEINS**

Veins dominated by calcite, with common but minor chlorite and very rare pyrite, occur throughout the deposit. They range from fracture coatings to dilatant veins many centimetres wide, are continuous and planar, have sharp contacts with their hosts, and lack alteration envelopes. Similar veins have been recognized throughout the northern end of the batholith; they have

been observed to cut Eocene dikes and are unrelated to mineralization in the Crescent deposit.

#### **OPEN SPACE BRECCIAS**

True open-space hydrothermal breccias are common. Fragments are typically angular and have not been milled. The matrix of breccias is usually dominated by calcite with lesser quartz and, less commonly, chalcedony. Typically the matrix contains little or no sulphide although rare, small examples with up to 10% chalcopyrite have been observed. Most sulphide contained in hydrothermal breccias occurs in the fragments. One sample shows two stages of brecciation. The later stage has an unmineralized calcite matrix. Fragments within this matrix are themselves an earlier breccia with a matrix of calcite and minor hematite, chalcopyrite and pyrite; the fragments in this earlier breccia are altered by potassium feldspar and chlorite, and contain over 5% sulphide with a high chalcopyrite to pyrite ratio. The sulphides are in part disseminated and in part contained within calcite-quartz veins that are restricted to the fragments. Larger examples of these breccias are spatially related to major faults.

#### **DISTRIBUTION OF ALTERATION MINERALS**

A visual estimate of the percentage of epidote, magnetite, potassium feldspar, chlorite, albite, calcite, pyrite, chalcopyrite, quartz and hematite was made for the bench face at stations spaced 15 metres apart. The

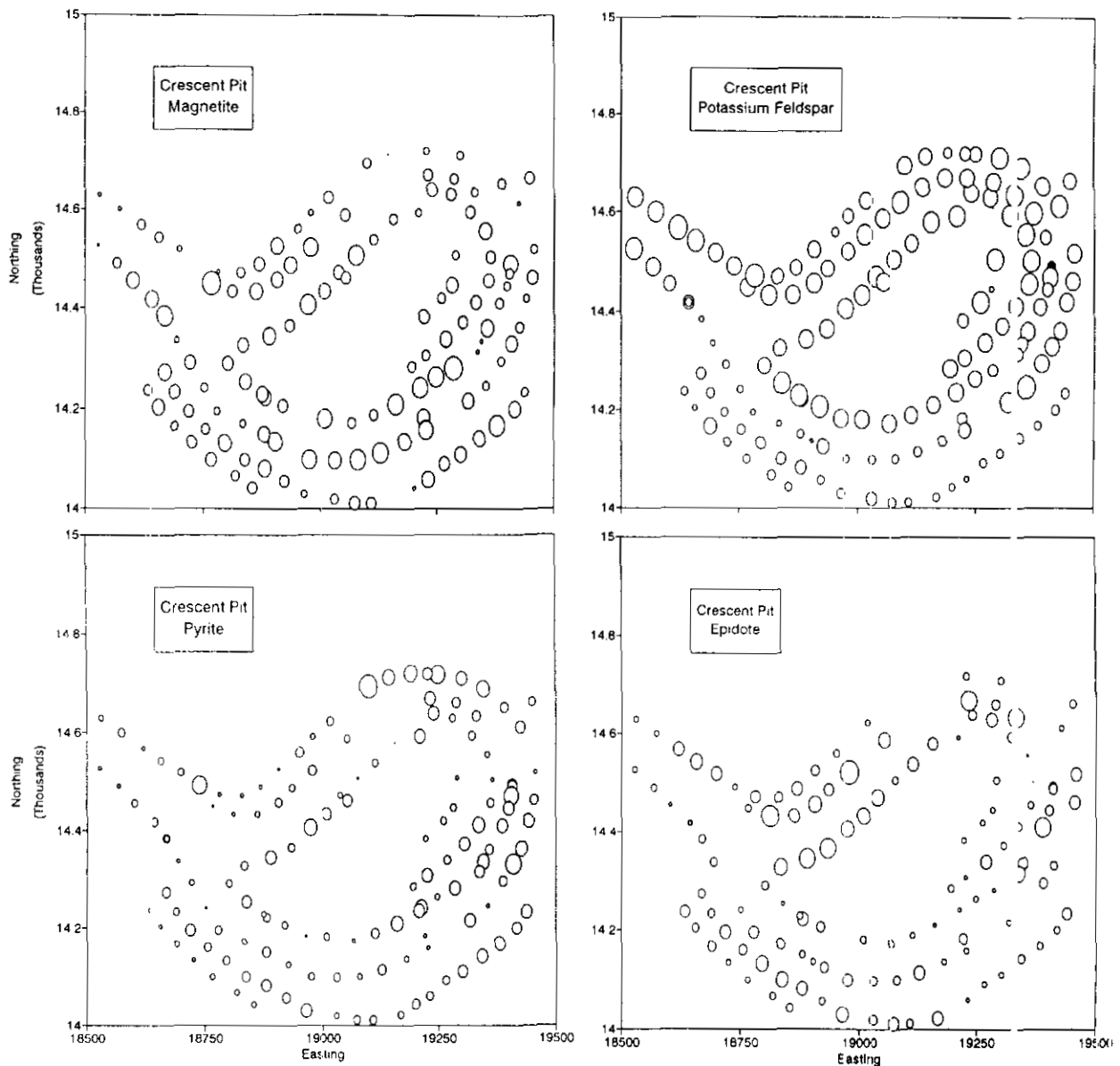


Figure 4. Bubble plots of alteration mineral distribution. Data are visual estimates at 15-metre stations along each accessible bench. Bubble diameter is proportional to value. Maximum values for potassium feldspar, magnetite, pyrite, and epidote are 65%, 15%, 7%, and 20%, respectively.

data were analyzed on bubble plots (Figure 4). Among the minerals not shown on Figure 4, calcite and chlorite are very evenly distributed, and quartz, hematite and albite are erratically distributed with no apparent pattern. A reconnaissance examination of thin sections has shown that visual estimates of chalcopyrite have unacceptably large errors because of its finely disseminated occurrence. Magnetite, potassium feldspar, pyrite and epidote are shown on Figure 4. Magnetite is largely disseminated and is consistently abundant throughout the deposit, even though the Pothook diorite contains nearly twice as much primary magnetite as the Cherry Creek monzodiorite; this reflects the partial destruction of magnetite during potassium metasomatism of the Pothook diorite.

Potassium feldspar is more abundant in the Cherry Creek monzodiorite and in the areas of Pothook diorite affected by strong potassium metasomatism; a sharp decrease is apparent on the south and west sides of the pit. The abrupt decrease on the west occurs at an atypically sharp contact between the Pothook and Cherry Creek units that is not characterized by the usual intrusion or hydrothermal brecciation present elsewhere; the 'tightness' of the contact may have limited fluid flow at this point. Pyrite and epidote abundance is highest at the margins of the deposit and reflects a propylitic, pyritic halo surrounding the ore zone.

At each alteration station (Figure 5), the relative abundance of each vein type was assigned a value from 0

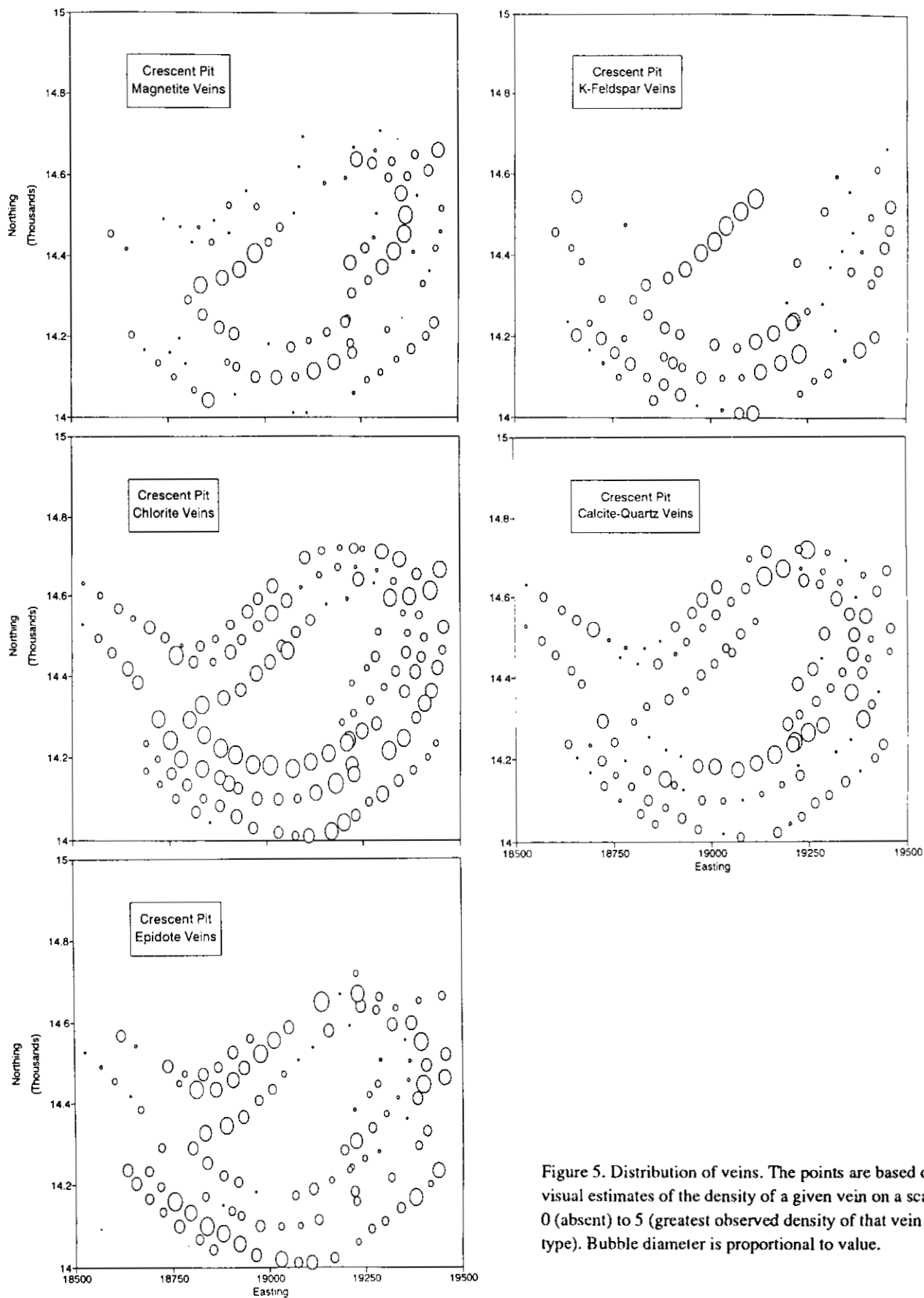


Figure 5. Distribution of veins. The points are based on visual estimates of the density of a given vein on a scale of 0 (absent) to 5 (greatest observed density of that vein type). Bubble diameter is proportional to value.

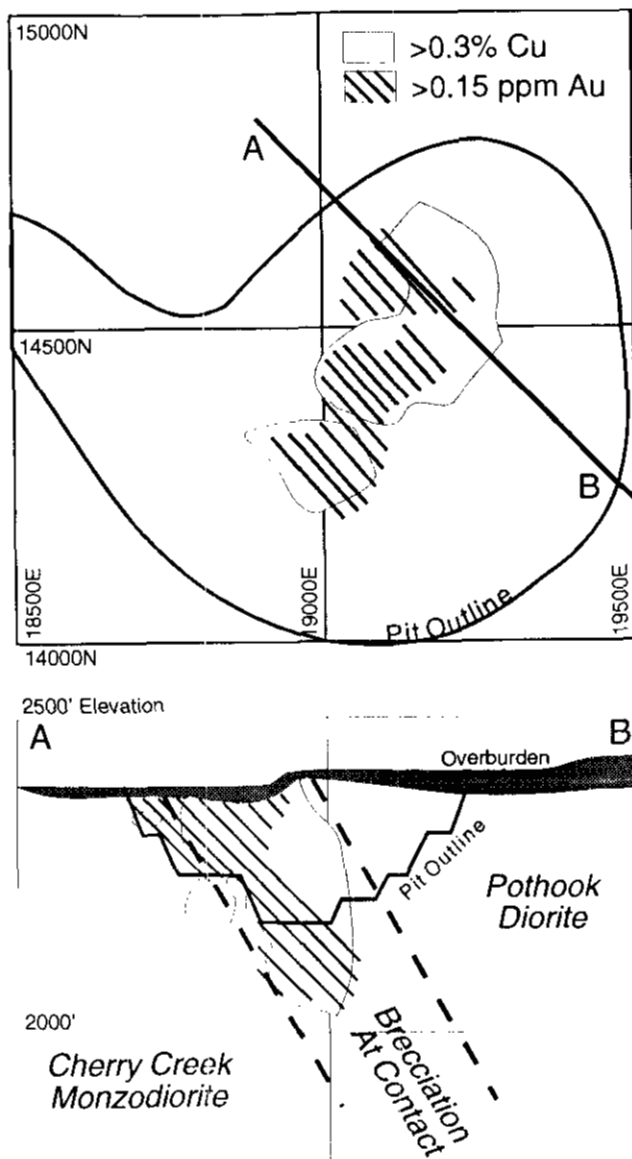


Figure 6. Plan and cross-section distribution of mineralization in the Crescent deposit. Simplified from Bond and Tsang (1988).

(absent) to 5 (greatest number of that particular vein type observed). Magnetite veins occur in both the Pothook diorite and the Cherry Creek monzodiorite but are most abundant near the contact zone. Potassium feldspar veins are more commonly developed in the Pothook diorite, but their greatest and most consistent abundance is on the 2245 level, near the contact zone. Chlorite-sulphide veins are more abundant in the hangingwall of the contact, roughly coincident with the ore zone. Calcite-quartz veins show no distinct distribution pattern. Epidote veins are most abundant on the margins of the pit. The only vein type that is well developed outside the confines of the pit is epidote-magnetite veins which occur sporadically in many exposures of the Pothook diorite throughout the northern end of the Iron Mask batholith;

these veins are indigenous to the Pothook diorite itself and are not directly related to the formation of the copper-gold deposits.

### DISTRIBUTION OF MINERALIZATION

The ore reserve in the Crescent pit formed a tabular zone oriented about 050° with a southerly dip of 60° (Figure 6; Bond and Tsang, 1988). Mineralization continues downward to at least the 300-metre limit of drilling (L.H.C Tsang, personal communication, 1993). Chalcopyrite was the dominant ore mineral and insignificant amounts of bornite and molybdenite are also reported (Bond and Tsang, 1988). Figure 7 illustrates the distribution of copper and gold as determined from blast-hole assays. A comparison with Figure 2 shows that the higher grades were present along the contact zone and its immediate hangingwall but that sporadic high values were present throughout the deposit. Gold has a more erratic distribution, but Figure 8 shows a good correlation between copper and gold at a nearly constant ratio of about 25,000. This ratio is consistent with values observed at other alkalic porphyry copper-gold deposits and is apparently a fundamental feature of this deposit type (Stanley, 1993). The absence of samples with lower Cu/Au ratios indicates that a late stage episode of gold enrichment, similar to that which has affected some deposits of this class such as the nearby Pothook deposit (Stanley, 1994) and the 66 zone at Mount Milligan (Stanley and DeLong, 1993), has not affected the Crescent deposit. In the Crescent deposit, gold was deposited with chalcopyrite in a single hydrothermal event.

### SUMMARY

The Crescent deposit formed in the earliest Jurassic in response to the intrusion of alkalic igneous rocks of the Iron Mask batholith. A proposed sequence of events is presented in Table 3. Mineralization, alteration, and vein formation were localized at the brecciated contact between the older Pothook diorite and the younger Cherry Creek monzodiorite. Relatively more permeable intrusion breccias may have focussed fluid flow. Early deuteric alteration related to intrusion of the Cherry Creek monzodiorite effected intense potassium metasomatism but did not deposit sulphide minerals in the system. This event was closely followed in sequence by magnetite, potassium feldspar, chlorite-sulphide, calcite-quartz, and epidote veins. Ore grade mineralization is associated with chlorite (after biotite?) veining and alteration, and forms a tabular zone along the contact that extends southward into Pothook diorite in the hangingwall. Epidote and pyrite extend beyond the deposit and form a weak halo surrounding the ore zone.

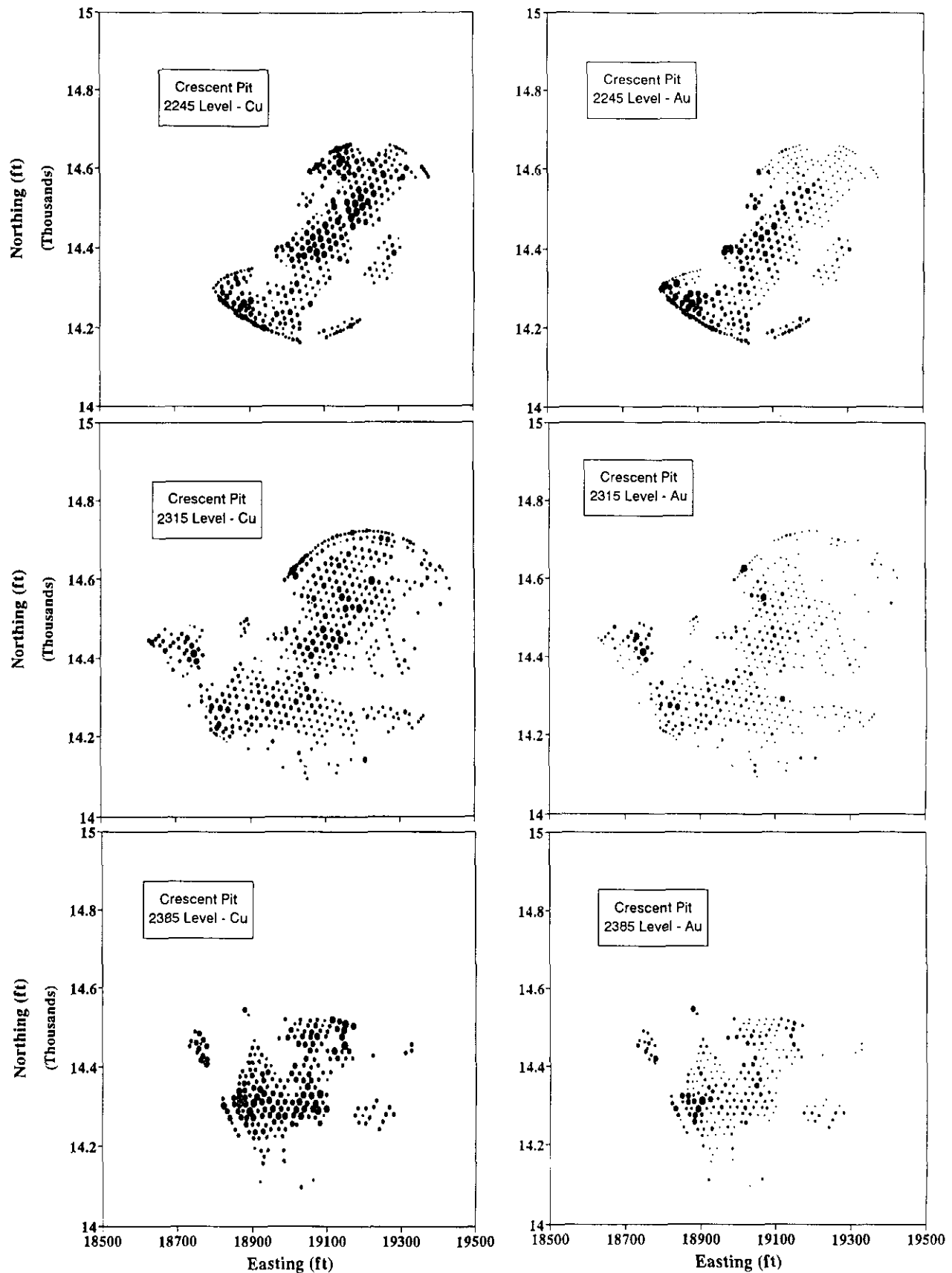


Figure 7. Bubble plots of copper and gold blast-hole assays. Data are shown for each of the four main benches. Bubble diameter is proportional to value. For each respective level N, the number of data points, maximum and minimum copper grade (wt. %), and maximum and minimum gold grade (g/t) are: 2175 level, 258, 2.09, 0.09, 0.82, 0.035; 2245 level, 349, 1.41, 0.06, 0.86, 0.00; 2315 level, 511, 1.83, 0.11, 1.82, 0.00; 2385 level, 236, 1.25, 0.13, 1.41, 0.035.

TABLE 3. SEQUENCE OF EVENTS AFFECTING THE CRESCENT DEPOSIT.

Timing	Geologic Event
1	Intrusion of Pothook diorite
2	Intrusion of Cherry Creek monzodiorite
3A	Formation of intrusion breccias at contact
3B	Potassium metasomatism at contact
3C	Formation of pseudobreccias by K-feldspar veining (Cu-Au mineralization)
4	Intrusion of plagioclase diorite porphyry dikes
5A	Formation of hydrothermal veins (Cu-Au mineralization)
5B	Movement along major faults; formation of major fractures
5C	Formation of barren calcite-quartz $\pm$ -pyrite veins
6	Intrusion of andesite dikes
7	Minor additional fault movement; formation of barren calcite veins

Hydrothermal breccias closely related to faults are common but generally postdate main-stage copper mineralization. A constant Cu/Au ratio of 25000 is similar to other alkalic suite porphyry deposits and indicates that copper-gold introduction was related to a single hydrothermal event.

## REFERENCES

Bond, L.A. and Tsang, L.H.C. (1988): Diamond Drilling on the CID1, CID2, and Winty C. G. Mineral Claims; Afton

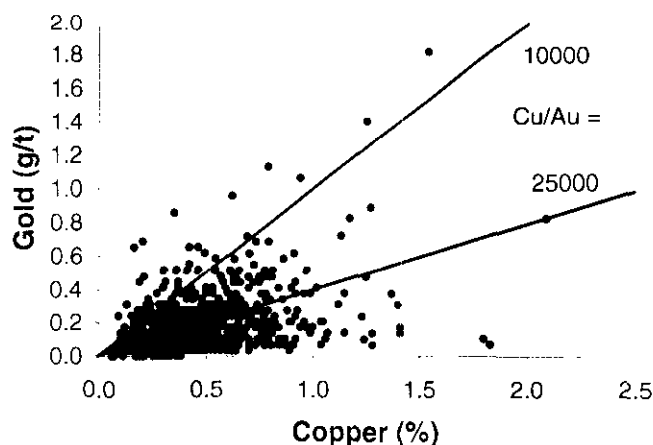


Figure 8. Copper and gold blast-hole assay data, Crescent deposit.

Operating Corporation, Private Report, 13 pages.  
 Cann, R.M. (1979): Geochemistry of Magnetite and the Genesis of Magnetite-Apatite Lodes in the Iron Mask Batholith, British Columbia; unpublished M.Sc. thesis, The University of British Columbia, 191 pages.  
 Ghosh, D.K. (1993): Uranium-Lead Geochronology; *Mineral Deposit Research Unit - The University of British Columbia, Copper-Gold Porphyry Systems of British Columbia, Annual Technical Report - Year 2*, pages 11.1-11.26.  
 Kwong, Y.T.J. (1987): Evolution of the Iron Mask Batholith and its Associated Copper Mineralization; *B.C. Ministry of Energy, Mines and Petroleum Resources, Bulletin 77*.  
 Lang, J.R., Stanley, C.R. and Thompson, J.F.F. (1992): Quartz-Alkalic and Nepheline-Alkalic: Two Distinct Subtypes of Porphyry Deposits Related to Alkalic Igneous Rocks; *Geological Society of America, Abstracts With Programs, Volume 24*, page A143.  
 Snyder, L.D. and Russell, J.K. (1993): Field Constraints on Diverse Igneous Processes in the Iron Mask Batholith (9219,10); in *Geological Fieldwork 1992*, Grant, B. and Newell, J.M., Editors, *B.C. Ministry of Energy, Mines and Petroleum Resources, Paper 1993-1*, pages 281-286.  
 Souther, J.G. (1992): Volcanic Regimes; in *Geology of the Cordilleran Orogen in Canada*, Gabrielle, H. and Yorath, C.J., Editors, *Geological Society of America, The Geology of North America Decade of North American Geology Series, Volume G-2* pages 457-493.  
 Stanley, C.R. (1993): A Thermodynamic Geochemical Model for the Co-precipitation of Gold and Chalcopyrite in Alkalic Porphyry Copper-Gold Deposits; *Mineral Deposit Research Unit-The University of British Columbia, Copper-Gold Porphyry Systems of British*

Columbia, Annual Technical Report - Year 2, pages 12.1-12.17.

Stanley, C.R. (1994): Geology of the Pothook Alkalic Porphyry Copper-Gold Deposit, Afton Mining Camp, British Columbia (92I/9,10); in Geological Fieldwork 1993, Grant, B. and Newell, J.M., Editors, *B.C. Ministry of Energy, Mines and Petroleum Resources*, Paper 1994-1, this volume.

Stanley, C.R. and DeLong, C. (1993): A Crystal Chemical Analysis of Hydrothermal Biotite From the MBX and 66 Zones, Mt. Milligan Cu-Au Porphyry Deposit; *Mineral Deposit Research Unit - The University of British Columbia*, Copper-Gold Porphyry Systems of British Columbia, Annual Technical Report - Year 2, pages 9.1-9.12.

Stanley, C.R., Lang, J.R. and Snyder, L.D. (1994): Geology and Mineralization in the Northern Part of the Iron Mask Pluton, Iron Mask Batholith, British Columbia (92I/9,10); in Geological Fieldwork 1993, Grant, B. and Newell, J.M., Editors, *B.C. Ministry of Energy, Mines and Petroleum Resources*, Paper 1994-1, this volume.



# PETROLOGY AND STRATIGRAPHIC SETTING OF THE KAMLOOPS LAKE PICRITIC BASALTS, QUESNELLIA TERRANE, SOUTH-CENTRAL B.C. (92I/9, 15, 16)

By Lori D. Snyder and J.K. Russell  
Mineral Deposit Research Unit, U.B.C.

(MDRU Contribution #34)

**KEYWORDS:** Petrology, picritic basalt, Nicola Group, Kamloops, mineral chemistry, olivine, ultramafic

## INTRODUCTION

Picritic basalt is exposed in the Intermontane Belt in the southern part of the Quesnellia Terrane, south-central British Columbia (Figure 1). It is found in four localities in the Kamloops Lake area (Figure 2): as small pods within the Early Jurassic Iron Mask batholith; on an isolated knoll near Jacko Lake just outside the southwestern margin of the Iron Mask batholith; near Carabine Creek on the

north side of Kamloops Lake; and north of Pass Lake near Watching Creek. These rocks are olivine±clinopyroxene-porphyrific, occasionally serpentinized and exhibit volcanic textures. They contain extremely high MgO, anomalously low Al<sub>2</sub>O<sub>3</sub>, low TiO<sub>2</sub> and are enriched in chromium and nickel.

We present petrographic and chemical data on the Kamloops Lake picritic basalts as well as the stratigraphic setting for these ultramafic lavas. Age constraints derive from field relationships. Mineral chemistry indicates that these ultramafic rocks represent mantle-derived material which has undergone minimal differentiation or crustal contamination and, based primarily on regional geology and whole-rock and mineral chemistry, they represent ultramafic magmatism in an island arc setting. Comparisons to other ultramafic rock suites provide a framework for further interpretation of these rocks.

## REGIONAL GEOLOGY

The majority of the rocks exposed within the study area are Nicola Group (Figure 2), an extensive sequence of Late Triassic volcanic, volcanoclastic and sedimentary rocks (Pretorius, 1979). In the Kamloops Lake area, Nicola Group consists mainly of abundant green and red agate porphyry flows and related breccias, bedded and massive tuffaceous siltstones, and minor cherty sediments. Nicola Group rocks have an alkaline chemical signature and characteristically exhibit low-grade greenschist metamorphism (Pretorius, 1979). The rocks are generally broadly folded, cut by prominent northwest-trending structures, and show a weak foliation.

Intruding and overlying the Nicola Group rocks are a variety of younger intrusive and volcanic rocks, including the Iron Mask batholith and the Kamloops Group. The Iron



Figure 1. Map showing the location of the Kamloops Lake picritic basalts in the southern Intermontane Belt, British Columbia.

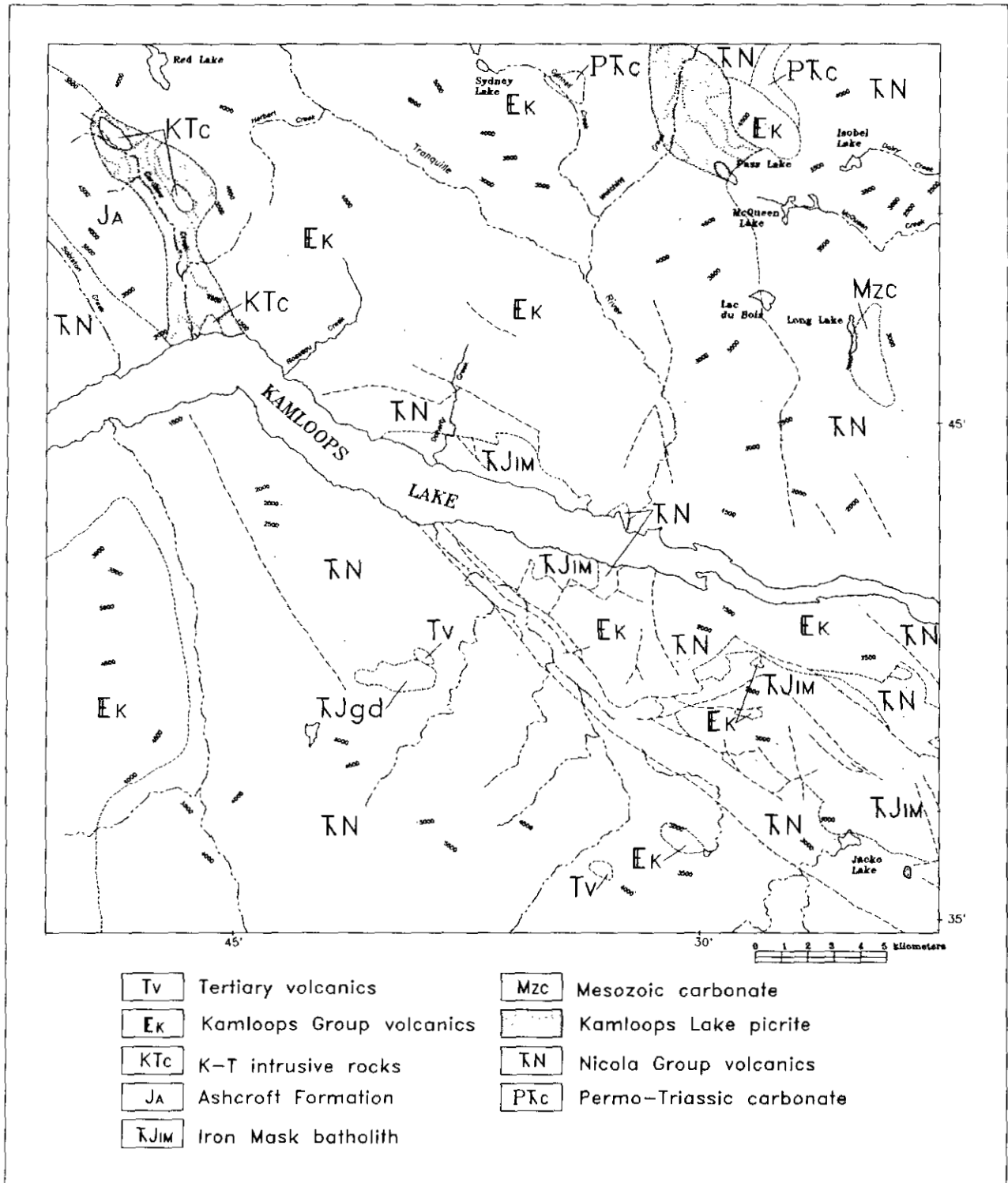


Figure 2. Geology of the Kamloops area. Nicola Group volcanic and sedimentary rocks underlie most of the map area. Picrite occurrences are shown in the stippled pattern.

Mask batholith, a northwesterly trending Early Jurassic composite alkaline intrusive complex, is exposed in the southeast part of the study area (Preto, 1968; Northcote, 1977; Kwong, 1987; Snyder and Russell, 1993). It is intruded along deep-seated structures and contains numerous xenoliths of serpentinitized picritic basalt. The Eocene Kamloops Group volcanic rocks overlie much of the study area and consist of abundant alkali basalt flows and minor sedimentary rocks (Ewing, 1982).

Picritic basalt occurs as small, poorly exposed, disconnected bodies in the vicinity of Kamloops Lake. The four locations described in this work are referred to as the Carabine Creek, Watching Creek, Jacko Lake and Iron Mask localities.

## HISTORICAL PERSPECTIVES AND PREVIOUS WORK

Mathews (1941) and Cockfield (1948) described two occurrences of picritic basalt exposed on the north side of Kamloops Lake near Watching Creek and Carabine Creek, assigning them to a Cretaceous or Tertiary package of volcanic rocks. They described the rocks as "effusive" and characterized by "vitreous bases". Mathews also identified similar rocks within the Iron Mask batholith and the presence of a small area of "peridotite" near Jacko Lake. The latter was presumed to be a small intrusion unrelated to either the Nicola Group or the batholith.

Carr (1957) noted that the picritic basalt in the Iron Mask batholith occurs as small, lenticular serpentinitized bodies, commonly associated with northwest-trending structures. He interpreted the serpentinites as non-batholithic, post-Nicola intrusions. Carr also suggested that the unaltered "peridotite" near Jacko Lake is similar to picritic basalt north of Kamloops Lake. Some of the outcrops he included as basalt are, in fact, augite porphyries of the Nicola Group. Preto (1968) suggested that the picritic basalt in the Iron Mask batholith was pre-Kamloops Group (Eocene) and noted the presence of dioritic dikes which crosscut outcrops of serpentinite; Northcote (1977) assigns the dikes to late-stage phases of the Iron Mask intrusive suite.

Snyder and Russell (1993) reinterpreted the relative age relationships of the phases of the Iron Mask batholith and concluded that the picritic basalt is pre-Iron Mask in age. They suggest that serpentinitization of the basalts resulted from interaction with the batholith

during emplacement. They also note the textural and mineralogical similarity in rocks from the four localities in the Kamloops Lake area. Ross *et al.* (1993) report that although lenses of picritic basalt are commonly associated with mineralized zones such as the Afton orebody on the northern margin and the Ajax properties near the southwest margin of the batholith, they are not mineralized.

## FIELD AND STRATIGRAPHIC RELATIONSHIPS

Picritic basalt crops out near Jacko Lake, approximately 1 kilometre from the southwest margin of the Iron Mask batholith on a small, isolated knoll. A distinctive feature of this locality is the presence of rounded aggregates of olivine and clinopyroxene ranging from 1 to 20 centimetres in diameter. The mineral grains in the aggregates are the equivalent size of the crystals in the groundmass. Outcrops have a subtle layering defined by the proportion of these aggregates. Basalt at Jacko Lake is cut by a small (0.6 m wide) felsic dike which is inferred to be a late phase of the Iron Mask batholith.

The picritic basalt exposed at Carabine Creek on the north side of Kamloops Lake is similar in appearance to the Jacko Lake outcrop but there is greater exposure. Although olivine and clinopyroxene aggregates are present, they are not as abundant. The basalt at Carabine Creek is intruded by small stocks of granitoid composition belonging to the post-Early Cretaceous Copper Creek Plutonic Suite (Cockfield, 1948).

Ultramafic rocks at the Watching Creek locality, north of Pass Lake, are massive; the outcrops are typically dense, black and structureless. The rocks contain more olivine phenocrysts (up to 50%) than observed at the other localities and are weakly porphyritic. Aggregates of olivine and clinopyroxene were not seen at Watching Creek, but hematite is ubiquitous at this locality, giving some samples a reddish colour.

Picritic basalt occurs in the Iron Mask batholith as small, serpentinitized xenoliths and septa. Olivine is generally the only primary mineral preserved, although clinopyroxene is locally present. Serpentine, replacing original minerals, commonly preserves fragmental textures. Contacts with Iron Mask units or Nicola Group rocks are generally sheared; one contact seen in drill core from near Jacko Lake

(Figure 2) is unsheared and shows the basalt in sharp contact with Nicola augite porphyry.

Picritic basalt at the Jacko Lake locality overlies Nicola volcanic rocks, indicating that it is younger than the Late Triassic. Because picritic basalt is found as xenoliths within the Early Jurassic (207±3 Ma, Ghosh, 1993) Iron Mask batholith, the ultramafic magmatism is definitively older. At Carabine Creek, the picritic basalt is overlain by Kamloops Group volcanic rocks, supporting a pre-Eocene age for the basalts. These relationships constrain the

age of the Kamloops Lake suite to the latest Triassic or earliest Jurassic.

## PETROGRAPHY

Picritic basalts in the Kamloops Lake area are olivine±clinopyroxene-porphyritic. Spinel occurs ubiquitously as microphenocrysts, inclusions in olivine and clinopyroxene, and in the groundmass. The groundmass is typically fine grained and altered to either serpentine or

**TABLE 1. REPRESENTATIVE ELECTRON MICROPROBE ANALYSES OF OLIVINE PHENOCRYSTS IN THE KAMLOOPS LAKE PICRITIC BASALTS.**

Sample	Carabine Creek				Watching Creek			
	224	224	225	225	240	240	241	241
Position	C	R	I	R	C	R	C	R
SiO <sub>2</sub>	41.24	41.16	40.83	40.39	39.95	39.66	40.03	40.04
Al <sub>2</sub> O <sub>3</sub>	0.04	b.d.	0.04	0.05	0.05	0.02	b.d.	0.04
Cr <sub>2</sub> O <sub>3</sub>	0.08	b.d.	b.d.	b.d.	b.d.	b.d.	b.d.	b.d.
FeO	6.96	7.66	9.03	8.88	10.07	10.10	10.33	10.07
MnO	0.12	0.17	0.18	0.13	0.24	0.22	0.18	0.24
MgO	51.25	50.94	49.39	49.19	48.67	48.43	48.82	48.91
CaO	0.05	0.06	0.38	0.42	0.28	0.28	0.26	0.25
NiO	0.43	0.33	0.22	0.32	0.30	0.31	0.28	0.33
TOTAL	100.17	100.32	100.07	99.38	99.56	99.02	99.90	99.88
Atoms/4(O)								
Si	0.997	0.997	0.998	0.995	0.988	0.987	0.988	0.987
Al	0.001	0.000	0.001	0.001	0.001	0.001	0.000	0.001
Cr	0.002	0.000	0.000	0.000	0.000	0.000	0.000	0.000
Fe <sup>2+</sup>	0.141	0.155	0.185	0.183	0.208	0.210	0.213	0.208
Mn	0.002	0.003	0.004	0.003	0.005	0.005	0.004	0.005
Mg	1.848	1.840	1.800	1.806	1.795	1.797	1.796	1.798
Ca	0.001	0.002	0.010	0.011	0.007	0.007	0.007	0.007
Ni	0.008	0.006	0.004	0.006	0.006	0.006	0.006	0.007
Fo%	92.4	91.9	90	90.2	89.7	89.9	89.8	89.9
Sample	Jacko Lake				Iron Mask			
Position	230	230	99	99	07	07	07	07
	R	C	R	I	C	R	I	R
SiO <sub>2</sub>	40.80	40.91	40.60	40.74	40.92	40.80	40.79	40.91
Al <sub>2</sub> O <sub>3</sub>	0.04	b.d.	0.05	0.03	0.04	0.02	0.05	0.05
Cr <sub>2</sub> O <sub>3</sub>	b.d.	b.d.	b.d.	b.d.	0.11	b.d.	b.d.	0.08
FeO	7.63	7.66	8.84	8.98	7.73	8.92	7.81	7.69
MnO	0.11	0.08	0.19	0.17	0.08	0.17	0.13	0.10
MgO	50.40	50.22	50.31	49.96	51.37	50.07	51.26	51.71
CaO	0.08	0.07	0.29	0.23	0.09	0.18	0.09	0.11
NiO	0.41	0.39	0.32	0.34	0.42	0.31	0.28	0.39
TOTAL	99.47	99.33	100.60	100.45	100.76	100.47	100.41	101.04
Atoms/4(O)								
Si	0.997	1.001	0.988	0.992	0.988	0.993	0.989	0.986
Al	0.001	0.000	0.001	0.001	0.001	0.001	0.001	0.001
Cr	0.000	0.000	0.000	0.000	0.002	0.000	0.000	0.002
Fe <sup>2+</sup>	0.156	0.157	0.180	0.183	0.156	0.182	0.158	0.155
Mn	0.002	0.002	0.004	0.004	0.002	0.004	0.003	0.002
Mg	1.836	1.831	1.825	1.815	1.850	1.817	1.852	1.857
Ca	0.002	0.002	0.008	0.006	0.002	0.005	0.002	0.003
Ni	0.008	0.008	0.006	0.007	0.008	0.006	0.005	0.008
Fo%	91.8	91.5	91.2	90.7	92.5	90.8	92.6	92.9

Sample numbers refer to whole-rock analyses in Table 4. Formulae calculated on 4 oxygens; C=core, I=interior, R=rim.

talc. The basalts can be subdivided texturally into cumulate and volcanic rocks. The Watching Creek locality typifies the cumulate phase; olivine phenocrysts occur in a groundmass of intercumulus clinopyroxene phenocrysts. Rocks from the three other localities are characterized by a volcanic texture, with olivine phenocrysts and smaller, euhedral clinopyroxene microphenocrysts in a fine-grained groundmass. At Carabine Creek, numerous small (< 0.2 cm) vesicles are filled with secondary fibrous thomsonite, a variety of zeolite.

Olivine phenocrysts are subhedral to euhedral and range in size from 0.5 to 3.5 millimetres. The grains show no resorption features and are generally altered only slightly at the rims and along fractures in the mineral grains. Olivine phenocryst abundances in the Kamloops Lake picritic basalts range from 20 to 30% at Iron Mask, Jacko Lake and Carabine Creek and 35 to 50% at Watching Creek. Anhedral inclusions of spinel within olivine grains are common in most samples. In the most altered rocks, olivine phenocrysts are rimmed by anhedral, fine-grained opaque material interpreted as secondary spinel produced through the breakdown of olivine.

Clinopyroxene occurs as anhedral phenocrysts (Watching Creek), and subhedral to euhedral microphenocrysts (Carabine Creek, Jacko Lake, Iron Mask). Clinopyroxene represents approximately 20 to 25% (Watching Creek) to 30 to 45% (Jacko Lake, Carabine Creek) of the rock and ranges in size from 0.05 to 0.25 millimetre (Jacko Lake, Carabine Creek) or 0.5 to 2.5 millimetres (Watching Creek). Grains generally exhibit a slight yellowish pleochroism and inclusions of subhedral to anhedral spinel in both forms of clinopyroxene are very common, indicating that olivine and spinel were the primary liquidus phases. Zoning is evident only in the microphenocrysts in the non-cumulate rocks. Pigeonite has been reported at the Jacko Lake locality by Mathews (1941), but none was recognized during this study.

Spinel in the picritic basalts occur throughout the crystallization sequence; small inclusions of subhedral to anhedral spinel within olivine and clinopyroxene are common. Spinel also occurs as subhedral to anhedral microphenocrysts up to 0.3 millimetre and is scattered throughout the groundmass in crystals ranging from 0.005 to 0.15 millimetre across. Serpentinized picritic basalt in the Iron Mask batholith has oxides as an alteration product through the breakdown of olivine and clinopyroxene to serpentine, talc and tremolite during hydrothermal alteration induced by the

Iron Mask intrusive suite. The majority of spinels from these samples are not primary and are not included in the following discussion of mineral compositions.

## MINERAL CHEMISTRY

The three major phases, olivine, clinopyroxene and spinel were analyzed on a Cameca SX-50 electron microprobe at The University of British Columbia, with operating conditions of 15 kilovolts and 20 or 30 nanoamps.

Representative olivine compositions for each of the four Kamloops Lake picritic basalt localities are shown in Table 1. Compositions of olivine phenocrysts range from  $Fe_{0.29-0.89.5}$ , reflecting the high magnesium content of the magma. Zoning in the olivine phenocrysts ranges from unzoned in the Watching Creek locality to slightly zoned (up to 1 mole % Fo from core to rim) at the Carabine Creek, Jacko Lake and Iron Mask localities.

The NiO content in the olivine phenocrysts from the Kamloops Lake suite ranges from 0.22 to 0.43 weight% but is not correlated to forsterite content (Figure 3). In contrast, data from some other ultramafic rock suites exhibits a well-defined positive trend of forsterite content versus NiO (Gorgona Island; Echeverria, 1980; Kilauea picritic basalts; Nicholls and Stout, 1988). Furthermore, NiO contents of olivine are slightly greater for a similar forsterite composition in these suites. Olivines from

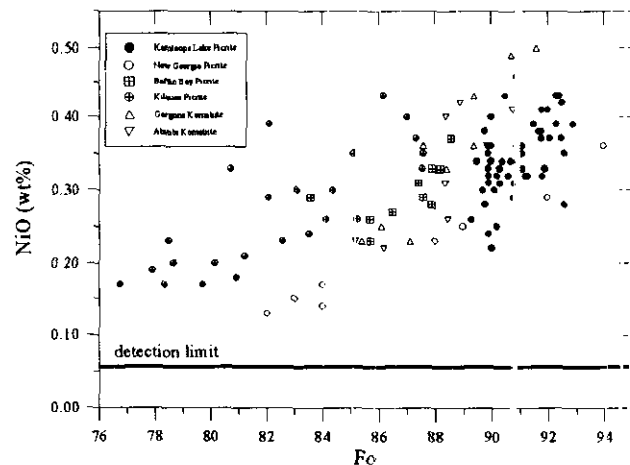


Figure 3. Forsterite content vs nickel (ppm) for olivine from the Kamloops Lake picrites and other ultramafic suites. Sources of data: New George (Ramsay *et al.*, 1984), Baffin Bay (Francis, 1985), Kilauea (Nicholls and Stout, 1988), Gorgona (Echeverria, 1980) and Abitibi (Barnes *et al.*, 1980).



**TABLE 3. REPRESENTATIVE ELECTRON MICROPROBE ANALYSES OF SPINEL IN THE KAMLOOPS LAKE PICRITIC BASALTS.**

Sample Position	Carabine Creek				Watching Creek			
	224 gm	224 inc-ol	225 inc-py-C	225 inc-ol-C	240 pheno-R	240 pheno-C	240 inc-py-I	240 inc-py-I
SiO <sub>2</sub>	0.15	0.06	0.06	0.03	0.04	0.06	0.07	0.04
TiO <sub>2</sub>	0.60	0.40	0.58	0.58	1.43	1.16	1.22	1.03
Al <sub>2</sub> O <sub>3</sub>	8.83	7.17	8.53	8.30	12.08	9.25	8.62	8.63
Cr <sub>2</sub> O <sub>3</sub>	28.70	49.46	30.60	27.92	10.82	13.65	16.04	15.81
Fe <sub>2</sub> O <sub>3</sub>	16.00	14.56	15.06	15.57	20.32	19.02	18.62	18.41
FeO	33.22	14.63	32.36	35.32	45.45	46.67	45.31	45.77
MnO	0.43	0.10	0.16	0.21	0.26	0.20	0.23	0.22
MgO	10.83	11.74	11.54	11.21	8.83	9.31	9.58	9.52
CaO	0.09	0.03	0.13	b.d.	0.03	b.d.	0.02	0.02
NiO	0.25	0.17	0.28	0.30	0.40	0.39	0.39	0.41
ZnO	0.09	0.10	b.d.	b.d.	b.d.	b.d.	0.09	0.08
<b>TOTAL</b>	<b>99.19</b>	<b>98.43</b>	<b>99.30</b>	<b>99.44</b>	<b>99.66</b>	<b>99.71</b>	<b>100.19</b>	<b>99.94</b>
<b>Atoms/32(O)</b>								
Si	0.040	0.016	0.016	0.008	0.011	0.016	0.019	0.011
Ti <sup>4+</sup>	0.122	0.081	0.117	0.118	0.291	0.238	0.249	0.211
Al	2.808	2.280	2.699	2.636	3.846	2.972	2.759	2.770
Cr <sup>3+</sup>	6.123	10.553	6.496	5.950	2.311	2.943	3.444	3.405
Fe <sup>3+</sup>	6.745	2.971	6.539	7.163	9.240	9.576	9.260	9.381
Fe <sup>2+</sup>	3.610	3.287	3.380	3.509	4.590	4.338	4.228	4.194
Mn <sup>2+</sup>	0.098	0.023	0.036	0.048	0.059	0.046	0.053	0.051
Mg	4.357	4.723	4.619	4.504	3.556	3.785	3.879	3.866
Ca	0.026	0.009	0.037	0.000	0.009	0.000	0.006	0.006
Ni	0.054	0.037	0.060	0.065	0.087	0.086	0.085	0.090
Zn	0.018	0.020	0.000	0.000	0.000	0.000	0.018	0.016
CR#	68.56	82.23	70.65	69.30	37.53	49.75	55.52	55.14
MG#	54.69	58.96	57.74	56.21	43.65	46.60	47.85	47.97
<b>Jacko Lake</b>								
Sample Position	230 pheno-C	230 pheno-I	230 gm	230 gm	99 inc-py-I	99 inc-py		
SiO <sub>2</sub>	0.03	0.05	0.56	0.92	0.06	0.74		
TiO <sub>2</sub>	0.48	0.56	0.40	0.72	0.55	0.51		
Al <sub>2</sub> O <sub>3</sub>	8.10	8.56	7.16	9.02	7.63	6.94		
Cr <sub>2</sub> O <sub>3</sub>	33.75	30.50	32.93	22.45	26.09	27.10		
Fe <sub>2</sub> O <sub>3</sub>	14.43	14.95	18.73	19.52	14.88	15.20		
FeO	30.89	33.91	30.56	37.08	38.34	36.08		
MnO	0.15	0.17	0.23	0.24	0.20	0.16		
MgO	12.10	12.03	9.60	9.53	11.50	11.64		
CaO	b.d.	b.d.	0.04	0.08	0.17	0.14		
NiO	0.29	0.28	0.24	0.31	0.31	0.34		
ZnO	0.08	b.d.	0.07	b.d.	b.d.	b.d.		
<b>TOTAL</b>	<b>100.29</b>	<b>101.01</b>	<b>100.52</b>	<b>99.86</b>	<b>99.73</b>	<b>98.85</b>		
<b>Atoms/32(O)</b>								
Si	0.008	0.013	0.151	0.249	0.016	0.201		
Ti <sup>4+</sup>	0.096	0.111	0.081	0.146	0.111	0.104		
Al	2.535	2.661	2.281	2.873	2.421	2.218		
Cr <sup>3+</sup>	7.086	6.361	7.038	4.797	5.555	5.810		
Fe <sup>3+</sup>	6.172	6.730	6.216	7.540	7.769	7.362		
Fe <sup>2+</sup>	3.203	3.297	4.234	4.410	3.350	3.448		
Mn <sup>2+</sup>	0.034	0.038	0.053	0.055	0.046	0.037		
Mg	4.790	4.731	3.869	3.840	4.617	4.706		
Ca	0.000	0.000	0.012	0.023	0.049	0.041		
Ni	0.062	0.059	0.052	0.067	0.067	0.074		
Zn	0.016	0.000	0.014	0.000	0.000	0.000		
CR#	73.65	70.51	75.52	62.54	69.65	72.37		
MG#	59.93	58.93	47.75	46.55	57.95	57.71		

CR# = 100\*Cr/(Cr+Al); MG# = 100\*Mg/(Mg+Fe<sup>2+</sup>). Sample numbers refer to whole-rock analyses in Table 4. Formulae calculated on 32 oxygens; P=phenocryst, MP=micropenocryst, GM=groundmass, INC=inclusion (host mineral indicated), C=core, I=interior, R=rim.

the New Georgia arc (Ramsay *et al.*, 1984), although also showing a positive correlation between NiO and forsterite content, are, in general, depleted in NiO with respect to the Kamloops Lake picritic basalts. Nickel concentrations and forsterite contents of olivines in Kamloops Lake picrites are consistent with mantle-derived olivine (Sato, 1977). The CaO concentration in olivines from the picritic basalts averages 0.25 weight% which for basaltic rocks would suggest an extrusive or hypabyssal crystallization environment for the magma (Simkin and Smith, 1970).

Analyses of representative clinopyroxene phenocrysts and microphenocrysts for the Kamloops Lake picritic basalts are given in Table 2. Clinopyroxenes are diopsidic in composition with a slightly sub-calcic signature and composition varies little between localities, and between phenocrysts, microphenocrysts or groundmass. Minor zoning is seen in clinopyroxene crystals, with the Watching Creek locality exhibiting minimal normal zoning (core to rim of 5 mol% Mg), while the non-cumulate rocks tend to be more strongly zoned (core to rim up to 16 mol% Mg). The overall range in  $100 \cdot \text{Mg}/(\text{Mg} + \text{Fe}^{2+})$  is from 87.1 to 99.7, probably indicating that the Mg/Fe ratio in the melt was large or that the oxygen fugacity during clinopyroxene crystallization was quite high. In addition, all clinopyroxenes contain a significant amount of  $\text{Fe}^{3+}$  (see Table 2), which also suggests that the melt crystallized under high oxygen fugacity (Barsdell, 1988).

Chromium contents in the clinopyroxenes range from below detection limit to 1.32 weight% with an average of 0.66 weight%, consistent with the chromium content of the rocks. No systematic differences with respect to chromium contents are apparent between the cumulate and non-cumulate rocks. The moderate  $\text{Al}_2\text{O}_3$  contents of the clinopyroxenes (1.63-4.70 wt%) are anomalous compared to the very low whole-rock  $\text{Al}_2\text{O}_3$  contents, but  $\text{Al}_2\text{O}_3$ ,  $\text{TiO}_2$  (0.12-0.43 wt%) and  $\text{Na}_2\text{O}$  (0.17-0.33 wt%) contents of the Kamloops Lake picritic basalts are comparable to other island arc picrite suites such as Grenada (Arculus, 1978) and New Georgia (Ramsay *et al.*, 1984). Clinopyroxenes from the komatiite suites of Gorgona Island (Echeverria, 1980) and the Abitibi greenstone belt (Barnes *et al.*, 1983) typically contain more  $\text{Al}_2\text{O}_3$ . Sun and Nesbitt (1979) report that titanium contents in clinopyroxene from island arc suites are typically lower than for oceanic suites.

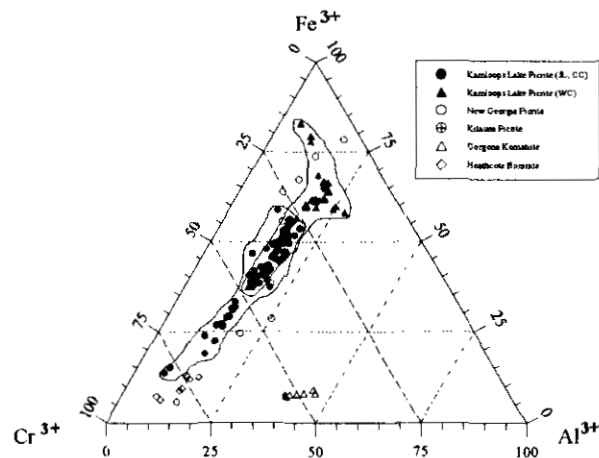


Figure 4. Ternary plot of the proportions of the cations  $\text{Cr}^{3+}$ ,  $\text{Al}^{3+}$ , and  $\text{Fe}^{3+}$  in spinels from Kamloops Lake picritic basalts. Fields are indicated for rocks with volcanic (Carabine Creek, Jacko Lake) vs cumulate texture (Watching Creek).

Spinels from the Kamloops Lake picritic basalts exhibit a wide range of chemistry; representative analyses are given in Table 3. Spinels have consistently low  $\text{Al}_2\text{O}_3$  contents (8.39 wt% average) and variable chromium and iron ( $\text{Fe}^{3+}$ ) contents (Figure 4). Systematic zoning in the spinels is not observed. In general, spinels from cumulate rocks at Watching Creek are higher in iron while spinels from non-cumulate rocks lie on the chromium-rich side of the spectrum. In comparison to the Kamloops Lake picritic basalts, komatiites from Gorgona Island (Echeverria, 1980) have higher  $\text{Al}_2\text{O}_3$  concentrations, while spinels from other ultramafic suites are comparable to the Kamloops Lake picritic basalts.

Figure 5 shows the range of spinel compositions. Again, the spinel compositions of the Kamloops Lake picritic basalts form two groups representing cumulate *versus* non-cumulate rocks, although there is a continuous spectrum of compositions with no obvious gaps in the spinel solid solution sequence. Spinel compositions from the Kamloops Lake picritic basalts are distinguished from spinels found in komatiites by depleted abundances of ZnO and MnO (Plaksenko and Smol'kin, 1990).

There is a weak correlation in spinels from the Kamloops Lake picritic suite between increasing  $\text{Cr}/(\text{Cr} + \text{Al})$  and increasing  $\text{Mg}/(\text{Mg} + \text{Fe}^{2+})$ . This trend is similar to spinels from lavas associated with arc magmatism (Ramsay *et al.*, 1984). In addition, the  $\text{Fe}^{3+}/(\text{Fe}^{3+} + \text{Cr} + \text{Al})$  ratios in the spinels of the Kamloops Lake picrites are all higher than the

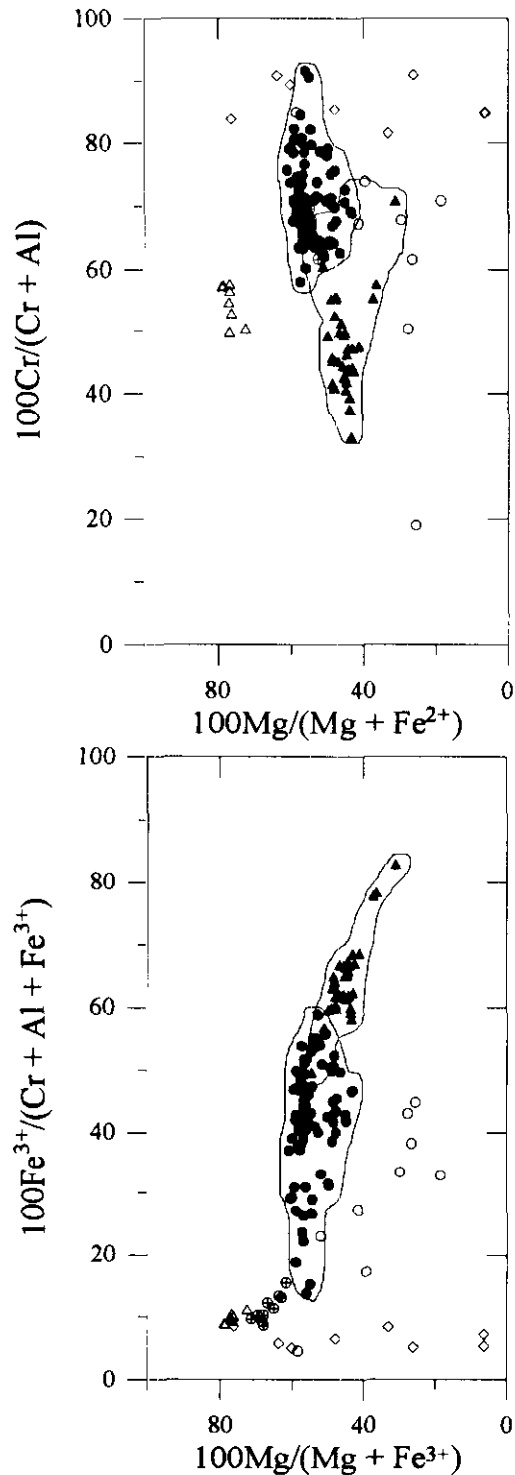


Figure 5. Spinel compositions for Kamloops Lake picritic basalts shown as: (a)  $Mg/Mg+Fe^{2+}$  vs  $Cr/Cr+Al$  and (b)  $Mg/(Mg+Fe^{2+})$  vs  $Fe^{3+}/(Fe^{3+}+Cr+Al)$ . Symbols as in Figure 4 represent data from: New Georgia (Ramsay *et al.*, 1984), Kilauea (Nicholls and Stout, 1988), Gorgona (Echeverria, 1980) and Heathcote (Crawford and Cameron, 1985)

highest value of this ratio for the majority of basic rocks (see Figure 5b), illustrating the oxidized nature of these spinels relative to sites found in other tectonic settings. All other occurrences of strongly oxidized spinels occur in lavas in an island arc setting (Ramsay *et al.*, 1984; Utter, 1978). In addition, Dick and Bullen (1984) would group spinels with a  $Cr/Cr+Al$  ratio similar to that observed in the Kamloops Lake picritic basalts into spinels derived from island arc sources.

## ROCK CHEMISTRY

Whole-rock major and trace element analyses and normative mineralogy for the Kamloops Lake picritic basalts are given in Table 4. These picritic basalts have exceptionally low  $Al_2O_3$  contents (2.17 to 6.34 wt%), low silica (38.4-43.2 wt%) and very high MgO (24.3-33.65 wt%).  $TiO_2$  and CaO contents are depleted with respect to some other picritic suites (Deccan, Baffin Bay) possibly due to the very high MgO. The Kamloops Lake picritic basalts also have large concentrations of nickel (920-1420 ppm) and chromium (1670-3040 ppm). The serpentinization of the Iron Mask localities does not significantly alter the rock chemistry.

Figure 6 shows Harker diagrams of  $MgO$ ,  $Al_2O_3$  and  $SiO_2$  for the Kamloops Lake picritic basalts and several other ultramafic suites. On all diagrams, the Kamloops Lake rocks fall at extreme ends of the chemical spectrum; they are enriched in MgO and depleted in  $SiO_2$  and  $Al_2O_3$  compared to other ultramafic suites. The extremely high MgO content is unlike many other picritic suites (Ramsay *et al.*, 1984; Krishnamurthy and Cox, 1997) and, taking MgO content alone into consideration, the Kamloops Lake picritic basalts are similar to some komatiite suites (Abitibi greenstone belt, Barberton Mountains). However, the Kamloops Lake magmas are enriched in strontium, barium, nickel and chromium relative to komatiite melts (Plaksenko and Smol'kin, 1990), distinguishing them as true picrites. Boninites contain more  $SiO_2$  and less MgO than either komatiites or picrites.

Testing for a cogenetic relationship between the four occurrences of the Kamloops Lake picritic basalts was undertaken using Pearce element-ratio diagrams (Pearce, 1968; Russell and Nicholls, 1988; Nicholls and Russell, 1991). The principal concept behind this method is that rocks that are related to each other through fractionation or accumulation of a given mineral

**TABLE 4. WHOLE-ROCK MAJOR AND TRACE ELEMENT CHEMICAL COMPOSITIONS OF THE KAMLOOPS LAKE PICRITIC BASALT WITH CALCULATED NORMATIVE MINERALOGY.**

	225 CC	222 CC	241 WC	230 JL	108* IM	309 IM	error
SiO <sub>2</sub>	40.40	38.70	38.40	41.30	39.33	43.20	0.197
TiO <sub>2</sub>	0.230	0.193	0.166	0.240	0.21	0.386	0.005
Al <sub>2</sub> O <sub>3</sub>	3.80	3.08	2.17	3.94	2.74	6.84	0.056
Fe <sub>2</sub> O <sub>3</sub>	2.63	6.42	10.30	4.48	11.00	5.01	0.063
FeO	3.97	2.64	—	4.72	—	4.40	0?
MnO	0.17	0.17	0.18	0.17	0.20	0.14	0.004
MgO	31.40	32.80	32.60	32.30	33.65	24.30	0.217
CaO	4.72	3.20	5.32	4.91	3.53	6.03	0.109
Na <sub>2</sub> O	0.09	0.02	0.08	0.18	0.15	0.30	0.012
K <sub>2</sub> O	0.95	0.22	0.15	1.50	0.57	2.21	0.012
P <sub>2</sub> O <sub>5</sub>	0.11	0.10	0.05	0.10	0.06	0.13	0?
H <sub>2</sub> O <sup>+</sup>	7.80	11.10	9.20	4.70	7.38	4.80	
CO <sub>2</sub>	0.08	0.08	0.36	0.04	0.08	0.03	
LOI	8.45	11.80	9.75	4.80	7.10	5.00	
SUM	100.44	100.08	99.57	99.61	99.45	98.68	
<i>Trace Elements</i>							
Ba <sup>1</sup>	213	147	226	521	129	354	
Rb <sup>2</sup>	31.11		3.83	26.03	16.30		
Sr <sup>2</sup>	216.44		41.00	112.92	14.00		
Nb <sup>2</sup>	0.59		0.13	0.37	0.31		
Zr <sup>2</sup>	11.80		4.35	10.85	10.55		
Y <sup>2</sup>	4.34		2.57	4.03	3.90		
Ni <sup>1</sup>	1350	1380	1420	1410	1254	920	
Cr <sup>1</sup>	2580	3040	2790	2990	2902	1670	
V <sup>2</sup>	110.91		61.90	103.12	74.95		
Sc <sup>2</sup>	18.27		21.41	17.41	20.73		
Th <sup>2</sup>	0.23		0.10	0.27	0.28		
U <sup>2</sup>	0.09		0.06	0.09	0.20		
Pb <sup>2</sup>	1.50		0.99	1.65	0.31		
Hf <sup>2</sup>	0.51		0.16	0.44	0.39		
Cl <sup>1</sup>	128	109	293	125	396	125	
Co <sup>1</sup>	80	85	87	85	92	66	
Cu <sup>1</sup>	25	15	20	30	25	17	
F <sup>1</sup>	75	110	20	90	45	192	
Ga <sup>1</sup>	16	16	16	16	17	19	
S <sup>1</sup>	-50	-50	1120	-50	1662	-50	
Sn <sup>1</sup>	10	10	7	12	4	10	
Ti <sup>1</sup>	1210	981	746	1160	1210	1780	
Zn <sup>1</sup>	58	60	61	60	50	58	
Li <sup>2</sup>	6.57		7.70	6.62	4.69		
Be <sup>2</sup>	0.65		0.01	0.82	0.81		
Mo <sup>2</sup>	0.11		0.47	0.25	3.40		
Cs <sup>2</sup>	0.63		0.24	1.43	0.80		
Ta <sup>2</sup>	0.37		0.08	0.17	0.15		
Tl <sup>2</sup>	0.23		-0.08	0.09	0.09		
Bi <sup>2</sup>	0.07		-0.06	0.17	0.10		
<i>Normative Mineralogy**</i>							
OR	6.38	1.50	1.01	6.59	3.74	14.15	
(AL)	0.86	0.19	0.77	0.00	1.40	2.75	
(AN)	8.10	8.82	5.78	6.68	5.66	11.67	
LU	0.00	0.00	0.00	2.30	0.00	0.00	
NE	0.00	0.00	0.00	0.09	0.00	0.00	
DI	14.03	6.94	18.89	15.01	10.58	15.84	
HY	7.93	16.04	0.60	0.00	3.67	2.39	
OL	61.94	65.80	72.48	68.62	74.32	52.13	
CR	0.63	0.75	0.68	0.69	0.69	0.39	
IL	0.50	0.42	0.36	0.49	0.44	0.79	
AP	0.30	0.27	0.13	0.26	0.16	0.33	

\* Average of six analyses; \*\* Calculated with FeO=FeT  
<sup>1</sup> XRF Pressed Pellet  
<sup>2</sup> Internally Coupled Plasma Mass Spectrometry  
 CC=Carabine Creek, WC=Watching Creek, JL=Jacko Lake, IM=Iron Mask

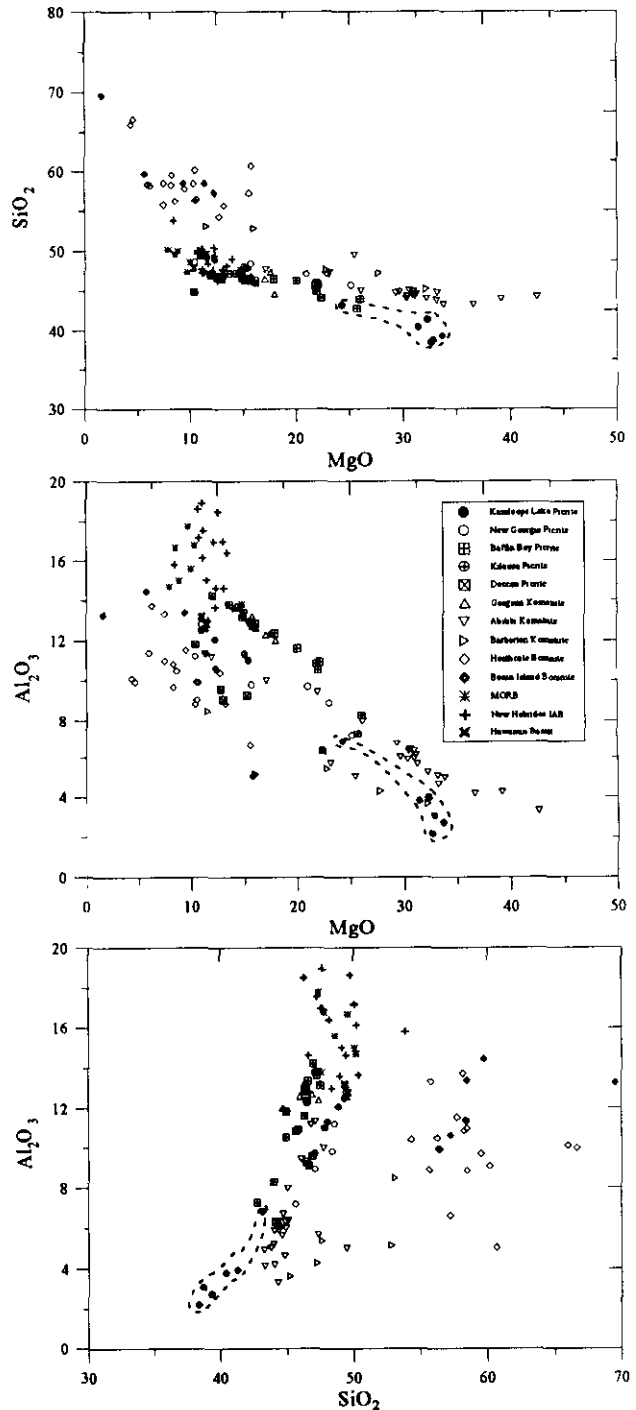


Figure 6. Chemical compositions of Kamloops Lake picritic basalts and other suites of ultramafic rocks: (a) MgO vs SiO<sub>2</sub>, (b) MgO vs Al<sub>2</sub>O<sub>3</sub> and (c) SiO<sub>2</sub> vs Al<sub>2</sub>O<sub>3</sub>. Data sources: New Georgia (Ramsay *et al.*, 1984), Kilauea (Nicholls and Stout, 1988), Baffin Bay (Francis, 1985), Deccan (Krishnamurthy and Cox, 1977), Abitibi (Barnes *et al.*, 1983), Barberton (Viljoen and Viljoen, 1969), Gorgona (Echeverria, 1980), Heathcote (Crawford and Cameron, 1985), Bonin Island (Hickey and Frey, 1982), MORB (Sun and Nesbitt, 1979), New Hebrides (Dupey *et al.*, 1982) and Hawaiian basalt (Wright, 1971).

or mineral assemblage will define a line with a predictable slope. The diagram (Figure 7) was designed by choosing an appropriate conserved element for the denominator (*e.g.*, Ti), and choosing a set of numerator elements for the x and y-axes that will model the effects of the target mineral assemblage. In Figure 7a, a cluster of open circles represents six duplicate analyses obtained from sample 92IM-108, a serpentinite from the Iron Mask batholith. An analytical error was calculated from these duplicates and applied to all other data points for the Kamloops Lake picritic basalts.

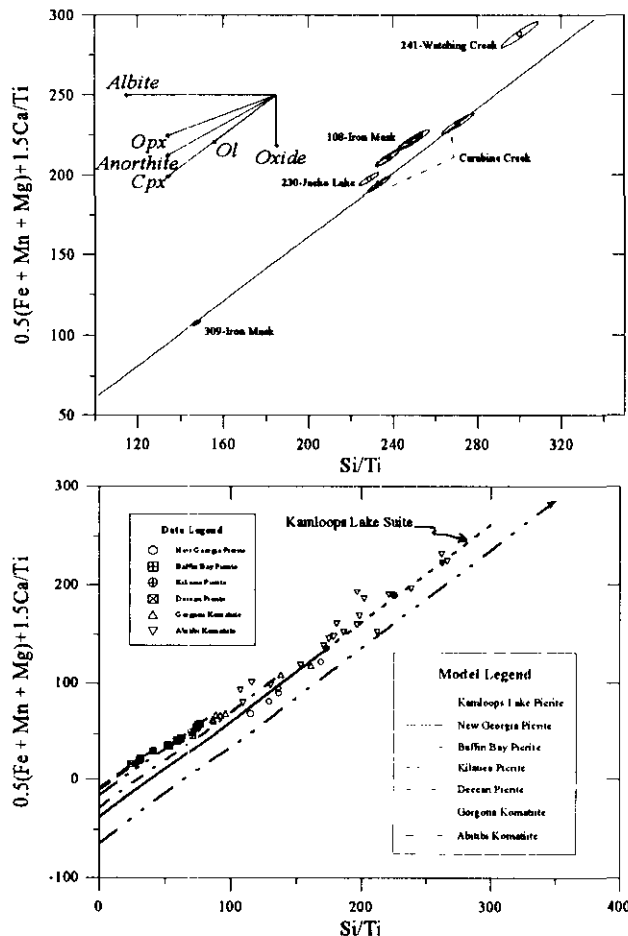


Figure 7. Chemical variation of (a) Kamloops Lake picritic basalts and (b) other mafic-ultramafic rock suites are shown as Pearce element-ratio diagrams that portray the effects of olivine and clinopyroxene. See text.

For this study, one sample from Carabine Creek (92IM-225) was chosen as the reference sample and is used as a basis for comparison for all other samples. Sample 92IM-225 is the least altered picrite obtained and displays a distinctive volcanic character.

Figure 7a tests for the cogenetic relationship of the Kamloops Lake picritic basalts through olivine and clinopyroxene fractionation. Both samples from Carabine Creek plot along a slope of one indicating that this process explains the chemical variation between these two samples. In addition, one sample from the Iron Mask batholith is also consistent with this scenario. Other samples from Watching Creek, Jacko Lake and the Iron Mask batholith still fail to be explained as comagmatic by this process. Given the field relationships and petrography, the most logical explanation is that the picritic basalts represent several magma batches (*cf.* Nicholls and Russell, 1991).

Other ultramafic suites have been plotted for comparison on the same diagrams that were developed for the Kamloops Lake suite. Boninite suites are not shown because of the inability to conclude that titanium would be a conserved element during crystallization. The results (Figure 7b) illustrate that this method appears to consistently explain some of the crystallization and fractionation processes of ultramafic volcanic rocks.

The dashed line on Figure 7b represents the differentiation trend of the Kamloops Lake suite from Figure 7a. Because these rocks are enriched in MgO, they lie to the upper left of most of the suites. However, the intercept of the differentiation trend is a function of the source region. It is apparent that the intercept of the Kamloops Lake suite is very close to the intercept of the New Georgia picrites, which are an island arc suite. This implies that the source regions for these two suites of rocks may be similar.

## CONCLUSIONS

The Kamloops Lake picritic basalts represent an episode of ultramafic volcanism at the later stages of Late Triassic Nicola volcanism. They lie stratigraphically above the Nicola Group arc rocks and occur as inclusions in the Early Jurassic Iron Mask batholith, which restricts the ultramafic lavas as a late Triassic to Early Jurassic event.

Based on relict mineralogy and textures and rock and mineral chemistry, the Iron Mask serpentinite bodies are equivalent to the picritic basalts found at Jacko Lake, Carabine Creek and Watching Creek.

The Kamloops Lake suite shows no appreciable contamination or fractionation. The extreme forsterite content of the olivine phenocrysts is indicative of an upper mantle

source. Therefore, the suite represents primary magmas derived from the upper mantle beneath the Nicola arc during the Late Triassic. In addition, the oxidized nature of the spinels and the trace and major element chemistry further indicate that they represent ultramafic magmatism in an island arc setting.

Modeling fractionation with the Pearce element-ratio methods indicates that some picrite exposures may be cogenetic rocks related through olivine and clinopyroxene sorting. Results also indicate that the Kamloops Lake picritic magmas most likely represent more than one magma series.

## ACKNOWLEDGMENTS

Funding for this study was supplied by Natural Sciences and Engineering Research Council of Canada, the Science Council of British Columbia, and industry through the Mineral Deposit Research Unit at The University of British Columbia on the research project "Copper-Gold Porphyry Deposits of British Columbia." The electron microprobe expertise of Dr. Mati Raudsepp is gratefully appreciated.

## REFERENCES

- Arculus, R.J. (1978): Mineralogy and Petrology of Grenada, Lesser Antilles Island Arc; *Contributions to Mineralogy and Petrology*, Volume 65, pages 413-424.
- Barnes, S.J., Gorton, M.P. and Naldrett, A.J. (1983): A Comparative Study of Olivine and Clinopyroxene Spinifex Flows from Alexo, Abitibi Greenstone Belt, Ontario, Canada; *Contributions to Mineralogy and Petrology*, Volume 83, pages 293-308.
- Barsdell, M. (1988): Petrology and Petrogenesis of Clinopyroxene-rich Tholeiitic Lavas, Merelava Volcano, Vanuatu; *Journal of Petrology*, Volume 29, pages 927-964.
- Carr, J.M. (1957): Deposits Associated with Eastern Part of the Iron Mask Batholith near Kamloops; *B.C. Minister of Mines*, Annual Report 1956, pages 47-69.
- Crawford, A.J. and Cameron, W.E. (1985): Petrology and Geochemistry of Cambrian Boninites and Low-Ti Andesites from Heathcote, Victoria; *Contributions to Mineralogy and Petrology*, Volume 91, pages 93-104.
- Cockfield, W.E. (1948): Geology and Mineral Deposits of Nicola Map-area, British Columbia; *Geological Survey of Canada*, Memoir 249.
- Dick, H.J.B. and Bullen, T. (1984): Chromium Spinel as a Petrogenetic Indicator in Abyssal and Alpine-type Peridotites and Spatially Associated Lavas; *Contributions to Mineralogy and Petrology*, Volume 86, pages 54-76.
- Dupey, C., Dostal, J., Marcelot, G., Bougault, H., Joron, J.L. and Treuil, M. (1982): Geochemistry of Basalts from Central and Southern New Hebrides Arc: Implication for their Source Rock Composition; *Earth and Planetary Science Letters*, Volume 60, pages 207-225.
- Echeverria, L.M. (1980): Tertiary or Mesozoic Komatiites from Gorgona Island, Colombia: Field Relations and Geochemistry; *Contributions to Mineralogy and Petrology*, Volume 73, pages 253-266.
- Ewing, T. (1982): Geologic Map of Tertiary Rocks of the Afton-Tranquille Area West of Kamloops, B.C. (92/9,10); *B.C. Ministry of Energy, Mines and Petroleum Resources*, Preliminary Map 48 and accompanying notes, 19 pages.
- Francis, D. (1985): The Baffin Bay Lavas and the Value of Picrites as Analogues of Primary Magmas; *Contributions to Mineralogy and Petrology*, Volume 89, pages 144-154.
- Ghosh, D. (1993): Uranium-Lead Geochronology; in Porphyry Cu-Au Systems of British Columbia, *Mineral Deposit Research Unit*, Annual Technical Report, pages 11.1-11.26.
- Hickey, R.L. and Frey, F.A. (1982): Geochemical Characteristics of Boninite Series Volcanics: Implications for their Source; *Geochimica et Cosmochimica Acta*, Volume 46, pages 2099-2115.
- Krishnamurthy, P. and Cox, K.G. (1977): Picrite Basalts and Related Lavas from the Deccan Traps of Western India; *Contributions to Mineralogy and Petrology*, Volume 62, pages 53-75.
- Kwong, Y.T.J. (1987): Evolution of the Iron Mask Batholith and its Associated Copper Mineralization; *B.C. Ministry of Energy, Mines and Petroleum Resources*, Bulletin 77.
- Mathews, H.M. (1941): Geology of the Ironmask Batholith; *The University of British Columbia*, unpublished M. Sc. thesis, 42 pages.
- Nicholls, J. and Russell, J.K. (1991): Major-element Chemical Discrimination of Magma-batches in Lavas from Kilauea volcano, Hawaii, 1954 - 1971 Eruptions; *Canadian Mineralogist*, Volume 29, pages 981-993.
- Nicholls, J. and Stout, M.Z. (1988): Picritic Melts in Kilauea - Evidence from the 1967-1968 Halemaumau and Hiiaka Eruptions; *Journal of Petrology*, Volume 29, pages 1031-1057.
- Northcote, K.E. (1977): Iron Mask Batholith; *B.C. Ministry of Energy, Mines and Petroleum Resources*, Preliminary Map 26 and accompanying notes, 8 pages.
- Pearce, T.H. (1968): A Contribution to the Theory of Variation Diagrams; *Contributions to Mineralogy and Petrology*, Volume 19, pages 142-157.
- Plaksenko, A.N. and Smol'kin, V.F. (1990): Typomorphism of Accessory Chromium Spinel in Highly Magnesian Volcanics; *International Geology Review*, pages 244-259.
- Preto, V.A. (1968): Geology of the Eastern Part of the Iron Mask Batholith; *B.C. Minister of Mines and Petroleum Resources*, Annual Report 1967, pages 137-147.
- Preto, V.A. (1979): Geology of the Nicola Group between Merritt and Princeton; *B.C. Ministry*

- of Energy, Mines and Petroleum Resources*,  
Bulletin 69.
- Ramsay, W.R.H., Crawford A.J. and Foden, J.D.  
(1984): Field Setting, Mineralogy, Chemistry,  
and Genesis of Arc Picrites, New Georgia,  
Solomon Islands; *Contributions to Mineralogy  
and Petrology*, Volume 88, pages 386-402.
- Ross, K.V., Dawson, K.M., Godwin, C.I. and Bond,  
L. (1993): Major Lithologies and Alteration of  
the Ajax East Orebody, a Sub-alkalic Copper-  
Gold Porphyry Deposit, Kamloops, South  
Central British Columbia; in *Current  
Research, Part A; Geological Survey of  
Canada*, Paper 92-1A, pages 87-96.
- Russell, J.K. and Nicholls, J. (1988): Analysis of  
Petrologic Hypotheses with Pearce Element  
Ratios; *Contributions to Mineralogy and  
Petrology*, Volume 99, pages 25-35.
- Sato, H. (1977): Nickel Content of Basaltic Magmas:  
Identification of Primary Magmas and a  
Measure of the Degree of Olivine  
Fractionation; *Lithos*, Volume 10, pages 113-  
120.
- Simkin, T. and Smith, J.V. (1970): Minor-element  
Distribution in Olivine; *Journal of Geology*,  
Volume 78, pages 304-325.
- Snyder L.D. and Russell, J.K. (1993): Field  
Constraints on Diverse Igneous Processes in  
the Iron Mask Batholith (92/9, 10); in  
*Geological Fieldwork 1992*, Grant, B. and  
Newell, J.M., Editors, *B.C. Ministry of  
Energy, Mines and Petroleum Resources*,  
Paper 1993-1, pages 281-286.
- Sun, S.-S. and Nesbitt, R.W. (1978): Petrogenesis of  
Archean Ultrabasic and Basic Volcanics:  
Evidence from Rare Earth Elements;  
*Contributions to Mineralogy and Petrology*,  
Volume 65, pages 301-325.
- Sun, S.-S. and Nesbitt, R.W. (1979): Geochemical  
Characteristics of Mid-ocean Ridge Basalts;  
*Earth and Planetary Science Letters*, Volume  
44, pages 119-138.
- Utter, T. (1978): The Origin of Detrital Chromites in  
the Klerksdorp Goldfield, Witwatersrand,  
South Africa; *Nues Jahrbuch für Mineralogie,  
Abhandlungen*, Volume 133, pages 191-209.
- Viljoen, R.P. and Viljoen, M.J. (1969): Evidence for  
the Composition of the Primitive Mantle and  
its Products of Partial Melting from a Study of  
the Mafic and Ultramafic Rocks of the  
Barberton Mountain Land; in *Upper Mantle  
Project, Geological Society of South Africa*,  
Special Publication No. 2, pages 275-295.
- Wright, T.L. (1971): Chemistry of Kilauea and  
Mauna Loa in Space and Time; *U.S.  
Geological Survey*, Professional Paper 735,  
pages 1-40.

## **NOTES**



**SILICA-UNDERSATURATED, ZONED, ALKALINE INTRUSIONS  
WITHIN THE BRITISH COLUMBIA CORDILLERA**

By Brian A. Lueck and J. K. Russell  
Department of Geological Sciences (MDRU), U.B.C.

(MDRU Contribution 038)

**KEYWORDS:** Petrology, pyroxenite, syenite, alkaline, silica-undersaturated, melanite, cumulates.

**INTRODUCTION**

Within the framework of cordilleran alkaline intrusions, there is a unique group of plutons characterized by pyroxenite and syenite (Lueck *et al.*, 1993). Some members of this plutonic suite host porphyry copper-gold mineralization and mineralized plutons show distinct petrological differences from barren plutons.

Individual plutons show variable plutonic zonation, the most prevalent being a pyroxenite border phase with a central core of syenite. The pyroxenite encloses syenite, which typically contains an abundance of aligned alkali feldspar megacrysts. This zoning suggests that individual silica-undersaturated magma bodies fractionate aegirine-augite in their early crystallization history, thus forming the enclosing pyroxenites. Intermediate phases are mela-syenites which occur adjacent to pyroxenite and are mineralogical mixtures of pyroxenite and syenite.

**THE PYROXENITE-SYENITE ASSOCIATION**

**DESCRIPTION**

Plutons of the pyroxenite-syenite association occur in widely dispersed regions of the Canadian Cordillera (Currie, 1976; Anderson, 1993). Previous studies of the Averill pluton (Keep and Russell, 1992) and the Rugged Mountain pluton (Neil and Russell, 1993) provide the framework for a description of the chemistry and mineralogy of this suite. Distinct similarities between the Averill and Rugged Mountain plutons include: the presence of a silica-undersaturated suite of rocks spanning the compositional range from pyroxenite to syenite, strong iron enrichment for the rock suite as a whole, the presence of a distinct igneous mineral assemblage comprising alkali feldspar, aegirine-augite, biotite, melanite, titanite and apatite, and plutonic-scale petrological zonation.

Field and literature research has defined at least twelve plutons in British Columbia which share these characteristics. These plutons (Figure 1) span the length of the British Columbia Cordillera. They intrude basement and volcanic arc rocks of both the Stikine and Quesnell terranes and were emplaced

during the time period from Late Triassic to Early Jurassic.

Field studies of the Zippa Mountain pluton (Lueck and Russell, in press) provide evidence of cumulate processes in the formation of this pluton. This field evidence includes the presence of strong concentric petrological zoning in the form of a 200 to 500 metre thick pyroxenite and mela-syenite unit enclosing a core of syenite, a pervasive, mappable, inwardly dipping, non-tectonic mineral fabric formed by the planar alignment of alkali feldspar and pyroxene, and fabric-concordant mineral zonation in the form of vishnevite-cancrinite, aegirine-augite and melanite-rich layers within the syenite. A low silica activity is implied by the presence of vishnevite-cancrinite and melanite.

**THE DEFINING CHARACTERISTICS OF THE SUITE**

The twelve plutons shown on Figure 1 are the minimum number of plutons which can be defined as silica-undersaturated, zoned alkaline plutons. All of the plutons shown have the critical elements that indicate they are part of this suite. Most of these attributes were detailed by Neil and Russell (1993).

**MINERALOGY**

The mineralogy of this plutonic suite shows little variation in the characteristic mineral suite of aegirine-augite, potassium feldspar, biotite, melanite, titanite and apatite. Various proportions of these minerals comprise the dominant rock types of pyroxenite, mela-syenite and syenite. Testing of the comagmatic hypothesis using Pearce element-ratio tests (Lueck *et al.*, 1993), was done for the Rugged Mountain pluton (Figure 2) using zirconium as a conserved constituent of the melt. This diagram tests for the sorting of feldspar and augite to explain the chemical diversity of the plutonic suite. The test does not reject the comagmatic hypothesis.

Notable variations on the above described mineralogy include the presence of major amounts of hornblende, magnetite and vishnevite-cancrinite in some plutons (Neil and Russell, 1993; Currie, 1976; Lueck and Russell, in press). The presence of both hornblende and magnetite in these plutons is an important criteria for the differentiation of mineralized from barren intrusions (Table 1).

Figure 1. Location map of silica-undersaturated zoned intrusions within the British Columbia cordillera.

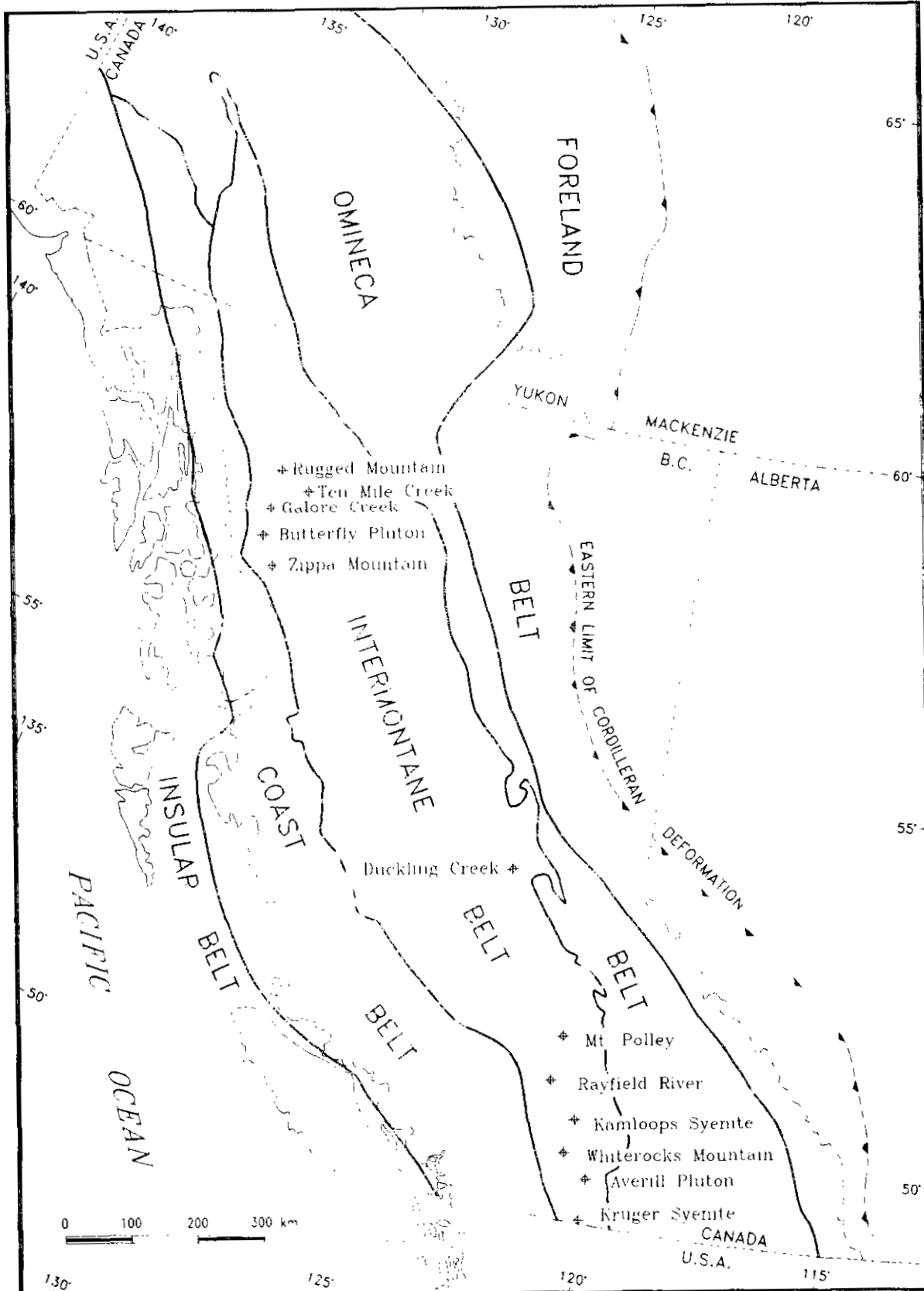


TABLE 1. Silica-undersaturated plutons and the relationship between mineralogy and Cu-Au mineralization.

Pluton	Dominant Mafic Phase	Abundant Magnetite	Terrane Affinity
<b>Mineralized (Cu-Au)</b>			
Galore Creek	Hornblende	Yes	Stik nia
Averill	Hornblende	Yes	Quest ellia
Duckling Creek	Hornblende	Yes	Quest ellia
Mt. Polley	Hornblende	Yes	Quest ellia
Rayfield River	Hornblende	Yes	Quest ellia
<b>No known reserves</b>			
Zippa Mountain	Augite	No	Stik nia
Rugged Mountain	Augite	No	Stik nia
Ten Mile Creek	Augite	No	Stik nia
Whiterocks Mountain	Augite	No	Stik nia
Kruger Mountain	Augite	No	Quest ellia
Kamloops Syenite	Augite	No	Quest ellia

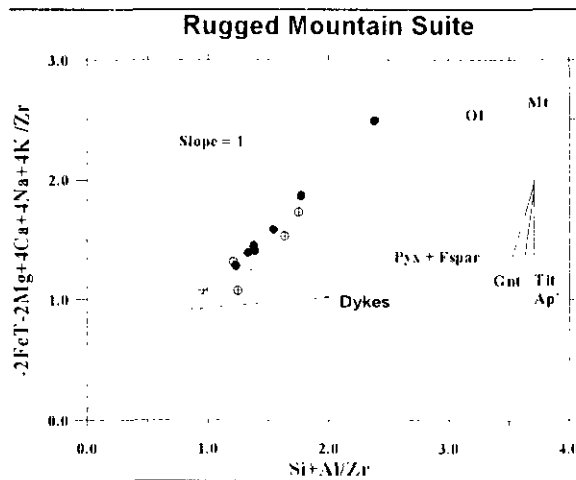


Figure 2. Pearce element-ratio diagram for rocks from the Rugged Mountain pluton. This diagram tests for the sorting of feldspars and augite to explain the chemical diversity of the suite. This test does not reject the comagmatic hypothesis.

Table 1 clearly shows the positive relationship between porphyry copper-gold mineralization and the presence of hornblende and magnetite. Plutons classified as unmineralized often contain sparse or discontinuous copper deposits. These areas of copper mineralization are generally associated with the mafic plutonic phases and are invariably associated with the local presence of hornblende and/or magnetite (e.g. Whiterocks Mountain pluton; Wilkins, 1981).

**CHEMICAL COMPOSITION**

Based on alkali and silica content, these plutons are chemically alkaline (Neil and Russell, 1993). They are strongly undersaturated with respect to silica and this is universally expressed both chemically and

mineralogically as normative feldspathoid and modal melanite. Other notable occurrences of silica-undersaturated phases include: nepheline in the Kruger syenite (Currie, 1976); pseudo-eucrite at Mount Polley and Galore Creek (Currie, 1976); and vishnevite-cancrinite at Zippa Mountain (Lueck and Russell, in press).

Figure 3 is a ternary AFM diagram which shows the representative compositions of rocks from both the Averill (Keep and Russell, 1992) and Rugged Mountain plutons (Neil and Russell, 1993). Both suites show a strong iron enrichment trend which is typical of this plutonic association. Iron enrichment is expressed mineralogically by iron-rich megirine-augite, melanite garnet, iron-rich biotite and magnetite.

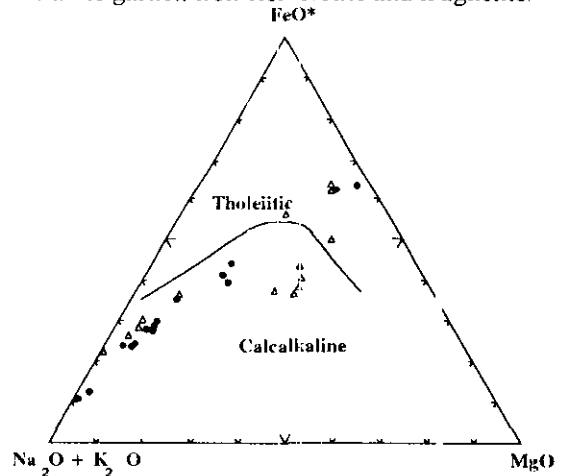


Figure 3. AFM diagram for rocks from the Averill and Rugged Mountain plutons.

**IGNEOUS MELANITE GARNET**

The presence of igneous melanite garnet, a titanium-bearing andradite, is a primary

distinguishing feature of these plutons (Lueck *et. al.* 1993). Melanite garnet occurs in varying amounts within these bodies and becomes a major phase locally. Melanite is a common phase in the Zippa Mountain pluton and occurs as rare cumulate bands (Lueck and Russell, in press). The presence of melanite and aegirine-augite suggests a high oxygen fugacity in these melts as these minerals require significant  $Fe^{3+}$  in their crystal structure.

The presence of titanium in the structure of andradite is problematic (Dingwell and Brearly, 1985; Howie and Wooley, 1968; Huckenholz, 1969; Huggins *et. al.*, 1977; Issacs, 1968; Moore and White, 1971; Schwartz, 1979; Tarte, 1979). The presence of aluminum in the andradite structure within natural melanites complicates the substitution behavior. A definitive solution to the problem has yet to be determined.

A plot of cationic titanium *versus* silica in melanite garnet (Figure 4) from the Rugged Mountain pluton (Neil and Russell, 1993) shows that there is more titanium in the garnet structure than can be accommodated by the silica vacancies. There is, however, a strong linear relationship between the two elements of 1.5 titanium atoms for every 1 silica absence. This suggests a coupled substitution of titanium in both the tetrahedrally coordinated silica site and also in the octahedrally coordinated  $Fe^{3+}$  site. The latter substitution would require the reduction of  $Fe^{3+}$  to  $Fe^{2+}$ .

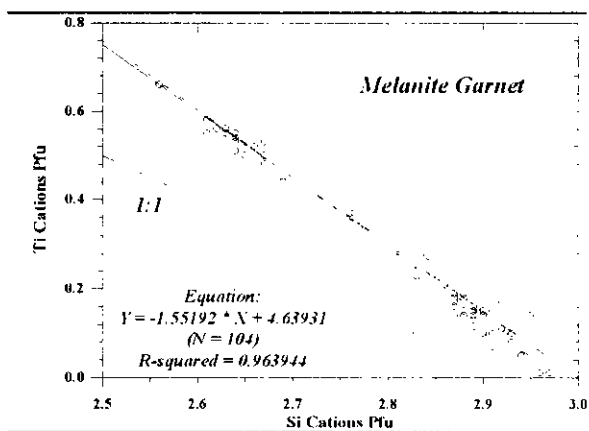


Figure 4. Plot of cationic silica vs. titanium in melanite garnet from Rugged Mountain pluton (Neil and Russell, 1993). Upper dashed line is ideal 1.5:1 substitution; solid line is fitted curve.

## PLUTONIC ZONATION

Plutonic zonation is another distinguishing feature of these undersaturated plutons. The suite is characterized by a zonation from pyroxenite to syenite. Pyroxenite encloses a core of trachytic syenite in many of these plutons (*eg.* Rugged Mountain, Ten Mile Creek [Morgan, 1976], Zippa Mountain, Whiterocks Mountain). Intermediate mela-syenites are found adjacent to pyroxenites (*eg.* Rugged Mountain, Zippa

Mountain) and are mineralogical mixtures of syenite and pyroxenite. This zonation suggests that the lithological diversity within these plutons is a result of magmatic differentiation processes. Magmatic fractionation of aegirine-augite early in the crystallization history of the pluton is a possible explanation for both the plutonic geometry and the lithological inhomogeneity of this pyroxenite-syenite association.

## PLUTONIC FABRIC

The presence of a prominent mineral fabric in the form of planar crystal alignment is another diagnostic feature of this plutonic association. Trachytic syenite is a dominant rock type in all of these plutons and this may reflect on the origins of the syenite phase. At Zippa Mountain (Lueck and Russell, in press) trachytic alignments of potassium feldspar crystals outline a well-developed and mappable fabric within the syenite phase of the pluton. This fabric is non-tectonic in origin, as evidenced by the lack of strain within the interlocking crystals that outline the fabric. The foliation outlines a map pattern which is inwardly dipping, concordant with the pluton margins and steepest at the pyroxenite border. This geometry is consistent with a crystal cumulate model for the formation of these plutons.

## CONCLUSIONS

Silica undersaturated, zoned alkalic intrusions occur in both the Stikine and Quesnell Terranes within British Columbia. These plutons intrude Paleozoic to Triassic assemblages, are latest Triassic to Early Jurassic in age and are formed from arc-related magmas. Pyroxenite and syenite are compositional end members within this plutonic suite that are believed to be comagmatic and related by the sorting of mineral phases within the cooling magma chambers.

Porphyry copper-gold deposits are found within several of these plutons and the presence of significant mineralization is restricted to plutons which contain an abundance of hornblende and magnetite.

## REFERENCES

- Anderson, R. G. (1993): A Mesozoic Stratigraphic and Plutonic Framework for Northwestern Stikinia (Iskut River Area), Northwestern British Columbia, Canada; in Dunne, G. and McDougall, K., Editors, *Mesozoic Paleogeography of the Western United States--II, Society of Economic Palaeontologists and Mineralogists*, Pacific Section, Volume 71, pages 477-494.
- Currie, K. L. (1976): *The Alkaline Rocks of Canada*; *Geological Survey of Canada*, Bulletin 239.

- Dingwell, D. B. and Brearley, M. (1985): Mineral Chemistry of Igneous Melanite; *Mineralogy and Petrology*, Vol. 90, pages 29-35.
- Howie, R. A. and Wooley, A. R. (1969): The Role of Titanium on Cell Size, Refractive Index and Specific Gravity in Melanite; *Mineralogical Magazine*, Volume 36, pages 775-790.
- Huckenholtz, H. G. (1969): Synthesis and Stability of Ti 646-665
- Huggins F. E. et al. (1969): The Crystal Chemistry of Melanites and Schorlomite; *American Mineralogist*, Volume 62, pages 646-665.
- Issacs, T. (1968): Titanium Substitutions in Andradite; *Chemical Geology*, Volume 3, pages 219-222.
- Keep, M. and Russell, J. K. (1992): Mesozoic Alkaline Rocks of the Averill Plutonic Complex; *Canadian Journal of Earth Sciences*, Volume 29, pages 2508-2520.
- Lueck, B. A. and Russell, J. K. (in press): Geology and Origins of the Zippa Mountain Igneous Complex; with Research, *Geological Survey of Canada*.
- Lueck, B. A., Neil, I. and Russell, J. K. (1993): The Rugged Mountain Pluton: an Example of the Melanite Bearing Pyroxenite-Syenite Association; *Geological Association of Canada/Mineralogical Association of Canada, Programs with Abstracts*, Volume 18, page A61
- Moore, R. K. and White, W.B. (1971): Intervalence Electron Transfer Effects in Melanite; *American Mineralogist*, Volume 56, pages 826-840.
- Morgan, T. (1976): Geology of the Ten Mile Creek Syenite-Pyroxenite Pluton, Telegraph Creek, E. C. unpublished B. Sc. thesis, *The University of British Columbia*.
- Neil, I. and Russell, J. K. (1993): Mineralogy and Chemistry of the Rugged Mountain Pluton: a Melanite-bearing Alkaline Intrusion; *Geological Fieldwork 1992*, Grant, B. and Newell, J. M., Editors, *U. C. Ministry of Energy, Mines and Petroleum Resources*, Paper 993-1, pages 149-157.
- Schwartz, K. B. (1979): Crystal Chemistry of Natural Fe-Ti Garnets; *Eos*, Volume 59, pages 395-396.
- Tarte, P. (1979): The Structural Role of Titanium in Synthetic Ti-Garnets; *Physical and Chemical Mineralogy*, Volume 4, pages 55-63.
- Wilkins, A. L. (1981): K-Ar and Rb-Sr Dating of the Whiterocks Mountain Alkaline Complex: in the Intermontane Belt West of Okanagan Lake; unpublished B. Sc. thesis. *The University of British Columbia*.

## NOTES

# MAJOR LITHOLOGIES OF THE BATTLE ZONE, BUTTLE LAKE CAMP, CENTRAL VANCOUVER ISLAND (92F/12E)

By Michelle Robinson and Colin I. Godwin

*Mineral Deposits Research Unit, U.B.C.*

Stephen J. Juras

*Westmin Resources Limited*

*(MDRU contribution 040)*

**KEYWORDS:** Economic geology, Westmin Resources Limited, Wrangellia, Buttle Lake camp, Price formation, Myra formation, H-W horizon, Battle zone, upper zone, Gap zone, volcanogenic massive sulphide, gold, silver, lead, zinc, barite, andesite, rhyolite, chert, flow-dome.

## INTRODUCTION

The Buttle Lake mining camp (49°34' north, 125°36' west) is located in Strathcona Park near the south end of Buttle Lake, 90 kilometres southwest of Campbell River, British Columbia (Figure 1). It is a major volcanogenic massive sulphide district hosted by the Myra formation of the Paleozoic Sicker Group. Past production has come from several mines: Lynx open pit, Lynx underground mine, Myra open pit and H-W underground mine. The Price deposit, discovered early in the history of the camp, has received sporadic work but has not been mined. Current production is from H-W mine, however, ore from the recently discovered Battle and Gap zones will be mined in late 1993. Between 1966 and 1992, 13.8 million tonnes of ore grading 1.9% copper, 5.6% zinc, 0.6% lead, 2.2 grams per tonne gold and 64.0 grams per tonne silver had been mined from the camp (Westmin Annual Report, 1992). Of this, 7.5 million tonnes are from H-W, 5.3 million tonnes are from Lynx and 1.0 million tonnes are from Myra mine (Pearson, 1993). Geological reserves as of 1992 are in Table 1 and total more than 12 million tonnes. Exploration within the camp has also defined several new prospective zones. These are: Trumpeter, Ridge and the Main Zone Extension (Figure 1).

Massive sulphides occur mainly at two stratigraphic levels within the Myra formation. The lowest member of the Myra formation, H-W horizon, hosts the H-W main lens and the Battle and Gap zones. The upper Lynx-Myra-Price horizon hosts several small sulphide lenses. This paper focuses on the lithologies in the Battle zone,

and establishes a detailed stratigraphy for the H-W horizon in this area.

## HISTORY

James Cross and associates from Victoria staked the claims covering the H-W, Lynx, Price and Myra mines in 1918 when Strathcona Park was first opened for prospecting. The Paramount Mining Co. of Toronto started developing the property, but depressed metal prices and inconclusive findings halted the operations in 1925. The property remained dormant until 1959, when the Reynolds Syndicate acquired the claims. An option to purchase agreement was negotiated with Western Mines Limited in 1961. Exploration initially focused on the Lynx showings. By mid-1964, 1.5 million tonnes of ore were defined on five levels. To service the new mine, Western Mines built the present 40-kilometre road along the east side of Buttle Lake. Previous access to the property had been by boat and barge. In 1956 the Lynx pit started production at 775 tonnes per day. Continued drilling established underground reserves and the pit was phased out in favour of underground production by 1975.

In 1970, the Myra deposit was evaluated. Open-pit production began in 1972 and continued until 1986 when the mine closed due to depletion of reserves. In 1976, Brascan Ltd. acquired control of Western Mines Limited and formed Westmin Resources Limited. The Price showings were evaluated between 1979 and 1981, but development has been put on hold indefinitely.

Exploration for new orebodies in 1976 resulted in the discovery of H-W deposit 3 years later: at about 1000 metres below the Myra valley floor. Production from H-W main lens began in 1985. Exploration continued into the 1990's, and in May of 1991 the high-grade Gap lens was discovered. Five months later the Battle zone was found. Current drilling on the property is focused on definition of the Battle and Gap zones.



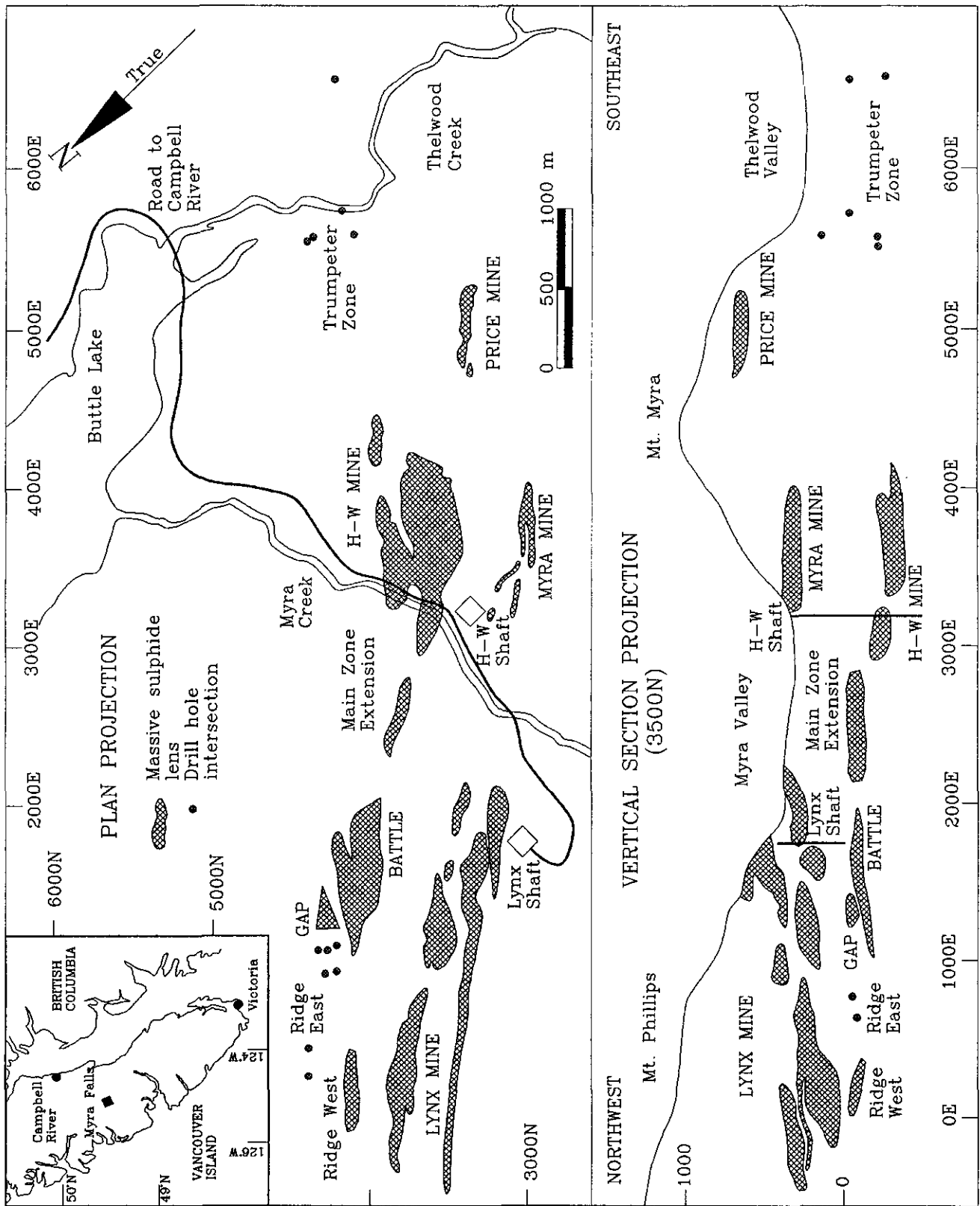


Figure 1. Buttle Lake mining camp, central Vancouver Island, southwestern British Columbia, showing the surface and vertical projections of major orebodies and prospective zones (Westmin Resources Limited Annual Report, 1992).

**TABLE 1. PROVEN AND PROBABLE GEOLOGICAL RESERVES IN BUTTLE LAKE CAMP, CENTRAL VANCOUVER ISLAND, AS OF 1 JANUARY 1993 (WESTMIN RESOURCES LIMITED ANNUAL REPORT, 1992)**

	Reserves (tonnes)	Gold (g/t)	Silver (g/t)	Copper (%)	Lead (%)	Zinc (%)
H-W	8 955 100	2.2	39.6	1.7	0.4	4.3
Lynx	315 300	3.0	94.0	1.7	1.1	10.0
Price	185 000	1.5	66.4	1.4	1.3	10.4
Gap	634 400	3.2	151.5	1.8	1.1	13.3
Battle	2 013 700	1.1	24.2	2.6	0.5	12.7
Extension	231 100	1.2	60.4	1.7	0.4	3.8
Trumpeter	61 200	3.2	68.9	6.3	6.3	4.6
6 Level	120 500	1.3	91.4	0.4	0.9	6.0
TOTAL	12 516 300	2.1	45.6	1.9	0.5	6.3

## REGIONAL GEOLOGY

The Buttle Lake massive sulphide deposits occur within the Myra formation of the Paleozoic Sicker Group. The Sicker Group is the oldest stratigraphic unit recognized on Vancouver Island, and represents the base of Wrangellia, an allochthonous terrane that underlies most of the Island (Jones *et al.*, 1977). The Sicker Group is exposed by three major uplifts: Buttle Lake, Cowichan - Horne Lake and Nanoose.

Table 2 presents an informal revised stratigraphy for the Buttle Lake uplift established by Juras (1987). This table of formations incorporates earlier work by Yole (1969), Jeffery (1970) and Muller (1980). In order of decreasing age the formations recognized are: Price, Myra, Thelwood, Flower Ridge, Buttle Lake and Henshaw.

The Price formation consists of feldspar-pyroxene-porphyrific basaltic andesite flows, flow breccias, hyaloclastites, pillowed flows and minor volcanoclastic sediments. Most flows contain 1 to 8 % quartz and chlorite-filled ovoid amygdules less than 1 millimetre long. The freshest rocks are moderately altered to chlorite-epidote-plagioclase-actinolite assemblages. Rocks below massive sulphide lenses are totally altered to sericite and pyrite with or without chlorite. This unit is known to be over 300 metres thick from diamond drilling; the base is not exposed in the Buttle Lake uplift. It is Late Devonian or older based on an isotopic Late Devonian age for the overlying Myra formation. The basaltic andesite probably represents a major period of early arc volcanism (Juras, 1987).

The Myra formation is 310 to 440 metres thick and is composed of rhyolitic to basaltic rocks with lesser sedimentary units. Most volcanic rocks are clastic, with lesser flows and intrusions. Sedimentary rocks are primarily volcanic greywacke with interbedded argillite and chert. Lithologic units are continuous along the

northwest trend of the ore zones (Figure 1), but have abrupt lateral northeast to southwest facies changes. Deposition of the Myra formation was complex, because material was deposited from three separate volcanic centres (Juras, 1987). Rhyolite flows and volcanoclastic rocks were formed within an ancient volcanic arc to the northeast, towards Buttle Lake. Massive sulphides, pelagic deposits, volcanogenic sediments and andesite flows fill an intra-arc basin. Mafic flows and volcanoclastic deposits mark an intra-arc or back-arc provenance to the northwest, towards Mount Myra. Uranium-lead zircon dating of rhyolite by Juras (1987) established a Late Devonian age of 370 Ma for the Myra formation. Details of the formation are outlined in the following section on mine geology.

The Thelwood formation unconformably overlies the Myra formation. It is 270 to 500 metres thick and consists of fine-grained siliceous tuffaceous sediments, volcanoclastic debris-flows and penecontemporaneous mafic sills. Tuffaceous sedimentary units may be 5 to 30 metres thick. They are generally massive, fine to coarse crystal-lithic tuff at the base and are capped by pale green to grey, locally cherty, thin-bedded tuffaceous mudstone and siltstone. Most units represent an A, E turbidite sequence. Volcanoclastic debris-flows are 4 to 25 metres thick, moderately well sorted, crudely stratified, and consist of vitric-lithic, fine lapilli-tuff and coarse tuff. Scoured bases and boulder sized rip-up clasts of tuffaceous sediment units are common. Mafic sills are 1 to 90 metres thick and consist of basaltic andesite. Contacts with the sediments are locally peperitic, indicating that the Thelwood formation was un lithified at the time of sill intrusion (Juras, 1987). Thus, this unit represents a sediment-sill complex of the Guyamas Basin type. The Thelwood formation has not been dated in the Buttle Lake uplift. However, the sediment-sill unit of Muller *et al.* (1974) in the Cowichan - Horne Lake uplift probably correlates with the Thelwood formation. The sediment-sill unit contains radiolaria of Mississippian age (Muller, 1980).

**TABLE 2. TABLE OF FORMATIONS FOR THE PALEOZOIC SICKER GROUP IN THE BUTTLE LAKE UPLIFT, CENTRAL VANCOUVER ISLAND, SOUTHWESTERN BRITISH COLUMBIA. MODIFIED FROM JURAS (1987).**

	<b>Formation</b>	<b>Thickness</b>	<b>Lithology</b>
<b>Paleozoic</b>	Early Permian (?)	Henshaw formation 5-100 m	Conglomerate, epiclastic deposits, vitric tuff
	Early Permian to Pennsylvanian	Buttle Lake formation 300 m	Crinoidal limestone <sup>3</sup> , minor chert
	Pennsylvanian or Mississippian	Flower Ridge formation 650+ m	Moderately to strongly amygdaloidal mafic lapilli tuff (scoria clast), tuff breccia, minor tuff and flows, and syndepositional(?) sills <sup>2</sup>
	Early Mississippian (?)	Thelwood formation 270-500 m	Subaqueous pyroclastic deposits, siliceous tuffaceous sediments, mafic sills
	Late Devonian	Myra formation 310-440 m	Intermediate to felsic <sup>1</sup> volcanics, volcanoclastics, minor sediments, massive sulphide mineralization
	Late Devonian or older	Price formation 300+ m	Feldspar-pyroxene porphyritic basaltic andesite flows, flow breccias, minor sediments

<sup>1</sup> 370 ± 6 Ma, U-Pb zircon (Juras 1987).

<sup>2</sup> 276 ± 8 Ma, K-Ar hornblende: Early Permian (unpublished data; C. Godwin, J. Harakal and D. Runkle, The University of British Columbia).

<sup>3</sup> Pennsylvanian to Early Permian based on brachiopods (Fyles, 1955), fusulinids (Sada and Danner, 1974), foraminifera (Muller *et al.*, 1974) and conodonts (Brandon *et al.*, 1986).

The Flower Ridge formation is dominantly basaltic volcanoclastic rocks in conformable contact with the Thelwood formation. It is over 650 metres thick and is characterized by strongly amygdaloidal feldspar and pyroxene porphyritic basaltic lapilli-tuff and pyroclastic breccia. Amygdules are filled with quartz, albite, clinzoisite and/or epidote and pumpellyite. Other rock units include tuffaceous siltstone and wacke, basalt flows and flow breccias, bedded tuffaceous mudstone and argillaceous sediments. The section is expanded by a large number of hornblende-phyric basaltic sills. The Flower Ridge formation marks the resumption of shallow marine mafic volcanism. A K-Ar date of 276±8 Ma on hornblende (unpublished data, C. Godwin, J. Harakal and D. Runkle, 1991) from the sills indicates that this unit may be Early Permian if the sills are penecontemporaneous.

The Buttle Lake formation is primarily massive to bedded crinoidal limestone with associated chert lenses and nodules, greywacke and argillite. This unit is 100 to 500 metres thick and conformably overlies the Flower Ridge formation. The age of this unit is Pennsylvanian to Early Permian based on brachiopods (Fyles, 1955), fusulinids (Sada and Danner, 1974), foraminifera (Muller *et al.*, 1974) and conodonts (Brandon *et al.*, 1986).

The Henshaw formation both overlies and locally scours out the Buttle Lake formation. It is 5 to 100 metres thick and is composed of conglomerate, distinctive purple epiclastic deposits and purple to grey vitric tuff beds. Crinoidal limestone boulders are characteristic. The Henshaw formation marks the unconformity between the Buttle Lake limestone and basalt of the overlying Triassic Karmutsen Group.

## MINE GEOLOGY: THE MYRA FORMATION

The Myra formation is a complex sequence of mafic to rhyolitic volcanoclastic rocks and lesser flow units that fill a basin that trends northwest. The formation is characterized by relatively continuous units in a northwest-southeast direction but by rapid northeast-southwest facies variations (Walker, 1985). Juras (1987) recognized ten lithostratigraphic units in the Myra formation, displayed on the schematic cross-section of Figure 3. They are: H-W horizon, hangingwall andesite, ore clast breccia, lower mixed volcanoclastics, upper dacite/SE andesite, Lynx-Myra-Price horizon, G-flow, upper mixed volcanoclastics, upper rhyolite and upper mafic.

## **LITHOLOGY**

### **H-W HORIZON**

The H-W horizon is predominantly felsic flows and volcanics. It is 15 to 200 metres thick and occurs throughout the mine area. There are five general members within H-W horizon (Juras, 1987): massive sulphide lenses; argillite; H-W mafic; pyroclastic and epiclastic deposits; and felsic flows and domes. H-W horizon is discussed in detail in the section on the geology of the Battle zone.

Massive sulphides are pyrite-rich, zoned lenses with chalcopyrite-rich core zones and zinc-rich margins. The H-W main lens is the largest on the property, and contained a total of 12 million tonnes of massive sulphide. The argillite member is 1.5 to 45 metres thick and consists of black siliceous argillite, fine to coarse rhyolitic tuff and minor chert. It is massive to thin bedded, and represents A, E and A, B, E turbidite sequences. The H-W mafic unit intrudes and flows over the argillite member. It is a pale green pyroxene-phyric basalt with peperitic, pillowed and quench brecciated (hyaloclastite) margins. Pyroclastic and epiclastic deposits make up most of H-W horizon in the central region. Pyroclastic deposits are quartz-feldspar crystalline-lithic lapilli tuff and coarse to fine tuff. Epiclastic deposits consist of debris flows, some of which contain up to 25% fragments of Price formation andesite. Felsic flows and domes are of three types: quartz-feldspar porphyritic; aphyric to feldspar porphyritic; and feldspar-porphyritic dacite (Juras, 1987).

### **HANGINGWALL ANDESITE**

Hangingwall andesite is mostly basaltic andesite flows and hyaloclastite flow breccias. This unit is up to 100 metres thick; individual flow members may be over 3 metres thick. Well-sorted greywackes are also present. The hangingwall andesite is thickest over the H-W main lens, probably because that lens was deposited in a topographic low (Pearson, 1993). The hangingwall andesite is discussed in detail in the next section.

### **ORE-CLAST BRECCIA**

The ore-clast breccia is characterized by massive sulphide clasts (Walker, 1985) and olistoliths of pyrite-mineralized rhyolite up to 50 metres long by 15 metres wide (Juras, 1987). The unit is up to 90 metres thick and consists of a series of submarine debris-flows and lesser pyroclastic deposits. There are three distinct members within the ore-clast breccia (Juras, 1987): rhyolite-rich volcanoclastic breccia with about 25% non-andesite or

mafic constituents; rhyolite-poor volcanoclastic breccia with less than 10% non-andesite or mafic constituents; and interzone pyroclastic rhyolite. Clast types within the volcanoclastic breccia members are highly variable. In decreasing order of abundance they are: feldspar-phyric andesite, amygdaloidal mafic, dacite, quartz-feldspar-porphyritic rhyolite, massive sulphide, fine rhyolite tuff, chert and argillite. Clast sizes range from 1 centimetre to 150 centimetres across. The interzone rhyolite member is up to 20 metres thick and consists of bedded felsic tuff, lapilli tuff and tuff-breccia. It represents a period of felsic phreatomagmatic activity (Juras, 1987) that interrupts slide and debris-flow sedimentation.

### **LOWER MIXED VOLCANICLASTICS**

Lower mixed volcanics are dominated by andesite with lesser dacite fragments. The unit also includes rare thin flows of andesite. This unit is up to 90 metres thick and contains bedded clastic sequences and coarse clastic deposits. Bedded clastic sequences contain mostly aphyric to plagioclase-phyric subrounded andesite fragments with lesser broken to euhedral plagioclase crystals. Coarse deposits contain two types of andesite and lesser dacite clasts. Most andesite fragments contain 15% feldspar crystals and are perlitic textured. Other andesite fragments are feldspar glomeroporphyritic. Lower mixed volcanics are distinguished from the ore-clast breccia by the absence of rhyolite and massive sulphide fragments (Juras, 1987).

### **UPPER DACITE/5E ANDESITE**

Upper dacite/5E andesite occurs at the southeast and northwest ends of the mine property respectively. The upper dacite is divided into upper and a lower members. The lower member is up to 60 metres thick and contains resedimented hyaloclastite and pillow breccia and subaqueous pyroclastic deposits. The upper member is mostly intermediate flows with yellow-green to dark grey to purple feldspar-porphyritic flow clasts. The flows are medium to dark green with 25% feldspar crystals. The 5E andesite sequence of massive to pillowed basaltic andesite flows and flow breccias is up to 250 metres thick. The upper dacite and the 5E andesite represent two contemporaneous, but different, eruptive events (Juras, 1987).

### **LYNX-MYRA-PRICE HORIZON**

Lynx-Myra-Price horizon is massive to bedded, fine to coarse quartz-feldspar crystalline-lithic rhyolitic tuff, lapilli tuff and lesser chert (Juras 1987, Walker 1985). Massive sulphides occur at two levels within the Lynx-Myra-Price horizon. Some lenses are located at the base

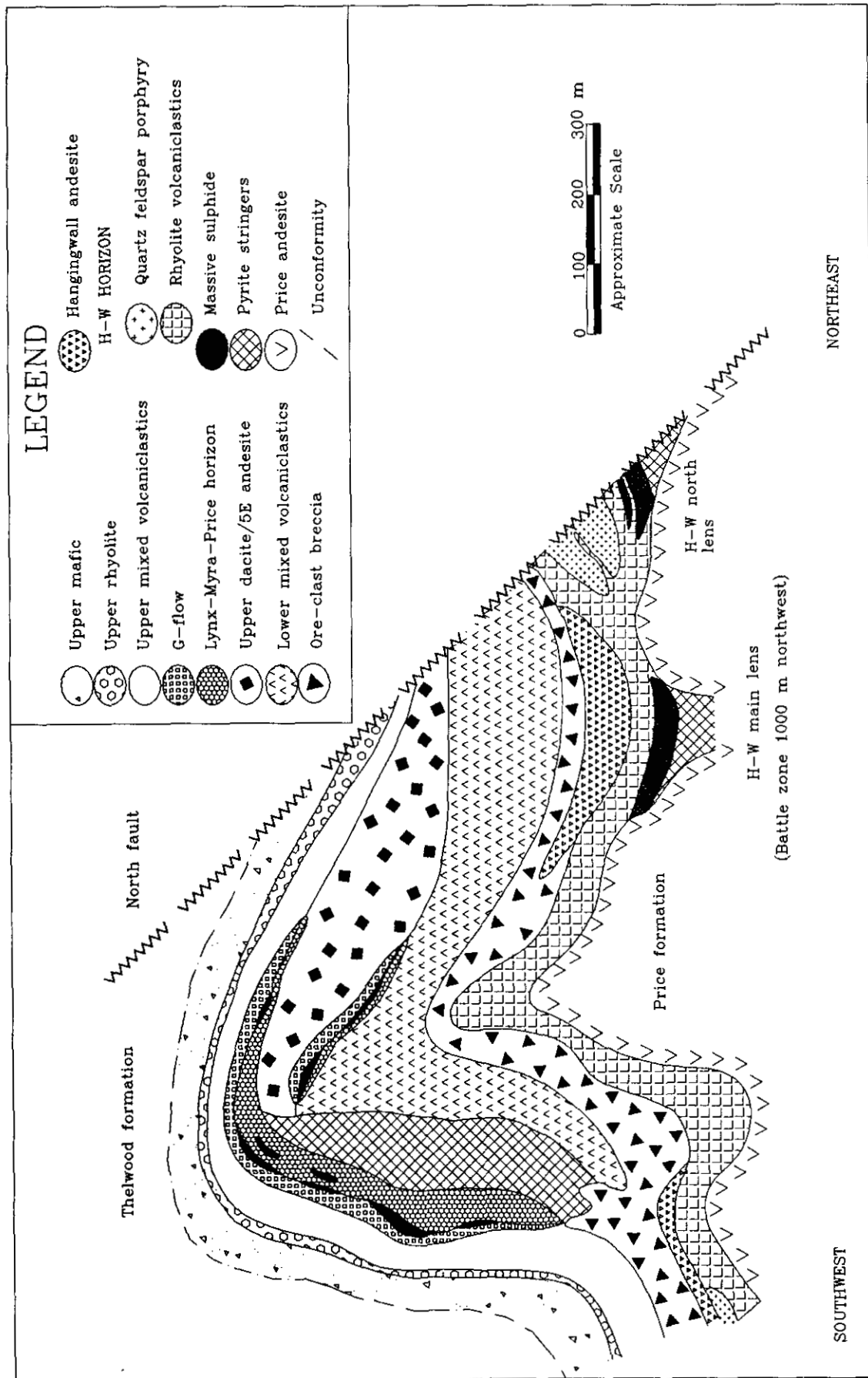


Figure 2. Schematic cross-section of the Myra formation, Buttle Lake camp, central Vancouver Island, southwestern British Columbia. The Myra formation hosts all known volcanogenic massive sulphide deposits in the camp. Figure is compiled from Juras (1987) and Pearson (1993).

of the horizon where they are underlain by schistose sericite-quartz-pyrite feeder zones within the 5E andesite. Other lenses occur at the upper contact with G-Flow. Upper sulphide lenses have no underlying feeder zones. The variably altered rhyolite tuffs and lapilli tuffs probably served as a conduit for mineralizing fluids, which channelled them laterally to hydrothermal discharge sites. Massive sulphide lenses are composed of banded sphalerite, barite, pyrite, chalcopyrite, galena and tennantite.

## G-FLOW

G-flow is a widespread but thin (2 to 15 m thick) package of komatiitic basalt flows and hyaloclastite breccias immediately above the Lynx-Myra-Price horizon (Juras, 1987). Least altered flow rocks consist of 5% augite glomerocrysts, trace chromite microphenocrysts and trace olivine phenocrysts. The groundmass is fine-grained actinolite, chlorite, plagioclase and relict clinopyroxene. Hyaloclastite breccias are locally hematite altered to a distinctive purple. Spherulitic textured jasper fills interstices between breccia fragments.

## UPPER MIXED VOLCANICLASTICS

The upper mixed volcanics are mafic to intermediate fine to coarse deposits up to 50 metres thick (Juras, 1987). Fine deposits are thin to medium-bedded, well-sorted, normally graded feldspar-crystal intermediate to mafic tuff. Locally, these deposits are capped by maroon fine tuff. Coarse deposits are characterized by a wide textural variety of mafic to intermediate clasts in a matrix composed of 5 to 15% feldspar crystals in an epidote-albite-chlorite groundmass. Lesser clast types include massive to flow-banded rhyolite, rip-up clasts of tuffaceous siltstone and white to black chert.

## UPPER RHYOLITE

The upper rhyolite is 50 to 65 metres thick and contains two members: a pyroclastic-rich and a siliceous argillite and chert dominant member (Juras 1987, Walker 1985). The pyroclastic member is up to 50 metres thick and generally coarsens upward, although individual beds are normally graded. The deposits are thin to medium-bedded crystal-lithic-vitric coarse tuff to lapilli tuff, and lesser fine tuff and tuff-breccia deposits. The siliceous argillite and chert member is 1 to 15 metres thick and consists of grey to black siliceous argillite, white to pale green chert, green to grey fine rhyolite tuff and minor jasper. Round radiolarian "ghosts" occur in the argillaceous material.

## UPPER MAFIC

The upper mafic unit is pyroxene-feldspar-porphyrific basalt. It is 5 metres to over 200 metres thick and is the uppermost unit within the Myra formation. Because the Myra formation is unconformably overlain by the Thelwood formation, the upper mafic unit is absent in some areas (Juras, 1987). Most of the unit is comprised of pyroclastic and hydroclastic deposits. Flows are present in the middle to upper parts of the upper mafic unit, and are 3 to 15 metres thick.

## STRUCTURE

The main structural feature of the Battle Lake camp is a megascopic subhorizontal, northwest-trending asymmetric anticline with a steeply dipping southwestern limb and a gently dipping northeast limb (Walker, 1985; Figure 3). Related mesoscopic fold structures are most common in massive sulphides and associated sericitic alteration zones. Axial planar foliation trends northwest with nearly vertical to steeply northeast dipping surfaces. Most fragmental rocks have stretched clasts that may reach length to width ratios of greater than 10:1. In general, the long axes of stretched clasts parallel the hinge (b-axis) of the anticline. Prominent  $\epsilon$ -c joints, locally quartz-carbonate veined, are present throughout the mine area.

Faults of various ages and orientations cut the mine stratigraphy (Juras, 1987; Walker, 1985). Most are high-angle normal faults with trends to the northeast, north, northwest and east-southeast; some are strike-slip. Figure 3 shows the North fault which dips around 45° and downdrops the northeastern part of the mine stratigraphy by about 800 metres. It is one of the youngest faults as it cuts the overlying Thelwood formation. Some of the oldest normal faults are synvolcanic faults within the Price andesite. These important structures commonly localize syn mineral feeder zones to massive sulphide mineralization. Later thrust faults dip 30° and displace both the orebodies and the overlying rocks. Many of these are filled with gouge, quartz veins and late mafic dikes.

## LITHOLOGY OF THE BATTLE ZONE

Battle zone massive sulphide lenses occur at three stratigraphic levels within the H-W horizon (Figures 3 and 4): main Battle; upper zone and Gap zone. Main Battle massive sulphides occur at the Price formation contact. Upper zone massive sulphides form thin lenses at the contact between rhyolitic volcanics and an overlying rhyolite flow-dome complex. Gap massive sulphides occur as high-grade lenses proximal to the rhyolite flow-dome complex.

The geology in the Battle zone is complex due to synmineral and postmineral faulting, rapid facies

changes and obliterating alteration. For these reasons, a detailed stratigraphy of the upper Price formation and the H-W horizon was established to unravel structural offsets and to help target ore zones. As most of the large orebodies occur in paleo-depressions within the Price formation, identification of synmineral normal faults is critical.

## **PRICE FORMATION**

The Price formation is a sequence of massive to pillowed basaltic andesite flows, volcanic breccias and inter-flow clastic sediments that include turbidites. It is over 300 metres thick, and is the lowermost unit in the mine area and the Buttle Lake uplift (Juras, 1987). The base has not been identified. Only the upper 75 metres of the formation have been intersected in Battle zone exploration drilling. All of the intersections are intensely altered; primary textures are only sporadically preserved. Individual flows are 5 to 30 metres thick and are the dominant volcanic facies (>80%) in the Price formation. Juras (1987) defined two types of andesite flows elsewhere on the property based on phenocryst assemblages. They are: pyroxene-feldspar-phyric flows with 5% euhedral clinopyroxene crystals 1 to 10 millimetres long and 3% plagioclase crystals 0.8 to 2.5 millimetres long; and feldspar-phyric flows with 15% plagioclase crystals 0.6 to 5 millimetres long and trace to 0.5% clinopyroxene phenocrysts 0.5 to 2.5 millimetres long. Feldspar-phyric flows are prevalent in the Battle zone (Plate 1a). Contacts to individual flow units may be massive, devitrified tachylite or quench brecciated (hyaloclastite). Devitrified tachylite is dark green-black, and altered to sericite and chlorite. Hyaloclastite breccias are 1 to 6 metres thick and poorly sorted with individual fragments up to 30 centimetres in diameter in a finely shattered matrix. Most show *in situ* jigsaw-fit breccia textures, indicating minimal resedimentation of the breccia fragments. Pillow breccia is also common (Plate 1b). Pillow fragments are pinkish, scoriaceous and have convex edges. Inter-flow sediments (Plate 1c) are moderately well sorted to well-sorted fining-upwards turbidites.

## **H-W HORIZON**

H-W horizon consists of the following eight members in the Battle zone: main Battle massive sulphide lenses, fine rhyolitic tuffaceous deposits, H-W mafic sills, coarse rhyolite pyroclastic deposits, rhyolite tuffaceous sediments, upper zone massive sulphides,

rhyolite flow-dome complex and Gap massive sulphide lenses. These members are described below.

## **MAIN BATTLE MASSIVE SULPHIDE LENSES**

The main Battle massive sulphide lens is tabular and occurs at the contact between the basaltic andesite of the Price formation and the felsic volcanics of H-W horizon (Figure 4). Current reserves are about 2 million tonnes of high-grade ore (Table 1). Massive sulphides are zoned with: pyrite and chalcopyrite rich core zones close to synmineral faults (Plate 2a); banded pyrite and dark sphalerite in the central parts of most sulphide lenses (Plate 2b); and pale yellow sphalerite at the top and periphery of the ore zone (Plate 2c). Bedding was found in sulphides at the top of the main ore zone (Plate 2d). Bedding to core axis angles in the sulphide unit are the same as in the overlying fine rhyolite tuffaceous deposits. Feeder zones to the main Battle lenses are in the Price andesite, and comprise widespread networks of pyrite-quartz-chalcopyrite veins. The number of veins increases towards synmineral normal faults.

## **FINE RHYOLITIC TUFFACEOUS DEPOSITS**

Fine rhyolitic tuffaceous deposits are mostly tuffaceous chert, thin-bedded fine tuff and tuffaceous sandstone. A typical sequence overlying the ore zone consists of: fine rhyolite tuff with compacted, devitrified, sericitized, pumice fragments; massive grey to purple tuffaceous chert (Plate 3a); and thin to medium bedded, graded, well sorted, variably silicified rhyolite tuff (Plate 3b). In some areas, fine rhyolite tuff is underlain by brown to grey, thin-bedded mudstone and shaly sandstone. These are not rhyolitic in composition, but are included in this unit because they are fine-grained, thin-bedded sediments above the ore zone. Tuffaceous chert forms a distinctive marker, and is described in detail below.

**Tuffaceous chert** (Plate 3a) occurs slightly above and peripheral to massive sulphides. Thin (<50 cm) chert beds locally occur at other levels within the H-W horizon. However, chert associated with the ore zone may attain thicknesses of up to 3 metres. This chert is massive to thin bedded, white-grey to purple or green and has a conchoidal fracture. Pure chert is rare; usually it contains a tuffaceous component and a minor sulphide component. The sulphide component is usually pyrite, although some sphalerite is locally present. Sulphides may occur as thin beds or laminae that form up to 2% of the rock, but epigenetic sulphide stringers are more common. These usually consist of chalcopyrite, sphalerite and pyrite.

## H-W MAFIC SILLS

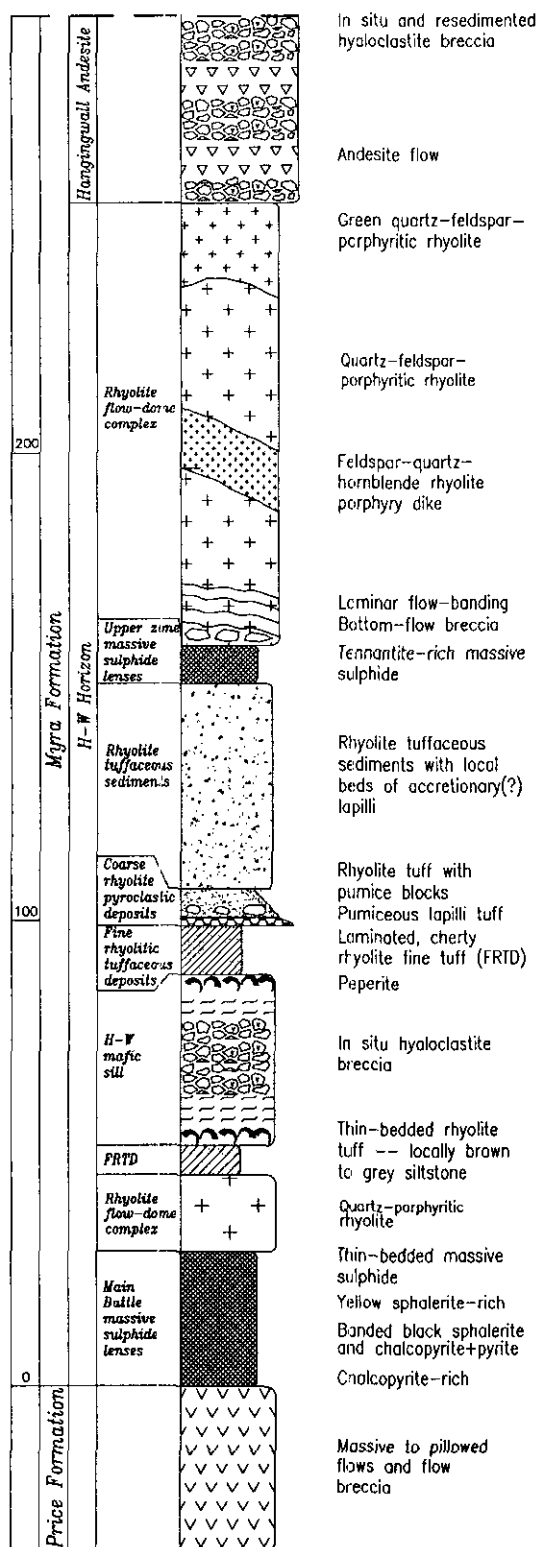


Figure 3. Stratigraphic column of H-W horizon as established mainly in the Battle zone, Battle Lake camp. Scale on the left is in metres.

Mafic sills from 5 to 30 metres thick cross-cut the lower strata within H-W horizon. They are pink-brown due to pervasive sericite-pyrite-quartz alteration and contain 20% sericite-filled amygdules 1 to 2 millimetres in diameter (Plate 4a). Unaltered examples of this unit were not observed in the Battle zone. Fresh samples from close to the H-W mine are medium olive-green with 5% clinopyroxene phenocrysts and glomerocrysts in a very fine grained groundmass containing feldspar, actinolite, calcite and epidote (Juras, 1987). Both upper and lower contacts of the sills are chaotic, with swirls of white material incorporated into the mafic rock (Plate 4b). The white material is siliceous, contains trace quartz eyes, and is most likely silicified felsic sediment that has been incorporated from the fine rhyolite tuffaceous deposits. The chaotic boundary is peperite, which implies intrusion into unconsolidated and felsic rocks. Peperite margins change laterally to pillow breccia. Hyaloclastite occurs at the base of most sills (Plate 4c and Figure 5). Fragments in the hyaloclastite are arcuate, generally less than 5 centimetres across, and occur in a finely shattered matrix. They retain *in situ* breccia textures, therefore they are not resedimented. The H-W mafic unit probably comprises number of shallow level sills that locally extruded past the sediment-water interface to form pillowed flows. It locally scours the main Battle zone massive sulphide and consequently contains sulphide fragments.

## COARSE RHYOLITE PYROCLASTIC DEPOSITS

Coarse rhyolite pyroclastic deposits are composed of two related members: pumiceous lapilli tuff and rhyolite tuff with pumice blocks. Pumiceous lapilli tuff is about 5 metres thick, but locally reaches thicknesses greater than 10 metres. It contains 15% quartz-porphyrific rhyolite cognate lithic fragments in a compacted, pumiceous, crystal-rich matrix with 10% quartz phenocrysts 1 to 2 millimetres across and lesser feldspar crystals (Plate 4a). The pumiceous component is dark grey to black, and devitrified to sericite. The lithic fragments are subrounded, normally graded, and fine from over 5 centimetres across at the base of the unit to 0.5 centimetres across at the top. They were probably incorporated at the vent, and indicate that the quartz-porphyrific rhyolite (see description below) related the pyroclastic eruption. The pumiceous component shows intense flattening which is restricted to this unit. It is definitely a compaction texture, and may be a result of subaqueous welding (Juras, 1987).

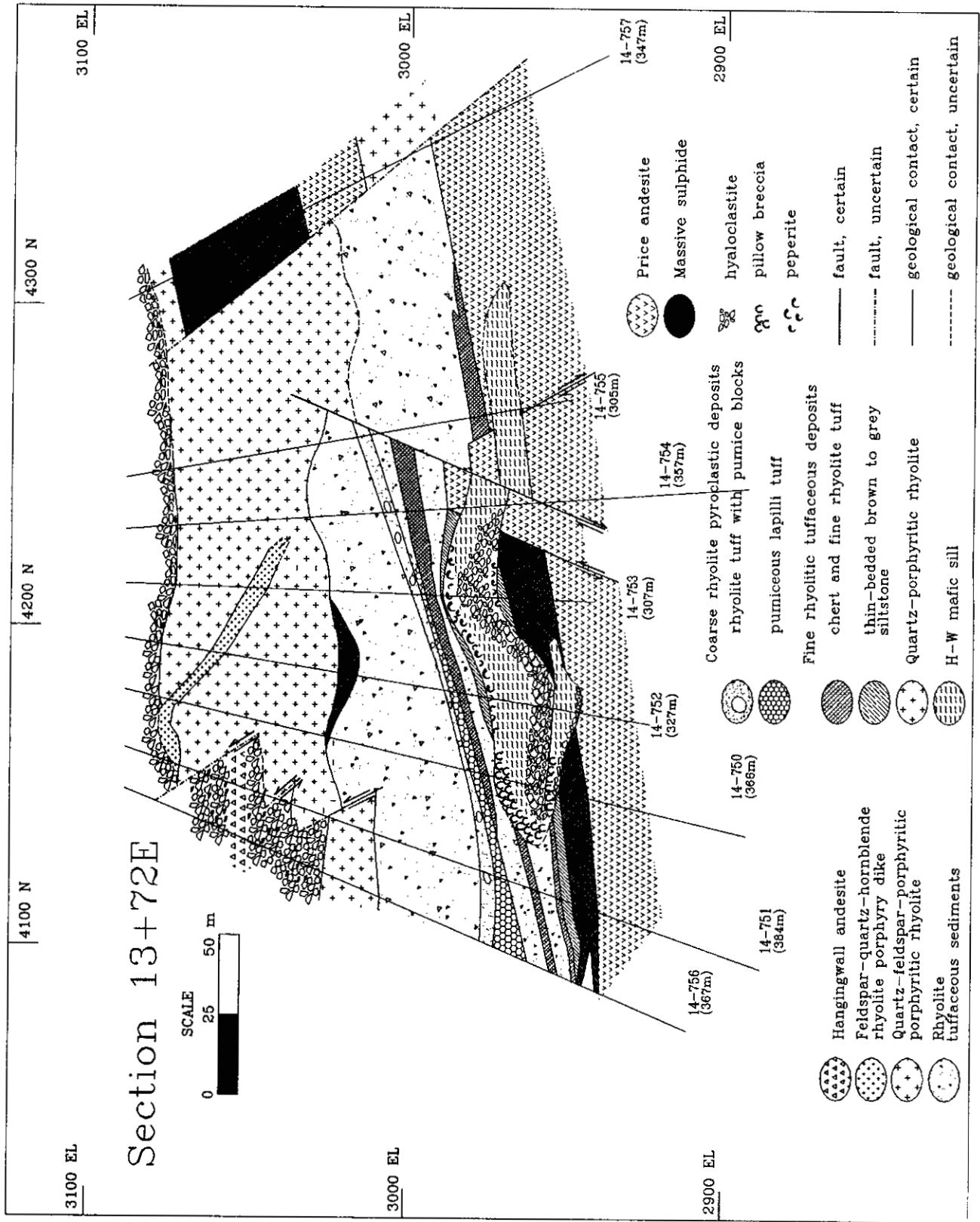
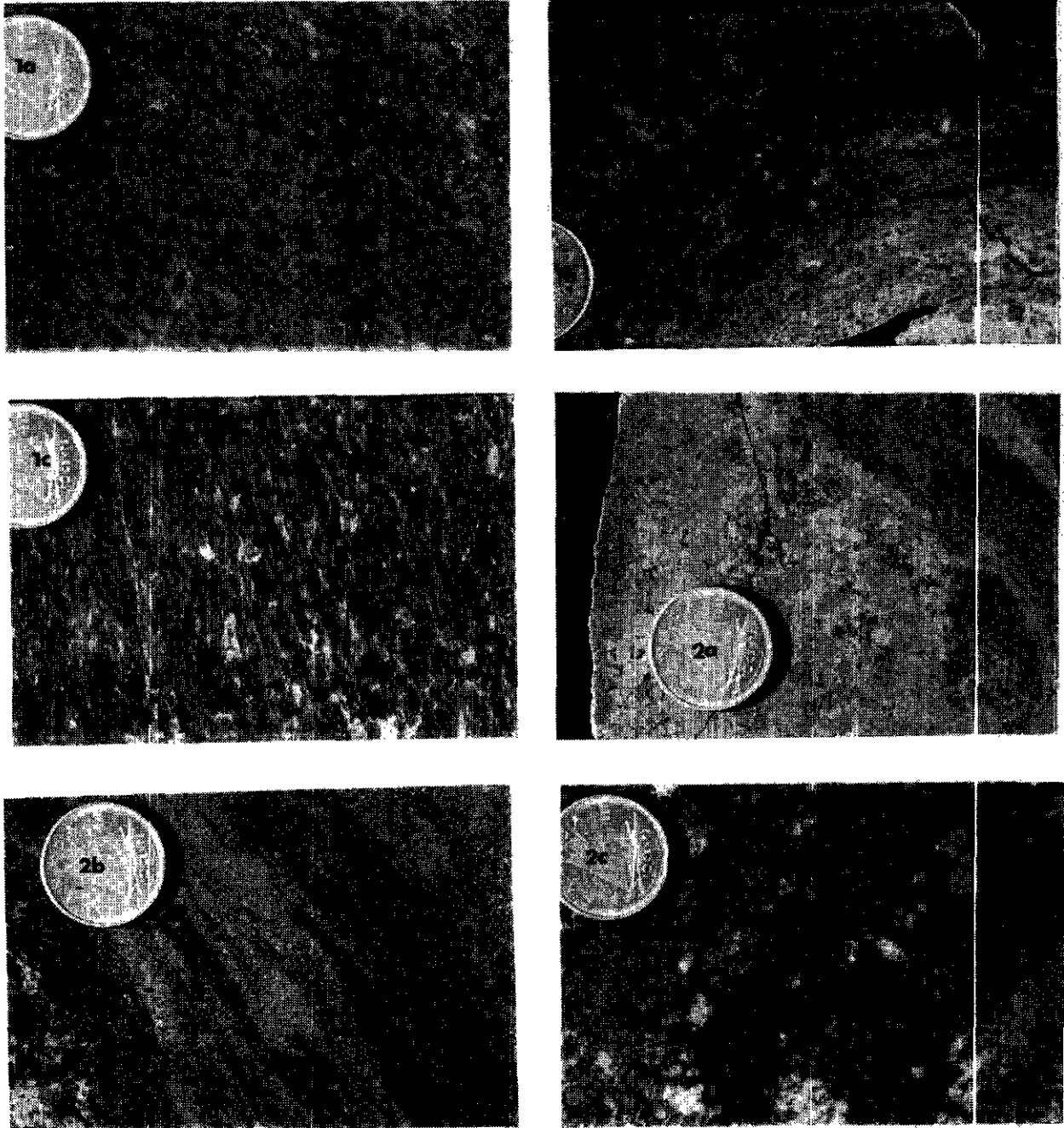
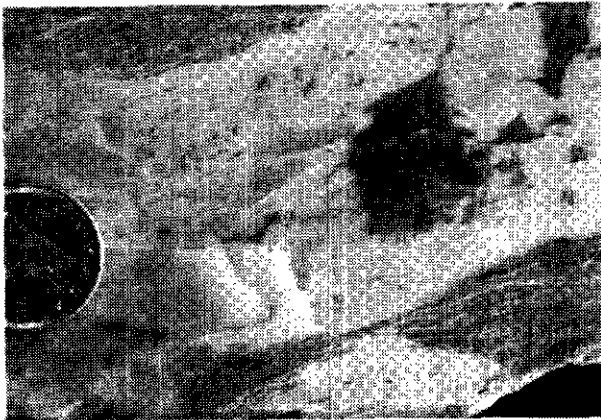
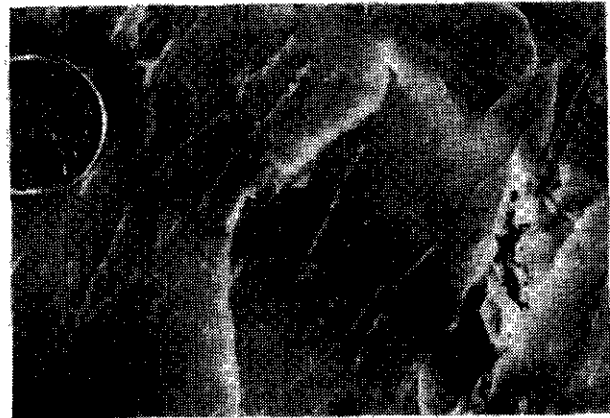


Figure 4. Cross-section of the Battle zone (13+72 E), Buttle Lake camp.



**Plate 1. Price formation.** (a) Massive andesite flow (DDH 14-751, 375 m or 1230 feet). Flows are the dominant volcanic facies (>90%) in the Price formation. Specimen has 25% green sausseritized feldspar, 1% pyroxene, 3% quartz-filled amygdules and 2% disseminated pyrite. (b) Andesite pillow breccia (DDH 14-757, 341.6 m or 1121 feet). Scoriaceous pillow fragments with 2 to 10 millimetre quartz-filled amygdules. (c) Interflow sediments (DDH 14-751, 354.5 m or 1163 feet). Fragments are stratified, moderately well sorted coarse sand to pebble-sized grains of Price andesite.

**Plate 2. Main Battle massive sulphide lenses.** (a) Chalcopyrite-rich ore from the basal part of the sulphide lens (DDH 14-751, 323.4 m or 1061 feet). Veins of coarse pyrite and chalcopyrite cross-cut and replace fine-grained dark brown sphalerite. (b) Banded pyrite and dark sphalerite from the middle part of the sulphide lens (DDH 14-751, 321.3 m or 1054 feet). Chalcopyrite-rich vein cross-cuts banded sulphides. (c) Pale yellow sphalerite from the top of the sulphide lens (DDH 14-751, 318.8 m or 1046 feet). Sample, almost pure sphalerite with 5% pyrite, has 15% chert inclusions. (d) Interbedded sphalerite, pyrite and shale from top of the sulphide lens (DDH 14-753, 280 m or 920 feet). Bedding to core axis angles in the sulphide unit are the same as in the overlying fine rhyolitic tuffaceous deposits. Chalcopyrite is concentrated in dewatering pillar structures that are perpendicular to the bedding.



**Plate 3. Fine rhyolitic tuffaceous deposits.** (a) White, distinctly laminated chert (DDH 14-751, 306 m or 1004 feet). Locally Battle zone chert may be silicified rhyolite tuff. Quartz and sulphide veins crosscut laminations at  $90^{\circ}$ . (b) Fine-grained rhyolite tuffaceous sandstone (DDH 14-751, 290 m or 953 feet). Dark grey layer on the left (base) is mostly flattened pumice fragments with 10% 1-millimetre quartz crystals. Pale grey layer is fine-grained, silicified rhyolite tuff with quartz veins perpendicular to bedding. Layer at right (top) is coarse-grained rhyolite tuff. It contains 0.5% quartz crystals and 2% black devitrified pumice fragments.

**Plate 4. H-W mafic sill.** (a) Massive sill (DDH 14-753, 268 m or 879 feet). The sample is pink due to pervasive sericite-pyrite alteration. (b) Swirly pink and white peperite from the top of sill (DDH 14-753, 263 m or 863 feet). White material is siliceous and contains euhedral quartz crystals; it is most likely incorporated felsic tuffaceous sandstone from overlying units. (c) *In situ* hyaloclastite (DDH 14-750, 299 m or 980 feet); the matrix is pyritized.

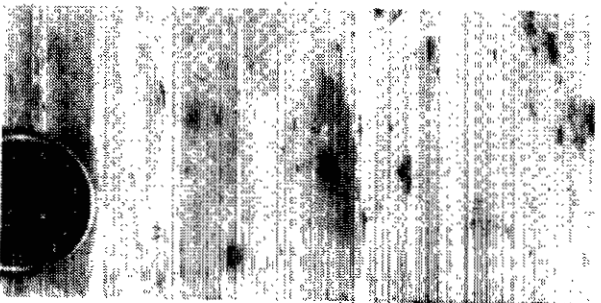
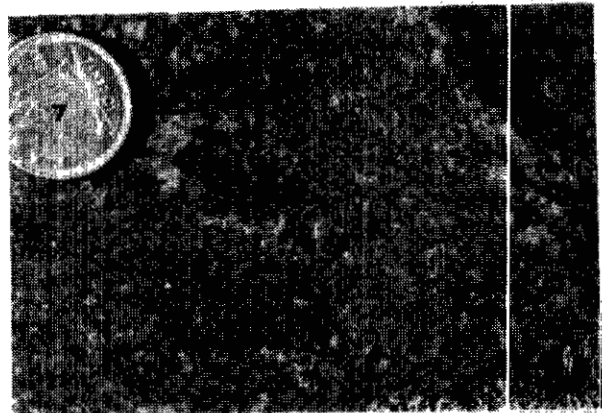
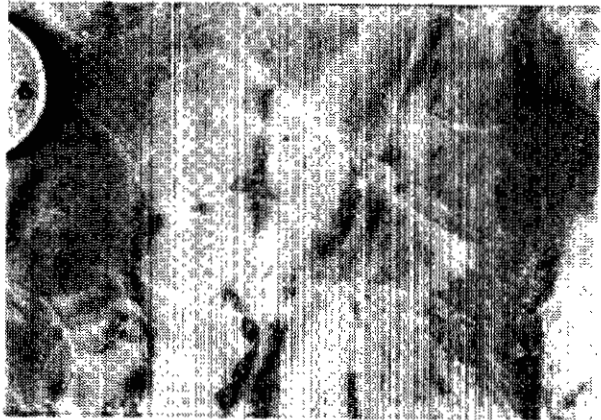
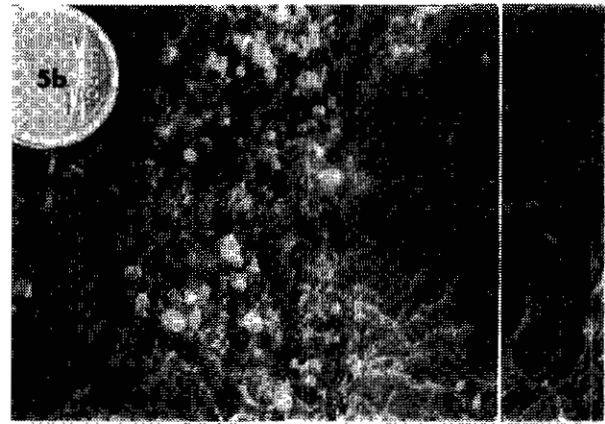


**Plate 5. Coarse rhyolite pyroclastic deposits.** (a) Pumiceous lapilli tuff (DDH 14-753, 254 m or 834 feet) contains 15% pale grey to white weakly quartz-porphyritic to aphanitic rhyolite fragments in a black, compacted, pumiceous, crystal-rich matrix with 10% 1 to 2-millimetre quartz eyes and 15% 2-millimetre feldspars. The flattened texture of the pumice fragments is restricted to this unit, and may indicate welding. (b) Rhyolite tuff with pumice blocks (DDH 14-753, 252 m or 828 feet). Pumice blocks are in a fine-grained, medium-bedded rhyolite tuff.

**Plate 6. Rhyolite tuffaceous sediments.** Tuffaceous sandstone (DDH 14-750, 260 m or 854 feet). This specimen is intensely altered by polymetallic quartz-sericite veins, but relict sedimentary bedding is still visible.

**Plate 7. Upper zone massive sulphide lenses** (DDH 14-723, 217.9 m or 715 feet). Specimen contains sphalerite > tetrahedrite > pyrite > galena > chalcopyrite.

**Plate 8. Rhyolite flow-dome complex.** (a) Vitric quartz-porphyritic rhyolite (QP) with 1 to 2% 1-millimetre quartz eyes (DDH 14-904, 281 m or 923 feet). There are only trace feldspar phenocrysts in this specimen. Fragments of this material are found in the batwing lapilli tuff. (b) Flow-banded quartz-porphyritic rhyolite (QFP) from the base of the flow-dome complex (DDH 14-753, 221.9 m or 728 feet). QFP contains 3-5% 1 to 2-millimetre quartz eyes and 15% 1 to 2-millimetre sericitized feldspar. Flow bands are marked by trails of pyrite grains.

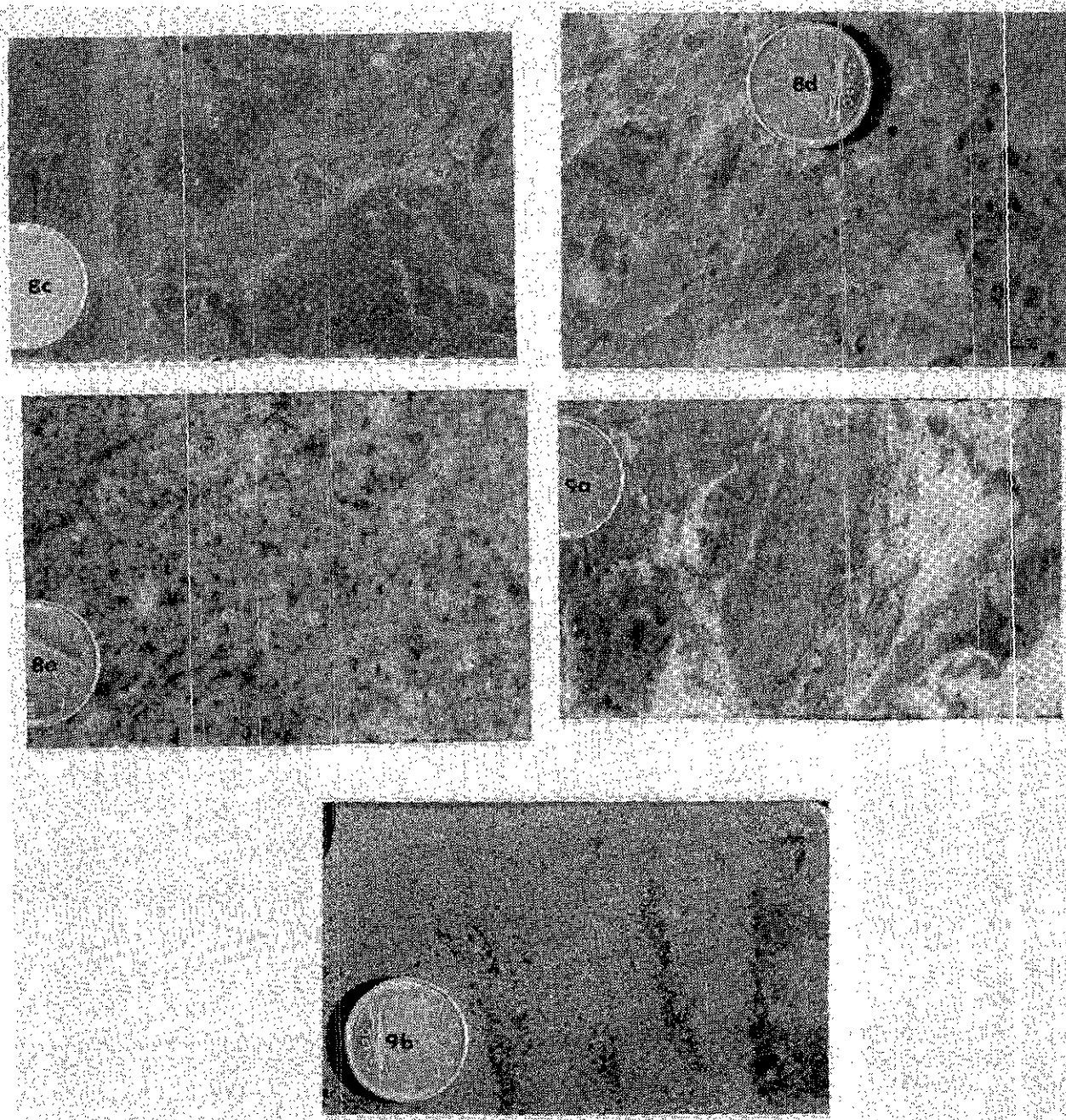


**Plate 8 continued...** (c) Massive to autobrecciated, chaotically flow-banded QFP from the top of the flow-dome complex (DDH 14-756, 242 m or 794 feet.); crystal contents are as in (b) above. (d) Monomict QFP breccia (DDH 14-751, 222 m or 729 feet) locally occurs on top of the rhyolite dome. (e) Feldspar-quartz-hornblende rhyolite porphyry dike (QFPD; DDH 14-753, 221.8 m or 728 feet). Massive, green-grey QFPD with 35% 2 to 3-millimetre feldspar crystals and 10% 1 to 3-millimetre quartz eyes. Green colour is due to chlorite alteration of hornblende. This unit crosscuts the QFP units described above.

**Plate 9. Gap massive sulphide lenses.** (a) Barite-rich massive sulphide from the upper part of the Gap lens (DDH 14-757, 200 m or 656 feet). Mineralogy is: sphalerite > barite > pyrite > quartz > galena > tetrahedrite. Barite in centre shows convex surfaces that face up-hole (to the right). (b) Copper-rich massive sulphides (DDH 14-757, 223.7 m or 734 feet). Sample is pyrite rich with black crystals of sphalerite that are characteristic of Gap-style mineralization. Mineralogy is: pyrite > sphalerite > bornite > chalcocite.

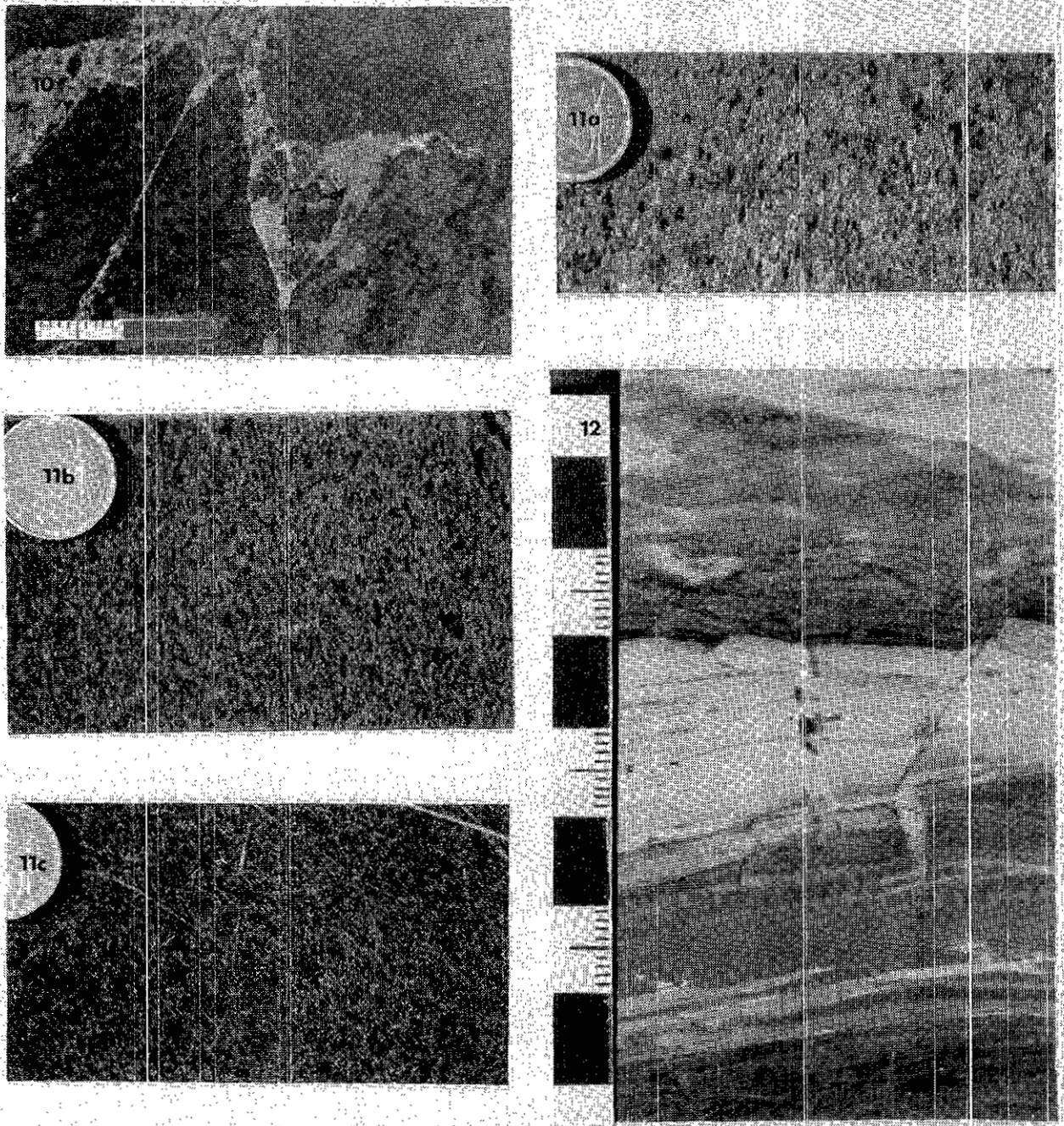


**Plate 10.** *Hangingwall andesite* hyaloclastite breccia (DDH 14-720, 169 m or 556 feet). Cusped fragments of andesite that can be jigsawed together are characteristic of this unit. 1% QFP fragments are also present.

**Plate 11.** *Dikes.* (a) Pale green, feldspar-phyric, trachytic mafic dike (DDH 14-920, 301.7 m or 990 feet). (b) Dark green, augite- and feldspar-phyric mafic dike (DDH 14-757, 282 m or 925 feet). (c) Dark blue-green, weakly feldspar-porphyrific andesite dike (DDH 14-750, 195.7 m or 642 feet); pale specks are leucoxene.

**Plate 12.** Miniature ore deposit (DDH 14-720, 194 m or 634 feet). Specimen contains a block-faulted layer at the base, with quartz-filled feeders along the 'faults'. Mineral zoning is normal with a pyrite-rich base and barite-sphalerite mineralization away from the feeder.

Well-sorted, laminated tuffaceous deposits between 20 centimetres and 2 metres thick cap the lapilli tuff in some areas of the Battle zone. Conspicuously large fragments of black, sericitized, flattened, crystal-rich pumice (Plate 5b) up to 30 centimetres across occur in these units. This type of deposit is characteristic of water-settled suspension deposition of ash and pumice.

## RHYOLITE TUFFACEOUS SEDIMENTS

Rhyolite tuffaceous sediments form a unit about 40 metres thick of fine to coarse, intensely silicified and sericitized tuff, tuffaceous sandstone (Plate 6) and lapilli tuff. There are no distinct marker horizons within this unit, however, fine-grained, thin-bedded sediments are more common in the south part of the Battle zone; coarse tuff, lapilli tuff and rare breccias occur mostly to the north. Devitrified, pale green to black pumice fragments occur throughout the entire package. Spherical, concentrically zoned grains up to 10 millimetres in diameter may be accretionary lapilli. They occur in a bed 3 metres thick at the top (drill hole 14-755; Figure 4).

Polymetallic sulphide stringer networks are common in the rhyolite tuffaceous sediments, probably because it was permeable. Stringer networks are characterized by sphalerite-pyrite-galena-tennantite veins with sericitic alteration envelopes in a pervasively silicified groundmass. Alteration obliterates most of the original textures and makes this rock type difficult to characterize.

## UPPER ZONE MASSIVE SULPHIDE LENSES

Upper zone massive sulphide lenses (Plate 7) occur mostly at the contact between rhyolite tuffaceous sediments and the overlying quartz-feldspar-porphyrific rhyolite. They are both exhalative (synsedimentary) and replacement (postsedimentary) in origin. Exhalative upper zone massive sulphides form lenses up to 5 metres thick. They are polymetallic with sphalerite > barite > tennantite > pyrite > galena > chalcopyrite. High tennantite contents make these lenses extremely silver rich (usually 150 g/t but locally up to 1000 g/t), although gold contents are not particularly high (1 to 3 g/t). Replacement upper zone lenses are thin (1 to 2 m thick) but they can be laterally extensive (over 40 m long). They are characterized by a coarse grained pyrite-quartz-sphalerite mineral assemblage. Feeder zones to upper zone massive sulphide lenses are diffuse polymetallic stockwork zones in the aphanitic rhyolite sediments described above.

## RHYOLITE FLOW-DOME COMPLEX

Rhyolite forms long linear bodies that are over 100 metres thick, 100 metres wide and 1000 metres long in the north Battle zone. There are four visually distinct

members within the rhyolite flow-dome complex. They are: quartz-porphyrific rhyolite; quartz-feldspar-porphyrific rhyolite; green quartz-feldspar porphyritic rhyolite and feldspar-quartz-hornblende rhyolite porphyry dikes. The type of phenocrysts and their morphology is unique within each member, and will be described in detail below.

**Quartz porphyritic rhyolite (QP)** occurs in the northernmost part of the Battle zone. It is up to 30 metres thick and forms the basal unit of the flow-dome complex (Plate 8a). It overlies and locally intrudes the Price andesite. QP rhyolite is white to pale grey-green with high proportions of sericitized, devitrified volcanic glass. It contains 1 to 2% euhedral hexagonal and square quartz phenocrysts about 1 millimetre in diameter and trace amounts of feldspar phenocrysts. This unit is intensely silicified and sericitized due to its proximity to the ore-forming hydrothermal systems. Silicified flows are often mistaken for cherty units but are distinguishable from chert by the presence of quartz eyes and a sericitic sheen on broken surfaces.

**Quartz-feldspar porphyritic rhyolite (QFP)** is the most common type of rhyolite within the flow-dome complex. The upper contact with overlying andesite flows and volcanoclastics is sharp or rubbly, and may be unconformable. The lower contact overlies the tuffaceous rhyolite sediments, and may be obscured by hydrothermal alteration. The QFP is characterized by 8% sericitized feldspar phenocrysts, about 3 millimetres long, and 4% euhedral to rounded quartz phenocrysts, 1 to 5 millimetres in diameter, in an aphanitic, weakly flow-banded matrix. There are several distinct morphological units preserved within the QFP. Most of the unit is massive, white-grey to pale green with variable degrees of quartz-sericite alteration. Flow-banding is present throughout, but is concentrated at the base and margins. Flow bands are laminar in the central and basal parts of the flow, and contain aligned phenocrysts and pyrite grains (Plate 8b). Upper and marginal parts of the QFP are strongly flow banded and more sericitic, indicating that they were once glassier. Two types of flow banding have been identified in the upper QFP: pumice-shard and chaotic flow bands. Pumice-shard flow bands are characterized by flattened black, devitrified, pumice fragments in a massive QFP matrix. The pumice fragments are stretched out in the direction of flow and define the flow banding. Chaotic flow-banded rhyolite is the most marginal facies (Plate 8c). It is characterized by wormy textured flow bands in autobrecciated and quench-brecciated rhyolite. Flow-banded fragments are rotated with respect to each other, making this a very chaotic looking unit. Coarse deposits of rounded QFP fragments occur locally at the top of the flow-dome complex (Plate 8d). This unit may be a reworked flow-top breccia.

**Green quartz-feldspar-porphyrific rhyolite** (QFP) contains 6% round quartz phenocrysts, 0.5 to 6 millimetres in diameter, and 10% feldspar phenocrysts, 1 to 4 millimetres long, in a green, aphanitic matrix. The green colour is due to tiny crystals of hornblende within the matrix that have altered to chlorite. Locally, this unit is purple tinged where trace amounts of magnetite have altered to hematite.

**Feldspar-quartz-hornblende rhyolite porphyry dikes** (QFPD) have sharp, quenched contacts with the QFP. This unit is crystal rich with 35% 2 to 3-millimetre feldspar crystals, 7% quartz eyes up to 7 millimetres in diameter, and 2% hornblende crystals (Plate 8e). The quartz eyes are partially resorbed and have quartz-feldspar coronas around them. It is mossy green due to chlorite alteration of hornblende.

### GAP MASSIVE SULPHIDE LENSES

The Gap massive sulphide lens occurs close to the contact between the rhyolite flow-dome complex and hangingwall andesite. Many appear to be located in depressions on the flow dome. The largest lenses are associated with quartz-porphyrific rhyolite, the lowest member within the flow-dome complex. Most lenses are zoned from lower copper and pyrite-rich mineral assemblages to upper and peripheral barite and sphalerite-rich zones. Barite-rich massive sulphide from the upper part of the Gap lens is: sphalerite-barite-pyrite-quartz-galena-tennantite (Plate 9a). Barite is locally mammillary; convex surfaces face up-hole. Copper-rich mineralization is: pyrite-sphalerite-chalcopyrite-bornite-tennantite-chalcocite (Plate 9b). Big black crystals of sphalerite up to 1 centimetre across are common in copper-rich zones and are characteristic. Feeder zones to the Gap are characterized by stockworks of coarse pyrite and quartz veins in the underlying rocks.

### HANGINGWALL ANDESITE

Hangingwall andesite is dark green, slightly amygdaloidal, and contains about 25% feldspar and 1% pyroxene phenocrysts. It is weakly altered to a chlorite-epidote assemblage; trace magnetite grains are altered to purple hematite. Amygdules are elongate to lenticular, 1 to 2 millimetres long, and are filled with quartz, epidote and chlorite. Most of the andesite is brecciated; about 30% forms coherent flows. Approximately 10% of the hangingwall andesite consists of inter-flow sedimentary units.

Andesite breccias are composed of poorly sorted, angular fragments with arcuate clast boundaries; many of the fragments also have *in situ* (jigsaw-fit) breccia texture (Plate 10). Exotic fragments of QFP, massive sulphides and pale green rhyolite comprise no more than 5% of the rock. The shape and arrangement of andesite

fragments, as well as the largely monomict rock composition are characteristic of hyaloclastite breccias that form by *in situ*, subaqueous quench fragmentation. Appropriately, the andesite breccias form marginal facies to coherent andesite flows in the Battle zone. A typical andesite flow consists of 2 metres of coherent andesite, with 3 metres of hyaloclastite breccia on both the top and bottom.

The contact between the underlying H-W horizon and hangingwall andesite is generally sharp, although fragments of QFP and QFPD are commonly scattered from the flow-dome complex and incorporated into the overlying andesites. Sericitic alteration that affects the Price formation and the H-W horizon does not extend into the hangingwall andesites. This suggests that there is a time gap between alteration associated with the ore deposits and deposition of the overlying andesites.

### DIKES

Most dikes in the Battle zone are mafic. Three distinct types of mafic dikes have been recognized: light green, feldspar-phyric, trachytic mafic dikes (Plate 11a); dark green augite and feldspar-phyric mafic dikes (Plate 11b) and andesite dikes (Plate 11c). Most of the pale green dikes are intensely altered to an epidote-fuchsite-chlorite-carbonate assemblage and have irregular, quartz-carbonate veined contacts with the country rock. They may have pink quartz-carbonate filled amygdules. Dark green augite-phyric dikes may be fresh or altered to epidote, fuchsite and chlorite; they tend to have sharp contacts. Andesite dikes are dark blue-green, weakly feldspar porphyritic and unaltered. All of the dikes crosscut H-W horizon and the hangingwall andesite.

Some felsic rocks, locally intersected by drill holes in the Price andesite, may be dikes. Their full significance is not known.

### DISCUSSION AND INTERPRETATION OF THE BATTLE ZONE GEOLOGY

Main Battle zone sulphides occur at the base of the felsic H-W horizon, which overlies Price formation. Price formation is a sequence of massive to pillowed flows and associated breccias that was deposited during a series of non-explosive, effusive events. Subsequent rifting formed the Butte Lake camp basin with **minimum** dimensions of 3 by 10 kilometres (Juras, 1987). The base of the H-W horizon probably marks the initial development of a rift basin, and the first cycle of sulphide deposition (main Battle zone, which is correlative with most mineralization in the H-W mine (Figure 1)). Rifting was probably contemporaneous with the onset of felsic volcanism in the volcanic arc. Massive sulphides of the main Battle zone were deposited in small

fault-bounded basins away from the locus of felsic volcanism. The faults provided conduits for metal-rich hydrothermal fluids, which upon reaction with cold sea water at and below the sea floor, deposited sulphide mud. Continued reaction of the mud with circulating fluids zoned most of these mounds to pyrite and chalcopyrite-rich cores with sphalerite-dominant upper and peripheral zones. Plate 12 shows the depositional style of the orebodies in miniature. The dominantly felsic volcanic package of the H-W horizon represents an intra-arc environment within an oceanic island-arc system (Juras, 1987).

Battle zone chert commonly, but not exclusively, occurs just above sulphide lenses (Figures 3 and 4) in the fine rhyolite tuffaceous deposits. A key question is whether or not the cherts are exhalites and therefore closely related to massive sulphides.

Exhalites are distal and proximal, contemporaneous and late-stage products of the hydrothermal systems responsible for forming massive sulphide deposits (Kalogeropoulos and Scott, 1983). They have two components, clastic and chemical. The clastic component may be volcanoclastic, epiclastic or pelagic. The chemical component is dominantly quartz, associated with either iron oxides or iron sulphides. Manganese oxides, iron-rich smectites, sericite, base metal mineralization and anomalous amounts of gold, silver, cobalt and nickel may also be present (Kalogeropoulos and Scott, 1983).

Battle zone cherts (Plate 4a) are probably not exhalites because: they do not contain significant amounts of iron sulphides or oxides; they are not enriched in gold, silver, manganese, cobalt or nickel (M. Robinson, unpublished inductively coupled plasma data from Chemex Labs Ltd., Vancouver, British Columbia, 1993); and they have the same immobile element chemistry as the overlying rhyolites (M. Robinson, unpublished data, X-Ray Laboratories Ltd, Toronto, Ontario, 1993). In addition, contact relationships between the massive sulphides and the associated cherts suggest a "competitive" (not a cogenetic) relationship between the two rock types. For example, two closely spaced drill holes with no intervening structures contain an equal thickness (about 4 m) of chert in one hole, and sulphide in the other. A most likely scenario is that the chert was originally deposited as a layer of fine rhyolite ash against which massive sulphides were deposited. Continued hydrothermal activity silicified the ash. The presence of chert layers that are not demonstrably related to sulphide lenses indicates that a hydrothermal source related to sulphide mineralization may not be necessary to their formation.

Emplacement of rhyolite is intimately associated with ore-forming processes in the Battle zone. Fine rhyolite tuffaceous deposits probably represent the first eruption associated with emplacement of the quartz porphyritic rhyolite (QP). These deposits competed with

the main Battle sulphide lenses for space during the waning stages of their deposition (see above). Massive to weakly flow-banded quartz-porphyrific rhyolite (QP) intrudes both the andesite basement and its own ejecta. This unit occurs in the footwall below the Gap massive sulphide lens. Pumiceous rhyolite lapilli tuff forms a pyroclastic flow up to 10 metres thick throughout the Battle zone (Figure 5). It contains fragments of QP and therefore postdates eruption of the QP.

The thick section of rhyolite tuffaceous sediments may represent a period of pyroclastic activity preceding the emplacement of the flow-banded quartz-porphyrific rhyolite. Alternatively, it may represent a period of epiclastic sedimentation. The high degree of alteration in this unit makes it difficult to determine the exact nature of this deposit. Local beds of accretionary lapilli(?) and devitrified pumice blocks occur throughout, supporting a pyroclastic origin for the sediments. However, the presence of locally preserved well-sorted fine turbidite units, especially distal to the dome, favours an epiclastic origin. Sericitized areas, which might be mistaken for pumice fragments, are commonly alteration envelopes surrounding sulphide veins. This unit was probably permeable and may have channeled hydrothermal fluids towards upper zone lenses of both exhalative and replacement type. The thicker lenses are exhalative, contain sphalerite > barite > tennantite and appear to mark a short hiatus between sedimentation and emplacement of the QFP, which intrudes and overlies the rhyolite tuffaceous sediments. The hydrothermal system continued to circulate, but fluids then became focused along the boundary between the QFP and the underlying sediments. Replacement-style upper zone massive sulphides were deposited against this boundary. These lenses are usually no more than 2 metres thick and are characterized by the presence of coarse-grained pyrite.

The Gap massive sulphide lens was deposited in depressions at the top and peripheral to the QP unit of the rhyolite flow-dome complex. They are overlain by thin flows of the QFP rhyolite. The QFP appears to have formed a cap over the Gap massive sulphide lenses which prevented their erosion. Green quartz-feldspar-porphyrific flows (GQFP) overlie the QFP in central regions of the Battle zone. The last felsic event in H-W horizon was the intrusion feldspar-quartz-hornblende rhyolite porphyry dikes (QFPD). Locally, these dikes may extrude on top of the QFP and feed crystal-rich flows. Rhyolite units within the flow-dome complex progressively increase in mafic mineral content and become more coarsely crystalline as they decrease in age. This suggests progressive, episodic emplacement from deeper regions of a crystallizing source magma chamber. Crystallization of the QFP could have driven off metal-rich magmatic waters which may be related to the unique character of Gap-style mineralization.

## ACKNOWLEDGMENTS

We thank Westmin Resources Limited for permission to publish this paper and for the support and input from the geologists at the H-W mine -- particularly C. Pearson, F. Bakker and I. McWilliams. Early work by G. Price and A. Hamilton contributed substantially to this study. R. Allen of Volcanic Resources provided insights into the physical volcanology. At the Department of Geological Sciences, The University of British Columbia, A.J. Sinclair, John Thompson and members of the Mineral Deposits Research Unit provided helpful discussions and advice. Funding to M. Robinson was provided by Westmin and MDRU. Funding to C. Godwin was provided by a Natural Sciences and Engineering Research Council Operating Grant. This study is part of the Volcanogenic Massive Sulphide project undertaken by the MDRU at UBC, funded by the Natural Sciences and Engineering Research Council of Canada, the Science Council of British Columbia, and ten mining and exploration member companies.

## REFERENCES

- Brandon, M.T., Orchard, M.J., Parrish, R.R., Sutherland Brown, A. and Ycrath, C.J. (1986): Fossil Ages and Isotopic Dates from the Paleozoic Sicker Group and Associated Intrusive Rocks, Vancouver Island, British Columbia; *in* Current Research, Part A, *Geological Survey of Canada*, Paper 86-1A, pages 683-696.
- Fyles, J.T. (1955): Geology of the Cowichan Lake Area, Vancouver Island, British Columbia; *B.C. Ministry of Energy, Mines and Petroleum Resources*, Bulletin 37.
- Jeffery, W.G. (1970): Buttle Lake: *B.C. Ministry of Energy, Mines and Petroleum Resources*, Miscellaneous Open File Report.
- Jones, D.L., Siberling, N.J. and Hillhouse, J. (1977): Wrangellia--A Displaced Terrane in Northwestern North America; *Canadian Journal of Earth Sciences*, volume 14, pages 2565-2577.
- Juras, S.J. (1987): Geology of the Polymetallic Volcanogenic Buttle Lake Camp, with emphasis on the Price Hillside, Central Vancouver Island, British Columbia, Canada; unpublished Ph.D. thesis, *The University of British Columbia*.
- Kalogeropoulos, S.I. and Scott, S.D. (1983): Mineralogy and Geochemistry of Tuffaceous Exhalites (Tetsusekiei) of the Fukazawa Mine, Hokuroku District, Japan; *Economic Geology*, Monograph 5, pages 412-432.
- Muller, J.E. (1980): The Paleozoic Sicker Group of Vancouver Island, British Columbia; *Geological Survey of Canada*, Paper 79-30.
- Muller, J.E., Northcote, K.E. and Carlisle, D. (1974): Geology and Mineral Deposits of the Alert Bay - Cape Scott Map-area, Vancouver Island, British Columbia; *Geological Survey of Canada*, Paper 74-8.
- Pearson, C.A. (1993): Mining Zinc-Rich Massive Sulphide Deposits on Vancouver Island, British Columbia; *International Symposium - World Zinc '93*, pages 75-84.
- Sada, D. and Danner, W.R. (1974): Early and Middle Pennsylvanian Fusulinids from Southern British Columbia, Canada and Northwestern Washington, U.S.A.; *Transactions of the Proceedings of the Palaeontological Society, Japan, New Series*, No. 93, pages 249-265.
- Walker, R.R. (1985): Westmin Resources' Massive Sulphide Deposits, Vancouver Island; *Geological Society of America*, Cordilleran Section Meeting, May 1985, Vancouver, B.C., Field Trip Guidebook, pages 11 to 1-13.
- Yole, R.W. (1969): Upper Paleozoic Stratigraphy of Vancouver Island, British Columbia; *Geological Association of Canada*, Proceedings, Volume 20, pages 30-40.

## **NOTES**

# GEOLOGICAL INVESTIGATIONS OF THE H-W DEPOSIT, BUTTLE LAKE CAMP, CENTRAL VANCOUVER ISLAND (092F/12E)

By T.J. Barrett, R.L. Sherlock  
Mineral Deposit Research Unit, U.B.C.  
S.J. Juras  
Westmin Resources Limited  
G.C. Wilson  
Turnstone Geological Services Limited  
R. Allen  
Volcanic Resources

(MDRU Contribution 041)

**KEYWORDS:** economic geology, Buttle Lake, Sicker Group, H-W horizon, lithogeochemistry, massive sulphide, gold, silver, copper, lead, zinc, andesite, rhyolite.

## INTRODUCTION

The Myra Falls deposits of the Buttle Lake mining camp (49° 34'N, 125° 36'W) occur in Paleozoic Sicker Group rocks of Vancouver Island, within the Wrangellia allochthonous terrane of the Insular Belt of the western Cordillera. The deposits are located at the south end of Buttle Lake, 90 kilometres by highway from Campbell River (Figure 1). The deposits include the past-producing Lynx and Myra orebodies, which were brought into production in 1967, and the producing H-W orebody and adjacent North Lens, discovered in 1979. In 1991 the Battle and Gap zones were discovered along strike and to the west of the H-W orebody and are scheduled to begin production in 1993. As of January 1, 1993 proven and probable geological reserves for the entire property are 12 516 300 tonnes grading 1.9 % copper, 0.5 % lead, 6.3 % zinc, 2.1 grams per tonne gold and 45.6 grams per tonne silver (Westmin Resources Limited Annual Report, 1992).

This paper is based on 1993 fieldwork involving relogging and sampling of selected drill-cores through the stratigraphic sequence hosting the H-W orebody, as well as preliminary lithogeochemistry and ore petrology. Robinson *et al.* (1994) describe stratigraphic relations in the Battle zone, which occurs at the same level in the camp stratigraphy as the H-W deposits. In order to avoid repetition of the general geology and mine stratigraphy the reader is referred to Robinson *et al.* (1994; this volume) for a detailed discussion. Earlier work on the geology and geochemistry of the volcanic hostrocks is summarized and discussed by Juras (1987); preliminary fluid inclusion results are reported by Hannington and Scott (1989).

## H-W STRATIGRAPHY

The stratigraphy at the H-W deposit comprises a series of relatively flat lying mafic and felsic volcanic units (Figure 2). Stratigraphic columns for two exploration holes that penetrated thick sections of the H-W orebody are given in Figures 3 and 4. The stratigraphically lowest unit, the Price andesite (DCp, Figure 2), forms the footwall to the sulphide mineralization and comprises at least 300 metres of massive to pillowed andesite flows and flow breccias, with minor volcanoclastic andesitic rocks. This unit is directly overlain by the Myra formation, the lowest part of which is the H-W horizon (unit 1, Figure 2). The H-W horizon comprises 50 to 100 metres of felsic subaqueous volcanoclastic and pyroclastic beds, lesser interbedded black mudstones, and a lens of quartz-feldspar-porphyrific rhyolite up to 50 metres thick.

Much of the footwall beneath the Main and North lenses is intensely altered to a sericite-pyrite-quartz assemblage, locally with significant chlorite. Lateral to this, the alteration is dominated by an albite-sericite-quartz assemblage. Least-altered samples are massive, feldspar-pyroxene-phyric andesite (Juras, 1987).

The massive sulphide lenses occur at the contact between the Price andesite and the H-W horizon (Figure 2). They are underlain by a strongly altered and pyritized feeder zone that extends at least 25 to 50 metres down into the andesitic footwall. Mineralization directly above the footwall andesite is typically massive pyrite with only trace disseminated chalcopyrite. This style grades vertically into massive pyrite with several percent disseminated chalcopyrite, that constitutes the bulk of the ore body. This massive sulphide is typically overlain by an upper interval of semimassive to disseminated polymetallic mineralization alternating with felsic mass-flow units. This upper interval of mineralization tends to be dominated by sphalerite, galena, tennantite and barite.

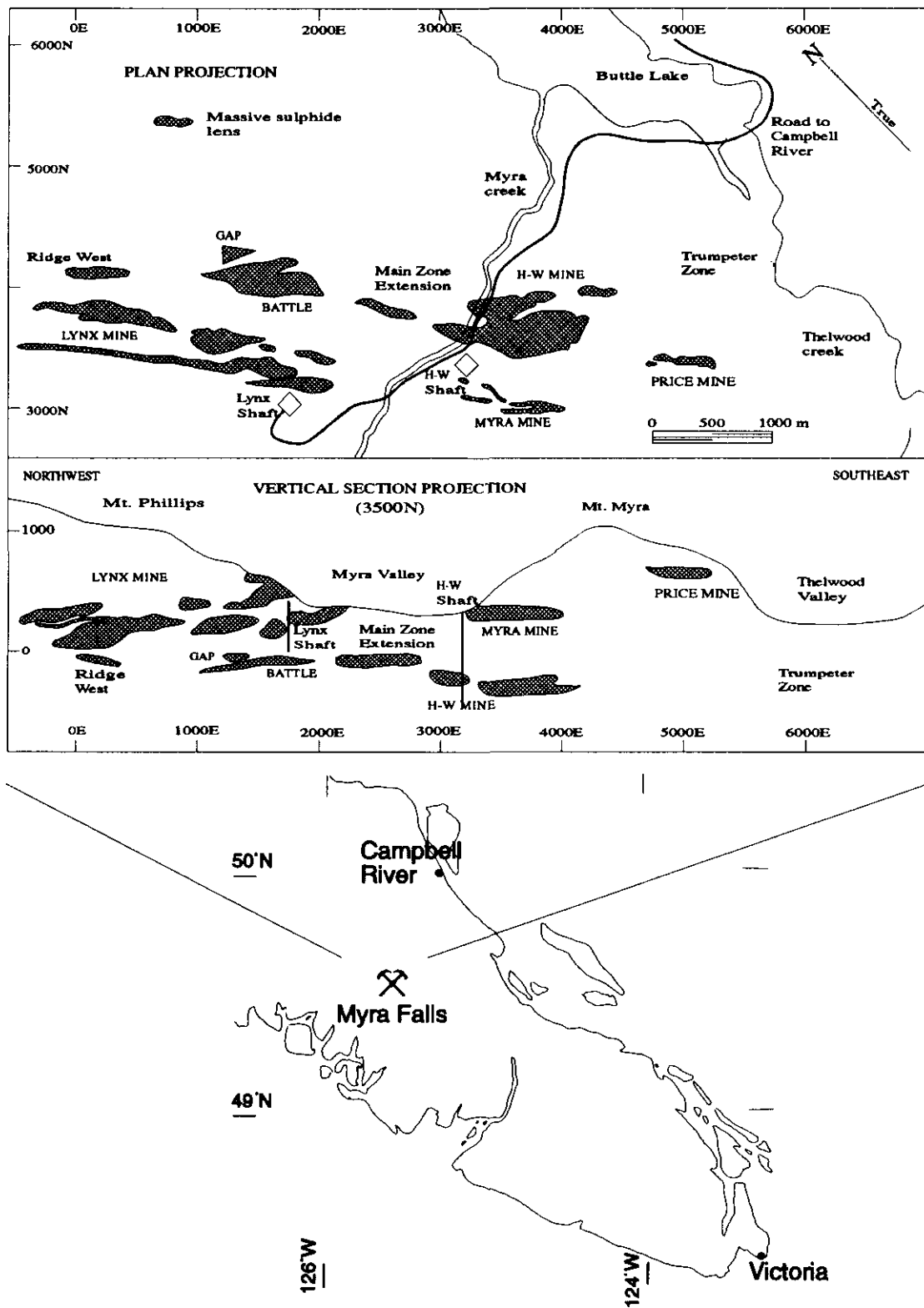


Figure 1. Location map for the Myra Falls massive sulphide deposits. Also shown is a longitudinal section of the relative locations of the various orebodies.

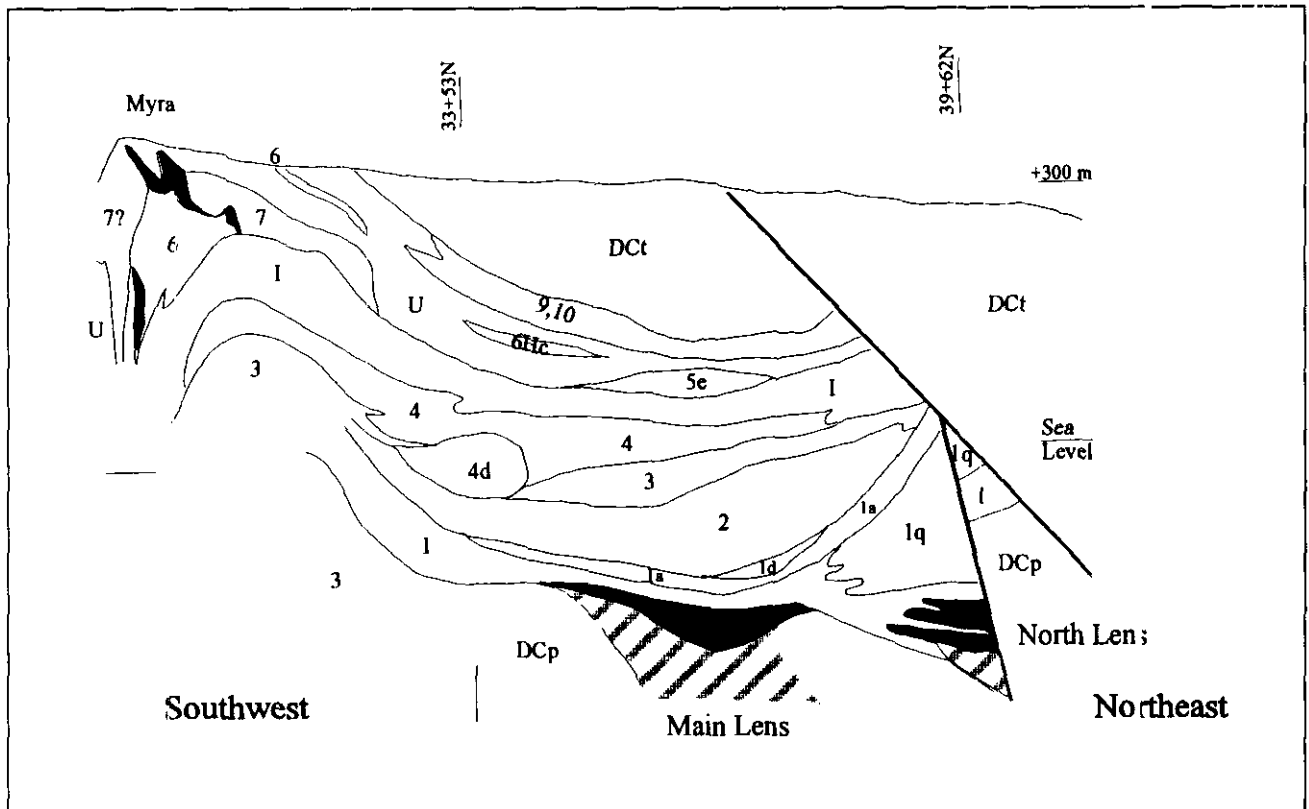


Figure 2. Stratigraphic section through the H-W area at 34+75E. DCp, Price Formation; 1, H-W horizon; 1a, argillite; 1d, dacite; 1q, quartz-feldspar-porphyritic rhyolite; 2, H-W andesite; 3, ore-clast breccia; 4, lower mixed volcanics; 4d, lower mixed volcanics, dacite; I, undifferentiated Myra formation, interzone units; 5e, andesite; 6, Lynx-Myra-Price horizon; 6Hc, Lynx-Myra-Price chert horizon; U, undifferentiated Myra formation, upper units; 7, G-flow unit; 9, upper rhyolite unit; 10, upper mafic unit; DCt, The Wood formation. Solid black areas represent massive sulphide lenses, striped areas represent zones of massive pyrite alteration. After: Juras (1987).

The felsic mass-flow units of the H-W horizon are composed of a monomict assemblage of rhyolite clasts. Beds range from 0.1 to 1 metre thick and are generally graded, with younging directions up-hole. Clasts range from rounded to subangular and appear to have been reworked.

A large body of quartz-feldspar-porphyritic rhyolite (QFP) wedges into the H-W horizon about 50 to 100 metres to the north of the H-W deposit, and thickens progressively northwards. It can be traced for more than 2 kilometres westwards to the Battle zone. The H-W horizon also contains distinctive black mudstone intervals with interbedded felsic volcanoclastic rocks. Black mudstones that occur just above the H-W orebody continue northwards above the QFP wedge, but not below it.

The H-W andesite is a sill-flow complex that is partially intrusive into the H-W horizon. It comprises flows and breccias of basaltic andesitic and andesite that form a lens of several hundred metres in diameter above the area of the H-W deposit. To the southwest, in the area of 33+50N, the H-W andesite is overlain by a lens of siliceous dacite up to 75 metres thick (Figure 2). Above the H-W deposit, in the area of 39+50N, a

smaller dacite lens intervenes between the H-W horizon and the H-W andesite.

Stratigraphically above the H-W andesite is the ore-clast breccia, which consists of mainly andesite volcanoclastic debris-flows, locally with some rhyolite and minor sulphide clasts. This is followed by green tuff breccias and bedded coarse to fineuffs which mark the end of the first volcanic cycle. An overlying thick sequence of mafic-rich volcanoclastics with lesser rhyolite forms the second volcanic cycle, and is host to the Myra-Lynx-Price orebodies.

## LITHOGEOCHEMISTRY

A suite of 27 whole-rock samples from exploration holes W-111 and W-123 was analyzed by X-ray fluorescence using glass beads for major elements, and pressed pellets for trace elements. The locations of the samples are shown next to the stratigraphic logs in Figures 3 and 4. The purpose of the lithogeochemical study was to identify the main volcanic units, particularly where core and petrographic identification is difficult due to severe alteration.

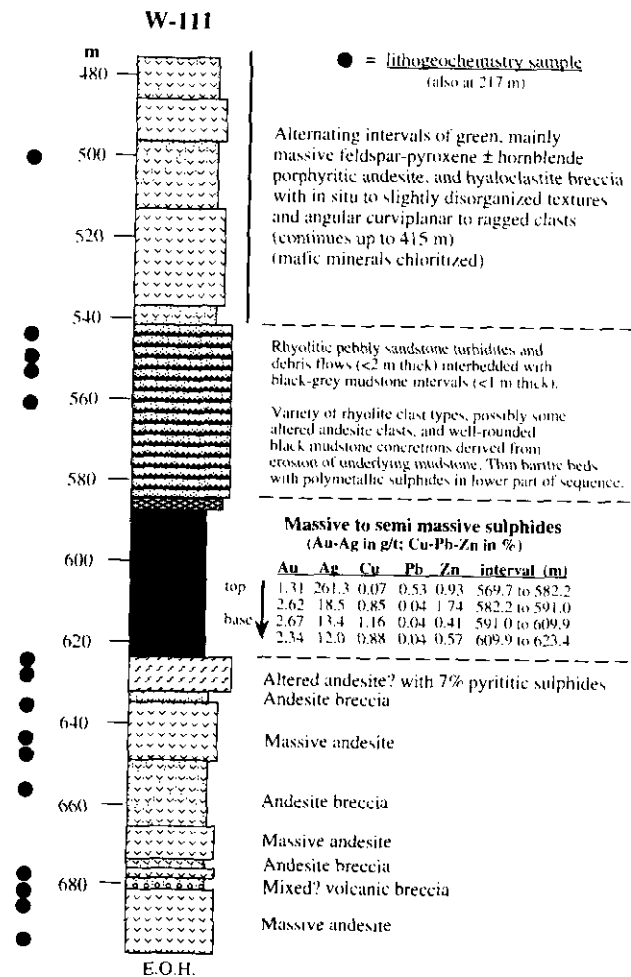


Figure 3. Stratigraphic column for drill hole W-111, H-W orebody. The black dots are lithogeochemical sample locations.

The lithogeochemical data for the H-W volcanic rocks have been examined using immobile element relationships (e.g. Ti-Al-Zr) to identify rock types and characterize alteration, as described by MacLean and Kranidiotis (1987), MacLean (1990), and Barrett and MacLean (1991). The results (Figure 5) define two main alteration trends in plots of both  $Al_2O_3$  versus  $TiO_2$  (a) and  $Al_2O_3$  versus Zr (b). These trends result from alteration of rhyolite and andesite precursors. Ideally, a single alteration line results from alteration of a homogeneous precursor, with the spread of points along a given alteration line reflecting the overall mass change in the mobile elements. Net mass gain in mobile elements moves a sample point from its precursor location along a line towards the origin, whereas net mass loss moves a point in the opposite direction.

The altered footwall andesites show a small compositional range in terms of their immobile element ratios. This primary range leads to a fan-like distribution for the altered samples (Figure 5). Of particular interest is the fact that the footwall andesite (DCp, Figure 2), which in places is altered

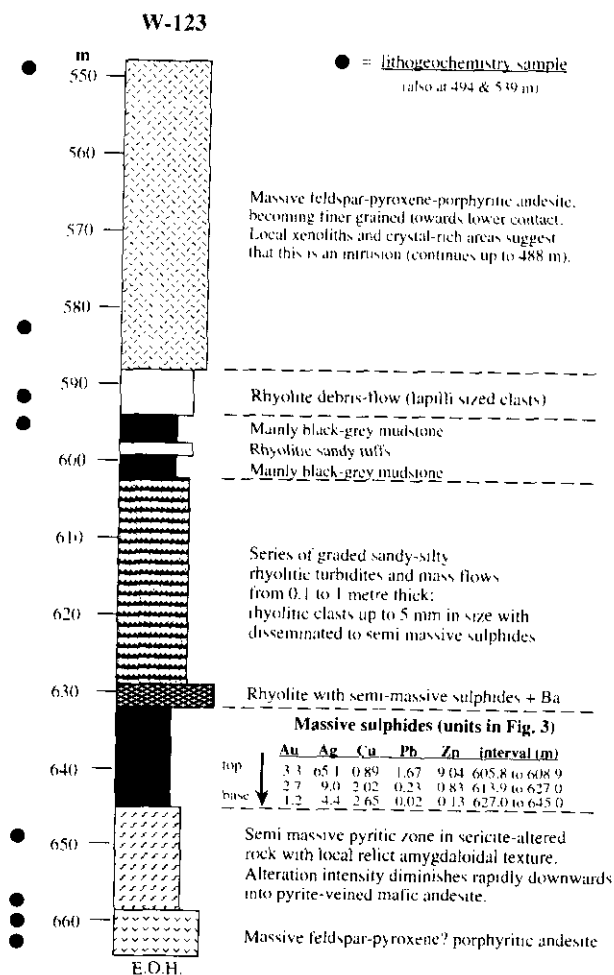


Figure 4. Stratigraphic column for drill hole W-123, H-W orebody. The black dots are lithogeochemical sample locations.

beyond recognition and contains up to 50% sulphides, yields a perfectly straight alteration line in the  $Al_2O_3$  versus  $TiO_2$  plot (Figure 5a). This indicates that the drilled interval from at least 636 to 682 metres was derived from an andesitic precursor with uniform immobile element ratios. A later study will present calculated elemental mass changes in the alteration zone of the H-W deposit.

Five samples of H-W andesite from the hangingwall (unit 2, Figure 2) have a tight  $Al_2O_3$  versus Zr composition (Figure 5b). Their major element composition, and lack of alkali exchange in particular, indicates that the H-W andesite is much less altered than the footwall andesite. Although the H-W andesite has slightly higher  $Al_2O_3$  versus Zr ratios than the footwall andesite, their  $Al_2O_3$  versus  $TiO_2$  ratios are similar, as are other trace element ratios. This suggests that the H-W and footwall andesites are compositionally closely related.

The single rhyolite alteration line (Figure 5) is rather unexpected, given the fact that the samples were taken from several felsic mass-flow or turbidite beds. These

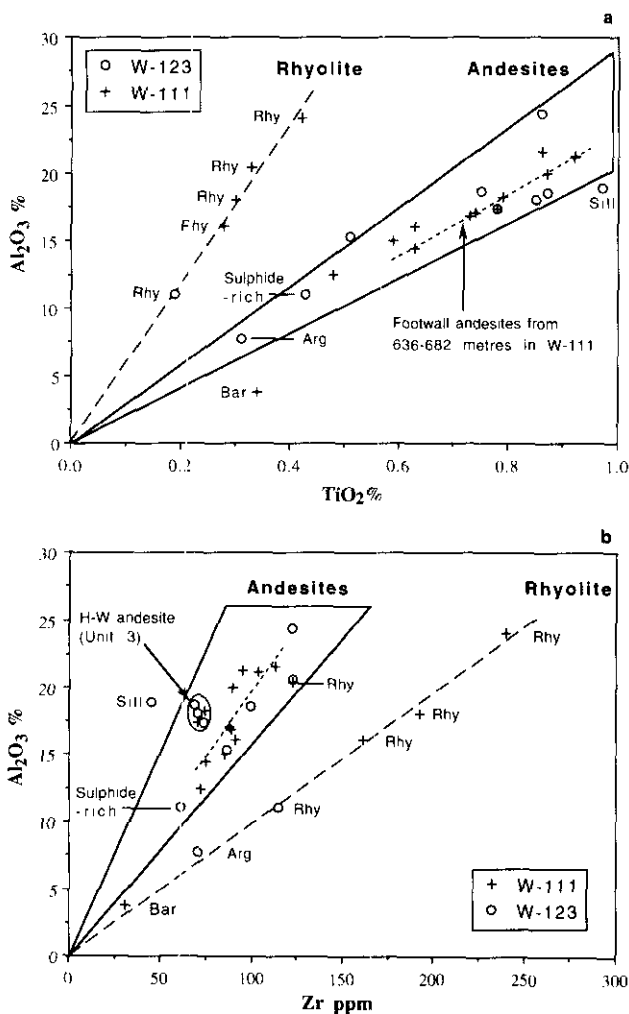


Figure 5. Plot of  $Al_2O_3$  versus  $TiO_2$  (a) and versus  $Zr$  (b) for volcanic rocks from the H-W lens, drill holes W-111 and W-123. Most of the samples fall along andesite or rhyolite alteration lines, making this technique a useful tool for discriminating between extremely altered rhyolites and andesites.

clastic rocks in fact had a heterolithic appearance due to the different textures and colours of the clasts. However, the slope of the felsic alteration line closely corresponds to a pure end-member rhyolite composition (based on Westmin Resources unpublished data for least-altered rhyolites). Thus, essentially all of the fragments must be of rhyolite composition. The monolithic nature of these beds suggests that they were rapidly emplaced (into a muddy basin at this particular locality).

It is of interest that the immobile element plots clearly indicate that several altered units logged by previous workers as rhyolites are actually andesite and vice versa. Thus, these plots can usefully serve to establish original rock types and improve stratigraphic correlation.

Samples in the H-W data set plot consistently in both  $Al_2O_3$  versus  $TiO_2$  and  $Al_2O_3$  versus  $Zr$  space, except for one rhyolite sample that has shifted onto the andesite alteration line, probably due to zirconium loss. This effect can occur in some felsic rocks if zirconium

becomes incompatible during magmatic fractionation or is lost by crystal sorting (MacLean and Barrett, 1993). For this reason,  $Al_2O_3$ - $TiO_2$  plots show the most consistent immobile element relations.

## SULPHIDE MINERALIZATION

The H-W deposit consists of the Main, North and Upper sulphide lenses, of which the first two occur at the base of the H-W horizon (unit 1). The lenses consist of fine-grained massive to thinly banded pyrite, sphalerite and chalcopyrite with minor bornite, galena and tennantite; gangue minerals are quartz, barite and sericite. The Main lens is some 1200 metres long, 500 metres wide and up to 80 metres thick (Juras, 1987). There is a general zoning from a pyrite core with sphalerite and chalcopyrite-rich areas, to a pyrite-poor barite-rich margin with notable sphalerite, chalcopyrite, galena and bornite (Walker, 1985). The Upper lens mineralization is near the top of the H-W horizon (unit 1). It comprises disseminated to locally massive polymetallic sulphides. Much of the intervening sequence of unit 1 felsic volcanoclastics is strongly altered, probably as a result of continued hydrothermal activity after formation of the Main and North lenses.

## MINERAL COMPOSITIONS

Polished mounts (total area  $\approx 92$  cm<sup>2</sup>) were prepared from six samples of disseminated, brecciated, banded and massive sulphide ores. These were characterized in terms of mineralogy, textures and mineral chemistry. The modal proportions of each ore and gangue phase were estimated visually: four stope samples from the H-W deposit contain 40 to 90 volume percent sulphides, averaging about 60%. Two drill-core samples from the Upper zone contain 8 to 15% sulphides. The five key ore minerals, in terms of average volume percent across the sample set, are: pyrite (28%), sphalerite (9%), chalcopyrite (7%), galena (1%) and tennantite (0.4%), averaging a total of 45% for all samples.

Four complementary techniques were used for mineral analysis. On scales ranging from about 0.01 to 1 millimetre, polished samples were analyzed for major, minor and trace elements. Elements expected at levels of 0.1 weight percent (1000 ppm) or more were analyzed by electron microprobe (EPM). A survey of minor and trace elements in the 5 to 5000 ppm range was conducted by proton microprobe (PIXE). A limited study of gold distributions (<10 ppm) was carried out using accelerator mass spectrometry (AMS) and ion microprobe (SIMS) methods.

The EPM and PIXE data indicate that common sulphides, particularly pyrite, almost always contain much less than 500 ppm (0.05 wt.%) arsenic. Silver occurs at significant levels in only two minerals, namely tennantite (0.1-1.2 wt.%) and galena (60-250 ppm, based on three PIXE analyses). Over 30 elements were analyzed by microprobe methods; the PIXE survey also yielded some minor element data. Cadmium is present in sphalerite and tennantite at concentrations of 0.33 and 0.1 weight percent, respectively. Chalcopyrite contains a

few tens of parts per million selenium and indium; tennantite contains up to 500 parts per million tellurium. Pyrite and chalcopyrite may each host tens of parts per million of molybdenum.

Good agreement in reconnaissance surveys of gold by SIMS, and its ultrasensitive variant AMS indicates that gold contents in pyrite and chalcopyrite are in the 25 to 1000 parts per billion range, with the higher values occurring in pyrite. This is inadequate to account for the 1.9 to 3.9 grams per tonne gold reported in the bulk assays. Contributions from submicroscopic inclusions at grain boundaries and scattered grains of gold or electrum (not seen in this study) may account for the balance. A third possibility not yet evaluated is a contribution from 'invisible gold' in tennantite (PIXE lacks the sensitivity required for a definitive check on gold).

## CONCLUSIONS

A preliminary interpretation of the lithological sequence in the H-W area is:

- i) Accumulation of a widespread mafic volcanic footwall of andesitic flows and sills.
- ii) Deposition of some massive sulphides on the mafic volcanic footwall.
- iii) Accumulation of felsic volcanoclastic debris-flows in the area of the H-W deposit but in felsic flows (or shallow sills) in the area of the north lens.
- iv) Continued sulphide deposition as infillings within porous unconsolidated felsic debris-flows, and local precipitation of barite and chert.
- v) Accumulation of pelagic black mud, with continued episodic deposition of felsic debris-flows in the black muds.
- vi) Emplacement of an andesite sill/flow complex (H-W andesite) into and onto the felsic debris-flow unit.
- vii) Accumulation above the H-W andesite of mafic-rich and lesser felsic volcanoclastics that form the second volcanic cycle and host the Myra-Lynx-Price orebodies.

Immobile element plots have been used to effectively identify heavily altered (and locally mineralized) rocks near the H-W orebody. These identifications allow the hangingwall-footwall contact to be established, and permit correlation of individual volcanic (and even volcanoclastic) units within the mine stratigraphy.

## FURTHER WORK

Our continued work at Myra Falls will include: definition of the H-W stratigraphy and extent of hydrothermal alteration using detailed litho geochemistry and petrography; comparison of H-W stratigraphy with that of the Battle zone 1 to 2 kilometres to the west (Robinson *et al.*, 1994, this volume); identification of the mineral assemblages in the H-W orebody and the trace metal composition of sulphides and sulphosalts; and characterization of the temperatures and compositions of the mineralizing fluids. Once these volcanic units are identified using immobile element relations mass changes will be calculated for each mobile element in

order to reveal the intensity and distribution of hydrothermal alteration around the H-W orebody.

## ACKNOWLEDGMENTS

We are indebted to Westmin Resources Limited for permission to publish information on the H-W deposit, and to Cliff Pearson, Finlay Bakker and Ivor McWilliams for geological information and discussions. The electron microprobe work and accelerator mass spectrometry were carried out at the Department of Geology and the Isotracer Laboratory, University of Toronto. The PIXE and SIMS analyses were conducted at the University of Guelph and at CANMET (Ottawa), respectively.

Research at the Myra Fall deposit forms part of a Mineral Deposit Research Unit project on Volcanogenic Massive Sulphide Deposits of the Cordillera, funded by the Natural Sciences and Engineering Council of Canada, the Science Council of British Columbia, and ten mining and exploration member companies.

## REFERENCES

- Barrett, T.J. and MacLean, W.H. (1991): Chemical, Mass and Oxygen Isotope Changes During Extreme Hydrothermal Alteration of an Archean Rhyolite, Noranda, Quebec; *Economic Geology*, Volume 86, pages 406-414.
- Hannington, M.D. and Scott, S.D. (1989): Sulfidation Equilibria as Guides to Gold Mineralization in Volcanogenic Massive Sulfides: Evidence from Sulfide Mineralogy and the Composition of Sphalerite; *Economic Geology*, Volume 84, pages 1978-1995.
- Juras, S.J. (1987): Geology of the Polymetallic Volcanogenic Buttle Lake Camp, with Emphasis on the Price Hillside, Central Vancouver Island, British Columbia, Canada; unpublished Ph.D. thesis, *The University of British Columbia*, 279 pages.
- MacLean, W.H. (1990): Mass Changes in Altered Rock Series; *Mineralium Deposita*, Volume 25, pages 44-49
- MacLean, W.H. and Barrett, T.J. (1993): Litho geochemical Techniques Using Immobile Elements; *Journal of Geochemical Exploration*, Volume 48, pages 109-133.
- MacLean, W.H. and Kranidiotis, P. (1987): Immobile Elements as Monitors of Mass Transfer in Hydrothermal Alteration: Phelps Dodge Massive Sulphide Deposit, Matagami, Quebec; *Economic Geology*, Volume 82, pages 951-962.
- Robinson, M., Godwin, C.I., Juras, S. and Allen, R.L. (1994): Major Lithologies of the Battle Zone, Buttle Lake Camp, Central Vancouver Island; in *Geological Fieldwork 1993*, Grant, B. and Newell, J.M., Editors, B.C. Ministry of Energy, Mines and Petroleum Resources, Paper 1994-1, this volume.
- Walker, R.R. (1985): Westmin Resources' Massive Sulphide Deposits, Vancouver Island; *Geological Society of America*, Cordilleran Section Meeting, May 1985, Vancouver, B.C., Field Trip Guidebook, pages 1-1 to 1-13.

# GEOLOGY OF THE SENECA PROPERTY SOUTHWESTERN BRITISH COLUMBIA (92H/5W)

By Sean McKinley, J.F.H. Thompson, T.J. Barrett, R.L. Sherlock,  
Mineral Deposit Research Unit, U.B.C.

R. Allen, Volcanic Resources

C. Burge, Metall Mining Corporation

(MDRU Contribution 043)

**KEYWORDS:** Economic geology, Harrison Lake Formation, Kuroko, synvolcanic, dacite, andesite, rhyolite, alteration.

## INTRODUCTION

The Seneca property in southwestern British Columbia is located approximately 120 kilometres east of Vancouver (Figure 1). The property is accessible from the Lougheed Highway at Harrison Mills by the Morris Valley Road and the Chehalis-Fleetwood logging road.

The property has been described as a zinc-copper-lead-barite volcanogenic massive sulphide environment similar in many aspects to the Kuroko-type deposits (Urabe *et al.*, 1983). Current geological reserves are estimated at 1.5 million tonnes grading 3.57% zinc, 0.60% copper and 0.14% lead. Mineralization occurs as replacement sulphides associated with volcanoclastic sediments and as stockwork-style stringer sulphides hosted in a sequence of felsic to intermediate volcanic rocks of the Harrison Lake Formation.

The objective of this study is to better constrain the spatial, temporal, and geochemical relationships of the various rock units and the accompanying alteration and mineralization. Fieldwork in the 1993 season involved logging of diamond-drill cores as well as some outcrop examination.

## EXPLORATION HISTORY

The Seneca Prospect, formerly known as the Lucky Jim property, was discovered in 1951 as an indirect result of logging operations and was optioned by Noranda Exploration Company at that time (Thompson, 1972). The sulphide mineralization was believed to be part of a steeply dipping vein or shear system. In 1961 stripping, trenching, and some underground work were carried out, but the results were not encouraging. The

property was held by Noland Mines, Ltd. from 1964 to 1965 and was bought by Zenith Mining Corporation, Ltd. in 1969. Cominco Ltd. optioned the property in 1971 and carried out further exploration based on the concept that the zone represented Kuroko-style conformable mineralization. The property was acquired by Chevron Standard Ltd. in 1977 and further diamond drilling was completed over the next ten years in joint ventures with International Curator Resources Ltd. and B.P. Canada Inc. Further logging in the area indirectly led to the discovery in 1986 of the Vent zone stockwork mineralization 1.75 kilometres to the west of the original discovery. In 1991 drilling by Minnova, Inc., 1 kilometre to the west of the Vent zone, led to the discovery of the Fleetwood zone. The property is currently held by International Curator Resources Ltd. and is under option to Metall Mining Corporation.

## REGIONAL GEOLOGY

The Harrison Terrane on the west side of Harrison Lake is a sequence of Triassic to Cretaceous volcanic and sedimentary rocks that are adjacent to Upper Jurassic quartz diorite batholiths that lie to the east of the property. The Harrison Formation is a Lower to Middle Jurassic succession that strikes north-northwest, with gentle to moderate easterly dips, and which may be up to 2500 metres thick. Although not fully constrained, the Seneca property is interpreted to lie within the Weaver Lake Member of the Harrison Lake Formation. Regionally, the Weaver Lake Member, which is dominated by intermediate to felsic volcanic rocks and related intrusions, is overlain by the Echo Island Member which comprises mostly volcanoclastic sediments (B. Mahoney; personal communication, 1993). Metamorphic grade is zeolite facies around the property. The regional geology is described in more detail by Monger (1970).



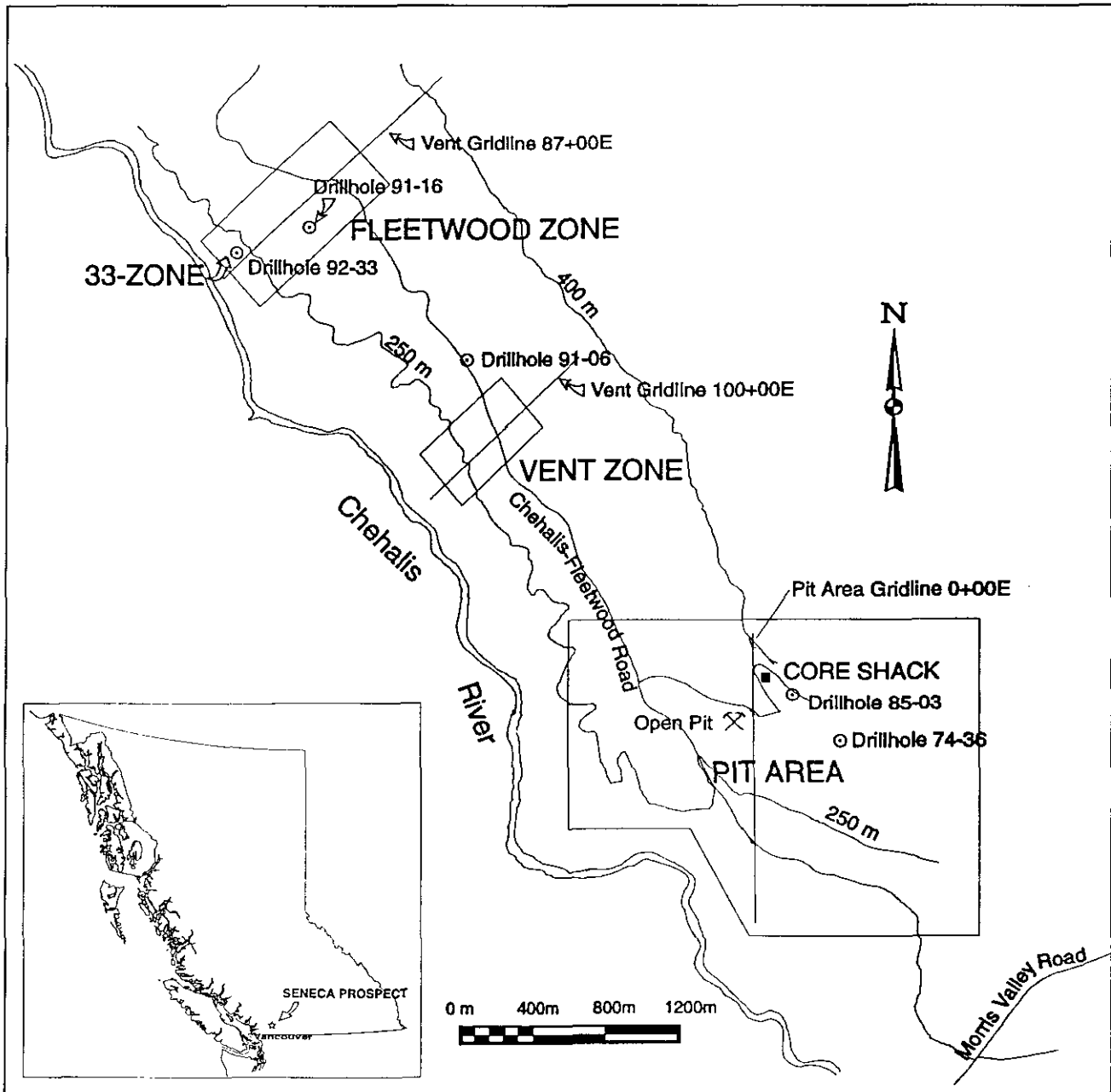


Figure 1. Location of the Seneca prospect showing location of zones of mineralization and selected drill holes.

## GEOLOGY OF THE SENECA PROPERTY

The geological setting of the Seneca property will be discussed using the volcanological models and terminology of Easton and Johns (1986) and McPhie and Allen (1992). The rock units at Seneca are subdivided into three principal volcanic facies as follows:

- dacite and andesite lavas and associated autoclastic breccias;
- juvenile to reworked volcanoclastic rocks;
- rhyolitic to andesitic synvolcanic intrusions.

A possible fourth facies consists of an argillite that

often contains flattened feldspar-phyric pumice clasts (fiamme). However, it is only observed in drillholes in the vicinity of the Pit Area and is usually a relatively thin layer. The three principal facies are generally observed in all drillholes, but their relative abundances vary greatly from hole to hole. The spatial and textural relationships of the facies in four representative drillholes are schematically depicted in Figure 2. Variations in the characteristics and abundances of each facies provide a means of interpreting the primary volcanic environment.

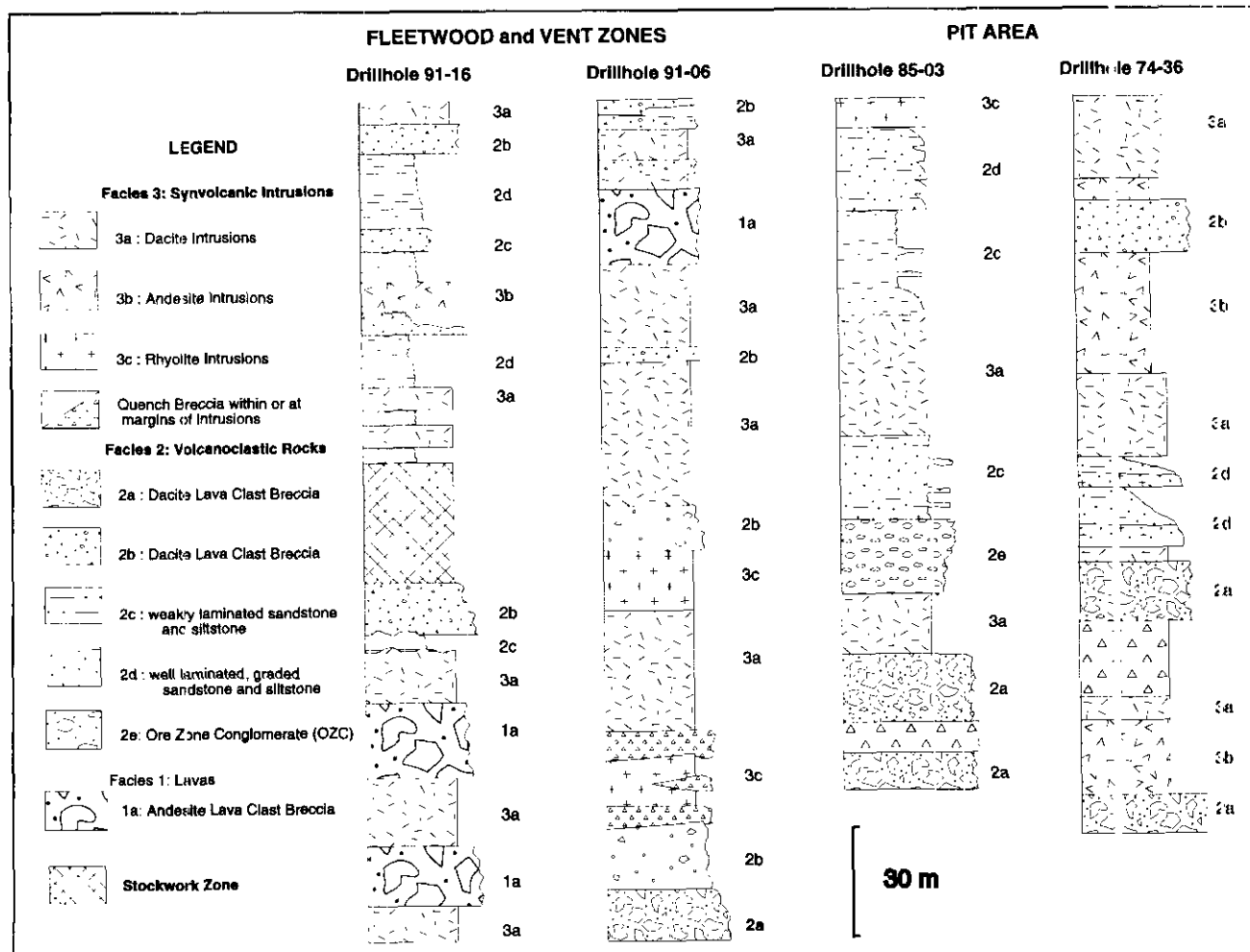


Figure 2. Stratigraphic logs for selected drill holes on the Seneca property.

### FACIES 1: LAVAS

Lava flows are defined by the presence of contact relationships, flow textures, and autobrecciation. The dacite lavas contain 5 to 15% subhedral to euhedral plagioclase phenocrysts that are typically 1 to 2 millimetres long. Quartz phenocrysts are much less common, but may comprise up to 5% of the rock. They are usually less than 5 millimetres in diameter and are subrounded. Chloritized hornblende laths are also usually present (up to 5%) and average 1 to 2 millimetres in size. Flow brecciation tends to be restricted to the upper part of flows whereas lower parts tend to be chilled and/or slightly brecciated. The upper brecciated zones range in thickness from 0.5 to 3 metres with subangular to angular lava clasts generally less than 10 centimetres across. The cores of the thicker flows are typically massive and greyish green in colour.

The occurrence of extrusive mafic flows at Seneca has not been confirmed as pillows were not observed and the unbrecciated andesites tend to be featureless.

However, a unit that consists of subrounded to amoeboid fragments of vesicular andesite surrounded by angular andesite clasts and hyaloclastite was logged in most holes in the vicinity of the Fleetwood and Vent zones (Unit 1a, Figure 2). These fragments are typically 1 to 10 centimetres in size, are light green or purplish grey in colour and consist of a core of massive andesite and chilled or cracked rims. The textures of the fragments, together with their elongate shape and tail-like ends, suggests that they were ejected as molten material either subaqueously or subaerially, but landed in water while still semi-molten. In either case, this unit must have formed close to a vent as the surrounding angular hyaloclastite does not appear to have been reworked. This facies is termed 'fire fountain debris' and is only seen in lower parts of the drillholes.

### FACIES 2: VOLCANICLASTIC SEDIMENTS

There are a variety of volcanically derived sediments and breccias on the Seneca property, which range from

mud size to block size (< 10 cm). These units probably represent the reworking of volcanic debris derived from lava flows and eruptions with the probable addition of fine sediments of a more distal origin.

One of the more economically important volcanoclastic units is seen in drillholes in the Pit Area and is referred to as the 'ore zone conglomerate' (OZC ; unit 2e). This unit, which varies from 1 to 15 metres in thickness, hosts some of the strongest mineralization on the property. It consists of moderately silicified, mostly subrounded dacite lava clasts ranging from sand size up to 3 centimetres in diameter in a sandy or silty matrix. The unit can be matrix or clast supported, and also contains clasts and matrix that have been replaced by sulphides.

A dacite lava clast breccia (units 2a and 2b) is present stratigraphically below the ore zone conglomerate in the Pit area and generally above the major andesitic units in the Fleetwood and Vent zones. Typically the unit is clast supported (up to 90% clasts up to 10 centimetres in diameter) and consists dominantly of subangular dense fragments of feldspar-phyric dacite lava, significant amounts of dark green vitric or pumiceous material, andesitic fragments and occasional silty rip-up clasts. The dacite clasts vary in colour from light grey to reddish tan, possibly representing subaerial deposition and later reworking. The unit is moderately to poorly sorted, suggesting deposition by debris flows. The drillholes in the Pit area usually terminate in this unit.

The Fleetwood and Vent zones show an increased abundance of reworked andesitic lava clast breccias consisting of centimetre-size, subangular, amygdaloidal andesite fragments and hyaloclastite, compared to the Pit area. It is not unusual to find up to 30% dacite lava clasts within this unit. The true thickness of the unit is difficult to determine due to synvolcanic intrusions, but individual intersections are in the order of 5 to 10 metres thick. Andesite lava clast breccias are less common at higher levels, and where they do occur, they have smaller clasts that are more rounded.

Fine-grained volcanoclastic sediments are common throughout the area, particularly in the upper part of the stratigraphy intersected by drilling (units 2c and 2d). The sediments form light to dark grey beds of mud to coarse sand-sized material. Individual beds range in thickness from a few centimetres to 5 metres, and vary from massive to well laminated and graded. The bases of normal graded beds are most often in sharp contact with the underlying beds, and are characterized by coarse sand to gravel-sized material, often with a component of dacite pumice fragments. These beds grade upward through massive or weakly laminated sands to well-laminated and occasionally cross bedded fine sand, silt and mud. These beds may represent individual turbidite layers. Graded beds become more common higher in the stratigraphy.

### ***FACIES 3: SYNVOLCANIC INTRUSIONS***

Synvolcanic intrusions were distinguished from flows by their contact relationships. Commonly, the contacts, where they are well preserved, are parallel to the local bedding. These units lack flow banding and autobreccia and are interpreted to be sills. Chilled margins and contacts at high angles to stratigraphy provide simple criteria for the recognition of dikes.

The most common intrusions are feldspar-phyric dacite porphyry sills (unit 3a). The sills range in thickness from 1 metre to more than 50 metres, and are columnar jointed in some outcrops. Mineralogically, and often texturally, these rocks are identical to the dacite flows described earlier and are only distinguishable by their contact relationships. Dacite sills commonly cut other intrusions with contacts that are chilled over widths of 10 centimetres to more than 1 metre, and are very slightly brecciated. Where sills intrude the volcanoclastic sediments and breccias, the contacts tend to be quenched and brecciated into angular to cusped hyaloclastic fragments less than 1 centimetre to 20 centimetres in size that are mixed with a matrix of the sediment. These zones of mixing, which reach thicknesses of several metres, are usually at the top of the sills. The textures suggest that the sills have intruded into wet, unconsolidated sediments as described by McPhie and Allen (1992).

Andesitic intrusions (unit 3b) are less common and are restricted to the lower part of the stratigraphy. Similar to the dacite porphyries, they have both crosscutting and bedding-parallel contacts with chilled margins. The andesites are generally massive and dark green with chlorite-filled amygdules 0.5 to 1 millimetre in diameter. Where they intrude sediments, they exhibit quenching, brecciation, and mixing similar to that described above, except that brecciated zones tend to be more extensive (in the range of several metres). In many of the drillholes in the Pit area, these andesitic sills are intimately associated with the ore zone conglomerate, intruding into it and into units immediately above and below it.

The third type of intrusions are quartz-feldspar-phyric rhyolite porphyry bodies (unit 3c). These are less common than the other two types (at least in the drill-cores studied) and their mode of emplacement is less clear. They occur at higher levels in the stratigraphy and their upper contacts are rarely seen. Their size and massive nature suggest they too may be synvolcanic sills, but they may also represent emergent domes. The rhyolite porphyries are easily distinguishable from the dacite porphyries by their greyish brown groundmass and by the presence of up to 10% subrounded quartz phenocrysts 2 to 5 millimetres in diameter. There are also 5 to 15% plagioclase phenocrysts 1 to 2 millimetres in size, as well as minor hornblende. The rhyolite

porphyry bodies range in thickness from a few metres to more than 30 metres. They have not been observed to exhibit the same intrusion-sediment relationships as the dacites and andesites.

## MINERALIZED ZONES

Three types of mineralized zones are present at Seneca:

- conformable massive sulphide lenses;
- semi massive and disseminated sulphides associated with volcanoclastics;
- stockwork and stringer mineralized zones.

Conformable, stratabound lenses of semi-massive sphalerite, pyrite, and chalcopyrite with lesser galena are exposed in the pit at the discovery site, and to a lesser degree in drillhole 92-33 which intersects the recently discovered "33-zone" in the Fleetwood area. The sulphides in both locations are hosted by fragmental rocks and occur as discontinuous pods. In the 33-zone, 2 metres of massive sulphides are underlain by a quartz-carbonate-chlorite zone and are sharply overlain by a cherty sulphide layer and a zone of strongly chloritized fragmental material. This zone is not correlatable to any other drillholes. Unlike the 33-zone, the massive sulphides in the pit are underlain by siliceous stringer mineralization. Blades of barite are seen together with the sulphides in both locations. In the 33-zone, the drillholes studied do not intersect mineralization of the type seen in the pit.

Semi massive to disseminated sulphides are associated with the volcanoclastic ore zone conglomerate. It should be noted that the term ore zone conglomerate refers to the entire unit which hosts this particular type of mineralization and that much of the unit does not contain sulphides. The sulphides, where present, tend to be restricted to upper parts of the conglomerate. The best such intersection is 0.5 metres of massive pyrite, sphalerite and barite with lesser chalcopyrite underlain by 3.5 metres of mostly semi massive pyrite in drillhole 85-03. More often the mineralization in the conglomerate consists of clasts and matrix that have been replaced by pyrite, and occasionally sphalerite. Some of the clasts are rimmed by a later pyrite.

Stockwork and stringer quartz-sulphide mineralization can be seen in outcrop and in drillcore from the Vent zone and in drillhole 91-16 from the Fleetwood zone (Figure 2). The Vent zone consists of veinlets up to 1 centimetre wide of sphalerite, pyrite, and quartz ( $\pm$  chalcopyrite) in altered dacite. The mineralization below the stockwork consists of occasional sphalerite-pyrite-chalcopyrite veinlets and disseminated sulphides in a moderately altered andesite lava clast breccia. Drillhole 91-16 in the Fleetwood zone intersects 1.1 metres of massive sphalerite, pyrite and chalcopyrite immediately above about 30 metres of

stockwork sphalerite-pyrite-chalcopyrite-a thyrhite-quartz veinlets in altered dacite similar to the Vent zone. Mineralization at Fleetwood ends fairly abruptly below the altered stockwork.

## ALTERATION

Typically most of the rocks at the Seneca property are unaltered with pristine volcanic textures preserved. Significant alteration is restricted to the Vent and Fleetwood zones where it is characterized by intense silicification and sericitization associated with a hydrothermally brecciated dacite porphyry (not necessarily the same porphyry in both areas). The brecciation is restricted to the dacites but alteration extends 10 to 20 metres into the surrounding fragmental rocks, obliterating the original textures. The dacites were identified on the basis of the relict feldspar "ghosts" left by the alteration. Petrography and lithogeochemistry will be used to confirm this and to further examine the alteration.

## DISCUSSION

The stratigraphy hosting the Seneca Prospect consists of massive to normal-graded dacitic and andesitic volcanoclastic sediments and lava flows that were intruded before consolidation by massive rhyolitic to andesitic synvolcanic sills and dikes. This succession comprises part of the Lower to Middle Jurassic Weaver Lake Member of the Harrison Lake Formation. The volcanoclastic rocks represent volcanically derived material that has been deposited by mass flows in the case of the coarser grained, poorly sorted units, and by turbidites in the case of the finer grained, graded units. These units become progressively finer grained and better graded upwards in the succession. Typically, andesitic units are restricted to the lower part of the examined stratigraphy. Rhyolite porphyry sills and dikes are generally restricted to the upper part of the stratigraphy. Dacite porphyries intrude at all levels of stratigraphy including the andesitic intrusives lower in the stratigraphy. Mineralization consists of conformable lenses of massive, semi massive and disseminated sulphides in the Pit area and the 33-zone, and stockwork-style sphalerite-pyrite-chalcopyrite-quartz veinlets and stringers in the Vent and Fleetwood zones. Major zones of silicification and sericitization are associated with the stockwork zones. Major and trace element lithogeochemical data and petrographic samples will be examined to determine the relationships between the intrusive units and the volcanoclastic rocks and lavas, and to determine the nature of alteration in the mineralized zones. Additional drill cores will be examined to better constrain the volcanic stratigraphy, lateral facies relationships, and paleotopography, and to

delineate potential horizons that would be favourable for the deposition of volcanogenic massive sulphide mineralization.

## ACKNOWLEDGMENTS

The authors wish to thank Metall Mining Corporation for its valuable cooperation and for providing access to maps, cross-sections and drill-core. We also thank Brian Mahoney (University of British Columbia) for his guidance in the field and helpful discussions of local stratigraphy. This M.Sc. study is part of the Mineral Deposit Research Unit project "Volcanogenic Massive Sulphide Deposits of the Cordillera" funded by the Natural Sciences and Engineering Research Council of Canada, the Science Council of British Columbia, and ten member companies involved in mining and mineral exploration.

## REFERENCES

- Easton, R.M. and Johns, G.W. (1986): *Volcanology and Mineral Exploration: The Application of Physical Volcanology and Facies Studies*; in *Volcanology and Mineral Deposits*, Wood, J. and Wallace, H., Editors, *Ontario Geological Survey*, Miscellaneous Paper 129, pages 2-40.
- McPhie, J. and Allen, R.L. (1992): *Facies Architecture of Mineralized Sequences: Cambrian Mount Read Volcanics, Western Tasmania*; *Economic Geology*, Volume 87, pages 587-596.
- Monger, J.W.H. (1970): Hope Map-area, West Half, British Columbia; *Geological Survey of Canada*, Paper 69-47.
- Thompson, R.I. (1972): *Report on Harrison, Lucky Jim Property*; in *Geology, Exploration and Mining in British Columbia 1972*, B.C. Ministry of Energy, Mines and Petroleum Resources, pages 102-114.
- Urabe, T., Scott, S.D. and Hattori, K (1983): *A Comparison of Footwall-rock Alteration and Geothermal Systems beneath some Japanese and Canadian Volcanogenic Massive Sulfide Deposits*; *Economic Geology*, Monograph 5, pages 345-364.



**GEOLOGICAL INVESTIGATIONS OF THE HIDDEN CREEK DEPOSIT,  
ANYOX, NORTHWESTERN BRITISH COLUMBIA  
(103/P5)**

By **R.W.J. Macdonald, T.J. Barrett, R.L. Sherlock, R.L. Chase, P. Lewis**  
**Mineral Deposit Research Unit, U.B.C.**  
and  
**D. J. Alldrick**  
**B.C. Geological Survey Branch,**

(MDRU Contribution 042)

**KEYWORDS:** Economic geology, Anyox, massive sulphide, pyrite, pyrrhotite, chalcopyrite, stratigraphy, metavolcanic, chert, turbiditic sediments

## INTRODUCTION

The Hidden Creek mine is an historic copper producer located within the Anyox pendant, a volcanic-sedimentary succession preserved as a roof pendant along the eastern margin of the Coast Plutonic Complex, approximately 160 kilometres north of Prince Rupert, British Columbia. (Figure 1)

This study is the first phase of a two-year program designed to examine the geological and geochemical relationships of sulphide mineralization in the Anyox pendant. This phase focuses on the volcanic-sedimentary contact at the Hidden Creek mine which is recognized as the main site of massive sulphide deposition in the Anyox camp. In this first year, the project utilized data and drill core from the exploration program completed by TVI Copper Inc. in the fall and winter of 1992-93. Sixteen holes totalling 3202 metres were logged and sampled for litho-geochemistry, fluid inclusion studies and petrographic analysis. Detailed mapping and sampling on a 1:2400-scale were carried out in the immediate area of the Hidden Creek mine with particular emphasis on the footwall metavolcanic sequence and the immediately overlying chemical and clastic sediments.

## REGIONAL GEOLOGY

The most recent regional geological mapping in the Anyox pendant was done by Sharp (1980), Grove (1986) and Alldrick (1986). These authors defined a simplified stratigraphy consisting of a basal mafic volcanic unit of primarily tholeiitic, andesitic to basaltic flows and subordinate volcanoclastic layers, and an overlying sequence of siltstone, greywacke and sandstone with minor calcareous and conglomeratic beds. A chert unit crops out discontinuously along the volcanic-sedimentary

contact. Most recently the geochemistry of volcanic rocks in the pendant has been described by Smith (1993).

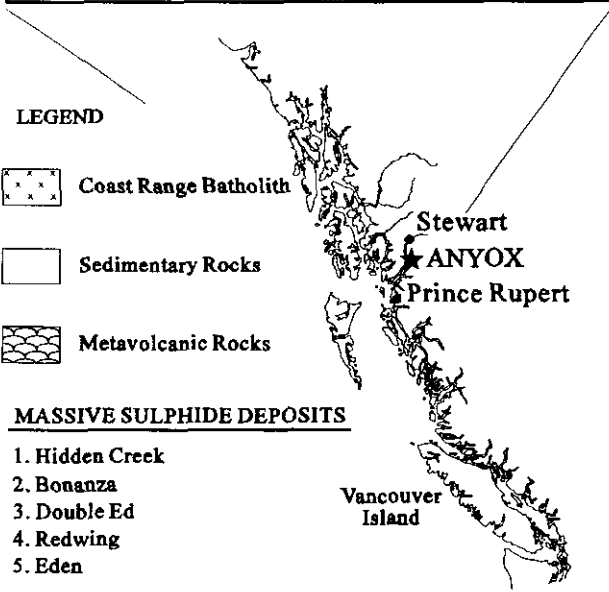
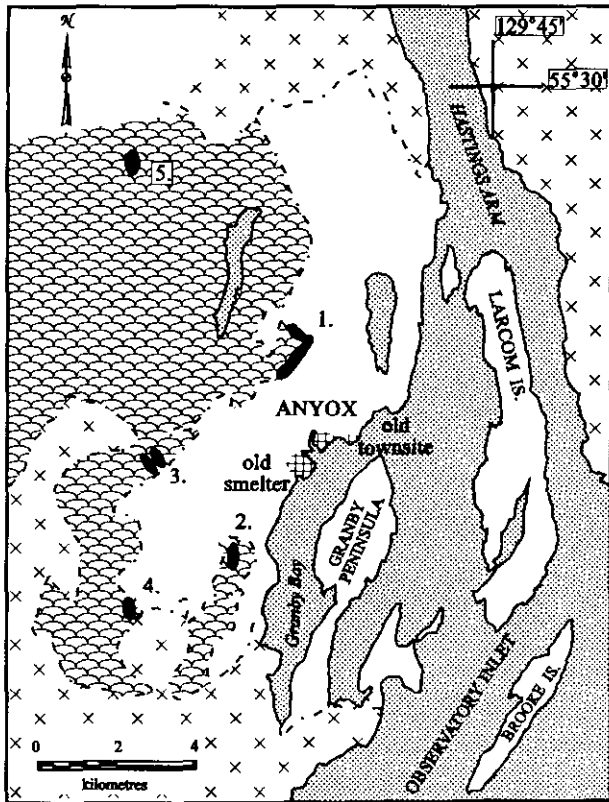
The structure of the pendant is dominated by large, north-trending, east-verging asymmetric or overturned folds. Superimposed on these are east-trending minor crossfolds that are most clearly recognized along the volcanic sedimentary contact. The area has been cut by several generations of faults. Fox (1989) identified a major décollement zone and tear fault in the Hidden Creek area, and related these to an early fold-thrust deformational event that generated the early north-trending folds. The entire succession is cut by late, mainly northerly trending extensional faults, one of which offsets the No. 2 and No. 3 ore zones at the mine.

Five major copper-rich massive sulphide deposits are recognized in rocks either along or adjacent to the metavolcanic-sedimentary contact (Figure 1).

## EXPLORATION AND MINING HISTORY

The Hidden Creek deposit was discovered in 1901 and was operated between 1914 and 1935 by Granby Consolidated Mining and Smelting Company. During this period, 21 681 800 tonnes of ore grading 1.5 % copper, 9.25 grams per tonne silver and 0.17 gram per tonne gold was mined from the Hidden Creek deposit and an additional 647 904 tonnes averaging 1.51 % copper from the Bonanza deposit. The mine was closed on August 1, 1935 and purchased by The Consolidated Mining and Smelting Company of Canada, Limited, now Cominco Ltd. on October 25, 1935 (Davis *et al.*, 1992).

From 1936 to 1989 a number of exploration programs were carried out by Cominco and various joint venture partners. Most of this work was completed on the Hidden Creek, Double Ed and Eden properties. During the course of these programs, 96 holes were drilled for an approximate total of 17 000 metres (Fox, 1989). Detailed geological studies and drilling from 1950-54 resulted in the discovery of the Double Ed and Eder deposits. The



**LEGEND**

-  Coast Range Batholith
-  Sedimentary Rocks
-  Metavolcanic Rocks

**MASSIVE SULPHIDE DEPOSITS**

1. Hidden Creek
2. Bonanza
3. Double Ed
4. Redwing
5. Eden

Figure 1. Location and general geology of the east Anyox pendant (after Alldrick, 1986).

work delineated a drill-indicated resource of 1 224 700 tonnes and a drill-inferred resource of 748 427 tonnes grading 1.3 % copper and 0.6 % zinc at Double Ed and a drill-indicated resource of 158 757 tonnes of 1.3 % copper and 1.9 % zinc at Eden (summarized in Davis *et al.*, 1992).

In a 1982 joint venture with Mitsui, 16 drill holes

were completed in the Hidden Creek area. Several new mineralized zones were identified under the No. 1 orebody although values were erratic or low grade. One intersection, obtained from a hole north of the old mine workings and within the sedimentary sequence, graded 2.5 % copper, 0.5% zinc, 100.4 grams per tonne silver and 1.8 grams per tonne gold over 6.1 metres.

From 1987 to 1988 a total of 13 drill holes were completed by Cominco Ltd. and Prospector Airlines Ltd. in the Hidden Creek, Bonanza Creek and Redlight areas, however, no significant mineralization was found. In 1990 Moss Management Ltd. and Boston Financial Corporation acquired the property and retained Glanville Management Ltd. to update the economic assessment of the property. This study indicated a geological reserve of 10.8 to 13.6 million tonnes grading 0.7 % to 0.75 % copper.

In the fall and winter of 1992-93, TVI Copper undertook a comprehensive exploration program that included geological mapping, prospecting, geochemical and geophysical surveys, and 4256 metres of diamond drilling in the Hidden Creek area and on other nearby copper occurrences. The program included eleven definition holes designed to confirm reserves and ten exploratory holes to test a number of targets (Davis *et al.*, 1993).

**GEOLOGY OF THE HIDDEN CREEK AREA**

The stratigraphy at the mine site consists of a basal metavolcanic unit overlain by a turbiditic sedimentary sequence with an intervening chert horizon of variable thickness. In most drill holes, intersections display consistent stratigraphic relationships across the contact and suggest that the original ocean-floor stratigraphy is, for the most part, preserved in this area (Figure 2)

**METAVOLCANIC ROCKS**

Massive to pillowed flows, fragmental metavolcanic and bedded volcanoclastic rocks form the footwall to the Hidden Creek sulphide lenses. These rocks are fine grained to porphyritic and have been metamorphosed to a lower greenschist assemblage of chlorite, actinolite, biotite, sericite, clinozoisite and zoisite. A biotite-chlorite assemblage forms a distinct subunit in the upper sections of the volcanic pile and may reflect hydrothermal alteration.

Pillows range from 10 centimetres to 1 metre in longest dimension and typically have length to width ratios of 2:1. Pillow rims are 1 to 2 centimetres thick, aphanitic and darker than the pillow cores. The interpillow fill consists of aphanitic to fine-grained, black to dark green to reddish coloured rock of predominately chlorite and biotite. Locally the pillow rims and interpillow fill are silicified and sulphide bearing in mineralized zones.

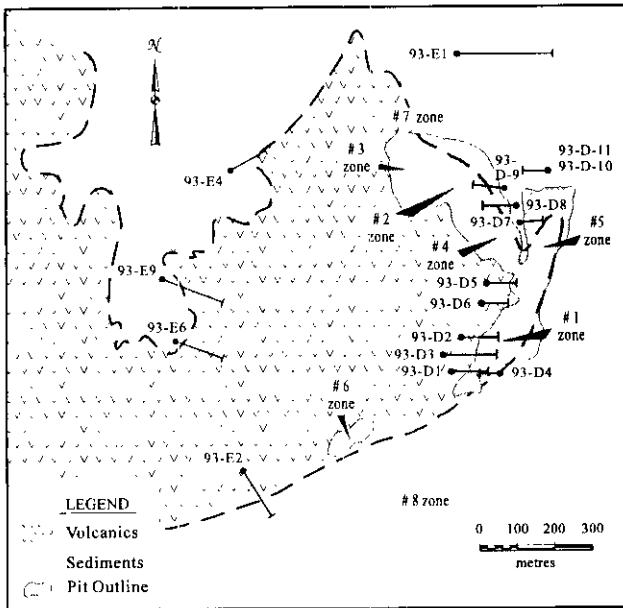


Figure 2. Generalized geology of the Hidden Creek mine area showing the distribution of the ore zones and the location of the drill holes logged during the first phase of this project. The number 7 and 8 zones are small subsurface deposits indicated by drilling (after Davis, 1993).

Fragmental rocks, described by Sharp (1980) as pyroclastic tuff horizons, crop out in several areas throughout the map area and are commonly recognized in drill core. The rocks consist of subangular to tear-shaped, actinolite-rich volcanic clasts, 5 to 30 centimetres long, separated by an anastomosing network of 0.2 to 1-centimetre, aphanitic quartz veins and fine-grained, granular to foliated volcanic rock. Individual clasts appear flattened and vein networks have consistent trends over tens of metres, imparting a banded appearance to these outcrops. The origin of these rocks is still in question as they have a similar appearance, on a small scale, to the silicified pillowed sequences that locally appear to grade into the fragmental rocks across zones of more intense deformation.

Bedded volcaniclastic horizons are readily recognized in drill core but are difficult to distinguish in outcrop. Beds are several centimetres thick, light olive-green in colour, and show normal grading. The distribution of these horizons is not well established within the volcanic stratigraphy, however, they appear most commonly near the top of the volcanic pile.

## CHERT

A thin to thickly bedded, foliated, saccharoidal chert unit is found along the volcanic-sedimentary contact at Hidden Creek mine. It varies in thickness from less than a metre to a maximum of about 70 metres (Sharp, 1980). The maximum thickness is in the vicinity of the No. 1

and No.5 orebodies where the chert contains interlayered massive sulphides and volcaniclastic rocks. The chert varies in colour from bone-white to grey, reddish or pale green as a result of impurities. Individual beds vary from less than a centimetre to several centimetres in thickness and are separated by sericitic laminae. At its base the chert is interbedded with a silicified chlorite-biotite-sericitic schist and at its top with silicified siltstone or argillite; transitions between these lithologies are gradational over distances of several metres.

To date no microfossils have been identified within the chert unit. Its variable thickness and close association with exhalative metal sulphides and chemically precipitated carbonate in the mineralized zones suggest that the chert is of exhalative origin.

## CLASTIC SEDIMENTARY ROCKS

The sedimentary rocks in the Hidden Creek area comprise laminated to interbedded siltstone, argillite and fine sandstone. Individual beds range from less than a centimetre to tens of centimetres thick, with sharp boundaries and thinly laminated tops and only rarely display good grading. Flame and load structures mark the boundaries of beds. Crosslamination is preserved in finer layers as thin wisps. Small, discontinuous limestone layers, less than a metre thick, occur near the base of the sequence immediately overlying the contact and decrease in frequency up-section.

The sedimentary rocks are variably metamorphosed and deformed, most strongly near the contact with the metavolcanic rocks. Metamorphism has formed phyllosilicates such as biotite, sericite and chlorite, and produced planar and crenulated fabrics through most of the unit. Medium to coarse-grained porphyroblasts of cordierite (Fox, 1989) are developed in pelitic rocks along the contact in the vicinity of the ore zones, and may be related to sub-seafloor hydrothermal alteration.

## STRUCTURE

The orebodies sit within the hinge zone and the overturned limb of the Hidden Creek anticline, a northerly trending, easterly verging structure that formed as part of a fold and thrust system that Fox (1989) correlates with the earliest deformation event in the area (Figure 3). Movement along a tear fault, immediately to the south of the deposit, is thought to be responsible for rotating the southern part of the contact to a northeast-southwest orientation, resulting in the arcuate distribution of the orebodies (Fox, 1989; Figure 2).

Deformation is reflected in the rocks as open to tight folding in the sedimentary sequence, as planar flattening fabrics in the alteration assemblages, and as shear fabrics in the metavolcanic rocks. Folds on the scale of metres to tens of metres occur throughout the sedimentary sequence. These are particularly noticeable along the walls of all the open pits and obviously affect the distribution of

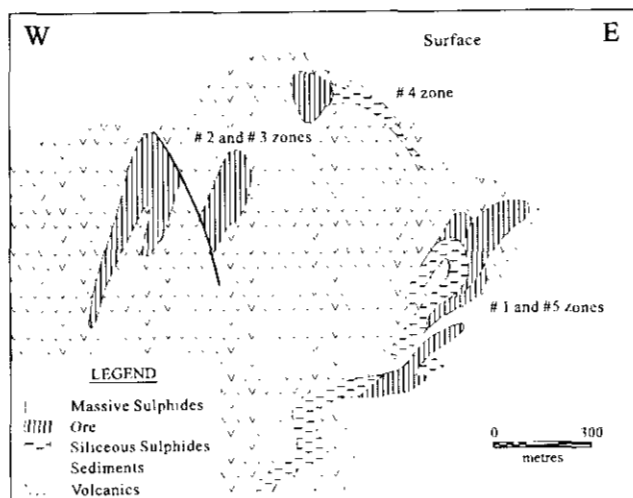


Figure 3. Schematic cross-section, from west to east, through the Hidden Creek mine (after Grove, 1986). Positions of the ore zones are approximate and are inferred from the literature.

mineralization within the larger scale anticline. The development of strong planar and crenulated fabrics adjacent to the volcanic-sedimentary contact suggests that this was a zone of high strain; however, movement along this zone has not been established.

## MINERALIZATION

The Hidden Creek orebodies constitute the largest accumulation of known sulphide mineralization in the Anyox district. Eight mineral deposits are known in the Hidden Creek area. Of these, seven contributed to mine production (Table 1; after Davis *et al.*, 1992).

The Nos. 1, 4, 5 and 6 orebodies are located at the contact between footwall metavolcanic rocks and hanging-wall sedimentary rocks and are intimately associated with cherty chemical sediments. The No. 2 and 3 orebodies are west of the contact within the footwall metavolcanic rocks. The Nos. 7 and 8 orebodies occur stratigraphically above the contact in hangingwall turbiditic sedimentary rocks (Sharp 1980; Figure 2). Average production figures for the mine give recovered grades of 1.6% copper, 0.17 gram per tonne gold and 9.25 grams per tonne silver. However, significant portions of the No. 1 and 5 orebodies graded in excess of 3% copper with higher than average gold and silver values. The best copper mineralization was always concentrated in fold closures and the best precious metal grades associated with massive sulphide bodies in proximity to sediments (Rhodes and Jackisch, 1988).

The orebodies are tabular to sheet like (Grove, 1986) and consist mainly of pyrite, pyrrhotite and chalcocopyrite, with minor sphalerite, galena and magnetite. The gangue minerals are principally quartz, calcite, chlorite and sericite. There is a strong association between

chalcocopyrite and pyrrhotite in the massive sulphide lenses and in vein networks in mineralized sections. Mineral zoning in the massive sulphide lenses is observed in drill hole D-9 and along the southern wall of the No. 6 zone pit. In these sections of chemical sediments and sulphides, pyrite dominates the stratigraphically lower horizons, occurring as alternating semimassive to massive bands in a matrix of silica and carbonate. In stratigraphically higher parts of these sections, pyrrhotite-chalcocopyrite forms more discrete and massive layers in a carbonate-dominated matrix. Transitions between the two types of sulphide ore are characterized by large euhedral pyrite crystals within a finer grained pyrrhotite-chalcocopyrite matrix.

TABLE 1  
TONNAGE AND GRADE OF HIDDEN CREEK  
PRODUCTION

Orebody	Tonnes Shipped	% Copper
1	8 879 803	1.55
2	6 279 157	1.48
3	2 896 192	1.14
4	420 600	1.12
5	2 651 610	2.27
6	485 738	2.19
8	9 022	0.69
slide	59 678	1.13
TOTAL	21,681,800	1.57

Quartz-pyrite-pyrrhotite-chalcocopyrite veins occurring stratigraphically below the sulphide lenses within the chert and the metavolcanic rocks probably represent footwall stockwork mineralization. These veins range from less than 0.2 to several centimetres wide. Associated gangue minerals include quartz, chlorite and biotite.

Fine to medium-grained disseminations of pyrite, pyrrhotite and chalcocopyrite occur throughout the basal units of the clastic sedimentary sequence in siliceous bedding-parallel layers and coarse sandstone layers. These sulphides form in both discrete spaced layers, typically less than 2 centimetres thick, and in more diffuse layers that coalesce into thick semimassive bands.

## STRATIGRAPHIC SECTIONS

Two of the sixteen holes logged during this phase of the study are illustrated in Figures 4 and 5. These holes demonstrate some of the stratigraphic relationships observed in the drill core.

Diamond-drill hole 93 D-1 (Figure 4) was collared in the footwall to the south of the No. 1 deposit at an azimuth of 090° and inclination of -60°. The hole was drilled up the stratigraphy, extending 146.3 metres to the hangingwall sedimentary rocks. The hole progresses from an interlayered chert and biotite-sericite schist, to a

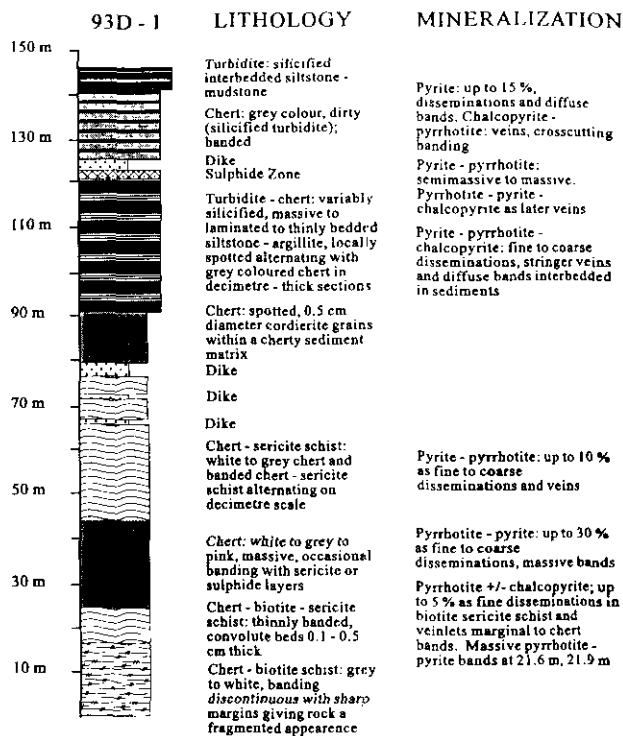


Figure 4. Summary log of diamond-drill hole 93D - 1. The scale on the left represents depth of the drill hole. The thickness of units has not been corrected for drilling angle

massive white to grey chert, to an alternating chert and banded chert-sericite schist, and ends in an interbedded chert and silicified siltstone-mudstone turbidite. Pyrite, pyrrhotite and chalcopyrite occur as fine disseminations, as semimassive to massive bands several centimetres thick, and as anastomosing vein networks throughout the section.

Diamond-drill hole 93 D-9 (Figure 5) was collared in the hangingwall in the north end of the mine, at an azimuth of 270° and inclination of - 60°. The hole was drilled down the stratigraphy, extending 136.6 metres to the footwall metavolcanic rocks. The hole passes stratigraphically upward from a stockwork zone in chlorite, biotite and talc-altered metavolcanic rocks through an intensely biotite-altered zone, and into a 40-metre semimassive to massive sulphide section of primarily pyrite with lesser pyrrhotite and chalcopyrite. The hole ends in laminated siltstone to mudstone turbidite. Pyrrhotite, pyrite and chalcopyrite occur as stockwork veins in the footwall basalts and in banded semimassive to massive layers in a carbonate and silica-rich matrix.

## PRELIMINARY CONCLUSIONS

Mineralization occurs at or near the top of a thick,

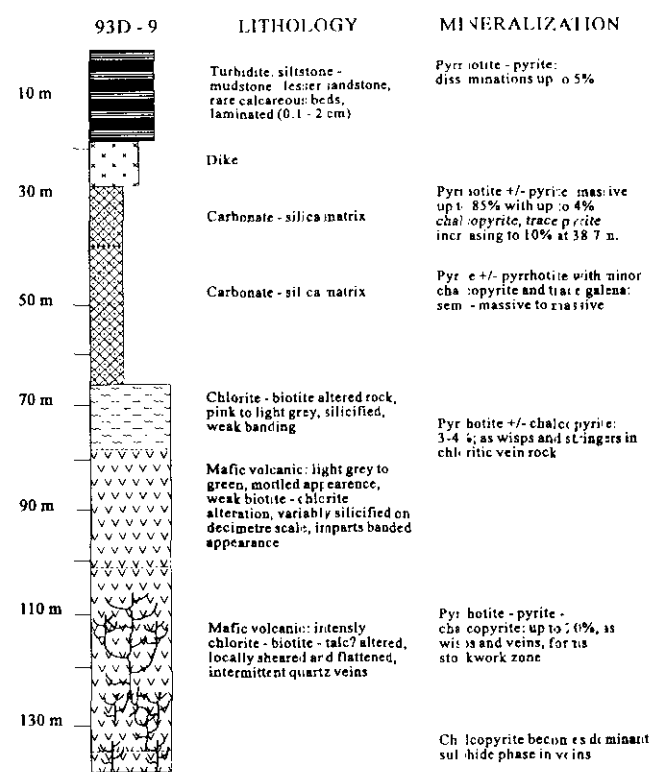


Figure 5. Summary log of diamond-drill hole 93D - 9. The scale on the left represents depth of the drill hole. The thickness of units has not been corrected for drilling angle

mafic volcanic pile which forms the base of the stratigraphic succession in the Anyox area. Although deformation has affected the area the original stratigraphy is still intact in many areas. The ore zones are tabular bodies and are closely associated with a thick chert horizon, and to a lesser extent, with silicified clastic sedimentary rocks at the base of the overlying turbiditic-mudstone sedimentary sequence. Some of the metal-rich chert intervals may represent lateral equivalents of the massive orebodies. These features suggest that the sulphide lenses were formed after volcanism, at the same time as the chert, and for the most part prior to the deposition of the turbiditic sediments.

## FUTURE WORK

Future research at the Hidden Creek mine will concentrate on characterizing volcanic and sedimentary stratigraphy, mineralization, intensity and characteristics of the hydrothermal alteration, and geometry of the hydrothermal system. This will utilize whole-rock geochemistry and petrography of various lithologic units and their altered equivalents, trace element and stable isotopic studies of the chert horizon and ores, and fluid inclusion studies of the ores and footwall stringer mineralization.

## ACKNOWLEDGMENTS

The authors would like to thank Dr. Cliff James and TVI Copper Inc. for granting permission to work on the Anyox property and for providing background geological material for the study. Justin Vandenbrink provided cheerful and capable field assistance throughout the summer. A special thanks is extended to Teddy and Jesse Watson, Lance and Rob for their hospitality, sound advice and spirited discussion throughout the summer.

This research forms part of the Mineral Deposit Research Unit's project on Volcanogenic Massive Sulphide Deposits of the Cordillera, supported by the Natural Sciences and Engineering Research Council of Canada, the Science Council of British Columbia and ten mining and exploration member companies.

## REFERENCES

- Alldrick, D.J. (1986): Stratigraphy and Structure of the Anyox Area (103P/5); in Geological Fieldwork 1985, B.C. Ministry of Energy, Mines and Petroleum Resources, Paper 1986-1, pages 211 - 216.
- Davis, J.W., Aussant, C.H. and Chisholm, R.E. (1992): Geological, Geochemical and Geophysical Report on the Anyox Property, Skeena Mining Division; *TVI Copper Inc.*, private company report.
- Davis, J.W., Aussant, C.H. and Chisholm, R.E. (1993): Diamond Drilling, Geochemical and Geophysical Report on the Anyox Property, Skeena Mining Division; *TVI Copper Inc.*, private company report.
- Fox, J.S. (1989): Structural Analysis of the Hidden Creek Area, Anyox Property, Observatory Inlet Region, B.C.; *Cominco Ltd./Prospector Airways Co. Ltd.*, private company report.
- Grove, E.W. (1986): Geology and Mineral Deposits of the Unuk River - Salmon River - Anyox Area; B.C. Ministry of Energy, Mines and Petroleum Resources, Bulletin 63
- Rhodes, D. and Jackisch I. (1988): 1987 Annual Project Report, Geology, Diamond Drilling, Anyox Property; *Cominco Ltd.*, private company report.
- Smith A.D., (1993): Geochemistry and Tectonic Setting of Volcanics from the Anyox Mining Camp, British Columbia; *Canadian Journal of Earth Sciences*, Volume. 30, pages 48-59.
- Sharp, R.J. (1980): The Geology, Geochemistry and Sulphur Isotopes of the Anyox Massive Sulphide Deposits; unpublished M. Sc. thesis, *University of Alberta*, 211 pages.

## GEOLOGICAL INVESTIGATIONS OF THE 21B DEPOSIT, ESKAY CREEK, NORTHWESTERN BRITISH COLUMBIA (104B/9W)

By R.L. Sherlock, T.J. Barrett, T. Roth, F. Childe, J.F.H. Thompson  
Mineral Deposit Research Unit, U.B.C.

D. Kuran, H. Marsden  
Homestake Canada Inc.

R. Allen  
Volcanic Resources

(MDRU Contribution 044)

**KEYWORDS:** economic geology, Eskay Creek, 21 zone, gold, silver, massive sulphides, Hazelton Group

### INTRODUCTION

The Eskay Creek property (56° 38'N, 130° 27'W) is located in the Iskut River area, about 80 kilometres north of Stewart, British Columbia. It is underlain by Triassic Stuhini Group and Jurassic Hazelton Group sediments and volcanic rocks described by Alldrick *et al.* (1989), Britton (1991), Lewis (1992); and Lewis *et al.* (1992). The mineral deposits of the 21 zone are hosted by a sequence of mainly bimodal volcanic rocks of Lower to Middle Jurassic Hazelton Group. The 21A and 21B zones occur within fine-grained sedimentary rocks that are underlain by rhyolite and intermediate volcanic rocks, and overlain by basalts. Studies by company geologists (Blackwell, 1990; Rye, 1992; Edmunds and Kuran 1992) have outlined the main stratigraphic, lithogeochemical and alteration characteristics at Eskay Creek, and documented the nature of the mineral deposits. Regional geological relations on the property have been described by Bartsch (1992a, 1992b, 1993a, 1993b); Roth (1992) and Roth and Godwin (1992).

The 21A and 21B zones are distinguished by their mineralogy and geochemical characteristics. For a more detailed account of the 21A deposit the reader is referred to Roth and Godwin (1992) and Roth (1992). Field work in 1993 by the Mineral Deposit Research Unit involved relogging and sampling of selected drill-holes through various styles of mineralization in the 21B zone. This report concentrates on the stratigraphy, sedimentology and mineralization of the 21B orebody. The currently defined mineable reserves in the 21B zone are 1.08 million tonnes grading 65.5 grams per tonne gold, 2930 grams per tonne silver, 5.6 % zinc, and 0.77 % copper (Homestake Canada Inc. Feasibility Report August, 1993).

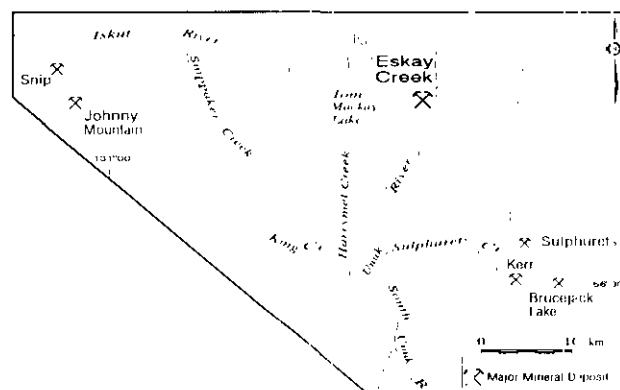


Figure 1. Location map of the Eskay Creek deposit, Iskut River Area

### MINE SEQUENCE STRATIGRAPHY

#### FOOTWALL VOLCANIC UNIT

The footwall volcanic unit has in the past been referred to as the footwall dacite unit. It overlies marine sediments and volcanoclastic rocks, of Hettangian through late Pliensbachian age, of the lower Hazelton Group, and underlies the footwall rhyolite.

The unit comprises aphanitic flows, sills and primary to reworked volcanoclastic material. Geochemically it is quite variable, ranging from dacite to basalt (Rye, 1992). The unit is generally altered to a characteristic pink-beige colour and is cut locally by a series of quartz-pyrite ± sphalerite-galena-chalcopyrite veinlets with grey, sericitic envelopes. A distinctive marker horizon is the dacite datum which commonly contains quartz-filled or locally chlorite-filled amygdules. The footwall volcanic unit is regionally in excess of 100 metres thickness (Britton *et al.*, 1950).

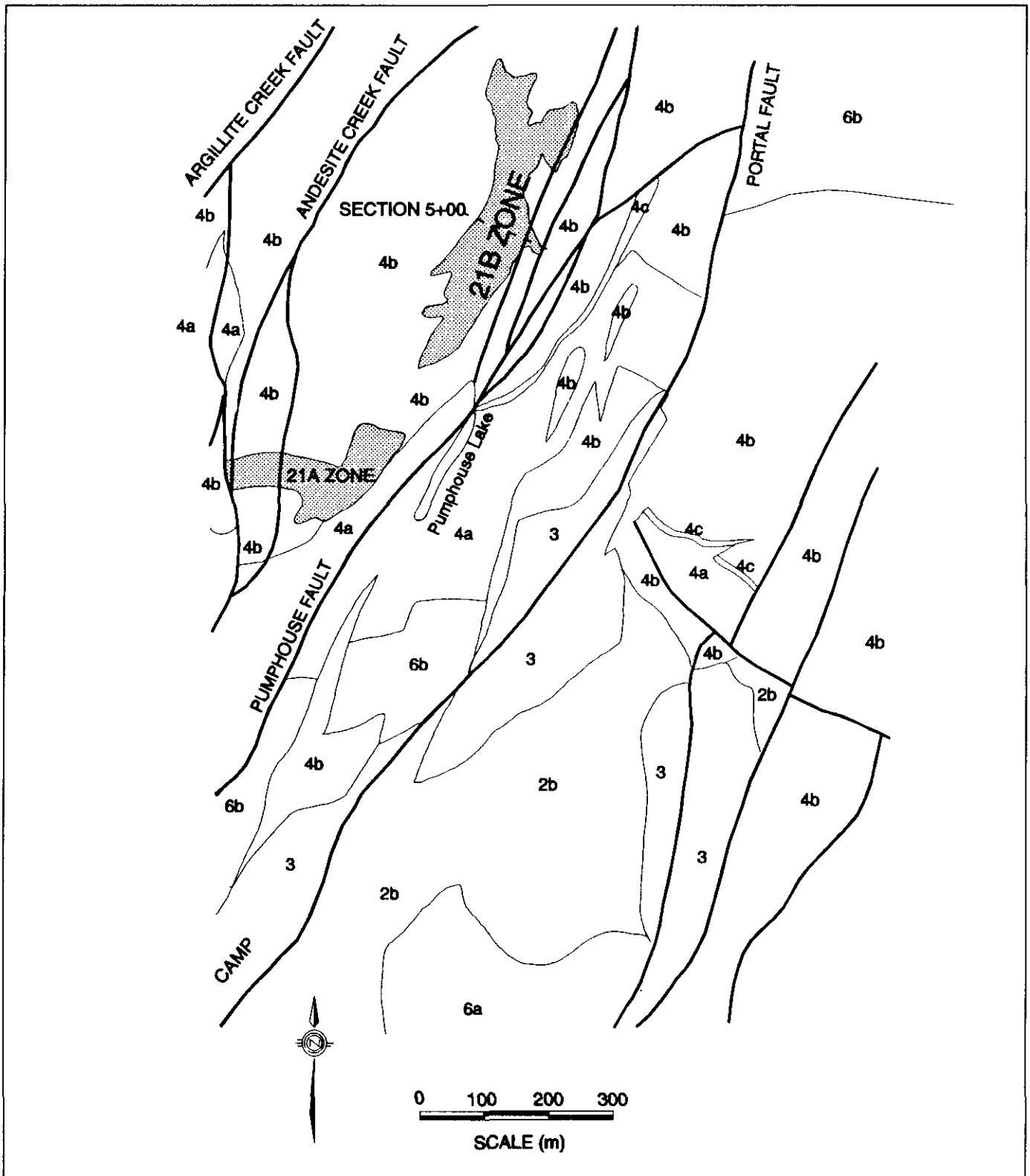


Figure 2. Geology of the Eskay Creek property. 2b, intermediate, coarse epiclastics with minor mudstone, limestone and andesite-derived conglomerates; 3, heterolithic felsic volcanic fragmentals, air fall welded tuffs, vesicular dacite fragmentals, and massive to perlitic dacite (lower volcanic unit); 4a, massive to flow-banded and autobrecciated rhyolite, with tuffs and fragmental units (footwall rhyolite); 4b, pillow basalts, hyaloclastites, debris flows, flow breccias, autobreccia with intercalated sediments, and unaltered mafic dikes (hangingwall basalt); 4c, argillite (contact zone argillite); 6a, monzodiorite; 6b, feldsparphyric siliceous, pyritic dikes/sills (felsite). Geology based on company reports.

The footwall volcanic unit is commonly separated from the overlying footwall rhyolite by a narrow (less than 1 to 3 metres thick) black mudstone horizon, which may contain low-grade gold, silver and base metal mineralization.

### **FOOTWALL RHYOLITE**

Rhyolite forms the immediate footwall to the 21B stratiform deposit and is the host to stringer-style discordant mineralization. This unit consists of massive to flow-banded rhyolite, flow and hydrothermal breccias, and pyroclastic deposits. Hyaloclastite and perlitic textures occur locally. Primary textures are commonly obscured by pervasive alteration. Within the mineralized zones, this unit is altered to an assemblage of quartz, potassium-feldspar, chlorite and sericite. The upper contact of the rhyolite with the argillite is commonly marked by a black-matrix breccia, consisting of matrix-supported white rhyolite fragments in a siliceous black matrix (Rye, 1992; Bartsch, 1993b; Roth, 1992). The footwall rhyolite ranges from 30 to 110 metres thick (Britton *et al.*, 1990).

### **CONTACT ARGILLITE (TRANSITION ZONE)**

The contact argillite occurs between the rhyolite and the overlying basalt, and is the host to the stratiform sulphide-sulphosalt mineralization of the 21B zone. The unit consists of a laterally extensive, well-laminated, carbonaceous mudstone that is variably calcareous and siliceous. Radiolaria, dinoflagellates, rare belemnites and corals have been identified within it, indicating deposition in a marine environment (Roth, 1992; Nadaraju, 1993). Prehnite porphyroblasts are locally abundant in the argillite; these have been referred to as crystallites in exploration drill logs.

The basal member of the contact argillite is termed the transition zone, which comprises fine sericitic flakes in mudstone. The flakes tend to decrease in abundance away from the rhyolite. The sericite material are similar in appearance to some of the underlying altered rhyolite and were probably derived from this unit. The contact argillite ranges from less than 1 metre to more than 60 metres in thickness (Rye, 1992; Britton *et al.*, 1990).

### **HANGINGWALL BASALT**

The hangingwall basalt occurs as both extrusive and intrusive phases, and ranges from aphanitic to medium grained with local feldspar phenocrysts. In places, basaltic sills and dikes are intrusive into the contact argillite. Elsewhere, well-preserved pillows and pillow breccias overlie the argillite. Chlorite and quartz-filled amygdules are common and tend to be concentrated at the upper contacts of flows (Rye, 1992). Thin argillite intervals are interbedded within

the basalt. The unit exceeds 150 metres in thickness (Britton *et al.*, 1990).

### **INTRUSIVE ROCKS**

Several intrusions are exposed on the property including monzodiorite (Eskay porphyry,  $185 \pm 5$  Ma, Macdonald *et al.*, 1992), mafic intrusives (Salmon River equivalents) and the "felsite". The felsite is chemically equivalent to the Eskay rhyolite and is strongly altered to an assemblage of silica, pyrite and minor sericite forming the gossanous bluffs prominent at the Eskay camp. The felsites crosscut stratigraphy and reach their highest stratigraphic level directly below the 21 zone deposits (Edmunds and Kuran, 1992; Bartsch, 1993b).

### **STRUCTURE**

The stratigraphy at Eskay Creek is folded about a gently plunging upright fold trending at  $035^\circ$ , called the Eskay anticline. The 21A and B deposits occur on the gently west-dipping, northeast-striking western limb of this fold. Faults striking north-northeast, notably the Andesite Creek, Pumphouse, Portal and East Break faults, crosscut and offset the stratigraphy (Edmunds and Kuran, 1992).

### **ALTERATION**

Footwall alteration is dominated by pervasive silicification of the rhyolite. In the immediate footwall to the 21 zone, the alteration is marked by the development of a chlorite-sericite ( $\pm$  potassium-feldspar) assemblage that increases in intensity towards the rhyolite-argillite contact. The metasomatic effects are depletion of sodium, and enrichment of potassium, magnesium and commonly silica.

### **MINERALIZATION**

Two main styles of mineralization are recognized in the 21B zone, stratiform and discordant. The relationship between the various styles of mineralization is poorly understood and is presently under investigation.

**Stratiform mineralization in the 21B zone** is dominated by detrital sulphide-sulphosalt beds. The stratiform segment of the zone is about 900 metres long, 60 to 200 metres wide and locally in excess of 40 metres thickness (Britton *et al.*, 1990). Individual clastic ore beds range from less than 1 centimetre to 50 centimetres in thickness and are composed dominantly of coarse-grained clasts of zoned sphalerite, with finer grained tetrahedrite, boulangerite, bournonite and minor galena and pyrite; also present are sericitized to chloritized rhyolite fragments. Gold and silver occur as electrum and in sulphosalts. In some holes, the stratigraphically lower clastic ore beds are rich in sulphide-sulphosalt cobbles and pebbles, and pass upwards into argillite containing

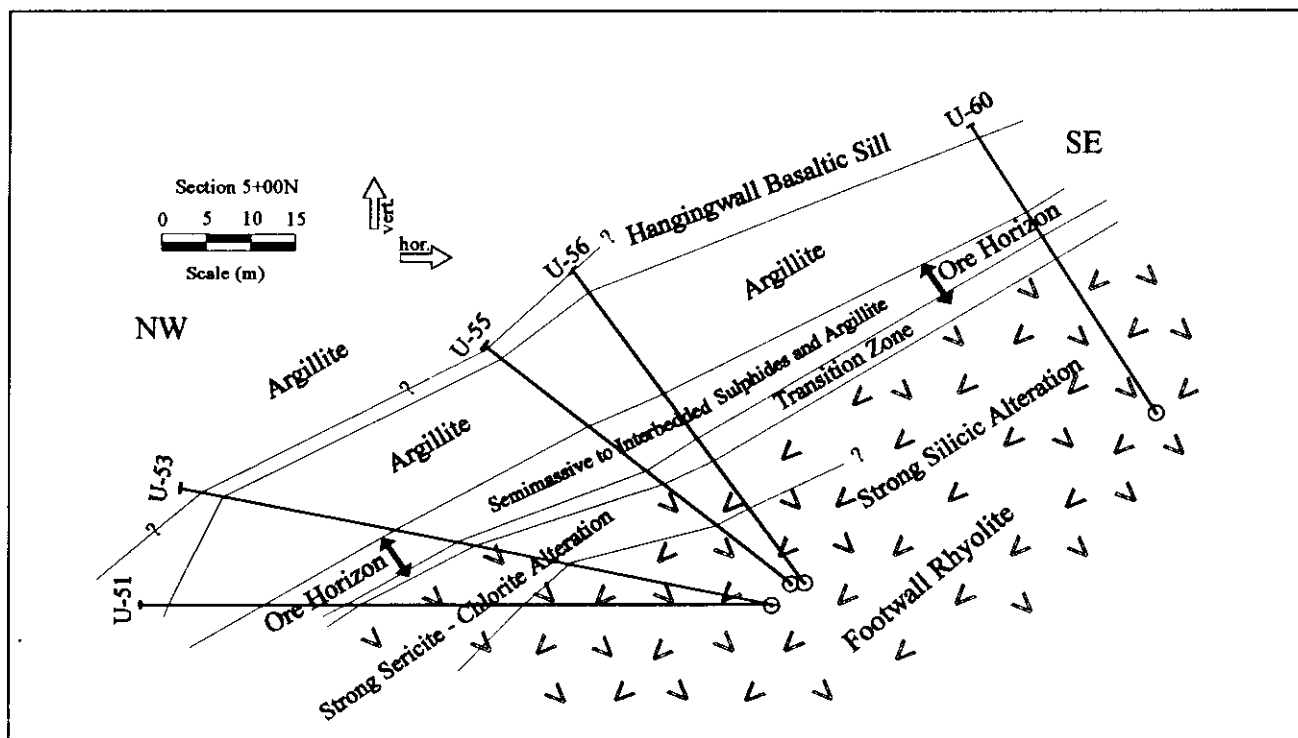


Figure 3. Cross-section through the 21B zone at section 5+00N. Based on company maps.

thinner rhythmically bedded and graded clastic ore beds. Thin, ungraded sulphide-sulphosalt beds and laminations are also present. Mineralization may have been localized in small synvolcanic seafloor depressions. The southernmost 600 metres of the 21B zone contains the highest grades and has the greatest lateral continuity; the northern 300 metres is mineralized at several stratigraphic intervals (Blackwell, 1990).

In the northern part of the 21B zone, a second interval of stratiform mineralization, termed the HW zone, is present within the contact argillite stratigraphically above the main zone of 21B stratiform mineralization. This interval is present as semimassive to massive sphalerite, galena, chalcopyrite and pyrite. The HW zone contains a much higher copper content than does the clastic ore in the lower part of the 21B zone.

**Discordant** mineralization occurs in the rhyolite-hosted 109 zone, which plunges down at a high angle to the rhyolite-argillite contact. The 109 zone is characterized by crustiform quartz veins and coarse-grained, zoned sphalerite, galena, minor pyrite and chalcopyrite and contains abundant carbonaceous material (Blackwell, 1990). Gold and silver occur as electrum and sulphosalts.

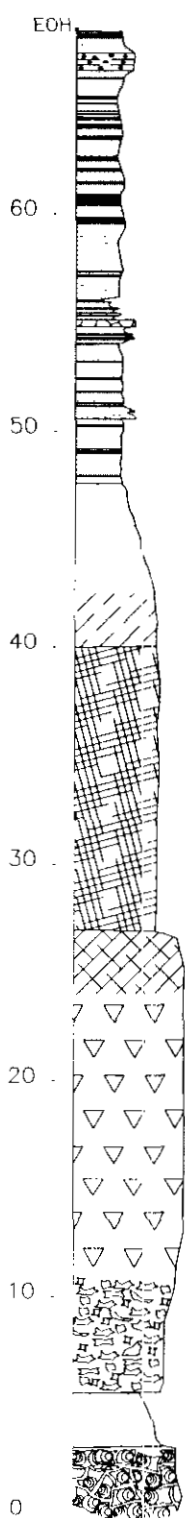
### SECTIONS 5+00N & 5+25N

Although the gross stratigraphic relationships of the 21B zone are well constrained, in detail they are complex. Geological relations in the 21B zone are perhaps best examined in section 5+00N (Figure 3).

Underground drilling on this section has provided high definition coverage allowing the geologic relationships to be investigated in detail. A total of eleven underground drill-holes and five surface holes penetrated the mineralized interval, although only five underground holes are shown, for clarity, in Figure 3.

In section 5+00N, the stratigraphy begins with silicified footwall rhyolite that becomes increasingly more sericitized and chloritized towards the argillite contact. The transition zone between the footwall rhyolite and the contact argillite is well developed with a variable thickness that increases to the east. The mineralized horizon comprises disseminated sulphides within the transition zone, and semimassive to thinly interbedded sulphides in the contact argillite. The contact between mineralized and overlying unmineralized argillite occurs over an interval of tens of centimetres, through a decreasing number of sulphide-sulphosalt beds. The overlying argillite is well laminated and composed of black mudstones with thin interbeds of brown ashy siltstone and grey calcareous sandstone. In section 5+00N, a basaltic sill, several metres thick, intrudes the contact argillite above the mineralized horizon.

Underground drill-hole U39, on section 5+25N, shows the stratigraphy in greater detail (Figure 4). The footwall rhyolite is divisible into several units beginning with *in situ* brecciated (hyaloclastite) and perlitically cracked rhyolite, overlain by an immature rhyolite sandstone. This is overlain by *in situ* rhyolite breccia of angular flow-banded fragments, which is probably an autoclastic flow breccia. The *in situ* breccia grades sharply into a zone of massive, waxy



U39

Mudstone, dark grey tuffaceous silt, and very fine to fine-grained sandstone

- silty to sandy laminae and beds range up to 5 cm thick within bedded intervals from 5 to 50 cm.
- fine-grained beds are khaki coloured
- 1 m sandstone interval near the end of the hole contains round to irregular calcareous concretions.

Mudstone and clastic sulphide beds

Laminated mudstone

- black mudstone containing <5% folded to crenulated, 1 to 5 cm, graded pyrite laminae and minor medium to coarse-grained volcanic sandstone beds, up to 5 cm thick, with normal grading.
- 2-3% irregular, anastomosing, fine-grained stibnite veinlets

Rhyolitic sandstone and pebbly sandstone - volcanoclastic

- sandstone is locally recognizable through strong sericitic alteration
- moderately sorted, overall normal grading
- white sericite streaks and spots occur throughout
- up to 1% disseminated pyrite and minor sphalerite.

Sericite-chlorite altered rhyolite

- primary textures are obscured; dark grey with white patches of sericite

"Massive chlorite"

- pale green to grey, massive to mottled, waxy chlorite rock
- contains batchy cream coloured quartz-carbonate blebs up to 3 cm across, through the central 6 m of the interval. Minor to 2% pyrite and sphalerite occur disseminated and in veinlets and streaks
- primary textures are not preserved.
- lower contact is sharp; upper contact is gradational, but changes rapidly to dark grey sericite-chlorite alteration.

In situ rhyolite breccia - autoclastic breccia

- clast-supported breccia of angular, flow-banded clasts of aphyric rhyolite
- variation from preferred alignment to locally disorganized, rotated flow-banded clasts
- lower 5 m contains abundant chloritic cusped clasts or patches suggesting possible altered glassy hyaloclastic margin
- alteration is mainly grey, pervasive to mottled quartz-sericite, partly controlled by flow bands and clast boundaries. Few thin chlorite veins occur locally
- minor disseminated pyrite occurs throughout. Minor sphalerite and tetrahedrite occur locally in thin (<2cm) veinlets with sericite or quartz-sericite.

Well sorted rhyolitic sandstone - pyroclastic deposit

- diffusely stratified, angular clasts range from 1 to 15 mm

In situ rhyolite breccia - hyaloclastite

- clast-supported breccia of broadly curved fragments containing arcuate to concentric perlitic fractures.

Figure 4. Detailed log of underground drill-hole U39, on section 5+25N.

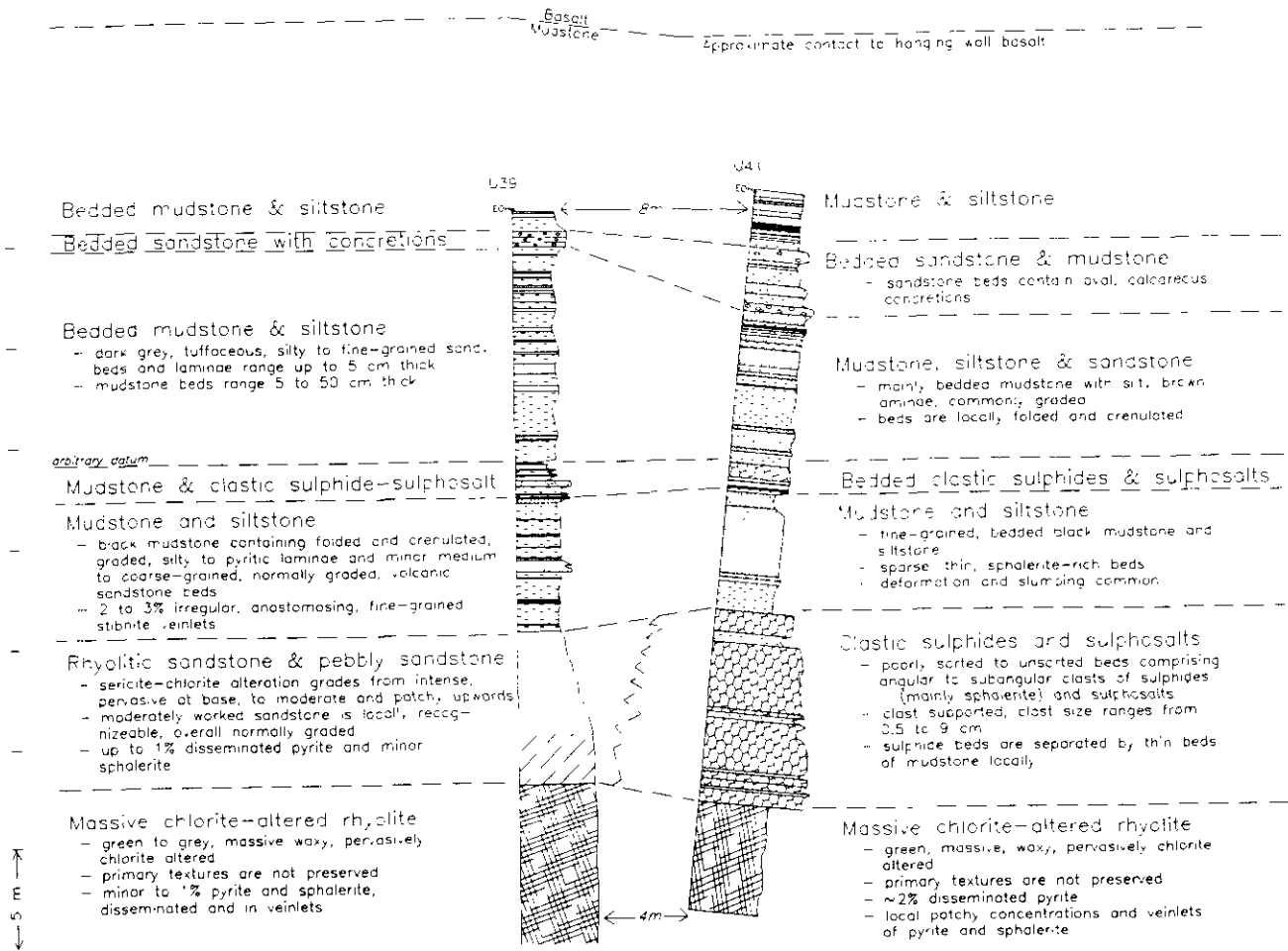


Figure 5. Detailed stratigraphy of underground drill holes U39 and U41, both from section 5+25N. Possible correlations are shown. Note the close spacing of the drill holes (4-8 metres).

green chlorite which is in turn overlain by a dark grey sericitized and chloritized rock. The actual field distinction between sericite-chlorite-altered rock and chlorite-altered rock is based on the physical appearance of the rock, not on chemical composition. This distinction may be misleading as some phases of the chlorite alteration are a pale brown colour and are often mistaken for sericite (R. Britten, personal communication, 1993). In U39, this intensely altered rock contains minor (3%) pyrite and sphalerite, disseminated and in thin veinlets. Intense sericite-chlorite alteration decreases gradually upward. Volcaniclastic rhyolitic sandstone is recognized locally at the top of the footwall. The footwall rhyolite is overlain by laminated mudstone with pyrite laminations and minor medium to coarse-grained, graded, volcanic sandstone beds. Within this interval are irregular anastomosing stibnite veinlets. The stratiform mineralized 21B horizon in hole U39 is entirely within the argillite unit, approximately 5 metres above the rhyolite-argillite contact. This mineralized horizon consists of eight clastic sulphide beds ranging between 0.5 and 25 centimetres thick;

separated by mudstone beds; the total thickness of this package is 1.7 metres. Angular to subrounded clasts in the ore range from less than 1 millimetre to 3 centimetres in diameter and are generally poorly sorted to unsorted; normal grading is locally weakly developed in the thinner beds. The clasts are mainly sphalerite, tetrahedrite and fine-grained sulphosalts; specks of electrum are visible locally within the clasts. Clasts include sericite and chlorite-altered rhyolite, and local rip-up clasts of argillite with pyritic or silty laminae. These lithic clasts comprise less than 5% of the ore beds and commonly increase in abundance toward the tops of the graded sulphide-sulphosalt beds. The mineralized horizon is overlain by a variably calcareous mudstone with thin interbeds of grey tuffaceous siltstone and sandstone.

Rapid thickness variations of individual units are exhibited between U39 and U41, two closely spaced drillholes in section 5+25N (Figure 5). The drill intersections of the mineralized intervals are only 4 to 8 metres apart but are markedly different in character, even though the stratigraphy above and below the mineralized intervals is correlatable. The datum used

in Figure 5 was the uppermost clastic sulphide-sulphosalt bed. This datum is preferred as it also brings into alignment the main igneous-sedimentary contacts. However, different geological interpretations are possible using a different datum. Mineralization in drill hole U41 is dominated by 8 metres of almost continuous, massive, thickly bedded, unsorted, coarse-grained, heterolithic, clastic sulphide-sulphosalt fragments which occur immediately above the pervasively chloritized interval. Minor mudstone interbeds within this sequence are less than 10 centimetres thick. Barite fragments are common near the base of the ore sequence, but decrease upward. Lithic fragments are minor. Clasts are angular to subangular and range from 0.1 to 10 centimetres across. Colloform banding of sulphides and sulphosalts observed in one large clast is sharply truncated at the clast margins.

This thick sequence of clastic ore is overlain by a sequence of mudstone and siltstone which contains thin beds and laminae of clastic sulphides and sulphosalts over another 8.5 metres; the latter beds become most prominent in the uppermost 1 metre which may correlate with bedded mineralization in hole U39. Notably, a thin zone of gouge underlies this upper zone of bedded mineralization in both drill holes, and may reflect a shallow-dipping fault which has displaced beds at this locality.

The lateral variations between individual mineralized beds in U41 and U39 probably reflect cross-strike variations in the deposition of the mineralized beds. The beds were probably deposited rapidly, perhaps as chaotic mass-flows that infilled local depressions, or as sheets of debris that paralleled the elongation of the 21B zone. Thickness variations presumably were influenced by basement topography as well as distance from source. In section 5+25N, the thick sulphide-sulphosalt sequence can be traced for at least 25 metres in other drill holes to the east of U41.

## DISCUSSION

Eskay Creek represents a precious metal enriched sea-floor deposit, with well-preserved stratiform mineralization as well as footwall stringer mineralization in areas such as the 109 zone. The overall geological relationships in the Eskay Creek camp have been documented by Rye (1992) and Edmunds and Kuran (1992). The present study is part of a detailed investigation into the physical nature of the volcanic and sedimentary environments during mineralization, and the mechanisms of emplacement of the mineralized beds. Many of these beds probably represent localized debris flows derived from *in situ* accumulation of sulphide-sulphosalt material but it is not yet understood if these beds are the product of seafloor mass wasting or fragmentation during volcanic activity.

Future work by the Mineral Deposit Research Unit will focus on measuring the composition of the fluids that formed the stratiform *versus* stringer

mineralization, and quantifying footwall alteration using recent lithochemical and X-ray diffraction methods to assess chemical and mineralogical changes. Continuing efforts are being made to constrain the age of the volcanic rocks and the lead isotopic composition of the various mineralized zones using radiogenic isotopes.

The 21B zone is a small but very attractive exploration target. Understanding the relations between footwall and stratiform mineralization through studies of fluid evolution, footwall alteration, metal-precipitating mechanisms, and ore redistribution on the seafloor may aid future exploration for these unique mineral deposits.

## ACKNOWLEDGMENTS

We are indebted to Homestake Canada Inc. for permission to publish information on the Eskay Creek property. We have benefited from discussion with Ron Britten of Homestake Canada Inc. and the previous work of Ken Rye and Carl Edmunds (now of Homestake Mineral Development Company) and Roland Bartsch (formerly of MDRU). Research at the Eskay Creek property forms part of a Mineral Deposit Research Unit project on Volcanogenic Massive Sulphide Deposits of the Cordillera, funded by the Natural Sciences and Engineering Research Council of Canada, the Science Council of British Columbia and ten mining and exploration companies.

## REFERENCES

- Alldrick, D.J., Britton, J.M., Webster, I.C.L. and Russell, C.W.P. (1989): Geology and Mineral Deposits of the Unuk Area (104B/7E, 8W, 9W, 10E) *B.C. Ministry of Energy, Mines and Petroleum Resources*, Open File 1989-10.
- Bartsch, R.D. (1992a): Eskay Creek Area, Stratigraphy Update (104B/9, 10); in *Geological Fieldwork 1991*, Grant, B. and Newell, J.M., Editors, *B.C. Ministry of Energy, Mines and Petroleum Resources*, Paper 1991-1, pages 517-520.
- Bartsch, R. D. (1992b): Lithostratigraphy - In situ Plateau; in *Metallogenesis of the Iskut River Area, Northwestern B.C.*; *Mineral Deposits Research Unit, The University of British Columbia*. Annual Technical Report for the period June 1991 to May 1992.
- Bartsch, R.D. (1993a): A Rhyolite Flow Dome in the Upper Hazelton Group, Eskay Creek Area (104B/9, 10); in *Geological Fieldwork 1992*, Grant, B. and Newell, J.M., Editors, *B.C. Ministry of Energy, Mines and Petroleum Resources*, Paper 1993-1, pages 331-334.
- Bartsch, R.D. (1993b): Volcanic Stratigraphy and Lithochemistry of the Lower Jurassic Hazelton Group, Host to the Eskay Creek Precious and Base Metal Volcanogenic Deposit; unpublished M.Sc. thesis, *The University of British Columbia*, 173 pages.

- Blackwell, J.D. (1990): Geology of the Eskay Creek #21 Deposits; *Mineral Deposits Division, Geological Association of Canada Newsletter*, The Gangué, Number 31, April, 1990, pages 1-4.
- Britton, J.M. (1991): Stratigraphic Notes from the Iskut-Sulphurets Area: in *Geological Fieldwork 1990*, B.C. Ministry of Energy, Mines and Petroleum Resources, Paper 1991-1, pages 331-334.
- Britton, J.M., Blackwell, J.D. and Schroeter, T.G. (1990) #21 Zone Deposits, Eskay Creek, Northwestern British Columbia: in *Exploration in British Columbia 1989*, B.C. Ministry of Energy, Mines and Petroleum Resources, pages 197-223.
- Edmunds, F.C. and Kuran, D.L. (1992): TOK-KAY and GNC 1991 Exploration Program, Geological and Diamond Drilling Program, *Prime Resources Group Inc.*, internal report.
- Lewis, P.D. (1992): Structural Geology of the Prout Plateau Region, Iskut River Map Area, British Columbia; in *Geological Fieldwork 1991*, Grant, B. and Newell, J.M., Editors, B.C. Ministry of Energy, Mines and Petroleum Resources, Paper 1992-1, pages 521-527.
- Lewis, P.D., Macdonald, A.J. and Bartsch, R.D. (1992): Hazelton Group / Bowser Lake Group Stratigraphy in the Iskut River Area: Progress and Problems; in *Metallogenesis of the Iskut River Area*, Northwestern B.C.; *Mineral Deposits Research Unit, The University of British Columbia*, Annual Technical Report for the period June 1991 to May 1992.
- Macdonald, A.J., van der Heyden, P. Lefebure, D.V. and Alldrick, D.J. (1992): Geochronometry of the Iskut River Area - An Update (104A and B); in *Geological Fieldwork 1991*, Grant, B. and Newell, J.M., Editors, B.C. Ministry of Energy, Mines and Petroleum Resources, Paper 1992-1, pages 495-502.
- Nadaraju, G.D. (1993): Triassic-Jurassic Biochronology of the Iskut River Map Areas, Northwestern British Columbia; unpublished M.Sc. thesis, *The University of British Columbia*, 268 pages.
- Roth, T. (1992): Geology of the 21A Zone-An Update; in *Metallogenesis of the Iskut River Area*, Northwestern B.C.; *Mineral Deposits Research Unit, The University of British Columbia*. Annual Technical Report-for the period June 1991 to May 1992.
- Roth, T. and Godwin, C.I. (1992): Preliminary Geology of the 21A Zone, Eskay Creek, British Columbia; in *Geological Fieldwork 1991*, Grant, B. and Newell, J.M., Editors, B.C. Ministry of Energy, Mines and Petroleum Resources, Paper 1992-1, pages 529-533.
- Rye, K. (1992): Geological and Geochemical Report on the 1991 Eskay Creek Diamond Drill Re-log Program; internal report, *Prime Resources Group Inc.*

## GEOLOGY AND ALTERATION ZONATION OF THE HANK PROPERTY, NORTHWESTERN BRITISH COLUMBIA (104G/1,2)

By Andrew W. Kaip, Mineral Deposit Research Unit, U.B.C  
and  
David Gaunt, Homestake Canada Ltd.

(MDRU Contribution 033)

**KEYWORDS:** Economic geology, Stuhini Group, epithermal, alteration, gold, Middle Jurassic, megacrystic porphyry.

### INTRODUCTION

The Hank property is situated in northwestern British Columbia 20 kilometres northwest of Bob Quinn Lake (Figure 1).

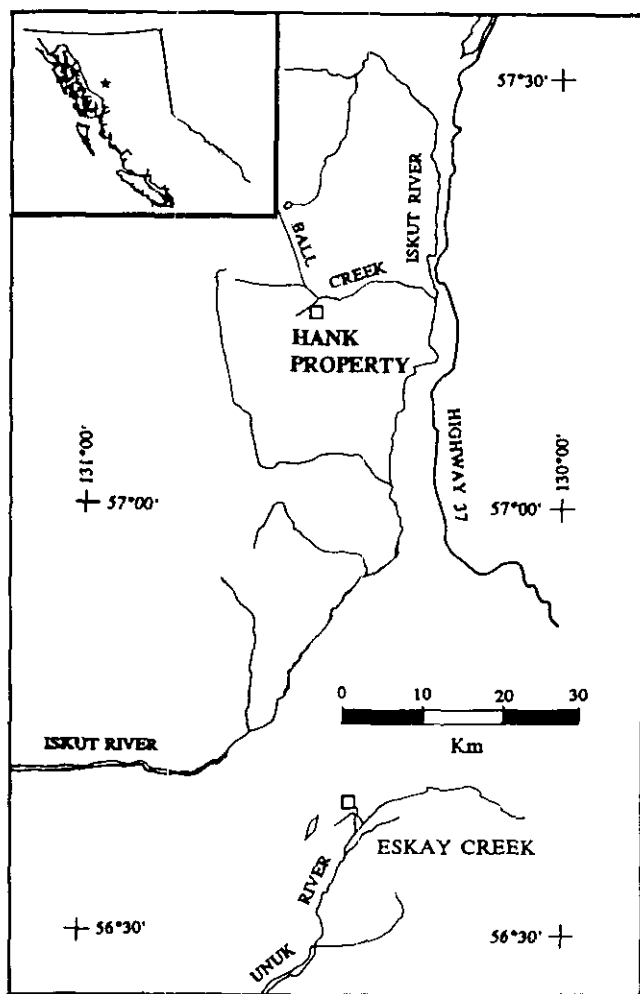


Figure 1. Location of the Hank property adapted from Anderson and Thorkelson (1990).

Access to the property is by helicopter from Bob Quinn Lake; the claims are served by a network of cat trails developed by Lac Minerals Ltd. between 1985 and 1989.

Fieldwork concentrated on relogging of core in the lower and upper alteration zones and logging of core from the Homestake Canada Ltd. 1993 diamond drilling program on Felsite Hill. The emphasis of fieldwork was to document the vertical changes in alteration from the lower alteration zone to Felsite Hill, to identify the lateral extent of the silicified zone beneath Felsite Hill, and to identify those features which characterize hydrothermal alteration on the Hank property as a low-sulphidation epithermal environment. Continued research at the University of British Columbia will comprise part of a M.Sc. thesis supervised by Dr. A.J. Sinclair and Dr. J.F.H. Thompson.

### EXPLORATION HISTORY

The Hank property comprises two groups of claims, the Hank claims, owned by Lac Minerals Ltd., which cover the majority of the hydrothermal alteration zones on the property, and the Panky claims, owned by Cominco Ltd., which lie to the east and south.

The Hank property was initially staked by Lac Minerals Ltd. in 1983. During 1984 to 1985 and 1987 to 1989 Lac Minerals Ltd. completed geological mapping, geochemical surveys, trenching, geophysical surveys, and diamond drilling totaling 11 604 metres in 88 holes in the upper, lower and flats alteration zones. Drilling outlined geological reserves of 245 000 tonnes with an average grade of 4.0 grams per tonne gold and 213 000 tonnes with an average grade of 2.0 grams per tonne in the 200 and 440 pit areas of the upper alteration zone, respectively (Figure 2).

Carmac Resources Ltd. (now Camner Resources Ltd.) optioned the Hank claims in 1990 and drilled five holes totalling 1 090 metres in the Upper and Lower zones, then terminated the option.

Homestake Canada Ltd. optioned the Hank and Panky claims in 1992 and completed a program of soil and rock sampling, an induced polarization survey and detailed geological mapping, concentrating on the Felsite Hill and Rojo Grande alteration zones (Figure 2, Kaip

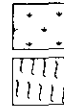
# LEGEND

## STRATIGRAPHY

East of the West Hank fault

West of the West Hank fault

Middle Jurassic



- 5a Dark green amygdaloidal aphyric flows and flow breccias
- 5b Rusty, pyritic, flow-banded rhyolite

Lower Jurassic



- 4 Undivided siltstone, well-bedded sandstone and heterolithic conglomerate

Unconformity

Upper Triassic  
Stuhini Group



- 2c Bioclastic and silty limestone



- 2b Andesitic, pyroxene+felspar-phyric volcanioclastic breccia



- 2a Andesitic to basaltic, magnetic, pyroxene+felspar-phyric flows



- 1d Maroon, magnetic, hornblende felspar+/- pyroxene flows, sills and dikes



- 1c Interbedded siltstone and well-bedded sandstone



- 1b Feldspar+/-biotite-phyric ash tufts and biotite phyric flows and breccias



- 1a Undivided green to maroon felspar+/-hornblende+/-pyroxene volcanioclastic tufts and breccias



- 3 Well-bedded, felspar-rich, volcanic derived sandstones, conglomerates, greywacke and siltstones

## INTRUSIONS



- A Bald Bluff porphyry: orthoclase megacrystic hornblende-phyric monzonite, bx=breccia, ex=possible extrusive equivalent of the Bald Bluff porphyry



- B Medium-grained hornblende diorite

## ALTERATION



- Clay+/-quartz+/-pyrite (For figure 3)



- Clay+/-quartz



- Quartz+/-pyrite



- Quartz+clay+/-pyrite



- Quartz+clay+pyrite



- Clay+pyrite+carbonate+/-quartz with carbonate stockwork



- Sericite+pyrite+/-chlorite+/-clay +/-carbonate



- Sericite+pyrite+/-carbonate



- Quartz+sericite+pyrite+/-clay

## SYMBOLS



Geologic contact (defined, assumed, inferred)



Fault



Alteration contact

and Macpherson, 1993). In 1993 Homestake Ltd. drilled five diamond-drill holes for a total of 657 metres targeting geochemical, and geophysical anomalies in the flats and Felsite Hill alteration zones.

## REGIONAL GEOLOGY

The Hank property lies within the Stikine Terrane along the western margin of the Intermontane Belt and the eastern margin of the Skeena fold belt. Regional mapping in the area (Logan *et al.*, 1992; Evenchick, 1991; Anderson and Thorkelson, 1990; Souther, 1972) has defined the following major units: Paleozoic volcanic and sedimentary rocks of the Stikine assemblage;

Mesozoic volcanic-plutonic arc assemblages, represented by Triassic Stuhini Group, and Jurassic Hazelton Group; a Middle and Upper Jurassic overlap assemblage, the Bowser Lake Group; and the Mesozoic to Cenozoic Coast Plutonic Suite.

The oldest rocks in the region are complexly folded schists and gneisses of middle Paleozoic age, which form the basement to the area and are exposed in Moore Creek south of the Hank property. Closer to the property, regional mapping has defined the stratigraphy surrounding the property as Upper Triassic augite andesite flows, pyroclastic rocks and volcanic-derived sediments overlain by Lower Jurassic grit, conglomerates and greywackes (Souther, 1972).

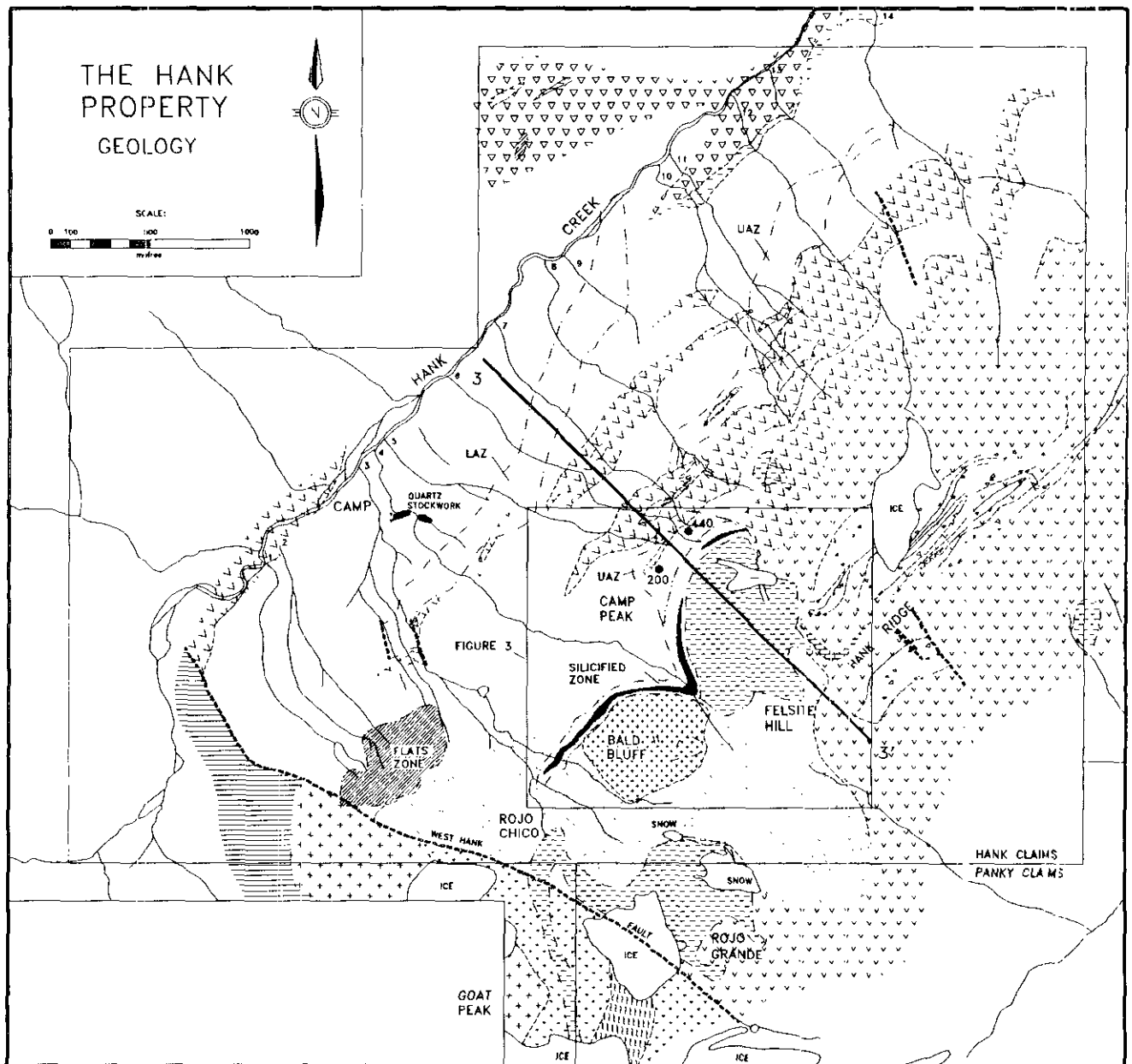


Figure 2. Geology of the Hank property.

Sedimentary rocks of the Middle Jurassic Ashman Formation of the Bowser Lake Group are exposed along the Iskut River valley to the east (Evenchick, 1991).

To the west of the property a northwest-striking fault is mapped at the head of Hank Creek (Souther, 1972). A subparallel fault, informally named the West Hank fault, adjacent and to the east of the regional fault, is exposed on the ridge to the northwest of the claims and traces across the southwest corner of the property (Figure 2).

## PROPERTY GEOLOGY

The Hank property is underlain by a succession of flows, sills, volcanoclastic and minor sedimentary rocks divided into five units and described in detail by Kaip and McPherson (1992; Figure 2). On the northeast side of the West Hank fault the stratigraphy consists of Upper Triassic Stuhini Group pyroxene-feldspar-phyric flows, sills, breccias and minor limestone overlying hornblende-pyroxene-feldspar-phyric flows, sills, and volcanoclastic breccias with intercalated siltstones, sandstones, biotite-phyric flows and breccias. On the property the Stuhini volcanic rocks strike northeast along Hank Ridge and dip 30 to 50° to the southeast.

Lower Jurassic calcareous siltstones, sandstones, wackes and pebble conglomerates which locally contain abundant fossilized wood fragments unconformably overlie the volcanic succession. The Lower Jurassic sediments are folded about a southeast-plunging syncline exposed between Felsite Hill and Rojo Grande (Figure 2). Diamond drilling by Homestake Canada Ltd. to the southeast of the flats zone intersected sedimentary rocks of this unit (Figure 2), and extended the known extent of unit 4 to the upper margin of the flats zone.

On the west side of the fault, well-bedded, feldspar-rich, volcanic derived sandstones, conglomerates, greywacke and thin bedded siltstones of the Upper Triassic Stuhini Group are exposed along the north flank of Goat Peak (Logan *et al.*, 1992).

A wedge of possible Middle Jurassic interlayered aphyric vesicular basalt flows and flow-banded rhyolites and minor volcanoclastic sediments exposed along the eastern flank of Goat Peak are bounded by the West Hank fault on the northeast side and hornblende diorite to the west (Figure 2).

Two intrusive plugs are exposed on the property, an orthoclase-megacrystic, hornblende-phyric monzonite which underlies the prominent knoll, Bald Bluff, and an elongate medium-grained hornblende diorite intrusion which crops out on Goat Peak. A sample of the Bald Bluff intrusion collected during the 1992 field season for zircon dating yielded a preliminary age of 185±3 Ma (J. K. Mortensen, personal communication, 1993).

## ALTERATION

Seven alteration zones are present on the Hank property with characteristic alteration assemblages described by Kaip and McPherson (1992). They include: the quartz stockwork consisting of quartz veining and silica flooding within chlorite+carbonate+pyrite altered volcanoclastic breccias of unit 1a; the lower alteration zone, dominated by intense sericite+pyrite±carbonate alteration; the upper alteration zone, dominated by sericite+pyrite±chlorite±clay±carbonate alteration; the Flats zone at the head of Creeks 1 to 3 and characterized by quartz+sericite+pyrite alteration hosting pods of more intense clay+pyrite±quartz alteration and quartz+potassium feldspar+pyrite alteration; the silicified zone characterized by intense silicification with or without pyrite and barite which displays multiple phases of brecciation; Felsite Hill and Rojo Grande dominated by intense quartz+clay+pyrite alteration and lesser quartz+clay±pyrite and clay±quartz alteration (Figure 2). Based on X-ray diffraction studies on type alteration assemblages, sericite refers to fine-grained muscovite, and clay refers to a mixture of dickite and kaolinite.

## SECTIONS 1 AND 2

Sections 1 and 2 (Figure 4), are located on Figure 3 and incorporate data collected from recent drilling on Felsite Hill and relogging of core from the 200 pit area of the lower alteration zone. Hydrothermal alteration in this area is continuous from the base of the lower alteration zone to the top of Felsite Hill and provides the opportunity to characterize the vertical changes in alteration style within a low-sulphidation epithermal environment.

## UPPER ALTERATION ZONE

The upper alteration zone is less continuous in the vicinity of the 200 pit area and comprises green sericite+pyrite+carbonate±chlorite alteration near the base and pale grey, intense clay+sericite+pyrite±carbonate alteration near the upper contact with the silicified zone (Figure 3). This change in style is characterized by a decrease in competency of core as clay becomes more abundant. In this area the upper zone strikes northeast and dips semiconformably to stratigraphy within volcanoclastic breccias of unit 1a. In outcrop and drill core the footwall to the upper alteration zone is defined by a flow or sill of unit 1d.

Six types of veining are recognized: quartz-carbonate veins carrying sphalerite, pyrite and minor chalcopyrite; barite±pyrite veins; quartz-pyrite veins; pyrite veinlets; white to pink carbonate veins and crustiform calcite veins.

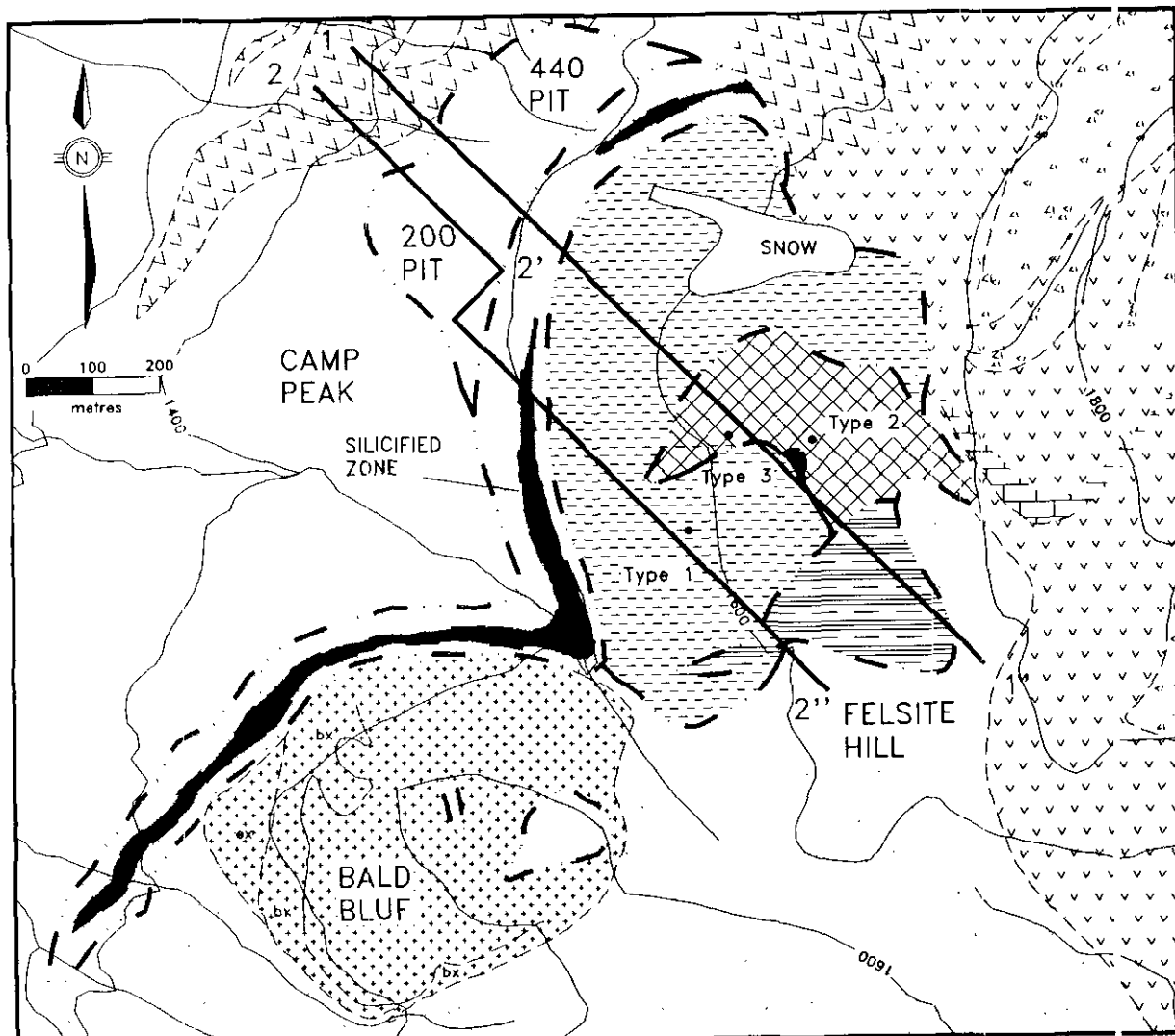


Figure 3. Distribution of alteration assemblages and of breccias types on Felsite Hill.

Barite veins are characterized by coarse-grained bladed barite with minor disseminated pyrite and frequently contain wallrock fragments. Quartz-pyrite veins, commonly less than 10 centimetres wide, contain euhedral coarse-grained pyrite concentrated along the margins. Pyrite veinlets, less than 1 centimetre in width are abundant in the upper zone and are cut and are cut by white to pink carbonate veinlets. Crustiform calcite veins up to 1 metre wide are exposed in the 200 and 440 pit area of the upper alteration zone. These veins contain *minor pyrite and bladed quartz after calcite*.

Gold mineralization occurs within a subhorizontal zone dipping gently to the southeast, approximately 30 metres above the base of the upper zone (Figure 4b). Gold concentrations correlate with an increase in pyrite veining, quartz-carbonate and quartz-pyrite veining enveloped by intense clay+sericite+pyrite±carbonate alteration. Veining strikes northeast and dips steeply to the southeast.

### SILICIFIED ZONE

The silicified zone is exposed along the base of Bald Bluff and Felsite Hill (Figure 3). It is hosted by sedimentary rocks of unit 4 and volcanic rocks of unit 1. Above the 200 pit area the trace of the silicified zone was intersected in drill core and consisted of grey, intense silicification hosting very fine-grained disseminated pyrite (Figure 4). The upper and lower margins of the silicified zone display evidence of brecciation with coarse-grained pyrite and barite filling open cavities.

On surface a poorly exposed zone of friable, recessive weathering alteration corresponds to the trace of the silicified zone. In drill core this zone, up to 70 metres wide, is marked by a general decrease in the degree of silicification downward from quartz+clay+pyrite alteration to friable clay+pyrite+carbonate±quartz which grades into typical upper zone alteration (Figure 4a and 4b). This zone is also characterized by a carbonate stockwork composed of

white to pink calcite veins 1 to 2 centimetres wide and abundant pyrite veinlets above and below the silicified zone. In addition, within this envelope several intervals of silicification occur above the main silicified zone (Figure 4b).

From surface exposure and the intersection of the silicified zone in core it is apparent that it is semiconformable to stratigraphy, strikes northeast and dips 15 to 20° to the southeast.

### FELSITE HILL

Alteration on Felsite Hill is hosted by sedimentary rocks of unit 4 and hornblende-feldspar-phyric flows or sills of unit 1d (Figure 3). Four types of alteration are present: quartz+clay+pyrite; quartz+clay±pyrite; clay±quartz and quartz±pyrite.

Quartz-clay-pyrite alteration is hosted by hornblende-feldspar-phyric flows or sills of unit 1d. Alteration is characterized by clay-altered plagioclase phenocrysts within a groundmass of grey quartz, clay and pyrite. Quartz+clay±pyrite alteration is hosted by units 4 and 1d and varies from texturally destructive vuggy, quartz and clay alteration to less intense alteration with relict primary textures and isolated pods of fine-grained pyrite. Quartz+clay±pyrite alteration overlies and extends to the southeast of quartz+clay+pyrite alteration; from drill core it is apparent that this type of alteration cuts quartz+clay+pyrite alteration along vertical structures which narrow at depth (Figure 4a). Clay±quartz alteration varies dramatically in intensity along the southern margin of the alteration zone on Felsite Hill and is hosted by sedimentary rocks of unit 4. Clay varies from white to maroon in colour and occurs initially as pervasive alteration of the hostrock.

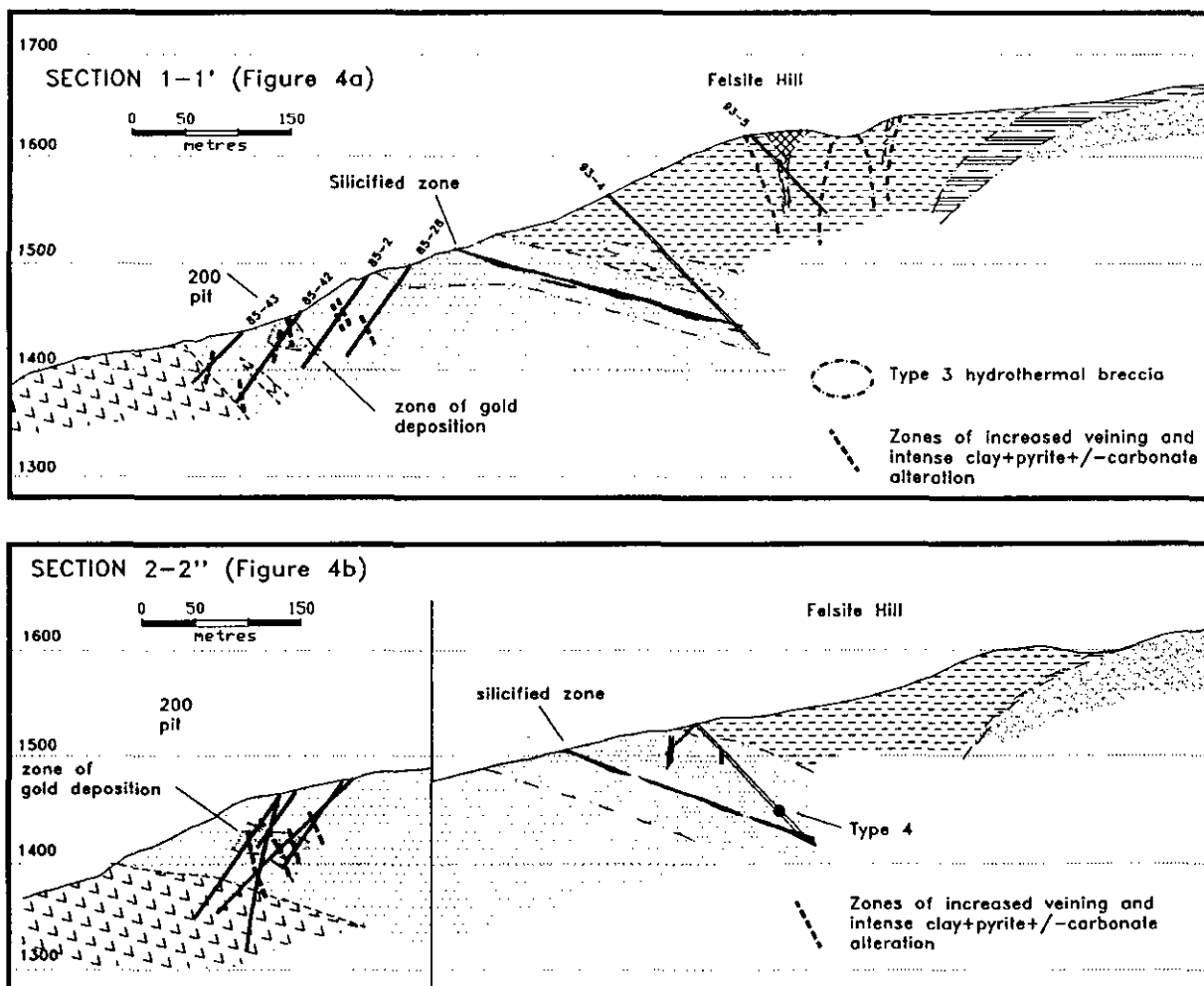


Figure 4: Cross-sections 4a and 4b through the upper alteration zone and Felsite Hill. Sections identify distribution of alteration, hydrothermal breccias, and level at which gold deposition occurred.

Four types of hydrothermal brecciation are observed in outcrop and core (Figures 3 and 4). Type 1 breccia is characterized by fragments of white quartz+clay±pyrite and grey quartz+pyrite+pyrite altered fragments within a matrix of quartz, clay and pyrite followed by white porcellanous clay. Type 2 breccia is characterized by white quartz+clay altered fragments within a matrix of black silica. This type of breccia is found in quartz+clay±pyrite altered siltstones with carbonaceous plant fragments. Type 3 breccia consists of quartz+clay+pyrite-altered angular fragments of feldspar-phyrlic volcanic rock with serrate margins. The matrix of the hydrothermal breccia is composed of quartz, clay and pyrite followed by white porcellanous clay. Diamond-drill hole 93-5 intersected type 3 hydrothermal breccia at depth (Figure 4a). In drill core type 3 breccia is cored by several 2 to 5 metre zones of vuggy quartz and clay alteration with limonite-covered fracture surfaces, similar to quartz+clay±pyrite alteration observed at surface. Type 4 breccia is observed in diamond-drill hole 93-2A, and consists of rounded quartz+clay+pyrite-altered fragments in a matrix of soft clay and pyrite (Figure 4b).

## DISCUSSION

The topography, combined with outcrop and diamond-drill hole data from the Hank property provides an excellent cross-section through an epithermal alteration system, as defined by Lindgren (1933). Alteration is characteristic of a low-sulphidation, near-surface environment with sericitic alteration at depth in the lower alteration zone (Kaip and McPherson, 1992) and clay alteration at higher elevations on Felsite Hill and Rojo Grande. The upper alteration zone is transitional between these two styles of alteration with sericite+pyrite+carbonate±chlorite near the base and clay

±sericite+carbonate+pyrite near the upper contact with the silicified zone. The latter is characterized by multiphase silicification within a broad zone of clay+pyrite+carbonate±quartz and carbonate stockwork.

The overall morphology of these alteration zones shown in Figure 5, suggests that the lower alteration zone may be a feeder zone as it cuts stratigraphy at a high angle. The upper alteration zone is semiconformable to stratigraphy, is hosted by rocks of unit 1a, and may indicate lateral movement of hydrothermal fluids along a permeable horizon. The presence of large crustiform banded carbonate veins with silica-replaced bladed calcite crystals suggests that bicarbonate fluids were present and that boiling may have taken place in the upper alteration zone (Simmons and Christenson, 1993). Alteration on Fe site Hill is dominated by clay and pyrite alteration with varying degrees of silicification and displays a vertical and lateral zonation of quartz+clay+pyrite to quartz+clay±pyrite to clay±quartz from core to periphery. Hedenquist (1993), indicates that clay-dominant alteration can occur on the margins of low-sulphidation epithermal environments where temperatures are cooler and alteration products are characteristic of vapour condensates. From drill hole 93-5, it is apparent that vuggy quartz+clay alteration forms along vertical structures and overprints quartz+clay+pyrite-altered hydrothermal breccia. This feature may represent the effects of encroaching surface water on the collapsing hydrothermal system. The silicified zone, which lies above the upper alteration zone and below Felsite Hill, may indicate a zone of increased permeability or the former presence of a phreatic table. Alternatively, the silicified zone may represent the level at which boiling fluids deposited silica, but this has yet to be determined from mineralogical and geochemical investigations.

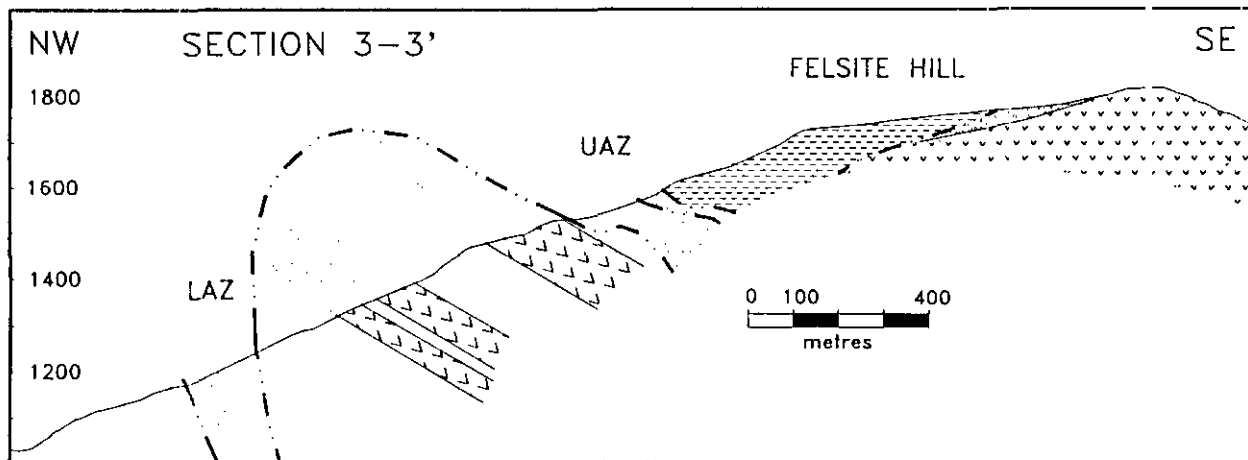


Figure 5. Cross-section 3-3' through the lower and upper alteration zones and Felsite Hill showing zoning in the type of alteration.

Based on field mapping there appears to be a genetic link between the intrusion of the Bald Bluff orthoclase megacrystic porphyry and hydrothermal alteration at the Hank property. This hypothesis is supported by the age of intrusion at  $185 \pm 3$  Ma. and a Middle Jurassic signature obtained from galena in precious metal bearing quartz-carbonate-sulfide veins from the lower alteration zone.

The Hank property is the first known occurrence of a Middle Jurassic epithermal system, apparently related to the intrusion of orthoclase megacrystic porphyries within the Iskut region. These porphyries have been shown regionally to be temporal and spatially related to other types of mineralizing environments in the region.

## ACKNOWLEDGMENTS

The authors would like to thank Homestake Canada Ltd. for financial, technical and logistical support of this study. We are grateful to R. Britten and H. Marsden of Homestake Canada Ltd. for insight and ideas on the Hank property and to Lac Minerals Ltd. and Cominco Ltd. for access to data. Thanks to J.F.H. Thompson, A.J. Sinclair and A.J. Macdonald for constructive editing. Continued financing for this study is provided under the Mineral Deposit Research Unit project "Metallogenesis of the Iskut River Area" funded by Natural Sciences and the Engineering Research Council of Canada, the British Columbia Science Council and member mining companies

## REFERENCES

Anderson, R.G. and Thorkelson, D.J. (1990): Mesozoic Stratigraphy and Setting for some Mineral Deposits in Iskut River Map Area, Northwestern British Columbia; in Current Research, Part E, *Geological Survey of Canada*, Paper 90-1F, pages 131-139.

Evenchick, C.A. (1991): Jurassic Stratigraphy of East Telegraph Creek and West Spatsizi Map Areas, British Columbia; in Current Research, Part A, *Geological Survey of Canada*, Paper 91-1A, pages 155-162.

Hedenquist, J.W. (1993): Environments of Volcanic-hosted Epithermal Mineralization: Recent Advances in Understanding the variable nature of Near-surface Hydrothermal Systems; in *Volcanoes and Ore Deposits*, Mineral Deposit Research Unit, The University of British Columbia, Short Course 14, 31 pages.

Kaip, A.W. and McPherson, M.D. (1993): Preliminary Geology of the Hank Property, Northwestern British Columbia (104G/1,2); in *Geological Fieldwork 1992*, Grant, B. and Newell, J.M., Editors, *B.C. Ministry of Energy, Mines and Petroleum Resources*, Paper 1993-1, pages 349-357.

Lindgren, W. (1933): *Ore Deposits*. 4th Edition; *McGraw-Hill*, New York, 930 pages.

Logan, J.M., Drobe, J.R. and Elsby, D.C. (1992): Geology of the Moore Creek Area, Northwestern British Columbia (104G/2); in *Geological Fieldwork 1991*, Grant, B. and Newell, J.M., Editors, *B.C. Ministry of Energy, Mines and Petroleum Resources*, Paper 1992-1, pages 161-178.

Simmons and Christenson (1993): Origins of Calcite in a Boiling Geothermal System; in *American Journal of Science*, in press.

Souther, J.G. (1972): Telegraph Creek Map Area, British Columbia; *Geological Survey of Canada*, Map 1623A.

# GEOLOGICAL INVESTIGATIONS OF THE TULSEQUAH CHIEF MASSIVE SULPHIDE DEPOSIT, NORTHWESTERN BRITISH COLUMBIA (104K/12)

By R.L. Sherlock, F. Childe, T.J. Barrett, J.K. Mortensen, P.D. Lewis  
Mineral Deposit Research Unit, U.B.C.

T. Chandler  
Redfern Resources Limited  
P. McGuigan, G.L. Dawson  
Cambria Geological Limited  
R. Allen  
Volcanic Resources

(MDRU Contribution 045)

**KEYWORDS:** economic geology, Tulsequah Chief, Big Bull, massive sulphides, volcanogenic, Mount Eaton Group

## INTRODUCTION

The Tulsequah Chief volcanogenic massive sulphide deposit (58° 30'N, 133° 35'W) is located along the east bank of the Tulsequah River, 100 kilometres south of Atlin, British Columbia and 70 kilometres northeast of Juneau, Alaska (Figure 1). At present, access to the site is limited to small aircraft via two nearby airstrips. The Tulsequah Chief deposit is accessible by adits at several levels on the west side of Mount Eaton. The Big Bull deposit is located along strike 10 kilometres south of Tulsequah Chief on the southern flank of Mount Manville at the confluence of the Tulsequah and Taku rivers (Figure 1).

Fieldwork in 1993 involved relogging and sampling of selected drill-core through sections of the Tulsequah Chief mine stratigraphy, as well as underground sampling on the 5400 level and surface sampling around both the Tulsequah Chief and Big Bull deposits. Samples are being analyzed for litho geochemistry, geochronology, mineralogy and fluid inclusions. This contribution describes the preliminary results and interpretations of the volcanic stratigraphy at the Tulsequah Chief deposit.

The objectives of the overall study are: to define the main stratigraphic units at Tulsequah Chief on the basis of detailed litho geochemistry and petrography; to determine if this stratigraphy can be correlated across the 4400E and 5300E faults, which divide the property into western, central and eastern blocks; to identify the different levels and styles of mineralization and their origins; to date both the host volcanic rocks and the associated intrusive rocks; and to determine the distribution and intensity of alteration associated with mineralization.

For a detailed discussion of the regional geology the

reader is referred to Kerr (1948), Souther (1971), Nelson and Payne (1984) and Mihalyuk *et al.* (1994).

## EXPLORATION AND PRODUCTION HISTORY

The Tulsequah Chief deposit was discovered in 1923 by W. Kirkham of Juneau. Subsequent activity in this area led to the discovery in 1929 of both the associated Big Bull massive sulphide deposit and the Polaris-Taku gold deposit. The Tulsequah Chief and Big Bull deposits were acquired by the Consolidated Mining and Smelting Company of Canada, Limited (Cominco) in 1946 and brought into production in 1951. The mines closed in 1957 due to depressed metal prices. Total production from the two orebodies was 933 520 tonnes with an average grade of 1.59% copper, 1.54% lead, 7.0% zinc, 3.84 grams per tonne gold and 126.5 grams per tonne silver. Of this ore, 622 136 tonnes were from the Tulsequah Chief orebody and the remaining 311 384 tonnes from the Big Bull deposit (McGuigan *et al.*, 1993).

A joint venture between Cominco and Redfern Resources Limited from 1987 to 1991 led to extensive exploration including over 21 000 metres of surface and underground diamond drilling (Casselman, 1988, 1989, 1990). In June 1992, Redfern Resources purchased Cominco's interest (60%) in the property and consequently now owns 100% of the Tulsequah Chief and Big Bull orebodies and adjacent ground. In 1992 an additional 4 579 metres of underground diamond-drilling was completed; in addition, surface mapping and relogging of drill core were carried out by Cambria Geological Limited. Reserve estimates made by Cambria Geological at the end of the 1992 program for all ore horizons and classes were 8 500 592 tonnes grading 1.48% copper, 1.17% lead, 6.86% zinc, 2.56 grams per tonne gold and 103.4 grams per tonne silver (McGuigan *et al.*, 1993).

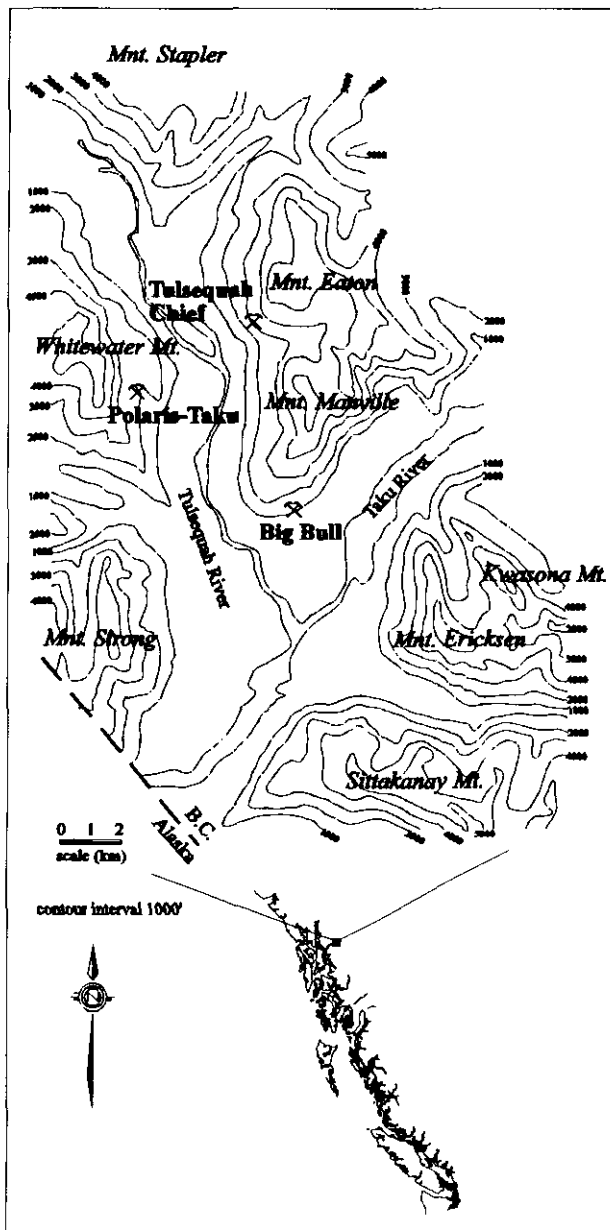


Figure 1. Location map for the Tulsequah Chief, Big Bull and Polaris-Taku deposits, from Nelson and Payne (1984).

Current exploration on the property, by Redfern Resources Limited, consists of geological mapping, geophysical surveys, underground and surface diamond-drilling at both the Tulsequah Chief and Big Bull orebodies. Diamond drilling in 1993 includes 8 060 metres from the surface and underground at Tulsequah Chief, and 3 700 metres from the surface at Big Bull.

### MINE SEQUENCE STRATIGRAPHY

The stratigraphy at the Tulsequah Chief deposit is composed of a series of northward-younging mafic and felsic volcanic rocks (Figure 2). The stratigraphically lowest unit (unit 1) is composed of mafic volcanic rocks forming the footwall to mineralization. This unit is

directly overlain by a series of dacitic flows, sills and volcanoclastic material (units 2 and 4). On the basis of contact relationships, units 2 and 4 are interpreted to have originally been a single felsic (dacitic) package which was subsequently intruded by a large mafic sill (unit 3). The upper felsic unit (unit 4) is overlain by a series of mafic flows or sills and volcanoclastic sediments (unit 5). All of these units are intruded by Tertiary Sloko dikes, mainly of felsic composition. The lithological units are based on field descriptions and limited petrology and may be modified as a result of future lithochemical results.

### UNIT 1

Unit 1 forms the stratigraphic footwall to the massive sulphide deposits and comprises mainly massive to flow-brecciated mafic volcanics with minor volcanic sediment. Alteration and metamorphism have modified the primary mineralogy to an assemblage of quartz, sericite, chlorite, biotite, pyrite and hematite. The top of the unit is strongly amygdaloidal and commonly contains hyaloclastic textured material. The amygdules are typically filled by quartz, pyrite and chalcopyrite. Cordierite porphyroblasts are variably developed in areas immediately underlying the sulphide mineralization.

### UNIT 2

Unit 2 is the principle host to sulphide mineralization in the lower mine stratigraphy, and comprises massive, flow-brecciated and volcanoclastic dacite. Several massive sulphide lenses, collectively termed the H-AB horizon, are hosted by dacite mass-flow material containing variable amounts of sulphide and cherty clasts. Intrusive into the mass-flow unit are dacite sills that locally dilate and split the package. This process, and subsequent fault dislocations, has separated the mineralized horizon into discrete sulphide lenses termed the F, AB<sub>1</sub>, AB<sub>2</sub>, H, I and G zones (Figure 2). Unit 2 thickens to the west, which may indicate a dacitic source in this direction. The dacite consists of plagioclase and quartz phenocrysts in a groundmass of quartz, sericite and epidote.

### UNIT 3

A thick massive mafic sill (unit 3) with chilled margins and intercalations of dacitic material at either margin separates the upper and lower felsic packages. Unit 3 is up to 50 metres thick and is slightly discordant to stratigraphy; it probably represents a low-angle sill that has intruded the dacitic (fragmental-rich) package. The margins of unit 3 are finer-grained than the interior which has a diabasic texture. The primary mineralogy of the sill comprises augite, plagioclase and olivine phenocrysts in a fine-grained plagioclase groundmass. This assemblage is overprinted by coarse-grained randomly oriented chlorite and amphibole of possible metamorphic origin. The unit appears to be relatively unaltered compared to units 1, 2 and 4, suggesting it was emplaced after the mineralizing event. Unit 3 may be the subvolcanic equivalent of unit 5.

## STRUCTURE

Stratigraphic units at Tulsequah Chief outline a series of north to northwest-plunging folds which are divided into three discrete structural blocks by the 5300E and 4400E faults (Figure 2). These faults are exposed in several locations in the 5400 level mine workings. The 5300E fault is the most significant and probably has the largest displacement of the faults on this level. Kinematic indicators record an early period of dextral motion with a gently northward-plunging slip vector, followed by movement along a southerly plunging slip vector of unknown sense. The dextral motion is probably the most important in terms of displacement, but determination of absolute displacements requires a detailed analysis of stratigraphy in the central and eastern mine blocks. The 4400E and minor unnamed faults of variable orientation cause no large-scale displacement of stratigraphic contacts.

## MINERALIZATION

The sulphide deposits described here occur primarily within volcanoclastic mass-flows of unit 2. Several sulphide facies have been defined by Cambria Geological Limited and Redfern Resources. The pyrite facies consists mainly of massive pyrite with little base metal content. The zinc facies is composed primarily of semimassive pale yellow sphalerite, pyrite, galena, chalcopyrite and tetrahedrite, with barite, quartz and sericitically altered lithic fragments. The copper facies is mainly massive pyrite with up to several percent disseminated chalcopyrite. Stringer mineralization is quite common in the footwall and is composed of thin, anastomosing quartz veins with dark red sphalerite and minor chalcopyrite.

The sulphides in unit 2 felsic volcanoclastics may have formed from hydrothermal fluids that precipitated metals within the highly permeable felsic mass-flow, close to the seafloor. Also present in unit 2 are near-massive sulphide beds that may represent precipitates directly onto the seafloor, where barite and chert also accumulated episodically. Finally, the presence of detrital massive sulphide fragments and chert and barite clasts in unit 2 indicates that some reworking has occurred. The different styles of mineralization are currently under study in terms of stratigraphic level and facies variations, mineralogical and isotopic variations, and temperature and composition of mineralizing fluids.

Although the overall mine stratigraphy is relatively consistent, the composition of the sulphide mineralization and its relationships to extrusive and intrusive rocks are quite variable. This is best demonstrated by drill holes TCU 90-22 (Figure 3) and TCU 92-36 (Figure 4). Although these two holes are located less than 200 metres apart, TCU 90-22 intersects an interval of uninterrupted sulphide mineralization, in contrast to TCU 92-36 which intersects two significant intervals of mineralization separated by about 24 metres of dacite sill and 7 metres of mafic sill.

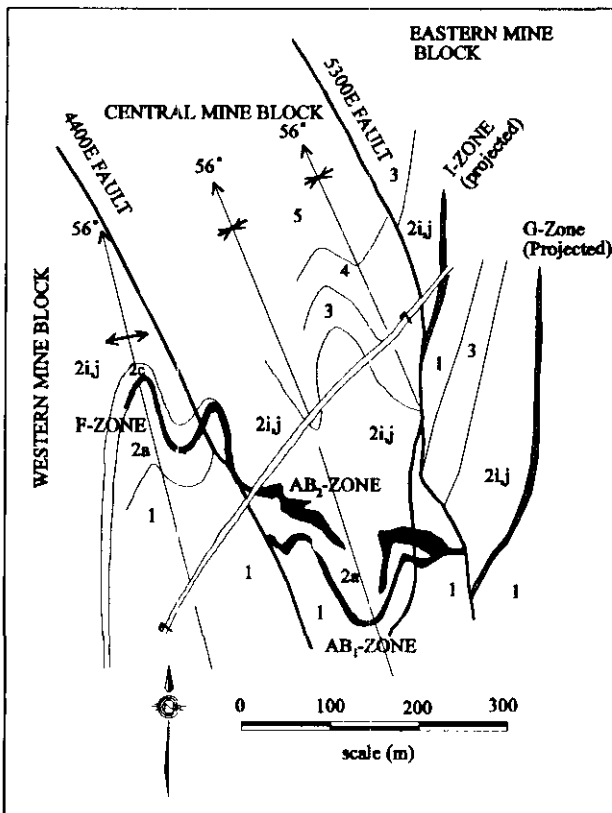


Figure 2. Tulsequah Chief 5400 level geology map: 1, undifferentiated basalt; 2a, mixed felsic fragmental rock; 2c, banded to massive chert; 2i,j, dacite flow, flow breccia and lapilli tuff; 3, undifferentiated mafic sill; 4, undifferentiated upper felsic horizon; 5, undifferentiated mafic flows and epiclastic rocks; 7, Sloko dike. Black areas are sulphide mineralization. Mapping from McGuigan *et al.*, 1993.

### UNIT 4

The upper felsic package (unit 4) is very similar to unit 2 but may contain a greater proportion of volcanoclastic material. Unit 4 is composed mainly of dacitic mass-flows with pumice, lithic, chert and barite fragments. The preservation of angular pumice fragments suggests that the volcanoclastic material has not been highly reworked. East of the 5300E fault felsic rocks, previously assigned to unit 4, are host to the I zone sulphide lens which was the main focus of early mining activity. Recent mapping and drill-hole interpretation suggest that the I zone may be a structural offset of the G zone and may correlate with the lower felsic stratigraphy of unit 2.

### UNIT 5

The upper mafic package (unit 5) is primarily massive mafic flows or sills, and intercalated sediments composed mainly of argillite, siltstone, ash tuff and minor chert. The unit is typically unaltered and lies above all known mineralization.

# DDH TCU 90-22

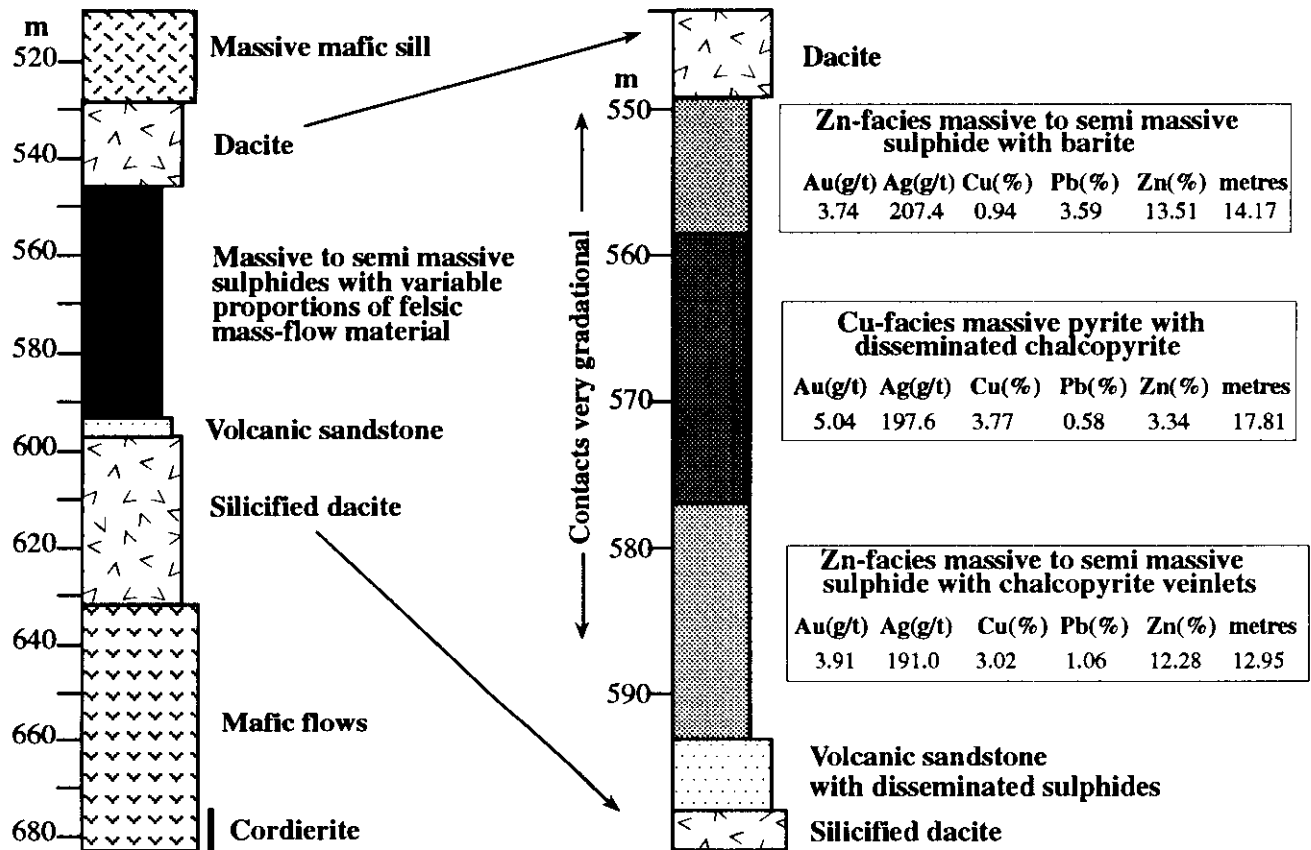


Figure 3. Stratigraphic section for diamond-drill hole TCU 90-22.

## GEOCHRONOLOGY

On the basis of mapping and biochronology by Nelson and Payne (1984), the Tulsequah Chief deposit was considered to be mid-Pennsylvanian to Early Permian in age. The fossil locality described by Nelson and Payne is about 2 kilometres northeast of the Tulsequah deposit, making its stratigraphic position with respect to the ore horizon uncertain. In order to help date the volcanic stratigraphy, a coarse-grained volcanoclastic rock from unit 4, near the 6400 portal, was analyzed by J. Mortensen. Results for this sample are presented below.

## ANALYTICAL TECHNIQUES

Approximately 50 kilograms of dacite from unit 4, the upper felsic volcanic unit, was collected by M. Casselman of Cominco for U-Pb dating. Zircons were separated using conventional Wilfley table and heavy liquid techniques. Most zircon fractions were abraded prior to analysis (Krogh, 1982) to minimize the effects of surface-correlated lead loss. Uranium-lead analyses were done at the geochronology laboratory at the Geological Survey of Canada (Ottawa). Criteria for selection of grains for analysis, and procedures used for dissolution, chemical extraction and purification of uranium and

lead, and mass spectrometry are described in detail by Parrish *et al.* (1987). Procedural blanks were 20 to 7 picograms for lead and less than 1 picogram for uranium. Uranium-lead analytical data are given in Table 1. Errors assigned to individual analyses were calculated using the numerical error propagation method of Roddick (1987). Age calculations employed the decay constants recommended by Steiger and Jäger (1975), and initial common lead compositions from the model of Stacey and Kramers (1975). Concordia intercept ages were calculated using a modified York-II regression model as described by Parrish *et al.* (1987), and the algorithm of Ludwig (1980). All errors in ages are given at the 2 $\sigma$  level.

## ANALYTICAL RESULTS

About one-half of the original dacite sample was processed initially. Only a small amount of zircon was recovered. The zircons form a relatively homogeneous population of mainly fine, very pale pink, clear grains with rare to abundant clear, bubble- and rod-shaped inclusions. Igneous zoning was faint to absent, and no cores were observed. The grains range from equant to

# DDH TCU 92-36

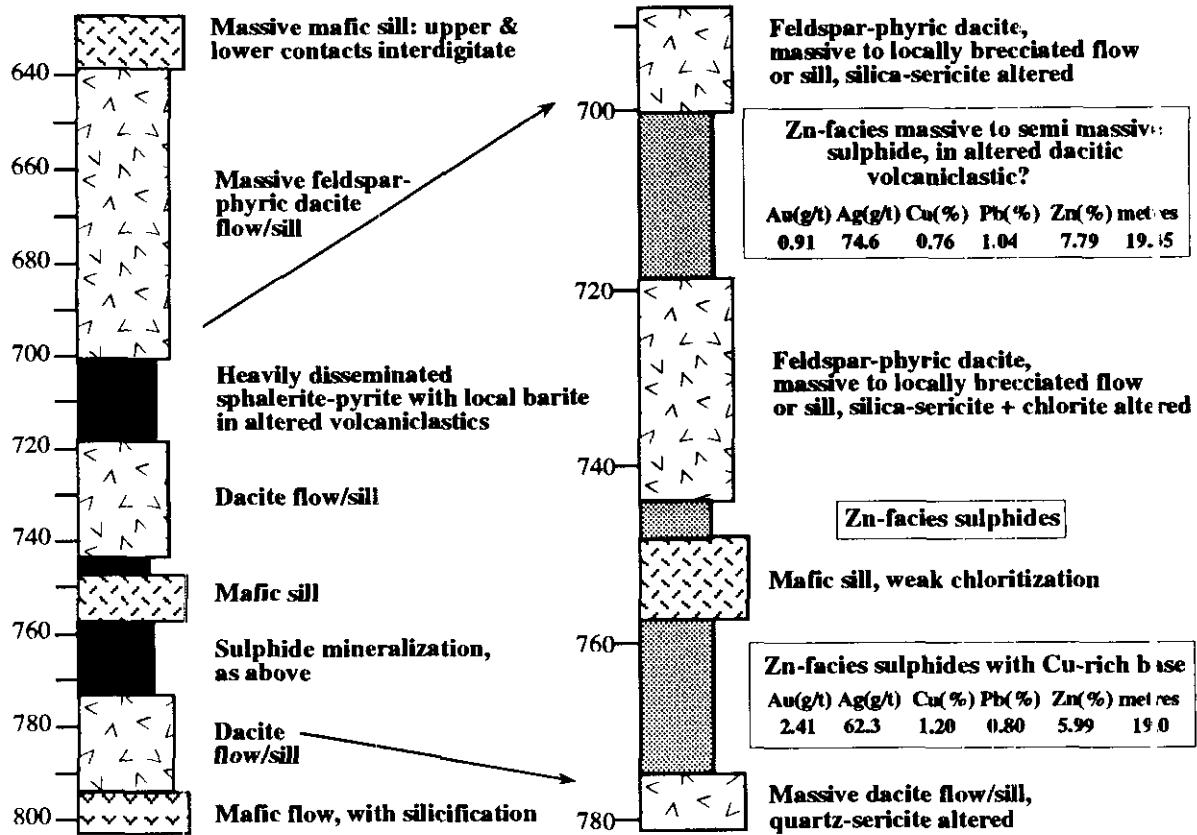


Figure 4. Stratigraphic section for diamond-drill hole TCU 92-36

**TABLE 1**  
**URANIUM-LEAD ANALYTICAL DATA FOR TULSEQUAH CHIEF UNIT 4 DACITE**

Sample Description	Wt. (mg)	U (ppm)	Pb <sup>2</sup> (ppm)	<sup>206</sup> Pb/ <sup>204</sup> Pb (meas.) <sup>3</sup>	% <sup>208</sup> Pb <sup>2</sup>	<sup>206</sup> Pb/ <sup>238</sup> U <sup>4</sup> (± % 1s)	<sup>207</sup> Pb/ <sup>235</sup> U <sup>4</sup> (± % 1s)	<sup>207</sup> Pb/ <sup>206</sup> Pb <sup>4</sup> (± % 1s)	<sup>207</sup> Pb/ <sup>206</sup> Pb <sup>4</sup> (M.a. ± % 2s)
A: N,+74,a	0.039	198	61.6	4291	20.0	0.26286(0.09)	3.6394(0.10)	0.10042(0.34)	1631.8(1.4)
B: N,+74,a	0.057	269	84.9	6950	12.4	0.28528(0.09)	4.9473(0.10)	0.12577(0.33)	2039.7(1.1)
C: N,-44	0.079	275	55.5	5519	8.8	0.19475(0.08)	2.6157(0.10)	0.09741(0.33)	1575.1(1.3)
D: N,-44	0.063	390	64.8	2876	8.3	0.16325(0.09)	1.9072(0.11)	0.08473(0.35)	1309.4(1.8)
EA: bulk,a	0.011	193	11.3	737	12.6	0.05633(0.14)	0.4162(0.40)	0.05358(0.35)	353.4(15.8)
EB: bulk,single,a	0.003	292	15.1	318	15.8	0.04805(0.21)	0.3566(0.89)	0.05383(0.79)	363.9(35.4)
F: bulk,best prisms,a	0.015	213	12.0	1237	11.6	0.05478(0.10)	0.4042(0.23)	0.05352(0.19)	351.7(3.7)

<sup>1</sup> +74, -74 refers to grain size in diameter (μ); N, nonmagnetic on Frantz magnetic separator; a, abraded

<sup>2</sup> radiogenic Pb; corrected for blank, spike and initial common Pb

<sup>3</sup> corrected for spike and fractionation

<sup>4</sup> corrected for blank Pb and U, and common Pb. Errors are 1 standard error of mean for isotopic ratios and 1σ for derived ages

stubby prismatic (1:w = 2-3) subhedral forms to irregular, anhedral, commonly broken grains showing smoothly corroded surfaces suggestive of magmatic corrosion. Four fractions were selected for analysis. Two of these were relatively coarse (>74 $\mu$  diameter) equant to prismatic grains, and were strongly abraded prior to dissolution. Two other fractions of finer unabraded grains were also analyzed. The four analyses are all moderately to highly discordant (Figure 5) and yield surprisingly old  $^{207}\text{Pb}/^{206}\text{Pb}$  ages (up to 2040 Ma). In view of the probable mid-Paleozoic crystallization age inferred for the volcanic rocks in the Tulsequah region, the data were taken to indicate the presence of a major component of older zircon in the sample, either as inherited cores or, more likely, as xenocrysts that did not differ greatly in appearance from the igneous grains. Zircon was subsequently separated from the remaining sample of dacite, and three fractions were selected and abraded. One fraction (F) was of the clearest, most euhedral prismatic grains in the sample, a second fraction (EA) consisted of very clear fragments with at least one well-preserved euhedral facet, and the third fraction was a single, faintly zoned, subhedral, stubby prismatic grain with a slightly more inclusion-rich core. These three fractions yield much younger  $^{207}\text{Pb}/^{206}\text{Pb}$  ages, and define a linear array (Figure 5) with calculated upper and lower intercept ages of  $350.6 + 14.7/-6.2$  and  $-72 \pm 267$  Ma, respectively. One of the fractions (EA) is concordant with a  $^{207}\text{Pb}/^{206}\text{Pb}$  age of  $353.8 \pm 15.8$  Ma. The similarity of the  $^{207}\text{Pb}/^{206}\text{Pb}$  ages of the three fractions suggests that they were all free of inheritance (despite the slightly cloudy core visible in single grain EB). We consider the best estimate of the crystallization age of the dacite sample to be given by the  $^{207}\text{Pb}/^{206}\text{Pb}$  and  $^{206}\text{Pb}/^{238}\text{U}$  ages of fraction EA, and therefore assign a latest Devonian to earliest Mississippian age of  $353.4 \pm 15.8/-0.9$  Ma to the sample.

## DISCUSSION

A preliminary interpretation of the early geological history of the mine area is:

- 1) accumulation of a widespread mafic volcanic basement composed of basaltic flows and sills and minor tuffaceous sediments;
- 2) accumulation of massive dacitic volcanic flows and flow breccias;
- 3) mass flows of dacitic to heterolithic volcanoclastic debris with local baritic to cherty intervals;
- 4) emplacement of sulphide mineralization at a number of stratigraphic levels associated with the dacitic volcanoclastic package; sulphides infilled porous unconsolidated debris flows and accumulated as exhalative units together with barite and chert between debris flows;
- 5) intrusion of the dacitic volcanoclastic package by one or more dacite sills which acted to dilate the original mineralized intervals;
- 6) intrusion of the unit 3 mafic sill, further dilating the felsic package to produce felsic units 2 and 4;

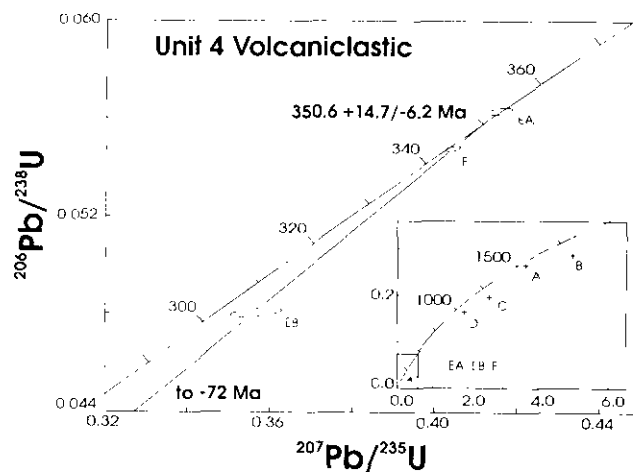


Figure 5.  $^{206}\text{Pb}/^{238}\text{U}$  vs.  $^{207}\text{Pb}/^{235}\text{U}$  concordia diagram for unit 4 (upper felsic horizon)

- 7) accumulation of the unit 5 mafic volcanic rocks. It is possible that unit 5 is coeval with, and genetically related to the unit 3 sill.

## FURTHER WORK

Further work will involve: examination of primary volcanic textures and facies relationships to determine the physical environment of ore formation; lithochemical and petrographic analysis of all units to determine the stratigraphic relationships and the effect of alteration throughout the camp; uranium-lead geochronology on newly collected samples from the upper and lower felsic volcanic packages within the central mine block, unit 3 mafic intrusion, a felsic volcanic sample from the Big Bull deposit and two regional felsic units.

Galena samples were collected from all mineralized horizons for lead isotope analysis. On a regional scale a detailed analysis of the lead isotopic signature may yield information on the tectonic setting and evolution of the Tulsequah Chief and Big Bull deposits. Locally, minor variations in the lead isotopic composition of the different ore lenses may assist in correlating mineralized horizons between the major fault blocks.

Mineralized intervals have been sampled for fluid inclusion and stable isotope analysis to determine the physical and chemical conditions of the ore-forming fluids and how they may have varied both temporally and spatially.

## ACKNOWLEDGMENTS

We are indebted to Redfern Resources Limited and Cambria Geological Limited for permission to publish information on the Tulsequah Chief deposit. We have benefited from discussions with Don Harrison, Bob Carmichael and Kerry Curtis of Redfern Resources on the geology of the Tulsequah Chief and Big Bull properties. We thank Mike Casselman of Cominco Ltd., previous owner of the property, for supplying the dacite

sample for U-Pb dating.

JKM thanks the staff of the Geochronology Section at the Geological Survey of Canada in Ottawa for assistance in producing the U-Pb analytical data, and R. W. Kirkham for arranging for collection of the geochronology sample and for many useful discussions regarding Tulsequah and other volcanogenic massive sulphide deposits in the Cordillera.

Research at the Tulsequah Chief - Big Bull properties forms part of a Mineral Deposit Research Unit project on Volcanogenic Massive Sulphide Deposits of the Cordillera funded by the Natural Sciences and Engineering Research Council of Canada, Science Council of British Columbia and ten mining and exploration member companies.

## REFERENCES

- Casselman, M.J. (1988): Tulsequah Chief Property; *Cominco Ltd.*, 1987 Year End Internal Report.
- Casselman, M.J. (1989): Tulsequah Chief Property; *Cominco Ltd.*, 1988 Year End Internal Report.
- Casselman, M.J. (1990): Tulsequah Chief Property; *Cominco Ltd.*, 1989 Year End Internal Report.
- Kerr, F.A. (1948): Taku River Map Area, British Columbia; *Geological Survey of Canada Memoir 248*, 84 pages.
- Krogh, T. (1982): Improved Accuracy of U-Pb Zircon Ages by the Creation of More Concordant Systems Using Air Abrasion Technique; *Geochimica et Cosmochimica Acta*, Volume 46, pages 637-649.
- Ludwig, K. R. (1980): Calculation of Uncertainties of U-Pb Isotope Data; *Earth and Planetary Science Letters*, Volume 46, pages 212-220.
- McGuigan, P., Melnyk, W., Dawson, G.L. and Harrison, D. (1993): Tulsequah Chief Mine, Northwestern B.C. 1992 Exploration Program: Diamond Drilling Geology and Reserve Estimation; *Cambria Geological Limited*, Vancouver, B.C. unpublished report in three volumes.
- Mihalynuk, M.G., Smith, M.T., Hancock, K.I. and Duda, S. (1994): Regional and Economic Geology of the Tulsequah River and Tulsequah Glacier Areas. (N.S. 104K-12 and 13); in *Geological Fieldwork 1993*, Grant, B., and Newell, J.M. Editors, *B.C. Ministry of Energy Mines and Petroleum Resources*, Paper 1994-1, this volume.
- Nelson, J. and Payne, J.G., (1984): Paleozoic Volcanic Assemblages and Volcanogenic Massive Sulphide Deposits near Tulsequah, British Columbia; *Canadian Journal of Earth Sciences*, Volume 21, pages 379-381.
- Parrish, R.R., Roddick, J.C., Leveridge, W.D. and Sullivan, R.W. (1987): Uranium-Lead Analytical Techniques at the Geochronology Laboratory, Geological Survey of Canada. in *Radiogenic Age and Isotopic Studies Report 1*, *Geological Survey of Canada*, Paper 87-2, pages 3-7.
- Roddick, J.C. (1987): Generalized Numerical Error Analysis with Applications to Geochronology and Thermodynamics; *Geochimica et Cosmochimica Acta*, Volume 51, pages 2129-2135.
- Stacey, J.S. and Kramers, J.D. (1975): Approximation of Terrestrial Lead Isotope Evolution by a Two-stage Model; *Earth and Planetary Science Letters*, Volume 26, pages 207-221.
- Steiger, R.H. and Jäger, E. (1977): Subcommittee on Geochronology: Convention on the Use of Decay Constants in Geo- and Cosmochronology; *Earth and Planetary Science Letters*, Volume 36, pages 359-362.
- Souther, J.G., (1971): Geology and Mineral Deposits of the Tulsequah Map-area, British Columbia. *Geological Survey of Canada*, Memoir 362, 84 pages.

## NOTES

## EXTERNAL PUBLICATIONS

- Alldrick, D.J., Godwin, C.I. and Sinclair, A.J. (1993): An Exploration Application for Lead Isotope Ratios, Stewart Mining Camp, Northwestern British Columbia; in *Exploration Mining Geology, Canadian Institute of Mining, Metallurgy and Petroleum*, Volume 2, Number 2, pages 121-128.
- Blais, A., Clague, J. and Bobrowsky, P.T. (1993): Marine Geological Studies of Coastal Areas, Saanich Inlet; in *Applied Quaternary Research*, Program with Abstracts and Field Guide, *CANQUA 1993*, pages G19-G22.
- Blyth, H. and Levson, V.M. (1993): Metchosin Gravel Pit; in *Applied Quaternary Research*; *Canadian Quaternary Association*, Program with Abstracts and Field Guide, pages 92-96.
- Bobrowsky, P.T. and Clague, J. (1993): Island View Beach Neotectonics Stop; in *Applied Quaternary Research*, Program with Abstracts and Field Guide, *CANQUA 1993*, pages G65-G67.
- Bobrowsky, P.T., Sansom, J. and Howes, D. (1993): Beacon Hill Sea Cliffs; in *Applied Quaternary Research*, Program with Abstracts and Field Guide, *CANQUA 1993*, pages G76-G80.
- Clague, J.J., Bobrowsky, P.T. and Hamilton, T.S. (1993): Documentation of a Tsunami Origin for a Sand Sheet at Port Alberni, British Columbia, by <sup>137</sup>CS analysis; *Estuarine and Coastal Shelf Science*, B.C. Geological Survey Contribution #003, in press.
- Cook, S.J. and Fletcher, W.K. (1993): Distribution and Behaviour of Platinum in Soils, Sediments and Waters of the Tulameen Ultramafic Complex, Southern British Columbia, Canada; *Journal of Geochemical Exploration*, Volume 46, pages 279-308.
- Cook, S.J. and Fletcher, W.K. (1992): Platinum-group Elements in Tulameen Coal, British Columbia, Canada - A Discussion; *Economic Geology*; Volume 87, pages 1677-1679.
- Cook, S.J. and Fletcher, W.K. (1992): Influence of Subsample Size on Pt Recovery: Analytical Pitfalls in Geochemical Exploration for Chromite-associated Pt Deposits; *Explore*, Number 75, pages 17-18.
- Cordey, F. and Schiarizza, P. (1993): Long-lived Panthalassic Remnant: The Bridge River Accretionary Complex, Canadian Cordillera; *Geology*, Volume 21, pages 263-266.
- Dawson, F.M. and Ryan B.D. (1992): Distribution and Quality of some Bowser Basin Coals, Northern British Columbia; *Geological Survey of Canada*, Open File 2555.
- Dostal, J. and Church, B.N. (1994): Geology and Geochemistry of the Volcanic Rocks of the Pioneer Formation, Bridge River Area, Southwestern British Columbia; in *Geological Magazine*, *Cambridge University Press*, Volume 131, in press.
- Grant, B. and Logan C. (1993): Geoscience and the Public: Bridging Communications Gaps in British Columbia; CO-GEOENVIRONMENT, Netherlands International Union of Geological Sciences, Commission on Geological Sciences for Environmental Planning - Circular 3, Fall 1993.
- Grieve, D.A. (1992): Phosphorus in British Columbia Coking Coals; *Proceedings of the Canadian Coal and Coalbed Methane Geoscience Forum*, Parksville, B.C., February 1992, pages 335-354.
- Grunsky, E.C. (1991): Strategies and Methods for the Interpretation of Geochemical Data; in *Exploration Geochemical Data Processing, Mineral Deposits Research Unit, University of British Columbia*, Short Course G, Interpretation of Geochemical Data, June 1991, 88 pages.
- Grunsky, E.C. and Agterberg, F.P. (1991): FUNCORR A FORTRAN 77 Program for Computing Multivariate Spatial Autocorrelation; *Computers and Geosciences*, Volume 17, Number 1, pages 115-131.
- Grunsky, E.C. and Agterberg, F.P., (1991): SPFA 2: A Fortran 77 Program for Spatial Relationships of Multivariate Analysis; *Computers and Geosciences*, Volume 17, Number 1, pages 133-160.
- Grunsky, E.C. and Agterberg, F.P. (1992): Spatial Relationships of Multivariate Data; *Mathematical Geology*, Volume 24, Number 6, pages 731-758.
- Grunsky, E.C., Easton, R.M., Thurston, P.C. and Jensen, L.S. (1992): Characterization and Statistical Classification of Archean Volcanic Rocks using Major Element Geochemistry; in *The Archean: Terrains, Processes and Metallogeny*, Glover, J.E. and Ho, S.E., Editors, *Proceedings for the Third International Archean Symposium*, pages 11-38.
- Harper, J. and Bobrowsky, P.T. (1993): Esquimalt Lagoon; in *Applied Quaternary Research*, Program with Abstracts and Field Guide, *CANQUA 1993*, pages G65-G67.
- Holuszko, M.E. (1992): Washability of Peace River and East Kootenay Coals; *Proceedings of the Canadian Coal and Coalbed Methane Geoscience Forum*, Parksville, B.C., February 1992, pages 189-210.
- Holuszko, M.E., Grieve, D.A. and Matheson, A. (1992): Sulphur in British Columbia Coals and its Implications for Cleaning; *International Journal of Environmental Issues in Minerals and Energy Industry*, Volume 1, pages 83-93.
- Höy, T., Dunne, K.P.E. and Wilton, P. (1993): Massive Sulphide and Precious Metal Deposits in Southeastern British Columbia; *Geological Association of Canada Mineralogical Association of Canada*, Joint Annual Meeting 1993, Field Trip A-7 Guidebook A-7, 74 pages.
- Hyndman, R.D., Dragert, H., Rogers, G.C., Wang, D., Clague, J.J. and Bobrowsky, P. (1993): Constraints on the Potential Megathrust Rupture Surface in the Northern Cascadia Subduction Zone; *EOS Transactions American Geophysical Union*, Volume 73, page 123.
- Jones, L.D. and Jakobsen, D. (1992): Geoscience Database and Geographical Information Systems with Examples from MINFILE; in *Geographical Information Systems Workshop Notes*, *Geological Association of Canada, Cordilleran Section*, February 1992, Simon Fraser University, Vancouver, Canada.
- Levson, V.M., Kerr, D.M. and Giles, T.R. (1993): Recognizing Late Pleistocene Paleoshoreline Levels from Geomorphic and Stratigraphic Records of Glaciofluvial Deltas; *Current Research in the Pleistocene*, in press.
- McMillan, W.J. and Panteleyev, A. (1992): Tectonic Setting of Mesozoic Gold Deposits in the Canadian Cordillera; in *Basement Tectonics 8: Characterization and Comparison of Ancient and Mesozoic Continental Margins*, Bartholomew, M.J., Hyndman, D.W., Mogk, D.W. and Mason, R., Editors, *Proceedings of the 8th International Conference on Basement Tectonics*, Butte, Montana, pages 633-651.

- Money, N.J., Tauchid, M., Jones, L.D., Pecnik, M. and Taylor, R.B. (1993): Proceedings of the Regional Training Course on Computerised Databases in Mineral Exploration and Development, 10-28 May 1993; Lusaka, Zambia; *International Atomic Energy Agency (IAEA) Vienna and Geological Survey Department, Ministry of Mines, Zambia*, in preparation.
- Owen, J.V., Dostal, J. and Church, B.N. (1993): Mineralogic Reaction Zones at a Calc-Silicate/Metapelite Interface: An Example of trace Element Mobility in a Metamorphic Environment; *Mineralogical Magazine*.
- Pell, J. and Hora, Z.D. (1993): Rifting, Alkaline Rocks and Related Magmatic Deposits in the Southern Canadian Cordillera; *Proceedings of the Eighth Quadrennial IAGOD Symposium*.
- Price, R.A., Grieve, D.A. and Patenaude, C. (1992): Geology, Tornado Mountain, British Columbia-Alberta; *Geological Survey of Canada*, Map 1823A, scale 1:50 000.
- Price, R.A., Grieve, D.A. and Patenaude, C. (1992): Geology and Structure Cross-section, Fording River (West Half), British Columbia - Alberta; *Geological Survey of Canada*, Map 1824A, scale 1:50 000.
- Rutter, N.W., Fenton, M., Levson, V.M., Pawlowicz, J., Reasoner M. and Beaudoin, A. (1993): Quaternary Geology of the Edmonton - Jasper - Rocky Mountain House Region; *Geological Association of Canada - Mineralogical Association of Canada*, Field Trip Guidebook A-2, 128 pages.
- Ryan, B.D. (1992): Estimation of Coal Washability Using Small Samples; *Journal of Coal Quality*, Volume 11, pages 13-19.
- Sibbick, S.J., Matysek, P.F., Cook, S.J. and Jackaman, W. (1992): Influence of Geology on Metal Concentrations within the Howe Sound Watershed; in Proceedings of the Howe Sound Environmental Science Workshop, Levings, C.D., Turner, R.B. and Ricketts, B., Editors, *Canadian Technical Report of Fisheries and Aquatic Sciences*, Number 1879, pages 35-42.
- Sibbick, S.J. and Fletcher, W.K. (1993): Distribution and Behavior of Gold in Soils and Tills at the Nickel Plate Mine, Southern British Columbia; *Journal of Geochemical Exploration*, Volume 47, pages 183-200.
- Simandl, G.J., Hancock, K.D., Paradis, S. and Simandl, J. (1992): Use of Sodium Polytungstate in Exploration for Magnesite Deposits in Sedimentary Rocks, Southeastern British Columbia, Canada; *Canadian Institute of Mining, Metallurgy and Petroleum*, Bulletin, Volume 86, Number 966, pages 68-72.
- Turner, R.W., Höy, T., Letich, C.H.B., Anderson, D. and Ransom, P.W. (1993): Guide to the Geological Setting of the Middle Proterozoic Sullivan Sediment-hosted Pb-Zn Deposit, Southeastern British Columbia; in *Geologic Guidebook to the Belt-Purcell Supergroup, Glacier National Park and Vicinity, Montana and Adjacent Canada*, Link, P.K., Editor, Belt Symposium III Fieldtrip Guidebook; *Belt Association Inc.*, Spokane, Washington, pages 53-94.
- Turner, R.J.W., Ames, D.E., Franklin, J.M., Goodfellow, W.D., Leitch, B.H.B. and Höy, T. (1993): Character of Active Hydrothermal Mounds and Nearby Altered Hemipelagic Sediments in the Hydrothermal Areas of Middle Valley, Northern Juan de Fuca Ridge; Shallow Core Data, *Canadian Mineralogist*, in press.

# UNIVERSITY RESEARCH IN BRITISH COLUMBIA

## THE UNIVERSITY OF BRITISH COLUMBIA, 1992

- Hunt, J.A.: Stratigraphy, Maturation and Source Rock Potential of Cretaceous Strata in the Chilcotin Nechako Region of British Columbia. (M.Sc.)
- Ke, P.: A New Approach to Mass Balance Modeling: Applications to Igneous Petrology. (M.Sc.)
- Lyatsky, H.: Structure, Evolution, and Petroleum Potential of the Queen Charlotte Basin. (Ph.D.)
- Taite, S.: The Geology of the Central Moresby Island Region, Queen Charlotte Island, (Haida Gwaii) British Columbia. (M.Sc.)

## THE UNIVERSITY OF BRITISH COLUMBIA, 1993

- Bartsch, R.D.: Volcanic Stratigraphy and Lithochemistry of the Lower Jurassic Hazelton Group, Host to the Eskay Creek Precious and Base Metal Volcanogenic Deposit. (M.Sc.)
- Bickford, C.: Geology and Petrography of the Wellington Seam, Nanaimo Coalfield, Vancouver Island. (M.Sc.)
- Bridge, D.: The Deformed Early Jurassic Kerr Copper-Gold Porphyry Deposit, Sulphurets Gold Camp, Northwestern British Columbia. (M.A.Sc.)
- Cookenboo, H.O.: Lithofacies, Provenance, and Diagenesis of Jura Cretaceous Strata of the Northern Bowser Basin, British Columbia. (Ph.D.)
- Cui, Y.: Geochemistry of Igneous Rocks from the Southern Coast Belts Plutonic Complex, Southwestern British Columbia. (M.Sc.)
- Delaney, T.: Distribution of Gold in Soils and Stream Sediments in a Variety of Weathering Environments, and the Use of Cyanidation in Exploration Geochemistry. (M.Sc.)
- Jardine, K.: Hydrogeological Decision Analysis: Monitoring Networks for Fractured Geologic Media. (M.A.Sc.)
- Lamberson, M.N.: Composition and Facies Variation in Mid-Cretaceous Gates Formation Coal, Northeastern British Columbia, Canada: Implications for the Interpretation of Paleo-Wetland Environments and Assessment of Coalbed Methane Characteristics. (Ph.D.)
- Nadaraju, G.T.: Triassic-Jurassic Geochronology of the Eastern Iskut River Map Area, Northwestern British Columbia. (M.Sc.)
- Rhys, D.A.: Geology of the Snip Mine, and its Relationship to the Magmatic and Deformational History of the Johnny Mountain Area, Northwestern British Columbia. (M.Sc.)
- Ross, K.V.: Geology of the Ajax East and Ajax West, Silica-Saturated Alkalic Copper-Gold Porphyry Deposits, Kamloops, South Central British Columbia. (M.Sc.)
- Roth, T.: Geology, Alteration and Mineralization in the 21A Zone, Eskay Creek, Northwestern British Columbia. (M.Sc.)

## UNIVERSITY OF ALBERTA, 1992

- Caplan, M.L.: Sedimentology, Stratigraphy and Petrography of the Middle Triassic Halfway Formation, Peeply Field, North-eastern British Columbia. (M.Sc.)
- Carey, J.S.: Origin and Geologic Significance of Holocene Temperate Carbonates, British Columbia Continental Shelf. (M.Sc.)
- Zaluski, G.S.: Hydrothermal Alteration and Fluid Sources Associated with the Babine Lake Porphyry Copper Deposits, West-central British Columbia. (M.Sc.)

## UNIVERSITY OF ALBERTA, 1993

- Lu, Z.: Landslides and Geotechnical Properties of Volcanic Tuff on Mount Cayley, British Columbia. (Ph.D.)
- Xiong, Y.: Geochemistry of the Vault Epithermal Mineralization and its Environs, Okanagan Falls, Southern British Columbia. (M.Sc.)

## UNIVERSITY OF CALGARY, 1993

- Lickorish, W.H.: Structure of the Porcupine Creek Anticlinorium and Tectonic Implications of the Lower Cambrian Gog Group of the Rocky Mountain Ranges. (Ph.D.)
- Porter, S.: Geology and Metamorphism of Elbow Mountain, Iskut River Map Area, Northwestern British Columbia. (B.Sc.)
- Simpson, G.: Early Diagenesis in the Fraser River Delta. (M.Sc.)
- Varsek, J.L.: Cordilleran Crustal Structure, Southern Canada and Northwestern United States. (Ph.D.)
- Vogl, J.J.: The Southern Tail of the Nelson Batholith, Southeast British Columbia. (M.Sc.)

## MCGILL UNIVERSITY, 1993

- Thiersch, P.: Mineralization and Ore Controls of the Shasta Ag-Pb Deposit, Toodoggone River Area, British Columbia. (M.Sc.)

## UNIVERSITY OF WESTERN ONTARIO

- Gunning, M.H.: Character and Evolution of an Upper Carboniferous to Upper Permian Succession in an Extensional Oceanic Tectonic Setting; Stikine Assemblage, Northwest Stikinia, Scud River Area (NTS 104G), British Columbia. (M.Sc.)

## QUEEN'S UNIVERSITY

- Castonguay, Sébastien (1993): Structure, Evolution and Tectonic Significance of the Misty Thrust: Kanaskis Country, Southern Canadian Rocky Mountains. (M.Sc.)
- Hall, Douglas C. (1991): A Petrological Investigation of the Cross Kimberlite Occurrence, Southeastern British Columbia, Canada. (Ph.D.)

## NOTES